

ADVANCES IN CHEMICAL PHYSICS  
VOLUME VII

## EDITORIAL BOARD

THOR A. BAK, Universitetets Fysik Kemiske Institut, Copenhagen, Denmark

J. DUCHESNE, University of Liège, Liège, Belgium

H. C. LONGUETT-HIGGINS, The University Chemical Laboratory, Cambridge, England

M. MANDEL, University of Leiden, Leiden, Holland

V. MATHOT, Université Libre de Bruxelles, Brussels, Belgium

P. MAZUR, Institut Lorentz, Leiden, Holland

A. MÜNSTER, Laboratoire de Chimie Physique, Université de Paris, Paris, France

S. ONO, Institute of Physics, College of General Education, Tokyo, Japan

B. PULLMAN, Laboratoire de Chimie Théorique, Université de Paris, Paris, France

S. RICE, Department of Chemistry, University of Chicago, Chicago, Illinois

G. SZASZ, General Electric Company, Zürich, Switzerland

M. V. VOLKENSTEIN, Institute of Macromolecular Chemistry, Leningrad, U.S.S.R.

B. H. ZIMM, School of Science and Engineering, University of California at San Diego, La Jolla, California



ADVANCES IN CHEMICAL PHYSICS—VOLUME VII

I. Prigogine—Editor

---

# The Structure and Properties of Biomolecules and Biological Systems

**Edited by J. DUCHESNE**

*University of Liège, Liège, Belgium*

**INTERSCIENCE PUBLISHERS**

**a division of John Wiley & Sons, Ltd., London—New York—Sydney**

FIRST PUBLISHED 1964                      ALL RIGHTS RESERVED  
LIBRARY OF CONGRESS CATALOG CARD NUMBER 58-9935

PRINTED IN GREAT BRITAIN  
BY SPOTTISWOODE, BALLANTYNE & CO. LTD.  
LONDON AND COLCHESTER

## CONTRIBUTORS TO VOLUME VII

- R. BRAAMS, Department of Radiobiophysics, Physics Laboratory, University of Utrecht, Utrecht, The Netherlands
- P. S. BRATERMAN, Inorganic Chemistry Laboratory, Oxford University, Oxford, England
- R. C. DAVIES, Inorganic Chemistry Laboratory, Oxford University, Oxford, England
- PIERRE DOUZOU, Biophysics Laboratory, National Museum of Natural History, Paris, France
- ANDERS EHRENBERG, Medicinska Nobelinstitutet, Biokemiska Avdelningen, Karolinska Institutet, Stockholm, Sweden
- D. D. ELEY, Department of Chemistry, University of Nottingham, Nottingham, England
- J. I. FERNÁNDEZ-ALONSO, Department of Physical Chemistry, Faculty of Science, University of Valencia, Valencia, Spain
- T. A. HOFFMANN, Research Institute for Telecommunications, Budapest, Hungary
- JOHN JAGGER, Biology Division, Oak Ridge National Laboratory, Oak Ridge, Tennessee
- OLEG JARDETSKY, Department of Pharmacology, Harvard Medical School, Boston, Massachusetts
- DAVID R. KEARNS, Department of Chemistry, University of California, Riverside, California
- MASAO KOTANI, Department of Physics, Faculty of Science, University of Tokyo, Bunkyo-ku, Tokyo, Japan
- YOSHIMASA KYOGOKU, Faculty of Pharmaceutical Sciences, University of Tokyo, Bunkyo-ku, Tokyo, Japan
- J. LADIK, Central Research Institute for Chemistry, Hungarian Academy of Sciences, Budapest, Hungary
- J. LECOMTE, Laboratoire de Recherches Physiques, Paris, France
- ROBERT B. LESLIE, The Institute for Muscle Research, The Marine Biological Laboratory, Woods Hole, Massachusetts
- CLAUDE S. NICOLAU, Centre of Research of the Ministry of Health and Institute of Petroleum, Gas and Geology, Bucharest, Rumania
- ERNEST C. POLLARD, Biophysics Department, The Pennsylvania State University, University Park, Pennsylvania

CHARLES SADRON, Biophysics Laboratory, National Museum of Natural History, Paris, France

G. SCHOFFA, Physics Department of the Technical University, Karlsruhe, Germany

TAKEHIKO SHIMANOUCHI, Department of Chemistry, Faculty of Science, University of Tokyo, Bunkyo-ku, Tokyo, Japan

BERNARD SMALLER, Argonne National Laboratory, Argonne, Illinois

ALBERT SZENT-GYÖRGYI, The Institute for Muscle Research, The Marine Biological Laboratory, Woods Hole, Massachusetts

MASAMICHI TSUBOI, Faculty of Pharmaceutical Sciences, University of Tokyo, Bunkyo-ku, Tokyo, Japan

G. VAN HERPEN, Department of Radiobiophysics, Physics Laboratory, University of Utrecht, Utrecht, The Netherlands

CHARLES WALTER, Cardiovascular Research Institute, University of California Medical Center, San Francisco, California

R. J. P. WILLIAMS, Inorganic Chemistry Laboratory, Oxford University, Oxford, England

## CONTENTS

Introduction. <i>By A. Szent-Györgyi</i> . . . . .	ix
--	----

### PART I: THEORETICAL

#### A. Electronic Structure of Proteins and Nucleic Acids

1. Electronic structures in quantum biochemistry. <i>By J. I. Fernández-Alonso</i> . . . . .	3
2. Quantum mechanical considerations on some properties of DNA. <i>By T. A. Hoffmann and J. Ladik</i> . . . . .	84
3. Electronic structure and magnetic properties of hemoproteins, particularly of hemoglobins. <i>By Masao Kotani</i> . . . . .	159
4. Magnetic susceptibilities and the chemical bond in hemoproteins. <i>By G. Schoffa</i> . . . . .	182

### PART II: EXPERIMENTAL

#### B. Influence of Physical Agents on Proteins and Nucleic Acids

5. Thermal effects on protein, nucleic acid and viruses. <i>By Ernest C. Pollard</i> . . . . .	201
6. Adsorption of water on solid proteins with special reference to haemoglobin. <i>By D. D. Eley and R. B. Leslie</i> . . . . .	238
7. The effects of ionizing radiations on some fibrous proteins. <i>By R. Braams and G. Van Herpen</i> . . . . .	259

#### C. Electrical and Magnetic Properties of Organic Molecular Solids, Proteins and Nucleic Acids

8. Electronic conduction in organic molecular solids. <i>By David R. Kearns</i> . . . . .	282
9. The electronic properties of deoxyribonucleic acid. <i>By Pierre Douzou and Charles Sadron</i> . . . . .	339
10. The properties of metal-porphyrin and similar complexes. <i>By P. S. Braterman, R. C. Davies and R. J. P. Williams</i> . . . . .	359

#### D. Applications of Spectroscopic Methods

11. Prospects for the use of infrared spectroscopy in biology. <i>By J. Lecomte</i> . . . . .	408
12. Infrared spectra of nucleic acids and related compounds. <i>By Takehiko Shimanouchi, Masamichi Tsuboi and Yoshimasa Kyogoku</i> . . . . .	435

13. The study of specific molecular interactions by nuclear magnetic relaxation methods. *By Oleg Jardetzky* . . . . . 499
14. Recent advances in EPR spectroscopy. *By Bernard Smaller* . . . . . 532

### **E. Physico-chemical Mechanisms in Biological Systems**

15. Photoprotection from far ultraviolet effects in cells. *By John Jagger* 584
16. Some recent developments in the study of paramagnetic species of biological interest. *By Anders Ehrenberg* . . . . . 602
17. ESR investigations on different plant systems. *By Claude S. Nicolau* . . . . . 628
18. The use of product inhibition and other kinetic methods in the determination of mechanisms of enzyme action. *By Charles Walter* 645

Author Index . . . . . 725

Subject Index . . . . . 739

## INTRODUCTION\*

Up to the Renaissance, man had no reason to doubt that his senses revealed to him the ultimate nature of the world. He thought his senses and mind were perfect and trusted his reasoning more than any crude experiment. Each of us being the center of his (or her) universe, there could have been no doubt that man was really the center of the universe which was created for his pleasure or temptation, with a "beyond", in which apparent inequities could be amended.

In that great reawakening of the western mind, the Renaissance, here and there men appeared who questioned our perfection. Copernicus pointed out that the apparent motion of the sun around our globe could be equally explained by our globe's moving around the sun, and so our impressions do not necessarily correspond to reality. Maybe our eyes are not perfect either! So, Galileo built his telescope by which he discovered the rings of Saturn and the satellites of Jupiter. These had never been seen by man before, indicating that the universe could not have been created, solely, for man's pleasure. A Dutch greengrocer, Leeuwenhoek, built the first microscope, with which he discovered a whole new world, too small to be seen by the unarmed eye. Kepler replaced crude observation by taking careful notes of measurements while Galileo asked questions of nature and did experiments. Thus began experimental science, which grew exponentially, accelerating its own development. This "classical science", which had reached maturity at the end of the last century, extended man's world, replaced divine whim by natural laws, corrected many of our ideas, but brought nothing into the picture that man could not "understand". What we commonly call "understanding" means correlating our observation with some earlier experience. If I am told that it is gravitation which holds the universe together "I understand", though I do not know what gravitation is. By "understand" I mean that gravitation is the same thing which makes apples fall and I have seen apples fall before. So classical science introduced nothing that man could not

\* The writer is supported by grants from the National Science Foundation, and the National Institutes of Health, H-2042R.

understand, that was beyond his experience and was based on the impressions mediated by his senses. Nor did it introduce new dimensions into man's life. All this holds true, also, for science's twin brother: technology. Stephenson's "iron horse", the train, could still be outrun by a good live horse. So man could still feel at home in this universe, built of indestructible matter and energy.

A new period of science, and with it a new period in man's history, was ushered in by two mysterious discoveries just before the turn of the century, in 1896. The one was the discovery of radioactivity, by Becquerell, the other the discovery of X-rays, by Röntgen. These were the first steps toward an entirely new world, hidden behind the directly observable one, a world in which no human experience comes to our help in "understanding". In a way, this mysterious world is the real one, while the one in which we live is more or less but a flickering shadow.

We are at the very beginning of the exploration of this new world. Not only can our senses not reveal it, they are made so as not to reveal it. Our senses are given us by Nature to help us to get through the day alive. If they showed the real nature of things they would be useless. If I could see my chair as it is, a queer-shaped vacuum with here and there an atomic nucleus in it with electrons moving around it at a crazy speed in crazy patterns, I could simply not sit on it. I cannot expect ever to "understand" these nuclei and electrons because there is nothing analogous in my everyday experience.

This "modern" science brought new dimensions into man's life, creating a new world in which we are, more or less, strangers ourselves. It replaced the speed of the horse with the speed of light, and replaced the flimsy little terrestrial fires with cosmic energies which we are clever enough to release but not clever enough to grasp, and which threaten us all, now, with extinction.

The penetration into this new world, with its new dimensions, spreading from the infinitely small to the infinitely big, is exceedingly difficult. Our main vehicle is mathematics, which is not linked to any dimension. But even this tool, mathematics, is highly inadequate, its methods clumsy. We need enormous computers to solve the equation of an electron jump, while that electron simply makes that jump without calculation, and never misses.

By the side of the mathematical methods we have also developed sophisticated experimental methods for penetration into this new



world, often equally as clumsy as the mathematical methods, using thousands of tons of hardware to observe the behavior of an elementary particle. The most important of the new tools is the human brain, trained in the new ideas and methods, equipped for participation in this grand expedition into the unknown.

Chemistry has grown up on the shoulders of classical science, and biochemistry on the shoulders of classical chemistry. The newly discovered world of quanta, with its wave mechanics has had, as yet, no real impact on biology. Biochemistry has hardly taken notice of it. Present biochemistry is still "classical", being closely connected with everyday experience. A molecule of sugar is still the same sugar which I know from my breakfast table. It is true, I cannot see its shape and structure, but, all the same, I can describe them with my human ideas, and I can symbolize my ideas with simple figures, drawn on paper. "Molecular biology", which dominates biochemistry, at present uses these human ideas when describing molecules, stating their length, width, charge, and the sequence and relative positions of atoms.

There can be no doubt that this molecular biology is still harvesting the most wonderful successes, such as the "breaking of the code" of DNA, but behind these achievements there are hidden failures, which we tend to forget, being blinded by our successes. The basic phenomena of life, by which we know life from death, like motion (mechanic work), secretion (osmotic work) and reflexes (electric work), we still do not understand. The electron microscope has revealed, in the cell, an unsuspected wealth of structures, dominated by laminar formations. What is the deeper meaning of these formations? One of the most basic principles of Nature is that of organization. When Nature puts two things together in a meaningful way it always generates something entirely new, the qualities of which cannot be described in terms of the qualities of components. Living Nature is not additive. This holds true through the whole gamut of levels of organization, from elementary particles up to complex societies. What, then, is the meaning of these lamellar structures? What is the meaning of the cell, this most basic unit of life? Why are all higher organisms built of such small, more or less uniform units? And what is that mysterious "living state" which needs a constant energy for its maintenance and the preservation of its low entropy, the "negentropy" of Brillouin,

Looking, unbiased, at biology one must come to the conclusion that we have hardly scratched the surface of its central problems and created, with the molecular approach, merely a frame from which the picture is still missing. There is no doubt in the author's mind that the real nature of life will remain a closed book as long as we try to approach it solely with ideas of "classical" chemistry.

Needless to say hopeful beginnings of a new approach are not missing. Suffice it to quote the pioneering work of B. and A. Pullman, who have made an extensive effort to translate molecular biochemistry into the new language of wave mechanics, looking at biomolecules as they really are, not as pieces of matter with a certain anatomy, but as structures of atomic nuclei, surrounded by electronic clouds of varying shape and density, finding the explanation of chemical reactivity and biological function in the changes of these electronic clouds. The writer himself, with his associates, has devoted his last decade to calling the attention of biologists to this new approach, trying to broaden the way leading into this new world.

In the present volume, the Editor is bringing together papers, all leading us one step deeper into this new world. The penetration into such a new domain is exceedingly difficult. It demands both a great deal of knowledge and courage to try to participate in this new epic of man's intellectual ascent. The final goal is far, the ascent difficult, which makes the effort still more laudable and significant.

Institute for Muscle Research  
The Marine Biological Laboratory  
Woods Hole, Mass.

ALBERT SZENT-GYÖRGYI

*Advance in Chemical Physics, Volume VII*  
Edited by J. Duchesne  
Copyright © 1964 by John Wiley & Sons, Inc.

**PART I**

**THEORETICAL**

A. Electronic Structure of Proteins and Nucleic  
Acids Chaps. 1–4



# 1

## ELECTRONIC STRUCTURES IN QUANTUM BIOCHEMISTRY \*

J. I. FERNÁNDEZ-ALONSO, *Faculty of Science*  
*University of Valencia, Valencia, Spain*

### CONTENTS

I. Introduction . . . . .	4
II. Fundamental Concepts and Methods of Quantum Mechanics . . . . .	6
A. Atomic Orbitals . . . . .	10
B. The Chemical Bond . . . . .	16
C. Bond Orbitals . . . . .	18
D. Bonding and Antibonding Molecular Orbitals . . . . .	19
F. Orbitals for Multiple Bonds . . . . .	20
G. Localized and Delocalized Bonds . . . . .	21
H. Principal Quantum Mechanical Methods . . . . .	21
I. Molecular Orbital Theory; LCAO Approximation . . . . .	22
(1) Hückel Approximation (HMO) . . . . .	26
(2) Mulliken–Wheland Method . . . . .	28
(3) Introduction of Heteroatoms and Substituents: Pauling–Wheland Method . . . . .	30
(4) Other Naïve Methods . . . . .	32
(5) Goeppert-Mayer and Sklar Method . . . . .	32
(6) Self-Consistent Molecular Orbital Method (Roothaan's Equations) . . . . .	33
(7) Generalized Hückel or “SCF-like LCAO-MO” Method (Semi-empirical Methods) . . . . .	35
J. Electronic Indices . . . . .	38
(1) Total $\pi$ -Electron and Delocalization Energies . . . . .	38
(2) $\pi$ -Electron Charges or Densities . . . . .	40
(3) Bond Order . . . . .	41
(4) Free-Valence Index . . . . .	42
(5) Localization Energies . . . . .	42
(6) Chemical Reactivity . . . . .	43
III. Biochemical Applications . . . . .	44
A. Theory of Electron Transfer . . . . .	45
B. Electronic Structures of Biomolecules . . . . .	47
(1) Purines . . . . .	47
(2) Pyrimidines . . . . .	52

\* Translated by Dr. L. C. Cusachs.

(3) Adenine-Thymine and Guanine-Cytosine Pairs . . . . .	54
(4) Pteridines . . . . .	55
(5) Basicity of the Aromatic Ring Nitrogens . . . . .	59
(6) Electronic Structure and Antitumor Activity in Cancer . . . . .	60
C. Electronic Interpretation of Some Biocatalyzed Reactions . . . . .	61
(1) Electronic Structure of Energy-Rich Bonds . . . . .	62
(2) Electronic Structure of the Coenzymes DPN and FAD . . . . .	67
(3) Electronic Structure of the Transelectronases (Cytochromes) . . . . .	71
(4) The Pullmans' Theory of Enzymatic Hydrolysis . . . . .	74
(5) Other Biochemical Processes . . . . .	77
IV. Conclusions . . . . .	77
V. Acknowledgements . . . . .	79
References . . . . .	79

## I. INTRODUCTION

Recent rapid progress in certain domains of biology is due fundamentally to the possibility of formulating problems in molecular terms. Powerful research methods and techniques of chemistry, physics, and engineering then become applicable. This impact is most evident in biophysics and biochemistry, which, with their mother science, physiology, constitute molecular biology.

Study of the organization of living systems and the processes which occur in them has followed two roads: the organismic or systems approach, and the analytic method.

The first method supposes that the cell, tissue, or organism conserves its individuality as a "physico-chemical machine" in the corresponding medium, and one investigates the properties which result from its interactions, its adaptation to the medium and tendency to form higher entities or systems characterized by new properties, many of which cannot be predicted from a knowledge of simpler systems.

The employment of the analytic method, which has contributed more to the development of biochemistry, is better understood by considering one of its characteristic studies, that of the enzymes which specifically and efficiently catalyze biochemical reactions, as for example, the metabolism of the glycidos. The results obtained have lead to an interpretation of the individual reactions, even though for many of them the structure and mode of action of the specific enzymes is still unknown. Moreover, the necessity of the

presence of enzyme systems has been demonstrated; without them complete cycles of reactions, such as the Krebs and the Calvin cycles would be impossible, or at least highly improbable.

In the beginning, biochemists determined the composition of biomolecules. Next, they investigated intermediate metabolism in detail, showing the existence of "energy-rich" compounds, which, by virtue of electronic rearrangement in undergoing hydrolysis, deliver the energy needed to sustain and repair organisms, thus overthrowing the old concept of vital force. At present, one focus of research is the study of the various ways in which this energy is related to biosynthetic processes, in particular the synthesis of proteins, lipoproteins, nucleic acids, and their derivatives. Another active research interest is the mechanism of action of enzyme models, according to which the prosthetic group produces chemical change in the corresponding substrate. A third and more recent aspect is the study of processes of electron transfer, to which we will return later.

The chemical study of biosynthetic processes and the parts played by enzymes in them now leads to the consideration of biochemistry, at least in one view, as the organic chemistry of enzymatic reactions.<sup>111</sup>

Thus, as the application of the concepts and methods of quantum mechanics to chemistry has lead to the establishment of quantum chemistry, in an analogous manner its more recent application to biochemistry has given rise to quantum biochemistry. It is possible to ask, nevertheless, what is the proper scope of these applications.

Recently, one of the most capable of contemporary quantum chemists, Longuet-Higgins,<sup>67</sup> expressed in this respect a conservative opinion, in contrast with the optimistic view of many other authors; he suggests that the methods of quantum mechanics will be really effective in those processes in which radiation plays a fundamental role (photosynthesis, retinal photosynthesis, bioluminescence) rather than in the case of "dark reactions" (synthesis of proteins, lipoproteins and nucleic acids, glycolysis, etc.).

The calculation of molecular electronic structures, which may be considered true "molecular fine structure" has made possible in chemistry, particularly organic chemistry, an extraordinary advance in the understanding of chemical processes. Though the situation in biochemistry is not completely analogous, as we shall

see later, it is reasonable to expect that the knowledge of electronic structures of molecules of biological interest will constitute a valuable contribution to the interpretation of biochemical reactions. These studies were not initiated directly; they developed as a result of efforts to arrive at a quantum mechanical interpretation of chemical carcinogenesis and of antitumor activity in cancer and leukemia. The pioneers in this field of quantum biochemistry are Alberte and Bernard Pullman.<sup>102</sup>

Before examining the most important molecules and biochemical processes, we will outline the fundamental concepts and methods of quantum mechanics, basing our development on the books of Kauzmann,<sup>57</sup> Daudel, Lefebvre and Moser,<sup>19</sup> and Streitwieser.<sup>119</sup> Readers with a limited mathematical background might begin with the book by Roberts.<sup>107</sup>

## II. FUNDAMENTAL CONCEPTS AND METHODS OF QUANTUM MECHANICS

The ideal goal of quantum mechanical calculation is to find a function,  $\Psi$ , called the "state function", or "wave function", which describes the behavior of the atomic or molecular system.

Suppose that a system is made up of  $p$  nuclei and  $q$  electrons. A possible arrangement of electrons in space and spin of the electrons of the system is called an "electronic configuration".<sup>64</sup> In the great majority of problems which interest the chemist, it is only necessary to deal with what are called "stationary", or "uniform states". The stationary state of lowest energy is called the "fundamental" or "ground state". For these stationary states,  $\Psi$  depends on the coordinates of the  $p$  nuclei and the  $q$  electrons, so that  $\Psi = \Psi(a, b, \dots, p; 1, 2, \dots, q)$ . The square of the absolute value of the wave function,

$$|\Psi(a, b, \dots, p; 1, 2, \dots, q)|^2 \quad (1)$$

is interpreted by a majority of quantum theorists as measuring the density of probability of finding the  $(p+q)$  particles with given values of the coordinates. Alternate interpretations are defended by even some of the more eminent theoreticians, but interpretations belong more to philosophy than to science. The quantum theory is entirely independent of them; they cannot in principle be either



proved or disproved by any physical phenomenon or experiment so far proposed. For scientific purposes it is quite sufficient to introduce the wave function,  $\Psi$ , defined as a solution of a Schrödinger equation and satisfying certain conditions of regular behavior, and in turn useful for calculating measurable properties of a system. It is perhaps significant that it is possible to interpret the square of the wave function in simple terms, but this quantity is inadequate for calculating many of the observable constants of motion of the system. The wave function corresponds less to any intuitive picture but leads to more generally useful results.

In order to calculate properties of molecular systems it is necessary to know their stationary states. Theoretically, these may be determined by solving the Schrödinger equation for the stationary state:

$$H\Psi = E_{\text{tot}}\Psi \quad (2)$$

where  $E$  is the energy of the systems and  $H$  is the *Hamiltonian operator*, or simply, *Hamiltonian*, for the system, which, neglecting relativistic effects, can be written:

$$-\frac{h^2}{8\pi^2} \sum_p \frac{\nabla_p^2}{M_p} - \frac{h^2}{8\pi^2 m} \sum_q \nabla_q^2 + \sum_{p < p'} \frac{Z_p Z_{p'} e^2}{r_{pp'}} - \sum_{p,q} \frac{Z_p e^2}{r_{pq}} + \sum_{q < q'} \frac{e^2}{r_{qq'}} \quad (3)$$

where  $e$  is the electronic charge,  $h$  Planck's constant,  $M_p$  and  $Z_p$  are the mass and atomic number of the  $p$ th nucleus,  $\nabla$  the Laplacian operator, and  $r$  the interparticle distance. The first two terms of Eq. (3) are the kinetic energy operators for the nuclei and electrons, respectively; the remaining three are potential terms corresponding to nucleus-nucleus, nucleus-electron, and electron-electron interactions. We recall that the operator  $H$  possesses two properties which simplify calculation; it is linear and Hermitian. Substituting Eq. (3) in Eq. (2) the Schrödinger equation takes the form:

$$\left[ -\frac{h^2}{8\pi^2} \sum_p \frac{\nabla_p^2}{M_p} - \frac{h^2}{8\pi^2 m} \sum_q \nabla_q^2 + \sum_{p < p'} \frac{Z_p Z_{p'} e^2}{r_{pp'}} - \sum_{p,q} \frac{Z_p e^2}{r_{pq}} + \sum_{q < q'} \frac{e^2}{r_{qq'}} \right] \Psi = E_{\text{tot}} \Psi \quad (4)$$

In general Eq. (4) has acceptable solutions for discrete (negative) values of the energy which correspond to bound states of the

molecule, usually the only ones of chemical interest. The functions  $\Psi$ , solutions of Eq. (4), are eigenfunctions and the values of  $E_{\text{tot}}$  eigenvalues of the Hamiltonian for the system. The condition

$$\int |\Psi|^2 d\tau = 1 \quad (5)$$

is ordinarily imposed on the eigenfunctions; Eq. (5) called the normalization integral. Another important property of the function  $\Psi$  is that of orthogonality; that is

$$\int \Psi_m \Psi_n d\tau = 0, \quad \text{if } m \neq n \quad (6)$$

In solving Eq. (4), the familiar quantum rules arise from the application of the boundary conditions. As the solutions have to satisfy the Pauli exclusion principle, the wave function has to satisfy the condition of antisymmetry; we will later show how this is expressed. Even though general theorems for the existence of solutions to the Schrödinger equation have not yet been proved, some basic advances have been made in this direction.<sup>69</sup>

Since the potential energy operator for the nucleus-nucleus interaction does not depend on the electronic coordinates, we may write:

$$E_{\text{tot}} - \sum_{p < p'} \frac{Z_p Z_{p'}}{r_{pp'}} = E_{\text{el}}$$

where  $E_{\text{el}}$  is the electronic energy of the system, depending parametrically on the nuclear coordinates. With this approximation, the Schrödinger equation, Eq. (4), may be transposed to the form called the Born-Oppenheimer approximation:

$$\left\{ \sum_q \left[ -\frac{\hbar^2}{8\pi^2 m} \nabla_q^2 - \sum_p \frac{Z_p e^2}{r_{pq}} \right] + \sum_{q < q'} \frac{e^2}{r_{qq'}} \right\} \Psi_{\text{el}} = E_{\text{el}} \Psi_{\text{el}} \quad (7)$$

defining  $\Psi_{\text{el}}$  the electronic wave function, which is a function of the electronic coordinates of the system, including spin. The term in square brackets is the mono-electronic operator which describes the movement of an electron in the field of the nuclei. Two approximations—neglect of relativistic effects and consideration of the nuclei as point masses—are already implicit in Eq. (7).<sup>15</sup>

It will be interesting to note the effect of correlation, which includes the instantaneous interaction of the electrons on their

positions in space, due partially to their being of like charge, and partially to the effects of spin. This has been a subject of much interest in recent years.<sup>63, 69</sup>

In order to be able to satisfy conditions (5) and (6), the wave function must be quadratically integrable. By use of the principle of superposition, it is possible to demonstrate that if 1, 2, ..., constitute a complete or closed set, then

$$\Psi_{\text{el}} = \sum_{j=1}^{\infty} c_j \chi_j \quad (8)$$

We should remember that this expression is exact only in the case where all functions of the complete set are included, but we shall see that use of a complete set requires the resolution of an infinite system of equations, which presents insuperable practical difficulties. In practice, a carefully chosen finite set is used. Löwdin<sup>69</sup> has investigated expansion theorems for the total wave function.

The substitution of Eq. (8) in Eq. (7) is extremely important because the search for the wave function,  $\Psi$ , then reduces to the numerical problem of determining the coefficients in Eq. (8). This way of writing the Schrödinger equation is called the vectorial form. In all that follows we will assume that  $\Psi$  is a real function, for this occurs in the great majority of chemical problems.

Since the wave equation, Eq. (7) (after substitution of expression (8)), cannot be solved directly, it is necessary to resort to applying approximate methods, especially the variation and the perturbation methods (the first in particular for questions of interest in this chapter), in order to find a good approximation to the function  $\Psi$ . We will not describe the details of these methods which can be found elsewhere.<sup>91, 112</sup> The variation theorem (or Rayleigh–Ritz method) establishes that the energy calculated using any normalized wave function is always equal to or greater than the energy of the ground state. Perturbation theory permits the improvement of an approximate wave function so that the wave function for a system can be constructed if the set of solutions for a slightly different system is available.

The problem of the validity of a given wave function and the limiting procedure applied are extraordinarily important and require a profound study because if special precautions are not taken the case may arise where a good wave function (one differing little

from the exact solution) may lead to a very poor calculated value of some property  $\langle P \rangle$ . Also, a good result does not generally imply a good wave function.<sup>69</sup>

### A. Atomic Orbitals

The Schrödinger equation for hydrogen-like atoms is:

$$-\left[\frac{\hbar^2}{8\pi^2 m} \nabla^2 + \frac{Ze^2}{r}\right]\psi = E\psi \quad (9)$$

where  $m$ ,  $e$ , and  $Z$  have the usual meaning as in Eq. (4). For hydrogen itself,  $Z$  is 1. The discrete solution of Eq. (9) is:

$$\psi_{n,l,m}(r, \theta, \psi) = R_{n,l}(Zr) e^{-Zr/n} \Theta_{l,m}(\theta) \Phi_m(\psi) \quad (10)$$

where  $r$  is the radial vector of a sphere on which points are determined by the angles  $\theta$  and  $\psi$ , latitude and longitude respectively. The functions of expression (10) are called hydrogenic wave functions or atomic orbitals. The term orbital means<sup>81</sup> "one-electron orbital wave function". The set constitutes the zero order wave function for perturbation calculations. As may be observed, the wave function is associated with an atom and depends only on electron coordinates. The wave functions (10) correspond to a united or bound system with a negative value of the energy; it follows that atomic orbitals (10) do not constitute a complete set.

The radial function,  $R_{n,l}(Zr)$ , is expressed in terms of Laguerre polynomials and depends on the values of  $n$  and  $l$ . The principal quantum number,  $n$ , takes on only positive integral values (1, 2, 3, ...) and is associated with the energy of the electron. The angular momentum quantum number,  $l$  ( $= 0, 1, \dots, (n-1)$ ) is associated with the orbital angular momentum of the electron. As  $Z$  increases, the atomic orbital is concentrated more near the nucleus, requiring a greater energy to separate the electron from the atom. The angular function,  $\Theta_{l,m}(\theta)$ , is expressed in the form of Legendre functions and depends on the quantum numbers  $l$  and  $m$ ; the latter is the magnetic quantum number which may take on values from  $-l$  to  $+l$ , a total of  $2l+1$  values. The quantum number  $m$  is also related to the orbital angular momentum. Finally,  $\Phi_m(\psi)$  depends exponentially on  $m$  and on the angle  $\psi$ .

The principal quantum number,  $n$ , serves to define precisely the

notion of electronic shell; thus for  $n$  equal to 1, 2, 3, ... there are the  $K$ ,  $L$ ,  $M$ , ... shells respectively. When  $l$  is zero, we have the atomic  $s$  orbitals, which are not degenerate, that is there is only one  $s$  orbital for each value of  $n$ . For  $l$  equal to 1 there are three  $p$  orbitals, the members of this degenerate set being taken as  $(p_0, p_{\pm 1})$  or, more frequently, as  $(p_x, p_y, \text{ and } p_z)$ ; for  $l$  equal to 2 there are five  $d$  orbitals,  $(d_0, d_{\pm 1}, d_{\pm 2})$ ; for  $l$  equal to 3 seven  $f$  orbitals,  $(f_0, f_{\pm 1}, f_{\pm 2}, f_{\pm 3})$ . Explicit forms of the different orbitals are found elsewhere.<sup>19</sup>

The radial dependence of an atomic orbital is the principal factor in determining its stability, which is of primary importance in forming a chemical bond. While atomic orbitals may differ very little in radial dependence, they are very different in their angular forms. In three-dimensional space, graphical representation shows  $l$  nodal surfaces for the angular functions and  $n - l$  nodes in the radial function; the total number of nodes for an atomic orbital is equal to  $n$ .

Polar representations of the angular part of atomic orbitals provide a useful qualitative picture of electronic charge distribution; about 90% of the electron density is included within the lines. We must remember that the orbitals  $\psi_{n,s}$  and the corresponding density functions, having spherical symmetry, have no preferred spatial orientation; they merely become more diffuse with increasing  $n$ . On the other hand, the orbitals  $\psi_{n,p}$  and their density functions show a preferred direction, an axis of symmetry; for the same value of  $n$  they are identical except for direction. The  $p$  functions are anti-symmetric with respect to their nodal planes, but their density functions, proportional to the square of the wave function, are always symmetric.

Until now we have not considered the fourth degree of freedom of the electron: spin, which corresponds to an intrinsic angular momentum, associated with a quantum number  $s$  (not to be confused with  $s$  orbital). We will not go into the details;<sup>57</sup> it is sufficient to indicate that the projection of this moment on a given axis may take on only two values, corresponding to  $+\frac{1}{2}$  and  $-\frac{1}{2}$  in units of  $\hbar/2\pi$ . Thus a complete atomic wave function is specified by four quantum numbers,  $n$ ,  $l$ ,  $m$ , and  $s$ , that is  $\psi_{n,l,m,s}$ . This one-electron wave function including spin is called a spin orbital.<sup>81</sup> The Pauli exclusion principle permits a maximum of two electrons per atomic orbital. They must necessarily have antiparallel spins.

If no operator involving spin is included in the Hamiltonian, as will always be our case, we can separate:

$$\psi(n, l, m, s) \sim \psi(n, l, m) \sigma(s) \quad (11)$$

The concept of natural spin orbitals is found elsewhere.<sup>69</sup>

Before considering many-electron atoms, it is useful to recall that generally only the outer, or valence, shells of an atom are responsible for chemical properties and electronic spectra. The core of internal filled shells is spherically symmetric and very slightly affected by excitation of the valence electrons.

The objective of the theory of many-electron systems is to express the exact total electronic wave function in simple fashion, that is, as an expansion as rapidly convergent as possible and with a dominant term admitting a simple physical interpretation.<sup>68</sup>

Suppose that an atom contains  $N$  electrons. If we neglect the term in the Hamiltonian corresponding to the Coulomb repulsion of the electrons, the Schrödinger equation for the atom is the sum of  $N$  terms analogous to the first member of Eq. (9), while the second member is identical, the energy  $E$  becoming that of the atom. The solution of this differential equation has the form:

$$\Psi^0 = \prod_{i=1}^N \phi(n_i, l_i, m_i, s_i) \quad (12)$$

$\Psi^0$  being the zero order function for the atomic state in further calculation.

There are many possible different zero order functions, but all have to satisfy the Pauli exclusion principle, that is to be antisymmetric in the exchange of any pair of electrons. The best way to construct antisymmetric zero order functions is, following Slater,<sup>114</sup> to use an atomic wave function expressed as a determinant of one-electron functions,

$$\Psi^0 = (N!)^{-1/2} |\phi(n_1, l_1, m_1, s_1) \dots \phi(n_N, l_N, m_N, s_N)| \quad (13)$$

where  $(N!)^{-1/2}$  is the normalization factor. An equivalent expression, following (11), is:

$$\Psi^0 = (N!)^{-1/2} |x(n_1, l_1, m_1) \sigma(s_1) \dots x(n_N, l_N, m_N) \sigma(s_N)| \quad (14)$$

Functions of the form (13) or (14), or a sum of such terms, represent the electronic configuration of the (ground) state of the atom in

question. A knowledge of them is very important because they are sufficient to explain many atomic properties, such as chemical periodicity, and the way atoms combine to form molecules.

The electrostatic repulsions of the electrons, which were left out of the Hamiltonian for many-electron atoms, are of three types: (a) mutual interaction of core electrons, (b) mutual interaction of external electrons, and (c) interaction between core and external electrons. Interactions of type (a) have little effect on the chemical behavior of atoms, so we need not consider them. Those of type (b) are very important, giving rise to atomic multiplet structure, but this is not our immediate interest. Repulsions of type (c) give rise to a penetration effect, or screening, which we now consider.

The interposition of the core electrons between the nucleus and the external or valence electrons keeps the spectra of non-hydrogenic atoms from having the same energy levels as hydrogen. The deviation measures the intensity of the effect, which varies inversely with the quantum number  $l$ . Thus the effect is most pronounced for  $s$  orbitals, less so for  $p$  orbitals, etc.

By virtue of the screening effect, the "true" atomic orbitals are not of the form given by (10), but are much less concentrated around the atomic nucleus. This can be translated by replacement of the nuclear charge,  $Z$ , by an effective nuclear charge,  $Z^*$ , defined as  $(Z - \delta)$ , where  $\delta$  is a screening constant which measures the screening of an electron by the rest. As may be expected,  $\delta$  has different values for different orbitals.

Zener<sup>44</sup> calculated wave functions for a number of atoms using screening constants. Since this is still a central field problem, the angular functions are the same as for hydrogen; he found that the dominant term corresponded to the highest power of  $r$ . Slater<sup>115</sup> used Zener's results to derive a system of semi-empirical atomic orbitals, the Slater-type orbitals (STO), which in unnormalized form are:

$$\chi = r^{n^*-1} e^{-(Z-\delta)r/n^*} \Theta_{l,m}(\theta) \Phi_m(\psi) \quad (15)$$

where  $n^*$  is called the effective principal quantum number. He provided rules for determining the numerical values of  $n^*$  and  $\delta$ . Fueno<sup>34</sup> recently discussed the use of variable  $Z$  in atomic  $p\pi$  orbitals.

The approximate nature of Slater orbitals is borne out by their

limitations, for example, they lead to the same radial function for  $(2s)$  and  $(2p)$  orbitals. However, the most serious limitation is that the radial function has no nodes, consequently the orbitals with the same angular functions are not orthogonal. There is then the dilemma of using non-orthogonal atomic orbitals, which make the calculation very laborious, or neglecting the non-orthogonality and running into serious mathematical difficulties.<sup>110</sup> Fortunately the dilemma can be resolved by simply using orthogonalized Slater orbitals, constructed from nodeless functions (by restoring the nodes). Duncanson and Coulson<sup>22</sup> have given improved semi-empirical atomic orbitals for elements of the first row of the periodic table. Boys<sup>7</sup> has utilized atomic orbitals with Gaussian functions,  $e^{-ar^2}$ , in the radial factor. This makes the integrals easier to evaluate.

Hartree<sup>47</sup> developed the self-consistent field (SCF) method of determining the atomic orbitals which lead to a "best" wave function for polyelectronic atoms.

Consider an  $N$ -electron atom; let  $\phi(i)$  ( $i = 1, 2, \dots, N$ ) be real spin orbitals which form an orthonormal set and let the coordinates of electron  $i$  correspond to the orbital  $\phi_i$ . Expressing the wave function for the atom as a product of spin orbitals we have:

$$\Psi = \prod_{i=1}^N \phi_i(i) \quad (16)$$

Suppose that electron 1 occupies the fixed point  $(r_1, \theta_1, \psi_1)$ ; then the average electrostatic interaction between electrons 1 and  $i$ , for example, is given, in atomic units, by:

$$\int \frac{\phi_i^2(i)}{r_{1i}} d\tau_1$$

Considering the interaction of electron 1 with the  $(N - 1)$  others, the total potential energy of electron 1, exclusive of the potential due to the nucleus, is:

$$V_1(r_1, \theta_1, \psi_1) = \sum_{i=2}^n \int \frac{\phi_i^2(i)}{r_{1i}} d\tau_1 \quad (17)$$

The wave function  $\phi'_1(1)$  corresponding to electron 1 in the potential field (17) is obtained by solving the wave equation:

$$\left[ \left\{ -\frac{\hbar^2}{8\pi^2m} \nabla_1^2 - \frac{Ze^2}{r_1} \right\} + \sum_{i=2}^n \int \frac{\phi_i^2(i)}{r_{1i}} \right] \phi'_1(1) = \epsilon_1 \phi'_1(1) \quad (18)$$



or simply:

$$H_{\text{eff}}(1) \phi'_1(1) = \epsilon_1 \phi'_1(1) \quad (18')$$

In general the Hartree equations have the form: <sup>19</sup>

$$\left[ H^N + \sum_{\substack{j=1 \\ j \neq i}}^n \int \frac{\phi_j^2(2)}{r_{12}} d\tau_2 \right] \phi'_i(1) = \sum_{j=1}^n \epsilon_{ji} \phi'_j(1) \quad (19)$$

where  $H_1^N$  is the Hamiltonian for electron 1 in the presence of the bare nucleus.

It is necessary to use digital calculators to solve Eq. (19). Once the functions  $\phi'_i(i)$  ( $i = 1, 2, 3, \dots, N$ ) are obtained, the calculation is repeated to obtain the functions  $\phi''_i(i)$ , etc., until self consistency is obtained. The total energy is <sup>19</sup>

$$E = \sum_{i=1}^n \epsilon_i^N + \sum_{\substack{i,j \\ i < j}}^n J_{ij} \quad (20)$$

where the  $\epsilon_i^N$  are the monoelectronic energies in the field of the nucleus and the  $J_{ij}$  are the Coulomb integrals.

The Hartree method has two important limitations. The first is that atomic total wave functions of type (16) do not take into account the effect of electron correlation. The other shortcoming of the Hartree SCF orbitals is the omission of the exchange of electrons between orbitals whenever there are two or more electrons with the same spin present in the system. Fock <sup>33</sup> eliminated this second difficulty by using a Slater determinant (14) for the total wave function, deducing the so-called Hartree-Fock equations: <sup>19</sup>

$$\left[ H^N + \sum_{\substack{j=1 \\ j \neq i}}^n \int \frac{\phi_j^2(2)}{r_{12}} d\tau_2 \right] \phi_i(1) - \left( \sum'_{\substack{j=1 \\ j \neq i}}^n \int \frac{\phi_j(2) \phi_i(2)}{r_{12}} d\tau_{12} \right) \phi_j(1) = \sum_{j=1}^n \epsilon_{ji} \phi_j(1) \quad (21)$$

Here the symbol  $\Sigma'$ , in exception to its usual meaning, indicates that only orbitals,  $\phi_j$ , with the same spin as  $\phi_i$  are included. This system of non-linear integrodifferential equations can be solved and the eigenvalues determined by the SCF method. The Hartree-Fock

method has been frequently used with various approximations in recent years; thus, for example, its solutions have been expressed in terms of localized orbitals,<sup>1</sup> and the so-called unrestricted Hartree-Fock<sup>5</sup> is beginning to come into general use.

Löwdin<sup>70</sup> has recently examined at length the Hartree-Fock approximation, which, until recently, was the most elaborate theoretical technique used in the treatment of the independent-particle model in many-particle systems. Good qualitative and often good quantitative results have been obtained in a variety of applications (electronic shell structure,  $\pi$ -electron systems of conjugated organic molecules, and the band structure of crystals). It appears that these are due to the electrostatic repulsions being relatively weak and the correlation effects satisfactorily considered as a small perturbation.

Brueckner's success in applying the independent-particle model to (nuclear) shell theory in atomic nuclei, where it is called the Brueckner approximation, seems to indicate that this model is also valid for strong interactions between particles. The new approximation includes exactly the correlation between two particles (correlation among three or more particles is neglected) in a scattering operator. When this approximation is extended to electronic systems, in which the electronic repulsion is long range, it is necessary to include correlation among three or more electrons. Löwdin<sup>70</sup> has developed the exact SCF theory, a step further in the Hartree-Fock-Brueckner direction, solving the wave equation in the independent-particle model using a SCF system with "average" potentials. He applied his new approximation to the theory of energy bands in crystals, establishing a diagram which shows the relations among the different SCF schemes.

## B. The Chemical Bond

From a pure phenomenological viewpoint, the hydrogen molecule is made up of two protons and two electrons which form a stable chemical entity characterized by a dissociation energy,  $D_e$ , of 4.7466 eV and an average internuclear distance,  $R_e$ , of 0.74116 Å. (The experimental values can be compared with the calculated ones obtained by Kolos and Roothaan,<sup>58</sup> who extended the well-known, now classical, calculations of James and Coolidge<sup>52</sup> to fifty terms,

finding  $D_e$  equal to 4.7467 eV and  $R_e = 0.74127$  Å. It appears that the calculated value of  $D_e$  is more reliable than the experimental.) We say that in the hydrogen molecule there is a two-electron chemical bond—the chemical bond par excellence according to G. N. Lewis—which unites the protons. The concept of bond is fundamental to the chemist, but it is a very complicated one; Coulson<sup>11</sup> records the words of Mulliken on this subject: “I believe the chemical bond is not so simple as some people seem to think.”

The formation of a chemical bond is attributed to the overlapping of two atomic orbitals. This physical concept can be expressed quantitatively by the overlap integral,  $S$ ,<sup>12</sup> defined as:

$$S_{ab} = \int \psi_a \psi_b d\tau \quad (22)$$

where  $\psi_a$  and  $\psi_b$  are normalized atomic orbitals which overlap.  $S_{ab}$  is a function of the internuclear distance,  $r_{ab}$ , for given orbitals. When  $r_{ab}$  is zero,  $S_{ab}$  is 1 for equivalent orbitals, reproducing the normalization condition. For  $r_{ab}$  tending to infinity,  $S_{ab}$  vanishes, expressing an orthogonality condition. Non-zero  $S_{ab}$  is a measure of the non-orthogonality of atomic orbitals. The orbitals  $1s$ ,  $2s$ ,  $2p$ , ... of the same atom are mutually orthogonal.

Mulliken<sup>79</sup> has calculated and plotted graphs of  $S_{ab}$  as a function of  $r_{ab}$  (Å) for different orbitals and hybrids often used for the carbon atom. For the pair of  $2p\pi$  C—C, which will be of special interest later,  $S_{ab}$  varies between 0.20 and 0.27 as  $r_{ab}$  ranges from 1.20 to 1.54 Å, the interatomic distances of triple and single bonds respectively.

The qualitative concept of Lewis of a covalent bond formed by two shared electrons, one furnished by each atom, can be explained by three postulates:

(1) A single bond is formed by two electrons of antiparallel spin which exert a force of attraction between the atomic nuclei.

(2) The principle of maximum overlap (Pauling–Slater Principle): The direction of the bond will be that for which the electron clouds of the bonding orbitals overlap the most for a given internuclear distance. In Coulson's opinion this principle follows the Pauli exclusion principle in importance.

(3) If there are two orbitals on an atom, the one which overlaps more with the other atom will form a stronger bond.

### C. Bond Orbitals

There are two principal different types of overlap which give rise to corresponding types of bonds, sigma ( $\sigma$ ), and pi ( $\pi$ ). If the overlap is axial or frontal, sigma bonding orbitals, or simply sigma orbitals, are formed. Analysis of the electronic clouds of sigma bonding orbitals leads to certain properties. They have cylindrical symmetry with respect to the internuclear axis, the origin of the almost free rotation around single bonds. At the same time they give an idea of the approximate size of the molecule. Finally, the charge distribution resulting from the overlap provides a slight but definite concentration in the internuclear region which, by virtue of the Hellman–Feynman theorem, can be shown to hold the nuclei together. This small excess of charge, of the order of  $0.1$  to  $0.5e$ , constitutes the substance of the binding energy; from its tendency to be localized comes the relative independence of bond properties in polyatomic molecules.

When two  $p$  orbitals overlap laterally a pi bond is formed. The electron clouds of the  $p$  atomic orbitals must be parallel to satisfy the principle of maximum overlap. Contrary to the case of  $\sigma$  orbitals,  $\pi$  bonds are not localized between the nuclei, but rather above and below the internuclear axis, in such a way that it is necessary to consider both parts of the cloud as inseparable and constituting a single bonding orbital.  $\pi$  orbitals do not possess cylindrical symmetry about the bond axis, rather a nodal plane passes through the nuclei.

If two adjacent orbitals are oriented so that their axis form an angle,  $\phi$ , it is possible to calculate the properties of the bent bond.<sup>107, 119</sup>

Another fundamental concept for the interpretation of the chemical bond is that of hybridization, developed by Slater and Pauling in the study of the behavior of the carbon atom.<sup>63, 90</sup>

Tetrahedral orbitals,  $sp^3$ , are formed by the linear combination of an  $s$  and three  $p$  orbitals; considered as simple vectors they would be directed to the vertices of a regular tetrahedron; they are not coplanar. These form a set of equivalent orbitals. Thus four electrons of like spin occupying these orbitals would have as their most probable arrangement the vertices of a regular tetrahedron. It is easy to show that an infinite set of such combinations is

possible, corresponding to different orientations of a tetrahedron in space.

Trigonal hybrids,  $sp^2$ , are formed by the carbon atoms of an  $s$  and two  $p$  orbitals and are directed toward the vertices of an equilateral triangle in the plane of the  $p$  orbitals. Digonal hybrids,  $sp$ , composed of an  $s$  and a  $p$  orbital are directed in opposite directions along the axis of symmetry of the  $p$  orbital.

The use of hybrid bonding orbitals is an improvement over pure atomic orbitals in two senses: modification of directional properties, and increasing bond strength. By Pauling's criteria,<sup>90</sup> the strength of the bonds formed by hybrid orbitals follows the sequence  $sp^3 > sp^2 > sp \gg p > s$ . If the numerical value of the overlap integral is used as the criterion,<sup>12</sup> the order is the reverse,  $sp > sp^2 > sp^3 \gg p$ .

Methods based on the principle of maximum overlap for constructing optimum hybrids have been described recently.<sup>83</sup>

It is important to note that the directed character of valence bonds can be explained on the basis of correlation of charge and spin. In the case of a pair of electrons, spin correlation tends to unite, and charge correlation to separate; in the interaction of pairs both effects act in the same direction and this appears to be the dominant factor operating in directed valence.

#### D. Bonding and Antibonding Molecular Orbitals

Wave functions  $\psi_{1s}, \psi_{2s}, \psi_{2p}, \dots$  are called atomic orbitals (AO) because they are functions for one electron referring to the different electrons of an atom. Wave functions describing the behavior of molecular systems are called molecular orbitals, MO's. When the MO's refer to two atoms, they are called two-center molecular orbitals. As we shall see below in full detail, the MO's may be constructed from linear combinations of atomic orbitals, LCAO's. For example, for the hydrogen molecular-ion,  $H_2^+$ , the unnormalized MO for the ground state is:

$$\sigma_g 1s = \psi_{1s_A} + \psi_{1s_B} \quad (23)$$

and for the next state,

$$\sigma_u^* 1s = \psi_{1s_A} - \psi_{1s_B} \quad (24)$$

$A$  and  $B$  label the two protons,  $\sigma$  indicates that the angular momentum about the internuclear axis is zero (it is denoted by  $\pi$  if it is 1 in

units of  $h/2\pi$ ), while  $g$  is used if the MO is symmetric and  $u$  if it is antisymmetric to an inversion through the center of the internuclear axis. A graph of the square of function (23), which measures the total electronic probability, shows that the electron has great probability of being found in the internuclear region, overcoming the nuclear repulsion. Even though a more complete calculation is necessary to show that this leads to a chemical bond, we may classify  $\sigma_g 1s$  as a bonding molecular orbital (BMO). On the contrary, the analogous representation for the MO  $\sigma_u^* 1s$  would show a nodal plane between the nuclei, indicating that the probability of finding the electron there is zero, so  $\sigma_u^* 1s$  is called an antibonding molecular orbital (ABMO).

The energy associated with the MO  $\sigma_g 1s$  is less than that associated with  $\sigma_u^* 1s$ , the more nodes, the higher the energy. The order of increasing energy for two-center MO's for the hydrogen molecule is

$$\sigma_g 1s < \sigma_u^* 1s < \sigma_g 2s \sim \pi_u 2p < \sigma_u^* 2s \sim \sigma_g 2p \sim \pi_g^* 2p < \sigma_g^* 2p.$$

## F. Orbitals for Multiple Bonds

The  $\sigma$ ,  $\pi$  formulation is the most used of the various possible descriptions of multiple bonds in terms of atomic orbitals.

Consider the double or ethylenic linkage. If two atoms of carbon are imagined in a state of trigonal hybridization and two hydrogen  $s$  orbitals brought up to each along the axes of two of the trigonal hybrids to a position of maximum overlap, the C—H bonding orbitals would be formed. Then, if the carbon atoms are oriented so that the remaining trigonal hybrids achieve maximum overlap, a C—C bonding orbital is constructed. Thus the hydrocarbon skeleton of the molecule is constructed entirely of  $\sigma$  bonding orbitals. As each carbon retains a pure  $2p_z$  orbital, these can be oriented laterally for maximum overlap (complying with the symmetry condition for forming a binding orbital); this is achieved when the axes of the  $p_z$  orbitals are perpendicular to the plane of the molecule and the molecular orbital formed from them is called a  $\pi$  bonding orbital. The two bonds which form the ethylenic bond have very different characteristics. The  $\pi$  bond is more easily broken, so that it disappears in addition reactions. The coplanarity of the ethylene molecule is a consequence of the trigonal hybridization, while the lack of free

rotation of the  $\text{CH}_2$  groups is due to the necessity of breaking the  $\pi$  bond, which requires considerable energy.

Recently, Pauling<sup>89,90</sup> has formulated a description of the double bond using Bayer-type hybrids. According to him, the double bond would be formed by two tetrahedral bent bonds from each carbon.

### G. Localized and Delocalized Bonds

When molecules react, the bonds are formed and are broken independently of each other. Because of this, the chemical bond is a "reality" to the classical chemist, with its experimental expression in the constancy of a series of properties, the most important of which are bond length, bond energy, characteristic infrared frequency, dipole moment, quadrupole coupling constant, and chemical "reactivity".

According to this view, the electrons forming a bond are supposed to be localized between the atoms they unite, forming localized bonds. This is expressed by localized two-center MO's. The localized electrons do not thus contribute appreciably to the electronic character of the remaining bonds of the molecule.

In conjugated and aromatic molecules it is no longer possible to speak of electron localization and we speak of delocalized or non-localized bonds.

The sigma electrons localized between the atomic nuclei constitute the molecular skeleton, determining the geometric properties (bond length, etc.). They are also important in those cases in which angular deformation results from the geometry or from molecular strain. On the other hand, they have a minimal role in molecular chemical behavior. The  $\pi$  electrons (which form the delocalized bonds in conjugated and aromatic molecules) have the primordial responsibility for chemical reactivity, ultraviolet absorption, carcinogenic activity, etc.

### H. Principal Quantum Mechanical Methods

There are two principal quantum mechanical methods employed in the study of molecular structure. One of these, the HLSP (Heitler-London-Slater-Pauling) or valence bond (VB) method has been applied extensively (Pauling<sup>90</sup>), despite certain shortcomings. One of its weaknesses is in the choice of resonance structures or

contributors, each one of which should be a reasonable approximation to the real electronic structure of the molecule. The only criterion of selection is chemical intuition. Another of its serious difficulties is that when applied to large organic molecules the calculation of the wave function is extremely laborious. (It leads to qualitatively incorrect assignments of the ultraviolet and visible spectra of complexes.) Furthermore, its application to heteronuclear molecules is excluded by mathematical difficulties. Even if now the major part of the studies of molecular structure are carried out using the other method, it should not be forgotten that the VB theory contains a large element of truth and corresponds more closely to the intuition of classical chemists.

The other method, the HM (Hund-Mulliken) or theory of molecular orbitals (MO), is the one we will apply in our study and is described in detail below.

We should remember that all judgement of the correctness of the results obtained applying both methods rests in the relative success obtained with approximations to them.<sup>63</sup>

### I. Molecular Orbital Theory: LCAO Approximation

We have already noted that in unsaturated molecules the localization of the  $\sigma$ - and  $\pi$ -electron clouds is different. The sigma orbitals are symmetric with respect to the molecular plane and form the molecular skeleton; the  $\pi$  orbitals are antisymmetric with respect to this plane and may be said to move in the field of the  $\sigma$  electrons and the nuclei. Thus if we neglect the interaction between these two types of electrons we can establish the first simplifying approximation, the " $\pi$ -electron approximation" <sup>88</sup> in the molecular orbital theory: the  $\pi$  electrons are considered independently. For a polyelectronic system one can write:  $\Psi_{\text{el}} = \Psi_{\sigma} \Psi_{\pi}$ .

If  $\Psi_{\sigma}$  is expressed as the product of localized two-center MO's, which are independent of the  $\pi$ -electron system, McWeeny<sup>74</sup> demonstrated that the  $\pi$  Hamiltonian is:

$$H_{\pi} = \sum_{\mu} H^c(\mu) + \sum_{\mu < \nu} \frac{e^2}{r_{\mu\nu}} \quad (25)$$

where  $H^c(\mu)$  is the energy of the electrons in the field of the core and the sum represents the energy of repulsion between  $\pi$  electrons.



The last few years have shown renewed interest in the problem of  $\sigma$ - $\pi$  interaction. It seemed reasonable to think that the electrostatic repulsion between  $\sigma$  and  $\pi$  electrons should be important, giving rise to  $\sigma$  and  $\pi$  polarizabilities affecting the calculation of dipole moments. However, recently Parks and Parr<sup>85</sup> studied the formaldehyde molecule by an SCF method taking into account  $\sigma$ - $\pi$  interaction and similarly, Brown and Hafferman<sup>34</sup> considered this and other heteronuclear molecules by the "variable electronegativity (VE) SCF-like LCAO-MO method". They concluded, discussing dipole moments, that "an unpolarized sigma core in heteroconjugated molecules seems to be more reasonable than is widely believed".<sup>34</sup> This and other calculations<sup>113</sup> appear to support the  $\sigma$ - $\pi$  separation. Another type of interaction to take into account is exchange between  $\sigma$  and  $\pi$  orbitals. Except for electron spin resonance, this interaction is negligible.<sup>119</sup>

Although any number of methods might be used to develop  $\Psi$ , we will follow general practice and consider only the approximation of linear combinations of atomic orbitals, the LCAO method.<sup>77</sup>

Very recently, Kasha<sup>55</sup> has given a diagram of the mode of operation of the MO theory in order to make it more readily understood by chemists and biologists. The steps in its development are given in Fig. 1.

*Step 1.* The point of departure is the detailed knowledge of the geometry of the molecule, which, for simplicity, we assume to be a hydrocarbon. Each carbon atom contributes one ( $2p_z$ )  $\pi$  electron to the  $\pi$  system of the molecule, which we associate with the atomic orbital,  $\chi_r$  ( $r = 1, 2, \dots, n$ , for  $n$  carbon atoms in the conjugated system). It is logical to suppose that, in the vicinity of each atom, the molecular orbital,  $\Psi_j$ , is very similar to the corresponding atomic orbital (which we have taken equivalent for all atoms), so that  $\Psi_j$  can be written as a linear combination of AO's,

$$\Psi_j = \sum_{r=1}^n c_{jr} \chi_r \quad (26)$$

where  $c_{jr}$  is the coefficient of the AO,  $\chi_r$ , in the MO  $\Psi_j$ . Expression (26) is the starting point for the basic LCAO formulation of the  $\pi$ -electron system in the one-electron theory.

The MO's (26) are polycentric, adapted to the symmetry of the molecule; beyond their symmetry they represent only a first

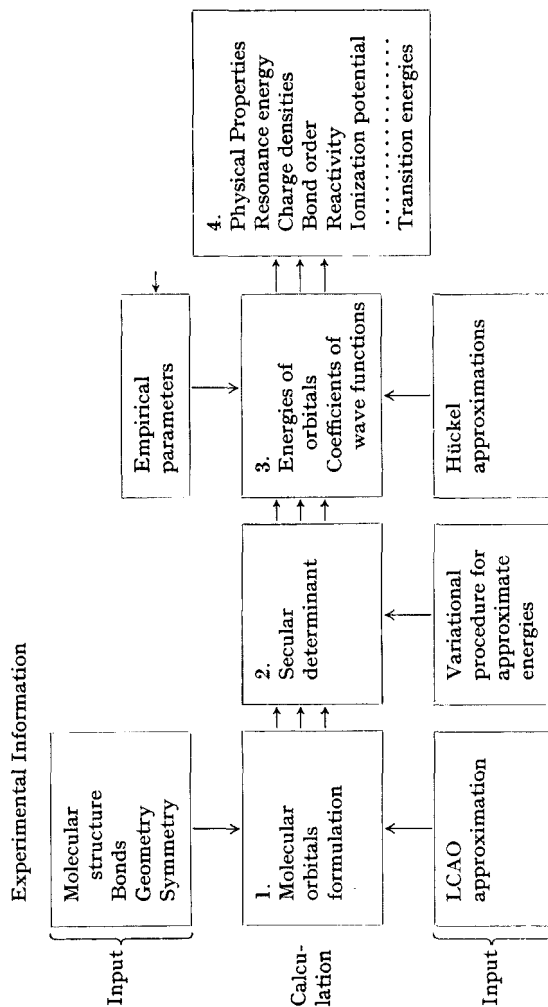


Fig. 1. Kasha's Flow Chart of simple semi-empirical molecular orbital calculations. (After Kasha,<sup>55</sup> p. 914.) (Figures 1, 3, 4 and 5 are reprinted with permission from *Deoxyribonucleic Acid—Structure, Synthesis and Function*, Pergamon Press Limited, 1962.)

approximation to the true MO's, as yet unknown for polyelectronic molecules. The orthogonality condition is fulfilled by requiring each molecular orbital to be an eigenfunction of a Hermitian Hamiltonian operator for one electron,  $H$ , whether or not it is possible to specify its explicit form.

By the Pauli exclusion principle, there can be no more than two electrons in each MO. Normally molecules have all their electrons paired, in which case the MO's are either doubly occupied or empty.

A deficiency of the LCAO-MO's is that they do not satisfy the virial theorem.

*Step 2.* To obtain the best set of coefficients,  $c_{jr}$ , for the expansion (26), the variational principle (Section II) is applied,  $\delta < H > = 0$ , leading to the best energy for each molecular orbital. This leads to the system of linear homogeneous equations,

$$\sum_s (H_{rs} - \epsilon S_{rs}) c_s = 0 \quad (27)$$

where  $\epsilon$  is the eigenvalue of orbital energy associated with  $\Psi$ . In these equations, we have employed the following standard symbols:

$$H_{rr} \equiv \int \chi_r H \chi_r d\tau \equiv \alpha_r \quad (28)$$

$$H_{rs} = H_{sr} \equiv \int \chi_r H \chi_s d\tau \equiv \beta_{rs} \quad (29)$$

$$S_{rs} = S_{sr} \equiv \int \chi_r \chi_s d\tau \quad (30)$$

The integral  $H_{rr}$ , called the Coulomb integral,<sup>50</sup> depends on the nuclear charge and the type of orbital. Since we supposed the molecule to contain only carbon atoms,  $\alpha_r$  represents, to a first approximation, the energy of a  $2p_z$  electron of the carbon atom in the presence of the other nuclei; it may be considered to measure approximately the electronegativity of that atom. Its numerical value, referred to the electron removed to infinity, is negative. We will see later how the value of  $\alpha_r$  is changed by neighboring heteroatoms.

$H_{rs}$ , the resonance or bond integral,<sup>50</sup> represents the energy of interaction of the two AO's,  $\chi_r$  and  $\chi_s$ . Its numerical value, also essentially negative, depends on the cores  $r$  and  $s$ , on the interatomic distance  $r-s$ , and, for  $p$  orbitals, on the angle between their symmetry axes and the internuclear axis. We have already discussed the overlap integral,  $S_{rs}$ ; we note that it is essentially positive

and less than unity, tending rapidly to zero with increasing inter-atomic distance.

*Step 3.* The secular determinant or secular equation formed by the bracketed term of equation (27) must be solved:

$$\det|H_{rs} - \epsilon_{rs}S_{rs}| \quad (31)$$

Different approximations in its solution lead to the different grades of sophistication in the simple LCAO-MO theory. Recently Ruedenberg<sup>109</sup> completed a formal study of the one-electron theory applied to  $\pi$  electrons with, in his words, "the help of such approximations as are *realistic and bona fide justifiable*".

### (1) *Hückel Approximation (HMO)\**

The most drastic of all approximations, or zero order approximation, it was first employed by Hückel,<sup>49</sup> hence its name. The form of the Hamiltonian is not specified; the  $\pi$  electron repulsion terms are eliminated from (25), leaving an effective one-electron operator:

$$H_{\pi} = \sum_r H_{\text{eff}}(r) \quad (32)$$

the base of the one-electron theory. The secular equation is simplified by (a) setting all diagonal matrix elements corresponding to  $H_{\text{eff}}$  equal to  $\alpha_{\text{eff}}$ , (b) taking all off diagonal elements between adjacent atoms equal to  $\beta_{\text{eff}}$ , neglecting the rest, (c) neglecting overlap. In compact form:

$$\begin{aligned} \alpha_r &= \text{constant} = \alpha_{\text{eff}} \\ \beta_{rs} &= 0, \text{ unless } r, s \text{ are adjacent} \\ \beta_{rs} &= \text{constant} = \beta_{\text{eff}}, \text{ for } r, s \text{ adjacent} \\ S_{rs} &= 0 \end{aligned} \quad (33)$$

We consider carefully these approximations. Since all the MO's extend over various identical cores, it appears to be a good approximation to admit the same value for the Coulomb integrals,  $\alpha_{\text{eff}}$ . As the resonance integrals depend on the distance between  $r$  and  $s$ , for constant bond distance we can suppose  $\beta_{rs} = \text{constant} = \beta_{\text{eff}}$  between bonded atoms, and for non-bonded atoms,  $\beta_{rs} = 0$ . These two

\* Notation introduced by Streitweiser.<sup>119</sup>

approximations introduce two empirical parameters in the secular determinant (31), indicating that the Hückel approximation is an empirical method.

It is customary to distinguish between "pure" or "non-empirical" theories and "semi-empirical" and "empirical" ones in quantum chemistry. This is a purely semantic distinction; there are no "non-empirical" theories since all relate some experimental data with others. Despite this, theories which permit the deduction of data of chemical interest from the Schrödinger equation, the numerical values of the electron charge and mass, Planck's constant, and quantum numbers, are called non-empirical. Greater or less deviation from this assumption leads to semi-empirical or empirical theories.

The approximation  $S_{rs} = 0$  is equivalent to supposing that the  $\chi_r$  are orthogonal (and for this reason called the orthogonality assumption). This is difficult to justify remembering that the overlap between two ( $2p_z$ ) STO's for carbon at the distance of adjacent atoms in an aromatic hydrocarbon is 0.25. The analysis of this approximation, to which we will return later, constitutes the central objective of Ruedenberg's recent study;<sup>109</sup> he concludes that "the outright neglect of neighbor overlap is not a bona fide first approximation". Results obtained using modern semi-empirical methods<sup>86</sup> appear to support this approximation, a question also analyzed by Ruedenberg.<sup>109</sup>

The adoption of approximations (33) leads to a secular determinant much simpler than (31). Solving it leads to the  $n$ th order characteristic equation whose real roots,

$$\epsilon_j = \alpha + m_j \beta \quad (34)$$

are the energies of the molecular orbitals. As we shall see, it is better to follow Ruedenberg<sup>109</sup> in calling them "one-electron energies" or "orbital contribution" to the total energy.

If  $m_j$  in expression (34) is positive, the  $j$ th  $\pi$  orbital is a binding  $\pi$  MO (BMO); if  $m_j$  is negative it corresponds to an antibonding  $\pi^*$  MO (ABMO). If  $m_j$  is 0,  $\epsilon_j = \alpha$  (which is taken as the zero of energy), corresponding to a non-bonding MO (NBMO), represented by the symbol  $n$ .

Non-bonding molecular orbitals are occupied by electrons of lone pairs of heteroatoms, such as O, N, or S.

Once the numerical values of  $\epsilon_j$  ( $j = 1, 2, \dots, n$ ) are known, an Aufbau process may be carried out, putting electrons in MO's as permitted by the Pauli principle. In the normal configuration of a

molecule, only bonding orbitals are occupied. When an electron, by a process called electron promotion, is excited and passes from a bonding MO to an antibonding one, the molecule is in an excited state.<sup>56</sup> In Fig. 2 are represented the molecular orbitals for the purine molecule.<sup>27</sup> We selected this example because we will later consider this and related molecules in detail. The conjugated system consists of ten  $\pi$  electrons accommodated in five BMO's, with four ABMO's vacant. There are, moreover, three NBMO's doubly occupied, corresponding to the aza-nitrogens.

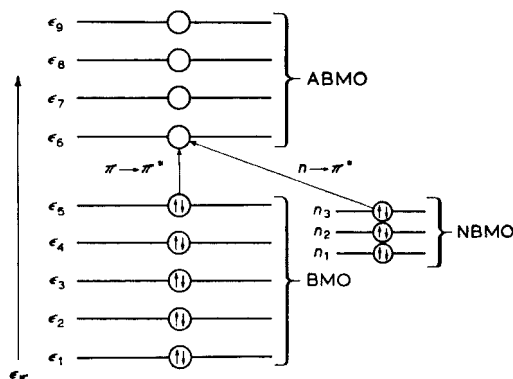


Fig. 2. Purine: Transitions and energies of the  $\pi$  orbitals (not to scale).

Despite the highly simplified nature of the HMO method, the chemist finds in it a valuable tool which has permitted the interpretation of many physical and chemical properties of conjugated molecules.<sup>119</sup> Its principal failings reside in its not permitting an interpretation of spectra<sup>88</sup> and its leading to the same numerical value for the ionization potentials for odd-alternant radicals, in contradiction with the experimental results.<sup>34,119</sup> These failings are undoubtedly due to the neglect of interelectronic repulsion.

## (2) Mulliken-Wheland Method

This method appears to have been introduced by Mulliken, Rieke, and Brown,<sup>82</sup> but was developed extensively by Wheland<sup>124</sup> (which explains its name). This method differs from the Hückel one

only in that the overlap between neighbors is not zero, but equal to a constant. Usually the value  $S=0.25$  is adopted. This method is also known as the "tight binding approximation".<sup>109</sup>

The values of the one-electron energies are now given by

$$\epsilon_j = \alpha + n_j \gamma \quad (35)$$

where  $\gamma$ , a new form of resonance integral, is

$$\gamma = \beta - S\alpha \quad (36)$$

and

$$n_j = m_j / (1 + m_j S) \quad (37)$$

We see then that once  $m_j$  has been calculated by the Hückel method, a simple step gives the values of  $n_j$  (37) and hence  $\epsilon_j$  from (35). If we call  $c_{ij}$  the coefficients of Hückel and  $c'_{ij}$  those of this method, Wheland demonstrated that the relation between them is:

$$c'_{ij} = c_{ij} / (1 - S m_j)^{1/2} \quad (38)$$

The tight binding approximation is, according to Ruedenberg,<sup>109</sup> a bona fide first approximation. Although the detailed study of that author refers to more refined theories which we will consider later, some of its consequences are applicable here. Thus he points out the existence of short-range forces, due to the neutral framework potential, and long-range, Coulomb-type forces, due to the ionic attraction of the skeleton and interelectronic repulsion. The short-range forces are determined by the topology of the molecule and are described by a so-called topological matrix, while the long-range forces determine the geometry of the molecule. Ruedenberg<sup>109</sup> demonstrates that the Hückel-Wheland MO's are topological molecular orbitals and that the tight binding approximation is a good approximation because the only forces operating are the short-range ones, the only ones in the Hamiltonian. The long-range forces cancel mutually in the average.

Likewise Ruedenberg<sup>109</sup> defines a one-electron orbital energy or energy contribution to the total energy,  $\epsilon_j$ , which corresponds to the short-range forces and is obtained as an eigenvalue of a topological one-electron problem. These are additive, and correspond to expression (35), defined as orbital energy. On the other hand, Ruedenberg uses this term for the energy of an electron which occupies an orbital,  $\epsilon_j$  (in particular in SCF orbitals). He also

deduces that when the orbital energy contribution,  $\epsilon_j$ , is negative, we have a BMO, and if positive an ABMO, which is consistent with the previous theory. Further, if the orbital energy  $\epsilon_j$  is negative, the orbital is bound; if it is positive, the orbital is unbound.

(3) *Introduction of Heteroatoms and Substituents:  
Pauling-Wheland Method*

Until now we have only considered homonuclear molecules, that is those containing only carbon atoms in the  $\pi$  system. In our biochemical studies we will be concerned exclusively with heteronuclear molecules, those which have one or more heteroatoms, usually nitrogen or oxygen, in addition to carbon. Similarly, we will consider homo- and heteronuclear with substituents, whether they be alkyl or other types. It is already possible to predict that the introduction of heteronuclei and substituents will affect to a greater or lesser degree the electronic organization of the hydrocarbons from which they are derived.

Pauling and Wheland<sup>92</sup> were the first to give a method for including heteronuclei in the MO theory.

The introduction of a heteroatom, X, requires the selection of a value for the Coulomb integral,  $\alpha_X$ , different from that for carbon. The resonance integral between the heteroatom, X, and a neighboring carbon,  $\beta_{CX}$ , should be different from that between two carbons,  $\beta_{CC}$ . Both differences are expressed in units of  $\beta_{CC}$ . For  $\alpha_C$  and  $\beta_{CC}$ , standard values are adopted, usually those for benzene.

The same parameters used in the Hückel-Wheland approximations are employed for the homonuclear remainder of the molecule. Following Pauling and Wheland,<sup>92</sup> an auxiliary inductive parameter,  $\eta$ , is used to take into account the inductive effect of X on neighboring carbon atoms,  $C_a - X$ . Thus, the new parameters have the form:

$$\begin{aligned}\alpha_X &= \alpha_C + \delta_X \beta_{CC} \\ \beta_{CX} &= \rho_{CX} \beta_{CC} \\ \delta_{C_a} &= \eta \delta_X\end{aligned}\tag{39}$$

Values of  $\delta_X$ ,  $\rho_{CX}$ , and  $\eta$  are introduced in the secular equations; these are solved for values of  $m_j$  which permit calculation of the one-electron energies. The choice of numerical values of these para-



meters is a difficult problem and far from having found a satisfactory solution. We will give only some general ideas about the way to attack this problem; a detailed study of it may be found elsewhere.<sup>19, 119</sup>

If it were possible to establish a relation between a physico-chemical property and a quantity calculable for homonuclear systems, and, after this, to extend the calculation to heteronuclear derivatives, systematically varying values of  $\delta_x$  and  $\rho_{cx}$  (the parameter  $\eta$  is unimportant), this would be a rational way to determine best numerical values and to find out whether or not there exists a unique consistent set. Unfortunately this procedure has not been applied fully.

Many difficulties are encountered in this problem. The following are among the more important. There are various degrees of sophistication in MO methods, different roles the same heteroatom may play, for example, pyrrolic or pyrimidinic nitrogen.

In general, methods for determining the parameters  $\delta_x$  and  $\rho_{cx}$  fall into two groups, those based on the use of eigenvalues (energy indices), and those based on eigenfunctions (structural indices). Usually the last methods are the least well specified in approximate quantum mechanical treatments.

Before leaving this question, we want to call attention to a fact that may be very important. Electron repulsion parameters are usually taken as the difference of the ionization potential and the electron affinity of the atom in its appropriate valence state. Pariser suggested reducing these values to obtain better agreement with experiment. This may be justified<sup>17</sup> by noting that the virial theorem requires that half the average potential energy be cancelled by kinetic energy for a system at equilibrium. The semi-empirical orbitals do not adjust their kinetic energies to changes in potential, but the modified integrals partially account for this effect.

Energies of atomic states not observed experimentally but desired for valence state calculations can be obtained from spectral data for observed states with adequate accuracy by using rescaled empirical orbitals. Preliminary study suggests the feasibility of including orbital rescaling in molecules semi-empirically.

The introduction of alkyl substituents and the general treatment of hyperconjugation can be found elsewhere.<sup>118</sup>

(4) *Other Naïve Methods*

Within the framework of the empirical MO method, the results of the methods already discussed may be improved by various refinements.<sup>19, 119</sup> We cite among them the inclusion in the secular equations of values of  $H_{rs}$  for non-neighboring atoms,<sup>24</sup> varying the integrals  $\alpha$  and  $\beta$ , leading among others to the “ $\omega$ -technique”. Besides the free-electron methods, there is the frontier-electron method developed by Fukui and collaborators<sup>36</sup> which has been successfully applied to molecules and processes of biological interest.

(5) *Goeppert-Mayer and Sklar Method*

We have seen (Section II-I (1) ) that the shortcomings of the simple Hückel method are due to the use of a one-electron Hamiltonian (Eq. (32) ) in which the  $\pi$ -electron repulsions are ignored. In more reliable calculation it is necessary to take this repulsion into account explicitly: for example, in the treatment of excited states of hydrocarbons, necessary for the interpretation of electronic spectra.

Goeppert-Mayer and Sklar<sup>40</sup> opened a new road beyond the one-electron theory, developing the first such method (GMS) which they applied to the study of the benzene molecule. Employing a Hamiltonian of the form (25) they represented the ground state by a single Slater determinant. Because of this, the GMS method is also called the antisymmetrized product of MO's method.

In the GMS method, the core Hamiltonian,  $H^c$  (neglecting the effects of the hydrogens), takes the form:

$$H^c(1) = -\frac{\hbar^2}{8\pi^2 m} \nabla^2 + \sum_i u_i^+(1) \quad (40)$$

where  $u_i^+$  is the potential of a hypothetical carbon ionized by the loss of a  $\pi$  electron. The sum extends over all the carbons of the system.

The eigenvalue function takes the form:

$$\left[ -\frac{\hbar^2}{8\pi^2 m} \nabla^2 + u_i^+ \right] \chi_i = W_{2p} \chi_i \quad (41)$$

where  $\chi_i (= 2p_z)$  is the AO contributed by atom  $i$  to the MO's and  $W_{2p}$  is a sort of ionization potential of the carbon atom in the valence state required. Equation (41) is theoretically inconsistent.<sup>109</sup>

Since in this method, one works with a  $H^c$  instead of a  $H_{\text{eff}}$ , the Coulomb integral,  $\alpha_p^c$ , and the resonance integral,  $\beta_{pq}^c$ , will be:

$$\alpha_p^c = \int \chi_p(1) H^c(1) \chi_p(1) d\tau(1) \quad (42)$$

$$\beta_{pq}^c = \int \chi_p(1) H^c(1) \chi_q(1) d\tau(1) \quad (43)$$

The introduction of electron repulsion ( $e^2/r_{12}$ ) gives rise to a new type of integral, the two-electron repulsion integrals:

$$(pq|rs) = \int \chi_p(1) \chi_q(1) (e^2/r_{12}) \chi_r(2) \chi_s(2) d\tau(1) d\tau(2) \quad (44)$$

For an asymmetric hydrocarbon with  $N$  atomic orbitals, it is necessary to calculate  $N^4/8$  integrals such as (44).

The two great drawbacks of the GMS method are<sup>88</sup> the  $N^4$  "difficulty" and the "purely theoretical" evaluation of all the integrals, discouraging its application to large molecules.

Since 1950 a new and very fruitful stage in the study of molecular systems by molecular orbital methods has been initiated with the development of two new methods of calculation. One, developed by Craig,<sup>16</sup> consists in the use of configuration interaction, CI, or the admixture of wave functions belonging to various states, including excited states of the independent-particle model. Strictly speaking, there is no essential difference between the CI and resonance methods, except that the MO configurations are orthogonal, therefore distinct or mutually exclusive, unlike the resonance structures which are usually not independent. The two methods correspond to different ordering of terms in an infinite series; the result of stopping at a few terms can be quite different. The other method, due to Roothaan,<sup>108</sup> is an application of the self-consistent field theory to the LCAO-MO approximation, so it is called the SCF LCAO-MO method.<sup>81</sup> A comparison of both methods is available elsewhere.<sup>116</sup> Only in the last few years with the intensive use of digital computers have these methods come to be widely applied.<sup>4</sup> We will consider only the second in detail as it is the one we apply.

### (6) *Self-Consistent Molecular Orbital Method* (Roothaan's Equations)<sup>15, 19, 66</sup>

The solution of the Hartree-Fock equations (21) for a system of  $\pi$  electrons provides SCF-MO's. In principle, it is possible to use an

iterative procedure for their solution. In practice, this procedure is effectively impossible because of the complexity and difficulty of the calculation, so it is necessary to impose certain preliminary restrictions on the MO to make the calculation feasible.

Roothaan<sup>108</sup> was the first to develop an explicit form for the application of the SCF-MO approximation to molecular systems, using as basis the LCAO-MO's. Since in practice a finite basis is used instead of a complete orthonormal set, the SCF-MO's calculated are approximate. Usually the form of the AO's is assumed, reducing the problem to the calculation of the coefficients.

For a molecule with a closed-shell ground configuration, Roothaan showed<sup>108</sup> that, in the LCAO approximation (26), the Fock equations take the form:

$$\sum_q c_{jq} F_{pq} = \epsilon_j \sum_q c_{jq} S_{pq} \quad (45)$$

where  $p, q, \dots$ , are the AO's. The molecular orbital energies,  $\epsilon_j$ , are solutions of the secular determinant,

$$\det |F_{pq} - \epsilon S_{pq}| = 0 \quad (46)$$

where  $S_{pq}$  is the overlap integral,  $F_{pq}$  is the matrix element between  $\chi_p$  and  $\chi_q$ ,

$$F_{pq} = H_{pq}^c + \sum_{r,s} P_{rs}[(pr|qs) - \frac{1}{2}(pr|sq)] \quad (47)$$

where  $H_{pq}^c$  expresses the interaction of an electron with the distribution  $[p(1)q(1)]$  and the molecular core; that is to say,  $H_{pp}^c \equiv \alpha_p^c$ , Eq. (42), and  $H_{pq}^c \equiv \beta_{pq}^c$ , Eq. (43).  $P_{rs}$  are expressions for the electron distribution of the molecule,

$$P_{rs} = 2 \sum_{i=1}^m c_{ir} c_{is}$$

The formulation of the system of nonlinear equations (45) requires prior knowledge of the overlap integrals, of the matrix elements  $H_{pq}^c$ , which depend, in turn, on the coefficients  $c_{jq}$ , and finally of the electron repulsion integrals of various types,  $(pp|qq)$ ,  $(pq|pq)$ , etc., integrals of two, three, and four centers. The evaluation of these integrals is the major difficulty of the Roothaan method and, in general, of non-empirical methods.

Starting with MO's determined by some other method (often those of the Hückel method, but it is easier to use orthogonal

MO's),<sup>83c</sup> the determinant (46) is solved to obtain values of the coefficients,  $c_{js}$ . The process is repeated until the MO's are consistent with those of the beginning of the last cycle.

The discussion developed until now corresponds to the closed-shell SCF method. In case of open shells in the SCF method, the problem is much more complicated because the variety of resulting equations cannot be reduced to the simple iterative determination of eigenvalues. Since we will not consider this question, the interested reader should consult other publications.<sup>2, 18, 61</sup>

(7) *Generalized Hückel or "SCF-Like LCAO-MO" Method*  
(Semi-empirical Methods)

Despite the fact that Roothaan's method represents a decisive step in the formal treatment of molecular systems, in practice its value has been severely limited by the extreme difficulty of evaluation of the electron-repulsion integrals. The method has only been applied to simple molecules.<sup>106</sup> If one wishes to apply this approach to more complex molecules, especially to the interpretation of aromatic hydrocarbon spectra, it is necessary to introduce certain simplifications to make practicable the numerical calculations. Among the semi-empirical methods, approximations begun about the same time by Pariser and Parr<sup>87</sup> and by Pople<sup>96</sup> have been developed. Essentially both methods reduce to the simplification of the SCF-MO method, devising semi-empirical procedures for evaluating some integrals and neglecting others, for which reason these approximations can be considered as belonging to the generalized HMO method, generalized to take account of electron repulsion. The authors cited above have observed that the neglect of differential overlap gives to the GMS method the mathematical simplicity of the one-electron schemes.

The Pariser and Parr method is a  $\pi$ -approximation in which an energy operator of the form (25) is employed, whose use is justified if certain conditions are fulfilled.<sup>71</sup> Among these is the  $\sigma$ - $\pi$  separation: that the  $\pi$  orbitals be orthogonal among themselves, the same for the  $\sigma$  ones, and that it is possible to express both types of orbitals in terms of STO's, although they may be of another form. The existence theorem for the operators  $H^c(\mu)$  indicates that they correspond to a fixed average  $\sigma$  structure for all states of interest.

The wave functions for various states are obtained by application of the variational theorem; the calculation involves the core integrals,  $\alpha_p^c$  (42) and  $\beta_{pq}^c$  (43), and electron-repulsion integrals (44).

The existence theorem for the operator  $H^c(\mu)$  permits the replacement of the purely theoretical calculations of the  $\alpha_p^c$  and  $\beta_{pq}^c$  integrals by semi-empirical procedure and suggests the use of semi-empirical calculation of electron repulsion integrals.

For the integrals it is assumed that

$$\beta_{pq}^c = 0, \quad \text{when } p \text{ and } q \text{ are not neighbors} \quad (48)$$

For neighbor atoms, an empirical value is adopted, chosen so that some calculated property will agree with experiment. This is equivalent to considering the  $\beta^c$  as empirical parameters, analogous to what occurs with  $\beta_{\text{eff}}$  of the simple HMO method.

Introducing the approximation of zero differential overlap (ZDO),

$$\chi_p \chi_q = 0, \quad \text{for } p \neq q \quad (49)$$

so that overlap integral  $S_{pq}$  is necessarily zero. For the electron repulsion integrals, it is found that:

$$(pq|rs) = 0, \quad \text{if } p \neq q \text{ or } r \neq s \quad (50)$$

For the justification of the zero differential overlap approximation one should consult the papers of Parr<sup>87d</sup> and of Ruedenberg.<sup>109</sup> Coulson and Schaad<sup>14</sup> have demonstrated, nevertheless, that the ZDO approximation is not valid for non-empirical calculations.

The use of the ZDO approximation reduces the problem of electron repulsion to that of the integrals of the type  $(pp|qq)$ .

In developing his theory of "atoms in molecules", Moffit<sup>78</sup> underlined the importance of a precise determination of the one-center repulsion integral,  $(pp|pp)$ , in molecular calculations; this is a true atomic parameter. Pariser and Parr also assign a fundamental role to this integral, from which follows the necessity of calculating it correctly. They determine formally that

$$(pp|pp) = -W_{2p} - A_p \quad (51)$$

where  $A_p$  is the electron affinity of the atom of carbon in its appropriate valence state.

The integrals  $(pp|qq)$  are calculated from  $(pp|pp)$  and values obtained by the uniformly charged sphere model for large values of

$r_{pq}$ . One should note also Ruedenberg's calculations.<sup>109</sup> The Pariser and Parr approximation can be applied to SCF theory. The matrix elements  $\alpha_p$  and  $\beta_{pq}$  which determine the coefficients  $c_{jq}$  are given by the expressions (with change of notation):<sup>18</sup>

$$\alpha_r = W_{2p} + \sum_{s \neq r} (q_s - 1) (rr|ss) + \frac{1}{2} q_r (rr|rr) \quad (52)$$

$$\beta_{rk} = \beta_{rk}^c - \frac{1}{2} p_{rk} (rr|kk)$$

where the  $q$  represent the electronic charges of the corresponding atoms, to be defined below.

Now we are prepared to justify the statement that the Pariser and Parr approximation can be considered as a generalized HMO. In fact, Pople<sup>96</sup> demonstrated that alternate hydrocarbons satisfy a pairing theorem similar to that of the HMO method; that is, the core energies are of the form  $\epsilon_\pi^c = \alpha^c \pm \beta^c$ . (If it is possible to divide the atoms of a hydrocarbon into two classes, starred and unstarred, such that no two atoms of one class are neighbors, it is alternant. Non-alternant hydrocarbons and heteromolecules do not satisfy the theorem.) Consequently, alternant hydrocarbons possess a unitary uniform distribution of charge, that is, all the  $q$ 's are 1. In this case, expressions (52) reduce to:

$$\alpha_r = W_{2p} + \frac{1}{2} (rr|rr) \quad (53)$$

$$\beta_{rk} = \beta_{rk}^c - \frac{1}{2} (rr|kk)$$

It is to be noted that the  $\alpha_r$  are independent of  $r$ . As for the  $\beta_{rk}$ , for neighbor atoms they differ so very little so that  $\beta_{12}^c$  is taken as an empirical parameter, while, for condensed aromatic hydrocarbons, the values of  $p_{rk}$  differ very little. This explains why the eigenvalues calculated by the HMO and the Pariser and Parr methods are much alike. And, it follows that the electronic indices calculated from these will also differ little. The Pariser and Parr method has characteristics in common with the HMO method but takes electron repulsion explicitly into account, hence the name "generalized Hückel method".

If the Pariser and Parr approximations are introduced into the non-empirical Roothaan equations (SCF-MO), the result is the Pople method.

One may consult the recent review by Fueno<sup>34</sup> for the development of other variants of the semi-empirical and non-empirical

methods. We cite only the semi-empirical method of Julg,<sup>53</sup> who takes correlation explicitly into account.

### J. Electronic Indices (Step 4)

The knowledge of the eigenvalues of one-electron energies and the eigenvectors, or molecular orbital coefficients, calculated by the approximations indicated in Step 3 (Section II-I) permits us to calculate a set of molecular electronic indices. Those obtained from eigenvalues are energy indices; those constructed from eigenvectors are structural indices. We will find that many of these indices correspond to "physico-chemical properties" which are not measurable directly or precisely.

In Fig. 3 we find these indices, their interrelations, and their applications. This is a slight variation from one proposed by the Pullmans.<sup>104</sup>

We proceed to describe, within the HMO approximation, the most important electronic indices which are frequently used in biochemical applications.

#### (1) *Total $\pi$ -Electron and Delocalization Energies*

The total  $\pi$ -electronic energy of a conjugated molecule is given by the expression:

$$E_{\pi} = \sum n_j \epsilon_j \quad (54)$$

Replacing  $\epsilon_j$  by its value given by Eq. (34) leads to

$$E_{\pi} = \sum n_j (\alpha + m_j \beta) \quad (55)$$

where  $n_j = 2, 1$  or  $0$  as there are 2, 1, or no electrons in the MO  $\Psi_j$ .

The delocalization energy, DE, is defined as the difference between the energy corresponding to  $E_{\pi}$ , and a system of localized double bonds. In the case of benzene, the one-electron energies are:  $\epsilon_1 = (\alpha + 2\beta)$  and  $\epsilon_2 = (\alpha + \beta)$  (this second is doubly degenerate). As  $n_j$  is 2, by Eq. (54) we have

$$E_{\pi} = 2(3\alpha + 4\beta) = 6\alpha + 8\beta$$

Now each ordinary double bond corresponds to an orbital of energy



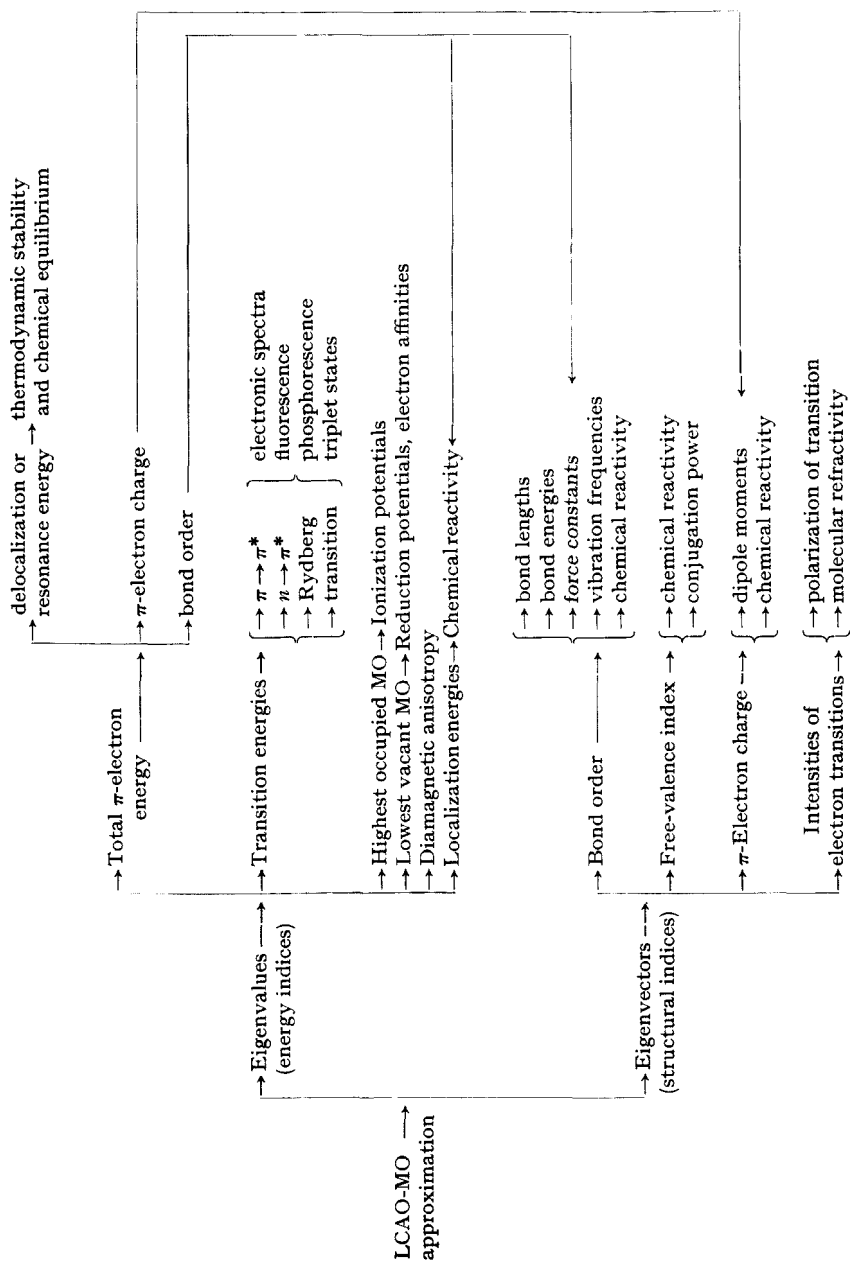


Fig. 3. Synoptic diagram of molecular electronic indices in the molecular orbital method and their applications. (After Pullman and Pullman, 1964 p. 904, Fig. 1.)

$(\alpha + \beta)$ , doubly occupied. The Kekulé structures suggest that in benzene there should be three double bonds, equivalent to:

$$E_{k\pi} = \sum n_j(\alpha + \beta) = 6\alpha + 6\beta$$

so that

$$DE = E_{k\pi} - E_{\pi} = -2\beta \quad (56)$$

This corresponds to an extra energy possessed by the molecule by virtue of the electronic delocalization. Usually the delocalization energy is called resonance energy,  $E_R$ .

The resonance energy thus calculated is the so-called vertical resonance energy because it is referred to a molecule with double and single bonds of equal length. But since this is not fulfilled in the Kekulé structures, it is necessary to add an energy of compression of the sigma bonds,<sup>12</sup>  $E_{kc}$ , to make all of the bonds equal. Therefore

$$E_R = E_{k\pi} - E_{\pi} - E_{kc} \quad (57)$$

For benzene, the value estimated for  $E_{kc}$  is about 35 kcal/mole.<sup>12</sup> In our later results we will not take  $E_{kc}$  into consideration.

Dewar and Schmeising<sup>21</sup> have presented considerable evidence to show that resonance is insignificant in all conventional aromatic systems, and here it is a small fraction of the value calculated by the simple methods; the main factor is the change in energy of the  $\sigma$ -bonded structure with hybridization changes, in line with the basic assumption that the molecular geometry is determined by the  $\sigma$  system of bonds. This more consistent and simpler formulation is still almost universally ignored in favor of the traditional approach.

There is no general agreement as to the value of  $\beta$ ; there are several reasons for this discrepancy.<sup>119</sup> We will use the value  $\beta = -20$  kcal/mole (0.87 eV).

## (2) $\pi$ -Electron Charges or Densities

The squares of the coefficients of the AO's in the MO  $\Psi_j$ ,  $c_{jr}^2$ , give the probability of finding the electron occupying that orbital in the proximity of that atom. Therefore, the total  $\pi$ -electron density, or  $\pi$ -electron charge at an atom,  $r$ , is defined by the expression:

$$q_r = \sum n_j c_{jr}^2 \quad (58)$$

where  $n_j$  is 1 or 2 as the MO is singly or doubly occupied.

In conformity with a theorem established by Coulson and Rushbrooke,<sup>13</sup> in alternant hydrocarbons, all the carbon atoms have unit charge. In non-alternant hydrocarbons and heteronuclear molecules, there is no longer a uniform unitary distribution of electronic charge, that is, there are migrations of charge. It is possible to interpret this as due to the following effects: (a) the tendency toward maximum delocalization of electrons, and (b) the power of the more electro-negative atom to attract electrons. The values of the  $\pi$ -electron charges calculated will be the result of a compromise between these effects. When the carbon atoms have a charge greater than one, they are negative, when it is less than one, positive.

### (3) Bond Order

A  $\pi$  electron in a MO (26) is free to move over the whole conjugated part of the molecular skeleton, contributing to the different bonds. If we suppose  $i$  and  $j$  to be neighboring, the contributions  $c_i c_j \chi_i \chi_j$  will be appreciable and can be interpreted as giving the probability that the electron be simultaneously associated with both cores. Coulson<sup>10</sup> gave the name partial bond order to the expression  $p_{ij}^* = c_i c_j$ . The total bond order, or simply bond order, containing contributions from all the MO's of the molecules, is:

$$p_{ij} = \sum n_r c_{ri} c_{rj} \quad (59)$$

where  $n_r$  is again equal to 1 or 2 as the MO  $r$  is singly or doubly occupied.

Even though the bond order is not a true physico-chemical property and therefore is not measurable, we may still interpret it as a bond-electron density and it may be related to the binding energy.

The  $\sigma$  part of carbon multiple bonds is normally supposed constant; therefore greater or lesser length is due to  $\pi$ -bond resonance. The greater the bond order, the greater the double-bond character, the lower the bond order the more single-bond character. (This view is not consistent with the  $\sigma$ - $\pi$  separation hypothesis.)

One of the more important applications of bond orders is the calculation of bond lengths, but this is not the place to discuss so important a question;<sup>12, 18, 119</sup> we content ourselves with indicating that in the case of aromatic hydrocarbons the agreement with

calculated and observed distances is generally acceptable, but in heteronuclear molecules less satisfactory. We will recall that a large bond order corresponds to a short bond.

#### (4) *Free-Valence Index*

This concept can be considered as the quantum mechanical expression of ideas advanced at the beginning of the century by Flürscheim, Werner (residual affinity) and Thiele (partial valency), according to which atoms in a molecule may not have used up their capacity to combine.

Each atom has a maximum power or capacity for uniting, and the difference between this maximum value and its real bonding capacity is called the free-valence index. If we call  $N_r$  the sum of the bond orders of all the bonds terminating in atom  $r$ , according to Coulson<sup>12</sup> the index of free valence is defined as:

$$F_r = N_{\max} - N_r$$

Ordinarily  $N_{\max}$  is taken as  $3^{1/2}$  or 1.732; therefore,

$$F_r = 1.732 - N_r \quad (60)$$

When numerical values are determined for  $q_r$ ,  $p_{rs}$ , and  $F_r$ , then a molecular diagram is available, a great advance over the classical chemical formula in representing molecular chemical behavior.

#### (5) *Localization Energies*

As it will be seen later the study of the chemical reactivity can be made using the so-called static structural indices ( $\pi$ -electron charge, free-valence index and bond order) and by the localization method.<sup>124</sup> In the last case, it is necessary to define first the following dynamic structural indices.

The atom localization energy is the index used to characterize the most reactive position of a molecule in substitution reactions. In the electrophilic substitution reactions it is necessary to fix two  $\pi$  electrons in the position where the localization occurs. This defines the electrophilic localization energy or cation localization energy. Its numerical value is the difference between the total  $\pi$ -electron energy and the energy of the molecular fragment which

results from the elimination of the substitution position. The nucleophilic localization energy corresponds to the localization of no  $\pi$  electron and the radical localization energy corresponds to the fixation of one  $\pi$  electron.

The *ortho*-localization energy or bond-localization energy is the energy necessary to localize simultaneously two  $\pi$  electrons in the two adjacent carbon atoms which are substrated from the total  $\pi$ -electron system. Therefore this is equivalent to fixing a double bond. The *para*-localization energy is the energy necessary to localize simultaneously two  $\pi$  electrons in *para* position. There are other localization energies which will not be mentioned here.<sup>119</sup>

The smaller the numerical values of the energies the more reactive the positions or bonds will be with respect to the corresponding substituents or additionants.

#### (6) Chemical Reactivity

One of the aspirations of quantum chemistry is to provide a theoretical interpretation of the chemical behavior of organic molecules. The problem is difficult because many factors enter the determination of the reactivity of a molecule; thus one tries to find certain characteristics of molecules and design a model of the process suitable for treatment by quantum mechanical methods.

One must distinguish two aspects of the study of chemical reactions: studying the reactivity of the different centers of a molecule or determining variations among molecules of a family of compounds. In both cases, the use of the molecular electronic indices just defined permits an attack on the theoretical study of the chemical reactivity of conjugated molecules, the only ones which interest us. Fueno<sup>34</sup> has recently reviewed the study of chemical reactivity by quantum mechanical methods.

Two methods, the static and the dynamic, are used for the prediction and interpretation of chemical reactivity. The first constitutes a nearly quantitative extrapolation of the classical qualitative treatment of organic reactions, according to which the reactivity of a position is determined by the  $\pi$ -electron density about the core in the first moment of attack. The static structural indices for atoms ( $q_r, F_r$ ) and for bonds,  $p_{rs}$ , are used. In the dynamic method, it is the stability of the hypothetical transition complex that

is calculated. This method is more general—but more complex—than the first because it provides a unifying explanation, not only of the reactivities of different positions in a molecule, but also of a whole series of conjugated molecules with respect to the three types of reaction.

The dynamic method is divided, in turn, into the “localized method”, due to Wheland, and the “delocalization theory”. To this second belongs the “frontier-electron theory” [Section II-I (4)], and the “charge-transfer theory” developed by Brown.<sup>34</sup>

Although it is difficult to establish general criteria for aromatic substitution, the position of maximum reactivity is usually given, according to the static and localization methods, by the following rules:

(a) Electrophilic substitution (positive ions) will occur where there is the highest electronic charge,  $q$ , the minimum for localization energy,  $A_e(-\beta)$ , and a high value of free valence,  $F$ .

(b) Nucleophilic substitution (negative ions) is favored by small values of  $q$  and of  $A_n(-\beta)$ , and in turn, a high value of free valence,  $F$ .

(c) Radical attack is expected where there is the highest free valence,  $F$ , and minimum  $A_r(-\beta)$ .

In addition reactions at neighboring atoms, the preferred bond will have the greater bond order,  $p_{rs}$ , or lesser energy of *ortho*-localization,  $O(-\beta)$ . *Para*- addition is favored between atoms where the sum of the indices of free valence is highest or the energy of *para*-localization minimal,  $P(-\beta)$ .

### III. BIOCHEMICAL APPLICATIONS

In this chapter we give the results obtained for the more important families of molecules and processes of biochemical interest. We want to indicate that we will exclude all reference to proteins, since these are considered in their various aspects in other chapters.

Despite the relatively short time since the first applications of quantum mechanical methods to the calculation of electronic structures of biomolecules, the publications are already numerous. Pullman, Pullman, and co-workers,<sup>103</sup> who initiated these studies, have calculated structures for some 300 biomolecules. Fernández-

Alonso and collaborators have also made calculations for a great number of molecules, as have Fukui and his group, Grabe, and others. Some of these results have been collected in recent publications.<sup>18, 75</sup>

### A. Theory of Electron Transfer

In recent years the formation of simple molecular complexes, for example, between a molecule of iodine and one of benzene, has become a well-known and amply studied phenomenon. Mulliken<sup>73, 78</sup> developed the theory of charge or electron transfer which permits predictions about molecular complexes. From a more chemical point of view we might call this the theory of electron donor-acceptor interaction.

Two types of electron transfer can be distinguished. If the charge passes from one part to another of the same molecule, we have intramolecular electronic transitions, which might better be called "transitions of electronic relocation". If the molecular complex is wholly or partially organic, 1:1 stoichiometry is observed and the electron is transferred partially or completely from one component to another of the complex, and we have the intermolecular electronic transfers. These are the principal cases considered by Mulliken. In these complexes, it is supposed that the electron passes spontaneously from the highest occupied MO of the donor compound to the lowest vacant MO of the acceptor. Generally the electron is only on the acceptor for a very short period of time; for definitive transfer an additional impulse of energy is needed.

If we represent the sum of the energies of the donor and acceptor molecules by  $W_0$ , and that of the ions  $D^+$  and  $A^-$  by  $W_1$ , we have for infinite internuclear separation,  $R_\infty$ :

$$W_1 - W_0 = I_D - A_A \quad (61)$$

where  $I_D$  is the ionization potential of the donor molecule,  $D$ , and  $A_A$  is the electron affinity of molecule  $A$ . It is easily shown that  $W_1$  varies with  $R$ . To determine  $W_1 - W_0$  it is necessary to know besides  $I_D$  and  $A_A$  the electrostatic interaction between the ions  $D^+$  and  $A^-$ .

For closed-shell configurations, according to Koopman's

theorem,<sup>60</sup>  $-I = \epsilon_m$ , where  $\epsilon_m$  is the energy of the highest occupied MO, but this theorem is only applicable strictly to the SCF-MO. However, when calculated potentials are compared with experiment, the former are larger. Apparently there are various causes for this discrepancy, of which the so-called "after effect" due to the stabilization of the conjugated systems after ionization is the most important. Introducing certain refinements permits the calculation of ionization potentials in fair agreement with experiment.<sup>34</sup>

In the Hückel approximation the above relation is but a crude approximation for polycyclic aromatics. Moreover, as we saw in Section II-I (1), the HMO method leads to the same value for the ionization of odd alternant radicals. Streitweiser<sup>119</sup> improved these results employing the " $\omega$ -technique". There are few values in the literature for  $I$  obtained by LCAO calculations on heteroatoms.<sup>119</sup> In general one can say that the HMO method is only applicable to ionization potentials for related groups of molecules.

Koopman's theorem, applied to electron affinity, identifies this with the energy of the lowest vacant MO,  $\epsilon_{m+1} = -A$ , where  $\epsilon_{m+1}$  is the energy of the lowest vacant MO. The electron affinities can be determined experimentally from polarographic half-wave reduction potentials. Although these contain the change of free energy from the solvated molecule to the solvated ion in addition to the electron affinity, the free-energy term is practically constant and a linear relation is found between the half-wave potentials and the roots of the secular equation,  $m_{m+1}$ . Here the agreement between  $A$  and  $\epsilon_{m+1}$  is good, superior to that found for ionization potentials.

Biochemical interest in electron transfer phenomena is recent.<sup>120</sup> Isenberg and Szent-Györgyi<sup>51</sup> demonstrated the formation of the complex tryptophan-riboflavin, Harbury and Foley<sup>46</sup> that of the molecular complex caffeine-riboflavin, and Fujimori<sup>35</sup> the tryptophan-pteridine complexes. These are intermolecular electron transfer complexes in which the donor transfers an electron to the acceptor. Szent-Györgyi<sup>120</sup> believes that these processes must occur frequently in biological systems, even in the ground state. Recently Goudot<sup>75</sup> postulated the formation of intramolecular electron transfer complexes to explain the catalytic activity of organo-metallic enzymes. Since the experimental values of  $I$  and  $A$  are not known for the majority of biomolecules, the theoretical calculations have provided a fundamental contribution.



### B. Electronic Structures of Biomolecules

Before discussing the molecular diagrams of the more important groups of biomolecules, we point out that (unless indicated to the contrary) they have been calculated by the method of Pauling and Wheland (Section II-I (3) ), neglecting overlap between neighboring atoms. The parameters used by Fernández-Alonso are indicated in Table I.

TABLE I. Numerical Values of the Parameters  $\delta$  and  $\rho$  in Expression (39)

Heteroatom	$\delta$	Bond	$\rho$
$=\text{N}-^{\text{a}}$	0.6	$\text{C}=\text{N}-$	1
$-\dot{\text{N}}-^{\text{a}}$	1	$\text{C}-\text{N}-$	1
$=\text{N}-^{\text{b}}$	0.9	$\text{C}=\text{N}-$	1
$-\text{N}-$	1.2	$\text{C}-\text{N}-$	1
$=\text{O}$	1.2	$\text{C}=\text{O}$	2
$-\ddot{\text{O}}-$	2	$\text{C}-\text{O}-$	$2^{1/2}$
F	1.7	$\text{C}-\text{F}$	1.1
Cl	1.6	$\text{C}-\text{Cl}$	0.9
Methyl ( $-\text{C}-\text{H}_3$ ):			
C	-0.1	$\text{C}-\text{C}$	0.7
$\text{H}_3$	-0.5	$\text{C}-\text{H}_3$	2

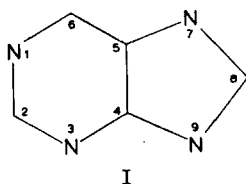
<sup>a</sup> Pyrimidinic nitrogen.

<sup>b</sup> Glyoxalic nitrogen.

#### (1) Purines

The group of fundamental purine bases is made up of two amino-purines, guanine and adenine, and two oxypurines, hypoxanthine and xanthine. The first two are constituents of nucleic acids; hypoxanthine plays a fundamental role in the *de novo* synthesis of them; xanthine is an essential product in degradation of these acids. For the purpose of comparison, we include here the product of metabolic degradation of the purines, uric acid. Diagram I indicates the numbering system used for this type of compound.

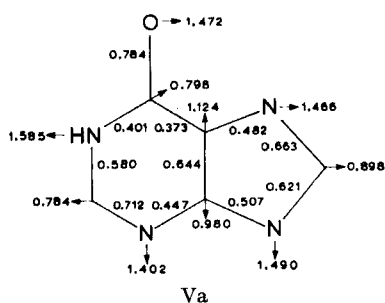
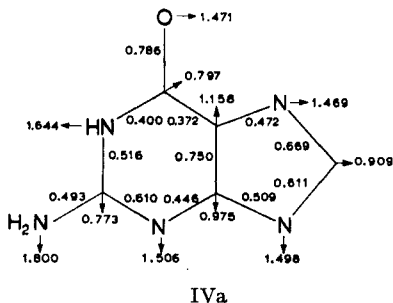
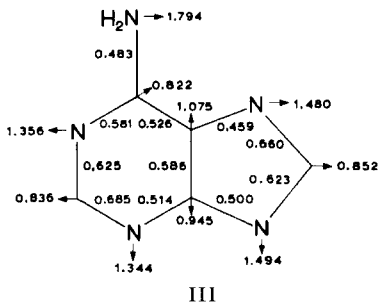
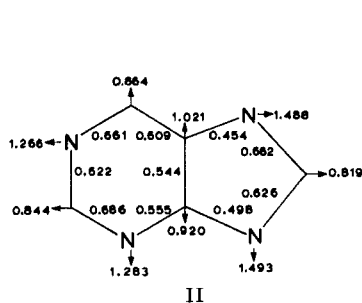
Guanine, xanthine, and hypoxanthine may show amino-imino

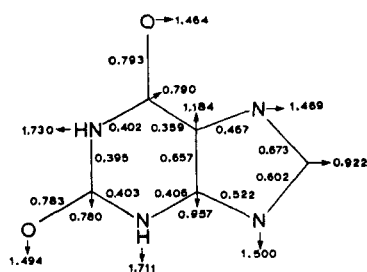


and lactam-lactim (the last, keto-enol) tautomerism; however, there is ample experimental evidence suggesting that these compounds are present exclusively in amino, and predominantly in lactam, forms.

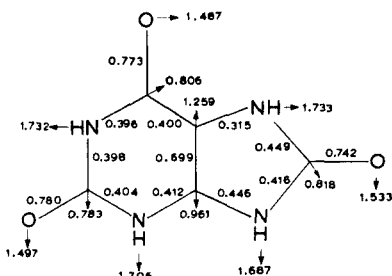
We give molecular diagrams obtained by Fernández-Alonso and Domingo <sup>27, 28</sup> for purine (II), adenine (III), guanine (IVa, lactam form), hypoxanthine (Va), xanthine (VIa) and uric acid (VIIa). (The "a" indicates keto forms and "b" denotes enol forms.) The values indicated by arrows correspond to the  $\pi$ -electron densities, the other ones to the bond orders.

In the original paper by Fernández-Alonso and Domingo <sup>27</sup> the diagrams for the ground states of IV, Va and V are accidentally interchanged with those of the first excited state.





VIa



VIIa

These diagrams (and those for the rest of the related compounds) have been calculated on the assumption that the hydrogen atom is not assigned to N<sub>9</sub>, as is done currently, but, following Mason,<sup>72</sup> is assumed shared by N<sub>7</sub> and N<sub>9</sub> by tautomeric exchange, hydrogen bonding, etc. This structural consideration results in the assignment of the same parameter to both nitrogens. Then N<sub>7</sub> and N<sub>9</sub> both contribute to the conjugated system with three  $\pi$  electrons.

Pullman and Pullman<sup>103</sup> have calculated molecular diagrams of the molecules above, but supposed that the hydrogen atom is at nitrogen 9. Since, in addition, they used different parameters, their diagrams are not identical, but agree closely, in general, as to distribution,  $\pi$ -electron charges, bond orders, and indices of free valence.

One can deduce from the preceding diagrams that in II, III, the gloxalic nitrogens are more charged than the pyrimidinics, while in IVa and in VIa the reverse is true. In the case of purine, the greater charge on N<sub>3</sub> with respect to N<sub>1</sub> is confirmed experimentally by the formation of the *N*-oxide of III.<sup>27</sup>

Very recently, Veillard and Pullman<sup>121</sup> have calculated the  $\pi$ -electron densities in purine, adenine, guanine, and 2,6-diaminopurine in the Pariser and Parr approximation, observing that their magnitudes and distributions correspond closely with those obtained in the Pauling-Wheland approximation. The same authors<sup>122</sup> have used the shifts in nuclear magnetic resonance to verify the calculations of  $\pi$ -electron charges in purine, adenine, and 2,6-diaminopurine. Baudet, Berthier, and Pullman<sup>6</sup> used the SCF method to calculate the distribution of spin density for the positive and negative radical-ions of adenine and guanine. These results are interesting in relation to electron paramagnetic resonance.

The treatment of the chemical reactivity of the fundamental purine bases, carried out by the static method, appears to lead to predictions in disagreement with the experimental results. Nevertheless, Pullman used the localization method to predict certain results for purine consistent with the experimental data. Recently special attention has been paid to the alkylation of guanine in position N<sub>7</sub>.<sup>20,104</sup> Perault, Valdemoro, and Pullman<sup>95</sup> studied the mechanism of the xanthine oxidase which regulates the catabolism of the biopurines. They studied the enzymatic oxidation of these biomolecules from the electronic point of view using the dynamic index, nucleophilic localization energy.

Bond orders permit the calculation of interatomic distances which, in view of the arbitrariness in the construction of the master curves, relating interatomic distances, C—N and C—O with their bond orders, are in acceptable accord with the experimental distances.<sup>27</sup>

Values of the energy indices are displayed in Table II. Besides the compounds already mentioned, the following are included: 2-methyladenine (VIII), 2,8-dihydroxyadenine (IX), 2,8-dichloro-adenine (X), 2-methylhypoxanthine (XI),<sup>26</sup> 2-hydroxypurine (XII), 6-fluoropurine (XIII), 6-chloropurine (XIV), 6-amino-2-hydroxypurine (iso-guanine) (XVa), 6-methylaminopurine (XVI),<sup>25</sup> 8-azahypoxanthine (XVII).<sup>32</sup>

Analysis of the delocalization energies in the table shows that it is greater for the keto than for enol forms; for example, it is  $0.18\beta$  ( $\sim 3.6$  kcal) for guanine,  $0.15\beta$  ( $\sim 3.0$  kcal) for hypoxanthine, and  $0.39\beta$  ( $\sim 7.8$  kcal) for xanthine. These theoretical results are in agreement with the experimental fact that the ketonic forms are more stable.

Pullman<sup>97,104</sup> has given the following interpretation of electron delocalization energies per  $\pi$  electron. It is known experimentally that the resistance of the purine bases to ultraviolet and ionizing radiation decreases in the order, adenine > guanine > xanthine > uric acid, while in relation to the pyrimidine bases which constitute the nucleic acids the order is adenine > guanine  $\gg$  cytosine > uracil  $\geq$  thymine. Gordy confirmed this by electron paramagnetic spectra of the irradiated solid bases.

From the beginning it became evident that these phenomena ought to be related to the electronic delocalization. Duchesne<sup>23</sup>

TABLE II. Energy Indices for the Purine Bases and Some Derivatives in Units of  $\beta$ 

Compound	Delocalization energy		h.o. MO <sup>a</sup>	l.v. MO <sup>b</sup>
	per molecule	per electron		
II	3.579	0.36	0.807	-0.672
III	3.636	0.30	0.593	-0.827
IVa	3.770	0.27	0.382	-1.100
IVb	3.594	0.26	0.593	-0.827
Va	3.696	0.31	0.457	-0.942
Vb	3.547	0.30	0.613	-0.878
VIa	3.894	0.28	0.403	-1.105
VIb	3.508	0.25	0.504	-0.918
VIIa	4.001	0.25	0.111	-1.281
VIIb	3.849	0.24	0.371	-1.047
VIII	3.795	0.27	0.580	-0.821
IX	3.942	0.25	0.373	-0.973
X	4.496	0.28	0.463	-0.919
XIa	3.858	0.27	0.447	-0.913
XIb	3.706	0.26	0.598	-0.868
XIIa	3.628	0.30	0.457	-0.650
XIIa'	3.668	0.31	0.493	-0.676
XIIb	3.535	0.29	0.613	-0.697
XIII	3.687	0.30	0.646	-0.823
XIV	3.814	0.32	0.683	-0.781
XVa	3.726	0.27	0.378	-0.840
XVa'	3.747	0.27	0.458	-0.856
XVb	3.596	0.26	0.498	-0.867
XVI	3.976	0.28	0.473	-0.845
XVIIa	3.957	0.33	0.534	-0.829
XVIIb	3.781	0.31	0.656	-0.734

<sup>a</sup> h.o. MO = highest occupied MO.<sup>b</sup> l.v. MO = lowest vacant MO.

was the first to suggest a quantitative interpretation, proposing diamagnetic anisotropy as a measure of radiation resistance. This was later confirmed by Veillard, Berthier, and Pullman.<sup>123</sup> Independently, the Pullmans<sup>97, 104</sup> suggested that the delocalization energy per  $\pi$  electron would be a good measure of radiation resistance, which was fully confirmed by them even if it is not clear what

this stabilization represents. The numerical results of Table II follow the sequence previously indicated for the enol forms of the purine bases, while the ketone series shows an inversion of guanine and xanthine.

The electron donor-acceptor properties of the fundamental purine bases are deduced from a study of the numerical values of the h.o. MO and l.v. MO. It can be generally shown that the bases should be good electron donors and poor acceptors. Their ionization potentials should follow the order: guanine < xanthine < hypoxanthine < adenine < purine. It can be said that the four fundamental purine bases will show intermediate activity. It is known that *N*-methylation of purines increases slightly their behavior as electron donors (but has little effect on their acceptor character). We can remember here that the alkylation of hydrocarbons reduces considerably their ionization potentials.<sup>27</sup> Uric acid should be an excellent electron donor, due to the very small numerical value of the energy of its h.o. MO. The previous theoretical considerations find experimental confirmation in the study of the solubilizer effect of the purines compared to that of the aromatic hydrocarbons, an effect which varies in the same direction as the electron donor properties.

From numerical values of the l.v. MO it is deduced that the polarographic reduction potentials should follow the order: purine < adenine < hypoxanthine < guanine < xanthine. The last two should be difficult to reduce, and uric acid should be even more so. It is known that adenine, adenosine, adenylic acid and the nucleotide adenine-cytosine are reduced at the dropping mercury electrode, while guanine, guanosine, guanylic acid and some other related compounds are not reduced.<sup>27</sup> Solutions of uric acid are not reduced if freshly prepared, but undergo reduction after a long exposure to air.

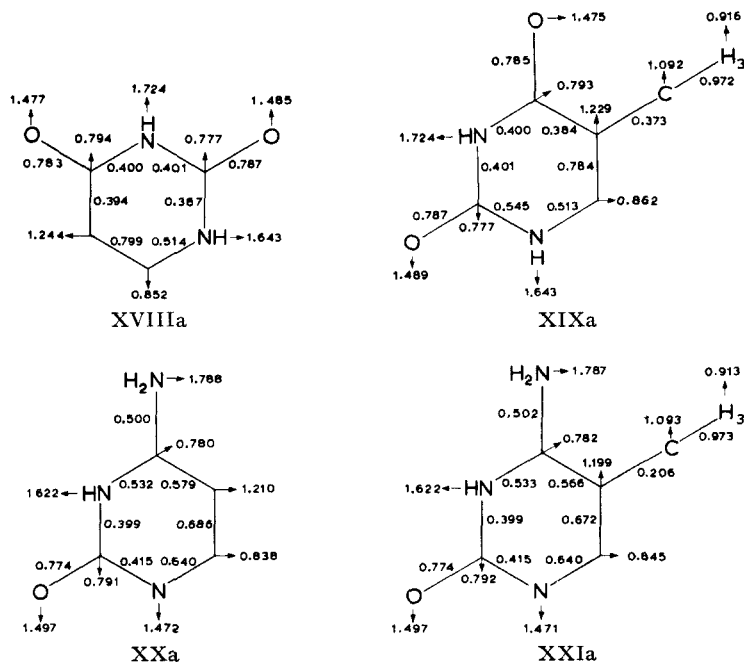
## (2) *Pyrimidines*

Pyrimidine constituents of nucleic acids are uracil, thymine, cytosine, 5-methylcytosine and 5-hydroxymethylcytosine.

A whole set of physico-chemical properties show that uracil is in tautomeric equilibrium between the lactam and lactim forms, but this is displaced strongly toward the former. An argument in favor

of the idea that the H atoms are joined to the N atoms of the ring and not to the oxygens is the considerable acidity of the hydroxyaromatics and large basicity of the nitrogen atoms of aromatic heterocyclics.

Distributions of  $\pi$ -electron densities and bond orders follow for the lactam forms of uracil (XVIIIa),<sup>29</sup> thymine (XIXa), cytosine (XXa),<sup>30</sup> and 5-methylcytosine (XXIa).<sup>32</sup> All have been calculated previously by the Pullmans.<sup>103</sup>



The values calculated for the energy indices are found in Table III. It includes, in addition, the molecules 5-fluorouracil (XXII), 6-azauracil (XXIII) and 2,4,5,6-tetraaminopyrimidine (XXIV).<sup>32</sup>

The keto forms have a DE superior to the enol forms. Our numerical results generally confirm the order of resistance to ionizing and ultraviolet radiation previously indicated in Section III-B (1) (although there is an inversion for the lactam forms of uracil and cytosine). At the same time, they corroborate the fact that the pyrimidine bases offer less radiation resistance than the purine bases.

TABLE III. Energy Indices for the Pyrimidine Bases and Some Derivatives in Units of  $\beta$ 

Compound	Delocalization energy		h.o. MO	l.v. MO
	per molecule	per electron		
XVIIIa	2.247	0.22	0.573	-1.011
XVIIIb	1.905	0.19	0.706	-0.920
XIXa	2.397	0.20	0.505	-0.998
XIXb	2.052	0.17	0.634	-0.915
XXa	2.139	0.21	0.549	-0.839
XXb	1.994	0.20	0.681	-0.879
XXIa	2.285	0.19	0.494	-0.837
XXIb	2.142	0.18	0.617	-0.877
XXIIa	1.473	0.12	0.226	-1.095
XXIIb	1.154	0.10	0.365	-0.949
XXIIIa	2.143	0.21	0.628	-0.730
XXIIIb	1.806	0.18	0.728	-0.672
XXIV	3.652	0.26	0.197	-1.050

From the data of Table III it turns out that the pyrimidines are poorer electron donors than the purines; at the same time they would be poor electron acceptors. We note that uracil is not reduced at the dropping mercury electrode.

### (3) *Adenine-Thymine and Guanine-Cytosine Pairs*

Pullman and Pullman<sup>104</sup> calculated the molecular diagrams for the guanine-cytosine and adenine-thymine pairs as they occur in the Watson-Crick model in order to interpret the electronic structure of the nucleic acids. Figures 4 and 5 show the charge distributions and the principal centers of physico-chemical behavior, respectively.

The authors cited above did a careful study of the electronic structure of nucleic acids; we will note that, according to their results, of the two pairs the guanine-cytosine pair is at the same time a better donor and a better acceptor. This is in accord with the higher denaturation temperature of the nucleic acids rich in this



pair. They suggest that it may be significant that the resonance energy for the first pair is  $6.328\beta$  and for the second only  $6.008\beta$ , that is, a difference of 6–7 kcal.

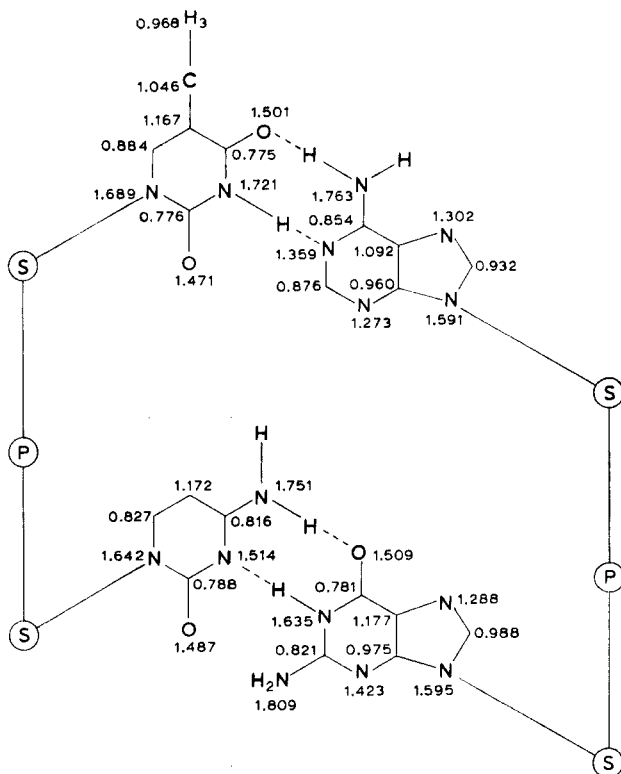


Fig. 4. Distribution of  $\pi$ -electron charges in the pairs adenine-thymine and guanine-cytosine. (S represents the sugar and P the phosphorus bridge.) (After Pullman and Pullman,<sup>104</sup> p. 905, Fig. 2.)

#### (4) Pteridines

In this group we include pteridine (XXV); 2,4-diaminopteridine (XXVI), a compound of great interest for the correlation between electronic structure and antitumor activity in cancer; xanthopterine (2-amino-4,6-dihydroxypteridine) (XXVII), which is naturally occurring, and is a strong catalyst of mitosis, similar to folic acid

which is believed to be a degradation product; leucopterine (2-amino-4,6,7-trihydroxypteridine) (XXVIII), the first naturally occurring pteridine for which a molecular structure was established;

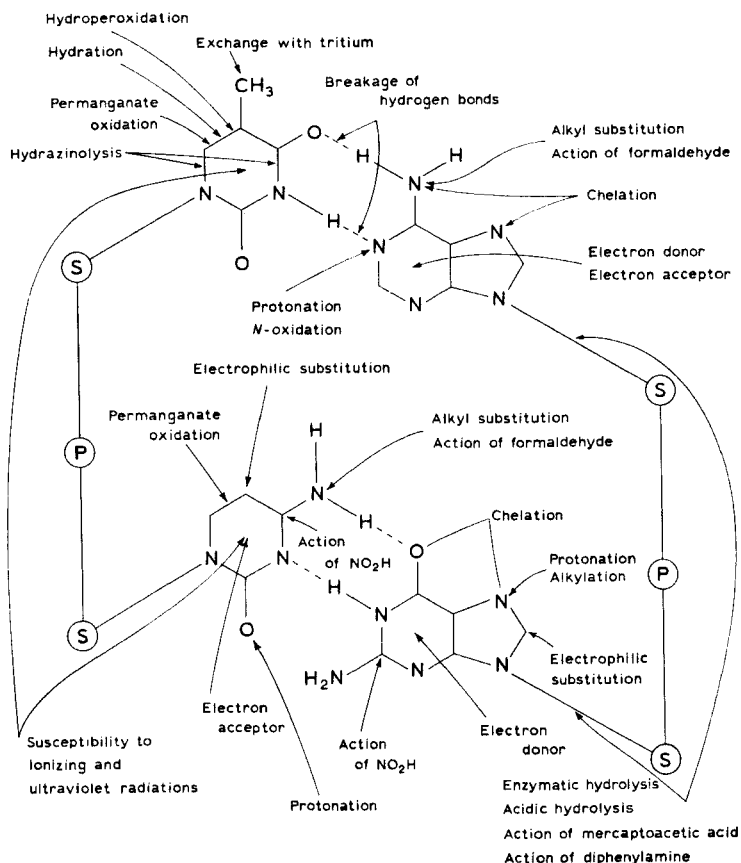
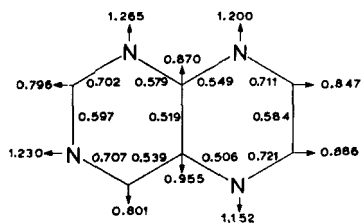


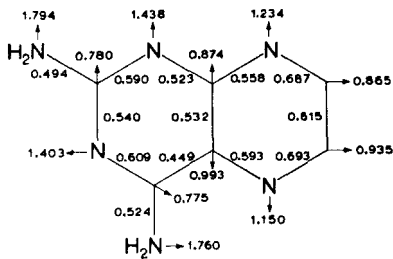
Fig. 5. Fundamental bases of the nucleic acids: Localization of the centers of the principal chemical and physico-chemical properties. (After Pullman and Pullman,<sup>104</sup> p. 911, Fig. 7.)

2,4,5,7-tetrahydroxypyrimido (5,4-g) pteridine (XXIX); 2,4,6,8-tetrahydroxypyrimido (4,5-g) pteridine (XXX); 2,4,5,7-tetraaminopyrimido (5,4-g) pteridine (XXXI); and 2,4,6,8-tetraaminopyrimido (4,5-g) pteridine (XXXII). Diagrams of these molecules

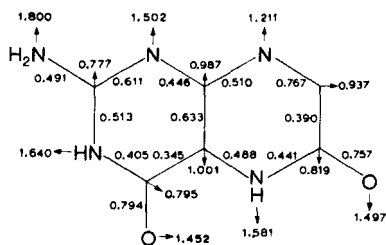
are given below.<sup>28, 31, 32</sup> Diagrams of XXVII and XXVIII were previously calculated by Pullman.



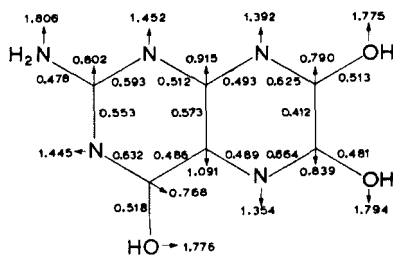
XXV



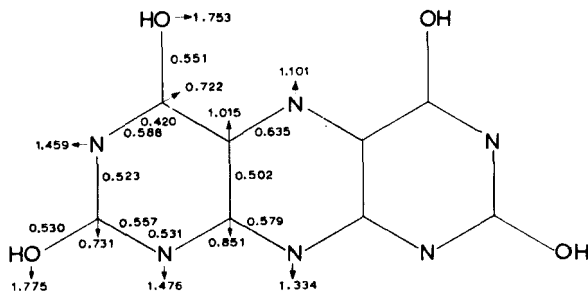
XXVI



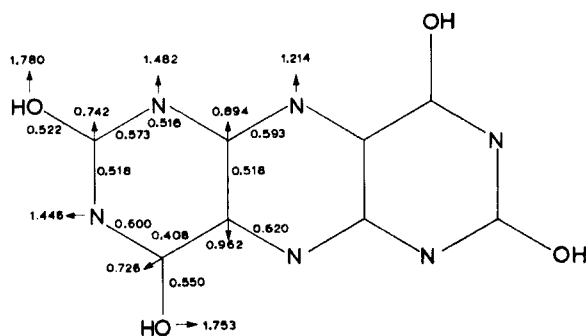
XXVIIa



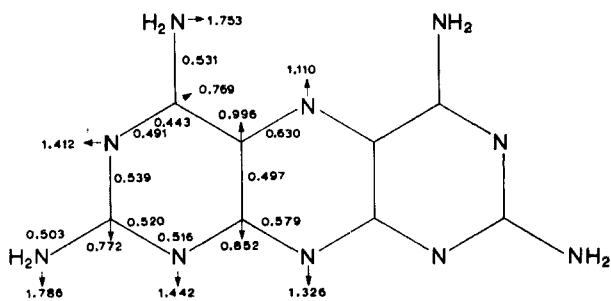
XXVIIIb



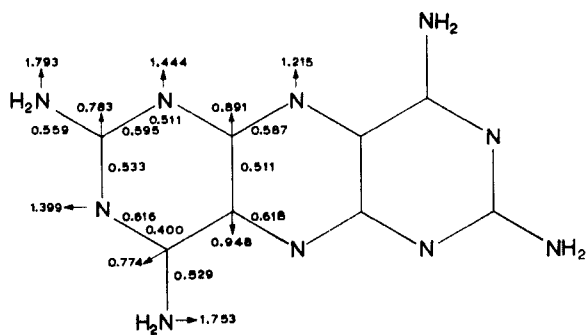
XXIX



XXX



XXXI



XXXII

The energy indices are shown in Table IV.

TABLE IV. Energy Indices for Some Pteridines in Units of  $\beta$

Compound	Delocalization energy		h.o. MO	l.v. MO
	per molecule	per electron		
XXV	3.588	0.32	0.764	-0.281
XXVI	3.775	0.31	0.651	-0.417
XXVIIa	3.865	0.30	0.260	-0.551
XXVIIb	3.593	0.25	0.483	-0.483
XXVIIIb	3.547	0.25	0.384	-0.666
XXIX	5.318	0.25	0.706	-0.352
XXX	5.259	0.29	0.503	-0.290
XXXI	5.636	0.31	0.662	-0.298
XXXII	5.585	0.31	0.492	-0.247

From the numerical values of the delocalization energy per  $\pi$  electron (for the enol forms, only one common to the hydroxylated compounds) the order of resistance to ultraviolet and ionizing radiations is deduced: XXV > XXVI = XXXI = XXXII > XXX > XXVIIb = XXVIII = XXIX.

On the other hand, XXVII, XXVIII, XXXII and XXX should be good electron donors while XXVI and XXXI should be average electron donors and the others, especially XXV, poor electron donors. It is to be observed that compounds which are at least average donors are those which have a substituent in position 6.

As electron acceptors, XXXII, XXV, XXX, XXXI and XXIX are excellent, while XXVI and XXVII are average acceptors. This is in agreement with Fujimori's results<sup>35</sup> for the formation of complexes between pteridines and tryptophan. We note that XXVII and XXVIII are reduced at the dropping mercury electrode.

The theoretical predictions of chemical reactivity of these compounds can be compared with the experimental results which are well known;<sup>3</sup> in general the agreement is good.

#### (5) Basicity of the Aromatic Ring Nitrogens

Nakajima and Pullman<sup>84</sup> demonstrated that the basicity of nitrogens of the conjugated rings was not directly related to their

formal charges. From the Pariser and Parr approximation, they deduced the expression

$$pK_a = B + \sum_p Q_p (dd|pp)$$

for the theoretical basicity, where  $B$  is a constant characteristic of each family of molecules,  $Q_p$  is the formal charge carried by the N atom and  $(dd|pp)$  is the Coulomb integral between a lone-pair electron on the N and the  $\pi$  electron on atom  $p$ , with the summation over the whole ring.

Graphical representation of the  $pK_a$ 's observed with those calculated by this expression shows agreement with experiment. They find that in guanine the most basic nitrogen is N<sub>7</sub> and in adenine N<sub>1</sub>.

The problem of the basicity of these compounds is, nevertheless, more complex, as has been observed recently by Chalvet and collaborators,<sup>9</sup> who found that the entropy of solvation is the factor which essentially influences the entropy of protonation of the aza-compounds studied.

#### (6) *Electronic Structure and Antitumor Activity in Cancer*

As indicated in Section I, one of the first applications of quantum mechanical methods to the study of biomolecules was the attempt to establish a relation between electronic structure and antitumor activity in cancer. This study was carried out first by Pullman and Pullman,<sup>102</sup> whose most important results on the purine anti-metabolites are summarized below.

Of all compounds of this type, antitumor activity is shown only by: 6-mercaptapurine, thioguanine, 2,6-diaminapurine, 8-azaguanine, 6-methylpurine, 2-azaadenine and purine. Related anti-metabolites not demonstrating antitumor activity are: 8-aza-6-mercaptapurine, 8-azapurine, 8-azaadenine, 8-azaxanthine, 6-carboxypurine, and 6-cyanapurine. From values calculated for the  $\pi$ -electron charges of the skeleton nitrogens of the purine, they established the following general rule: The inactive antimetabolites have a formal charge on N<sub>9</sub> higher than on the active ones; in the latter it is of the same order as in the fundamental purine bases. In addition all the active compounds are more basic than the inactive ones, where the basicity is calculated using the formula of Section III-B (5). The most basic nitrogens of the active metabolites are

N<sub>1</sub> and N<sub>7</sub>, which are also the most basic in adenine and guanine respectively.

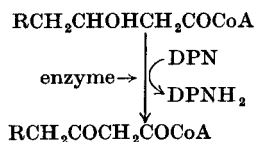
Recently, Fukui and his collaborators<sup>39</sup> have studied the relation between the electronic structure and the antitumor activity of carcinostatic compounds. According to their work, it seems that the tumor-inhibitory action of an anti-cancer agent depends on the interaction of its reactive sites with nucleophilic centers in the body which act as growth regulators. These workers establish the following policy as an operating norm in the search for active compounds in cancer chemotherapy: "To synthesize and test the compound which has a sufficiently large reactivity toward nucleophilic reagents". Now, our knowledge of the electronic structural characteristics of molecules can then help us in this search, from a theoretical standpoint, since the reactivity of a compound toward nucleophilic reagents is greater, the less the numerical value of its l.v. MO. The Japanese authors cite as compounds interesting in this respect the quinones, the fulvalenes and their derivatives.

The preceding considerations are in the line of reasoning developed by Perault and Pullman,<sup>93</sup> according to whom the actions of coenzymes and of the antimetabolites of folic acid seem to be related to the property of electron acceptor of the pteridinic ring which, as we have already seen (Section III-A), is characterized by the l.v. MO.

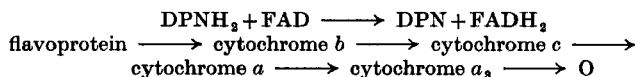
### C. Electronic Interpretation of Some Biocatalyzed Reactions

Metabolic processes proceed by the gradual liberation of energy at the expense of the oxidation of substrates. This energy is used directly or is stored in the form of organic compounds with "energy-rich bonds".

Consider one of the many possible examples of a link in the chain of degradation of fatty acids in which there is a smooth liberation of energy. This requires the presence of an enzyme which specifically catalyzes it, and a coenzyme, DPN, which acts as acceptor of the hydrogen removed from the molecule in question,



Since the supply of the coenzyme, in this case DPN, is depleted rapidly, it is necessary that there be a mechanism for its regeneration. The organism achieves this by way of the respiratory chain of the cytochromes, which makes possible the transfer of the hydrogen (from the reduced coenzymes) to molecular oxygen. This process liberates energy which the organism utilizes for the phosphorylation and resynthesis of substrates rich in energy. The successive steps in the respiratory chain are<sup>62</sup>

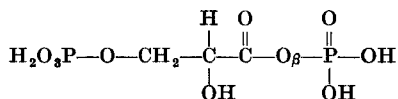


where FAD is the coenzyme flavine-adenine dinucleotide (flavoprotein).

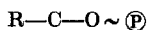
The theoretical analysis of the complex process of the respiratory chain was realized by B. Grabe,<sup>41</sup> constituting the subject of her dissertation. Recently Fischer-Hjalmars<sup>75</sup> summarized these results.

### (1) *Electronic Structure of Energy-Rich Bonds*

Hydrolyzable linkages fall into two groups with respect to their energy levels, low- and high-energy types. The bonds of carboxyl esters, phosphoric esters, peptide and glycoside belong to the first group. Their hydrolysis is characterized by a small standard free energy change ( $\Delta F^0 \sim -3$  kcal/mole). In comparison, the high-energy type bonds liberate much more energy ( $\Delta F^0 \sim -10$  kcal/mole), which can promote endergonic reactions. The first to point out this large liberation of energy were Kalckar<sup>54</sup> and Lipman.<sup>65</sup> This group includes the bonds of  $\beta$ -keto acids, thioesters, pyrophosphate, guanidine phosphate, enol phosphate, and carboxyl phosphate. We take as an example the molecule of diphosphoglyceric acid,

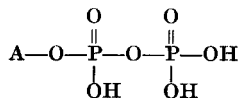


The bond  $\text{O}_\beta-\text{P}$  is a high-energy phosphate bond, usually represented by the symbol  $\text{O} \sim \text{P}$ . Consequently, the molecule above can be written thus:

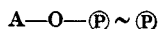




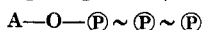
The adenosine diphosphate (ADP) molecule:



is represented by



and that of adenosine triphosphate (ATP) by



Recent results tend to suggest that the hydrolysis of ATP does not liberate as much energy as was previously supposed, but an amount similar to that released by the simple polyphosphates.<sup>38</sup>

From the beginning, attempts were made to explain the origin of the high energy of these compounds. The first theoretical interpretations were based on resonance theory,<sup>54, 65</sup> introducing the concept of opposing resonance, but no quantitative results were produced.

More recently, Grabe<sup>41c</sup>, Pullman and Pullman,<sup>101</sup> and Fukui, Morokuma, and Nagata<sup>38</sup> have used the molecular orbital method to study these compounds. The more important results are given below.

(a) *Grabe's results.* Electronic structures of the carboxylphosphate, carboxyl, and phosphate ions, adenosine diphosphate (ADP) and adenosine triphosphate (ATP) were calculated; we summarize the carboxylphosphate calculation as an example. In Fig. 6 the spatial arrangement and notation for the atoms are indicated.

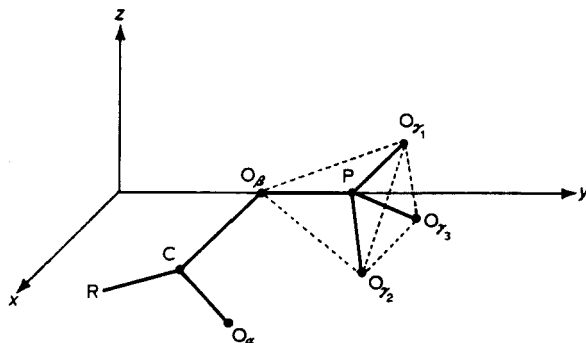


Fig. 6. The spatial arrangement and notation for the atoms in the carboxylphosphate. (After Grabe,<sup>41c</sup> p. 214, Fig. 1.)

Method of calculation: Pauling-Wheland approximations (Section II-I (3)) including overlap.

Number of electrons: 6. This corresponds to one from the carbon atom, one from the  $O_\alpha$  atom, two from the  $O_\beta$  atom, one from the P atom and one from the group  $(O_3)_\gamma$ . The AO's of the carbon and oxygen atoms are  $2p$ 's, those of phosphorus  $3p$  (or  $4p$ ) and for the three oxygen atoms of the group, one (unnormalized) orbital, assuming hyperconjugation, of the form

$$\Psi_{gr} = 2p_{\gamma_1} - \frac{1}{2}(2p_{\gamma_2} - 2p_{\gamma_3})$$

Evaluation of the integrals  $\alpha$ ,  $\gamma_{\lambda\mu}$ , and  $S_{\lambda\mu}$ : Numerical values of  $\alpha$  and  $\gamma$  were determined semi-empirically from experimental data. The integral  $\alpha$  was calculated from the ionization potentials estimated by Skinner and Pritchard.<sup>117</sup> The integral  $\gamma$  was obtained from the expression:

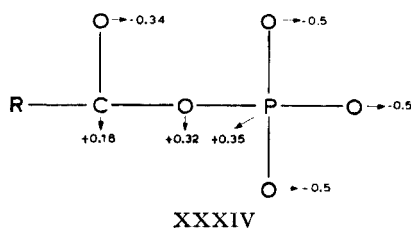
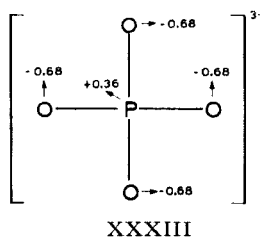
$$\gamma_{\lambda\mu} = -\frac{D' S_{\lambda\mu}}{2} \pm \sqrt{\frac{1}{4}[D'^2 - (\alpha_\lambda - \alpha_\mu)^2]}$$

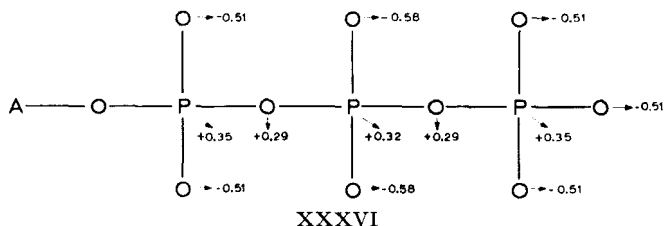
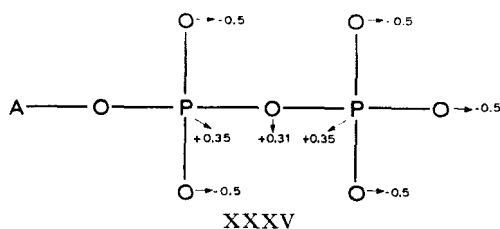
where  $D'$  is approximately the difference between the energy of a single and a double bond.

Overlap integrals were taken from tables of Mulliken and of Floodmark.

$\pi$ -electronic charges were calculated as defined by Mulliken.<sup>80</sup>

Grabe carried out different types of calculations to determine the effect of parameter value choice and type of atomic orbitals assumed for the phosphorus atom, for different distances and angles. Distributions calculated from the phosphate ion (XXXIII), carboxyl phosphate (XXXIV), adenosine diphosphate (XXXV), and adenosine triphosphate (XXXVI) are indicated below.





Analysis of these distributions shows the bridge O-atoms to possess a positive formal charge, while the remaining O-atoms have negative formal charges. That is to say that the bridge O-atoms have a  $\pi$ -electron charge defect and are bonded to P-atoms of positive formal charge constituting an atomic chain (of 3 atoms in ADP and 5 in ATP) of positive charge surrounded by an atomic system of negative formal charges. Fischer-Hjalmars<sup>75</sup> called these tri-positive bonds. According to Grabe, the atoms with positive formal charge are easily attacked by the negative ions of enzymes.

Fischer-Hjalmars' calculations of the share of the increased energy of the rich bond attributed to opposed resonance in the ADP and ATP molecules does not coincide with the results of Kalckar and Oesper.<sup>75</sup> Likewise, she calculated the increase corresponding to the electronic repulsion between like charges, finding them to contribute a third of the energy of the rich bond, confirming the results of Hill and Morales.<sup>48</sup>

Finally, another contribution to the energy of the rich bond, according to Grabe, is the  $\sigma$ -polarization energy, coming from a modification of the  $\pi$ -electron charge due to  $\sigma$  polarization, resulting in an increased positive formal charge on the carbon and phosphorus atoms. This awakens the bonds and leads to a competition among the three atoms of the bond for the electrons. This competition is what stabilizes the molecule and produces the so-called high-energy of the molecule.

It is known experimentally that energy-rich bonds may react in two ways:



In case (A), the group  $-PO_3H_2$  behaves as the active group; in case (B) it is the CO group. That is to say that the energy of the group bound to the bridge O-atom diminishes. According to Grabe, this is due to the transfer of a pair of  $\sigma$  electrons with the atom  $O_{\beta}$ .

(b) *Pullman and Pullman's results.* Using a calculation method analogous to Grabe's, they studied carboxyl phosphate, ADP, ATP, phosphoenol pyruvate (PEP) and guanidine phosphate.

They suppose that the energy of the rich bonds is the sum of the following contributions: (1) the fundamental contribution, that is, the energy liberated in the hydrolysis of low energy phosphates ( $\sim 3$  kcal/mole), (2) the energy of electrostatic repulsion due to formal charges analogous to those found in XXXIV, XXXV, and XXXVI (1.4 kcal/mole for ADP and 2 kcal/mole for ATP), and (3) the difference in energy between the delocalized bonds in the energy-rich phosphates and those in the constituent fragments. For example, in the case of ADP

$$\begin{aligned} -\Delta E_{\pi} &= E_{\pi}(CH_2-O) + 2E_{\pi}(PO_4^{3-}) - E_{\pi}(ADP) \\ &= 0.137\beta + 2 \times 1.185\beta - 2.412\beta = 0.095\beta \end{aligned}$$

The Pullmans adopt the value  $\beta = 40$  kcal/mole, and this difference comes to 4 kcal/mole, or 2 kcal/mole for each phosphate group. Electronic charges calculated by these authors differ quantitatively but not qualitatively from those of Grabe. They conclude that the energy-rich phosphates release some 4 kcal/mole more energy on hydrolysis than the low energy phosphates.

(c) *Results of Fukui, Morokuma and Nagata.* Using the Pauling-Wheland method without overlap, they studied ADP, ATP, PEP and acetyl phosphate (AcP). For comparison they considered the low-energy compounds adenosine monophosphate (AMP) and glycerol-1-phosphate (GLP). They carried out calculations for various values of  $\delta_p$  (Eq. (39)).

From the energy point of view, they calculate only the difference of the  $\pi$ -electron energies,  $\Delta E_{\pi}$ , between the products of hydrolysis

and the original molecule. They find  $\Delta E_{\pi}$  to be between 2.5 and 3 kcal/mole ( $\beta = 20$  kcal/mole) greater in the high-energy phosphates than in the low-energy ones. This, it will be noticed, is larger than that calculated by Pullman and Pullman as contribution (3). This is not surprising since the quantity defined by the Japanese workers corresponds to the difference in energy between the various phosphates, while that defined by the French authors refers to the constituent groups of the phosphates.

Supposing that the hydrolysis begins with a nucleophilic attack on the phosphorus atom, they considered the ease of hydrolysis of the different phosphates calculating the superdelocalizability of the phosphorus atom,  $S_P^{(N)}$ . They came to the conclusion that although there are differences between values of this index from the high- and low-energy phosphates, it should not have biochemical consequences. To consider the hydrolysis as beginning with the attack of a proton or other electrophilic reagent on the bridge oxygen, they calculated the superdelocalizability of the oxygen atom, but these results do not explain the singular behavior of ATP.

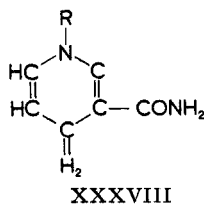
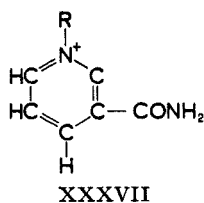
As the conclusion of their studies, the Japanese authors suggest that an interpretation of the exceptional behavior of the energy-rich phosphates should include the remainder of the adenine part as well as the polyphosphate part. These are joined by the saturated ribose group and interaction is possible either directly or by way of a metal cation. In addition, the method of calculation should also be refined to take into account the electron interaction. The effect of metal cations is considered by Goudot.<sup>75</sup>

## (2) *Electronic Structure of the Coenzymes DPN and FAD*

Oxidative processes in the living cell require the presence of carriers in the enzymatic chain to transfer electrons (hydrogen) from the substrate to oxygen, as was indicated in Section III. These electron carriers, called respiratory coenzymes, are reduced by the nearest neighbor on the substrate side and oxidized by the nearest neighbor on the oxygen side. Thus they alternate between oxidized and reduced states.

In this section we will analyze the electronic structures of di-phosphorpyridine nucleotide (DPN), which belongs to the group of pyridine nucleotide enzymes, and that of flavine adenine dinucleotide (FAD), of the flavoprotein group. The theoretical study of these

molecules was carried out by Grabe,<sup>41f</sup> who calculated electronic structures of the oxidized and reduced forms of both molecules, DPN<sup>+</sup> (XXXVII), DPNH (XXXVIII), FAD, and FADH<sub>2</sub>. In addition, Pullman and Pullman<sup>98</sup> have studied the molecules of DPN<sup>+</sup> and the flavine mononucleotide (FMN) which has the same flavine group as FAD.



Since these are extremely large molecules, a theoretical treatment would be practically impossible without drastic approximations. Thus, only that part of the molecule which changes with oxidation and reduction is considered, i.e. the pyridinic ring in DPN and the isoalloxazine ring in FAD.

Grabe used the LCAO-MO-AP-SCF method (AP, antisymmetrized products of MO's) in the Pariser and Parr approximation without configuration interaction. To start the interaction process of this method, she first applied the method of Pauling-Wheland.

The  $\pi$ -electronic system for the following molecules is:

DPN <sup>+</sup>	6 electrons
DPNH	8 „
FAD	10 „
FADH <sub>2</sub>	12 „

and for the radicals:

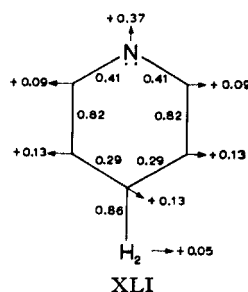
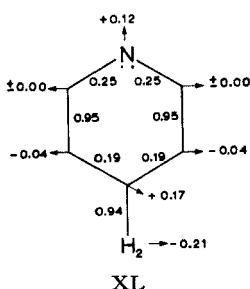
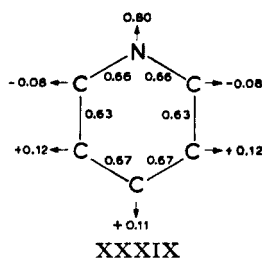
DPNH <sup>+</sup>	7 electrons
FAD <sup>-</sup>	11 „

Because of the careful selection of the parameters, the molecular integrals evaluated, and the method of calculation followed, these biomolecules are perhaps the best studied so far from a theoretical point of view.

Pullman and Pullman used the Pauling-Wheland method with parameters also judiciously chosen. The calculations are different in

that these workers considered greater number of electrons: ten for  $\text{DPN}^+$ , twelve for  $\text{DPNH}$ , and twenty-two for  $\text{FMN}$ .

$\pi$ -electron charge and bond-order distributions calculated by Grabe<sup>41c</sup> are listed below for  $\text{DPN}^+$  (XXXIX),  $\text{DPNH}$  (XL) and



for the radical  $\text{DPNH}^+$  (XLI). Energies (in atomic units) of the h.o. MO and l.v. MO of these molecules are indicated in Table V.

TABLE V. Respiratory Coenzymes: Energies of the h.o. MO and l.v. MO in Atomic Units

Molecule	h.o. MO	l.v. MO
$\text{DPN}^+$	-0.694	-0.265
$\text{DPNH}$	-0.414	-0.006
FAD	-0.449	-0.088
$\text{FADH}_2$	-0.390	-0.021

Analysis of the  $\pi$ -electron charge distributions of the systems

considered shows that the formal positive charge on the N atom is much greater in  $\text{DPN}^+$  than in  $\text{DPNH}$  (XL), with an intermediate value in  $\text{DPNH}^+$  (XLI).

The results of Table V are very illuminating with respect to the electron donor-acceptor properties of these compounds. It is observed that in the pair  $\text{DPN}^+ - \text{DPNH}$ ,  $\text{DPN}^+$  should be a good electron acceptor, that is easily reduced, while  $\text{DPNH}$  should be a good electron donor, easily oxidized. Analogous conclusions follow for  $\text{FAD} - \text{FADH}_2$ . As is observed, these theoretical predictions are in total agreement with experiment. The values obtained by Pullman and Pullman for the orbital energies of  $\text{DPNH}$ ,  $\text{FAD}$ , and  $\text{FADH}_2$  agree very well with those of Grabe; on the other hand, there is a big difference for  $\text{DPN}^+$ . Grabe supposes that this is due to the difficulty of choosing a parameter for the  $\text{N}^+$  of  $\text{DPN}^+$ .

Since the values calculated for the energy difference ( $W_1 - W_0$ ) [Eq. (61)] in the system  $\text{DPNH} + \text{FAD}$  are similar to that calculated by Mulliken for the system  $\text{C}_6\text{H}_6 + \text{I}_2$ , Grabe supposes that a charge transfer complex is formed. This supports her hypothesis about the formation of the high-energy phosphate bond due to oxidation taking place in the  $\text{DPN} - \text{FAD}$  part of the respiratory chain.

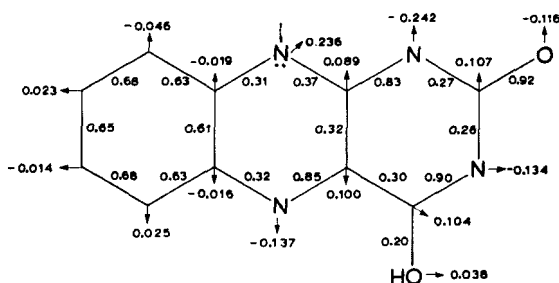
Until now we have not discussed the results calculated for the alloxazine ring of  $\text{FAD}$ . Grabe has recently carried out new calculations,<sup>42</sup> extending them and revising the choice of parameters. The recent work treats the oxidized form of isoalloxazine, comparing the enol and keto forms in energy and electronic distribution, investigating the effect of differing sets of parameters on  $\pi$  charges and orbital energies. All  $\pi$  electrons of the isoalloxazine ring were considered explicitly, including the lone pairs. From these new calculations Grabe<sup>42</sup> concludes that flavine is present in the enol form when it is united to a protein, for this is more stable. Consequently, she calculated the electronic structure of the enol form.  $\pi$ -charge distributions and bond orders calculated for this compound are indicated below (XLII).\*

Finally, we indicate that Pullman and Pullman<sup>98</sup> have investigated the chemical reactivity statically and dynamically for the

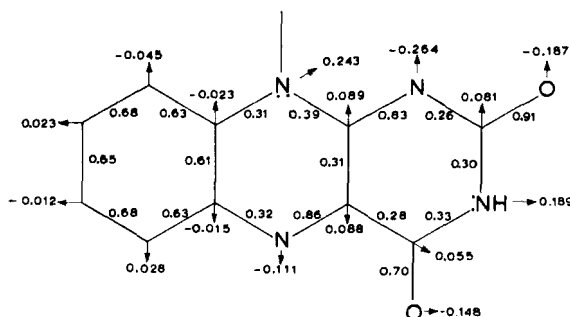
\* After this article was written we were informed by Miss Grabe that according to experiments the keto form of isoalloxazine is more stable than the enol form in the oxidized state. The molecular diagram calculated (with the same parameter values as for the enol form) is indicated in XLIIa.



molecules  $\text{DPN}^+$ , FMN,  $\text{FMH}_2$ , and some free radicals of these compounds.



XLII



XLIIa

### (3) *Electronic Structure of the Transelectronases (Cytochromes)*

Transelectronases or cytochromes are hemoproteins which, as indicated in Section III, act as agents of electron transfer, giving rise to the oxidation of nutrients by a series of carefully controlled steps leading finally to the storing of chemical energy in the form of ATP and the production of carbon dioxide and water as degradation products. In essence this is a chain of oxi-reductions. For this to occur, the carriers in the chain have to be substances easily oxidized and reduced. This fundamental role (aside from other highly specific functions) is played by the cytochromes whose active group, heme, is attached to a protein which permits controlled oxidation of the iron atom.

The main cytochrome chain includes the intermediates *c*, *b*, *a*, and

*a*<sub>3</sub>. Only *c* is extracted from tissues and has been obtained in crystallized form. Its porphyrin belongs to type IX. Saturated groups, each containing an atom of sulfur, have replaced in cytochrome *c* the (unsaturated) vinyl groups of the protoporphyrin, IX, as peripheral ring substituents. The proteins are bonded to the porphyrin ring of cytochrome *c* by way of two lateral chains,  $-(CH_2)_2-COOH$ , by the two sulfur atoms of the other chains, and above and below the central cation (Fe). Cytochrome *b* conserves the lateral vinyl groups while *a* has a vinyl and a formyl. The unsaturated lateral groups of these cytochromes conjugate directly with the porphyrin ring.

Recently Pullman, Spanjard, and Berthier<sup>105</sup> have calculated the  $\pi$ -electron charge distributions semi-empirically.

The ferro-porphyrin complexes are classified in two groups:

A. Ionic (Pauling's nomenclature) or "high spin" complexes (Griffith and Orgel<sup>43</sup>) in which the iron has a large number of unpaired electrons ( $Fe^{2+}$ , 4 $e$ ;  $Fe^{3+}$ , 5 $e$ ). The best-known examples are hemoglobin and myoglobin.

B. Covalent or "low spin" complexes in which one (ferricytochrome) or no electrons (oxyhemoglobin, ferrocytochrome *c*) are unpaired.

The details of the calculations are to be found in the original paper. We will specify only the electronic characteristics of the complexes.

$\pi$ -Electronic system:

porphyrin—26 electrons, 24 MO's

ionic porphyrins—26 electrons, 25 MO's

covalent ferroporphyrin—30 electrons, 27 MO's

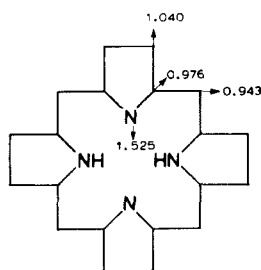
covalent ferriporphyrin—29 electrons, 25 MO's

$\sigma$ -Electronic system (corresponding to the interaction between the Fe cation and the 4 central nitrogens of the porphyrin ring):

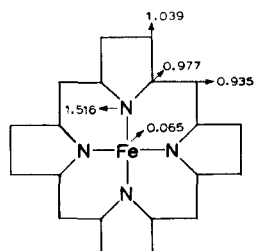
ionic porphyrins—8 electrons, 7 MO's

covalent porphyrins—8 electrons, 9 MO's

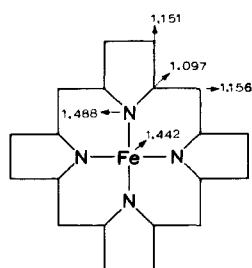
In the calculations, only the porphyrin-cation interactions were considered; interaction between the cation and the protein groups was neglected. The  $\pi$ -electron charge distributions are indicated for porphyrin (XLIII), ionic porphyrin (XLIV), covalent ferroporphyrin (XLV), and covalent ferriporphyrin (XLVI).<sup>105</sup>  $\sigma$ -electron



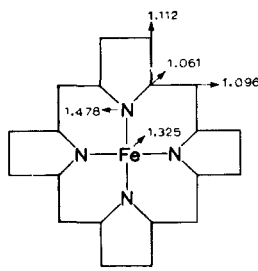
XLIII



XLIV



XLV



XLVI

charges are found in the original papers. Numerical values of the h.o. MO and l.v. MO are found in Table VI. While these are for cytochrome *c*, they give a general idea of the distribution of the MO's in the rest of the cytochromes.

TABLE VI. Porphyrins: Energies of the h.o. MO and l.v. MO in Units of  $\beta$

Porphyrins	h.o. MO	l.v. MO
Porphyrin	$0.309 \pi$	$-0.252 \pi$
Ionic porphyrins	$0.331 \pi$	$-0.252 \pi$
Ferroporphyrin covalent	$-0.085 \pi^a$	$-0.645 \sigma$
Ferriporphyrin covalent	$-0.075 \pi^b$	$-0.682 \sigma$

<sup>a</sup> Doubly degenerate MO occupied by 4 electrons.

<sup>b</sup> Doubly degenerate MO occupied by 3 electrons.

The different electron donor-acceptor behavior of the porphyrin ionic complexes and protoporphyrin from that of the covalent

complexes is shown by the table. We consider each compound separately.

The protoporphyrin IX should be a rather good electron donor and acceptor. The same behavior is to be expected of the ionic porphyrins. Naturally this refers to the  $\pi$  electrons of the complexes. But the  $3d$  electrons of the iron atom, which are not used in bonding, will be those involved in cellular oxi-reduction where these porphyrins enter.

The behavior of the covalent porphyrins is completely different, for the  $\pi$  MO's contain  $4p_z$  electrons from the porphyrin ring and  $3d$  Fe electrons. Consider first ferroporphyrin. Its h.o. MO is doubly degenerate and has a negative value which we found corresponded to an antibonding orbital. This is an unstable electron configuration and consequently the compound should be an energetic electron donor. At the same time, it should be a poor acceptor. Pullman, Spanjard, and Berthier suppose that the oxidation of these complexes should imply the elimination of an electron from the  $\pi$  h.o. MO.

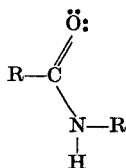
The situation is rather different in the covalent ferroporphyrins even though this is not apparent at first glance. Its h.o. MO is also doubly degenerate, but contains only three electrons. Thus one of the MO's contains only one electron and can accept another. In consequence, we can consider that this is the l.v. MO and the complex should be an energetic electron acceptor. The possibility of being a good electron donor can be excluded because the loss of another electron would lead to a very unstable configuration.

These considerations explain why the cytochromes act as electron carriers. In the case of the ferrocytochromes, which have an antibonding h.o. MO, we expect excellent electron donors while the ferricytochromes with a semi-occupied l.v. MO in the oxidized form should be excellent electron acceptors.

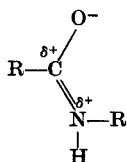
#### (4) *The Pullmans' Theory of Enzymatic Hydrolysis*

Hydrolases are enzymes which catalyze hydrolytic reactions, reactions in which the elements of water are added across the broken bond. They fall into groups according to the type of bond hydrolyzed:<sup>8</sup> esterases (carboxylesterases, thiolesterases, sulphatases, phosphatases, anhydrophosphatases), glycosidases, peptidases, aminidases and hydrolytic deaminases.

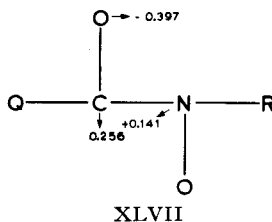
Except for the glycosidases which break  $\sigma$  bonds, the hydrolases rupture bonds with both  $\sigma$  and  $\pi$  character, that is, bonds with electron delocalization. They belong to the group which Pullman and Pullman<sup>100</sup> call "dipositive bond", or bonds between atoms with positive formal charges. (The concept tripositive bond applied to the energy-rich bonds by Fischer-Hjalmars<sup>75</sup> comes from this.) For clarification, let us select the example given by the French authors, the peptide link:



Since in this case the inductive and mesomeric effects act in the same sense, the electronic structure can be represented by:



where we see that the atoms C and N have formal positive charges. The MO method permits quantitative calculation of the  $\pi$ -electron charges in the peptide linkage. This constitutes a system of four  $\pi$  electrons (1 each from C and O, 2 from N) and three orbitals. In XLVII we give the values obtained by Pullman and Pullman.<sup>98</sup>



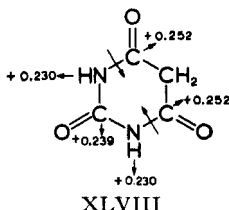
Goudot<sup>75</sup> also studied the peptide linkage by the MO method. The values calculated by this author for the charges are rather different from those of Pullman and Pullman.

The theory of enzymatic hydrolysis developed by Pullman and Pullman is based on three hypotheses:

*First hypothesis.* Except where glycosidases act, in all biological substrates where enzymatic hydrolysis is observed the bond broken is dipositive.

*Second hypothesis.* The greater the electron deficiency of the dipositive bond, the more readily will it be hydrolyzed. One concludes from this proposition that the introduction of substituents which increase the electron deficit (in certain phenolic esters groups in *ortho*- and *para*-) facilitates hydrolysis, while those of contrary effect reduce it.

*Third hypothesis.* When a molecule contains several dipositive bonds (excluding steric hindrance or specificity) enzymatic hydrolysis will occur in the most dipositive. The example of barbituric acid (XLVIII), calculated by the Pullmans,<sup>100</sup> confirms this. The arrows perpendicular to the bonds indicate the points of rupture.



Until now nothing has been said about the mechanism of enzymatic action. Recalling the formal charges of the extremes of the dipositive bond, the Pullmans suggested that a possible one consists of attack by a nucleophilic center (negative) of the enzyme on one or both positive ends of the bond which is broken. In support of this they cite the action of acetylcholinesterase on acetylcholine. Another possible explanation of this mechanism, also suggested by the Pullmans, is that the enzyme tends to increase the formal positive charges, augmenting the electron deficiency of the dipositive bond. This is closely related to Rowin's theory, according to which the enzyme's action is to "originate" a dipositive charge in the bond which breaks on hydrolysis.

Goudot<sup>75</sup> has studied the breaking of the peptide link in the presence of divalent metallic cations, such as  $Mg^{2+}$ ,  $Mn^{2+}$ ,  $Co^{2+}$ , etc. Calculation of the charges on the atoms of N, O, and C of the peptide

bond of the complex enzyme-metal-substrate showed that the carbon atom is depleted (that is, increases its positive formal charge) to the benefit of the atom of oxygen and the metal ion, favoring the rupture of the C—N bond.

#### (5) *Other Biochemical Processes*

To complete the applications of quantum mechanical methods to the study of biochemical processes we indicate that, in addition to those cited previously, published studies include among others: electronic aspects of the reactions of pyridoxal phosphate enzymes,<sup>94</sup> electronic structure and biochemical function of folic acid coenzymes,<sup>93</sup> the mechanism of action of xanthine oxidase,<sup>95</sup> metabolic breakdown of hemoglobin,<sup>99</sup> electronic structure and nicotine-like stimulant activity in choline phenyl ethers,<sup>37a</sup> electronic structure and biochemical activities in diethyl phenyl phosphates.<sup>37b</sup>

### IV. CONCLUSIONS

In Section III we have given an account of the results obtained by means of the application of the MO theory to the study of electronic structure of the most important biomolecules, and those which occur in some fundamental biochemical processes. We have asked ourselves, consequently, what value will these theoretical results have in the interpretation of the biological processes.

The goal of the application of calculations of quantum mechanics in biochemistry is to try to establish quantitative relations between certain electronic and energetic molecular indices and the biological activity of molecules. This will not only permit researchers to make predictions about the behavior of biomolecules, but what is yet more important, it will provide a theoretical criterion which both unifies the obtained results and offers new possibilities of research.

Conventional physical and chemical activities frequently permit the establishment of well-defined comparisons between theory and experimentation. Biological activity, nevertheless, does not belong to this group, since it is the result of the coming together of diverse and complex factors and it is not easy to know when we find the totality of an activity in a biological system.

The correct theoretical study of a biochemical process requires careful consideration of the following two aspects. In the first place, it is necessary to know as well as possible the biochemical mechanisms of the processes under study, since the procedures that we apply in the calculations and the quantities that we try to determine depend on these mechanisms. Unfortunately, many of these mechanisms are partially or totally unknown. On the other hand, it is assumed that biochemical reactions follow the mechanism of the Eyring and Polanyi theory, which is not evident, since as we have seen many of these reactions are enzymatic and involve only a limited number of very large molecules.

The other aspect is properly related to the methods of quantum mechanics. In Section II, we have carefully studied the approximations introduced in the MO theory: the separation of  $\sigma$  and  $\pi$  electrons, devoting attention to the electronic  $\pi$  cloud. Besides, in the most simple methods electronic interaction is neglected and we assume as known the effective potential which acts over these electrons ( $\pi$ ). Also within the mathematical apparatus of the theory it is possible to introduce more approximations, such as the neglect of overlapping. On the other hand, in the theoretical study of chemical reactivity, a great number of factors are frequently neglected, which many times are later seen to be important.

Consequently, when we compare the experimental results with the theoretical we are not often able to establish whether the differences are due to faulty assumptions in the original idea of the theory or to the use of poor approximations.

At present the state of this problem seems to be summed up in the following considerations. Instead of investigating whether the calculated values for the electronic structures of biomolecules are in themselves correct (which is possibly not true at all), it is better to consider series of similar molecules and make comparisons between electronic indices and see how a wise choice of parameters and the use of more refined calculating methods influence the obtained results.\* In this respect we call attention to the latest calculations of the Pullmans and Miss Grabe.

\* These opinions agree with the ones expressed recently by J. Ladik and K. Appel (*Tech. Note No. 79*, Uppsala Quantum Chemistry Group, Uppsala, Sweden 1962) in the "Investigation of the  $\pi$  electron system of uracil with different semi-empirical methods".



In conclusion, the time is here to thoroughly investigate the different calculations used and to carefully judge the experimental data of the processes studied for the purpose of including them in the laying-out of the quantum mechanical problem. It is evident that we have already advanced a great step forward in the application of quantum mechanics to biochemistry, and as Coulson<sup>11</sup> recently brought to mind when referring to this question: "*Ce n'est que le premier pas qui coûte.*"

## V. ACKNOWLEDGEMENTS

I express my sincere appreciation to Dr. L. C. Cusachs for his fine translation and his criticism of Section II. I also wish to thank Professor C. A. Coulson, Professor R. Daudel and to Mr. F. Peradejordi for their valuable suggestions, and Dr. B. Grabe for allowing me to use her results on isoalloxazine before its publication. I also express my gratitude to Professor J. García-Blanco and Professor J. Viña for their discussions on the biochemical problems.

## References

1. Adams, W. H., *J. Chem. Phys.* **34**, 89 (1961).
2. Adams, O. W., and Lykos, R. G., *J. Chem. Phys.* **34**, 1444 (1961); Hoyland, J. R., and Goodman, L., *ibid.* **34**, 1446 (1961).
3. Albert, A., *Quart. Rev. London* **6**, 197 (1952).
4. Allen, L. C., and Karo, A. M., *Rev. Mod. Phys.* **32**, 275 (1960).
5. Amos, A. T., *Mol. Phys.* **5**, 91 (1962).
6. Baudet, J., Berthier, G., and Pullman, B., *Compt. Rend.* **254**, 762 (1962).
7. Boys, S. F., *Proc. Roy. Soc. (London)* **A200**, 542 (1950); **A201**, 125 (1950).
8. Cantarow, A., and Schepartz, B., *Biochemistry*, 3rd Ed., W. B. Saunders, Philadelphia, 1962.
9. Chalvet, O., Daudel, R., and Peradejordi, F., *Compt. Rend.* **254**, 1283 (1962).
10. Coulson, C. A., *Proc. Roy. Soc. (London)* **A169**, 413 (1939).
11. Coulson, C. A., *Rev. Mod. Phys.* **32**, 170 (1960).
12. Coulson, C. A., *Valence*, 2nd Ed., Oxford University Press, London, 1961.
13. Coulson, C. A., and Rushbrooke, G. S., *Proc. Cambridge Phil. Soc.* **36**, 193 (1940).
14. Coulson, C. A., and Schaad, L. J., *J. Chem. Phys.* **35**, 294 (1961).
15. Coulson, C. A., and Lewis, J. T., in R. Bates, *Quantum Theory*, Academic Press, New York, 1962, Vol. II.
16. Craig, D. P., *Proc. Roy. Soc. (London)* **A200**, 474 (1950).

17. Cusachs, L. C., private communication.
18. Daudel, R., *Structure Électronique des Molécules*, Gauthier-Villars, Paris, 1962.
19. Daudel, R., Lefebvre, R., and Moser, C., *Quantum Chemistry*, Interscience Publishers, New York, 1959.
20. Dekker, C. A., *Ann. Rev. Biochem.* **29**, 453 (1960).
21. Dewar, M. J. S., and Scheimising, H. N., *Tetrahedron* **5**, 166 (1959); **11**, 96 (1960).
22. Ducanson, W. E., and Coulson, C. A., *Proc. Roy. Soc. Edinburgh* **67**, 37 (1944).
23. Duchesne, J., *Arch. Sci. (Geneva)* **10**, 257 (1957).
24. Fernández-Alonso, J. I., Mira, J., and Alcañiz, *Anales Fis. Quim. (Madrid)* **53B**, 101 (1957).
25. Fernández-Alonso, J. I., and Domingo, R., *Compt. Rend.* **250**, 2371 (1960).
26. Fernández-Alonso, J. I., and Domingo, R., *Compt. Rend.* **250**, 2576 (1960).
27. Fernández-Alonso, J. I., and Domingo, R., *Anales Fis. Quim. (Madrid)* **56B**, 687 (1960).
28. Fernández-Alonso, J. I., and Domingo, R., *Anales Fis. Quim. (Madrid)* **56B**, 757 (1960).
29. Fernández-Alonso, J. I., and Domingo, R., *Anales Fis. Quim. (Madrid)* **56B**, 759 (1960).
30. Fernández-Alonso, J. I., and Domingo, R., *Anales Fis. Quim. (Madrid)* **56B**, 1047 (1960).
31. Fernández-Alonso, J. I., and Domingo, R., communication to the International Biophysics Congress, Stockholm, 1961.
32. Fernández-Alonso, J. I., and Domingo, R., unpublished results.
33. Fock, V., *Z. Physik* **61**, 126 (1930).
34. Fueno, T., *Ann. Rev. Phys. Chem.* **18**, 303 (1961).
35. Fujumori, E., *Proc. Natl. Acad. Sci. U.S.* **95**, 133 (1959).
36. Fukui, K., Yonezawa, T., and Schingu, H., *J. Chem. Phys.* **20**, 722 (1952); Fukui, K., Yonezawa, T., Nagata, C., and Schingu, H., *ibid.* **22**, 1433 (1954).
37. (a) Fukui, K., Nagata, C., and Imamura, A., *Science* **131**, 87 (1960); (b) Fukui, K., Morokuma, K., Nagata, C., and Imamura, A., *Bull. Chem. Soc. Japan* **34**, 1224 (1961).
38. Fukui, K., Morokuma, K., and Nagata, C., *Bull. Chem. Soc. Japan* **33**, 1214 (1960).
39. Fukui, K., Nagata, C., Yonezawa, T., Morokuma, K., and Imamura, A., *Gann* **52**, 1 (1961).
40. Goepfert-Mayer, M., and Sklar, S. L., *J. Chem. Phys.* **6**, 645 (1938).
41. Grabe, B. (a) *Arkiv Kemi* **9**, 29 (1955); (b) *Exptl. Cell Res.* **9**, 447 (1956); (c) *Arkiv Fysik* **15**, 207 (1959); (d) *Exptl. Cell Res.* **13**, 588 (1957); (e) *Biochim. Biophys. Acta* **30**, 560 (1958); (f) *Arkiv Fysik* **17**, 97 (1960); (g) *Arkiv Kemi* **15**, 393 (1960).
42. Grabe, B., private communication.

43. Griffith, J. S., and Orgel, L. E., *Quart. Rev. London* **11**, 381 (1957).
44. Guillemin, V., and Zener, C., *Z. Physik* **61**, 199 (1930); Zener, C., *Phys. Rev.* **36**, 51 (1930).
45. Haddow, A., in *Ciba Found. Symp., Carcinogenesis: Mechanisms Action*, 1959.
46. Harbury, H. A., and Foley, K. A., *Proc. Natl. Acad. Sci. U.S.* **44**, 6636 (1958).
47. Hartree, D. R., *Proc. Cambridge Phil. Soc.* **24**, 89 (1928); *Rep. Progr. Phys.* **11**, 113 (1946-7).
48. Hill, T. L., and Morales, M. F., *J. Am. Chem. Soc.* **73**, 1656 (1951).
49. Hückel, E., *Z. Physik* **70**, 204 (1931).
50. Hückel, E., *Z. Physik* **76**, 628 (1932).
51. Isenberg, I., and Szent-Györgyi, A., *Proc. Natl. Acad. Sci. U.S.* **44**, 857 (1958).
52. James, H. M., and Coolidge, A. S., *J. Chem. Phys.* **1**, 825 (1933).
53. Julg, A., *J. Chim. Phys.* **57**, 196 (1960); Julg, A., Francois, P., and Mourre, R., *ibid.* **59**, 363 (1962).
54. Kalckar, H., *Chem. Rev.* **28**, 71 (1941).
55. Kasha, M., *J. Chim. Phys.* **58**, 914 (1961).
56. Kasha, M., *J. Chim. Phys.* **58**, 916 (1961).
57. Kauzman, W., *Quantum Chemistry*, Academic Press, New York, 1957.
58. Kolos, W., and Roothaan, C. C. J., *Rev. Mod. Phys.* **32**, 219 (1960).
59. Kon, H., *Bull. Chem. Soc. Japan* **27**, 265 (1954); **28**, 275 (1955).
60. Koopmans, T., *Physica* **1**, 104 (1934).
61. Lefebvre, R., *Thèses, Revue d'Optique*, Paris, 1959.
62. Lehninger, A. L., *Rev. Mod. Phys.* **31**, 136 (1959).
63. Linnett, J. W., *Wave Mechanics and Valency*, London, 1960.
64. Linnett, J. W., and Poe, A. J., *Trans. Faraday Soc.* **47**, 1033 (1951).
65. Lipman, F., *Advan. Enzym.* **1**, 99 (1941).
66. Longuet-Higgins, H. C., *Advan. Chem. Phys.* **1**, 239 (1958).
67. Longuet-Higgins, H. C., *Biophys. J.* **2**, 207 (1962).
68. Löwdin, P. O., *Rev. Mod. Phys.* **32**, 328 (1960).
69. Löwdin, P. O., *Ann. Rev. Phys. Chem.* **11**, 107 (1960).
70. Löwdin, P. O., *J. Appl. Phys. Suppl.* **33**, 251 (1962).
71. Lykos, P. G., *J. Chem. Phys.* **35**, 1249 (1961).
72. Mason, S. F., in *Ciba Found. Symp., Chem. Biol. Purines*, 1957.
73. McGlynn, S. P., *Chem. Rev.* **58**, 1113 (1958).
74. McWeany, R., *Proc. Roy. Soc. (London)* **A223**, 306 (1954).
75. *Mecanique Ondulatoire et Biologie Moleculaire*, Revue D'Optique, Paris, 1961.
76. Moffit, W. E., *Proc. Roy. Soc. (London)* **A210** 245 (1951).
77. Mulliken, R. S., *J. Chim. Phys.* **46**, 497, 675 (1949).
78. Mulliken, R. S., *J. Am. Chem. Soc.* **72**, 600 (1950); *J. Phys. Chem.* **56**, 801 (1952).
79. Mulliken, R. S., *Record Chem. Progr.* **13**, 67 (1952).
80. Mulliken, R. S., *J. Chem. Phys.* **17**, 1248 (1955).
81. Mulliken, R. S., *Rev. Mod. Phys.* **32**, 232 (1960).

82. Mulliken, R. S., Rieke, C., and Brown, W. G., *J. Am. Chem. Soc.* **23**, 41 (1941).
83. Murrell, J. N., (a) *J. Chem. Phys.* **32**, 767 (1960); (b) Guilbert, T. L., and Lykos, P. G., *ibid.* **34**, 2199 (1961); (c) Lykos, P. G., and Schmeising, H. V., *ibid.* **35**, 288 (1961).
84. Nakajima, T., and Pullman, A., *J. Chim. Phys.* **56**, 493 (1958).
85. Parks, J. M., and Parr, R. G., *J. Chem. Phys.* **32**, 1657 (1960).
86. Parr, R. G., *J. Chem. Phys.* **33**, 1184 (1960).
87. Parr, R. G., (a) *J. Chem. Phys.* **20**, 1499 (1952); (b) Pariser, R., and Parr, R. G., *ibid.* **21**, 466, 767 (1953); **23**, 711 (1955); (c) Pariser, R., *ibid.* **21**, 568 (1953); (d) Parr, R. G., *ibid.* **33**, 1184 (1960).
88. Parr, R. G., and Ellison, F. D., *Ann. Rev. Phys. Chem.* **6**, 171 (1955).
89. Pauling, L., *The Kekulé Symposium*, Butterworths, London, 1959.
90. Pauling, L., *The Nature of the Chemical Bond*, Cornell University Press, Ithaca, 1960.
91. Pauling, L., and Wilson, E. B., *Introduction to Quantum Mechanics*, McGraw-Hill, 1935.
92. Pauling, L., and Wheland, G. W., *J. Am. Chem. Soc.* **57**, 2086 (1935).
93. Perault, A., and Pullman, B., *Biochim. Biophys. Acta* **44**, 251 (1960); **52**, 266 (1961).
94. Perault, A., Pullman, B., and Valdemoro, C., *Biochim. Biophys. Acta* **46**, 555 (1961).
95. Perault, A., Valdemoro, C., and Pullman, B., *J. Theoret. Biol.* **2**, 180 (1961).
96. Pople, J. A., *Trans. Faraday Soc.* **49**, 1375 (1953).
97. Pullman, B., in *Application à la Biochimie et à la Chimie Structurale de la Spectroscopie des Radiofréquences*, Acad. Roy. Belgique, Bruxelles, **33**, 174 (1961).
98. Pullman, B., and Pullman, A., *Proc. Natl. Acad. Sci. U.S.* **45**, 136 (1959).
99. Pullman, B., and Perault, A., *Proc. Natl. Acad. Sci. U.S.* **45**, 1476 (1959).
100. Pullman, A., and Pullman, B., *Proc. Natl. Acad. Sci. U.S.* **45**, 1572 (1959).
101. Pullman, B., and Pullman, A., *Compt. Rend.* **249**, 1827 (1959); *Radiation Search Suppl.* **2**, 161 (1960).
102. Pullman, B., and Pullman, A., *Rev. Mod. Phys.* **32**, 428 (1960).
103. Pullman, B., and Pullman, A., *Results of Quantum Biochemical Calculations of the Electronic Structures of Biochemicals*, Institut de Biologie Physico Chimique, Paris, Vol. I, 1960, and Vol. II, 1961.
104. Pullman, A., and Pullman, B., *J. Chim. Phys.* **58**, 904 (1961).
105. Pullman, B., Spanjard, C., and Berthier, G., *Proc. Natl. Acad. Sci. U.S.* **46**, 1011 (1960); Spanjard, C., and Berthier, G., *J. Chim. Phys.* **58**, 169 (1961).
106. Ransil, J., *Rev. Mod. Phys.* **32**, 245 (1960); Clementi, E., *J. Chem. Phys.* **34**, 1468 (1961); **36**, 750 (1962); Clementi, E., and McLearn, A. D., *ibid.* **36**, 563, 745 (1962).
107. Roberts, J. D., *Molecular Orbital Calculations*, W. A. Benjamin, New York, 1961.
108. Roothaan, C. C. J., *Rev. Mod. Phys.* **23**, 69 (1951).

109. Ruedenberg, K., *J. Chem. Phys.* **34**, (a) 1681, (b) 1878, (c) 1884, (d) 1892, (e) 1897, (f) 1907 (1961).
110. Scherr, C. W., *J. Chem. Phys.* **23**, 569 (1955).
111. Schmitt, F. C., *Rev. Mod. Phys.* **31**, 5 (1959).
112. Sinanoğlu, O., *J. Chem. Phys.* **34**, 1237 (1961).
113. Sinanoğlu, O., and Mortensen, E. M., *J. Chem. Phys.* **34**, 1078 (1961).
114. Slater, J. C., *Phys. Rev.* **34**, 1293 (1929).
115. Slater, J. C., *Phys. Rev.* **36**, 57 (1930).
116. Slater, J. C., *Quantum Theory of Atomic Structure*, McGraw-Hill, Vol. II, New York, 1961.
117. Skinner, H. A., and Pritchard, M. O., *Trans. Faraday Soc.* **49**, 1254 (1953).
118. Streitwieser, A., *Conference on Hyperconjugation*, Pergamon Press, London, 1959.
119. Streitwieser, A., *Molecular Orbital Theory for Organic Chemistry*, John Wiley and Sons, New York, 1961.
120. Szent-Györgyi, A., *Discussions Faraday Soc.* **27**, 111 (1959).
121. Veillard, A., and Pullman, B., *Compt. Rend.* **253**, 2277 (1961).
122. Veillard, A., and Pullman, B., *Compt. Rend.* **253**, 2418 (1961).
123. Veillard, A., Berthier, G., and Pullman, B., *Compt. Rend.* **252**, 2321 (1961).
124. Wheland, G. W., *J. Am. Chem. Soc.* **63**, 2025 (1941).

## 2

# QUANTUM MECHANICAL CONSIDERATIONS ON SOME PROPERTIES OF DNA

T. A. HOFFMANN, *Research Institute for Telecommunication,  
Budapest*, and J. LADIK, *Central Research Institute for  
Chemistry of the Hungarian Academy of Sciences, Budapest*

## CONTENTS

I. Introduction . . . . .	84
II. The General Plan of the Quantum Mechanical Treatment of the Electronic Structure of DNA . . . . .	86
III. The Electronic System of the Single Bases and Their Spectro- scopical Properties . . . . .	90
IV. The Problem of Mutation and the Tautomerism of the Single Bases . . . . .	103
V. The Electronic Structure of the Base Pairs . . . . .	108
VI. Interaction Between the Superimposed Bases; Spectroscopical Consequences . . . . .	116
VII. Genetical Considerations: the Coding Problem . . . . .	130
VIII. Calculation of the Band Structure of Polynucleotides in the Hückel Approximation . . . . .	136
IX. Considerations on the Band Structure of Real DNA and Its Conducting Properties . . . . .	142
X. Working Hypothesis for the Mechanism of DNA Duplication and Tumour Development . . . . .	148
XI. Acknowledgements . . . . .	155
References . . . . .	156

## I. INTRODUCTION

In the last few years the investigation of the properties and function of nucleic acids has become a central problem in molecular biology. On the basis of the large body of experimental material collected in this field it is generally accepted that deoxyribonucleic acid (DNA) is the carrier of genetic information. It seems very probable that through ribonucleic acid (RNA) DNA determines the sequence of amino acids in proteins and with this the secondary and tertiary structure of proteins. Since many of the different

proteins synthesized in the living cell are enzymes (catalysts) of different biochemical reactions, they determine the reactions possible in a cell. Thus in the last analysis DNA determines the structure and function of the whole cell.

It is the basic assumption of biochemical genetics that the genetic information is carried in DNA first of all by the sequence of the four different nucleotide bases: adenine (A), thymine (T), guanine (G) and cytosine (C). Any effect, therefore, able to cause a change in the sequence of these bases may change the whole cell. Further, it seems very probable that DNA plays a crucial role in the control of mitosis. In consequence the problems of spontaneous and radiation-, or chemically induced mutation, the very important problems of ageing and of cancer are intimately connected with the structure of DNA. Further, the question of genetic stability is primarily the problem of the stability of the base sequences against environmental effects and internal changes in DNA.

The chemical and stereochemical structure of DNA is well known today; in other words, the positions of the atomic nuclei in this macromolecule have been determined. Thus, using the Born-Oppenheimer approximation, according to which the motion of the nuclei and the electrons may be separated in a good approximation, it is possible to begin the quantum mechanical calculation of the electronic structure of DNA. In the last five years there have been performed some calculations on the electronic structure of the nucleotide bases and base pairs.<sup>39,40</sup> In this review we shall try to describe also the results of the first approximations which we have performed, taking into account the interaction between the bases in the same chain and treating the electronic structure of the whole macromolecule as a common one.

It seems probable that on the basis of the quantum mechanical calculations performed on the electronic structure of DNA it will be possible to understand better the different important biological problems mentioned above and to elucidate the finer details of the mechanisms of many biological processes which are associated with DNA.

On the other hand, measurements have been made in the last few years of such physical properties of DNA as ultraviolet absorption spectra, conductivity, ESR spectra, ferro-, and piezoelectricity, which can be interpreted only on the basis of the electronic structure

of the molecule. We shall try to give the interpretation of some of these properties in this chapter, but most of them can be obtained only after much more extensive calculations have been performed.

## II. THE GENERAL PLAN OF THE QUANTUM MECHANICAL TREATMENT OF THE ELECTRONIC STRUCTURE OF DNA

According to the Watson-Crick stereomodel,<sup>3,57</sup> valid for the *in vivo* stable B form of DNA, the turn of the helix including 10 nucleotides (Fig. 1) has a height of 33.6 Å. Since according to the

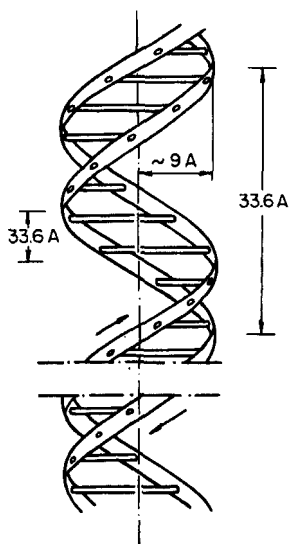


Fig. 1. Schematic representation of the double helix of DNA.

model all the planes of the nucleotide bases are perpendicular to the axis of the double helix, the distance between the planes of two superimposed bases belonging to the same chain is 3.36 Å and the adjacent bases are turned by  $36^\circ$  relative to each other in the plane perpendicular to the axis. Further, it was shown by Watson and Crick that the bases belonging to different polynucleotide chains of the double helix are joined together by hydrogen bonds in such a



way that A is always bound to T, and G always to C. The A-T, G-C base pairing relations are in good accordance with the results of the chemical analyses of the base compositions of different DNA molecules.

The X-ray investigations of the nucleotide bases: adenine, guanine, thymine and cytosine, have shown that these bases are planar and that their internuclear distances fall between the values characteristic for pure single and pure double bonds.<sup>50</sup> One has to assume on this basis that in these molecules delocalized  $\pi$ -electron systems are present, extending all over the rings. In consequence of the hydrogen bonds, the two bases of a base pair are in the same plane in a fixed position relative to each other. This makes it very

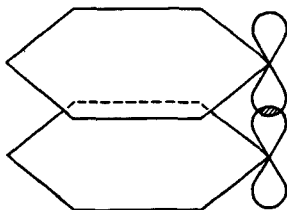


Fig. 2. Overlap of electron clouds of two atoms in superimposed rings.

probable that in the A-T, G-C base pairs the electron clouds of the single bases are in interaction through the hydrogen bonds and thus we have to take into account common delocalized  $\pi$ -electron systems for these base pairs.

On the other hand, there is also an interaction between the  $\pi$ -electron orbitals of the adjacent, superimposed bases belonging to the same chain (see Fig. 2).<sup>26</sup> This also means that two superimposed bases may be treated as common systems. In reality, however, we have to take into account not only interacting superimposed single bases, but interacting superimposed base pairs. This calculation, which requires much more numerical work, has not been performed until recently and therefore will not be treated at present in this chapter.

Considering that there is a  $\pi$ -electron interaction between all the adjacent bases of the macromolecule and knowing that the number of bases in a DNA molecule is of the order of magnitude of  $10^5$ , we

can investigate the delocalized  $\pi$ -electron system of the whole macromolecule with methods generally used in solid state physics. As a first step it is possible to calculate the electronic structure of an infinite single chain consisting of only one kind of base (homopoly-nucleotide). The second step will be the treatment of an infinite double helix, consisting of either the A-T, or the G-C base pair, but not a mixture of them.

With high-speed computers it will be possible later to make better approximations for the electronic structure of a real DNA double helix. For this purpose it is necessary to perform calculations first for infinite single chains consisting of two, three or all the four different nucleotides arranged in some predetermined sequences with periodicity. (This means that as a model for the calculation we have to use sequences, as for instance ATTG ATTG ATTG ATTG..., where we have a periodically repeated unit.) The calculations should then be extended to infinite double chains consisting of base pairs, but again with predetermined sequences with some periodicity.

It should be mentioned that for a sequence without any periodicity, which is most probably the case for a real DNA molecule, the simple methods of solid state theory cannot be applied and therefore the calculations cannot be performed at present. It seems, however, probable that with the aid of the results obtained for different complicated periodic model sequences it will be possible to get a rather good approximation of the electronic structure of a real DNA molecule.

All the different steps of approximation of the electronic structure of DNA mentioned above may be performed with the most simple form of the LCAO-MO method (the so-called Hückel approximation) and with other more refined methods. Up to the present we have performed all calculations only within the framework of the simple Hückel method with one exception: the electronic structure of a single uracil (U) molecule has been calculated in some higher approximations. We shall return to this calculation in the next section which deals with the electronic structure of the single bases.

For the sake of convenience we have summarized in Fig. 3 the different steps of the approximation of the electronic structure of DNA. In the further sections of this chapter we shall review the

results obtained in the steps (a), (b), (c) and (e) and at the same time try to interpret with their aid some physical and biological properties of DNA (Sections III–VIII).

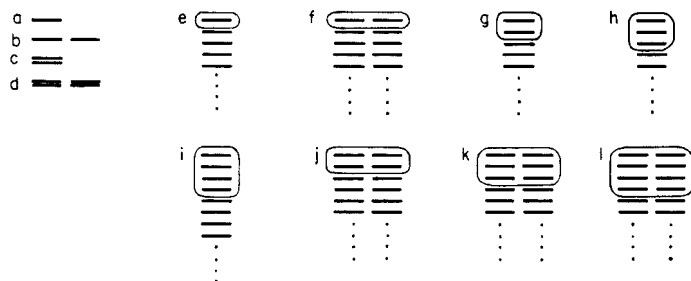


Fig. 3. The different steps for the approximation of the electronic structure of DNA. Each line in the figure indicates schematically a single base in side-view: (a) single base; (b) base pair; (c) two superimposed bases; (d) two superimposed base pairs; (e) infinite chain of the same nucleotide (the smallest periodically repeated unit is surrounded by a thin line); (f) infinite chain of the same base pair; (g) infinite chain of periodically repeated two different bases (e.g. ATATAT ...); (h) infinite chain of three different bases periodically repeated; (i) infinite chain of periodically repeated four different bases; (j) infinite chain of periodically repeated two different base pairs; (k) infinite chain of periodically repeated three different base pairs (e.g.  $\begin{pmatrix} \text{A G T A G T A G T} \dots \\ \text{T C A T C A T C A} \end{pmatrix}$ ); (l) infinite chain of periodically repeated four different base pairs.

In the final two sections we shall give a qualitative estimation for the electronic structure of a real DNA molecule (Section IX) and on its basis we present a working hypothesis for the correlation between the electronic structure of DNA and its duplication (Section X). In this section also we shall give some ideas on the possible connection between the problem of mitosis and of tumour development with the electronic structure of DNA. In connection with this last section we have to emphasize that it will contain, of course, only our personal points of view on these problems. We hope, however, that they will prove stimulating for further theoretical and experimental work in this very important, but rather complicated field.

### III. THE ELECTRONIC SYSTEM OF THE SINGLE BASES AND THEIR SPECTROSCOPICAL PROPERTIES

For the approximation of the delocalized  $\pi$ -electron system of A, T, G and C in their tautomeric form, which is stable *in vivo* (see Fig. 4), the LCAO-MO method has been used in the Hückel

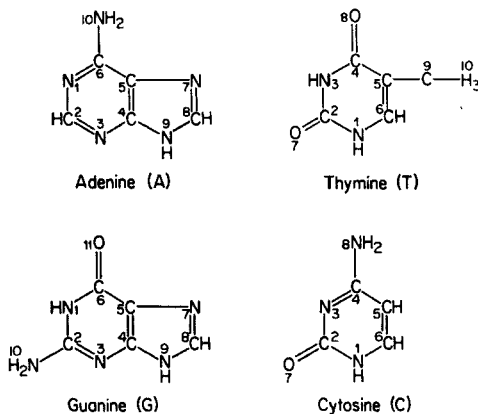


Fig. 4. The classical chemical formulae of the nucleotide bases in those tautomeric forms which are stable *in vivo*. The numbering of the atoms indicated here is used throughout the chapter.

approximation neglecting overlap. (For the detailed description of this method see the chapter by J. I. Fernández-Alonso: Electronic Structures in Quantum Biochemistry, in this volume.) We have determined the MO energies  $\epsilon_i$  and the coefficients  $c_{ik}$  of the different MO's of the nucleotide bases,

$$\Psi_i = \sum_{k=1}^n c_{ik} \psi_k \quad (1)$$

Here  $n$  denotes the number of atoms which give a  $\pi$ -type atomic orbital  $\psi_k$  to the delocalized  $\pi$ -electron system. In the calculation we have taken into account all the substituents which have a  $\pi$ -electron orbital and in the case of T also the hyperconjugation of the  $\text{CH}_3$  group. The set of  $\alpha_i$  and  $\beta_{ij}$  integrals given in Table I was used.

TABLE I. The Values of  $\alpha_i$  and  $\beta_{ij}$  Integrals Used in the Hückel Approximation of the Nucleotide Bases in  $\beta$  Units

$\alpha_i$	$\beta_{ij}$
$\alpha_C = 0.00$	$\beta_{CC} = 1.00$
$\alpha_{\text{C}_N} = 0.07^a$	$\beta_{\text{CN}} = 1.00$
$\alpha_{\text{N}_C\text{N}} = 0.14^b$	$\beta_{\text{CN}} = 1.10^k$
$\alpha_{\text{C}_O} = 0.20^c$	$\beta_{\text{CN}} = 1.00^l$
$\alpha_{\text{N}_C\text{O}} = 0.27^d$	$\beta_{\text{CO}} = 2.00$
$\alpha_{\text{C}_{\text{NON}}} = 0.34^e$	$\beta_{\text{CCH}_3} = 0.10^m$
$\alpha_{\text{N}} = 0.58^f$	$\beta_{\text{CH}_3} = 2.00^n$
$\alpha_{\text{N}} = 0.90^g$	
$\alpha_O = 1.30$	
$\alpha_{\text{C}_{\text{CH}_3}} = -0.10^h$	
$\alpha_{\text{C}_{\text{H}_3}} = -0.20^i$	
$\alpha_{\text{H}_3} = -0.25^j$	

<sup>a</sup> C atom, the nearest neighbours of which are an N atom and a C atom.

<sup>b</sup> C atom which has two N atoms as nearest neighbours.

<sup>c</sup> C atom the nearest neighbours of which are an O and a C atom.

<sup>d</sup> C atom which has an N and an O atom as nearest neighbours.

<sup>e</sup> C atom which has two N and one O nearest neighbours.

<sup>f</sup> Aromatic (pyridine type) N atom.

<sup>g</sup> Hybridized (pyrrole type) N atom.

<sup>h</sup> C atom which is the nearest neighbour of a methyl group.

<sup>i</sup> C atom of the methyl group.

<sup>j</sup> Pseudo-atom H<sub>3</sub> of the methyl group.

<sup>k</sup> Within the ring.

<sup>l</sup> Between a C atom of the ring and the N atom of a —NH<sub>2</sub> substituent.

<sup>m</sup> Between a C atom of the ring and the C atom of a methyl group.

<sup>n</sup> Between the C atom of the methyl group and its pseudo-atom H<sub>3</sub>.

We have taken, as usual, for the zero point of the energy scale the  $\alpha$  integral of a C atom (therefore in Table I we have  $\alpha_C = 0$ ) and all the integrals in Table I are expressed as multiples of the resonance integral  $\beta_{CC} = \beta$  between two C atoms. Some of the other parameter values were taken from the literature<sup>2,7,41</sup> and some we have obtained on the basis of some parameter-varying calculations for the nucleotide bases.

With the aid of the parameters given in Table I, it is very easy to construct the appropriate secular determinants for all the five nucleotide bases. (We have performed the calculations also for uracil, which does not occur in DNA but in RNA. U differs from T only by the lack of the methyl substituent of C atom 5.) The MO energies calculated by solving the determinantal equations with the aid of a computer are indicated in Table II.

TABLE II. The MO Energies of the Single Bases in  $\beta$  Units

	T	U	C	A	G
$\epsilon_i$	3.521	3.523	3.341	2.770	3.337
	3.035	3.037	2.125	2.132	2.572
	1.798	1.785	1.719	1.754	2.224
	1.755	1.043	0.792	1.146	1.340
	1.043	0.555	0.586	1.028	1.121
	0.507	-1.008	-0.846	0.530	0.945
	-1.025	-1.610	-1.404	-0.786	0.386
	-1.619	-2.246	-2.083	-1.003	-1.091
	-2.213			-1.386	-1.200
	-2.274			-2.016	-1.475
					-2.239
$\Delta E$	1.53	1.56	1.43	1.32	1.48
$E$	23.32	19.89	17.12	18.72	23.85

In Table II the MO's which have negative energies (the bonding MO's) occur with positive multiples of  $\beta$  because  $\beta$  is a negative quantity and the antibonding orbitals have negative values in  $\beta$  units. All bonding orbitals are of course in all the five cases completely filled, having two electrons with antiparallel spins on each

bonding MO. The vertical lines indicate the highest filled and lowest unfilled orbitals. In the row  $\Delta E$  we have given the first excitation energy of the bases which is, according to the Hückel approximation, the difference of the MO energies of the lowest unfilled and highest filled orbital:

$$\Delta E = \epsilon_{n^*+1} - \epsilon_{n^*} \quad (2)$$

where  $n^*$  denotes the highest filled orbital. In the last row of Table II the total  $\pi$ -electron energy of the bases is given by

$$E = 2 \sum_{i=1}^{n^*} \epsilon_i \quad (3)$$

Solving also the systems of secular equations belonging to the different  $\epsilon_i$  values we have obtained the sets of  $c_{ik}$  coefficients of Eq. (1) for all the bases. Now one can calculate without difficulty the  $\pi$ -electron charge densities

$$q_k = 2 \sum_{i=1}^{n^*} c_{ik}^2 \quad (4)$$

and the  $\pi$ -electron bond orders

$$p_{kl} = 2 \sum_{i=1}^{n^*} c_{ik} c_{il} \quad (5)$$

for the different bases. With their aid we have constructed the molecular diagrams of the bases, which are shown in Fig. 5.

It is possible to calculate in an approximate form also the transition moment integrals

$$\mathbf{R} = \int \Psi_f \Psi_i \mathbf{r} dV \quad (6)$$

which determine theoretically the probability of the electron transition from the state with the non-degenerate MO  $\Psi_i$  to the state with the non-degenerate MO  $\Psi_f$ .<sup>5</sup> (In the cases of the nucleotide bases we have always non-degenerate levels and therefore Eq. (6) may be used.) In Eq. (6)  $\mathbf{r}$  stands for the position vector of the electron and the integration is to be extended to the whole space. Further it can be shown<sup>5,6</sup> that if we are neglecting overlap the integral of Eq. (6) is equal to the expression

$$\mathbf{R} = \sum_{k=1}^n c_{fk} c_{ik} \mathbf{r}_k \quad (7)$$

where  $\mathbf{r}_k$  denotes the position vector of the  $k$ th nucleus;  $c_{fk}$  and  $c_{ik}$

stand for the coefficient of the  $k$ th atomic orbital in the MO's  $f$  and  $i$ , respectively. It is also proved<sup>5</sup> that expression (7) is invariant with respect to the choice of the origin of the coordinate system.

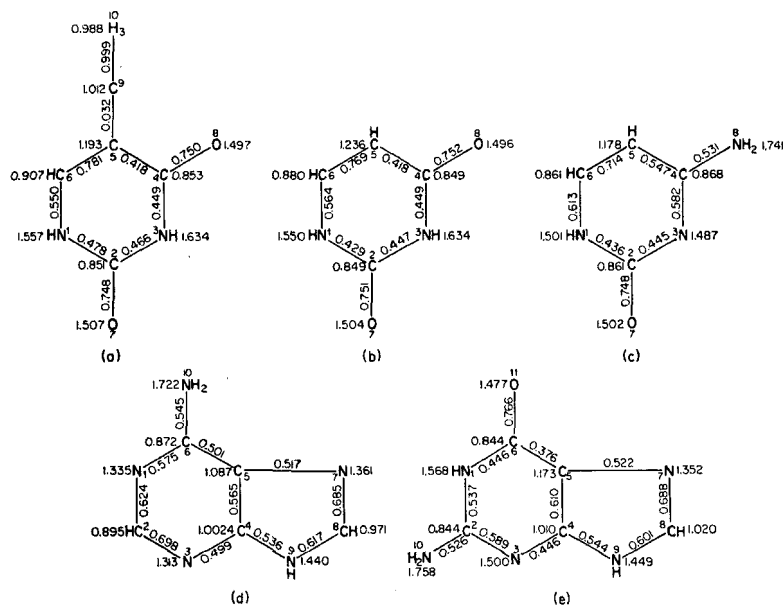


Fig. 5. The molecular diagrams of the nucleotide bases in their *in vivo* stable forms: (a) thymine, (b) uracil, (c) cytosine, (d) adenine, and (e) guanine.

Knowing the geometry of the bases it is very easy to calculate their  $\mathbf{R}$  vectors for the  $i \rightarrow f$  transition. The results obtained for  $i = n^*$  and  $f = n^* + 1$  are indicated in Fig. 6. It may be seen that the transition moment vectors of the pyrimidine bases are approximately parallel; this is the case for the two purine bases as well.

On the basis of the  $\mathbf{R}$  vectors so obtained we have calculated the oscillator strengths ( $f$ ), which give the intensity of the electronic transitions according to the well-known formula:<sup>5</sup>

$$f_{fi \text{ theor}} = 8\pi^2 m c \nu |\mathbf{R}_{fi}|^2 / 3h = 1.085 \times 10^{-5} \tilde{\nu} |\mathbf{R}_{fi}|^2 \quad (8)$$

In the second expression

$$\tilde{\nu} = \frac{\epsilon_f - \epsilon_i}{hc} = \frac{1}{\lambda} \quad (9)$$



is the wave number of the transition in  $\text{cm}^{-1}$ ,  $\lambda$  its wavelength,  $h$  the Planck constant,  $c$  the velocity of light, and  $\mathbf{R}$  should be measured in A. This quantity should be compared with the average oscillator

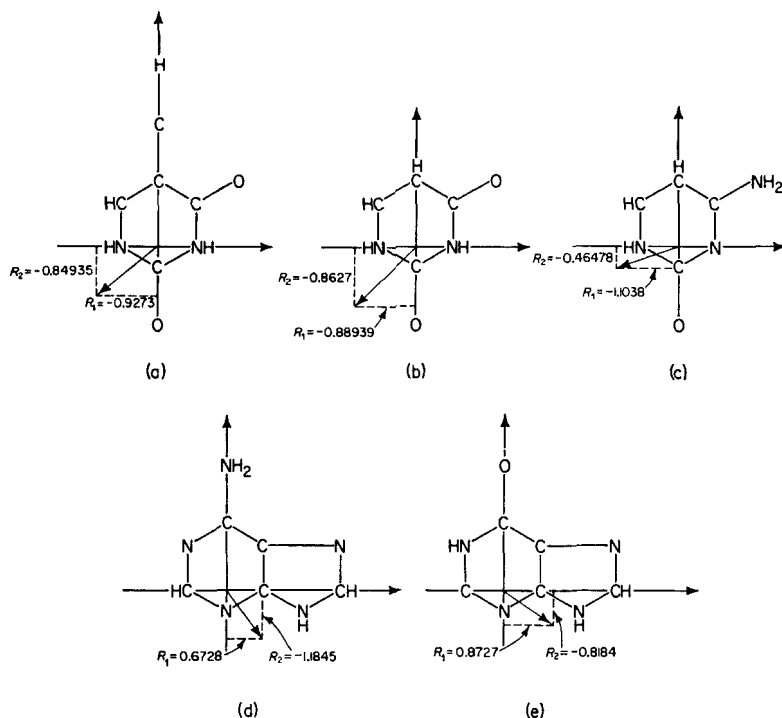


Fig. 6. The transition moment vectors of the nucleotide bases. All the vectors lie in the planes of the bases and have the components (in Å units) indicated in the figures: (a) thymine, (b) uracil, (c) cytosine, (d) adenine, and (e) guanine.

strength of the transition, which may be determined from the intensity of the observed spectra of a band system extending from the frequency  $\nu_1$  to  $\nu_2$ , according to the equation

$$f_{\text{exp}} = \frac{mc^2}{\pi e^2 N} \int_{\nu_1}^{\nu_2} \epsilon(\nu) d\nu \quad (10)$$

Here  $m$  is the mass of the electron,  $e$  the elementary charge,  $N$  the

Avogadro number and  $\epsilon(\nu)$  the molar extinction coefficient, which is of course a function of the frequency.

In Table III we give the calculated and experimental wavelength and intensity of the first excitation. The calculated excitation energy values (row  $\Delta E$  in Table II) are converted to  $m\mu$ 's using the values  $\beta_{Py} = -3.07$  eV (fitted to the spectrum of uracil) and  $\beta_{Pu} = -3.41$  eV (fitted to the spectrum of guanine). The  $f$ -values were calculated according to Eq. (8) using the theoretical  $\Delta E$  values again. The experimental wavelengths of the first  $\pi$ -electron excitations were taken from the first absorption maxima of the extinction curves of the free bases at neutral pH<sup>1</sup> with the exception of G, where the second maximum was used. The experimental  $f$ -values have been estimated by Tinoco.<sup>55</sup> (The  $f$ -value for U is our estimation.)

From Table III we can see that agreement between the theoretical and experimental excitation energies and primarily the intensities

TABLE III. Wavelengths and  $f$ -Values of the First Excitation of the Nucleotide Bases

	Theoretical		Experimental	
	$\lambda, m\mu$	$f$	$\lambda, m\mu$	$f$
U	259	0.67	259	0.25
T	264	0.67	264	0.21
C	283	0.57	267	0.17
A	276	0.73	262	0.30
G	246	0.63	246	0.40 (0.27)

is not good. It should be emphasized, however, that the very simple Hückel approximation, which does not take into account the difference between the energies of the singlet-singlet and singlet-triplet excitations, provides only the midpoint of the energies of the two types of excitations. Since the experimental excitation energies belong to singlet-singlet transitions, the Hückel approximation gives lower excitation energies (longer wavelengths) than the experimental values. The  $f$ -values obtained in the simple Hückel approximation are in general in all known cases larger than the

experimental ones. This discrepancy can be resolved only by taking into account the configuration interaction (CI) for the excited states.

It is interesting to note that in the case of the pyrimidines U, T and C, at least, the tendency of the excitation energies and  $f$ -values agrees with the tendency of the experimental values. In the case of the purines A and G we get this agreement of tendencies only when we do not take into account the shoulder of the band system of A at  $268 \text{ m}\mu$ <sup>1</sup> and do not consider the first absorption maximum of G at  $276 \text{ m}\mu$ <sup>1</sup> but only the second one at  $246 \text{ m}\mu$ . This may probably be interpreted in the following way: \* the pyrimidines U and T do not contain aromatic N atoms (see Fig. 4), which have a lone pair of electrons. Cytosine has an aromatic N atom, but since the absorption maximum of 5-methylcytosine shows a red shift compared to cytosine of approximately the same amount ( $5\text{--}6 \text{ m}\mu$ ) as 5-methyluracil (T) compared to uracil it seems to be very probably that the first absorption maximum of cytosine arises also from a so-called  $\pi \rightarrow \pi^*$ -type transition (a transition from a filled to an unfilled delocalized  $\pi$ -electron MO). On the other hand, in A we have three and in G two aromatic N atoms with lone pairs of electrons. It is therefore very probable that the first excitation of these molecules is an  $n \rightarrow \pi^*$ -excitation (transition of a  $\sigma$ -type lone pair electron from its AO to an unfilled  $\pi$ -electron MO) which has usually smaller excitation energy than a  $\pi \rightarrow \pi^*$ -type excitation. Thus, the shoulder of the band system of A at  $268 \text{ m}\mu$  and the first absorption maximum of G at  $276 \text{ m}\mu$  arise very probably from  $n \rightarrow \pi^*$ -type transitions and therefore these were not taken into account. Since the  $n \rightarrow \pi^*$ -type transitions have transition moments perpendicular to the plane of the molecule, whereas a  $\pi \rightarrow \pi^*$ -type transition is polarized in the plane of the ring, absorption experiments with polarized light could lead to the solution of the assignments of the different band systems in the spectra of the nucleotide bases.

It should be mentioned that the  $f$ -value given by Tinoco for G (0.40) seems to be rather high. Its value can be estimated from the spectrum to be  $\sim 0.27$  (the value in parenthesis in Table III) for the more intensive band system with a maximum at  $246 \text{ m}\mu$ . Further we have to note that while in the series of pyrimidine- (Py)

\* The authors are greatly indebted to Prof. L. Goodman for several useful discussions about this problem.

or purine- (Pu) type bases, at least, the relative values of excitation energies and intensities show an approximate agreement with experiment, this is not the case between Py- and Pu-type bases. For this reason we are using two different  $\beta$  values for the Py-type and Pu-type bases.

To interpret better the absorption spectrum and to compare critically the different semi-empirical methods in the case of U, some higher approximations have also been performed.<sup>21</sup> In this calculation an approximation was used in which the interaction of the electrons has been explicitly taken into account; also, a limited configuration interaction (CI) for the excited states was considered. (It should be mentioned that for the nucleotide bases Veillard and Pullman<sup>56a</sup> have already performed a SCF-LCAO-MO calculation. They have, however, not taken into account CI and therefore it seemed to be interesting to compare the results of the different methods.)

According to Pariser and Parr<sup>35</sup> and Pople<sup>36</sup> the elements of the secular determinant are given by the equations

$$\alpha_i^* = -I_i + \frac{1}{2}q_i^{(0)}(I_i - E_i) + \sum_{j \neq i} (q_j^{(0)} - Z_j)\gamma_{ij} \quad (11)$$

$$\text{and} \quad \beta_{ij}^* = \beta_{ij} - \frac{1}{2}p_{ij}^{(0)}\gamma_{ij} \quad (12)$$

(For the detailed description of the method of Pariser and Parr and the neglects introduced by Pople, see the chapter by J. I. Fernández-Alonso in this volume.)

In these equations  $I_i$  is the ionization potential and  $E_i$  the electron affinity of the  $i$ th atom in its appropriate valence state. It should be mentioned that for a hybridized (pyrrole type) N atom which gives two  $\pi$  electrons to the delocalized  $\pi$ -electron system, it is necessary to use the ionization potential and electron affinity of the  $N^+$  ion, and not those of the neutral atom. All the  $I_i$  and  $E_i$  values used in the calculation have been taken from the compilation of Pritchard and Skinner.<sup>38</sup> For the charge densities  $q_i^{(0)}$  and bond orders  $p_{ij}^{(0)}$ , the values used were obtained from a simple Hückel calculation which was performed with the parameters given in Table I with the exception of  $\beta_{C,N}$  for which the value  $1.25\beta$ , and  $\beta_{C,O}$  for which the value  $1.50\beta$  seemed to be more advantageous.<sup>17</sup> The same  $\beta_{ij}$  values have been used also in Eq. (12). For the effective

nuclear charge  $Z_j = 1$  was taken for a C or O atom, and  $Z_j = 2$  for a hybridized N atom.

The  $\gamma_{ij}$  Coulomb integrals between two  $\pi$ -electrons belonging to atom  $i$  and to atom  $j$  have been taken in one set of the calculations in the Mataga-Nishimoto<sup>32</sup> approximation,

$$\gamma_{ij}^{(1)} = \frac{e^2}{R_{ij} + a_{ij}} \quad (13)$$

where  $e$  is the elementary charge, and  $R_{ij}$  the internuclear distance between the atoms  $i$  and  $j$ , which was determined by the experimentally known geometry of uracil.<sup>50</sup> The constants  $a_{ij}$  were determined by the equation

$$\gamma_{ii} = \frac{e^2}{a_{ii}} = I_i - E_i \quad (14)$$

which gives the Coulomb repulsion between two  $\pi$  electrons on the same atom.<sup>32</sup> In the case when atoms  $i$  and  $j$  are of different kinds, the  $a_{ij}$  constants should be determined by the equation

$$\frac{e^2}{a_{ij}} = \frac{1}{2} (I_i - E_i + I_j - E_j) \quad (15)$$

In a second set of calculations the expression

$$\gamma_{ij}^{(2)} = \frac{e^2}{\sqrt{R_{ij}^2 + a_{ij}^2}} \quad (16)$$

suggested by Ohno<sup>34</sup> was used for the electron interaction integrals. Here the  $a_{ij}$  constants were determined by Eqs. (14) and (15) again.

In the last time Koutecký and his co-workers<sup>18</sup> have obtained good results for the spectra of aromatic hydrocarbons with the approximation described above stopping the iterations before self-consistency was reached, but taking into account a limited CI for the excited states. Therefore, in one approach only the first iteration has been performed, but the CI of the excitations  $5 \rightarrow 6$ ,  $5 \rightarrow 7$ ,  $4 \rightarrow 6$  and  $4 \rightarrow 7$  has been taken into account (the 5th MO of uracil is the highest filled and the 6th is the lowest unfilled MO).

In the case of the CI calculation the elements of the secular determinant

$$\begin{vmatrix} G_{5 \rightarrow 6}^{5 \rightarrow 6} - E & G_{5 \rightarrow 6}^{5 \rightarrow 7} & G_{5 \rightarrow 6}^{4 \rightarrow 6} & G_{5 \rightarrow 6}^{4 \rightarrow 7} \\ G_{5 \rightarrow 7}^{5 \rightarrow 6} & G_{5 \rightarrow 7}^{5 \rightarrow 7} - E & G_{5 \rightarrow 7}^{4 \rightarrow 6} & G_{5 \rightarrow 7}^{4 \rightarrow 7} \\ G_{4 \rightarrow 6}^{5 \rightarrow 6} & G_{4 \rightarrow 6}^{5 \rightarrow 7} & G_{4 \rightarrow 6}^{4 \rightarrow 6} - E & G_{4 \rightarrow 6}^{4 \rightarrow 7} \\ G_{4 \rightarrow 7}^{5 \rightarrow 6} & G_{4 \rightarrow 7}^{5 \rightarrow 7} & G_{4 \rightarrow 7}^{4 \rightarrow 6} & G_{4 \rightarrow 7}^{4 \rightarrow 7} - E \end{vmatrix} = 0 \quad (17)$$

whose roots give the first four singlet-singlet excitation energies ( $E$ ) of uracil are determined by the equation

$$G_{i \rightarrow k}^{j \rightarrow l} = - \sum_{p=1}^n \sum_{r=1}^n (c_{ip} c_{jp} c_{kr} c_{lr} - 2c_{ip} c_{jp} c_{kr} c_{lr}) \gamma_{pr} + (\epsilon_k - \epsilon_i) \delta_{ij} \delta_{kl} \quad (18)$$

where  $i, j = 4$  or  $5$ , and  $k, l = 6$  or  $7$ .

In Eq. (18) which may be easily derived using LCAO-MO's (see the chapter of J. I. Fernández-Alonso in this volume),  $c_{ip}$  stands for the coefficient of the  $p$ th atom in the  $i$ th MO obtained by solving the eighth order secular problem of uracil, with the determinantal elements (11) and (12).  $\delta_{ij}$  and  $\delta_{kl}$  are Kronecker symbols ( $\delta_{ij} = 0$ , if  $i \neq j$ ,  $\delta_{ij} = 1$  if  $i = j$ ),  $\epsilon_k$  and  $\epsilon_i$  are the energies of the  $k$ th and  $i$ th MO's respectively, and  $\gamma_{pr}$  stands for the interaction integral between a  $\pi$  electron on atom  $p$  and another on atom  $r$ . The  $\gamma_{pr}$  integrals have been approximated again with Eqs. (13) and (16).

Solving the determinantal Eq. (17) and the corresponding systems of linear equations, the first four excitation energies and the weights of the different one-electron excitations in the different excited states have been determined. Knowing the coefficients of the different one-electron excitations it was possible to calculate also the oscillator strength values of the first four excitations by a simple generalization of the equations giving the expressions of the transition moment integral and oscillator strength in the Hückel case (for the details see ref. 21).

In a second approach a self-consistent field (SCF) calculation has been performed with the determinantal elements (11) and (12). In each step the secular problem was solved, the  $q_i$  charge densities and  $p_{ij}$  bond orders were constructed and these values were substituted

in Eqs. (11) and (12). The self consistency has been reached in 4 or 5 iteration steps. Having the SCF-LCAO-MO energies and coefficients, the excitation energy and oscillator strength values have been calculated without and with CI. In the first case the energy of the first excitation is given according to Eq. (18) by

$$\Delta E_1 = G_{5 \rightarrow 6}^{5 \rightarrow 6} = - \sum_{p=1}^8 \sum_{r=1}^8 (c_{5p}^2 c_{6r}^2 - 2c_{6p} c_{5p} c_{6r} c_{5r}) \gamma_{pr} + \epsilon_6^{\text{SCF}} - \epsilon_5^{\text{SCF}} \quad (19)$$

The  $f$ -value may be calculated in the same way as in the Hückel approximation but the SCF coefficients should be used. In the case of the SCF-CI calculation the same equations are to be used, as above, for the CI approximation without the self-consistent treatment but now with the SCF-MO energies and coefficients.

In Table IV, we reproduce the results of the different approximations only for the first excitation of uracil, because experimental data are available only for this one.

TABLE IV. The Excitation Energy and Oscillator Strength Values of the First Singlet Excitation of Uracil Obtained with Different Semi-empirical Methods

	Simple Hückel method	Pariser and Parr method						Experi- mental
		1-Iteration-CI		SCF		SCF-CI		
		$\gamma_{ij}^{(1)}$ Eq. (13)	$\gamma_{ij}^{(2)}$ Eq. (16)	$\gamma_{ij}^{(1)}$	$\gamma_{ij}^{(2)}$	$\gamma_{ij}^{(1)}$	$\gamma_{ij}^{(2)}$	
$\Delta E_1$	-1.628 <sup>a</sup>	-1.955	-1.813	-2.395	-2.321	-2.374	-2.312	-1.970
$f_1$	0.632	0.602	0.492	0.816	0.723	0.680	0.653	~0.25

<sup>a</sup> In  $\beta$  units. For the Hückel case the  $\beta = -3.07$  eV should be used to fit the experimental spectrum. The other theoretical values and the experimental one are expressed in  $\beta = -2.39$  eV units.

From the results it is possible to see that the Pariser and Parr method gives much better results if we use only one iteration than

if the whole self-consistent calculation is performed. Using the first form of the  $\gamma_{ij}$  integrals there is a fairly good agreement between the theoretical excitation energy ( $-1.955\beta$ ) and the experimental one ( $-1.970\beta$ ). On the other hand, all methods give oscillator strength values which are too high indicating that the approximation of the wave function is rather poor. It should be noted that the second form of the  $\gamma_{ij}$  integrals in the Pariser and Parr method with one iteration process gives comparatively the lowest  $f$ -values. Therefore the picture is somewhat confused.

The reason why the semi-empirical SCF-LCAO-MO gives quite incorrect results in the case of a somewhat complicated heterocyclic molecule as uracil seems to be the inadequacy of the closed shell form of the SCF-LCAO-MO method<sup>46</sup> for the treatment of excited states. Perhaps a more complicated open shell SCF calculation<sup>47</sup> would give more reliable results.

The SCF-LCAO-MO calculation has given, however, rather reliable results for the electronic distribution of uracil in its ground state. The molecular diagrams obtained are shown in Fig. 7.

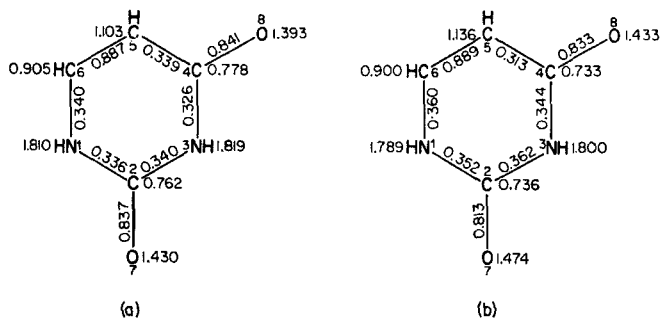


Fig. 7. The molecular diagrams of uracil obtained with the semi-empirical SCF-LCAO-MO method: (a) with  $\gamma_{ij}^{(1)}$ , (b) with  $\gamma_{ij}^{(2)}$ .

To summarize the conclusions obtained from the treatment of the electronic structure of uracil with different semi-empirical methods, it seems as though the present methods successfully used in the literature for simpler systems (pyridine, pyrimidine, etc.) were not very appropriate for heterocyclic systems with different kinds of heteroatoms. It is hoped, however, that by the improvement of the



present methods and with the construction of some new semi-empirical methods, quantum chemistry will be in the near future in the position to give a quantitative interpretation of the spectra for such complicated systems as the nucleotide bases.

#### IV. THE PROBLEM OF MUTATION AND THE TAUTOMERISM OF THE SINGLE BASES

The nucleotide bases at neutral pH are usually in their tautomeric forms, given in Fig. 4, but there is a non-zero probability for them to undergo a tautomeric rearrangement.<sup>14</sup> On the other hand, Watson and Crick have assumed<sup>58</sup> that mutation occurs when, during the duplication of DNA, one of the bases is in such an unusual tautomeric form that the base pairing relations

$$A^*-C; A-C^*; G^*-T; G-T^* \quad (20)$$

are valid instead of the relations

$$A-T; G-C \quad (21)$$

(The asterisk denotes the unusual tautomeric form of a base.) Thus in the new growing chains of DNA an error is introduced in the genetic information which is preserved in the further duplication cycles and may manifest itself in a mutation. An example of this mutation mechanism is shown in Fig. 8.

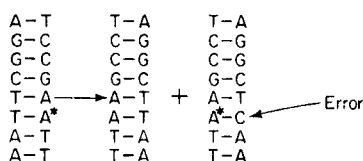


Fig. 8. Schematic representation of the mutation mechanism suggested by Watson and Crick.

For the nucleotide bases there are several possibilities for a tautomeric rearrangement but only the tautomeric forms shown in Fig. 9 can bind through hydrogen bonds to the base of the second chain of the DNA double helix according to the relations (20).

We have performed an LCAO-MO calculation in the Hückel approximation for the nucleotide bases in their tautomeric forms

given in Fig. 9.\* The same parameter values given in Table I have again been used; further for the O atom in the  $-\text{OH}$  group the  $\alpha_{\text{O}} = 1.80\beta$  value, for the resonance integrals  $\beta_{\text{N,C}}$  ( $\text{HN}=\text{C}$  bond) the value  $1.30\beta$  and finally for the resonance integral  $\beta_{\text{O,N}}$  ( $\text{HO}-\text{C}$  bond) the value  $1.20\beta$  has been applied. In Table V we give the MO energies,  $\epsilon_i$ , the energies of the first excitation and the total  $\pi$ -electron energies for the four bases in their unusual tautomeric forms.

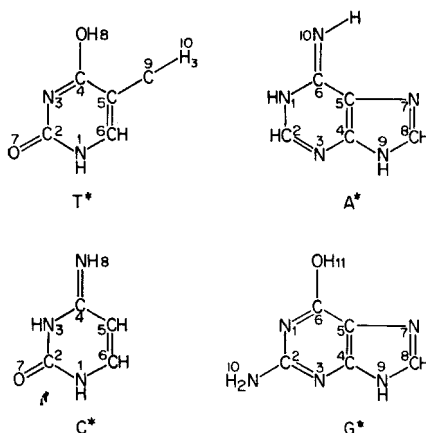


Fig. 9. Those unusual tautomeric forms of the nucleotide bases which may cause an error in the sequence of the bases.

Comparing the results given in Table V with the results for the nucleotide bases in their usual tautomeric forms reproduced in Table II it is apparent that from the point of view of electronic structure the four bases can be divided into two groups,  $\text{T}^*$  and  $\text{G}^*$  on the one hand, for which the enolic forms are the unusual tautomeric forms and  $\text{C}^*$  and  $\text{A}^*$  on the other hand, for which the imino (keto) forms are the unusual ones. Thus  $\text{T}^*$  and  $\text{G}^*$  have weaker electron-donor properties (the energy of the highest filled MO is lower) and stronger electron-acceptor properties (the energy of the lowest unfilled MO is lower) than T and G. At the same time  $\text{C}^*$

\* Note added in proof: With a somewhat different set of parameters the same calculation has been performed independently by Pullman and Pullman.<sup>42a</sup>

TABLE V. The MO Energies of the Single Bases in Their Unusual Tautomeric Form in  $\beta$  Units

	T*	C*	A*	G*
$\epsilon_i$	3.355	3.423	2.855	2.982
	2.666	2.290	2.325	2.513
	1.799	1.761	1.788	2.148
	1.755	0.876	1.145	1.367
	1.080	0.482	1.101	1.158
	0.582	-0.951	0.417	0.894
	-0.807	-1.497	-0.890	0.472
	-1.410	-2.154	-1.059	-0.818
	-2.079		-1.417	-1.186
	-2.232		-2.100	-1.394
				-2.037
$\Delta E$	1.39	1.43	1.31	1.36
$E$	22.48	17.66	19.26	23.07

and A\* have stronger electron-donor and weaker electron-acceptor properties than C and A. Further the energies of the first excitation (the row  $\Delta E$  in Tables II and V) are in the case of T\* and G\* lower than, while in the case of C\* and A\* practically the same as for the appropriate bases in their usual tautomeric form.

The total  $\pi$ -electronic energy (row  $E$  in Table V) is in the case of T\* and G\* smaller than for T and G by an amount of  $\sim 0.8\beta$ . Taking into account that the increase of the sum of the  $\sigma$ -bond energies of the systems T\* and G\* are probably not enough to compensate for this decrease of  $\pi$ -electron energy, one can understand that the systems T and G are more stable than the systems T\* and G\*. This is not the case, however, for the bases C\* and A\* which have a total  $\pi$ -electron energy larger by an amount of  $\sim 0.5\beta$  than that of C and A. At the same time it seems probable that also the sum of the  $\sigma$ -bond energies is larger for C\* and A\* than for C and A, as one may see from the chemical formulae given in Figs. 4 and 9. On the other hand, according to the experimental evidence<sup>14</sup> the energetically less stable tautomeric forms C and A exist in the crystalline

phase and also in neutral aqueous solution, not the energetically more stable  $C^*$  and  $A^*$ . The reason for this discrepancy is not clear at present. For its resolution we intend to make a semi-empirical SCF-LCAO-MO calculation for all four nucleotide bases in their two tautomeric forms to get more refined values for their total  $\pi$ -electronic energy. At the same time we intend to investigate

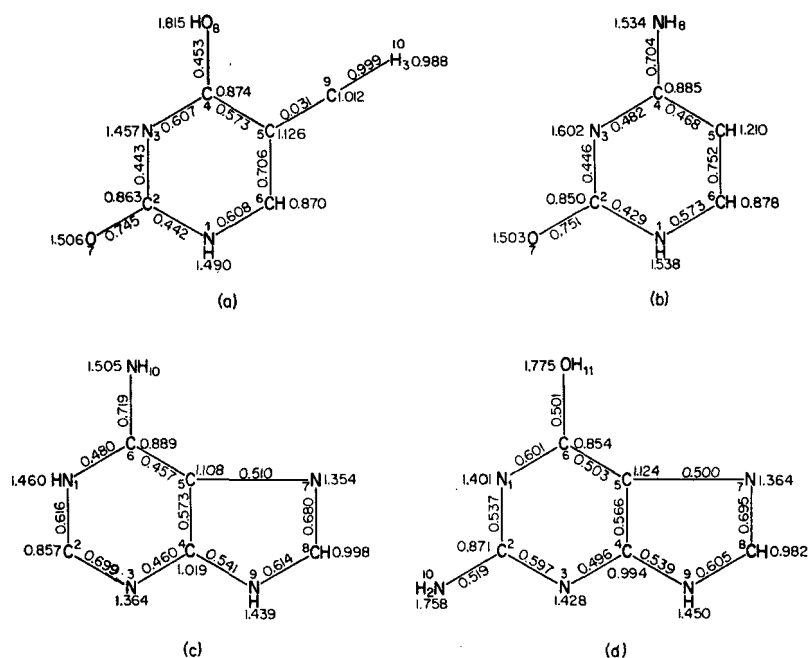


Fig. 10. The molecular diagrams of the nucleotide bases in their unusual tautomeric forms: (a)  $T^*$ , (b)  $C^*$ , (c)  $A^*$ , and (d)  $G^*$ .

also more thoroughly the change of the sum of the  $\sigma$ -bond energies by the tautomeric rearrangement of the nucleotide bases.

With the aid of the calculated  $c_{ik}$  coefficients of the different MO's of the bases in their unusual tautomeric forms we have constructed their molecular diagrams, consisting of the charge densities and bond orders. These are shown in Fig. 10.

It is interesting to note that according to the general experimental experience, the number of mutations can be increased in different biological objects by radiation. Thus, if the mutation

mechanism proposed by Watson and Crick is correct, it should be expected that the excitation or ionization of the bases caused by the radiation increases the probability of the tautomeric rearrangement of the bases.

For the first approximation to this problem which is rather complicated from a theoretical point of view one can compare the total  $\pi$ -electron energy differences of the bases in their two tautomeric forms

$$\Delta E_1 = E_{\pi_n} - E_{\pi_t} \quad (22)$$

with the appropriate quantities

$$\Delta E_2 = E_{\pi_n^+} - E_{\pi_t^+}$$

of the positively ionized bases. (In the equations the subscripts  $n$  and  $t$  refer to the usual (normal) and unusual (*tautomeric*) forms of the bases.) In the Hückel approximation the total  $\pi$ -electron energies of the positively ionized bases can be obtained very simply by subtracting from the total  $\pi$ -electron energy of the neutral base the energy of the highest filled MO (by ionization the electron with the largest probability is removed from this orbital). The quantities  $\Delta E_1$  and  $\Delta E_2$  are shown in Table VI.

TABLE VI. The  $\pi$ -Electron Energy Differences of the Two Tautomeric Forms of Neutral and Ionized Nucleotide Bases in  $\beta$  Units

Base	$\Delta E_1$	$\Delta E_2$
T	0.84	0.91
C	-0.54	-0.65
A	-0.54	-0.65
G	0.78	0.86

From Table VI one can see that according to the Hückel approximation in the case of T and G the  $\pi$ -electron energy difference between the more stable usual and the less stable unusual tautomeric forms is larger when the bases are ionized than when they are

neutral. In other words from the energetical point of view the tautomeric rearrangement of  $T^+$  and  $G^+$  would be less probable than for T and G.

In the case of C and A the energy differences of the tautomeric forms are also greater for ionized bases than for neutral ones. Since here, however, the unusual tautomeric form has the greater total  $\pi$ -electron energy, this means that by ionization the probability of the tautomeric shift will be increased.

It should be emphasized, however, that the very simple Hückel approximation which gives rather inaccurate results also for the ground states of the molecules provides a yet poorer approximation for excited or ionized molecules which have an open shell configuration.<sup>47</sup> Therefore, to get more reliable results for the ionized bases it would be necessary to perform more accurate open shell calculations and it would be yet more important to take into account the distortion of atomic orbitals in consequence of the net electronic charge.\*

Further it is to be noted that the equilibrium between the different tautomeric forms is not only the function of the energy difference between the two tautomeric forms, but also that of their standard entropies. This fact further complicates the situation, but may be at the same time one reason for the anomaly mentioned in connection with the tautomeric forms C and A. Therefore the investigation of the entropies of the different tautomeric forms of the bases would also be very interesting.

## V. THE ELECTRONIC STRUCTURE OF THE BASE PAIRS

According to the Watson-Crick stereomodel, in DNA the base pairs A-T and G-C occur usually. With the aid of the mutation mechanism described in the previous section, however, with much less probability, the so-called anomalous base pairs including the unusual tautomeric form of one base may also occur (see Eq. (20)). Figure 11 shows the classical chemical formulae of the normal and anomalous pairs.

\* The authors are greatly indebted to Prof. P. O. Löwdin for his useful remarks in connection with this problem.

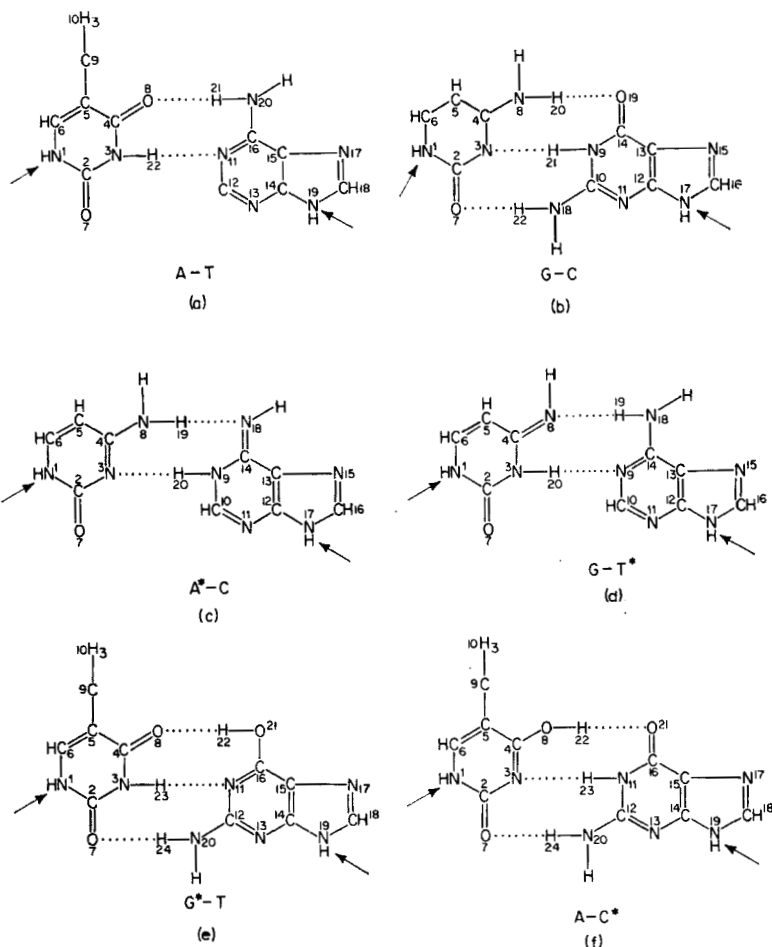


Fig. 11. The schematic representation of the normal and anomalous base pairs of DNA. The dotted lines indicate the hydrogen bonds, the arrows show the places where the bases are bound to deoxyribose.

All these base pairs are planar and the hydrogen bonds between them hold the bases in a fixed position relative to each other. Detailed stereochemical investigations<sup>51</sup> based on X-ray diffraction measurements have shown that in the A-T and G-C base pairs the hydrogen bonds have lengths between 2.95 and 3.05 Å and the H atoms lie approximately on the straight line joining the atoms X

and Y in an  $X-H\cdots Y$ -type hydrogen bond ( $X = N$ ;  $Y = N$  or  $O$ ). (The largest deviation has been found in the case of the  $N-H\cdots O$  hydrogen bond of the A-T base pair, where the angle between the  $N-H$  line and  $N-O$  line is  $\sim 8^\circ$ .)

Considering the above-mentioned geometry of the base pairs, it seems probable that the  $\pi$ -electron clouds of the delocalized  $\pi$ -electron systems of the single bases are in interaction through the hydrogen bonds. It should be mentioned that the same assumption was made by B. and A. Pullman in their calculation of the electronic structure of the base pairs.<sup>40</sup> We are, however, of the opinion, following Paoloni's suggestion,<sup>34a, b</sup> that if this assumption is correct, the empty  $2p_z$  orbitals of those H atoms which are taking part in the hydrogen bonds should be taken into account, too. In connection with this it should be mentioned that the  $^3P$ -excited state of a free  $H^-$  ion (a proton and one electron in the  $1s$  and another one with parallel spin in a  $2p$  state) does not exist. It is very probable, however, that the  $2p$  orbital of a  $H^-$  which is bonded to another atom lies yet below the ionization continuum (it is a stable orbital) because, in consequence of the chemical binding, the other electron will be in the neighbourhood of the  $2p$  electron with less probability than on the free ion; and so the repulsion between them will decrease\*.

For the first approximation of the problem we have performed a Hückel-type calculation for the two normal and the four anomalous base pairs, once without taking into account the H atoms as separate centres and once considering them. In the calculation we have taken into account three hydrogen bonds in the G-C base pair, hence there is no stereochemical reason to assume that the third hydrogen bond between the  $NH_2$  group of guanine and the O atom of cytosine does not exist.<sup>51</sup> In one set of calculations, in addition to the parameter values given in Table I, we have used for an  $X-H\cdots Y$  hydrogen bond the parameter values following B. and A. Pullman,<sup>40</sup>

$$\begin{aligned}\alpha'_X &= \alpha_X - 0.20\beta & \beta_{X,Y} &= 0.20\beta \\ \alpha'_Y &= \alpha_Y + 0.20\beta\end{aligned}\tag{24}$$

where  $\alpha_X$  and  $\alpha_Y$  are the  $\alpha$  integrals of atoms X and Y if they are not

\* The authors are greatly indebted to Dr. L. Hofacker for his remarks on this problem.



taking part in a hydrogen bond. In the second set of calculations in which the H atoms have been treated as separate centres, we have taken the parameter values:

$$\begin{aligned}\alpha'_X &= \alpha_X - 0.20\beta & \beta_{X,H} &= 0.80\beta \\ \alpha'_Y &= \alpha_Y + 0.20\beta & \beta_{H,\dots Y} &= 0.40\beta \\ \alpha_H &= -0.60\beta\end{aligned}\tag{25}$$

This choice of the  $\alpha_H$ ,  $\beta_{X,H}$  and  $\beta_{H,\dots Y}$  values is of course somewhat arbitrary. A moderate parameter-varying investigation of the  $N-H\cdots O$  simplified system has, however, shown that the total  $\pi$ -electron energy and the energy differences of the different levels are rather insensitive to the choice of these parameters.<sup>22</sup> Therefore it seems probable that also in the case of the base pairs the results of the Hückel-type calculation will not be very sensitive with respect to the choice of these parameters. In connection with the  $\alpha_H$  integral it should be mentioned that we have taken a negative value for it (in negative  $\beta$  units !) because in consequence of the repulsion between the two electrons of the  $H^-$  ion its value will be much more positive than the value of  $\alpha_C$ , which we have taken as the zero point of the energy scale.

The Hückel approximation is of course only the first step in the treatment of  $\pi$ -electron systems interacting through hydrogen bonds. The problem is complicated enough, especially when we are taking into account that as a result of the high mobility of protons the Born–Oppenheimer approximation is a rather poor approximation to the treatment of  $\pi$ -electron interaction through hydrogen bonds (the position of the H atoms cannot be regarded as fixed).<sup>30</sup>

In Table VII, we show the MO energies of the A–T and G–C base pairs in both approximations, and in Table VIII the total  $\pi$ -electron energies are given for the two normal and four anomalous base pairs, again in both approximations.

In the cases where the H atoms of the hydrogen bonds are not taken into account as separate centres, the levels of the A–T and G–C base pairs can be ordered unambiguously to the levels of the appropriate single bases, also reproduced in the table. In the cases, however, where the H atoms are taken into account as separate centres (A–T(H) and G–C(H)) new levels appear which are coming from the H atoms (these are shown on the right-hand side in

TABLE VII. The MO Energies of the A-T and G-C Base

	A-T	A	T	A-T(H)
$\epsilon_i$	3.529		3.521	3.551
	3.110		3.035	3.118
	2.775	2.770		2.784
	2.162	2.132		2.199
	1.798		1.798	1.800
	1.755		1.755	1.769
	1.736	1.754		1.756
				1.289
	1.149	1.146		1.148
	1.086		1.043	1.057
	0.903	1.028		
	0.533	0.530		0.624
	0.451		0.507	0.525
				-0.494
	-0.803	-0.786		-0.719
	-0.945	-1.003		-0.980
	-1.043		-1.025	-1.089
				-1.221
	-1.389	-1.386		-1.407
	-1.603		-1.619	-1.626
	-2.006	-2.016		-2.027
	-2.216		-2.213	-2.223
	-2.284		-2.274	-2.337
$\Delta E_1$	1.25	1.32	1.53	1.02
$\Delta E_2$	1.34 (A)			1.34 (A)

columns A-T(H) and G-C(H)). The perturbation of the original single-base levels is also larger in the latter cases, as we should expect.

In the row  $\Delta E_1$  the first excitation energies (the energy differences of the highest filled and lowest empty levels) of the base pairs and single bases are given. We find a decrease of  $0.07\beta$  of the excitation energy going from the case of A to the case of the A-T base pair (T has a larger excitation energy), while the excitation energy of the

Pairs in the Two Approximations Given in the Text in  $\beta$  Units

	G-C	G	C	G-C(H)
$\epsilon_i$	3.457		3.341	3.459
	3.382	3.337		3.417
	2.593	2.572		2.597
	2.177	2.224		2.247
	2.123		2.125	2.183
	1.730		1.719	1.759
	1.335	1.340		1.375
				1.215
	1.107	1.121		1.134
	0.991	0.945		0.923
	0.648		0.792	
	0.554		0.586	0.672
	0.355	0.386		0.443
				-0.464
				-0.673
	-0.832		-0.846	-0.928
	-1.079	-1.091		-1.066
	-1.241	-1.200		-1.163
	-1.388		-1.404	-1.406
	-1.474	-1.475		-1.446
				-1.554
	-2.041		-2.083	-2.071
	-2.248	-2.239		-2.303
$\Delta E_1$	1.19	1.48	1.43	1.01
$\Delta E_2$	1.39 (C)			1.51 (G)

G-C base pair is smaller by  $0.24\beta$  than that of C. On the other hand, in the cases A-T(H) and G-C(H) the first excitation energies are only about  $1\beta$  unit and so their decrease is in the A-T(H) case  $0.30\beta$  and in the G-C(H) case  $0.42\beta$ .

It should be mentioned, however, that the transitions with these decreased excitation energies are very improbable. In the A-T case it corresponds to a transition from the perturbed highest filled level of T to the perturbed lowest empty level of A and in the A-T(H) case

TABLE VIII. The Total  $\pi$ -Electron Energies of the Two Normal and Four Anomalous Base Pairs in Both Approximations in  $\beta$  Units

A-T 41.98	A + T 42.04	A-T(H) 43.24
G-C 40.91	G + C 40.97	G-C(H) 42.85
A*-C 36.39	A* + C 36.38	A*-C(H) 37.63
A-C* 36.34	A + C* 36.38	A-C*(H) 37.62
G*-T 46.19	G* + T 46.39	G*-T(H) 47.99
G-T* 46.23	G + T* 46.33	G-T*(H) 48.03

from the perturbed highest filled level of T to a new level originating from a H atom. In the G-C case the transition from the perturbed highest filled level of G to the perturbed lowest empty level of C has the smallest energy and in the G-C(H) case again the perturbed highest filled level of G and a H level are combined. Since all the transitions with the smallest excitation energies can thus be classified as transitions between levels originating from different bases they must have rather small probability. (See also ref. 13b.) This assumption is supported by the calculation of the oscillator strength values in two cases of superimposed bases (see Section VI), where we have found extremely small oscillator strength values for such. The improbability of the transitions with the decreased excitation energy is in agreement with the experimental fact that the position of the ultraviolet absorption maximum of DNA does

not differ from the one obtained by the superposition of the absorption curves of the single bases.<sup>1</sup>

In the last row of Table VII, the  $\Delta E_2$  values give the excitation energies of such transitions in the base pairs, which can be classified as transitions between levels originating from the same base and having at the same time the lowest excitation energy. The letter in parentheses indicates the base to which these much more probable transitions belong in the different cases. We see that the excitation energy of A-T and A-T(H) is greater than that of A by  $0.02\beta$ . In the case of G-C, the excitation energy is lower than that of C by  $0.04\beta$ , and finally in the case of G-C(H) there is again an increase of  $0.03\beta$  compared to G. Since these changes are not too large, it is easy to understand that in the experimental spectrum of DNA, which is influenced also by numerous interactions, they will not have a detectable effect.

Comparing the total  $\pi$ -electron energies of the normal base pairs (A-T, G-C) given in Table VIII with the sum of the energies of the constituent bases, they are smaller by an amount of  $0.06\beta$  in both cases, which is a very small deviation as compared to the magnitudes  $\sim 42\beta$  and  $\sim 41\beta$ , respectively, of the total  $\pi$ -electron energies of these base pairs. On the other hand when we are also taking into account the H atoms as separate centres this will give an extra stabilization which is too large.

In the case of the anomalous base pairs consisting of one base in its unusual tautomeric form we find that the total  $\pi$ -electronic energy is always larger for the G\*-T and G-T\* pairs by about  $10\beta$  than that for the A\*-C and A-C\* pairs, respectively. We can see further that by considering the H atoms as separate centres, the  $\pi$ -electron energy is increased by too great an amount. It is interesting to note that the energies of the A\*-C and A-C\*, and of the G\*-T and G-T\* base pairs are practically equal in both approximations. The energies of the anomalous base pairs, when we are not taking into account the H atoms explicitly, are in a first approximation equal to the sum of the energies of the constituent single bases again (we find the largest deviation,  $0.20\beta$ , in the case of the G\*-T base pair:  $E_{G^*-T} = 46.19\beta$ ,  $E_{G^*} + E_T = 46.39\beta$ ).

It should be emphasized, however, that the energies of the anomalous base pairs are not very interesting from the point of view of tautomeric rearrangement, because a G-C base pair is not

able to undergo a rearrangement to the most stable G\*–T base pair within a DNA double helix. Such a change is possible only during the duplication process, as described in the preceding section in connection with the mechanism of mutation.

We are of the opinion that the problem of the interaction of the  $\pi$ -electron system through H bonds should be investigated in more detail to get more reliable results.\* The results reported in this section give only a first orientation and therefore we have not discussed them in more detail.

## VI. INTERACTION BETWEEN THE SUPERIMPOSED BASES; SPECTROSCOPICAL CONSEQUENCES

The nucleotide bases within one chain are parallel, according to the Watson–Crick model, and therefore there is an interaction between their delocalized  $\pi$ -electron orbitals (see Fig. 2). To perform a Hückel-type LCAO-MO calculation for two superimposed bases as a common system, it is necessary to have some estimation of the  $\beta_{ij}$  integrals between atoms  $i$  and  $j$  belonging to two different rings. It may be shown that for the pair of atoms  $i$  and  $j$  the relation

$$\frac{\beta_{ij}(R_1)}{\beta_{ij}(R_2)} = \frac{S_{ij}(R_1)}{S_{ij}(R_2)} \quad (26)$$

holds in a good approximation between the resonance ( $\beta_{ij}$ ) and overlap ( $S_{ij}$ ) integrals.<sup>19</sup> In Eq. (26)  $\beta_{ij}(R_1)$  stands for the resonance integral taken at the internuclear distance  $R_1$  and  $\beta_{ij}(R_2)$  the same quantity at the distance  $R_2$ . On the basis of Eq. (26), which is valid for  $\sigma$ - as well as for  $\pi$ -type interactions between  $2p$  orbitals<sup>19</sup> (see Fig. 12), we may write

$$\beta_{ij}(R_2) = k S_{ij}(R_2); \quad k = \frac{\beta_{ij}(R_1)}{S_{ij}(R_1)} \quad (27)$$

Thus knowing the value of the overlap integral between the atoms  $i$  and  $j$  at distance  $R_1$  and, at the same time, the  $\beta_{ij}$  value used in the

\* *Note added in proof:* A recent detailed investigation of the  $\pi$  electron system of protein interacting through hydrogen bonds has shown that if one takes a much larger negative value for  $\alpha_H$ , it is possible to reach more reliable results for the delocalization energies.<sup>42b, 42c</sup> Further, it was possible in this way to reach similar results also for the nucleotide base pairs.<sup>42b</sup>

Hückel approximation for this distance, on the basis of the value of the overlap integral at another distance,  $R_2$ , the value of the resonance integral at this distance,  $\beta_{ij}(R_2)$ , can be easily estimated. It should be emphasized, however, that for each kind of atom pair another proportionality constant  $k$  has to be used.

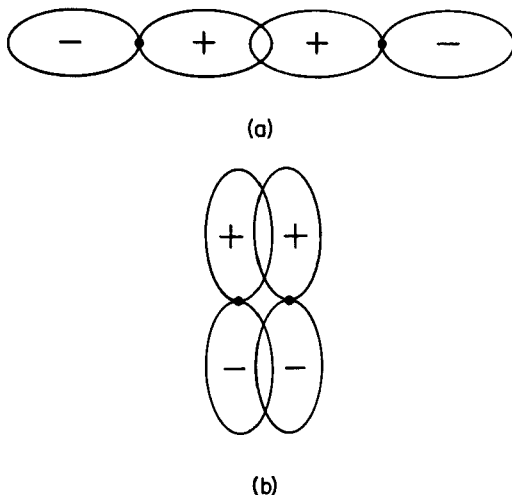


Fig. 12. (a)  $\sigma$ -type interaction between  $2p$  atomic orbitals. (b)  $\pi$ -type interaction between  $2p$  atomic orbitals.

For the determination of the  $\beta_{ij}$  integrals we have calculated the overlap integrals between all combinations of atoms of the  $4^2 = 16$  possibilities of two superimposed bases.<sup>13a</sup> In the calculation of the approximately 1600 occurring overlap integrals the relative geometrical position<sup>27</sup> of the superimposed bases has been taken into account with some unessential neglects. In consequence of the rotation of the bases around the long axis of the molecule  $36^\circ$  relative to each other, the  $\pi$ -electron orbitals of the atoms belonging to different rings will not be directed towards each other, but they will be shifted in different degrees in the plane perpendicular to the axis. However, by constructing the projections of the superimposed bases it is very easy to determine the distances by which the axes of the atomic  $2p$  orbitals are shifted relative to each other.

Since the  $2p$  wave functions are proportional to one of the

rectangular coordinates they can be treated as vectors and so they can be decomposed to perpendicular components. Thus if we have two  $2p$  atomic orbitals, shifted relative to each other by a distance  $\rho$  (see Fig. 13), we may write for them

$$\psi_i(2p) = \psi_{\sigma_i} \cos \vartheta + \psi_{\pi_i} \sin \vartheta \quad (28a)$$

$$\psi_j(2p) = \psi_{\sigma_j} \cos \vartheta - \psi_{\pi_j} \sin \vartheta. \quad (28b)$$

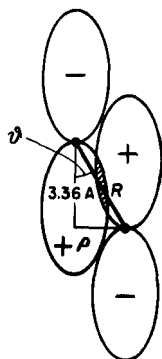


Fig. 13. Two  $2p$  orbitals of atoms in adjacent parallel planes shifted relative to each other by the distance  $\rho$  in their plane.

(see Fig. 14). Here  $\psi_{\sigma}$  stands for an atomic  $2p$  orbital directed from centre  $i$  towards centre  $j$  and  $\psi_{\pi}$  denotes a  $2p$  orbital perpendicular to it, while  $\vartheta$  is the angle between the line connecting the two centres

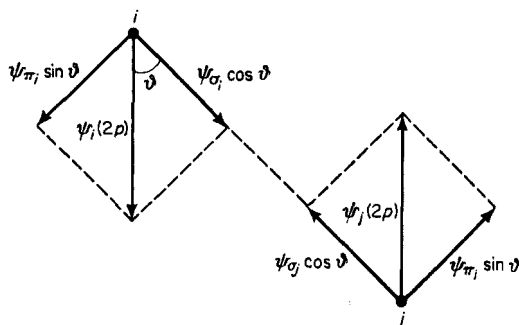


Fig. 14. The decomposition of two  $2p$  orbitals into components directed towards the centres of each other and into ones perpendicular to these directions.



and the direction perpendicular to the plane of the bases (see Fig. 13.) The negative sign before the second member of the second Eq. (28) can be understood from Fig. 14.

Substituting the expressions, Eqs. (28a) and (28b), into the overlap integral

$$S_{ij} = \int \psi_i(2p) \psi_j(2p) dV \quad (29)$$

we get

$$S_{ij} = \cos^2 \vartheta \int \psi_{\sigma i} \psi_{\sigma j} dV - \sin^2 \vartheta \int \psi_{\pi i} \psi_{\pi j} dV + \\ + \sin \vartheta \cos \vartheta \int (\psi_{\pi i} \psi_{\sigma j} - \psi_{\sigma i} \psi_{\pi j}) dV \quad (30)$$

Since the last integral vanishes by the orthogonality of the  $\sigma$  and  $\pi$  orbitals, we may write

$$S_{ij}(R) = S_{ij}^{\sigma\sigma} \cos^2 \vartheta - S_{ij}^{\pi\pi} \sin^2 \vartheta \quad (31)$$

Here  $S_{ij}^{\sigma\sigma}$  stands for the first  $\sigma$ -type overlap integral and  $S_{ij}^{\pi\pi}$  for the  $\pi$ -type second one. These integrals have been calculated by the appropriate  $R = \sqrt{(3.36^2 + \rho^2)}$  distances between the centres  $i$  and  $j$  (see Fig. 13), where 3.36 Å is the distance between the planes of two superimposed bases.

Using the Slater-type approximate atomic orbitals,<sup>49</sup> if  $i$  and  $j$  are the same kind of atom, it holds<sup>11</sup> that

$$S_{ij}^{\sigma\sigma} = (-1 - x - \frac{1}{5}x^2 + \frac{2}{15}x^3 + \frac{1}{15}x^4)e^{-x} \quad (32)$$

and

$$S_{ij}^{\pi\pi} = (1 + x + \frac{2}{5}x^2 + \frac{1}{15}x^3)e^{-x} \quad (33)$$

where  $x = (c/2)R$ . Here  $R$  is the internuclear distance and  $c$  the effective nuclear charge which is to be calculated according to the rules given by Slater.<sup>49</sup>

In the case where  $i$  and  $j$  are different kinds of atoms the overlap integrals may be expressed with the aid of auxiliary functions:<sup>37</sup>

$$S_{ij}^{\sigma\sigma} = \frac{1}{16}(\bar{\alpha}\bar{\beta})^{5/2} [A_2(B_0 + B_4) - B_2(A_0 + A_4)] \quad (34)$$

$$S_{ij}^{\pi\pi} = \frac{1}{32}(\bar{\alpha}\bar{\beta})^{5/2} [(A_4 - A_2)(B_0 - B_2) + (A_2 + A_0)(B_4 - B_2)] \quad (35)$$

Here  $\bar{\alpha} = (c_A/2)R$ ;  $\bar{\beta} = (c_B/2)R$ ;  $A_n = A_n(1; k) = \int_1^\infty e^{-kx} x^n dx$ ;  $k = (\bar{\alpha} + \bar{\beta})/2$  and

$$B_n = B_n(k') = A_n(-1; k') - A_n(1; k') \quad (36)$$

where

$$A_n(-1; k') = \int_{-1}^{\infty} e^{-k'x} x^n dx; \quad k' = (\bar{\alpha} - \bar{\beta})/2 \quad (37)$$

Since not all the necessary  $A_n(1; k')$ ,  $A_n(1; k)$  and  $A_n(-1; k')$  functions tabulated in the literature are at the appropriate distances used in our investigations, we have calculated all of them with the aid of the following series

$$A_n(g; l) = \frac{e^{-l}}{l} \sum_{r=0}^n \frac{n!}{(n-r)!} g^{n-r} \quad (38)$$

where  $g = +1$  or  $-1$ ;  $l = k$  or  $k'$ ; and  $n = 0, 2, 4$ .

The evaluation of all the occurring overlap integrals has been programmed and calculated on a computer using Eqs. (31)–(38).<sup>13a</sup> For orientation we give in Table IX the values of some overlap integrals for the case in which the atomic orbitals are directed towards each other. We give for comparison also the appropriate values for the  $\pi$ – $\pi$  type overlapping integrals *within one ring*.<sup>26</sup>

From Table IX one can see that the interactions between the different rings are of course much smaller than the  $\pi$ -electron interactions within one ring, but they are not negligible. Thus the value of  $S_{C,C}^{\sigma\sigma}$  is more than 12% of the value of  $S_{C,C}^{\pi\pi}$  and about 15% that of  $S_{C,N}^{\pi\pi}$ .

TABLE IX. Overlap Integrals Between Atoms Belonging to Different Rings and to the Same Ring

Pair of atoms	$S_{A,B}^{\sigma\sigma}, \rho = 0$	$S_{A,B}^{\pi\pi}$
C—C	0.032 ( $R = 3.36$ Å)	0.263 ( $R = 1.39$ Å) <sup>a</sup>
C—N	0.015 „	0.216 ( $R = 1.34$ Å) <sup>b</sup>
N—N	0.008 „	

<sup>a</sup> The distance between two C atoms in benzene.

<sup>b</sup> The average distance between a C and an N atom in the nucleotide bases.

Since, in reality, with two superimposed bases there are inter-

acting not single atomic orbitals, but delocalized molecular orbitals, the measure of their interaction is

$$S_{kl}^{AB} = \sum_{i=1}^{n_A} \sum_{j=1}^{n_B} c_{ki}^A c_{lj}^B S_{ij} \quad (39)$$

the overlap integral between their LCAO-MO's. Here  $S_{kl}^{AB}$  means the overlap integral between the  $k$ th MO of base  $A$  and the  $l$ th MO of base  $B$ ,  $c_{ij}^A$  is the coefficient of the  $j$ th atom in the  $l$ th MO of base  $A$ .  $S_{ij}$  stands for the overlap integral between the  $i$ th AO of base  $A$  and the  $j$ th one of base  $B$  and finally  $n_A$ , and  $n_B$  denote the number of centres in base  $A$  and base  $B$ , respectively.

To get an idea of the average interaction between the superimposed bases, instead of calculating the numerous overlap integrals between the individual MO's, we have calculated as a crude approximation the average overlap integrals between them defined by the equation:

$$S_{av}^{AB} = \frac{1}{\sqrt{(n_A n_B)}} \sum_{i=1}^{n_A} \sum_{j=1}^{n_B} \sqrt{q_i^A} \sqrt{q_j^B} S_{ij} \quad (40)$$

Here  $q_i^A$  and  $q_j^B$  are, respectively, the  $\pi$ -electron charge density of atom  $i$  in base  $A$ , and that of atom  $j$  in base  $B$ . It should be mentioned that the average overlap integrals defined by Eq. (39) will give, of course, an overestimation of the overlap between the bases, because contrary to the coefficients of the overlap integrals of the true MO's their  $\sqrt{q_i}$  and  $\sqrt{q_j}$  coefficients are always positive. It is our opinion, however, that they give *some measure* of the overlapping between the bases. In Table X we give these values for all the sixteen combinations of two superimposed bases.

From the values given in Table X which have been calculated with the aid of the charge densities given in Fig. 5, it can be seen that in the case where two Py-type bases (T or C) are superimposed, or when two Pu-type bases (A or G) are superimposed, the value of  $S_{av}^{AB}$  is approximately the same (values between 0.0220 and 0.0280.) On the other hand when we have a Pu-type base below a Py-type one, the interaction will be larger (values between 0.0330 and 0.0370), while in the reversed case, when we have a Py-type base below a Pu-type one it will be smaller (values between 0.0150 and

TABLE X. The Values of the Average Overlap Integrals Between Superimposed Bases Defined in Eq. (40)

Py-Py	T-T	0.0220
	C-C	0.0241
	T-C	0.0240
	C-T	0.0220
Pu-Pu	A-A	0.0256
	G-G	0.0260
	A-G	0.0230
	G-A	0.0284
Pu-Py	A-T	0.0331
	A-C	0.0351
	G-T	0.0340
	G-C	0.0368
Py-Pu	T-A	0.0166
	T-G	0.0150
	C-A	0.0160
	C-G	0.0150

0.0170)\*. Also within the mentioned three groups of interaction there are some differences, but the overall picture is given by the regularities described. These regularities are in agreement with the geometry of the different types of superimposed bases as may be seen from Fig. 15.

From Fig. 15 it is easy to see which atoms are playing the most important role in the interaction between the superimposed bases. These are, in agreement with the values of the calculated  $S_{ij}$  integrals, those shown in Table XI. In connection with Table XI it is interesting to note that in the interactions of a Py ring the C<sub>5</sub> atom plays an important role.<sup>13d, 26</sup> On the other hand T occurring in DNA and U occurring in RNA differ only in a CH<sub>3</sub> substituent at this position. Since the CH<sub>3</sub> group according to general experience changes the electron density at the position of its substitution, a T

\* Since the DNA chains are directed (right-handed helices), Pu → Py is not the same as Py → Pu from a geometrical point of view (the arrow indicates the direction of the chain).

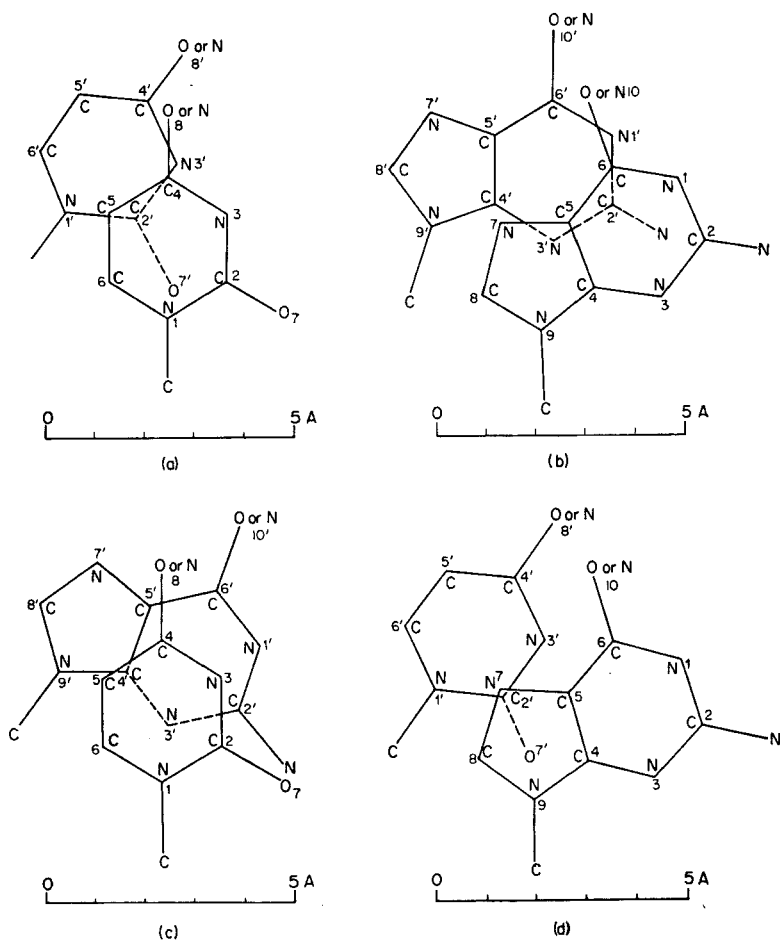


Fig. 15. The relative geometrical positions of superimposed bases. (a) Py-Py, (b) Pu-Pu, (c) Pu-Py, and (d) Py-Pu.

base will interact somewhat differently with its neighbours than a U base in the same position. The same considerations may hold between C(cytosine) on one hand and 5-methyl-C or 5-oxymethyl-C occurring in T-phages on the other hand. These things, as we shall try to show in the next section, may have some biological significance.

TABLE XI. The Most Strongly Interacting Atoms (Active Centres) in the Superimposed Bases

Type of interaction	Active centres
Py-Py	N <sub>3</sub> , C <sub>2</sub> , C <sub>6</sub> , C <sub>5</sub>
Pu-Pu	C <sub>2</sub> , N <sub>3</sub> , C <sub>4</sub> , C <sub>5</sub> , C <sub>6</sub>
Pu-Py	Pu: C <sub>2</sub> , N <sub>3</sub> , C <sub>4</sub> , C <sub>5</sub> Py: N <sub>3</sub> , C <sub>2</sub> , C <sub>6</sub> , C <sub>5</sub>
Py-Pu	Py: C <sub>2</sub> Pu: C <sub>2</sub>

Having all the  $S_{ij}$  overlap integrals between the AO's of the superimposed bases, using relation (27) we have estimated the appropriate  $\beta_{ij}$  resonance integrals. With the aid of the latter quantities it was very easy to perform a Hückel approximation for all sixteen superimposed bases by writing out the appropriate secular determinants. Solving the determinantal equations we have obtained the MO energies of two superimposed bases treated as a common system. In Table XII we give the calculated energies of their highest filled ( $\epsilon_{n^*}$ ) and lowest unfilled ( $\epsilon_{n^*+1}$ ) MO's as compared with the appropriate quantities of the constituent bases; their first excitation energies ( $\Delta E = |\epsilon_{n^*+1} - \epsilon_{n^*}|$ ), the data for the single bases and their total  $\pi$ -electron energies ( $E$ ) are also given.

From the data given in Table XII one can see that, in agreement with the quantum mechanical perturbation theory, the shifts of the highest filled and of the lowest unfilled levels from the appropriate levels of the single bases are largest ( $0.01$ – $0.03\beta$ ) when we have one kind of base (T–T, C–C, A–A and G–G). Further it turned out from more detailed analyses of the calculated energy levels that this shift is yet larger at many levels, reaching an amount of  $\sim 0.10\beta$  at the lowest levels. On the other hand, however, it is possible in almost all cases to determine that level of the single base from which a particular level pair has originated.

In the twelve other cases, when two different bases are superimposed, it is always possible to determine those levels of the constituent bases from which the levels of the common system were

TABLE XII. Energy Data in  $\beta$  Units for Superimposed Bases

Super-imposed bases	$\mathcal{E}_n^*$	$\mathcal{E}_n^*$ s.b. <sup>a</sup>	$\mathcal{E}_{n+1}^*$	$\mathcal{E}_{n+1}^*$ s.b. <sup>a</sup>	$\Delta E$	$\Delta E$ s.b. <sup>a</sup>	$E$
Py-Py							
T-T	0.485	T: 0.507	-1.019	T: -1.025	1.504	T: 1.532	46.64
C-C	0.563	C: 0.586	-0.837	C: -0.846	1.400	C: 1.432	34.24
T-C	0.501	T: 0.507	-0.846	T: -1.025	1.347	T: 1.532	40.44
C-T	0.502	C: 0.586	-0.845	C: -0.846	1.347	C: 1.432	40.44
Pu-Pu							
A-A	0.504	A: 0.530	-0.766	A: -0.786	1.260	A: 1.316	37.44
G-G	0.361	G: 0.386	-1.074	G: -1.091	1.435	G: 1.477	47.70
A-G	0.382	A: 0.530	-0.785	A: -0.786	1.167	A: 1.316	42.57
G-A	0.381	G: 0.386	-0.786	G: -1.091	1.167	G: 1.477	42.57
Pu-Py							
A-T	0.487	A: 0.530	-0.786	A: -0.786	1.273	A: 1.316	42.04
		T: 0.507		T: -1.025		T: 1.532	
A-C	0.519	C: 0.586	-0.786	C: -0.846	1.305	C: 1.432	35.84
G-T	0.379	G: 0.386	-1.018	G: -1.091	1.397	G: 1.477	47.17
		T: 0.507		T: -1.025		T: 1.532	
G-C	0.380	C: 0.586	-0.845	C: -0.846	1.225	C: 1.432	40.97
Py-Pu							
T-A	0.505	T: 0.507	-0.785	T: -1.025	1.290	T: 1.532	42.04
		A: 0.530		A: -0.786		A: 1.316	
T-G	0.385	G: 0.386	-1.025	G: -1.091	1.410	G: 1.477	47.17
C-A	0.529	C: 0.586	-0.786	C: -0.846	1.315	C: 1.432	35.84
		A: 0.530		A: -0.786		A: 1.316	
C-G	0.386	G: 0.386	-0.846	G: -1.091	1.232	G: 1.477	40.97

<sup>a</sup> s.b. = single base.

originated. Comparing with them the highest filled and lowest unfilled levels of the superimposed bases we find a shift of  $\sim 0.005\beta$  for the Py-Py (T-C and C-T) and Pu-Pu (A-G and G-A) cases, a larger,  $0.01-0.02\beta$ , shift for the Pu-Py cases and a very small,  $\sim 0.001\beta$ , shift for the Py-Pu cases. These results are in agreement with the relative amounts of the average overlap integrals between

the superimposed bases given in Table X. Further, it should be mentioned that also in the case of two different superimposed bases we have found larger shifts at some levels other than the highest filled and lowest unfilled ones. To review, in Table XIII we give all the MO energies of the G-G and G-C cases. For comparison we have reproduced in this table the levels of a single G and C base too.

TABLE XIII. MO Energies of G-G and G-C in  $\beta$  Units

G-G	G	G-C	C
3.430		3.409	3.341
	3.337	3.290	
3.256			
2.633	2.572	2.593	
2.519			
2.234	2.224	2.223	
2.205			2.098
			1.723
1.366	1.340	1.337	
1.312			
1.141	1.121	1.118	
1.098			
0.951	0.945	0.946	
0.937			
			0.788
			0.585
0.410	0.386	0.380	
0.361			
			-0.845
-1.074			-0.846
	-1.091	-1.091	
-1.106			
-1.196			
	-1.200	-1.200	
-1.206			
			-1.403
-1.462	-1.475	-1.478	-1.404
-1.489			
			-2.083
-2.238			-2.083
	-2.239	-2.240	
-2.241			



Referring to Table XII we see that the first excitation energies ( $\Delta E$ ) given show that in the homogeneous cases (T-T, C-C, A-A, G-G), the excitation energies are lowered by an amount of  $0.03-0.06\beta$  compared to the appropriate values for single bases. In most of the cases of different superimposed bases we find a much greater decrease in the first excitation energy compared to that for the two constituent bases, which has the smaller excitation energy (compare columns  $\Delta E$  and  $\Delta E$  s.b.). The reason for this is that in most cases when the highest filled level of one of the constituent bases lies higher, at the same time the first unfilled one of the same constituent also lies higher. When the two bases are united in a common system, since the interaction is not too large, the positions of these levels are retained approximately. Since, however, the first excitation means a transition from the highest filled to the lowest unfilled MO, the transition in the common delocalized system will take part from the filled level of the one base (from that lying higher) to the unfilled level of the other base (to that lying lower). This can well be seen from Table XII and XIII. This however sometimes causes a drastic decrease of the first excitation energy. For instance in the cases of G-C and C-G this decrease is  $0.20\beta$  and  $0.25\beta$  respectively as compared with the excitation energy of C and G. On the other hand in the cases of A-C and C-A we get a very small change in excitation energy ( $0.01\beta$ ), because A has at the same time a higher lying last filled and a lower lying first unfilled level than C.

In connection with the large decrease of excitation energies by interaction between different bases the question arises as to whether there is a strong red shift in the maximum of the absorption curve of DNA compared to the spectra of the single bases. The experimental spectra of DNA differs, however, essentially only in intensity from the spectrum calculated on the basis of superposition of the spectra of the single nucleotides, but not in the position of the maximum.<sup>1</sup> This discrepancy can be resolved, however, if we are taking into account that the transitions with decreased excitation energy have very low probabilities, as the calculations of the oscillator strength values (see below) suggest. Therefore they practically do not influence the shape of the absorption curve.

In connection with Table XII, finally, it should be mentioned that the total  $\pi$ -electron energies ( $E$ ) of two superimposed bases given in the last column are exactly equal to the sum of the

$\pi$ -electron energies of the two constituent bases (see also the last row of Table II). This means that the shifts of the levels of the superimposed bases are symmetrical around the appropriate level of the single base in the homogeneous cases; with two different superimposed bases the shifts of the levels in opposite directions cancel each other.

It is well known<sup>1</sup> that the intensity of the absorption spectrum of DNA is only about 60% of the intensity calculated on the basis of the superposition of the spectra of the single nucleotides. For the interpretation of this so-called hyperchromicity (more correctly hypochromicity) Tinoco<sup>55</sup> has calculated the electrostatic interaction between the dipoles induced by the exciting light. He has found that if these dipoles are lying in parallel planes, as is the case for the superimposed bases in DNA, the oscillator strength of DNA per nucleotide will be between 90 and 70% of the average oscillator strength of the single nucleotides (in calf thymus DNA,  $f_{av} = 0.27$ ). Since the directions of the transition moment vectors of the bases are not known Tinoco has assumed that they are all parallel and has given the value of the oscillator strength of DNA as a function of this unknown direction characterized by the azimuth angle. The limits given above (90 and 70%) refer to different angles. Later it was shown by Rhodes<sup>44</sup> that Tinoco's theory for the hypochromicity of DNA should be corrected taking into account not the interaction of parallel transition dipoles having the same frequency (exciton interaction<sup>16</sup>), but only the electrostatic interaction of parallel transition dipoles having different frequencies (dispersion interaction).

Having performed Hückel-type calculations for adjacent superimposed bases as common systems it was easy to investigate this problem of hypochromicity in the framework of the MO theory.<sup>13c</sup> For this reason we have solved also the systems of linear equations occurring in the Hückel theory for the superimposed bases and we have so obtained the  $c_{ik}$  coefficients of the

$$\Psi_i = \sum_{k=1}^{n_{A-B}} c_{ik} \psi_k \quad (41)$$

LCAO-MO's, which are now extending to both the superimposed bases ( $n_{A-B}$  denotes the number of atoms with  $\pi$  orbitals in both superimposed bases,  $A$  and  $B$ ). Having these coefficients we have

calculated in the usual approximation<sup>5</sup> the transition moment integrals for three cases with the aid of the formula

$$\mathbf{R} = \sqrt{2} \sum_{k=1}^{n_{A-B}} c_{fk} c_{ik} \mathbf{r}_k \quad (42)$$

where the summation is to be extended to both superimposed bases. In the calculation we have used the exact geometry of the bases given by Langridge *et al.*<sup>27</sup> Having the transition moment vectors (42), using Eq. (8) we have obtained the oscillator strength values of the superimposed bases. The calculation has been performed for all the 16 dinucleotides. Here we give results for the C-C system for the  $n^* \rightarrow n^* + 1$  and  $n^* \rightarrow n^* + 2$  transitions, and for the G-C system for the  $n^* \rightarrow n^* + 1$  transition. The values obtained are indicated in Table XIV.

TABLE XIV. Oscillator Strength Values for Superimposed Bases

	C-C	G-C
$n^* \rightarrow n^* + 1$	0.050	0.003
$n^* \rightarrow n^* + 2$	0.504	

Comparing the values given in the table it is apparent that the  $n^* \rightarrow n^* + 1$  transitions, which have the lowest excitation energies, have very low intensities. This can be easily understood, however, if we consider that the energy levels of two superimposed bases treated as a common system are originating from the levels of the constituent single bases (see above). Thus in the C-C system the highest filled MO ( $n^*$ ) originates from one base and the lowest unfilled one ( $n^* + 1$ ) from the other. We find the same situation in the case of the  $n^* \rightarrow n^* + 1$  transition of the G-C system, where the highest filled level originates quite clearly from G and the lowest unfilled one from C. Thus the very low  $f$ -values of the  $n^* \rightarrow n^* + 1$  transitions simply reflect the improbability of such transitions in which the preference region of the electron in its final state is far removed from its preference region in its initial state. For a similar interpretation of spectra of other organic molecules see ref. 13b.

On the other hand, the oscillator strength value of the  $n^* \rightarrow n^* + 2$  transition of C-C is ten times as large as the  $f$ -value of the  $n^* \rightarrow n^* + 1$  transition and with two orders of magnitude larger than the  $f$ -value of the  $n^* \rightarrow n^* + 1$  transition of the G-C system. It should be mentioned that the relative  $f$ -values of the two first transitions in the C-C system are in agreement with the results obtained by Kasha *et al.*<sup>16</sup> on the basis of their molecular exciton model, according to which the first transition from the highest filled level of two parallel interacting bases is forbidden and the second one is allowed.

Further, it is interesting to compare this value of 0.50 also with the theoretical  $f$ -value of a single C base (0.57, see Table III), which shows a 12% deviation. On the other hand, from the experimental investigations of some dinucleotides it is known that their spectra are practically the same as the spectra obtained by superposition of the spectra of their constituent nucleotides.<sup>48</sup> In a dinucleotide, however, the two bases are parallel to each other only with a very low probability and therefore the  $\pi$ -electron interaction between them, which causes the decrease of the intensity, does not exist.

On the basis of these first calculations one can hope that by calculating the oscillator strength values of the  $n^* \rightarrow n^* + 1$ ,  $n^* \rightarrow n^* + 2$  and  $n^* - 1 \rightarrow n^* + 1$  transitions of all the sixteen superimposed bases, and later by extending the calculations to superimposed base pairs, taking into account not only the interactions between nearest neighbours, it will be possible to give a better theoretical interpretation of the hypochromicity of DNA.

## VII. GENETICAL CONSIDERATIONS: THE CODING PROBLEM

It is the basic assumption of biochemical genetics that the genetical information carried by DNA is determined by the sequence of the four nucleotide bases.

Therefore it is interesting to point out that according to the arguments given in the preceding section, the interaction between the superimposed bases is a function of the sequence.<sup>26</sup> In other words different DNA molecules having the same base composition but different sequences will have somewhat different electronic structures. This statement, which could be rigorously proved only by calculating the energy band structures of the whole macro-

molecule assuming different model sequences, can be approximately verified also on the basis of the average overlap integrals given in Table X and of the MO energies of the superimposed bases.

The average overlap integrals in Table X show the largest interaction between a Pu-type base below a Py-type one, the smallest interaction when a Py-type base is below a Pu-type one and a medium interaction for the Py-Py and Pu-Pu cases. We may take as the zeroth approximation the values of the average overlap

(a)	(b)	(c)	(d)	(e)	(f)	(g)	(h)	(i)	(j)	(k)	(l)
A	T	T	A	T	A	G	C	C	G	C	G
A	T	T	A	A	T	G	C	C	G	G	C
A	T	T	A	T	A	G	C	C	G	C	G
A	T	T	A	A	T	G	C	C	G	G	C
A	T	T	A	T	A	G	C	C	G	C	G
A	T	A	T	A	T	G	C	G	C	G	C
A	T	A	T	T	A	G	C	G	C	C	G
A	T	A	T	A	T	G	C	G	C	G	C
A	T	A	T	T	A	G	C	G	C	C	G
A	T	A	T	A	T	G	C	G	C	C	G
A	T	A	T	A	T	G	C	G	C	G	C
0.2304	0.1980	0.2235	0.2070	0.2319	0.2154	0.2340	0.2169	0.2372	0.2154	0.2440	0.2222
(m)	(n)	(o)	(p)	(r)	(s)	(t)	(u)	(v)			
C	A	C	A	T	G	T	G	A			
C	A	A	C	T	G	G	T	G			
C	A	C	A	T	G	T	G	G			
C	A	A	C	T	G	G	T	C			
C	A	C	A	T	G	T	G	T			
A	C	A	C	G	T	G	T	G			
A	C	C	A	G	T	T	G	T			
A	C	A	C	G	T	G	T	C			
A	C	C	A	G	T	T	G	C			
A	C	A	C	G	T	G	T	A			
0.2339	0.2148	0.2395	0.2204	0.2260	0.2070	0.2300	0.2110	0.2236			

Fig. 16. Different model sequences containing 10 bases together with the sums of the average overlap integrals.

integrals as measures of the interactions between the superimposed bases. To get a crude picture for the interactions in larger sequences, we sum these values for nearest neighbours. For different sequences we obtain in this way somewhat different values. In Fig. 16 we give several model sequences containing ten bases and the values obtained by the summation of their average overlap integrals taken from Table X.

From Fig. 16 it is possible to see that with the same base composition the values are somewhat dependent on the sequence (compare for instance *d* to *f* and *i* to *k*). Further sequences belonging to different base compositions show rather different values

(compare  $b$  to  $g$  and to  $k$ ). It is possible that for longer model sequences the values would deviate even more.

It should be emphasized, however, that the average overlap integrals given in Table X are quantities somewhat arbitrarily defined and therefore the changes of the energy levels due to the interaction between adjacent bases is a more critical test for the dependence of the electronic structure of DNA on the sequence of bases. The most simple quantity which could characterize the interaction between the superimposed bases would be

$$\Delta E = E_{A-B}^{\pi} - (E_A^{\pi} + E_B^{\pi}) \quad (43)$$

the change of the total  $\pi$ -electron energy. Here  $E_{A-B}^{\pi}$  denotes the total  $\pi$ -electron energy of the common  $A$ - $B$  system, and  $E_A^{\pi}$  and  $E_B^{\pi}$  that of the constituent base  $A$  and base  $B$ , respectively. Comparing, however, the data given in Table XII for the superimposed bases and in Table II for the single bases it turns out that in all the 16 cases the  $\pi$ -electron energy of the superimposed two bases is exactly the sum of the  $\pi$ -electron energies of the single bases.

On the other hand, a comparison of the individual energy levels of the superimposed bases and the single bases (see Tables II, XII and XIII) shows that these levels are shifted in consequence of the perturbation by a greater or smaller amount in the different cases from the appropriate single base levels. In Table XV we have summarized the level splittings ( $\Delta$ ) of the highest filled MO's in the homogeneous cases (T-T, C-C, A-A and G-G, see Fig. 17). Further

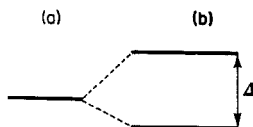


Fig. 17. Level splitting by perturbation.

we have indicated in Table XV for the 12 additional cases of different bases the double value of the shifts ( $\Delta = 2\delta$ ) of the highest filled MO's from the highest filled levels of their parent single bases (see Fig. 18).

From Table XV it is obvious that we find the largest perturbations of the energy levels when we have superimposed the same kind of bases (T-T, C-C, A-A, G-G). This result is in agreement with

perturbation theory according to which levels lying in the same position or near to each other perturb each other strongly. We find yet a relatively high  $\Delta$ -value for the A-T case ( $\Delta = 0.040\beta$ ), which can be understood if we are taking into account that the highest filled MO's of A and T lie rather near to each other (A:  $\epsilon_{n*} = 0.530\beta$  T:  $\epsilon_{n*} = 0.507\beta$ ; see Table II). The rather high  $\Delta$ -value of the A-C system ( $\Delta = 0.022\beta$ ) is the consequence of the same reason (see Table II). All the other  $\Delta$ -values are smaller, between  $0.008\beta$  and

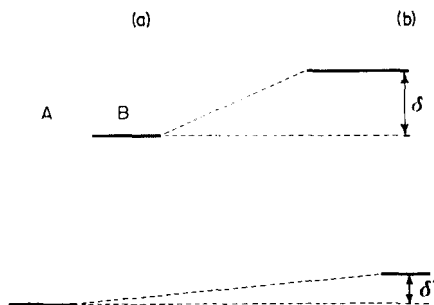


Fig. 18. Shift of the levels by the interaction of two different bases.  $\Delta$  is defined as  $2\delta$  for the highest filled level,  $\delta'$  of a lower lying level not being taken into account at all.

$0.014\beta$  in the Py-Py, Pu-Pu and Pu-Py cases, and about  $0.002\beta$  in the Py-Pu cases. The Py-Pu cases have the smallest interaction due to their geometry (see the overlap integral values in Table X) and this is why the perturbation of their energy levels is very small.

Thus the amount of perturbation of the energy levels is first of all determined by the relative position of the appropriate levels of the interacting systems, but it is also influenced by the amount of overlapping between them. It should be further mentioned that we could find similar regularities not only at the highest filled MO's, but at all the other energy levels.

If we define in a first approximation as an index of the interactions in larger base sequences the sum of the  $\Delta$ -values given in Table XV, we can calculate these quantities for the model sequences given in Fig. 16. The values obtained are presented in Table XVI.

In Table XVI we have denoted by a double asterisk the cases in which only one kind of base is repeated, and a single asterisk denotes the model sequences in which there are two kinds of bases but the same bases are arranged one after the other (see Fig. 16). It

TABLE XV. The Splittings and Doubles of the Shifts of the Highest Filled Energy Levels of the Superimposed Bases in  $\beta$  Units

	Case	$\Delta$
Py-Py	T-T	0.042
	C-C	0.042
	T-C	0.012
	C-T	0.010
Pu-Pu	A-A	0.051
	G-G	0.049
	A-G	0.008
	G-A	0.010
Pu-Py	A-T	0.040
	A-C	0.022
	G-T	0.014
	G-C	0.012
Py-Pu	T-A	0.004
	T-G	0.002
	C-A	0.002
	C-G	0.000

TABLE XVI. The Sum of  $\Delta$ -Values for the Model Sequences Given in Fig. 16 in  $\beta$  Units

(a) 0.459**	(g) 0.441**	(m) 0.394*	(t) 0.078
(b) 0.378**	(h) 0.378**	(n) 0.374*	(u) 0.066
(c) 0.412*	(i) 0.376*	(o) 0.118	(v) 0.161
(d) 0.376*	(j) 0.364*	(p) 0.098	
(e) 0.216	(k) 0.060	(r) 0.378*	
(f) 0.180	(l) 0.048	(s) 0.366*	

is quite evident from the table that in the mentioned cases there is a much larger interaction (sum of the  $\Delta$ -values, between  $0.460\beta$  and  $0.360\beta$ ) than in the cases  $e, f, k, l, o, p, t$  and  $u$ , when we have the different bases arranged alternately (values between  $0.120\beta$  and  $0.050\beta$  with the exceptions of cases  $e$  and  $f$ ). The comparatively



larger values of the model sequences  $e$  and  $f$  are the consequences of the high value of  $\Delta_{A-T} = 0.040\beta$  (see Table XV). In the last case (model sequence  $v$ ), we have taken a sequence without any regularity and have found for it a medium value ( $0.161\beta$ .)

The more detailed investigation of the splittings and shifts of the other levels showed the same regularities. Thus we can conclude that in base sequences we will find the larger interactions the more times the same kinds of bases are superimposed on each other. When the very important experimental problem of determining base sequences of DNA molecules coming from different sources has been solved, it will be interesting to investigate the experimentally found sequences also from the point of view of the interactions between them. On the other hand the nearest neighbour frequencies of the nucleotide bases in DNA determined by Josse *et al.*<sup>15</sup> show no correlations with these theoretically found regularities. Since, however, the larger interactions do not mean greater stability (the total energy of the interacting bases is always equal to the sum of the energies of the bases, see Tables II and XII), it is not to be expected at all theoretically that nearest neighbours with a larger interaction will be more frequent.

In connection with the DNA-RNA-P (protein) coding problem we should like to mention only two things. In the last year, on the basis of the experimental investigation of the polypeptides synthesized in the presence of polyribonucleotides with known composition, there has been considerable progress.<sup>28, 33, 52</sup> It is yet not quite clear, however, whether the code is degenerate or not, i.e. whether one trinucleotide of RNA determines more than one, or only one, amino acid in the protein. Ochoa and his co-workers<sup>28, 52</sup> are of the opinion that the code is non-degenerate, while other authors concluded that it is degenerate.<sup>4, 59</sup> Further elementary estimations show that the information content of DNA is probably ten times greater than the information content transferred through RNA to different protein molecules coded by it.<sup>23</sup> The reason for this redundancy is that perhaps some regions of DNA are not carrying genetic information (coil regions) but—according to our opinion—it supports the point of view that the code is non-degenerate.

In the case of a non-degenerate code we have immediately the problem of how to select from the sixty-four possible trinucleotides

those twenty trinucleotides of RNA which code the twenty essential amino acids of the proteins. It is interesting that the regularities found for the interaction between adjacent superimposed bases give a possible means of selecting twenty trinucleotides from the sixty-four. Namely, if we want to construct trinucleotides with largest possible interaction we have to put the same base in them as many times as possible. So we can select the four trinucleotides containing only one kind of base and can exclude all the possibilities when we have three different bases. Further, to increase the interaction we have to put in a trinucleotide containing two similar and one different base, the two similar bases always adjacent to each other. Finally knowing that when a Py-type base is below a Pu-type base the interaction will be smaller than in all other cases, we can exclude those possibilities from our trinucleotides containing one Py-type for every two of the same Pu-type base, or one Pu-type for every two of the same Py-type base. In this way we select exactly twenty of the most strongly interacting trinucleotides (for the details see ref. 24.) The described selection of the twenty trinucleotides refers, of course, to DNA. Since, however, the base sequence of DNA determines the base sequence of RNA, another set of twenty trinucleotides in RNA belongs to the twenty trinucleotides in DNA depending upon the coding principle between DNA and RNA.<sup>29</sup> It should be further mentioned that the twenty trinucleotides obtained in this way are not in agreement with the experimentally found coding trinucleotides of Ochoa and his co-workers.<sup>28, 52</sup> Therefore if it is the case that in nature there is a general biological code, the possibility for the selection of the twenty most strongly interacting trinucleotides may be only by chance. In the case, however, that the code is not general (in different biological systems there are different trinucleotide-amino acid correlations) the selection by largest interaction may have in some cases some importance.

### VIII. CALCULATION OF THE BAND STRUCTURE OF POLYNUCLEOTIDES IN THE HÜCKEL APPROXIMATION

Since in DNA all the superimposed bases are in interaction, it seemed to be of interest to perform a calculation for the whole chain of interacting bases. The number of bases in one chain of DNA is of the order of magnitude of  $10^5$ , so it can be treated as an infinite chain

in a very good approximation. If we have some periodically repeated unit in such a chain, it can be considered as the elementary cell of a one-dimensional crystal and therefore the methods of solid state physics can be applied to it.

The quantum mechanical treatment of the delocalized  $\pi$ -electron system of DNA is simplest when we are considering as the first step only a single chain consisting of only one kind of base (polynucleotide). In polyU, polyT, polyC, polyA and polyG for which the calculation has been performed,<sup>13a,25</sup> the U, T, C, A and G bases are the elementary cells and for these polynucleotides the same geometry has been assumed as for a chain of the real DNA double helix.

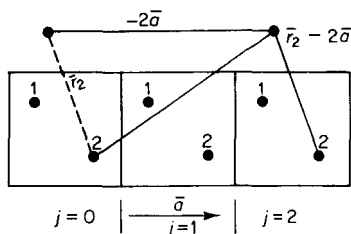


Fig. 19. Correlation of radius vectors of corresponding atoms in different elementary cells.

The calculation has been performed again with the simple LCAO-MO method using the simple Hückel approximation with the neglect of overlap. In this treatment, when we have  $N$  elementary cells (where  $N$  is a very large number), and in each elementary cell  $n$  atoms, we may write the LCAO-MO's of the  $\pi$  electrons delocalized in the whole chain in the form<sup>20</sup>

$$\Psi_{ps} = \sum_{j=1}^N \sum_{l=1}^n c_{ps,jl} \psi_l(\mathbf{r}_l - j\mathbf{a}) \quad (44)$$

Here the  $c_{ps,jl}$  constant belongs to the  $l$ th atom of the  $j$ th elementary cell in the MO denoted by the two indices  $p$  and  $s$ ;  $\psi_l(\mathbf{r}_l - j\mathbf{a})$  is the atomic  $2p_z$  orbital of the same atom (see Fig. 19.),  $\mathbf{a}$  is the primitive translation vector and the radius vector  $\mathbf{r}_l$  is taken from the  $l$ th atomic nucleus of the first cell (see Fig. 19). The possible values of the index  $p$  are the integers  $0, 1, \dots, N-1$  and those of  $s$  are the integers  $1, 2, \dots, n$ .

Substituting the quasi infinite chain by a cyclic chain where the first and  $N$ th elementary cells adjoin, we get the Born-von Kármán periodic boundary condition

$$\Psi_{ps}(\mathbf{r}) = \Psi_{ps}(\mathbf{r} + N\mathbf{a}) \quad (45)$$

according to which the wave function must have the same value after  $N$  elementary translations. From Eq. (45) it is very easy to derive the condition (the Bloch condition)

$$c_{ps,jl} = \exp(2\pi i j p / N) c_{ps,l} \quad (46)$$

for the coefficients of Eq. (44) (see, for instance, ref. 43). If  $N$  is a large number, it is possible to introduce the variable

$$k = (2\pi p / N) \quad (47)$$

which changes, in a very good approximation, continuously from 0 to  $2\pi$ . With the aid of Eq. (47) we can write

$$c_{ps,jl} = \exp(ikj) c_{ks,l} \quad (48)$$

Substituting (48) into (44) and calculating the expectation value of the Hamiltonian of a delocalized electron moving in the periodical potential of the one-dimensional crystal, we get

$$\bar{H} = \int \Psi_{ks}^*(\mathbf{r}) \mathbf{H} \Psi_{ks}(\mathbf{r}) dV = \bar{H}(\{c_{ks,l}\}) \quad (49)$$

This expression for the expectation value is a function of all the coefficients  $c_{ks,l}$ . ( $\{c_{ks,l}\}$  symbolizes the ensemble of all these constants.) The minimum of the expectation value, which approximates the energy of the electron, as in the case of simple molecules (see the chapter of I. Fernández-Alonso in this volume), can be determined again from the conditions

$$\frac{\partial \bar{H}}{\partial c_{ks,l}} = 0 \quad (50)$$

where  $0 \leq k < 2\pi$ ;  $s = 1, 2, \dots, n$ ;  $l = 1, 2, \dots, n$ .

From the conditions (50), using the neglects used already in the derivation of the Hückel approximation for simple molecules and neglecting overlap, one can get the system of linear equations

$$c_{ks,l}(\alpha_l - \epsilon) + \sum_{t=1}^n \beta_{lt} c_{ks,t} + \sum_{t=1}^n (\beta_{lt}^+ e^{ik} + \beta_{lt}^- e^{-ik}) c_{ks,t} = 0 \quad (51)$$

where  $0 \leq k < 2\pi$ ;  $s = 1, 2, \dots, n$ . Here the meaning of the integrals  $\alpha_l$  and  $\beta_{lt}$  is the same as in the Hückel method for simple molecules

( $\beta_{ll}$  means the resonance integral between atoms  $l$  and  $l$  belonging to the same elementary cell; in the case of DNA to the same base) and the asterisk in the first summation denotes that the summation should be extended only to those atoms,  $t \neq l$ , which are the nearest neighbours of atom  $l$  within the elementary cell.  $\beta_{ll}^+$  and  $\beta_{ll}^-$  stand for the resonance integrals between the  $l$ th atom of one elementary cell and the  $l$ th atom of the nearest neighbouring cell on the right and left in the chain, respectively.

The condition of the non-trivial solution of the system of equations (51) for the coefficients  $c_{ks,t}$  gives the determinantal equation

$$\begin{vmatrix} \gamma_{11} - \epsilon & \gamma_{12} & \gamma_{13} & \dots & \gamma_{1n} \\ \gamma_{21} & \gamma_{22} - \epsilon & \gamma_{23} & \dots & \gamma_{2n} \\ \gamma_{31} & \gamma_{32} & \gamma_{33} - \epsilon & \dots & \gamma_{3n} \\ \dots & \dots & \dots & \dots & \dots \\ \gamma_{n1} & \gamma_{n2} & \gamma_{n3} & \dots & \gamma_{nn} - \epsilon \end{vmatrix} = 0 \quad (52)$$

where

$$\gamma_{ll} = \alpha_l + \beta_{ll}^+ e^{ik} + \beta_{ll}^- e^{-ik} \quad (53)$$

and

$$\gamma_{ll} = \beta_{ll} + \beta_{ll}^+ e^{ik} + \beta_{ll}^- e^{-ik}, \quad (l \neq t) \quad (54)$$

The different roots  $\epsilon_s(k)$  of Eq. (52) ( $0 \leq k < 2\pi$ ;  $s = 1, 2, \dots, n$ ) will give the possible energy levels\* of an electron delocalized in the whole macromolecule. The energy levels belonging to a particular  $s$ -value, but to different  $k$ -values will form an energy band,† while the levels having a particular  $k$ -value but belonging to different  $s$ -values will be situated in different energy bands. Thus if we have in the elementary cell of the macromolecule  $n$  atoms, we will get  $n$  different energy bands. From a physical point of view it is most important to know the highest and lowest levels of these energy bands.

\* From the translational symmetry it follows that  $\beta_{ll}^+ = \beta_{ll}^-$ , therefore  $\gamma_{ij} = \gamma_{ji}^*$ , where  $\gamma_{ji}^*$  is the complex conjugate of  $\gamma_{ji}$  (see Eq. (54)). This has the consequence that all the roots of Eq. (52) are real.

† In reality, to a particular  $s$ -value there belong only  $N$  different near lying levels, but in consequence of taking  $k$  as a continuous variable (Eq. (47)), we will get a continuum for the allowed energy values. This is called in solid state physics an energy band.

In the calculation for the mentioned five polynucleotides the same  $\alpha_i$  and  $\beta_u$  parameter values have been used as for the single bases (see Table I). For the  $\beta_u^+$  and  $\beta_u^-$  ( $l, t = 1, 2, \dots, n$ ) integrals, the values estimated on the basis of the  $S_u$  overlap integrals between atoms belonging to superimposed bases have been applied again. Using these values not only the translational symmetry, but also the turning of the superimposed bases in the helix around the axis of the macromolecule, has been considered.

Substituting different  $k$ -values into Eq. (52) and solving it by standard mathematical methods (the solution of the eigenvalue problem of a complex hermitic matrix), it was possible to construct  $\epsilon_s$  as a function of  $k$ . With the aid of this it was very easy to determine the boundaries of the different energy bands and the  $k$ -values belonging to them (for the details of some of these calculations see ref. 25). In Table XVII we reproduce from these results the boundaries of the highest filled and lowest unfilled energy bands of the five polynucleotides and we give for comparison also the appropriate levels of the single bases.

From Table XVII one can see that the widths of the highest filled energy bands are about  $0.10\beta$  and their boundaries have positions symmetrical to the level of the appropriate single base in a good approximation. The lowest empty bands have at the same time smaller widths between  $0.02\beta$  and  $0.07\beta$ , located again symmetrically around the position of the appropriate single levels. It should be further mentioned that the  $k$ -value belonging to the lower ends of the highest filled and lowest unfilled band is in all the five cases equal to  $\pi$  and that belonging to the upper ends to  $k = 0$ .

An analysis of the detailed band structure of the five different polynucleotides<sup>25</sup> shows that the widths of the different bands varies between  $0.35\beta$  and  $0.01\beta$ . Again, as in the cases of two superimposed bases, the lowest filled levels are perturbed most strongly and therefore the energy bands originating from them have the largest widths. There is, however, in no case an overlapping between the different bands and therefore in all five cases one may get as many distinct energy bands as the number of the MO's of the appropriate single base.

It can be seen also that approximately all the bands are symmetrical around the positions of the levels of the single bases. Therefore, if we assume a uniform level density within the bands,

TABLE XVII. The Boundaries of the Highest Filled and Lowest Unfilled Energy Bands of the Five Polynucleotides in  $\beta$  Units

PolyT	T	PolyU	U	PolyC	C	PolyA	A	PolyG	G
Lowest empty band									
-1.036 ( $k = 0$ )	-1.025	-1.021 ( $k = 0$ )	-1.008	-0.867 ( $k = 0$ )	-0.846	-0.823 ( $k = 0$ )	-0.786	-1.122 ( $k = 0$ )	-1.091
-1.014 ( $k = \pi$ )		-0.995 ( $k = \pi$ )		-0.824 ( $k = \pi$ )		-0.749 ( $k = \pi$ )		-1.058 ( $k = \pi$ )	
Highest filled band									
0.464 ( $k = 0$ )		0.510 ( $k = 0$ )		0.537 ( $k = 0$ )		0.480 ( $k = 0$ )		0.336 ( $k = 0$ )	
0.547 ( $k = \pi$ )	0.507	0.597 ( $k = \pi$ )	0.555	0.631 ( $k = \pi$ )	0.586	0.576 ( $k = \pi$ )	0.530	0.433 ( $k = \pi$ )	0.386

the total  $\pi$ -electron energy of the polynucleotides will be equal to the sum of the  $\pi$ -electron energies of their constituents. Thus the situation is the same as in the case of two superimposed bases (see Tables II and XII). It is necessary, however, to perform a more detailed investigation of this problem.

In connection with the  $k$ -values belonging to the ends of the different bands the more detailed data <sup>13a, 25</sup> show that in many cases, as opposed to the cases of the highest filled and lowest unfilled bands,  $k = 0$  belongs to the lower and  $k = \pi$  to the upper ends of the bands and, in several cases, also  $k$ -values differing from 0 or  $\pi$  belong to them.

The broadening of the single levels due to the interaction between the superimposed bases causes a decrease in the first excitation energies. In Table XVIII these values (the energy differences of the upper ends of the highest filled bands and the lower ends of the lowest empty bands, the so-called forbidden band widths) are given.

TABLE XVIII. First Excitation Energies  
of Polynucleotides in  $\beta$  Units

	$\Delta E$ (polynucleotide)	$\Delta E$ (single base)
T	1.48	1.53
U	1.51	1.56
C	1.36	1.43
A	1.23	1.32
G	1.39	1.48

From Table XVIII it is obvious that in consequence of the interactions in the polynucleotide chain the decrease in the first excitation energy changes between  $0.05\beta$  and  $0.09\beta$ . This decrease is not too large, but it is not negligible ( $0.09\beta \approx 0.30$  eV).

## IX. CONSIDERATIONS ON THE BAND STRUCTURE OF REAL DNA AND ITS CONDUCTING PROPERTIES

In a real DNA macromolecule there are interacting A-T and G-C base pairs superimposed. The calculation of the band structure of an

$$\begin{array}{ccccccc} & \text{A} & \text{G} & \text{A} & \text{G} & \text{A} & \text{G} \dots \\ & | & | & | & | & | & | \\ \text{of an} & \text{T} & \text{C} & \text{T} & \text{C} & \text{T} & \text{C} \dots \end{array}$$

model for instance would require the solution of



a complex determinantal equation of the order of 40 which is equivalent to a real determinantal equation of the 80th order (see for instance refs. 13a and 25). Such calculations have at present been performed only for smaller determinantal equations because of the enormous amount of numerical work required.

TABLE XIX. The MO Energies of the A-T and G-C Base Pairs and the Approximate Levels of the  $\frac{A-T}{G-C}$  System in  $\beta$  Units with an Indication of the Qualitative Band Structure

A—T		A—T G—C		G—C	
		—1.079	III	—1.079	II
—0.945	II	—0.945	II		
		—0.832	I	—0.832	I
—0.803	I	—0.803			
		0.355	1	0.355	1
0.451	1	0.451			
0.533		0.533			
		0.554		0.554	2
		0.648		0.648	
0.903	2	0.903	2	0.991	3
1.086	3	0.991			
		1.086		1.107	4
1.149		1.107			
		1.149	3	1.335	5
		1.335		1.730	6
		1.730	4		
1.736	4	1.736			
1.755		1.755			
1.798		1.798			
		2.123	5	2.123	7
2.162	5	2.162		2.177	
		2.177			
		2.593	6	2.593	8
2.775	6	2.775	7		
3.110	7	3.110	8		
		3.382	9	3.382	9
		3.457		3.457	
3.529	8	3.529			

We can, however, qualitatively estimate the band structure of a real DNA molecule with the aid of the energy levels of the A-T and G-C base pairs given in Table VII. If we are taking on the basis of the results obtained for the polynucleotides an average band width of  $0.10\beta$  we can determine which levels of the base pairs will broaden to bands which overlap and form a common band. In Table XIX we reproduce the bonding and the first two anti-bonding levels of the A-T and G-C base pairs without taking into account the H atoms as separate centres and we indicate the approximate levels of the  $\begin{smallmatrix} \text{A-T} \\ \text{G-C} \end{smallmatrix}$  model system, and show which levels will have overlapping bands.

In Table XX we reproduce from Table VII the levels and approximate levels of the same systems now taking into account the H atoms as separate centres and we indicate again the probable band structure.

We can see from Tables XIX and XX that with the assumption of  $0.10\beta$  as band width we get for a DNA molecule which is built up of interacting adenine-thymine units only eight distinct filled bands in both approximations [A-T and A-T(H)]. These are indicated in the left-hand columns of Tables XIX and XX with Arabic numbers (the Roman numbers indicate the empty bands).

At the same time for a DNA molecule which consists only of superimposed G-C base pairs we get in both approximations nine filled bands (indicated in the right-hand columns of the tables).

Assuming as model system a DNA double helix which has the periodic sequence  $\begin{smallmatrix} \text{A G A G A G} \dots \\ | \quad | \quad | \quad | \quad | \quad | \\ \text{T C T C T C} \dots \end{smallmatrix}$  we get nine filled bands in both approximations again. These are shown in the middle of the tables. The MO energies of the superimposed interacting A-T and G-C base pairs treated as a common system will of course differ somewhat from the levels of the free A-T and G-C base pairs indicated in the tables. We have seen, however, from the comparison of the levels of two superimposed bases and their constituent bases (see Section VI) that the perturbation of the original levels of the subsystems is not too large. Thus it is to be expected that the levels given in the middle of the tables will not differ very much from the bands of the  $\begin{smallmatrix} \text{A-T} \\ \text{G-C} \end{smallmatrix}$  common system. Therefore it seems probable, that the band structure of a DNA macromolecule with this model sequence will be very similar to the qualitative band structures given in the middle

TABLE XX. The MO Energies of the A-T(H) and G-C(H) Base Pairs and the Approximate Levels of the  $\frac{\text{A-T(H)}}{\text{G-C(H)}}$  Model System in  $\beta$  Units with the Indication of the Qualitative Band Structure

A-T(H)		$\frac{\text{A-T(H)}}{\text{G-C(H)}}$		G-C(H)	
-0.719	II	-0.719	II	-0.673	II
-0.494	I	-0.673		-0.464	
		-0.494	I	0.443	I
		-0.464			
0.525	1	0.443	1	0.672	2
0.624		0.525		0.923	
		0.624	2	1.134	4
		0.672		1.215	
1.057	2	0.923	3	1.375	5
1.148		1.057		1.759	
1.289	3	1.134	4	2.183	7
		1.148		2.247	
		1.215	5	2.597	8
		1.289		3.417	
1.756	4	1.375	6	3.459	9
1.769		1.756			
1.800		1.759	7		
		1.769			
		1.800	8		
		2.183			
2.199	5	2.199	9		
		2.247			
		2.597			
2.784	6	2.784			
3.118	7	3.118			
		3.417			
		3.459			
3.551	8	3.551			

columns of Tables XIX and XX. In a real DNA macromolecule, however, according to our present knowledge, there are no periodical sequences of the bases. It is probable, however, that its energy-band structure will not differ greatly from the qualitative scheme given above. Of course, further investigations on the band structure of DNA are necessary to get a more accurate picture.

Taking the band structures given in the middle of Tables XIX and XX as zero order approximations for the energy bands of the real DNA molecule we can arrive at some conclusions regarding its conducting properties. Since according to this scheme DNA in its ground state has completely filled valence and completely empty conduction bands (bands 1 and I), it will be in its ground state an insulator. At the moment, however, when by natural radiation (sunshine, radioactive radiation, cosmic radiation), or by thermal excitation some electrons will get into the conduction band there remain some positive holes in the valence band, it will be conductive. Assuming again the widths of the energy bands to be  $0.10\beta$ , we can estimate the width of the forbidden band between the highest filled and lowest empty band in DNA. We obtain in the case where we are not considering the H atoms as separate centres (see Table XIX),  $\Delta E = (0.355 + 0.803 - 0.10)\beta = 1.058\beta = 1.058 \times 3.33 = 3.52 \text{ eV}$  and, with the data given in Table XX,  $\Delta E = (0.443 + 0.464 - 0.10)\beta = 0.807\beta = 2.69 \text{ eV}$ . ( $|\beta| = 3.33 \text{ eV}$  is the average of the  $\beta$  values fitted to the absorption maxima of the single bases occurring in DNA.) Taking into account that both simple approximations of the interaction of the  $\pi$ -electron clouds through the hydrogen bonds in the base pairs are only very crude first approximations (see Section V), we can conclude only that the forbidden band width in DNA is probably between these two values. It is to be hoped, however, that with the improvement of the approximations involved it will be possible to get a more well-defined value for this quantity.

Recently, Eley and Spivey<sup>10</sup> have measured the d.c. conductivity of dry DNA samples and have found at  $400^\circ\text{K}$  a specific resistance of  $\rho = 5.10^{11} \text{ ohm. cm}$ . They have concluded that the semiconductivity found in DNA is purely electronic and from the change of the specific conductivity with temperature they have obtained for the forbidden band width the value  $\Delta E = 2.42 \pm 0.05 \text{ eV}$ . These measurements have supported, from experimental point of view, the theoretically predicted delocalization of the  $\pi$  electrons along the long axis of the whole macromolecule.<sup>13,26</sup> On the other hand Duchesne and his co-workers<sup>8</sup> have concluded from their previous conductivity measurements the value for a forbidden band width of  $1.80 \text{ eV}$ .\*

\* See Note added in proof, p. 158.

It should be mentioned that we have obtained the qualitative band structures described above within the framework of the simple Hückel approximation. When we are also taking into account explicitly the interactions between the  $\pi$  electrons it may happen that the band structure will change essentially. Further the probability for the transition between the highest filled and lowest empty bands is also rather low. (See Sections V and VI.) Therefore it seems very probable that the excitation energy by light will not be very different in the case of the DNA molecule from those in the cases of the single bases ( $\Delta E \approx 4.80$  eV).

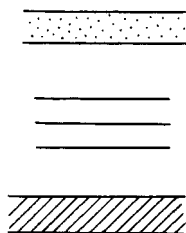


Fig. 20. Impurity levels between two energy bands.

The experimentally found activation energy (forbidden band width) refers, however, to an equilibrium state of the electron distribution which does not include a photoconductive property with the same activation energy. Therefore the triplet band may be inpopulated although the singlet-triplet transition by electromagnetic transition is forbidden. In this case also transitions between different bases may be more probable. Since the experiments show finite conductivity, there probably must be electrons in the triplet band or holes in the singlet band. The development of such a state is probably promoted by the fact that in a real DNA molecule there are always impurities and crystal imperfections which cause additional energy levels in the system. Thus an electron may go to the conduction band stepwise with the aid of these additional levels (see Fig. 20). For the further investigation of the problem it will be necessary in the future to calculate the energy band structure of DNA also in higher approximations.

## X. WORKING HYPOTHESIS FOR THE MECHANISM OF DNA DUPLICATION AND TUMOUR DEVELOPMENT

As we have seen in the preceding section, in consequence of thermal excitations and the natural radiation background, DNA has some charge carriers in its conduction band and positive holes in its valence band. It should be mentioned that when DNA comes into interaction with electron donor or acceptor molecules (molecules with low-lying first unfilled or high-lying highest filled levels), it is probable that it will take up or give off an electron and thus its conductivity will be increased. This is supported by the position of the levels of the base pairs given in Table VII, according to which the base pairs may be donors or acceptors (Fig. 22).

We may further assume the presence of strong local electric fields within the cell produced by dipole molecules, ion concentration fluctuations, etc., and by the inner field of a nucleoprotein.\* Thus a DNA molecule which has mobile charges will be polarized depending on its orientation with respect to the direction of the field (see Fig. 21). For the details of the polarization mechanism and the problem of recombination of excitons (electron-positive hole pairs) see ref. 13.

If the mobile  $\pi$  electrons or positive holes in the DNA double helix are separated by an electrostatic field, there will be a repulsion between the charges situated at the same end of the two helices. To have a rough estimate of the potential energy of this repulsion, we have calculated the classical repulsion energy between two elementary charges, one situated at the centre of a Py ring and the other at the midpoint of that C—C bond which is in annelation in the Pu ring. Using the geometry of the Watson-Crick base pairs,<sup>51</sup> we get for the distance of the two charges 6.70 Å (see Fig. 23). With this value we get for the potential energy

$$V = \frac{e^2}{r} = \frac{4.82 \times 10^{-20}}{6.7 \times 10^{-8}} = 3.44 \times 10^{-12} \text{ erg} \approx 50 \text{ kcal/mole} \quad (55)$$

\* An ideal DNA double helix would not have any resulting inner field but if there are impurities or lattice imperfections in the macromolecule, these may cause a resultant field. Further, in a nucleoprotein there is around the DNA double helix only one protein chain which has a resultant electric field due to its dipole moments and this may also contribute to the electric field within the DNA molecule.

On the other hand according to the Watson-Crick duplication mechanism of DNA which proved to be correct,<sup>53</sup> the duplication begins with the unwinding of the two helices. For this unwinding

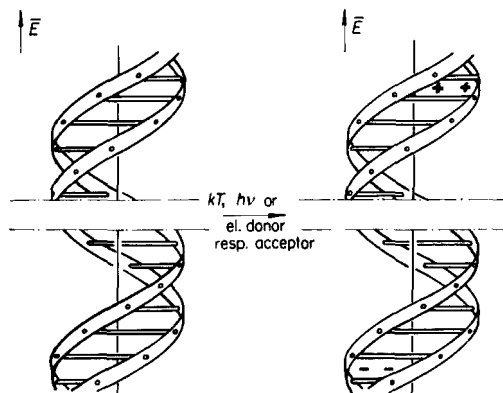


Fig. 21. Schematic representation of the polarization of a DNA double helix.

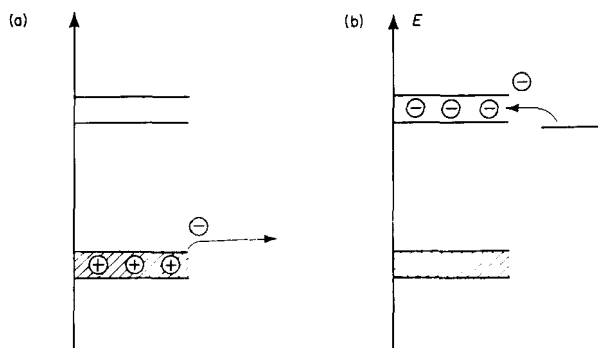


Fig. 22. Schematic representation of the effect of an (a) electron acceptor, (b) electron donor molecule on DNA. The donor molecules give electrons to the conduction band, the acceptor molecules take away electrons from the valence band and so increase the number of positive holes in it. Both cases lead to increased conductivity.

it is necessary to break the hydrogen bonds of the base pairs and to overcome also their extra stability provided by the delocalization of their  $\pi$ -electron systems through the hydrogen bonds.

The energy of the hydrogen bonds is for A-T  $\sim 4.0$  kcal/mole and for G-C  $\sim 6$  kcal/mole.<sup>13</sup> For the delocalization energies we have obtained (see Section V) in the A-T case  $1.20\beta$ , in the G-C case  $1.90\beta$ , when we are taking into account the H atoms as separate centres, while without H centres we have obtained practically no delocalization energy. Since both approximations of the electronic structure of the base pairs are very crude, the

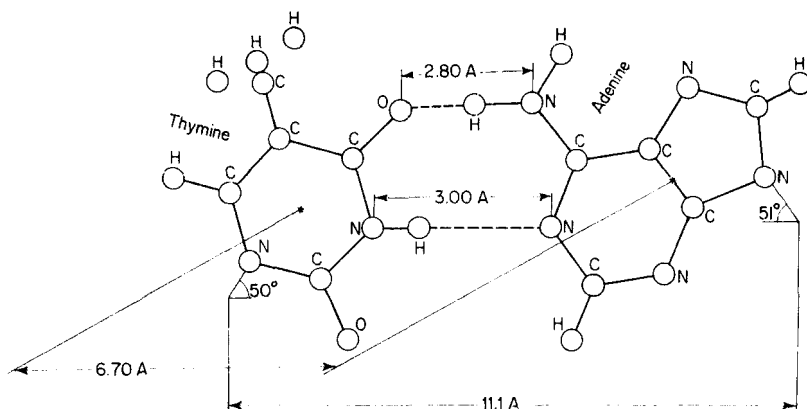


Fig. 23. Geometry of positions of charges in an A-T base pair.

delocalization energies obtained do not seem to be trustworthy. It seems probable that their real values are essentially smaller than the figures obtained in the second approximation. Therefore taking 16 kcal/mole for the value of  $\beta$ ,\* we may write for the energies necessary for breaking a base pair

$$\begin{aligned}\Delta E_{A-T} &= \epsilon_{H.b.} + \epsilon_{deloc.} < 4 + 19 = 23 \text{ kcal/mole} \\ \Delta E_{G-C} &= \epsilon_{H.b.} + \epsilon_{deloc.} < 6 + 30 = 36 \text{ kcal/mole} \quad (56)\end{aligned}$$

Here  $\epsilon_{H.b.}$  denotes the sum of the energies of the H bonds and  $\epsilon_{deloc.}$  stands for the delocalization energy.

\* It is a consequence of the semi-empirical nature of the simple Hückel approximation that for the calculation of delocalization (resonance) energies we have to use for  $\beta$  the value 16 kcal/mole to fit the experimental data, while for the calculation of excitation energies the much larger  $\beta = 3.33$  eV = 77 kcal/mole value has to be used to reach an agreement with the experiments.



Comparing the values in Eqs. (55) and (56) we can see that the repulsion between two elementary charges may cause the breaking of at least one base pair. Of course it is necessary to perform quantum mechanical calculations for the repulsion between two negatively or positively charged bases and it is probable that in the interacting  $\pi$ -electron system of DNA there will be only partial net charges on the bases at the end of the molecule due to the assumed polarization mechanism. Therefore it seems probable that the value

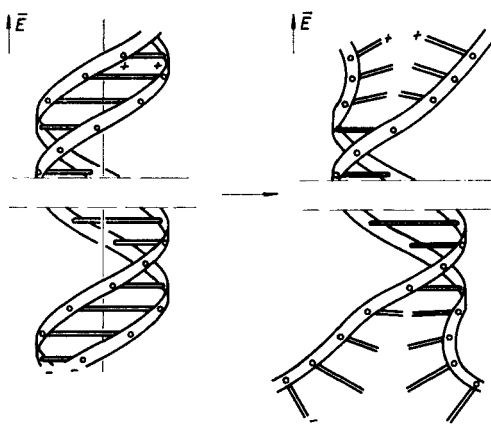


Fig. 24. The beginning of the unwinding of DNA in consequence of the repulsion between the two charged helices at the ends of the molecule.

in Eq. (55), as well as the values given in Eqs. (56) are overestimated. We feel, however, that more accurate calculations will give results of the same order of magnitude. Therefore it seems plausible to us to accept the qualitative statement that the repulsion energy between the net charges of polarized bases may cause the breakage of base pairs and may thereby induce step by step the unwinding of the two helices of DNA (see Fig. 24).

In connection with the assumption of unwinding induced by the repulsion of electric charges it should be pointed out that since DNA is a polyelectrolyte which is also *in vivo* partially dissociated and surrounded by counter-ions in an aqueous solution, the effect of the above-mentioned local electric fields within the cell can cause the polarization of this inner ionic atmosphere too. This polarization may induce very large dipole moments ( $10^6$  Debye units), as found

by Eigen and Schwartz<sup>9</sup> in their investigations of DNA in aqueous solution exposed to an outer electric field. Therefore it seems very probable that the unwinding process of DNA is not only a function of the polarization of the mobile  $\pi$  electrons, but also a function of the polarization of the ions surrounding the DNA molecule.

It is well known that the mitosis frequency of different cells is a function of species, age, the kind of cells and the state of the tissues to which the cells belong. It is evident that a control mechanism must function which determines the frequency of mitosis. It is not known, however, what the physical mechanism of this regulating system is. On the basis of the considerations described above, we are of the opinion that there are two factors, the number of mobile charges in DNA and the electrostatic field strength in it, which determine the frequency of DNA duplications. The number of mobile charges is determined by (1) the temperature within the cell, (2) the natural radiation level (sunshine, radioactive, cosmic radiation), (3) the concentration of molecules with electron-donor or -acceptor properties in the neighbourhood of DNA, and (4), in the case where the mobile "inner" ionic atmosphere of DNA also takes part in the regulation, all the factors which influence the dissociation of DNA molecules. The electrostatic field strength in DNA is determined, first of all, by (1) the impurities and crystal imperfections in DNA, (2) the dissociation of DNA, and (3) the concentration of molecules with large dipole moments in the neighbourhood of DNA. We assume that all these factors together form a very complicated self-regulating system for DNA duplication and mitosis.

In the case where the level of radiation to which the DNA molecules are exposed or the concentration of electron-donor or -acceptor molecules in the cell is increased, the number of mobile charges will also increase in DNA. It is known, on the other hand, that in some cases almost all condensed aromatic hydrocarbons have electron donor or acceptor properties. It has been reported by Szent-Györgyi<sup>54</sup> that carcinogenic hydrocarbons form charge transfer complexes with a  $I_2$  acceptor, but the non-carcinogenic ones do not. On the other hand Tüdös and Turcsányi<sup>56</sup> have found that carcinogenic and non-carcinogenic hydrocarbons form charge transfer complexes with different quinones. The apparent discrepancy of the two results can be resolved if we take into account

that according to Szent-Györgyi<sup>54</sup> the charge-transfer formation reaction of the aromatic hydrocarbons takes place through the local reaction of one or two highly charged C atoms with  $I_2$ , while in the cases of the reaction with quinones there is a great probability for such an interaction when the planes of the two interacting molecules are parallel ( $\pi$  complexes<sup>55</sup>).

Thus the carcinogenic hydrocarbons form charge-transfer complexes probably with "localized" interaction of their so-called *K* zone with protein or DNA constituents\* and this is expressed by the criteria for their specificity. Further experimental and theoretical investigations are of course necessary to elucidate the mechanism of the carcinogens. It is our opinion, in agreement with Mason,<sup>31</sup> that the charge transfer by carcinogens is the crucial point of their mechanism of action.

Assuming that the carcinogens are able to increase the number of mobile charges in DNA, their effect on DNA duplication will be the same as that of excitations or ionizations by irradiation. In both cases the increase of mobile charges in DNA will result in a higher degree of polarization and cause a DNA duplication sooner, as determined by the control system of the cell.

In the case where a large number of DNA particles within many cells of a tissue will duplicate at an irregular time as the result of irradiation or the action of carcinogens, it is probable that the stationary equilibrium of these cells will change to a new stationary equilibrium with a higher DNA, RNA and protein synthesis rate, thus with higher metabolic rate and with an increase of the mitosis frequency. This assumption is supported by the kinetic analysis of the rates of syntheses of nucleic acids and proteins in bacteria performed by Hinshelwood<sup>12</sup> who has found that the rate of protein synthesis is proportional to the nucleic acid concentration and the rate of the nucleic acid synthesis is proportional to the protein concentration. Thus it is imaginable that a rapid increase of

\* It is at present not clear as to which compound the carcinogenic hydrocarbons are primarily bound. According to some experimental results<sup>45</sup> they are bound to the protein of the ribosomes, but A. and B. Pullman<sup>40</sup> do not exclude the possibility of direct interaction with nucleotide bases. It should be mentioned that in the case where the carcinogens are primarily really bound to proteins, according to our opinion the possibility of secondary action on the electronic structure of DNA cannot be excluded.

the DNA content of a cell may increase the rate of the messenger RNA synthesis, the latter the rate of the synthesis of proteins. Since proteins form the enzymes necessary to DNA synthesis, these can keep the DNA synthesis on the new higher level and so we have a new stationary state for the cell. For the proof of this assumption it would be very interesting to perform an irreversible thermodynamical investigation of the problem taking into account the known control mechanisms of DNA, RNA and protein syntheses. More detailed experimental investigations are needed too.

The assumed new stationary state of the cells with a high rate of DNA synthesis and more frequent mitoses is preserved also after the radiation or carcinogenic effect. If it takes place in many cells of an organism it will lead as a first step to an increased normal growth. Perhaps the known growth stimulating effects of small doses of radiation can be interpreted in this way.

Turning now to the problem of tumour development it is a widely accepted assumption of the biochemists that the base sequence of the DNA molecules in tumour cells is changed from the sequence of the appropriate normal cells. Further it seems probable that the development of this "cancerous information" is the cause in the last analysis of the development of tumours. A normal cell can reach this cancerous sequence also by chance with the accumulation of the errors<sup>60</sup> which can be introduced in the original base sequence with the aid of the mutation mechanism described in Section IV.

Thus by each duplication cycle there is a small but non-zero  $P_i(j)$  probability that at a definite position instead of the base  $j$ , the base  $i$  will enter into the DNA chain. It is assumed that this is the mechanism of the development of spontaneous tumours in old age.<sup>60</sup>

In the case where the frequency of the DNA duplications will be increased with the assumed mechanism of radiations or of carcinogens, this accumulation of errors will also be increased and so the cancerous sequence can be reached sooner. Thus the increased normal growth can be easily transformed into a cancerous state.

On the other hand, as we have mentioned in Section IV, it seems probable that the excitations or ionizations caused by radiations (and the ionizations caused by carcinogens) increase the probabilities of the tautomeric rearrangements also within one duplication cycle.

Thus, in consequence of this second assumed effect of radiations and carcinogens, the number of errors in one duplication cycle will also be increased and so the carcinogenic state can be reached yet more quickly.

We should like to emphasize again that the working hypothesis described reflects only our personal points of view based on our present knowledge of the electronic structure of DNA. This means that on the basis of more detailed theoretical and experimental investigations\* to be done in the future, its details should be continuously corrected. It seems, however, to be a useful framework for our investigations and we hope that some parts of it may be stimulating for other investigators too.

## XI. ACKNOWLEDGEMENTS

We should like to express our gratitude to Professor I. Rusznyák, President of the Hungarian Academy of Sciences, for his valuable remarks on the biological aspects and his encouraging interest; to Professor P. O. Löwdin for his useful remarks and advice, and for making possible for one of us (J. L.) to perform a part of the calculations in his group; to Professor C. A. Coulson for several useful remarks; to Professor B. Pullman and Dr. A. Pullman for their criticism and helpful remarks; to Professor G. Schay for calling our attention to important data in the literature; and to Professors I. Törö and F. B. Straub for their valuable remarks on the biological side of the problem.

We are greatly indebted to Professor L. Goodman, Professor D. Shugar, Dr. J. Koutecký, Dr. K. Ohno, Dr. M. Eigen, Dr. L. Hofacker, Dr. J. Paldus, Dr. C. Valdemoro and Mr. G. Biczó for putting at our disposal some of their results before publication, and for stimulating and valuable discussions. We are very grateful to Dr. K. Appel, Mr. J. Szelezsán, Mrs. H. Hoffmann and Miss J. Rédly for performing the programming and numerical calculations. Finally we should like to express our thanks to the CHINOIN Pharmaceutical Factory for its financial support of this research.

\* In another paper which was published recently,<sup>1a</sup> some results about the observed changed behaviour of some biological objects placed in a strong electrostatic field were reported.

## References

1. Beaven, G. H., Holiday, E. R., and Johnson, E. A., "Optical Properties of Nucleic Acids and Their Components", in Chargaff, E. and Davidson, J. N., Eds., *The Nucleic Acids*, Vol. I, Academic Press, New York, 1955.
- 1a. Bozóky, L., Kiszely, Gy., Hoffmann, T. A., and Ladik, J., *Nature* **199**, 1306 (1963).
2. Coulson, C. A., and de Heer, J., *Trans. Faraday Soc.* **74**, 681 (1951).
3. Crick, F. H. C., and Watson, J. D., *Proc. Roy. Soc. (London)* **A223**, 80 (1954).
4. Crick, F. H. C., Barnett, L., Brenner, S., and Watts-Tobin, R. I., *Nature* **192**, 1227 (1961).
5. Daudel, R., Lefebvre, R., and Moser, C., *Quantum Chemistry*, Interscience, New York-London, 1959, Chapter X.
6. Daudel, R., *et al.*, *loc. cit.* Chap. IX.
7. Davies, D. W., *Trans. Faraday Soc.* **51**, 449 (1955).
8. Duchesne, J., Depireux, J., Bertinchamps, A., Cornet, N., and van der Kaa, J. M., *Nature* **188**, 405 (1960).
9. Eigen, M., and Schwartz, G., "Structure and Kinetic Properties of Polyelectrolytes in Solution, Determined from Relaxation Phenomena in Electric Fields", in *Electrolytes*, Pergamon Press, Oxford-London-New York-Paris, 1962, p. 309.
10. Eley, D. D., and Spivey, D. I., *Trans. Faraday Soc.* **58**, 411 (1962).
- 10a. Héden, C. G., and Rupprecht, A., personal communication.
11. Hellmann, H., *Einführung in die Quantenchemie*, Deutsche Verlag, Leipzig-Wien, 1937, pp. 338 and 339.
12. Hinshelwood, C. N., *The Chemical Kinetics of the Bacterial Cell*, Clarendon Press, Oxford, 1946.
13. Hoffmann, T. A., and Ladik, J., *Cancer Res.* **21**, 474 (1961).
- 13a. Hoffmann, T. A., and Hoffmann, H., unpublished results.
- 13b. Hoffmann, T. A., *Acta Phys. Acad. Sci. Hung.* **14**, 177 (1962).
- 13c. Hoffmann, T. A., and Ladik, J., *J. Theoret. Biol.* (in press).
- 13d. Hoffmann, T. A., Ladik, J., and Udvardy, A., *Acta Phys. Acad. Sci. Hung.* **13**, 113 (1961).
14. Jordan, D. O., "The Physical Properties of Nucleic Acids" in E. Chargaff and Davidson, J. N., Eds., *The Nucleic Acids*, Vol. I, Academic Press, New York, 1955.
15. Josse, J., Kaiser, A. D., and Kornberg, A., *J. Biol. Chem.* **236**, 864 (1961).
16. Kasha, M., Ashraf El Bayoumi, M., and Rhodes, W., *J. Chim. Phys.* **58**, 916 (1961).
17. Koutecký, J., personal communication.
18. Koutecký, J., Paldus, J., and Zahradník, R., *J. Chem. Phys.* **36**, 3129 (1962).
19. Koutecký, J., and Paldus, J., *Collection Czech. Chem. Commun.* **27**, 599 (1962).
20. Koutecký, J., and Zahradník, R., *Collection Czech. Chem. Commun.* **25**, 811, (1960).

21. Ladik, J., and Appel, K., *Technical Note of the Quantum Chemistry Group*, University of Uppsala, No.78 (1962).
22. Ladik, J., *Acta Phys. Acad. Sci. Hung.* **15**, 287 (1963).
23. Ladik, J., unpublished result.
24. Ladik, J., *Acta Phys. Acad. Sci. Hung.* **13**, 473 (1961).
25. Ladik, J., and Appel, K., *Technical Note of the Quantum Chemistry Group*, University of Uppsala, No.79 (1962).
26. Ladik, J., *Acta Phys. Acad. Sci. Hung.* **11**, 239 (1960).
27. Langridge, R., Wilson, H. R., Hooper, C. W., Wilkins, M. H. F., and Hamilton, L. D., *J. Mol. Biol.* **2**, 38 (1960).
28. Lengyel, P., Speyer, J. F., and Ochoa, S., *Proc. Natl. Acad. Sci. U.S.* **47**, 1936 (1961).
29. Leslie, J., *Nature* **189**, 260 (1961).
- 29a. Liang, C. Y., and Scalco, E. G., *Nature* **198**, 86 (1963).
30. Löwdin, P. O., personal communication.
31. Mason, R., *Nature* **181**, 820 (1958).
32. Mataga, N., and Nishimoto, K., *Z. Physik. Chem.* **13**, 140 (1957).
33. Nirenberg, M. W., and Matthaei, J. H., *Proc. Natl. Acad. Sci. U.S.* **47**, 1588 (1961).
34. Ohno, K., personal communication.
- 34a. Paoloni, L., *Nuovo Cimento* **4**, 410 (1956).
- 34b. Paoloni, L., *J. Chem. Phys.* **30**, 1045 (1959).
35. Pariser, R., and Parr, R. G., *J. Chem. Phys.* **21**, 466 (1953); **21**, 767 (1953).
36. Pople, J. A., *Trans. Faraday Soc.* **49**, 1375 (1953).
37. Preuss, H., *Integraltafeln zur Quantenchemie*, Vol. I, Springer Verlag, Berlin-Göttingen-Heidelberg, 1953, pp. 43, 78 and 82.
38. Pritchard, H. O., and Skinner, H. A., *Chem. Rev.* **55**, 745 (1955).
39. Pullman, A., and Pullman, B., *Bull. Soc. Chim. France* 766 (1958); 594 (1959).
40. Pullman, A., and Pullman, B., *Biochim. Biophys. Acta* **36**, 343 (1959).
41. Pullman, B., and Pullman, A., *Rev. Mod. Phys.* **32**, 428 (1960).
42. Pullman, A., and Pullman, B., *Advan. Cancer Res.* **3**, 117 (1955).
- 42a. Pullman B., and Pullman, A., *Biochim. Biophys. Acta* **64**, 403 (1962).
- 42b. Pullman, A., *Compt. Rend.* (in press).
- 42c. Valdemoro, C., personal communication.
43. Reitz, J. R., *Solid State Physics*, Vol. I, Academic Press, New York, 1955, p. 1.
44. Rhodes, W., *J. Am. Chem. Soc.*, **83**, 3609 (1961).
45. Rondoni, P., *Advan. Cancer Res.* **3**, 171 (1955).
46. Roothaan, C. C. J., *Rev. Mod. Phys.* **23**, 61 (1953).
47. Roothaan, C. C. J., *Rev. Mod. Phys.* **32**, 179 (1960).
48. Shugar, D., personal communication.
49. Slater, J. C., *Phys. Rev.* **36**, 57 (1930).
50. Spencer, M., *Acta Cryst.* **12**, 59 (1959).
51. Spencer, M., *Acta Cryst.* **12**, 66 (1959).
52. Speyer, J. F., Lengyel, P., Basilio, C., and Ochoa, S., *Proc. Natl. Acad. Sci. U.S.* **48**, 63 (1962).

53. Stent, G. S., *Genetic Experiments on the Replication of Bacteriophage DNA*, Plenary lecture at the First Intern. Biophysics Congress, Stockholm, 1961.
54. Szent-Györgyi, A., "On Charge Transfer", in *Application a la Biochimie et a la Chimie Structurale de la Spectroscopie des Radiofrequences*, Palais des Academies, Bruxelles, 1961, p. 162.
55. Tinoco, I., *J. Am. Chem. Soc.* **82**, 4785 (1960).
56. Tüdös, F., and Turcsányi, B., *Magy. Kém. Folyóirat.* **68**, 228 (1962).
- 56a. Veillard, A., and Pullman, B., *Compt. Rend.* **253**, 2277 (1961); *J. Theor. Biol.* **4**, 37 (1963).
57. Watson, J. D., and Crick, F. H., *Nature* **171**, 737 (1953); **171**, 964 (1953).
58. Watson, J. D., and Crick, F. H. C., *Cold Spring Harbor Symp. Quant. Biol.* **18**, 123 (1953).
59. Woese, C. R., *Nature* **194**, 1114 (1962).
60. Yockey, H. P., "A Study of Aging, Thermal Killing and Radiation Damage by Information Theory", in H. P. Yockey, Ed., *Symposium on Information Theory in Biology*, Pergamon Press, London-New York-Paris-Los Angeles, 1958, p. 297.

*Note added in proof.* The measurements are very sensitive to the change of water content of the sample and this explains the large difference in the measured values. Recently the measurements of Liang and Scalco<sup>29a</sup> of photoconductivity and those of Héden and Rupprecht<sup>10a</sup> on oriented DNA have shown similar values to those obtained by Eley and Spivey.



### 3

## ELECTRONIC STRUCTURE AND MAGNETIC PROPERTIES OF HEMOPROTEINS, PARTICULARLY OF HEMOGLOBINS

MASAO KOTANI, *Department of Physics, Faculty of Science,  
 The University of Tokyo, Bunkyo-ku, Tokyo, Japan*

### CONTENTS

I. Introduction . . . . .	159
II. Energy Levels of Free Atoms and Ions Containing Incomplete Shells . . . . .	161
III. Magnetic Moment . . . . .	164
IV. Cubic Ligand Field; Splitting of <i>d</i> Orbitals; High and Low Spin	167
V. Incomplete Quenching of Orbital Magnetic Moment in ( <i>dε</i> ) <sup>5</sup> .	170
VI. Analysis of EPR Data on a Ferrihemoglobin Derivative with Low Spin . . . . .	172
VII. Property of <sup>6</sup> S State in Ferrihemoglobin Fluoride . . . . .	174
VIII. Electronic Structure of Iron in Ferrohemoglobin . . . . .	177
References . . . . .	181

### I. INTRODUCTION

Studies on the *electronic* structure of biological substances are essential to the fundamental understanding of their biological activities. Electronic structures can be studied by optical spectroscopy, dielectric polarization, hyper- and hypochromism, rotatory dispersion and other methods, and some of them provide powerful means of determining higher order structures of these macromolecules.

Magnetic methods are, however, characterized by a unique feature that particularly detailed information about the electronic structures of molecules can be obtained but the applicability is limited to special group of molecules. Electron paramagnetic resonance (EPR) and measurement of static magnetic susceptibility are the two major magnetic methods; these methods are applicable only when the molecules of the substance shows paramagnetism. This condition restricts the use of the method rather

severely. This intrinsic limitation however, is not necessarily a shortcoming of the method; it may be regarded even as a merit in the sense that a very small number of electrons with unpaired spins can be sensitively detected without destroying the structure of the sample examined.

Biological substances having electrons with unpaired spins can be classified into two groups. The first group is comprised of free radicals with an odd number of electrons and those molecules with an even number of electrons in which spins of two electrons are coupled parallel yielding a triplet state. Semiquinone, which is formed in the process of oxidation of hydroquinone or reduction of quinone, is a typical example of such free radicals. Quite a number of papers have been published on EPR and susceptibility studies of these free radicals.<sup>1</sup>

The other group of biological substances which can be used as objects of magnetic studies consists of molecules containing atoms or ions of transition metal elements. Biological molecules are known which contain V, Mn, Fe, Co, Mo, etc.; but among them the most important and thoroughly studied substances are the hemoproteins, including hemoglobin, myoglobin, catalase, peroxylase, cytochromes, etc. In this chapter the results of magnetic studies on hemoproteins and the theoretical interpretations of these results will be briefly described.

A hemoprotein has a heme as its prosthetic group, which forms the active center of the molecule as far as its biological activity is concerned. Iron in the heme of hemoglobin or myoglobin binds an oxygen molecule reversibly, a function which is important to the transport and storage of oxygen in the animal body. In cytochromes, the valency of the iron alternates between 2 and 3 during its catalytic action in the electron transport processes involved in cellular respiration. Thus the hemoproteins are particularly convenient and profitable objects for research among proteins in general, because their active centers have been identified and their electronic structures are known fairly accurately. Furthermore, in the cases of myoglobin and hemoglobin, their higher order structures have been unveiled through elaborate X-ray analysis of crystalline samples by Perutz<sup>2</sup> and by Kendrew,<sup>3</sup> which is another point favoring choice of these molecules as objects of detailed studies.

## II. ENERGY LEVELS OF FREE ATOMS AND IONS CONTAINING INCOMPLETE SHELLS

In this section some basic features are explained concerning the electronic structure of atoms and ions in free states, i.e. in the absence of any external fields.

In the orbital approximation developed essentially by Hartree and Hartree-Fock, each electron in an atom is assigned to a definite orbit. In a quantum-mechanical description an orbit is represented by a one-electron wave function, which is called an orbital function or simply an "orbital". These orbitals are classified into  $s$ ,  $p$ ,  $d$ , and other orbitals according to the angular dependence of the orbital functions. In terms of Cartesian coordinates  $x$ ,  $y$ ,  $z$  of the electron, with its origin at the nucleus, an  $s$  orbital is a function of  $r = \sqrt{x^2 + y^2 + z^2}$  only, while the  $p$  orbital and  $d$  orbital, respectively, can be expressed in the following way:

$$R_p(r) \frac{1}{r} (ax + by + cz), \quad a, b, c, \text{ arbitrary}$$

$$R_d(r) \frac{1}{r^2} (ax^2 + by^2 + cz^2 + 2dyz + 2ezx + 2fxy),$$

$$a + b + c = 0, \text{ otherwise } a, b, c, d, e, f, \text{ arbitrary}$$

Thus,  $s$ ,  $p$ , and  $d$  orbitals have, respectively, 1, 3, and 5 linearly independent functions and a convenient set of orthonormal  $d$  orbitals is given by

$$\xi = R(r) \frac{yz}{r^2}, \quad \eta = R(r) \frac{zx}{r^2}, \quad \zeta = R(r) \frac{xy}{r^2} \quad (1)$$

$$u = R(r) \frac{2z^2 - x^2 - y^2}{2\sqrt{3}r^2}, \quad v = R(r) \frac{x^2 - y^2}{2r^2} \quad (2)$$

The electron has an intrinsic angular momentum, called spin; the spin of an electron can assume only two directions in space, i.e. there are only two linearly independent spin functions for a single electron. Let these two functions be denoted by  $\alpha$  and  $\beta$ . When an electron is describing an orbit, say  $\xi$ , and its spin is in the state  $\alpha$ , the complete description of the state of this electron is given by the combination  $(\xi, \alpha)$ . Such a combination of an orbital and a spin

state is called a "spin-orbital". According to the Pauli principle, a single spin-orbital can accommodate one electron at most. Since  $s$ ,  $p$ , and  $d$  states have, respectively, 2, 6, and 10 spin-orbitals, they are completely filled by these numbers of electrons, and form the so-called closed shells. Each closed shell has a spherically symmetric distribution of the charge, and the resultant spin angular momentum vanishes.

In the case of divalent or trivalent ions of the transition metal elements in the first long period, 18 electrons are filled in 5 closed shells  $1s$ ,  $2s$ ,  $2p$ ,  $3s$ ,  $3p$  and the remaining electrons are accommodated in the  $3d$  orbitals. Thus, we have the following electron configuration:

$$(1s)^2 (2s)^2 (2p)^6 (3s)^2 (3p)^6 (3d)^n \quad (3)$$

$n$  is equal to 5 for  $\text{Fe}^{3+}$ , and to 6 for  $\text{Fe}^{2+}$ .

As long as  $n$  satisfies  $1 \leq n \leq 9$ , the electron configuration (3) has an incomplete shell of  $(3d)^n$ , and the interaction among  $n$  electrons in the  $3d$  orbitals gives rise to a number of energy levels. These levels are separated by the difference in the effect of electrostatic Coulomb repulsions on electrons. These energy levels are characterized by sets of quantum numbers  $(S, L)$ , where  $S$  denotes the magnitude of the resultant spin angular momentum and  $L$  the magnitude of the resultant orbital angular momentum; more precisely, the resultant spin angular momentum possesses the magnitude  $\hbar\sqrt{S(S+1)}$ , while the resultant orbital angular momentum has the magnitude  $\hbar\sqrt{L(L+1)}$ . Symbols such as  $^3P$ ,  $^1D$ ,  $\dots$ , are employed to designate  $(S, L)$  states, in which  $L = 0, 1, 2, \dots$ , are denoted by  $S, P, D, \dots$ , respectively, and the spin multiplicity  $2S+1$  is added as the left superscript.

Since the separations between different  $(S, L)$  levels arising from a single configuration are due to the interelectronic Coulomb repulsions, they are of the order of several electron volts, or of several thousand inverse centimeters. Among the different  $(S, L)$  states arising from a single configuration, the lowest state is the one with the highest  $S$ , and if there is more than one  $(S, L)$  state for the highest  $S$ , then the state with the highest  $L$  among them gives the real ground state (Hund's rule). According to this rule the  $S$ -value of the ground state for configuration (3) is  $\frac{1}{2}n$  for  $n \leq 5$  and is  $\frac{1}{2}(10-n)$  for  $n \geq 5$ . The  $L$ -value of the ground state is  $\frac{1}{2}n(5-n)$

for  $n \leq 5$  and is  $\frac{1}{2}(10-n)(n-5)$  for  $n \geq 5$ . These  $(S, L)$  values are shown diagrammatically in Fig. 1.

If we introduce the spin-orbit interaction, an  $(S, L)$  state, which was considered to be  $(2S+1)(2L+1)$ -fold degenerate, is split into a number of states, each of which corresponds to a definite value

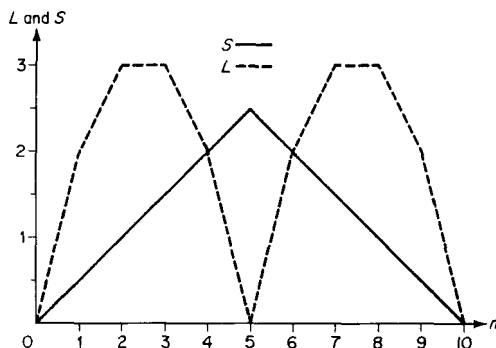


Fig. 1. Magnitude of resultant spin and orbital angular momenta in ions with  $nd$  electrons.

$J$  of the total angular momentum  $\mathbf{J} = \mathbf{S} + \mathbf{L}$ . The spin-orbit interaction is represented by an expression of the form

$$a \sum_i \mathbf{l}_i \cdot \mathbf{s}_i \quad (4)$$

where  $\mathbf{l}_i \cdot \mathbf{s}_i$  are the orbital and spin angular momenta of the  $i$ th electron, measured in the unit of  $\hbar$ , and  $a$  is the "spin-orbit coupling constant". It can be shown that the matrix of (4) within the substrates belonging to a single  $(S, L)$  level is identical to that of

$$A \mathbf{L} \cdot \mathbf{S} \quad (5)$$

if  $A$  is chosen as a suitable multiple of  $a$ . These coefficients for the normal  $(S, L)$  states of configuration (3) are given in Table I. From this table one notes that for  $1 \leq n < 5$ ,  $A$  is positive, and favors the antiparallel coupling between  $\mathbf{L}$  and  $\mathbf{S}$ , whereas for  $5 < n \leq 9$ ,  $A$  is negative, and favors the parallel coupling. In fact, expression (5) can be written as

$$\frac{A}{2} [\mathbf{J}^2 - \mathbf{S}^2 - \mathbf{L}^2] = \frac{A}{2} [J(J+1) - S(S+1) - L(L+1)] \quad (6)$$

TABLE I. Spin-Orbit Coupling Constants for the Normal States of  $(3d)^n$  Configurations

$n$	Ground ( $S, L$ )	$A$ in terms of $a$
1	$^2D$	$A = a$
2	$^3F$	$A = \frac{1}{2}a$
3	$^4F$	$A = \frac{1}{3}a$
4	$^5D$	$A = \frac{1}{4}a$
5	$^6S$	—
6	$^5D$	$A = -\frac{1}{4}a$
7	$^4F$	$A = -\frac{1}{3}a$
8	$^3F$	$A = -\frac{1}{2}a$
9	$^2D$	$A = -a$

so that for  $n < 5$  the lowest  $J$  ( $= |S - L|$ ) gives the normal state, but for  $n > 5$  the highest  $J$  ( $= L + S$ ) gives the normal state. The multiplet, i.e., the manifold of levels arising from a single  $(S, L)$ , is said to be normal for  $n < 5$ , and inverted for  $n > 5$ .

### III. MAGNETIC MOMENT

Classical electrodynamics teaches us that an electric current flowing along a small closed circuit behaves as a small magnetic dipole, and that its magnetic dipole moment  $\mu_L$  is proportional to the mechanical angular momentum  $\mathbf{l}$  of the electron; in fact

$$\mu_L = \frac{-e}{2mc} \mathbf{l} \quad (7)$$

where  $-e$  and  $m$  are the charge and the mass of the electron, respectively. According to the relativistic theory of the electron, due to Dirac, the spin angular momentum has also a magnetic dipole moment associated with it:

$$\mu_S = \frac{-e}{mc} \mathbf{S} \quad (8)$$

When there are more than one electron in the incomplete  $d$  shell,

one obtains similar formulas for the magnetic dipole moments associated with the resultant orbital and spin angular moment

$$\mu_L = \frac{-e}{2mc} \mathbf{L} \quad (9)$$

$$\mu_S = \frac{-e}{mc} \mathbf{S} \quad (10)$$

simply by adding (7) and (8) for each electron.

It is to be noted that the coefficient  $-e/mc$  in (8) and (10) is just twice the corresponding factor in (7) and (9). This situation leads to the result that the total magnetic moment of an atom

$$\mu = \mu_L + \mu_S = \frac{-e}{2mc} (\mathbf{L} + 2\mathbf{S}) \quad (11)$$

is not in general colinear with  $\mathbf{J} = \mathbf{S} + \mathbf{L}$ . This  $\mu$  can be split into two parts  $\mu_{\parallel}$  and  $\mu_{\perp}$ , the former being parallel, and latter perpendicular, to  $\mathbf{J}$ . It is easily shown that

$$\mu_{\parallel} \left( = \frac{(\mu \cdot \mathbf{J})}{\mathbf{J}^2} \mathbf{J} \right) = g \frac{-e}{2mc} \mathbf{J} \quad (12)$$

where

$$g = \frac{3}{2} + \frac{S(S+1) - L(L+1)}{2J(J+1)} \quad (13)$$

This dimensionless parameter  $g$  is called the Landé  $g$ -factor or the spectroscopic splitting factor. Since  $\mathbf{J}$  is a constant of motion in the case of a free atom,  $\mu_{\parallel}$  is also a constant of motion, but  $\mu_{\perp}$  executes a uniform precessional motion around  $\mathbf{J}$ , with an angular velocity of the order of  $\hbar/a$ .

When a uniform magnetic field  $H$  in the  $z$  direction is applied to the atom in question, a term

$$\Delta E = -\mu_z H \quad (14)$$

is added to the energy of the system. Substituting (11) into (14) one gets

$$\Delta E = -g \frac{-e}{2mc} J_z H - (\mu_{\perp})_z H \quad (15)$$

Taking the  $z$  axis as the axis of quantization of  $\mathbf{J}$ , one can write

$J_z = M\hbar$  ( $M = J, J-1, \dots, -J$ ), and the first term in (15) can be written as

$$g\mu_B MH \quad (16)$$

where  $\mu_B$  denotes the "Bohr magneton", defined by

$$\mu_B = \frac{e\hbar}{2mc} \quad (17)$$

which is the natural atomic unit of the magnetic moment.

In a state  $(S, L, J, M)$  expression (16) gives an energy proportional to  $H$ , and states for different  $M$ 's are split in such a way that they form  $2J+1$  levels equally spaced (Zeeman splitting). The second term in expression (15) has no term diagonal in  $J, M$  and gives a term quadratic in  $H$  as a result of the second-order perturbation. Then we have

$$\Delta E = g\mu_B MH - \frac{1}{2}\alpha_M H^2 \quad (18)$$

The explicit expression for  $\alpha_M$  is given elsewhere.<sup>4,5</sup> The effective magnetic moment for the state  $(J, M)$  is given by

$$(\mu_z)_{JM} = -\frac{\partial \Delta E}{\partial H} = -g\mu_B M + \alpha_M H \quad (19)$$

The first term originates from the orientation of the "permanent" dipole moment, while the second term may be considered as the magnetic moment "induced" by the applied magnetic field.

In the thermal equilibrium at an absolute temperature  $T$ , the statistical average of the  $z$  component of the magnetic moments of atoms is given by

$$\langle \mu_z \rangle = \frac{\sum (\mu_z)_{JM} e^{(-\Delta E/kT)}}{\sum e^{(-\Delta E/kT)}}$$

which reduces to

$$\langle \mu_z \rangle = \left( \frac{g^2 \mu_B^2 J(J+1)}{3kT} + \langle \alpha_M \rangle \right) H \quad (20)$$

by neglecting the quadratic and higher order terms in  $H$ . If Eq. (20) is multiplied by  $N$ , the number of magnetic atoms in a unit volume, it represents the macroscopic magnetization. Hence the paramagnetic susceptibility  $\chi$  is given by

$$\chi = N \frac{g^2 \mu_B^2 J(J+1)}{3kT} + N \langle \alpha_M \rangle \quad (21)$$



The first term is inversely proportional to the absolute temperature (Curie's law), while the second term represents the so-called "temperature-independent paramagnetism", first discussed by Van Vleck.<sup>4</sup> Equation (21) can be written as

$$\chi = N \left( \frac{\mu^2}{3kT} + \alpha \right) \quad (22)$$

where

$$\mu = g\mu_B \sqrt{J(J+1)} \quad (23)$$

is the magnitude of the magnetic moment for the state  $J$ .

It is sometimes very convenient to express the observed paramagnetic susceptibility in the form

$$\chi = N \frac{\mu_{\text{eff}}^2}{3kT}$$

and define  $\mu_{\text{eff}}$ , the effective magnetic moment, which may be temperature dependent. If we denote  $\mu_{\text{eff}}$  as a multiple of  $\mu_B$ :  $\mu_{\text{eff}} = n_{\text{eff}}\mu_B$ ,  $n_{\text{eff}}$  is called "the effective Bohr magneton number".

#### IV. CUBIC LIGAND FIELD; SPLITTING OF $d$ ORBITALS; HIGH AND LOW SPIN

In the preceding section we discussed the behavior of the  $d$  electrons of a metal ion located in a free space. In biophysics or biochemistry we are of course not much interested in free atoms, but rather we are concerned with metal ions bound in some organic structure, such as in hemes. In hemes the Fe atom, situated at the center, is surrounded by four nitrogen atoms forming a planar square, i.e. the four nitrogen atoms are symmetrically coordinated to Fe in a plane. We call these positions 1, 2, 3 and 4. In hemoproteins two further coordination positions, 5 and 6, which are in the direction normal to the heme plane, are occupied by nitrogens or other atoms or molecules. In the case of cytochromes both positions 5 and 6 are occupied by the nitrogen atoms in the imidazole ring of the histidine contained in the polypeptide chain of the protein; but in the case of myoglobin and hemoglobin, position 5 only is occupied by an imidazole nitrogen and in the sixth position a water molecule, a halogen atom, or some other molecule or radical may be found. In this way the Fe atom in a hemoprotein is surrounded by 6 atoms rather symmetrically, and these atoms

form a more or less regular octahedron. In the terminology of complex ions, these atoms (or molecules) of coordination are called ligands.

One of the most successful theories of coordination compounds is the so-called ligand-field theory,<sup>5,6</sup> in which the main effect of the ligands on the central metal ion is considered to produce a shift and splitting of the orbital energies of  $d$  electrons residing on the central ion. These changes in the orbital energies must be due to the combination of an electrostatic field and an exchange field due to ligands, but one need not worry about the details of these fields. In the ligand-field theory the effect of these fields is taken into account through the introduction of a certain number of parameters which are essentially the orbital energies of  $d$  electrons in coordination compounds, and in most cases values of these parameters are adjusted so as to achieve agreement with suitably selected experimental data.

As explained in the chapter by Dr. Schoffa, the molecular-orbital theory is more general than the ligand-field theory, the latter being an extreme case of the former.<sup>7</sup> In the case of hemes the situation may be considered as being not very far from this extreme, because the  $d$  orbitals, particularly  $d\epsilon$  orbitals to be defined below, do not form strong covalent bonds. In the molecular-orbital description, these  $d$  orbitals form linear combinations with ligand orbitals to give bonding and antibonding molecular orbitals, but all the bonding orbitals are fully occupied by electrons originally localized on ligands and can well be left out of account. The orbitals about which we are concerned are antibonding ones, and in these antibonding orbitals the relative percentage of the  $d$  orbitals is greater than that of the ligand orbitals. Particularly in the case of the  $d\epsilon$  orbitals, which can form only  $\pi$  bonds with the ligands, the coefficients for the ligand orbitals are fairly small, and the antibonding molecular orbitals are almost "non-bonding". Furthermore, small distortions of the  $d$  orbitals caused by the formation of a molecular orbital can be partly taken into account by reducing the numerical values of parameters such as the electrostatic repulsion integrals  $B$ ,  $C$ , and the spin-orbit coupling constant  $a$ .

The symmetry of the ligand field plays an essential role in the ligand-field theory. The exact symmetry of the ligand field in the case of hemoproteins is very low, but the essential contribution

comes from a cubic one. Since cubic, or octahedral, symmetry is typical of various 6-coordinated complexes, we discuss the cubic case first. The symmetry group is then  $O_h$ .

When the ligand field is cubic, the  $d$  level is split into two levels,  $d\epsilon$  and  $d\gamma$ .  $d\epsilon$  has three independent basic functions  $\xi$ ,  $\eta$  and  $\zeta$  of (1), while  $d\gamma$  has two independent bases  $u$  and  $v$  of (2). Thus in the cubic case  $d\epsilon$  and  $d\gamma$  are triply and doubly degenerate, respectively, and have different orbital energies  $E_\epsilon$  and  $E_\gamma$ . In the terminology of the group theory,  $d\epsilon$  and  $d\gamma$  functions belong to the irreducible representations  $t_{2g}$  and  $e_g$  of  $O_h$  respectively. These group theory properties of  $d\epsilon$  and  $d\gamma$  persist even when these orbitals are combined with ligand orbitals to form molecular orbitals.

In the case of hemes, six ligands are more or less electronegative, so that  $d\gamma$  orbitals, whose charge distribution extends to the ligands, have a higher orbital energy compared with  $d\epsilon$  orbitals, whose charge density vanishes along the  $x$ ,  $y$ , and  $z$  axes. The separation  $\Delta = E_\gamma - E_\epsilon$  is a measure of the strength of the cubic ligand field.

Now, we have seen in Section II that for a free atom or an ion the ground state has the largest possible  $S$ -value (Hund's rule). This is still true in the case of transition metal ions in coordination complex, provided that the cubic field is not too strong. Thus  $\text{Fe}^{3+}$  and  $\text{Fe}^{2+}$  in complexes can retain their high spin values  $S = \frac{5}{2}$  and  $S = 2$  respectively. If, however, the ligand field becomes very strong and  $\Delta$  is sufficiently large, then 6  $d$  electrons in  $\text{Fe}^{2+}$  and 5 electrons in  $\text{Fe}^{3+}$  have to be accommodated in the 3 sublevels of  $d\epsilon$ , in which case the resultant spin quantum number  $S$  will be 0 and  $\frac{1}{2}$  respectively. Thus, ferrohemoglobin and ferromyoglobin can have either a high spin value  $S = 2$  or a low spin value  $S = 0$ , and ferrihemoglobin and ferrimyoglobin can have either  $S = \frac{5}{2}$  or  $S = \frac{1}{2}$ . As a matter of fact, ferrohemoglobin in the natural physiological condition, with a water molecule coordinated at the sixth position, has a high spin value  $S = 2$ , and is paramagnetic, but it becomes diamagnetic ( $S = 0$ ) when an oxygen molecule is attached to the sixth position (oxygenated ferrohemoglobin). Furthermore, ferrihemoglobin fluoride has a high spin  $S = \frac{5}{2}$ , while ferrihemoglobin azide belongs to the low spin group  $S = \frac{1}{2}$ , as shown in Table II.

Paramagnetic susceptibilities of ferrihemoglobin derivatives and ferrohemoglobin with  $S = 2$  were measured at room temperature

TABLE II. Spin Values of Ferri- and Ferrohemoglobins

	Ferrohemoglobin (Ferromyoglobin)	Ferrihemoglobin (Ferryoglobin)
High spin type	$S = 2$ (hemoglobin)	$S = \frac{5}{2}$ (ferrihemoglobin fluoride)
Low spin type	$S = 0$ (oxyhemoglobin)	$S = \frac{1}{2}$ (ferrihemoglobin azide)

by several investigators since the pioneer work done by Pauling and his collaborators.<sup>8</sup> These are discussed in the chapter by Schoffa, but the expected temperature dependence of the effective magnetic moment on the ligand field theory will be discussed in Section V of this chapter. EPR measurements on ferrihemoglobin and ferryoglobin have successfully been carried out by Ingram and his collaborators,<sup>9,10</sup> and have yielded valuable information concerning the electronic structure of the heme iron. We discuss the EPR results in Sections VI and VII.

## V. INCOMPLETE QUENCHING OF ORBITAL MAGNETIC MOMENT IN $(d\epsilon)^5$

The magnetic susceptibility of the system of free atoms or ions is given by Eq. (21). This formula, however, is not applicable to hemoproteins because a fairly strong ligand field removes the degeneracy of the  $d$  orbitals, at least partially, and this destroys the contribution of the magnetic moment from the orbital motion of electrons considerably. This phenomenon is known as the "quenching" of the orbital magnetic moment.

If the contribution of the orbital moment is completely quenched, the effective magnetic moment arises from the spin only, and since  $g = 2$  for the spin, we should have

$$\mu = 2\mu_B \sqrt{S(S+1)} \quad (24)$$

instead of Eq. (23). This is the so-called "spin-only" value, and

is equal to  $1.73\mu_B$ ,  $2.83\mu_B$ ,  $3.91\mu_B$ ,  $4.95\mu_B$ ,  $5.98\mu_B$  for  $S = \frac{1}{2}$ , 1,  $\frac{3}{2}$ , 2,  $\frac{5}{2}$ , respectively.

Experimentally, the effective magnetic moment  $\mu_{\text{eff}}$  is obtained by expressing the paramagnetic part,  $\chi_{\text{para}}$ , of the susceptibility in the form

$$\chi_{\text{para}} = N \frac{\mu_{\text{eff}}^2}{3kT} \quad (25)$$

To derive  $\chi_{\text{para}}$  from the observed susceptibility one has to subtract the large diamagnetic contribution due to the protein, which can be determined experimentally by changing the heme into a diamagnetic state.

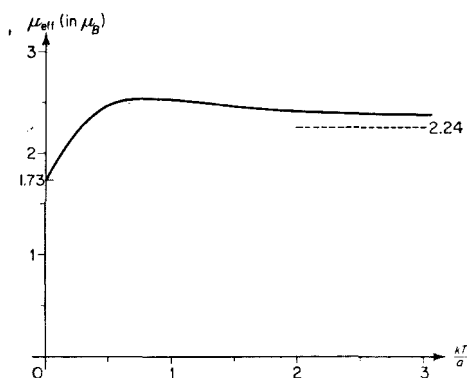


Fig. 2. Effective magnetic moment (Bohr magneton number) of an ion with 5  $d\epsilon$  electrons.

Now, the values of the effective magnetic moment of ferri-hemoglobin derivatives with low spin,  $S = \frac{1}{2}$ , are not very far from the spin-only value  $1.73\mu_B$ , but most of them fall in the region  $2.0\mu_B \sim 2.5\mu_B$ , which is clearly higher than  $1.73\mu_B$ . This increase of the effective magnetic moment above the spin-only value is due to the residual contribution of the orbital moment, which is quenched only incompletely. If we assume that the ligand field is cubic, and  $\Delta$  is much larger than the thermal energy  $kT$ , we can derive the theoretical formula for the effective magnetic moment:

$$\mu_{\text{eff}} = \mu_B \left[ \frac{3x + 8 - 8e^{-(3/2)x}}{x(1 + 2e^{-(3/2)x})} \right]^{1/2} \quad (26)$$

where  $x = a/kT$ .<sup>12</sup>

According to Eq. (26)  $\mu_{\text{eff}}$  assumes the spin-only value  $1.73\mu_B$  in the low temperature limit, and as the temperature increases  $\mu_{\text{eff}}$  manifests a broad maximum  $2.5\mu_B \sim 2.6\mu_B$  in the intermediate temperature  $kT = 0.5a \sim a$ , and then gradually decreases toward the high temperature limit  $2.24\mu_B$ . If we take  $a \sim 400 \text{ cm}^{-1}$ , room temperature corresponds to  $(kT/a) \sim 0.45$ .

If the symmetry of the ligand field becomes lower, say rhombic, the contribution from the orbital moment should decrease.<sup>11</sup> The fact that a rather high  $\mu_{\text{eff}}$  is observed for some of the low spin ferrihemoglobin derivatives seems to suggest that the symmetry of the ligand field is not very far from cubic. A more decisive test of this question could be given by the measurement of the effective magnetic moment in the wide temperature range, as well as the measurement of the principal values of the susceptibility tensor on single crystal samples.

Formulas similar to (26), applicable to the cases of 1, 2, 3 and 4  $d\epsilon$  electrons, were derived by the author.<sup>12</sup>

## VI. ANALYSIS OF EPR DATA ON A FERRIHEMOGLOBIN DERIVATIVE WITH LOW SPIN

The EPR experiment carried out by Gibson and Ingram<sup>9</sup> on a single crystal of ferrihemoglobin azide,  $\text{HbN}_3$ , gave the following values for the principal values of the  $g$  tensor:

$$g_x = 1.72, \quad g_y = 2.22, \quad g_z = 2.80 \quad (27)$$

where the  $z$  axis is perpendicular to the heme plane. Griffith<sup>13</sup> analyzed this result and succeeded in determining the relative energies of  $d\epsilon$  orbitals  $\xi$ ,  $\eta$  and  $\zeta$  for this substance. This seems to be the only reliable determination of energies of split orbitals at the present time.

In the case of ferrihemoglobin azide, five magnetic electrons are accommodated in three  $d\epsilon$  orbitals. There are three ways of distributing electrons:  $\xi\eta^2\zeta^2$ ,  $\xi^2\eta\zeta^2$ ,  $\xi^2\eta^2\zeta$  leaving an electron hole in  $\xi$ ,  $\eta$  and  $\zeta$  respectively, and since the resultant spin is  $\frac{1}{2}$ , each of these states is actually a doublet. The spin-orbit interaction tends to mix these three "sub-configurations", but Kramer's theorem<sup>6</sup> states that the degeneracy of these doublets cannot be removed as long as a magnetic field is not applied. The mixing of the doublets mentioned above modifies the principal  $g$ -values of the ground state,

and inversely we can determine the wave function from the observed  $g$ -values (27).

Eigenfunctions of our Hamiltonian corresponding to three Kramers doublets,  $k = 1, 2$ , and  $3$ , can be expressed in the form<sup>6</sup>:

$$\left. \begin{aligned} \psi_{k+} &= A_k \xi \alpha + i B_k \eta \alpha + C_k \zeta \beta \\ \psi_{k-} &= -A_k \xi \beta + i B_k \eta \beta + C_k \zeta \alpha \end{aligned} \right\} k = 1, 2, 3 \quad (28)$$

We understand (28) represents the wave function of the "hole", rather than of the electron, and treat our system as if it were a single-particle one. Normalization of (28) gives the condition:

$$|A_k|^2 + |B_k|^2 + |C_k|^2 = 1, \quad k = 1, 2, 3 \quad (29)$$

By examining the matrix elements of  $(-e/2mc)(\mathbf{L} + 2\mathbf{S})_z$  among doublet functions (28), we find that the principal  $g$ -values are given by

$$\begin{aligned} g_x &= 2|A^2 - (B + C)^2| \\ g_y &= 2|-(A - C)^2 + B^2| \\ g_z &= 2|(A - B)^2 - C^2| \end{aligned} \quad (30)$$

For the normal state  $k = 1$ , coefficients  $A_1, B_1, C_1$  should be chosen so as to satisfy (27) as closely as possible. By putting  $g_x:g_y:g_z = 1.72:2.22:2.80$  and using (29), we obtain a set of  $A_1, B_1$ , and  $C_1$ , which gives

$$g_x = 1.706, \quad g_y = 2.202, \quad g_z = 2.778 \quad (31)$$

satisfactorily close to (27).

Now we know  $\psi_{1+}$  and  $\psi_{1-}$ , which must be the lowest eigenfunctions of the Hamiltonian containing spin-orbit interaction, and  $\xi, \eta$ , and  $\zeta$  orbital energies. If  $a$  and  $E_\xi, E_\eta$ , and  $E_\zeta$  were known, we could solve the secular equation and determine  $A_k:B_k:C_k$  but here we have the reverse situation. We know the lowest eigenfunction, and we ask what relations should exist among the parameters  $a, E_\xi, E_\eta$ , and  $E_\zeta$  contained in the Hamiltonian. The spin-orbit interaction is taken as  $-a\mathbf{l} \cdot \mathbf{s}$ , so that  $a$  is positive. The answer is that we can determine relative values of  $E_\zeta - E_\xi, E_\eta - E_\xi$  and  $a$  quantitatively. The calculation gives

$$E_\eta - E_\xi = 2.398a, \quad E_\zeta - E_\xi = 5.943a \quad (32)$$

It is to be noted that these  $E$ 's are orbital energies of the *hole*, so

that the orbital energies of the real *electron* are of the reversed sign. Thus we have, for electrons

$$E_{\xi} - E_{\eta} = 2.398a, \quad E_{\xi} - E_{\zeta} = 5.943a \quad (33)$$

and this result shows that the  $\zeta$  orbital has the lowest energy.

It is remarkable that the  $\zeta$  orbital has the lowest energy, although it cannot form  $\pi$  bonds with nitrogens in the porphyrin ring. Griffith suggested that the  $\xi$  orbital is raised on account of the electronic repulsion between charges due to the  $\pi$  electrons of the imidazole ring and that of the  $\xi$  orbital itself. If this interpretation is correct, the azimuth of the imidazole ring, which is perpendicular to the heme plane, must be such that the ring is contained in the  $xz$  plane.

Two other eigenfunctions for excited doublets can easily be obtained, and we can calculate the expected temperature dependence of the effective magnetic moment.<sup>11</sup>

Since  $a$  is of the order of  $400 \text{ cm}^{-1}$ ,  $\xi$  and  $\eta$  orbitals lie above the  $\zeta$  orbital by about  $2400 \text{ cm}^{-1}$  and  $1500 \text{ cm}^{-1}$ , values much larger than the thermal energy  $kT \sim 200 \text{ cm}^{-1}$ . The excitation energies fall in the region of infrared spectroscopy.

## VII. PROPERTY OF ${}^6S$ STATE IN FERRIHEMOGLOBIN FLUORIDE

Ferrihemoglobin derivatives such as ferrihemoglobin fluoride have a high spin value  $S = \frac{5}{2}$  in their normal state, as shown by susceptibility measurements. In the case of free ions with five  $d$  electrons, the normal state is  ${}^6S$  and is six-fold degenerate. In the case of ferrihemoglobin derivatives, however, this six-fold degeneracy is partly removed, and we have three Kramers doublets. A simple representation of this situation is given by the use of a spin Hamiltonian

$$E_0 + D_x S_x^2 + D_y S_y^2 + D_z S_z^2 \quad (34)$$

where  $D_x + D_y + D_z = 0$ .  $E_0$  denotes the average energy of three Kramers doublets. A more exact spin Hamiltonian will have quartic terms in spin components, but they are assumed to be small. If the local symmetry at the iron is tetragonal we have

$$D_x = D_y = -\frac{1}{2}D_z$$



and (34) becomes as follows:

$$E_0 + \frac{3}{2}D_z(S_z^2 - \frac{1}{3}S^2) \quad (35)$$

In this case three doublets are characterized by  $S_z = \pm \frac{1}{2}$ ,  $S_z = \pm \frac{3}{2}$  and  $S_z = \pm \frac{5}{2}$  respectively, and the doublets  $S_z = \pm \frac{3}{2}$  and  $S_z = \pm \frac{5}{2}$  are separated from the lowest doublet  $S_z = \pm \frac{1}{2}$  by  $3D_z$  and  $9D_z$ , respectively.

Gibson, Ingram and Schonland<sup>10</sup> carried out EPR experiments on single crystals of ferrimyoglobin and ferrihemoglobin derivatives, and observed a high anisotropy of  $g$ -values. The  $g$ -value attains its minimum value 2 when the magnetic field is applied in a specific direction, and it increases to 6 when the field is perpendicular to this direction. This result can be accounted for nicely if the spin Hamiltonian is of the form (35),  $z$  being the specific direction mentioned above. It is natural to assume that this  $z$  direction is normal to the heme plane, so that from EPR experiments we can determine the orientation of hemes in the crystal. In ferrimyoglobin the unit cell contains two hemes inclined to each other, and in ferrihemoglobin the unit cell contains only one molecule, but each molecule has four hemes in different orientations. The information concerning the orientation of hemes in these crystals was very helpful in the determination of atomic positions of the hemoglobin molecule by X-ray diffraction studies, and Fig. 3 shows the relative position and orientation of four hemes in a single hemoglobin molecule determined in this way.

Now, the EPR experiment has been able to determine only the lower limit for  $D_z$ , because the resonance corresponding to transitions between levels arising from different doublets could not be observed within the range of the magnetic field employed. From this fact  $D_z$  is estimated as  $\gtrsim 7 \text{ cm}^{-1}$ . It is difficult to determine  $D_z$  by the EPR method, but spectroscopy in the far infrared, or the susceptibility measurement at very low temperatures, will be able to provide valuable information. The theoretical formulas for the effective magnetic moment  $\mu_{\text{eff}}$ , which are derived on the assumption of the spin Hamiltonian (35), have been given by the author.<sup>11</sup>

It is rather surprising that three Kramers doublets from  $^6S$  are separated by several tens of  $\text{cm}^{-1}$ . In a cubic or nearly cubic inorganic crystal  $^6S$  is split into a doublet and quartet, but the separation is very small ( $\lesssim 0.01 \text{ cm}^{-1}$ ). In tetragonal or rhombic

environment the separation becomes larger, but this separation is not the first-order effect because the spherically symmetric  $S$  state cannot feel the anisotropy of the ligand field directly. Through the spin-orbit interaction  ${}^6S$  has small contamination of  ${}^4P$  and other asymmetric states, and the splitting of these states due to the ligand field has some indirect effect on the ground state. Among

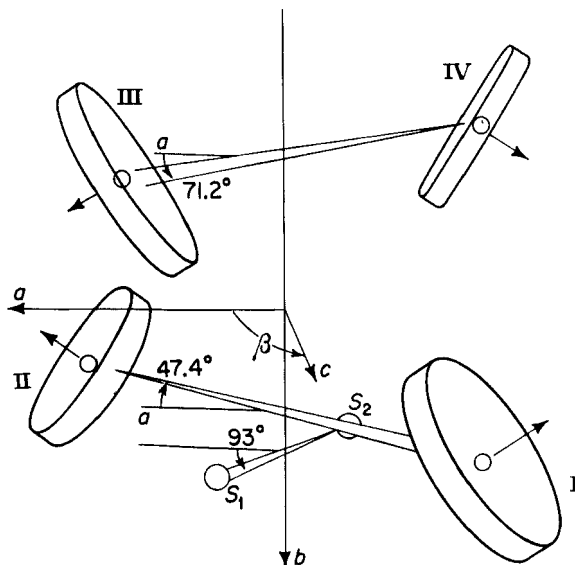


Fig. 3. Relative positions of four hemes in a single molecule of hemoglobin. (From Perutz *et al.*<sup>2</sup>)

various  $(S, L)$  states arising from the configuration  $(3d)^5$ , the only term which can combine with  ${}^6S$  through the spin-orbit interaction is  ${}^4P$ . This term is higher than the ground state  ${}^6S$  by about  $350,000 \text{ cm}^{-1}$  in the free  $\text{Fe}^{3+}$ , but in ferrihemes the excitation energy can be expected to be much lower. The main reason for this is found in the fact that in the limit of strong cubic ligand field  ${}^6S$  goes up to  $(d\epsilon)^3(d\gamma)^2$  but the lowest  ${}^4T_1$  level, which contains  ${}^4P$  to an appreciable extent, goes down to  $(d\epsilon)^4(d\gamma)$ . Thus, even such crossing must occur. In reality the symmetry of the ligand field is lower than cubic, and the  ${}^4T_1$  is split into three levels, lying above the normal

$^6S$  state by  $E_1$ ,  $E_2$ ,  $E_3$ , respectively. On these assumptions we can derive the formula

$$D_z = \frac{c^2 a^2}{3} \left( \frac{1}{E_3} - \frac{1}{2E_1} - \frac{1}{2E_2} \right)$$

where  $a$  is the spin-orbit coupling constant and  $c^2$  is the percentage of  $^4P$  in the lowest  $^4T_1$ . A rough estimate of this splitting between  $E_1$ ,  $E_2$ , and  $E_3$  can be obtained by using the values of orbital energies of  $E_\xi$ ,  $E_\eta$ , and  $E_\zeta$  obtained for ferrihemoglobin azide. If we further assume that the lowest component of  $^4T_1$  is situated about  $2000 \text{ cm}^{-1}$  above the normal state  $^6S$ , we have  $D_z \sim 5 \text{ cm}^{-1}$ , which is in the right order of magnitude.\*

### VIII. ELECTRONIC STRUCTURE OF IRON IN FERROHEMOGLOBIN

So far EPR experiments have not been successful in the study of ferrohemoglobin derivatives. One reason for this situation is the absence of a Kramers doublet in the system with an even number of electrons, such as  $\text{Fe}^{2+}$ . In this case all degeneracies are removed by the ligand field if the latter is sufficiently asymmetric, and the resonance absorption can be observed only when two levels are accidentally quite near to each other.

By the measurement of the static susceptibility, however, we learn that the resultant spin  $S$  is equal to 2. In order to discuss the paramagnetism of this substance in general, we have to work out the energy levels for  $S = 2$  of  $d^6$  configuration, taking the ligand field, or the orbital energy difference, and the spin-orbit energy into account. Although this is simple in principle, the actual calculation becomes fairly complicated unless we assume some sequence in the order of magnitude of different energies.

Practically, the following two cases deserve our consideration:

- (1) Cubic ligand field > lower symmetry ligand field > spin-orbit interaction > Zeeman energy.
- (2) Cubic ligand field > spin-orbit interaction > lower symmetry ligand field > Zeeman energy.

\*Note added in proof: Separation between  $E_\xi$  and  $E_\eta$  seems to be much smaller in ferrihemoglobin fluoride than in ferrihemoglobin azide. See the author's paper in the *Proceedings of the Conference on Quantum Aspects of Polypeptides and Polynucleotides*, to be published.

In both cases we start from  $(d\epsilon)^4(d\gamma)^2 {}^5T_2$ , which is  $5 \times 3 = 15$ -fold degenerate. In (1) this is first split into three levels corresponding to the following configurations:

$$\xi\eta\zeta^2(d\gamma)^2, \quad \xi\eta^2\zeta(d\gamma)^2, \quad \xi^2\eta\zeta(d\gamma)^2 \quad (36)$$

Since  $S = 2$ , each of these three levels is five-fold degenerate, and this degeneracy is removed by the spin-orbit interaction. The spin-orbit interaction has non-vanishing matrix elements only between different configurations in (36) so that the splitting of these quintets is of the order of  $a^2/\Delta E$ , where  $\Delta E$  stands for the differences between orbital energies. If for  $\Delta E$  we tentatively use values determined for HbN<sub>3</sub>,  $\Delta E \sim 1000 \text{ cm}^{-1}$  and  $a^2/\Delta E$  is of the order of  $100 \text{ cm}^{-1}$ , so that sequence (1) seems to be a consistent one. Since  $\Delta E$  is fairly large compared with  $kT$ , we have to deal with only the lowest quintet, which is  $\xi\eta\zeta^2(d\gamma)^2$  according to the order of orbital energies obtained in Section VI. The splitting of this quintet is represented by the spin Hamiltonian  $DS_z^2 + E(S_x^2 - S_y^2)$  with

$$D = \frac{a^2}{32} \left( \frac{1}{E_\eta - E_\zeta} + \frac{1}{E_\xi - E_\zeta} \right) \quad \text{and} \quad E = \frac{a^2}{32} \left( \frac{1}{E_\eta - E_\zeta} - \frac{1}{E_\xi - E_\zeta} \right).$$

We omit the details of calculation, and give the results in Figs. 4 and 5. In these figures the calculated  $n_{\text{eff}}$  is represented, taking  $x = a^2/(16\Delta kT)$  as the abscissa, where  $\Delta = \frac{1}{2}(E_\xi + E_\eta) - E_\zeta$ . In Fig. 4,  $E_\xi$  and  $E_\eta$  are assumed to be equal, while in Fig. 5,  $E_\xi - E_\eta$  is equal to  $0.5 \times \{\frac{1}{2}(E_\zeta + E_\eta) - E_\zeta\}$ . This latter choice corresponds approximately to the orbital energies in HbN<sub>3</sub>. From these figures we observe that as the temperature gets lower the average  $n_{\text{eff}}$  decreases gradually from the spin-only value of  $\sqrt{24}$  to zero.

The observed value of  $n_{\text{eff}}$  for ferrohemoglobin at room temperature is 5.4. This value cannot be fitted into the present approximation. Therefore, if the increase of  $n_{\text{eff}}$  above the spin-only value  $\sqrt{24}$  is really significant, case (1) cannot be true, and we have to consider case (2), or intermediate situations between (1) and (2).

In case (2) we start again from  $(d\epsilon)^4(d\gamma)^2 {}^5T_2$ , but first take into account the splitting due to spin-orbit interaction. This can be studied by the quasi-angular momentum method: the 15-fold level splits into a triplet, a quintet and a septet, as shown in Fig. 6. This

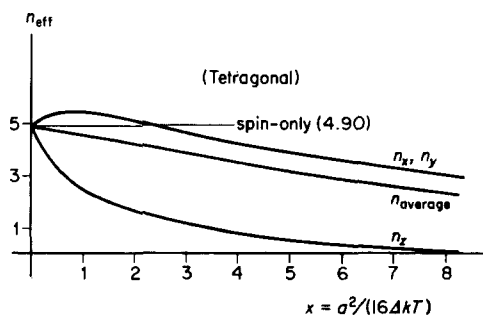


Fig. 4. Effective magnetic moment (Bohr magneton number) of a ferrous ion in a tetragonal ligand field.

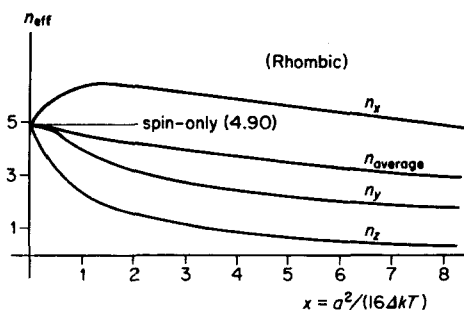


Fig. 5. Effective magnetic moment (Bohr magneton number) of a ferrous ion in a rhombic ligand field.

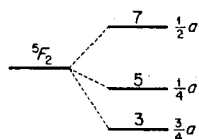


Fig. 6. Splitting of a quintet  $F$  state due to spin-orbit interaction in a cubic field.

corresponds to the energy level scheme in the absence of a lower symmetry ligand field, and Griffith has already given the formula for  $n_{\text{eff}}$  for this case as a function of  $x = a/kT$ . This function is illustrated in Fig. 7. A remarkable point is that in this case  $n_{\text{eff}}$  is greater

than  $\sqrt{24}$ , the maximum value being approximately 5.8. This increase above  $\sqrt{24}$  is due to the incomplete quenching of orbital magnetic moment inherent in  $d\epsilon$  orbitals. If we introduce the lower symmetry ligand field the degeneracy of each of the three levels in Fig. 6 is lifted, and  $n_{\text{eff}}$  tends to zero as the temperature is lowered indefinitely; but as long as the lower symmetry field, or  $\Delta E$ , is not very large,  $n_{\text{eff}}$  rises above  $\sqrt{24}$  in the medium temperature region. Anyway, the lower symmetry ligand field seems to be smaller in ferrohemoglobin than in ferrihemoglobin azide.

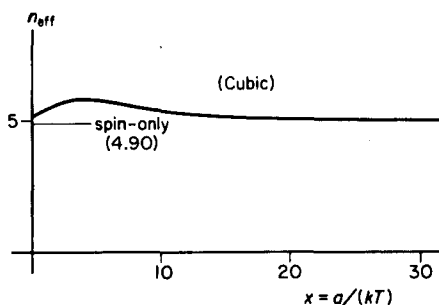


Fig. 7. Effective magnetic moment (Bohr magneton number) of a ferrous ion in a cubic ligand field.

We have dealt with magnetic properties of hemoproteins in this chapter and have paid little attention to other properties such as optical spectra and biological activity. To understand these properties it is essential to take into account the behavior of  $\pi$  and other electrons in the porphyrin ring and the imidazole. There have been several investigations along these lines, but a satisfactory molecular-orbital treatment of the whole system seems to still be in the infant stage. Much work has to be done before we can have a satisfactorily coherent view of the different properties of hemoproteins.

The author is indebted to Professor M. Mizushima for valuable discussions; he appreciates Miss Anyohji's faithful help in preparing the manuscript.

### References

1. Androes, G. M., and Calvin, M., *Biophys. J.* **2**, 217 (1962). (For a review of EPR studies on biological substances.)
2. Perutz, M. F., Rossmann, M. G., Cullis, A. F., Muirhead, H., Will, G., and North, A. C. T., *Nature* **185**, 416 (1960).
3. Kendrew, J. C., Dickenson, R. E., Strandberg, P. E., Hart, R. G., Davies, D. R., Phillips, D. C., and Shore, V. C., *Nature* **185**, 422 (1960).
4. Van Vleck, J. H., *The Theory of Electric and Magnetic Susceptibilities*, Clarendon Press, Oxford, 1932.
5. Orgel, L. E., *Transition Metal Chemistry*, Methuen, London, and Wiley, New York, 1960. (For a general introduction to the ligand-field theory.)
6. Griffith, J. S., *Theory of Transition Metal Ions*, Cambridge University Press, 1961, pp. 205–208. (This book provides a good general introduction to the ligand-field theory.)
7. Van Vleck, J. H., *J. Chem. Phys.* **3**, 807 (1935).
8. Pauling, L., and Coryell, C. D., *Proc. Natl. Acad. Sci. U.S.* **22**, 210 (1936).
9. Gibson, J. F., and Ingram, D. J. E., *Nature* **180**, 29 (1957). (EPR measurements of ferrihemoglobin azide.)
10. Gibson, J. F., Ingram, D. J. E., and Schonland, D., *Discussions Faraday Soc.* **26**, 72 (1958). (EPR measurements of ferrimyoglobin and ferrihemoglobin.)
11. Kotani, M., *Prog. Theoret. Phys. (Kyoto), Suppl.* No. 17, 4 (1961).
12. Kotani, M., *J. Phys. Soc. Japan* **4**, 193 (1949).
13. Griffith, J. S., *Nature* **180**, 30 (1957).

## 4

# MAGNETIC SUSCEPTIBILITIES AND THE CHEMICAL BOND IN HEMOPROTEINS

G. SCHOFFA, *Physics Department of the Technische Hochschule,  
 Karlsruhe*

## CONTENTS

I.	Introduction . . . . .	182
II.	Experimental Approach . . . . .	184
	A. Magnetic Susceptibility Measurements . . . . .	184
	B. Visible Absorption Spectra . . . . .	185
III.	Theoretical Aspects . . . . .	186
	A. Magnetic Susceptibility and the Chemical Bond . . . . .	186
	(1) The Valence-Bond Method . . . . .	188
	(2) The Ligand-Field Theory . . . . .	190
	(3) The Molecular-Orbital Method . . . . .	191
	References . . . . .	197

## I. INTRODUCTION

Biochemical systems in which metal ions are essential for activity are common. Among them are systems which contain iron, and the iron-porphyrin complexes such as hemoglobin, myoglobin, peroxidase, catalase, the cytochromes, etc. are of special importance. The hemoproteins of the naturally occurring metal complexes have received the greatest amount of attention and the application of techniques of proved value in coordination chemistry has yielded precise information about the association of the iron atom with the remainder of the molecule and, in addition, has thrown some light on the mechanisms involved in individual biological function of these molecules.

The iron in these complexes can exist in ferrous or ferric forms and is held in tetragonal or distorted octahedral coordination with porphyrin, protein and any small molecule such as H<sub>2</sub>O, O<sub>2</sub>, CO, F<sup>-</sup>, CN<sup>-</sup>, etc. The structure of the ferrihemoglobin is shown in



Fig. 1. The nomenclature for hemoglobin complexes has been given by Pauling and Coryell.<sup>15</sup>

This review is restricted to a discussion of some ferrihemoprotein complexes. A detailed understanding of their properties and biological effectiveness demands a knowledge of the chemical bond. During the last twenty years many new experimental and theoretical works have become available, greatly increasing our understanding of the interaction between ferric or ferrous ions at the center of porphyrin and ligands.

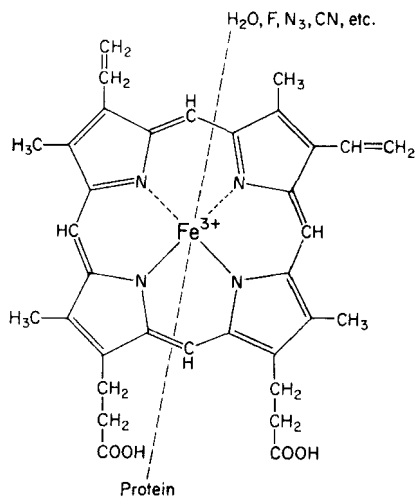


Fig. 1. Ferrihemoglobin.

Measurements of magnetic susceptibilities have been especially useful in the investigation of the chemical bond of many biologically important hemoglobin complexes. Pauling and his co-workers have derived results of great interest from their experimental and theoretical studies.<sup>3,6,14,15,16</sup> According to Pauling, these proteins fall into two characteristic groups. In the first group (acid-ferrihemoglobin, ferrihemoglobin fluoride, etc.), the total spin of the complex is the same as that of the ferric ion in its ground state in the gas phase ( $\mu = 5.92$  B.M.). These complexes Pauling calls "ionic" complexes. The second group called "covalent" complexes (ferrihemoglobin cyanide, ferrihemoglobin hydrosulfide, etc.) are those

in which the effective value of the spin may be very much lower ( $\mu = 2.0\text{--}2.5$  B.M.).

The first theoretical interpretation of both these groups of complexes given by Pauling was based on directed wave functions. For a detailed account of this work the reader is referred to the literature.<sup>14,17</sup> The sharply alternative modes of spin coupling which lead to high and low values for the susceptibility with the exclusion of intermediate values are of particular interest.

Most hemoglobin compounds fall satisfactorily into Pauling's classification as either "ionic" or "covalent" complexes. Thus in the ferrihemoglobin fluoride the paramagnetic moment is 5.9 B.M., the value for a fully "ionic" complex. In ferrihemoglobin cyanide which has a paramagnetic moment of 2.3 B.M., we have a "covalent" complex. There are, however, certain derivatives of ferriporphyrins, for example ferrihemoglobin hydroxide, for which the magnetic susceptibility has an intermediate value. Whether the chemical bond in such compounds is ionic or covalent, or a combination of the two, has not yet been decided from the investigation so far.

We have investigated magnetic susceptibilities and optical spectra of some new ferriprotein complexes.<sup>18,19</sup> Surprisingly, several of these derivatives have magnetic moments of intermediate values, and intermediate positions of the optical bands. It is the purpose of this review to explain these new experimental results and their bearing on the nature of the chemical bond in such intermediate complexes.

## II. EXPERIMENTAL APPROACH

### A. Magnetic Susceptibility Measurements

The methods which were used for measurement of diluted and also lyophilized ferric hemoproteins may be found in the author's papers.<sup>19,20</sup> The magnetic moments were calculated from molar susceptibility with the formula

$$\mu_{\text{eff}} = 2.84\sqrt{(\chi_M \cdot T)}$$

where  $\mu_{\text{eff}}$  is the effective magnetic moment in Bohr magnetons,  $\chi_M$  the molar magnetic susceptibility and  $T$  the temperature in degrees

absolute. In the table of specified magnetic moments (Table I), calculations are made on the assumption that the Curie law is fulfilled.

Surprisingly, some ferriprotein complexes show a great variation in magnetic moment. Regardless of what the protein is, the magnetic moments decrease along the series  $F > H_2O > HCOO^- > CH_3COO^- > OCN^- > SCN^- > OH^- > NO_2^- > SeCN^- > \text{imidazole} > N_3^- > CN^-$ , and intermediate values of magnetic moments, i.e. between 5.9 and 2.3 B.M., are also suggested.

TABLE I. Effective Magnetic Moments of Some Ferrihemoglobin and Ferrimyoglobin Complexes

Ligand	Horse hemoglobin		Horse myoglobin	
	pH	$\mu_{\text{eff}}$	pH	$\mu_{\text{eff}}$
$F^-$	7.10	5.76	6.84	5.77
$H_2O$	6.36	5.65	6.44	5.73
$HCOO^-$	6.92	5.44	6.54	5.69
$CH_3COO^-$	6.84	5.44	6.98	5.70
$OCN^-$	7.58	5.40	9.60	4.41
$SCN^-$	6.60	5.06	6.62	5.47
$OH^-$	9.73	4.66	11.60	5.04
$NO_2^-$	6.84	4.13	6.63	5.12
$SeCN^-$	6.91	3.88	7.36	4.89
Imidazole	6.92	2.87	6.81	2.44
$CN^-$	6.72	2.50	7.41	1.96
$N_3^-$	6.72	2.35	6.80	3.30

## B. Visible Absorption Spectra

Light absorption measurements have been made to verify the above magnetic susceptibility results. Table I and Fig. 2 include data on the magnetic moments and optical bands of many hemoproteins and their complexes. The positions of visible bands have been studied in ferrihemoproteins bound by a series of additional ligands. No matter what the protein is, the positions of the bands move to longer wavelengths along the series, like the magnetic moments series (Section II-A), while the magnetic susceptibility decreases.

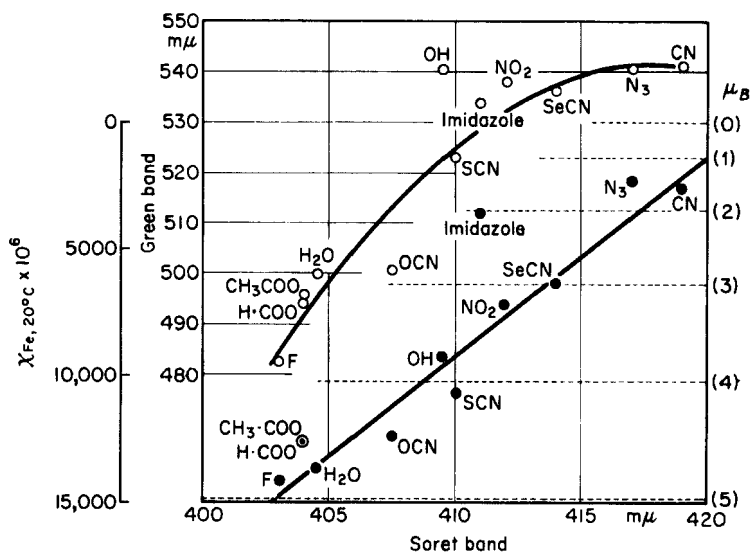


Fig. 2. Correlation given between magnetic susceptibilities and optical spectra in some horse ferrihemoglobin derivatives (Scheler, Schoffa and Jung<sup>18</sup>).

In horse ferrimyoglobin the Soret band shifts from 403  $m\mu$  to 420  $m\mu$ , the green band from 482 to 540  $m\mu$ , while the red band moves from 604  $m\mu$  to longer wavelengths and vanishes in "covalent" complexes.

### III. THEORETICAL ASPECTS

#### A. Magnetic Susceptibility and the Chemical Bond

In most salts of the iron group and also in hemoproteins, the molar magnetic susceptibility has approximately the value

$$\chi_M = \frac{4N\beta^2 S(S+1)}{3kT}$$

where  $\beta$  is the Bohr magneton and the spin,  $S$ , has the value given by the Hund rule that the ground state is that of maximum multiplicity compatible with the Pauli principle ( $S = \frac{5}{2}$  for  $\text{Fe}^{3+}$  or

$\mu_{\text{eff}} = 5.92$  B.M.). In some ferric complexes, e.g.  $\text{K}_3[\text{Fe}(\text{CN})_6]$ , the ligand field is strong enough to destroy the Russell-Saunders coupling and then  $S = \frac{1}{2}$ . Therefore  $\text{K}_3[\text{Fe}(\text{CN})_6]$  or ferrihemoglobin cyanide show a magnetic susceptibility corresponding to about one free spin, i.e.  $S = \frac{1}{2}$  or theoretically  $\mu = 1.73$  B.M. Since the orbital contribution is not negligible, the experimental magnetic moment is given approximately by  $\mu_{\text{eff}} = 2.3$  B.M.<sup>9</sup> (See Section II.)

Since in the first case we have the same magnetic moment as in the free ferric ion, and in the second case a magnetic moment which is lowered by ligands, we must then ask what factors favor and what inhibit the spin pairing of any particular electrons. A detailed understanding of the properties of all these complexes demands an acquaintance with the current concepts used in the description of the bonds between cations and ligands.

The behavior of electrons and the chemical bond in complexes can in principle be represented by the Schrödinger differential equation. If electron interaction is neglected, the calculation of the total wave function of a system is reduced to the resolution of an equation which depends on only one set of variables. Because we have 23 electrons in  $\text{Fe}^{3+}$  and even more electrons in the ligands, an exact solution of the Schrödinger equation is impossible, and approximation methods have to be used. The problem has to be reduced to that of a single electron moving in a spherically symmetrical field of force provided by the nucleus and the average effect of all the other electrons. The complete wave function is then written as the product of a number of one-electron wave functions. Two approximations are used: the Heitler-London-Slater-Pauling approximation (HLSP method), which is also called the valence-bond method, and an alternative treatment, known as the molecular-orbital method (MO theory) developed by Hund, Mullikan, Lennard-Jones and others. The two procedures represent different approximations in the solution of a complicated secular equation.

Another theoretical method is the crystal- or ligand-field theory. It can be shown<sup>24</sup> that all of these approximations have the same theoretical origin and represent different ways of solving the many-electron problem. The valence-bond theory and the ligand-field theory can be considered as special cases of the molecular-orbital method.<sup>1</sup> Since the magnetic properties and the chemical bond in

hemoproteins were explained first using the valence-bond method, we shall begin with this approximation.

### (1) *The Valence-Bond Method*

A possible procedure to describe the chemical bond in molecules consists in using as an approximate expression for the molecular orbital,  $\Psi$ , a linear combination of atomic orbitals (LCAO)  $\psi_A$ ,  $\psi_B$ , .... In spin-state approximation<sup>4,7,21</sup> we have a function of the following type

$$\Psi = \frac{1}{N} [\psi_A(1) \psi_B(2) \pm \psi_A(2) \psi_B(1)]$$

where  $A$  and  $B$  are the indices for the nuclei, and (1) and (2) are indices for the electrons. In valence-bond approximation certain combinations of spin states are made before the matrix elements are computed. The calculation is thereby somewhat simpler, but because it neglects some combinations of spin states, the criticisms of this method are well founded.<sup>1,4</sup> The above equation neglects the "ionic" terms  $\psi_A(1) \psi_A(2)$  and  $\psi_B(1) \psi_B(2)$  because these terms assume that the mutual repulsion between electrons reduce to a negligible value the probability that the electrons would be found simultaneously on the same nucleus.

With regard to magnetic properties and the chemical bond in hemoprotein complexes, the concept of hybrid orbitals is of great importance in valence-bond theory. The five electron orbitals in  $\text{Fe}^{3+}$

$$\left. \begin{matrix} d_{xy} \\ d_{yz} \\ d_{xz} \end{matrix} \right\} d\epsilon \qquad \left. \begin{matrix} d_{x^2-y^2} \\ d_{z^2} \end{matrix} \right\} d\gamma$$

can form suitable linear combinations with ligand electron orbitals to create equivalent or hybridized orbitals. In octahedral ferri-complexes the electronic configuration  $(3d\epsilon^m)(3d\gamma^4 4s^2 4p^6)$  is then possible ( $d^2 sp^3$  hybridization). These new hybrid orbitals have strong directional characteristics and the strength of a covalent bond is approximately proportional to the amount of overlap of the hybridized orbitals.

An explanation of magnetic susceptibilities in hemoproteins was

first given by Pauling on the basis of the valence-bond approximation. Until recently most biologists working with hemoprotein complexes have been mainly interested in the application of Pauling's theory.

Pauling<sup>14</sup> suggested that the bonding in the complexes with the high spin value was predominantly ionic, whereas in the low-spin complexes covalent bonds were formed from  $3d^2 4s 4p^3$  hybridization. Consider the case of ferrihemoglobin fluoride: this complex involves the six ligands held electrostatically to the ferric ion, so that the iron atom would have the electrostatic configuration of a free ferric ion with five unpaired electrons and a corresponding magnetic moment of 5.9 B.M. In the ferrihemoglobin cyanide the  $\text{Fe}^{3+}$  ion attaches its six atoms of coordination by means of  $d^2 sp^3$  hybridization, i.e. six electron pair bonds. These six bonds consume the  $3d\gamma$ ,  $4s$  and  $4p$  states, and house six electrons of  $\text{Fe}^{3+}$ , which has 11 electrons. In order to make two of the five  $3d$  orbitals available for bond formation, two electrons in the  $3d$  orbitals of the ferric ion become paired and two of  $d\epsilon$  orbitals will be filled twice. These electrons must have their spins antiparallel because of the Pauli principle and, hence, make no contribution to the susceptibility. The fifth electron, however, has a free spin,  $S = \frac{1}{2}$ . In this case the susceptibility will be much lower than without electron pair bonding.

It is difficult to believe that the iron in such complexes has the structure  $\text{Fe}^{3+}$  since the iron certainly is unwilling to accept three extra electrons. There are also other difficulties. Thus this theory cannot explain 5-coordinated complexes of  $\text{Ni}^{2+}$ ,  $\text{Pd}^{2+}$ ,  $\text{Pt}^{2+}$  and  $\text{Au}^{2+}$  ( $d^8$  ions). The formation of square-planar cupric complexes, involving  $dsp^2$  hybridization and the promotion of one electron from the  $3d$  orbital to some high level is very uncertain.

The source of the deficiencies is that in the valence-bond approximation the antibonding  $d\gamma$  orbitals have been neglected, and so the theory goes astray in describing molecules in which these orbitals are occupied.

In Pauling's theory, there is a sharp discontinuity between covalent and ionic bonding. In covalent complexes the free electrons of iron cannot go into  $d\gamma$  orbitals because here we have no bonding and antibonding orbitals as in the molecular-orbital theory.

There are, however, a number of ferric complexes with magnetic moments of 5.9 B.M. which have properties incompatible with ionic

bonds.  $\text{Fe}^{3+}$ -tris-acetylacetonate, for instance, behaves as a typical covalent substance. Ferriheme ( $\mu = 5.7$  B.M.) also has a high degree of covalent character.

In the foregoing section we have shown some new experimental results which cannot be explained with the Pauling theory. Intermediate magnetic susceptibilities are also shown by  $\text{Fe}(\text{CNS})_2$  and  $\text{Co}(\text{CN})_2$  complexes with *o*-phenantroline and 2,2'-bipyridyl.<sup>2</sup>

## (2) *The Ligand-Field Theory*

The ligand-field theory of Van Vleck and others<sup>12</sup> assumes that the central cation is held together by electrostatic forces, and that the behavior of the paramagnetic ion depends on the electric field arising from the surrounding ligands. This theory, originally called the "crystal-field theory", was applied to the behavior of metal ions in a crystal lattice, but it may be used equally well to describe metal complexes in which the metal ion is under the influence of the charge field created by the ligands. The basic assumption is that the effect of neighboring atoms can be represented by means of a static potential.

The crystal field splits the orbital levels of the paramagnetic ion into groups with an energy separation of about  $\Delta = 10^3$ – $10^4$   $\text{cm}^{-1}$ . The effect of a cubic force field is to split the five-fold orbital degeneracy of the ground state  $^6\text{S}$  of  $\text{Fe}^{3+}$  into an orbital doublet ( $d\gamma$ ) and an orbital triplet ( $d\epsilon$ ), the latter lower by about  $\Delta = 10$  Dq. (Dq is the crystal-field parameter usually used.) The consequent tetragonal component of the electric field and the spin-orbit coupling acting together partly remove the remaining degeneracy of each orbital level. The value of  $\Delta$  depends upon the charge on the ion, since a large ionic charge causes a large polarization of the ligand electrons and thereby increases the electrostatic field.

The presence of bonding increases the splitting between the  $d\gamma$  doublet and the  $d\epsilon$  triplet, and is in this respect similar in effect to an increase in the crystal-field strength, i.e. the value of  $\Delta$  increases as the ligand field increases.

The magnetic properties of the complexes can be explained on a ligand-field basis in the following way. If the ligand field is weak,  $\Delta$  is small and five magnetic  $d$  electrons of  $\text{Fe}^{3+}$  will occupy all five  $d$  orbitals. In the strong ligand field the  $d\gamma$  orbitals are very much



higher than the  $d\epsilon$  orbitals. Therefore, only  $d\epsilon$  orbitals are occupied and we obtain only one unpaired electron in ferric complexes.

The magnetic moments of some hemoproteins reported in the experimental part of this paper correspond to around three or four unpaired electrons per molecule. This is incompatible with the assumption that we have here essentially ionic or covalent bonds. An alternative explanation of these results is possible with the ligand-field theory.<sup>22, 25</sup> It can be shown that the intermediate spin type is possible if the ligands in the axis perpendicular to the heme plane are replaced by groups producing a low ligand field thus creating asymmetry which will split the two  $E_g$  levels.<sup>5, 11</sup>

The value  $\Delta$  depends upon the charge of the ligands on the perpendicular to the heme plane, since a large ionic charge causes a large polarization of the ligand electrons and thereby increases the electrostatic field. The ligands may be placed in order of decreasing electronegativity. This order is often found in spectrochemical investigations.<sup>23</sup> In  $F^-$  the electrons are held more tightly to the nucleus of the fluoride ion, and they are not distorted by the metal ion as much as they are in the  $CN^-$  ion. Therefore in  $F^-$  complexes we have purely electrostatic forces; in  $CN^-$  complexes, on the other hand, there is a strong bond between the metal ion and the  $CN^-$  ligand.

A comprehensive theoretical description of the ligand-field theory is given in this volume by Kotani, and elsewhere by Orgel,<sup>12</sup> and we will therefore not go into further detail.

### (3) *The Molecular-Orbital Method*

The molecular-orbital method also neglects in the Schrödinger equation the effect of interelectronic repulsion but it gives equal weight to the ionic and covalent terms. By using linear combinations of atomic orbitals (LCAO method) we obtain, e.g. for the hydrogen molecule, the equation

$$\Psi = \frac{1}{N} \{ [\psi_A(1) \pm \psi_B(1)] [\psi_A(2) \pm \psi_B(2)] \}$$

where after multiplication we have the ionic terms  $\psi_A(1), \psi_A(2)$  and  $\psi_B(1) \psi_B(2)$ , which are neglected in valence-bond theory. The solution of secular problems in molecular-orbital theory gives upper

and lower roots of the secular equation. The lower roots are bonding, the upper roots are antibonding. The bonding molecular orbitals represent lower energy and the antibonding orbitals represent higher energy than for the free atoms.

According to Van Vleck<sup>24</sup> there are in  $\text{Fe}(\text{CN})_6^{3-}$  and other  $\text{MX}_6$  complexes linear combinations of ligand  $\sigma$  and  $\pi$  orbitals with  $d\epsilon$  and  $d\gamma$  orbitals of cation possible:

$$\Psi = \alpha\psi(3d\gamma) + (1 - \alpha^2)^{1/2}\psi \sum \sigma_{i,k}$$

$$\Psi = (1 - \beta^2)^{1/2}\psi(3d\epsilon) + \beta\psi \sum \pi_{i,k}$$

$\alpha$  and  $\beta$  are here admixture coefficients for  $\sigma$  and  $\pi$  bonds. If  $\alpha^2 = 0$  and  $\beta^2 = 0$ , there is no contribution from the  $\sigma$  and  $\pi$  orbitals of ligands and the bonding is purely ionic. If  $\alpha^2$  and  $\beta^2$  are 0.5 we have a purely covalent bond. The value for  $\alpha$  or  $\beta$  can be determined, at least in principle by solving a secular equation. Unfortunately, there are great difficulties in solving secular matrices.  $\alpha$  and  $\beta$  may be obtained by empirical methods, and by other methods such as electron spin resonance.

The method of molecular orbitals has been used by Van Vleck<sup>24</sup> to investigate the anomalous magnetic properties of  $\text{Fe}(\text{CN})_6^{3-}$  and Van Vleck has shown that the same result is obtained by use of the crystal-field theory, the valence-bond method, or the molecular-orbital method. One can only enquire as to which procedure involves the most reasonable hypothesis.

We have shown experimentally that intermediate values of magnetic moments and also intermediate bonding in some hemoprotein complexes cannot be explained by Pauling's approximation. The ligand-field theory is suitable for interpreting the magnetic properties. Unfortunately the ligand-field theory is inadequate in its description of the chemical bond. The usual calculation of the energy states of the  $d$  electrons in a ligand field leaves the strength of the ligand field,  $Dq$ , undetermined. Moreover, the ligand-field theory treats all ligands *en bloc*. It seems that in the case of complexes of the transition elements one must probably decide in favor of the molecular-orbital method as the best description of the chemical bond.

In lieu of the octahedral space group ( $O_h$ ) in hemoproteins, lower symmetries  $\text{MX}_4\text{A}_2$  with the point group  $D_{4h}$  or  $\text{MX}_4\text{AB}$  with the

point group  $C_{4v}$  are present. The linear combinations for such complexes are collected in Table II.<sup>8,10</sup>

On the  $\text{Fe}^{3+}$  we have five  $3d$ , one  $4s$  and three  $4p$  wave functions. These may be combined with ligand functions to form six wave functions which are directed toward the central ion and are commonly called  $d\sigma$  orbitals, and twelve others which are oriented at right angles to the  $d\sigma$  orbitals and are called  $d\pi$  orbitals (Fig. 3).

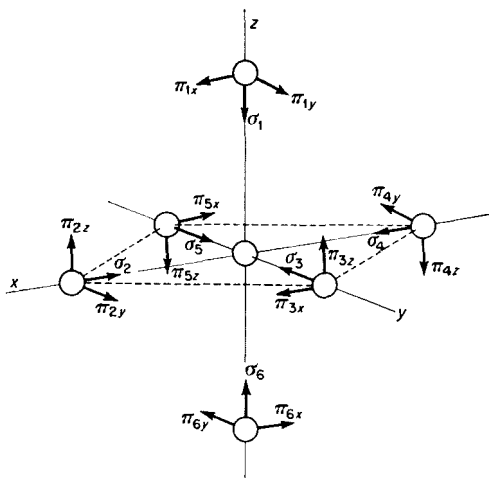


Fig. 3. Orientations of the orbitals.

We also have bonding and antibonding orbitals. Since the bonding orbitals are of greater potential energy than the antibonding orbitals the electrons occupy the bonding orbitals first. The covalency decreases with the number of antibonding electrons. The total spin which is measured as magnetic susceptibility does not necessarily indicate the nature of the bonding, but will sometimes give the bonding constants  $\alpha$  and  $\beta$ . Owen<sup>13</sup> has shown for which cases it is possible to calculate  $\alpha$  or  $\beta$  constants from the magnetic susceptibility data in  $\text{MX}_6$  complexes. Thus in purely ionic bonds we have  $\alpha = \beta = 1$  and the total spin has the value given by the Hund rule that the ground state is that of maximum multiplicity compatible with the Pauli principle. In covalent bond  $\alpha$  or  $\beta$  can be obtained only under favorable conditions. Here the magnetic susceptibilities give information about unpaired  $d$  electrons and,

hence, only approximate and qualitative values of  $\alpha$  and  $\beta$ , if at all. The values of  $\alpha$  for the covalent  $\text{Fe}^{3+}$  complexes ( $d\epsilon^5$ ) cannot be found because there are no  $d\gamma$  electrons. The measurements of magnetic susceptibility provide only an indirect method of determining the chemical bond.

In hemoproteins we do not have purely ionic but only "essentially ionic" complexes which show  $\sigma$  bonds between the ferric ion and the

TABLE II. Molecular Orbital Combinations

			$d\sigma$ bond	$d\pi$ bond
$\text{MX}_6$ $(O_h)$ ionic, e.g. $\text{HbF}$	$A_{1g}$	$4s$	$\frac{1}{\sqrt{6}} (\sigma_1 + \sigma_2 + \sigma_3 + \sigma_4 + \sigma_5 + \sigma_6)$	
	$E_g$	$3d_{z^2}$	$\frac{1}{\sqrt{12}} (2\sigma_1 + 2\sigma_6 - \sigma_2 - \sigma_3 - \sigma_4 - \sigma_5)$	
		$3d_{x^2-y^2}$	$\frac{1}{2} (\sigma_2 + \sigma_4 - \sigma_3 - \sigma_5)$	
	$F_{1u}$	$4p_x$	$\frac{1}{\sqrt{2}} (\sigma_2 - \sigma_4)$	
		$4p_y$	$\frac{1}{\sqrt{2}} (\sigma_3 - \sigma_5)$	
		$4p_z$	$\frac{1}{\sqrt{2}} (\sigma_1 - \sigma_6)$	
	$F_{2g}$	$3d_{xy}$		
		$3d_{yz}$		
		$3d_{zx}$		
$\text{MX}_5\text{A}$ $(C_{4v})$ M-A-bond essentially ionic, e.g. $\text{HbNCO}$	$A_1$	$4s$	$\frac{1}{\sqrt{8}} (\sigma_2 + \sigma_3 + \sigma_4 + \sigma_5 + 2\sigma_6)$	
		$3d_{z^2}$	$\frac{1}{\sqrt{8}} (\sigma_2 + \sigma_3 + \sigma_4 + \sigma_5 - 2\sigma_6)$	
		$4p_z$	$\sigma_1$	
	$B_1$	$3d_{x^2-y^2}$	$\frac{1}{2} (\sigma_2 + \sigma_4 - \sigma_3 - \sigma_5)$	
		$4p_x$		$\pi_x$
		$4p_y$		$\pi_y$
		$3d_{xx}$	$\frac{1}{2} (\sigma_2 + \sigma_3 - \sigma_4 - \sigma_5)$	
		$3d_{yz}$	$\frac{1}{2} (\sigma_2 - \sigma_3 - \sigma_4 + \sigma_5)$	

TABLE II—*continued*

			$d\sigma$ bond	$d\pi$ bond
MX <sub>4</sub> A <sub>2</sub> ( <i>D</i> <sub>4h</sub> ) M-A- bond essentially covalent, e.g. HbN <sub>3</sub>	<i>A</i> <sub>1g</sub>	4s	$\frac{1}{\sqrt{2}}(\sigma_1 + \sigma_6)$	
		4d <sub>z</sub>	$\frac{1}{2}(\sigma_2 + \sigma_3 + \sigma_4 + \sigma_5)$	
	<i>B</i> <sub>2g</sub>	3d <sub>y<sup>2</sup>-z<sup>2</sup></sub>	$\frac{1}{2}(\sigma_2 - \sigma_3 + \sigma_4 - \sigma_5)$	
	<i>A</i> <sub>2u</sub>	4p <sub>z</sub>	$\frac{1}{\sqrt{2}}(\sigma_1 - \sigma_6)$	
	<i>E</i> <sub>g</sub>	4p <sub>x</sub>	$\frac{1}{\sqrt{2}}(\sigma_3 - \sigma_5)$	$\frac{1}{\sqrt{2}}(\pi_{1x} - \pi_{6x})$
		4p <sub>y</sub>	$\frac{1}{\sqrt{2}}(\sigma_2 - \sigma_4)$	$\frac{1}{\sqrt{2}}(\pi_{1y} - \pi_{6y})$
	<i>E</i> <sub>g</sub>	3d <sub>zz</sub>		$\frac{1}{\sqrt{2}}(\pi_{1x} + \pi_{6x})$
		3d <sub>yz</sub>		$\frac{1}{\sqrt{2}}(\pi_{1y} + \pi_{6y})$
	<i>B</i> <sub>2g</sub>	3d <sub>xy</sub>		
MX <sub>6</sub> ( <i>O</i> <sub>h</sub> ) covalent, e.g. HbCN	<i>A</i> <sub>1g</sub>	4s	$\frac{1}{\sqrt{6}}(\sigma_1 + \sigma_2 + \sigma_3 + \sigma_4 + \sigma_5 + \sigma_6)$	
	<i>E</i> <sub>g</sub>	3d <sub>z</sub> <sup>2</sup>	$\frac{1}{\sqrt{12}}(2\sigma_1 + 2\sigma_6 - \sigma_2 - \sigma_3 - \sigma_4 - \sigma_5)$	
		3d <sub>x<sup>2</sup>-y<sup>2</sup></sub>	$\frac{1}{2}(\sigma_2 + \sigma_4 - \sigma_3 - \sigma_5)$	
	<i>F</i> <sub>1u</sub>	4p <sub>x</sub>	$\frac{1}{\sqrt{2}}(\sigma_2 - \sigma_4)$	$\frac{1}{2}(\pi_{3x} - \pi_{5x} + \pi_{1x} - \pi_{6x})$
		4p <sub>y</sub>	$\frac{1}{\sqrt{2}}(\sigma_3 - \sigma_5)$	$\frac{1}{2}(\pi_{2y} - \pi_{4y} + \pi_{1y} - \pi_{6y})$
		4p <sub>z</sub>	$\frac{1}{\sqrt{2}}(\sigma_1 - \sigma_6)$	$\frac{1}{2}(\pi_{2z} - \pi_{4z} + \pi_{3z} - \pi_{5z})$
	<i>F</i> <sub>2g</sub>	3d <sub>xy</sub>		$\frac{1}{2}(\pi_{2y} + \pi_{3x} + \pi_{4y} + \pi_{5x})$
		3d <sub>yz</sub>		$\frac{1}{2}(\pi_{2x} + \pi_{4z} + \pi_{1z} + \pi_{6x})$
		3d <sub>zz</sub>		$\frac{1}{2}(\pi_{3z} + \pi_{5z} + \pi_{1y} + \pi_{6y})$

ligands. In "essentially covalent" complexes there are six  $\sigma$  and six  $\pi$  bonds between the metal ions and the ligands. The antibonding  $d$  orbitals are occupied by  $\pi$  bonds and the five magnetic  $d$  electrons must go into three bonding  $d\epsilon$  orbitals. Therefore we have  $S = \frac{1}{2}$ . In

these complexes the  $\sigma$  bonding is likely to be stronger, but the  $\pi$  bonding will also increase the bond strength. Such a bond is present in ferrihemoglobin cyanide. A magnetic moment of about 2.3 B.M. instead of 1.73 B.M. is due to orbital contribution.

Molecular-orbital theory is also able to explain intermediate magnetic susceptibilities and intermediate chemical bonds. In Section II it is shown that ferrihemoglobin and other ferrihemoproteins can bind a large number of small molecules which can combine and have intermediate magnetic susceptibilities and chemical bonds. In Table II it is shown that in succession ionic  $\text{MX}_6$ ,  $\text{MX}_4\text{A}_2$ ,  $\text{MX}_4\text{AB}$ , and covalent  $\text{MX}_6$  have the systematical increase of the  $d\pi$  bond. The hemoproteins therefore can be classified in four groups:

(a) "essentially ionic" complexes (e.g. ferrihemoglobin fluoride). (In these complexes there are only six  $d\sigma$  bonds.)

(b) ionic bonds with a stronger bond on the perpendicular to the heme plane ( $\text{MX}_5\text{A}$  complexes). (In these hemoproteins we also have a  $d\pi$  bond to the ligand A. This group comprises, for instance, the alkaline ferrihemoglobin, ferrihemoglobin salts with CNS, CNO,  $(\text{COOH})_2$ , etc.)

(c) complexes with strong bonding of the two ligands on the perpendicular to the heme plane ( $\text{MX}_4\text{A}_2$  complexes). (In these complexes both ligands A have not only  $d\sigma$  but also  $d\pi$  bonds; ferrihemoglobin azide possibly falls in this group.)

(d) "essentially covalent" bonds with six  $d\sigma$  and twelve  $d\pi$  bonds. (The chemical bond in such complexes is very strong. In this group falls the ferrihemoglobin cyanide.)

All hemoproteins show  $d\sigma$  bonds and differ only in the  $d\pi$  bonds. Because the coefficient of the linear combination for the  $d\pi$  bond is  $\beta$ , we can describe the chemical bond in these complexes in terms of  $\beta$ . Analogous to the shifting of the  $g$  factor in the electron spin resonance we can describe deviations from ionic bond as

$$\mu_{\text{eff}} = [2 - (1 - \beta^2)] \sqrt{S(S + 1)}$$

because the electrons which are responsible for the magnetic susceptibility occupy antibonding orbitals.  $\beta$  is 1 if all unpaired electrons are on the Fe atom and 0.5 if these electrons spend the same time in the Fe atom and on the ligands. The  $\beta$  for some ferrihemoglobin complexes are shown in Table III. For "essentially

TABLE III. Chemical Bond of Ferrihemoglobin Complexes

Complex	$\beta$
$F^-$	0.95
$H_2O$	0.93
$HCOO^-$	0.92
$CH_3COO^-$	0.92
$SCN^-$	0.85
$OH^-$	0.70
$NO_2^-$	0.73
$SeCN^-$	0.65

covalent" bonds this formula is not valid because the interatomic forces are sufficiently powerful to destroy Russell-Saunders coupling and we have  $S = \frac{1}{2}$ , very strong  $d\pi$  bonds and a large contribution of orbital paramagnetism.

### References

1. Ballhausen, C. J., *Theories of Bonding in Coordination Compounds*, Lecture at the Coordination Meeting in Detroit, August 1961.
2. Cambi, L., and Cagnasso, A., *Rend. Ist. Lombardo Sci.* **67**, 741 (1934).
3. Coryell, Ch. D., Stitt, F., and Pauling, L., *J. Am. Chem. Soc.* **59**, 633 (1937).
4. Daudel, R., Lefebvre, R., and Moser, C., *Quantum Chemistry*, Interscience, New York and London, 1959.
5. Griffith, J. S., *Proc. Roy. Soc. (London)* **235A**, 23 (1956).
6. Hartree, E. F., *Ann. Rept. Progr. Chem. (Chem. Soc. London)* **43**, 287 (1947).
7. Heitler, W., and London, F., *Z. Physik* **44**, 455 (1927).
8. Kida, S., Fujita, J., Nakamoto, K., and Tsuchida, R., *Bull. Chem. Soc. Japan* **31**, 79 (1958).
9. Kotani, M., *J. Phys. Soc. Japan* **4**, 293 (1949).
10. Nakamoto, K., Fujita, J., Kobayashi, M., and Tsuchida, R., *J. Chem. Phys.* **27**, 439 (1957).
11. Orgel, L. E., in J. E. Falk, R. Lemberg, and R. K. Morton (Eds.), *Hematin Enzymes*, Part I, Pergamon Press, London, 1961, p. 1.
12. Orgel, L. E., *An Introduction to Transition-Metal Chemistry*, Methuen, London, and Wiley, New York, 1960.
13. Owen, J., *Discussions Faraday Soc.* **19**, 127 (1955).
14. Pauling, L., *J. Am. Chem. Soc.* **53**, 1367 (1931).

15. Pauling, L., and Coryell, Ch. D., *Proc. Natl. Acad. Sci. U.S.* **22**, 210 (1936).
16. Pauling, L., and Coryell, Ch. D., *Proc. Natl. Acad. Sci. U.S.* **22**, 159 (1936).
17. Pauling, L., *The Nature of the Chemical Bond*, Oxford University Press, London, 1939.
18. Scheler, W., Schoffa, G., and Jung, F., *Naturwissenschaften* **43**, 159 (1956).
19. Scheler, W., Schoffa, G., and Jung, F., *Biochem. Z.* **329**, 232 (1957).
20. Schoffa, G., Scheler, W., Ristau, O., and Jung, F., *Acta Biol. Med. Germ.* **3**, 65 (1959).
21. Slater, J. C., *Phys. Rev.* **38**, 1109 (1931).
22. Tanabe, Y., and Sugano, S., *J. Phys. Soc. Japan* **9**, 753 (1954).
23. Tsuchida, R., *J. Chem. Soc. Japan* **13**, 388, 426 and 471 (1938).
24. Van Vleck, J. H., *J. Chem. Phys.* **3**, 807 (1935).
25. Williams, R. J. P., *Chem. Revs.* **56**, 299 (1956).



## **PART II**

# **EXPERIMENTAL**

- |   |              |
|---|--------------|
| B. Influence of Physical Agents on Proteins and Nucleic Acids                                 | Chaps. 5–7   |
| C. Electrical and Magnetic Properties of Organic Molecular Solids, Proteins and Nucleic Acids | Chaps. 8–10  |
| D. Applications of Spectroscopic Methods  | Chaps. 11–14 |
| E. Physico-chemical Mechanisms in Biological Systems  | Chaps. 15–18 |



# THERMAL EFFECTS ON PROTEIN, NUCLEIC ACID AND VIRUSES

ERNEST C. POLLARD, *Graduate School Committee on  
Biophysics,\* The Pennsylvania State University,  
University Park, Pennsylvania*

## CONTENTS

I. Introduction . . . . .	201
II. The Nature of Thermal Action . . . . .	203
III. Experimental Findings . . . . .	211
A. Enzyme Reaction Rates . . . . .	211
B. Enzyme Inactivation . . . . .	212
C. Denaturation of Proteins . . . . .	216
D. Denaturation of Nucleic Acids: Melting Out . . . . .	217
E. Loss of Biological Activity of Nucleic Acids . . . . .	220
F. The Effect of Heat on Viruses . . . . .	222
G. The Thermal Expansion of Proteins . . . . .	224
IV. Theoretical Discussion . . . . .	225
A. Inactivation . . . . .	225
B. The Role of Water in the Inactivation Process . . . . .	227
V. Theoretical Partition Functions for Proteins and DNA . . . . .	229
VI. Energy of the Hydrogen Bond . . . . .	232
VII. Loss of Infectivity of Viruses . . . . .	233
VIII. Conclusion . . . . .	235
IX. Acknowledgements . . . . .	235
References . . . . .	236

## I. INTRODUCTION

The nature of heat has occupied the interest of physicists for several centuries. One of the triumphs of the combined experimental and theoretical approach has been the achievement of a high degree of understanding of the behavior of many substances over very wide temperature ranges. It is almost true to say that the physicist is only interested in very high and very low temperatures and considers the intermediate range as offering no new problems.

\* Much of the experimental background was developed while aided by U.S.P.H.S. Grants E1131 and RG9557.

In recent years, it has been shown that living systems behave in manners controlled by very large molecules, so large as to come within the definition suggested by Schrödinger of "aperiodic crystals". These large molecules are not simple repetitive structures; they have a definite essential order to their components, an order which seems to be very much analogous to the letters in a message and which needs to be intact to preserve the purpose of the molecule. What is more, the irregular, but definite, order also controls two other kinds of structure: the *secondary structure* which governs the coiling of a long molecular chain and the *tertiary structure* which governs the arrangement of the coils. It seems certain that the biological action of these large molecules depends on all three factors—order in the chain, secondary order and tertiary order. The problem presented to the physicist is thus both clear cut and complex. On the one hand the new evidence suggests that living systems are indeed controlled by molecular "behavior" and on the other hand this behavior involves a triple character. Thus the precise description of almost any physical variation in a molecule of protein or nucleic acid will almost certainly find application in some aspect of living behavior and yet the precision of description has to be three-fold.

Great advances in our understanding of protein and nucleic acid molecules have been made by a basically chemical approach whereby molecular alterations are made chemically or biochemically. Such experiments call attention to the effect of alterations in the assembly order of the molecules, but they are not necessarily concerned with secondary and tertiary structure. Studies of thermal effects have not been pushed so energetically because it has been hard to interpret the observations of these effects. The effect of thermal action is most usually on the secondary and tertiary structure, and so thermal studies should be an admirable complement to chemical studies. One object of this article is to review the evidence bearing on the nature of thermal action in the hope of showing that it is understandable and hence useful in further studies.

With this in mind, the following section will be devoted to a consideration of the nature of thermal action, as seen from the physical point of view. As far as can be done the experimental work will then be described in such a way as to make it possible to compare it with theory. Whenever it proves feasible, deductions regarding

molecular character will be made. Finally, suggestions as to the direction of future studies will be made.

## II. THE NATURE OF THERMAL ACTION

It is almost as difficult to describe the nature of heat as it is to describe a landscape. Almost all classes of energy take part in thermal behavior and their interplay is mainly regulated by statistics. For this reason it is easiest to take a particular case and to describe the various parts which contribute to thermal behavior and then to see what kind of generalization can be made.

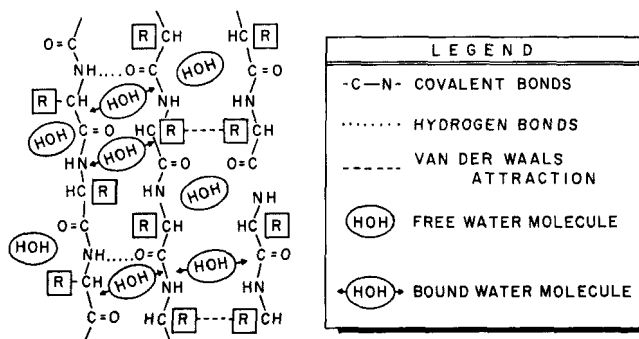


Fig. 1. A representation of three polypeptide chains lying close to each other. The various kinds of bonds are indicated together with the molecules of free and bound water.

In Fig. 1 we show three segments of polypeptide chains lying close to one another so that there are, in addition to the covalent bonds of the chains themselves, hydrogen bonds and van der Waals (or London) attractions. The chains are also supposed to have some bound water, indicated by the two arrows on the HOH, and free water. While this system is by no means inclusive of all the features of a protein molecule or a virus, there is sufficient complexity to enable us to begin to describe the factors which are operating.

In this system there are two main types of motion which are concerned with heat—vibration and rotation. In addition, there is also a continual exchange between electromagnetic radiation and the whole molecular system. There exist other forms of energy, for example the energy of excitation of an electron to a higher orbital or the energy of rupture of a bond. These forms of energy are only

rarely coupled to the more normal thermal processes. In physical measurements these rare events can essentially be ignored; in biological studies the opposite is true—it is these rare occasions when bonds are ruptured or excitation produced which cause the biological actions. Thus there is some divergence between the findings of physicists on thermal action and the kind of results of heat which are commonplace in biology. Nevertheless, the physical description is clearly adequate to describe the biological events; any inadequacy is a result of incomplete knowledge of the molecule on the one hand, or the inability to include the great complexity of bond structure on the other. In any event we shall proceed with the description.

Two quantities are of paramount importance in describing the thermal properties of a system such as we have chosen. The first is the *internal energy* and the second the *free energy*. To understand both these it is necessary to describe the various forms of energy in the system. There are two in the main: *vibration* and *rotation*. Both are governed by quantum mechanical rules. For the simplest form of vibration, the harmonic oscillator, the kind of motion is confined to a set of energy values,  $E_0, E_1, E_2$ , which are prescribed by integers and which obey the relation

$$E_n = \frac{h}{2\pi}(n + \frac{1}{2})\sqrt{\frac{b}{M}} \quad (1)$$

where the force relation for the harmonic oscillator is given by  $F$  (force) =  $-bx$  (distance),  $M$  is the mass which is oscillating,  $n$  is an integer and  $h$  is Planck's constant. The values of  $E$  are equally spaced, with a spacing dependent on  $b$  and  $M$ , and each value of energy can be obtained in only one way.

Looking at Fig. 1, it can be seen that many forms of oscillation exist and that the vibrational energy for the system will have many parts, governed by the force constants and masses concerned. Clearly the relationship of these many forms of vibration to the statistical distribution of energy is of great importance. A discussion of this distribution will be deferred for the moment.

A molecule which may rotate about a fixed axis has allowed energy values  $E_m$  given by

$$E_m = \frac{h^2 m^2}{8\pi^2 I} \quad (2)$$

where  $m$  is an integer and  $I$  is the moment of inertia of the molecule about its axis. These energy levels steadily become further and further apart. Also, there are several ways of attaining the same energy and the number of ways increases with  $m$ , being  $2m + 1$  for any particular value. This *degeneracy* is an important feature of this kind of motion.

Just as there are many forms of vibration, so in the liquid state there are many forms of rotation, ranging from hindered rotation which is really a rotational oscillation, to freely rotating units. The point to be made is that the spacing of the levels is determined by  $I$ , the moment of inertia, and this may well be large so that rotational levels can be close together and, because of their degeneracy, large in number. In Table I we give some values for the energies of

TABLE I. Rotational and Vibrational Energies

System	Kind of motion	Energy values (ergs)	Ratio to $kT$ at 37°C
HCl	Vibration	$2.97 \times 10^{-13}$	7.0
		$8.91 \times 10^{-13}$	20.6
		$14.85 \times 10^{-13}$	34.7
CO	Vibration	$2.15 \times 10^{-13}$	5.0
		$6.45 \times 10^{-13}$	15.1
		$10.75 \times 10^{-13}$	25.1
H <sub>2</sub> O	Rotation	$5.53 \times 10^{-17}$	$1.29 \times 10^{-3}$
		$2.21 \times 10^{-16}$	$5.16 \times 10^{-3}$

vibration and rotation in a few simple cases. Although the two methods of containing energy within the system which we have chosen are by no means the only ones possible, it is now feasible to describe the two functions, internal energy and free energy.

The internal energy  $U$  is the sum total of the energy in all its forms

$$U = \sum N_{\text{vib}} E_{\text{vib}} + \sum N_{\text{rot}} E_{\text{rot}} \quad (3)$$

where  $N_{\text{vib}}$  and  $N_{\text{rot}}$  represent the numbers of vibrational and rotational conditions of energy  $E_{\text{vib}}$  and  $E_{\text{rot}}$  respectively. It is a very simple and appealing idea and it is very useful. It lacks a means of

relating an energy change to the statistics of energy distribution. To consider the latter, the *partition function* or *zustandsumme*,  $Z$ , is most useful.  $Z$  is defined for any one kind of vibration or rotation as

$$Z = \sum e^{-E_n/kT} \quad (4)$$

where  $k$  is Boltzmann's constant and  $T$  is the absolute temperature. Where there are several forms of energy content coexisting, the partition function is the product of the separate partition functions. Thus  $Z$  for a system of one form of vibration and one form of rotation is

$$Z = Z_{\text{vib}} \cdot Z_{\text{rot}}$$

where  $Z_{\text{vib}}$  and  $Z_{\text{rot}}$  refer to the two separate partition functions.

Explicit values for partition functions can be derived for some simple cases. These are given below;  $m$  refers to mass.

Translation in a volume, $V$	Free rotation for three moments of inertia $I_1, I_2, I_3$	Linear vibration, frequency, $\nu$
$\frac{(2\pi mkT)^{3/2}}{h^3}$	$\frac{\pi^{1/2}(8\pi^2 kT)^{3/2} (I_1 I_2 I_3)^{1/2}}{h^3}$	$\frac{kT}{h\nu}$

In terms of these ideas, the free energy  $F$  is defined as

$$F = -NkT \ln Z \quad (5)$$

where  $N$  is the number of separate units to which the partition function  $Z$  applies. It can be seen that the free energy has three components: first a quantity component,  $N$ ; second an average energy component,  $kT$ ; third a component  $\ln Z$ , which describes the number of ways in which energy *could* be distributed. It is not surprising that a function with this three-fold content is extremely useful in describing thermal change.

Before going on to describe the way in which heat can cause a permanent change in a molecular structure, it is worth a moment to consider the factors which can change the size of  $F$ . Clearly the larger the number of separate units  $N$ , the larger is the numerical value of  $F$ . The greater the temperature, the larger is the value. Also a system such as a loose vibration, or a free rotation of a molecule with a high moment of inertia, will contribute a large value of  $Z$  and hence of  $\ln Z$ . Thus we look to a large, complex system with many loose vibrations and many free rotations to produce a large



numerical value. Such a value is *negative* and therefore such a system has a lower free energy than one which is simpler and has stiffer bonds with no rotation. In general the difference in free energy is of importance, particularly the difference between configurations of the same molecule. Thus consider Fig. 1. If the chains are tightly bonded by many effective hydrogen bonds, and if the amount of water free to rotate is small, the free energy which is measured downward, is not very far down and so is relatively high. A change in configuration which causes the bonding to become weaker and allows more water to rotate will have a higher negative value of  $F$  and so will be lower down on the scale. Such a transition might therefore be expected to occur under some circumstances.

We can now see how to describe the action of heat in terms of Fig. 1 and the function  $F$ . Raising the temperature produces two major effects. The first is explicitly to increase the value of  $T$ ; the second is to alter the nature of the bonds, thus producing a change in  $Z$  and hence in  $\ln Z$ . The consequences of these changes are, for the most part, quite trivial. Thus a solution of an enzyme can be warmed slightly and cooled slightly with no effects of any importance at all. On the other hand what is observed as thermal action on these molecules is a definite configurational change in which the loosening of bonds has caused a change to a wholly new method of bonding in one region. Such a change might be the breaking away of a whole chain to produce a dissociation of the molecule, or the uncoiling of a helical form to become a random coil. When this occurs the whole basis of reckoning of the free energy changes, because now there is a different number,  $N$ , of ways of dividing the energy and there is also a different set of energy levels and hence a different value of  $Z$ . The nature of thermal action is therefore very largely concerned with two factors. The first is a gradual change as the temperature increases, a change in which the system stays fundamentally unaltered, except in degree. The second is a relatively fast process of a shift to a new form in which the system is drastically altered and can be clearly seen to be different by the change of some measurable property.

The passage to the new form must, of necessity, be a process which happens relatively rarely and thus can be described primarily as a statistical event involving a probability. If it were not relatively rare then the whole system would need to be described in terms of

the new form, and thus a steady state condition of change would be the normal process.

In order to describe the nature of this process two factors have to be considered. The first is the measure of the statistical probability that enough energy will be available to permit the change of form to take place, and the second is an estimate of the rate at which the change takes place when energy is actually available. A third factor, that of a specific collision, which is often present in considering reaction rates, is generally not involved as the molecule is so large in the case of proteins and nucleic acids that the change we are describing is essentially internal. In order to consider these two factors, acquisition of energy and rate of change, the kind of energy must be understood and also the kind of change.

The most commonly used description, which is that of Eyring and his associates,<sup>11</sup> treats the process of change in form as involving three states: original, activated and final. On an energy diagram they appear as in Fig. 2. Eyring considers the process of acquisition of energy as being that of equilibrium between the original and the activated state. If the difference in free energy between these two states is denoted by  $\Delta F^*$  then the ratio of the number of molecules in the activated state,  $N^*$ , to the number in the original state,  $N$ , is given by

$$\frac{N^*}{N} = e^{-\Delta F^*/RT} \quad (6)$$

This ratio does not explicitly say how many of the molecules which do acquire the necessary energy will finally go on to change form. Actually the decision about this part of the process is not nearly so easy to describe in a satisfying way as the ratio just given. Eyring treats the process of actual passage as a translational process and deduces the rate per second per activated molecule as  $kT/h$  to a first approximation, where  $k$  is Boltzmann's constant,  $T$  is Kelvin temperature and  $h$  is Planck's constant. The actual number of changes of form per second is then  $dN/dt = (kT/h)N^*$  and by substitution in Eq. (6) we obtain

$$\frac{dN}{dt} = N \frac{kT}{h} e^{-\Delta F^*/RT}$$

This can be rewritten as

$$\frac{dN}{N} = \frac{kT}{h} e^{-\Delta F^*/RT} dt$$

Also, for this kind of internal rearrangement we have the very simple relation, which states that the fraction undergoing transition is a constant times the time,

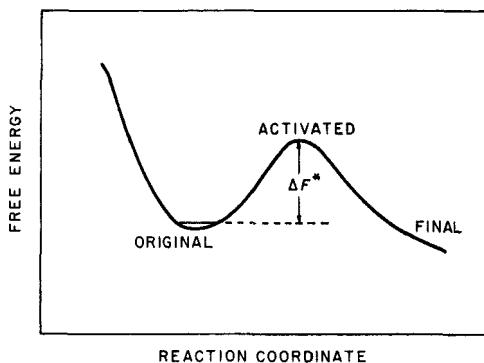


Fig. 2. A plot of the supposed variation of the free energy of a macromolecule as some chain starts to move away. The position of the chain is designated as the "reaction coordinate" and the free energy passes through a maximum at the "activated state". The free energy of activation is indicated.

$$\frac{dN}{N} = -k_1 dt \quad (7)$$

where  $k_1$  is the reaction constant. Thus we get

$$k_1 = \frac{kT}{h} e^{-\Delta F^*/RT} \quad (8)$$

This formulation is not universally deemed to be satisfactory. One may well object on the grounds that in a macromolecule where the final process of change of form may occur deep within the structure, the actual change is not really translation as considered above. This is not as important as it seems. Any process of actual transition is bound to be very rapid and almost any method of final passage will depend on the absolute temperature,  $T$ . So long as this term is of the order of  $10^{10} T$  per second, the effect on the primary variable,  $\Delta F^*$ , will not be great. For example, the value  $kT/h$

appears in Eyring's formulation as the product of the partition function for translation in a confined space of length  $\delta$ , which is  $(2\pi mkT)^{1/2}\delta/h$  and the frequency of passage for half the molecules, which is  $(2kT/\pi m)^{1/2}/\delta$ . In these formulas  $m$  is the effective mass which moves. The result is  $kT/h$ . If we suppose that the same term is the product of a vibration frequency  $\nu_0$  for a large mass oscillating, times the partition function for vibration which, for small values of  $\nu_0$  is  $1/(h\nu_0/kT)$  we again obtain  $kT/h$ . Thus we should probably regard Eq. (8) as representing a very large rate term which expresses of the speed of internal molecular changes and a term which measures the acquisition of energy.

We are now in a position to understand the general nature of the action of heat on biological macromolecules. The situation is dominated by the highly critical nature of a biological action by a macromolecule where, in very many cases, the exact features of structure in the chain, of folding of the chain and even tertiary structure, must be preserved for the biological function. Thus an enzyme may operate so that the actual region of molecular contact with the substrate is a particular amino acid (often a histidine residue) but the actual reaction will not take place unless the rest of the enzyme is correctly folded. Or a virus may have a nucleic acid chain, all of which is by no means essential, yet an unfolding of this chain within the protein shell may block the separation of protein and nucleic acid. Since the formation of a biological macromolecule within a living cell can be presumed to lead to a special configuration there are many other possible configurations not so formed and these will not function.

The process of heating combines a *general acquisition of energy*, with an associated increased probability of one special region acquiring energy, with a *kind of swelling*, in which a change in the number of molecules free to rotate takes place, a process which alters the distribution of energy. The combination of these two can produce a relatively rare situation in which energy is available to cause the molecule to change its configuration. This rare situation would be unimportant but for the fact that each such occurrence can be followed by an actual change, from the natural state to one which is stable but inactive. The effect of heat is then to cause a slow but persistent alteration of the molecular structure and also a slow loss of biological activity. It is this process which is responsible

for loss of enzyme activity and transforming activity, and causes the sterilization of cultures of viruses.

With some modification, the statistical thermodynamic description we have already given can be used to explain the action of heat. Rather than giving this theory now, we propose to describe several sets of experiments to show the kind of work that can be done and then to attempt a theoretical analysis of some of these experiments.

### III. EXPERIMENTAL FINDINGS

#### A. Enzyme Reaction Rates

One of the most commonly encountered effects of heat is the change in reaction rate of an enzyme with temperature. In Fig. 3 the rate of action of betagalactosidase on the substrate ONGP

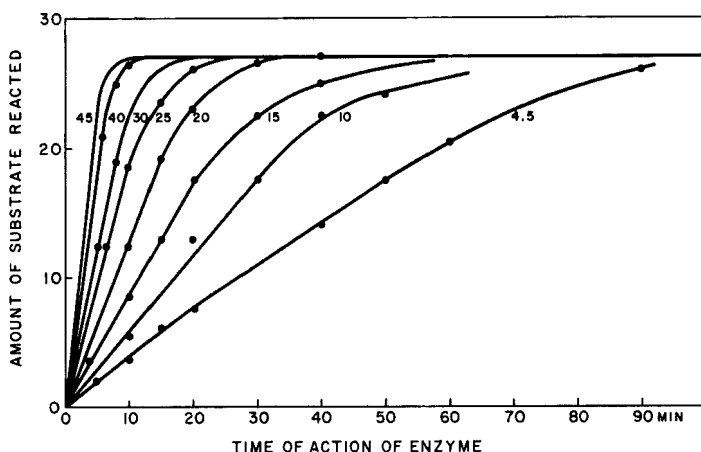


Fig. 3. The action of betagalactosidase on substrate (ONGP) as a function of time for temperatures ranging from 4.5°C to 45°C. The increase in the rate of action is apparent. Data due to Barbara Ruud.

(*ortho*-dinitrophenyl- $\beta$ -D-galactopyranoside) as a function of time and temperature is shown. These data were obtained in the author's laboratory by Barbara Ruud. The values of the rate constants are shown in Table II.

TABLE II. Rate Constants for the Action of Betagalactosidase at Different Temperatures

Temperature, °C	Temperature (T), °K	1/T	Rate constant (arbitrary units)
4.5	277.5	0.00361	0.36
10.0	283.0	0.00354	0.58
15.0	288.0	0.00347	0.87
20.0	293.0	0.00342	1.29
25.0	298.0	0.00336	1.82
30.0	303.0	0.00330	2.48
40.0	313.0	0.00320	2.80
45.0	318.0	0.00315	4.52

It can be seen that the rate constants increase rapidly as the temperature increases. In this case the rates are those of the initial rise when the substrate is in excess and they represent the break up of the enzyme-substrate complex into the products and the original enzyme. The rapid increase in the rates indicates that there is an energy of activation to be supplied and that this energy is acquired more readily and so with higher probability as the temperature increases. For this reaction the value of the activation energy varies slowly with temperature. An average value is 12,000 calories per mole. This is very typical value for the energy of activation in enzymatic processes. In this particular case the rate constants have also been measured in buffer made in D<sub>2</sub>O. The value of the activation energy found to be higher: it is 14,500 calories per mole. This is a general finding also and will be discussed later.

### B. Enzyme Inactivation

If an enzyme is heated for varying lengths of time at elevated temperatures it shows a loss of activity. An enzyme which can withstand drying without loss of activity loses its biological effectiveness in rather a simple way. Some data taken on invertase by the late Dr. W. F. Powell are shown in Fig. 4. The activity remaining is plotted on a logarithmic scale against the time elapsed. It can

be seen that the loss of activity is described by a simple relation

$$\ln (n/n_0) = -k_1 t \quad (9)$$

where  $n$  and  $n_0$  denote the activity at a time  $t$  and the initial activity, respectively, and  $k_1$  is a constant. This relation is the integral of a very simple, decay-type reaction already given in Eq. (7),  $dn/n = -k_1 dt$  and values for the reaction constant are given in Table III.<sup>18</sup>

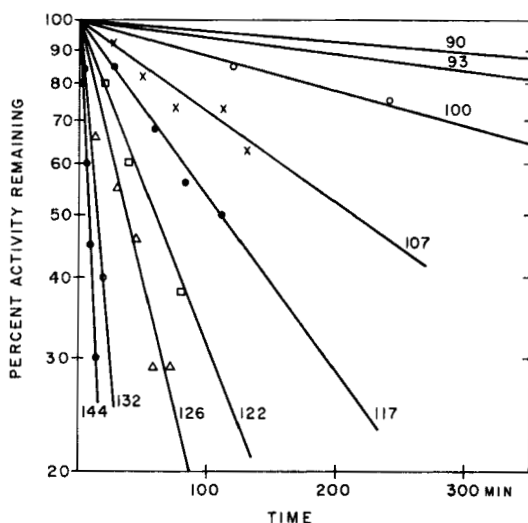


Fig. 4. The inactivation of invertase in the dry state as observed by Powell. The activity is lost in a simple way over a wide range of temperatures and corresponds to a free energy of activation which is constant.

This particularly simple example of thermal inactivation should be capable of accurate description by Eq. (8). According to this  $k_1$  is given by  $k_1 = (kT/h) e^{-\Delta F^*/RT}$  and if the relation holds, the value of  $\Delta F^*$  deduced in each case should be a constant. The last column of Table III shows the derived values<sup>18</sup> and it can be seen that quite good agreement with theory is found.

If the same enzyme is heated in the wet state in citrate phosphate buffer the inactivation is quite different. Results for pH 7 and pH 4.5, again data taken by Dr. W. F. Powell, show loss of activity

TABLE III. Rate Constants for the Inactivation of Dry Invertase

Temperature, °C	Temperature (T), °K	1/T	$k_1$ , fraction/sec	Calories per mole
90	363	$2.75 \times 10^{-3}$	$5.8 \times 10^{-6}$	30,250
100	373	2.68	$2.04 \times 10^{-5}$	30,100
107	380	2.63	$5.55 \times 10^{-5}$	29,900
117	390	2.56	$9.7 \times 10^{-5}$	30,100
126	399	2.51	$3.30 \times 10^{-4}$	30,200
144	417	2.40	$1.39 \times 10^{-3}$	30,250

as in Fig. 5. At the much lower temperatures used the activity decreases to a certain value and then remains the same. The constant residual value becomes less as the temperature increases. Chilling a sample which is at the residual value causes some increase in

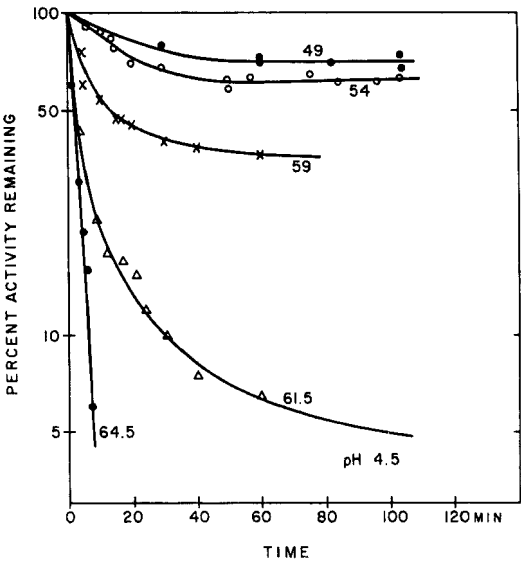
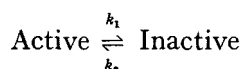


Fig. 5. The inactivation of invertase at pH 4.5 as observed by Powell. It can be seen that the relatively rapid initial inactivation is followed by a leveling out to a value which depends on the temperature.



activity. The loss in activity can be explained in part by an equilibrium in which we put



Setting  $a$  for initial activity,  $a_e$  for equilibrium activity and  $x$  for the amount rendered inactive, we have

$$\frac{dx}{dt} = k_1(a-x) - k_2x$$

giving 
$$a-x = \frac{k_2x + k_1ae^{-(k_1+k_2)t}}{k_1}$$

At infinite time, which corresponds to equilibrium, we find  $a_e/(1-a_e) = k_2/k_1$  and at very short times, when  $x$  is nearly zero,  $(a-x)/a = e^{-(k_1+k_2)t}$ . Thus both  $k_1$  and  $k_2$  can be found. Values for these are given in Table IV.

TABLE IV. Rate Constants for the Inactivation of Invertase in Solution

pH	Temperature, °C	$k_1$ , fraction/sec	$k_2$ , fraction/sec	$\Delta F_1^*$	$\Delta F_2^*$
4.5	48.5	$1.7 \times 10^{-4}$	$4.1 \times 10^{-4}$	24,500	28,800
	54.0	$3.8 \times 10^{-4}$	$6.8 \times 10^{-4}$	24,500	28,600
	59.0	$1.4 \times 10^{-3}$	$8.0 \times 10^{-4}$	23,950	28,700
	61.5	$3.3 \times 10^{-3}$	$2.1 \times 10^{-4}$	23,550	29,700
	64.0	$5.7 \times 10^{-3}$	—	23,350	
7.2	41.5	$4.1 \times 10^{-3}$	$4.3 \times 10^{-4}$	23,550	27,600
	44.0	$9.5 \times 10^{-4}$	$3.9 \times 10^{-4}$	23,150	27,800
	46.5	$1.6 \times 10^{-3}$	$3.9 \times 10^{-4}$	23,000	28,100
	49.0	$2.8 \times 10^{-3}$		22,800	
	54.0	$1.2 \times 10^{-2}$		22,150	
	59.0	$3.2 \times 10^{-2}$		21,900	

These figures indicate that the value of  $\Delta F_1^*$  decreases slightly as the temperature rises. This type of behavior is quite common and will be discussed in the next section. The reverse reaction, where

a rather sharp increase in  $\Delta F_2^*$  is observed at higher temperatures, indicates something abnormal and can be taken to suggest that the return process is complicated by some additional configuration change made possible at the higher temperatures.

### C. Denaturation of Proteins

The illustrations of the action of heat so far have been concerned with a loss of biological activity. However, proteins can be isolated and purified and their physical properties can be studied. Over a range of low temperatures many of these properties vary reversibly in the usual way. As the temperature is raised a new phenomenon of an irreversible change is seen. The most familiar is the change of ovalbumin from a clear, soluble protein to a white insoluble mass. This phenomenon, which is referred to as denaturation, is generally more drastic than loss of function although this certainly is often associated with it. Since any readily measurable change in physical properties usually requires some definite molecular alteration, such an alteration must occur in denaturation. It is usually associated with an unfolding of the secondary and tertiary structure of the protein and the formation of a new, or a mixture of several new, forms which are different from the original, generally by being much less accurately structured.

One very interesting method of studying this alteration of the secondary structure is by means of optical rotation, the rotation of the plane of polarization by a solution. The classical agent for such optical activity is an asymmetric carbon atom. A set of identical atoms arranged in a helix is another agent and such is to be found in proteins. Accordingly, a solution of a protein will show a rotation of the plane of polarization. If the protein solution is heated, there is, at lower temperatures, a gradual change in the rotation, but as the process of denaturation begins, the value rapidly increases. The following figures, taken from a graph of data due to Schellman,<sup>27</sup> indicate the kind of behavior. The protein is insulin. The denaturation process begins between 50 and 60°C and proceeds rapidly above 70°C. This type of experiment is valuable because the physical measurement is related to the degree of helical coiling of the polypeptide chain.

TABLE V. Optical Rotation ( $\alpha$ ) at Various Temperatures as Found by Schellman

Temperature, °C	Optical rotation
20	-38.5
30	-38.8
40	-39.5
50	-40.5
60	-44.0
70	-57.5
80	-72

#### D. Denaturation of Nucleic Acids: Melting Out

While in proteins the secondary structure is relatively complex, as it consists of partially helical sections in which the helix is held in place by bonds between amino acids within the helix, in one form of nucleic acid the secondary structure is very simple. In DNA two complementary chains of four bases—adenine (A), thymine (T), guanine (G) and cytosine (C)—form a double helix in which each adenine is hydrogen bonded to its complementary base thymine, and each guanine is bonded to cytosine in the other chain. While in this double helical form the molecule is relatively rigid. Also, the pyrimidine bases, thymine and cytosine, absorb ultraviolet light in the vicinity of 260 millimicrons wavelength, and when these bases are stacked in a relatively parallel and overlapping manner they are, so to speak, deployed wastefully for the purpose of absorbing light. Thus any agent which will separate the chains causes a better use to be made of the absorbing molecules and increases the absorption of light. The low absorption is called hypochromicity.

Upon heating DNA under conditions where the absorption of ultraviolet light can be measured, the absorption is observed to increase over quite a narrow temperature range. One such curve taken on a bacterial DNA preparation by Edgell is shown in Fig. 6. The sharpness of the transition is readily apparent. The process consists of a gradual severance of hydrogen bonds over limited segments of the giant double molecule, a severance which still

leaves the bases close together, followed at higher temperatures by a complete separation of the strands, which converts the double helix, in relatively stiff configuration, into two loose random coils. In these random coils the bases are more effectively used for absorbing light, hence the increased absorption is observed. This very useful phenomenon was first observed in DNA by Shack and Thompson.<sup>29</sup> Similar effects can be observed if the physical property studied is viscosity or the scattering of light. This process, referred to as

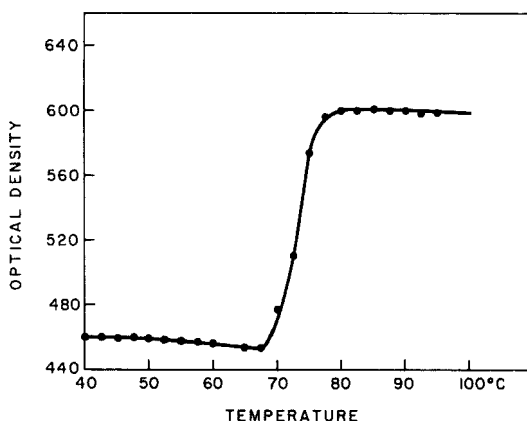


Fig. 6. The increase in ultraviolet adsorption as DNA passes from the double strand variety to the single strand due to thermal action. The ordinate is optical density times 1000. Data due to Edgell.

“melting,” is reversible. If the temperature is gradually lowered “hybrid” molecules will reform. Rapid chilling prevents such formation and can be used to prepare single strand DNA.

The fact that only two kinds of base pairs exist makes this phenomenon relatively simple to comprehend. The hydrogen bonding between adenine and thymine (AT) is not as strong as between guanine and cytosine (GC) where some bonding is present between three groups instead of two, a fact which makes a DNA sample rich in GC pairs more closely packed and hence more dense than high-AT DNA. This difference in bonding modifies the melting of high-GC DNA, which takes place at higher temperatures. Thus melting temperature and density are two physical parameters which can be used to characterize the DNA of different biological species.

While melting is quite sharp in DNA it is still a factor in single strand nucleic acids, notably in RNA found in ribonucleoprotein particles (or ribosomes), in RNA which can form hybrids with complementary single strand DNA (usually called "messenger RNA" or mRNA), and in the low molecular weight RNA (usually called SRNA) which has a specific relation with each amino acid. These strands can fold back on themselves, and tend to do so in such a way as to allow a high proportion of base pairing with hydrogen bonds. These also "melt," though not nearly so sharply and at such elevated temperatures. The safe temperature above which mRNA is found to be a single strand is 60°C. DNA very often melts well above this point.

In addition to the phenomenon of melting there are two other effects of heating. One is the rupture of the sugar-phosphate-sugar bond, known as the phospho-diester link. This is the rupture of a covalent bond, which we referred to earlier as improbable but highly important. A DNA molecule can have 100,000 such bonds in a single strand and if one of these is broken, while in the single strand form, two molecules will result in place of one. This molecular weight degradation can be caused by heating. Eigner, Boedtger and Michaels<sup>4</sup> observed an activation energy for such scission for RNA of 19 kcal/mole and for DNA of 25 kcal/mole. The other process is the removal of a purine from the chain and this again involves the rupture of a covalent bond. The rate of removal of purines from a DNA chain was measured by Greer and Zamenhof<sup>29</sup> at 81°C and found to be  $1.8 \times 10^{-5}$  removals per base pair per minute. The rate of scission was found by Doty, Marmur, and Sueko<sup>2</sup> to be  $10^{-6}$  events per base pair per minute at 79°C. Thus the removal of a purine is more probable. It is very interesting that in the RNA chain purines are much harder to remove and Ginoza<sup>7</sup> has suggested that this is due to the possibility of a further bonding of the phosphate with the OH of the ribose sugar.

Thus a picture emerges, as suggested by Ginoza and Zimm,<sup>8</sup> that DNA is vulnerable in three ways to the action of heat: first by melting of the hydrogen-bonded strands, which takes place sharply in a narrow temperature range; second by removal of purines, which takes place slowly at lower temperatures; and third by scission of the chain. For RNA the process is simpler, being primarily scission.

### E. Loss of Biological Activity of Nucleic Acids

The biological activities of nucleic acids have been the subject of intensive and remarkable work in the last two decades. Among these activities are the conferring, or rather carrying, of genetic markers (DNA), the forming of an ordered polypeptide chain which has enzymatic properties (messenger RNA), and in the specific carrying of amino acids to their place in an ordered synthesis (SRNA). Until recently it has not been easy to work with the nucleic acids alone while studying these basic biological properties. However, two

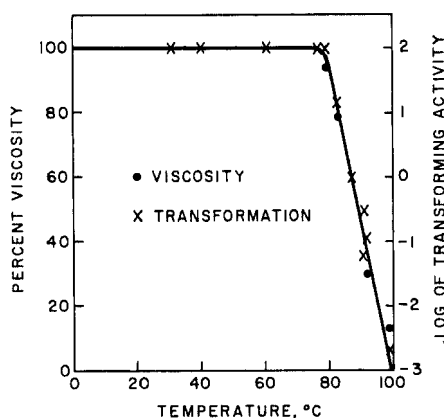


Fig. 7. Drop in viscosity and in transforming ability of DNA action on *Hemophilus influenzae* as a function of temperature as observed by Zamenhof, Alexander and Leidy. (From Zamenhof, Alexander and Leidy.<sup>32</sup>)

systems have developed which have been suitable for study—the transforming DNA of bacterial cells, notably *Pneumococcus*, *Hemophilus influenzae* and *Bacillus subtilis*, and the infectious RNA of viruses. Recent work on these systems has been most informative and promises still more information.

Thermal effects were studied on transforming principle in valuable early work by Zamenhof, Alexander and Leidy.<sup>32</sup> In Fig. 7 a plot of their data is given showing the reduction in activity of the transforming principle for *H. influenzae* and the reduction of viscosity by the effect of heat applied for one hour at the temperature shown. The sharpness of the process and its clear relation to a major

change in physical properties is dramatically apparent. Among the more recent papers of great significance is the work of Marmur and Lane<sup>13</sup> who showed that the inactivation of DNA which had the ability to transform pneumococcus to streptomycin-resistance at 100°C could be restored by slow cooling over a period of an hour or more. This process is called "annealing" and its physical characteristics were studied by Doty, Marmur, Eigner and Schildkraut.<sup>3</sup> The loss of biological function is due to the melting process already described and the annealing is due to the formation of recombined molecules.

The inactivation process has been carefully experimentally studied and considered theoretically by Ginoza and Zimm.<sup>8</sup> Using carefully prepared pneumococcus, in which protein is removed by phenol, they were able to show that two types of inactivation predominate. These can be seen in Fig. 8 where a wide series of plots of surviving activity versus time from 82.2 to 100.8°C are given. At the lower temperatures the inactivation follows the simple relation of Eq. (7) while in the very narrow range from 88.5°C to 90.8°C a completely different process develops and rapidly becomes predominant. These experiments indicate the change in character of one genetic marker on the DNA and are almost certainly to be explained in terms of two kinds of effect. The first is the alteration of a single base in the chain—the depurination process already discussed. This process, though most improbable, nevertheless can occur and when it does the DNA chain lacks one region which must specify correctly the amino acid order in an enzyme and so the activity is lost. This process is not likely to occur while the strands are still together and the fact that it does occur at temperatures below the melting temperature suggests that regions of strand separation are present even below the point of melting. The second process is strand separation, which occurs very sharply as discussed before. The parameters which characterize these two processes are most interesting and will be discussed later.

A considerable series of heat inactivation studies made by Roger and Hotchkiss<sup>24</sup> in which a great variety of genetic markers were studied leads to a similar conclusion, though there are differences in detail. Their work also shows clearly that there is some residual activity even after the DNA chains have collapsed. In the curves of Ginoza and Zimm shown in Fig. 8 this residual activity can also

be seen and it is of interest that the depurinating process seems to be observable even in the single strand condition.

For the case of RNA the system most studied is virus RNA which, in some cases, notably tobacco mosaic virus (TMV) and polio virus, has been found to be infectious even after separation from the protein shell. The effect of heat on TMV ribonucleic acid has been

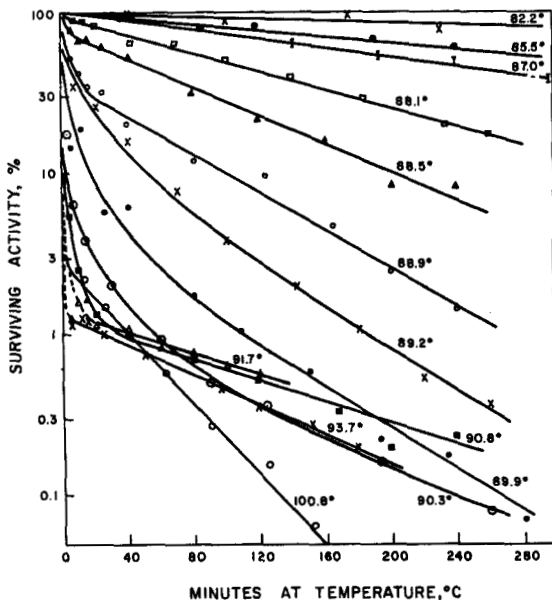


Fig. 8. Loss of transforming ability as observed by Ginoza and Zimm. The very rapid change between 89.9°C and 90.8°C is to be noted and also the fact that a small fraction retains its activity.

studied by Ginoza<sup>7</sup> who found a very simple inactivation, following the type of Eq. (7). He formed the conclusion that the effect of heat was to cause scission at the sugar-phosphate-sugar bond and that one such break would result in the loss of the biological activity.

#### F. The Effect of Heat on Viruses

The physical nature of nearly all viruses is now quite clear. With the possible exception of some large animal viruses such as *Vaccinia*, *Herpes simplex* and *Rabies*, a virus consists of a protein coat surrounding a very tightly and precisely wound chain of nucleic acid. The



essential portion proves to be the nucleic acid; this statement, however, must be qualified by saying that the protein part is very important in assisting with the process of entry into the host cell. In many cases the protein is still required for the process of infection to occur even though quite ingenious experimentation has been directed at securing the entry of pure nucleic acid. Thus, for an ordinary virus infection, unaided by skilled laboratory technique, the action of a virus is two-fold—first the process of attachment and entry, predominantly governed by the protein coat, and second the process of multiplication, predominantly governed by the nucleic acid. Thus the effect of heat on viruses should be two-fold, reflecting the heat sensitivity of protein as regards attachment, and the heat sensitivity of nucleic acid as regards multiplication. In a few experiments this dual character has been apparent. In most cases, however, the method of assay of the virus has simply been in terms of the process of infection and as this is the sum of attachment and multiplication the inactivation has reflected a double process, which has often appeared to be a kind of average of both. Early and informative experiments by Lauffer and Price<sup>12</sup> showed the course of loss of infectivity and of denaturation of tobacco mosaic virus. The denaturation proceeds rapidly at 90°C and the loss of infectivity follows it. However, at lower temperatures the loss of infectivity is more rapid. Work by Price<sup>13</sup> and Pollard and Dimond<sup>18</sup> showed that at still lower temperatures the kinetics of inactivation are quite different from those of denaturation.

Two contrasting studies have been made on T1 bacteriophage by Pollard and Reaume<sup>16</sup> and Pollard and J. Setlow.<sup>20</sup> In the first the loss of infectivity, as measured by the ability to form plaques in sheets of developing bacteria, was used as the means of assay. The inactivation both in the dry and wet state followed Eq. (7) and using the analysis of Eq. (8) gave  $\Delta F^*$  values, in calories per mole, of 27,500 constant with temperature for the dry condition and 26,200 varying down to 23,000 from 60° to 75°C in the wet state. The second study concerned quite a different property of the virus, the ability to combine with antiserum. This is certainly a property of the external protein coat and not of the nucleic acid interior. The reaction to heat was strikingly different. In the dry state it was hard to observe any inactivation until above 141°C and the resulting value for  $\Delta F^*$  was 31,900 which slowly fell to 21,000 at 173.5°C. In the wet state there

was no observable inactivation until 89.5°C and the ability to combine with antiserum could still be observed after 30 minutes at 102°C. The  $\Delta F^*$  value was 30,300 at 89.5°C and fell rather sharply to 26,400 at 102°C. Thus the behavior of the protein part as regards heat is strikingly different from the infectivity, which presumably is largely controlled by the nucleic acid.

Many viruses, particularly animal viruses, show an inactivation curve with heat which does not simply obey Eq. (7) but which has two components, one inactivating rapidly and one relatively slowly. The two do not represent a simple case of a resistant and sensitive population mixture, for the proportions of the two vary with the temperature at which the inactivation is studied. A very valuable review of this feature of inactivation has been given by Woese.<sup>31</sup> He also analyses the results in terms of a collapse property and something akin to a scission property. His analysis will be considered later.

Rather than summarizing the behavior of viruses as regards thermal action in terms of the experimental data, such summary will be reserved for the theoretical discussion because the known material can be set forth much more compactly when associated with theory.

### G. The Thermal Expansion of Proteins

A very important topic, which has received relatively little attention, is the thermal expansion of proteins. Some simple preliminary measurements have been made by the author<sup>22</sup> on egg albumin both in the dry state and in solution. In the dry state the thermal expansivity was found to be  $1.6 \times 10^{-4}$  fraction per °C, which is very large. It is so large that it could not be due to the elongation of even very weak bonds but must correspond to a kind of swelling process in which the secondary and tertiary structure enlarges. In solution a similar high expansivity is observed as can be seen from Fig. 9. The method used was an adaptation of the pycnometer to radioactive counting and the volume extruded by expansion was measured by the radioactivity which collected in liquid outside the expansion vessel. It can be seen that the expansion is definitely greater than that of water, which is itself high, and also that when denaturation occurs the expansion becomes less. From the values of expansion at the two concentrations shown,

the expansivity of fully hydrated egg albumin was found to be  $5.7 \times 10^{-4}$  volume fraction per  $^{\circ}\text{C}$ .

This high expansion must also carry with it an increased entraining of water, a fact which must also in turn have an effect on the kinetics of heat inactivation.

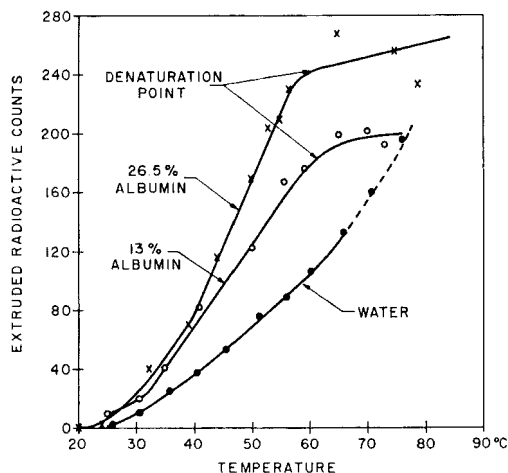


Fig. 9. The expansion of a solution of egg albumin as observed in a radioactive pycnometer. The high expansivity can be seen; also the drop at active denaturation.

Similar experiments were attempted on RNA but, other than the finding that RNA expands no more and probably definitely less than water, no figures can be given.

## IV. THEORETICAL DISCUSSION

### A. Inactivation

The process of inactivation, in its experimentally simplest form, obeys Eq. (7) and the reaction constant is found to fit Eq. (8),  $k_1 = (kT/h) e^{-\Delta F^*/RT}$ . In all these experiments the process is studied at constant pressure and the appropriate free energy is the Gibbs free energy which is the sum of the free energy as defined by Eq. (5), and  $PV$ , the product of pressure and volume for the system under

study. In terms of the partition function the Gibbs free energy, which we denote \* by  $F$ , is

$$F = -NkT \left\{ \ln Z - \left( \frac{d \ln Z}{d \ln V} \right)_T \right\} \quad (9)$$

and for the kind of studies we are considering, where we are dealing with processes in solution where volumes do not change greatly, the second term is usually only a few percent, at most, of the first.

One very simple method of theoretical extension of the above equation is to invoke the thermodynamic relation between Gibbs free energy, enthalpy,  $H$ , and entropy,  $S$ , namely  $F = H - TS$ . Then at constant temperature

$$\Delta F^* = \Delta H^* - T \Delta S^* \quad (10)$$

and Eq. (8) becomes

$$k_1 = \frac{kT}{h} e^{\Delta S^*/R} e^{-\Delta H^*/RT} \quad (11)$$

To a first approximation  $\Delta H^*$  and  $\Delta S^*$  are found to have constant values for particular processes and they form rather useful ways of describing the thermal inactivation process numerically for comparative purposes. Beyond this usefulness they are rather limited in giving understanding. Because  $\Delta H^*$ , the enthalpy difference, includes the energy difference due to very many bonds in the molecule and because  $\Delta S^*$ , the entropy difference, also involves the distribution of energy among many states, the values found are not easy to interpret directly. Thus, in terms of the partition function we have

$$S = -Nk \left\{ \ln Z + T \left( \frac{d \ln Z}{dT} \right)_V \right\} \quad (12)$$

which is certainly not a simple quantity to discuss.

In Table VI we give some experimentally found values of the enthalpy and entropy of activation for various processes. One or two generalizations can be made. The first, as already pointed out by the author,<sup>17</sup> is that for inactivations in the dry state the value of  $\Delta S^*$  is usually low, often being zero or negative. The second is that for processes concerned primarily with the inactivation of

\* The internationally accepted symbol for this quantity is " $G$ ". However, in all this kind of work " $F$ " has been so universally used that we hesitate to change the usage.

RNA the value of  $\Delta S^*$  is low and  $\Delta H^*$  is usually near 20,000 calories per mole. The third is that for denaturation of proteins the entropy can be very high, with a consequently high value of the enthalpy. The fourth is that for inactivation of proteins in  $D_2O$  the value of  $\Delta S^*$  is higher than in  $H_2O$ .

TABLE VI. Statistics of Inactivation\*

Subject inactive	$\Delta H^*$ , kcal/mole	$\Delta S^*$ , cal/mole/ degree	Covalent bond rupture energy	$n$	$Z_{gm}$	Ref.
RNA-ase	33	19	—	8	2.6	<sup>b</sup>
Pepsin	56	113	—	14	32	<sup>c</sup>
Catalase in						
$H_2O$	87	191	—	22	54	22
$D_2O$	145	360	—	36	118	—
Invertase	53	95	—	13	23	2
Invertase (dry)	30	0	30,000	—	—	2
RNA from TMV	19	-19	—	—	—	—
TMV (dry)	27	0	—	—	—	<sup>d</sup>
T1	95	207	24,000	17	25	18
T1 (dry)	27	0	27,500	0	—	18
T1 serological affinity (wet)	165	372	—	14	92	19
T1 serological affinity (dry)	56.5	57	—	14	9	19

\* The values of  $n$ , the number of hydrogen bonds broken, and  $Z_{gm}$ , the number of configurations available on rupture, have been made from an approximation to the theory of Gibbs and DiMarzio using an energy of 4000 calories per mole for the energy of one bond.

<sup>b</sup> Gajewska, E. and Shugar, D., *Bull. Acad. Polon. Sci.* **4**, 157 (1956).

<sup>c</sup> Stearn, A., *Advan. Enzymol.* **9**, 25 (1949).

<sup>d</sup> Thornberry, H. H., Valleau, W. D., and Johnson, E. M., *Phytopathology* **28**, 129 (1938), Table VI.

### B. The Role of Water in the Inactivation Process

Two of the generalizations given above concern the presence of water during the inactivation. The first is the relatively simple kind of kinetics encountered for dry inactivations in which water presumably does not play a part, and the second is the different

behavior in  $D_2O$  solutions. A brief discussion of these, using the idea of partition functions is helpful as it shows a simple way in which the presence of water exerts an influence.

We have already mentioned that proteins appear to expand, or swell, rather considerably in the normal range of temperatures involved with inactivation. We can suppose that the activated state represents a constant condition in which the molecular rearrangement is about to take place. If the necessary temporary amount of energy has to be attained from various temperatures, then the lower the temperature the less the molecule has swollen. Now the act of swelling will be expected to entrain and hinder the rotation of molecules of water which were formerly free to rotate. This stopping of rotation will cause the partition function for the complex of molecule plus water to be different, and because the free energy is related to the partition function the free energy is different. This idea can be represented very simply in mathematical form. Suppose that for the part of the molecule not involved with water we represent the partition function at the temperature of inactivation by  $Z_M$  and at the point of activation by  $Z_M^*$ ; the partition function per trapped or released water molecule as  $Z_{H_2O}$ ;  $y^*$  the number of such molecules in the activated state,  $y_0$  the number in a reference state and  $\alpha t$  the increase in the number trapped by swelling due to an increase in temperature  $t$ . Then we have

$$\frac{\Delta F^*}{RT} = -\{(\ln Z_M^* - \ln Z_M) + (y^* - y_0) \ln Z_{H_2O} - \alpha t \ln Z_{H_2O}\} \quad (13)$$

A plot of  $\Delta F^*/RT$  determined from the rate constants should then have a constant intercept with an increasing slope determined by  $\alpha \ln Z_{H_2O}$ . Since  $Z_{H_2O}$  can be calculated, we can make an estimate of the number of molecules of water entrained per degree increase in temperature. In the dry state  $\Delta F^*/RT$  should be constant unless there is a variation of  $\ln Z_M^* - \ln Z_M$  with temperature.

A very useful check in the validity of this very simple approach to the influence of water on inactivation is given by the observation of the rates of inactivation in  $D_2O$  medium. Under such circumstances, using  $Z_{D_2O}$  to represent the partition function for  $D_2O$  we should have

$$\frac{\Delta F^*}{RT} = -\{(\ln Z_M^* - \ln Z_M) + (y^* - y_0) \ln Z_{D_2O} - \alpha t \ln Z_{D_2O}\}$$

Thus if  $\Delta F^*/RT$  is plotted versus temperature the slope of the line in  $D_2O$  should exceed that in  $H_2O$  by the ratio of  $\ln Z_{D_2O}$  to  $\ln Z_{H_2O}$ . The effect of heat on catalase was studied by Guild and VanTubergen.<sup>10</sup> They found an increased slope for  $\Delta F^*/RT$  for the case of heating in  $D_2O$ . The increase is approximately what is expected, though it is rather more than is suggested by the two partition functions. Thus one action of water (certainly not the only action) is to increase the free energy of the hydrated protein molecule by becoming entrained in increasing numbers as the molecule swells.

## V. THEORETICAL PARTITION FUNCTIONS FOR PROTEINS AND DNA

The relatively recent ideas that one form of protein structure is a hydrogen bonded helix and that DNA is two complementary helical chains, quite heavily hydrogen bonded, have presented a relatively simple system for theoretical analysis. Gibbs and DiMarzio<sup>6</sup> have worked out the partition function for a solvated helical polypeptide chain in which there are various groupings of triplets of adjacent broken hydrogen bonds. The final result is naturally somewhat complicated but it nevertheless permits the calculation of the internal energy and entropy for various kinds of bonding and so puts a firm theoretical base under the description of the transition from a helix to a more random condition.

Their theory involves three parameters of importance, of which the first,  $Z_{gm}$ , is the number of conformations which can result from the release of three hydrogen bonds in a helix. This is a measure of the "power of confusion" of the random coil, or other form of altered structure. The higher the value of  $Z_{gm}$  the more ways of obtaining a non-helical form and the more readily such a form is produced. The second is the number,  $n$ , of units in a chain and the third,  $\epsilon$ , is the energy of each hydrogen bond. The procedure is to evaluate  $Z$ , the partition function and then determine the internal energy  $U$ , for any set of broken hydrogen bonds by the relation

$$U = kT^2 \frac{\partial \ln Z}{\partial T} \quad (15)$$

The fraction broken,  $f$ , is then given by  $U/\epsilon n$ , which is the actual internal energy divided by the total possible. When this is done a family of curves relating  $f$  and  $kT/\epsilon$  for various values of  $Z_{gm}$  can be

plotted. They show a characteristic sigmoidal form with a low value of the fraction until the transition process starts, after which there is a steady rise until a high value of the fraction is reached. The transition process shifts to low values of  $kT/\epsilon$  for high values of  $Z_{gm}$ . For  $Z_{gm} = 12$  the fraction broken approaches 0.5 for  $kT/\epsilon = 0.4$ .

When the problem is broadened to include the behavior in solution, an added factor is the effect of polar molecules, such as water, on the broken hydrogen bond. The hydrogen bond originates in the uneven charge distribution produced by molecular covalent bonds and a broken bond does not release this charge asymmetry. Therefore polar molecules will react with the exposed ends of the bond and they will modify the value of  $\epsilon$ . With allowance for this, a somewhat similar plot of the fraction broken results. The theory can be used to explain the behavior of synthetic polypeptides in solution rather well.

The process of separation of two strands of DNA is treated in a similar way. A particular case of some interest is that of "unzippering", or unraveling from one end. This gives a rather simple expression for the partition function  $Z$ , namely,

$$Z = \frac{1 + nx^{n+1} - (n+1)x^n}{(1-x)^2} + Z_{gm}^4 x^n \quad (16)$$

where  $x = Z_{gm}^2 e^{-\epsilon/kT}$ . This expression can be brought into relation with the thermodynamic analysis we have previously used. It contains two terms, the first of which is predominant for small values of  $x$  and which is moreover, generally close to unity. The second term, which corresponds to the complete opening up of the two chains becomes the dominant term for  $x$  when greater of unity. For purposes of aiding our intuition let us suppose that only the second term is important. The free energy corresponding to this condition, by Eq. (5), is  $F$ , where

$$\begin{aligned} F &= -NkT \ln Z \\ &= -NkT \ln \{Z_{gm}^{(4+2n)} e^{-n\epsilon/kT}\} \\ &= -NkT \{(4+2n) \ln Z_{gm} - n\epsilon/kT\} \\ &= -RT \{(4+2n) \ln Z_{gm} + N\epsilon\} \end{aligned}$$

where we have put  $R = Nk$ . Now  $N\epsilon$  is the energy of a mole of hydrogen bonds and  $n$  is the number of such per DNA molecule.



Therefore the last term is the energy involved in the bond breakage. The first term is related to the number of conformations,  $Z_{gm}$ , which can be reached by the broken bonds, and it is therefore the measure of the entropy difference. Thus, with our previous notation we can identify  $Nn\epsilon$  with  $U$  (or for intuitive purposes if volume changes are unimportant, with  $H$ ) and  $R(4+2)\ln Z_{gm}$  with  $S$ .

It must be remembered that this only applies to a special case, but it is nevertheless useful as a means of relating two apparently different approaches.

A rather less general but very valuable account of the transition from helix to random coil has been given in a series of papers by Schellman.<sup>25, 26</sup> He considers that the change in free energy  $\Delta F_u$  on unfolding  $n$  residues is given by

$$\Delta F_u = (n-4) \Delta H_r - (n-1) T \Delta S_r \quad (17)$$

where  $\Delta H_r$  and  $\Delta S_r$  are the changes in entropy on breaking one mole of hydrogen bonds and  $\Delta S_r$  is the entropy change on releasing one mole of amino acids from the helical form. The values of  $\Delta H_r$  and  $\Delta S_r$  are 1.5 kcal/mole and 3 to 4 cal/mole/°C. For small values of  $n$  the free energy is negative so that small helical polypeptide chains are not stable. Equation (17) shows that as  $n$  increases the temperature range in which the second term overcomes the first becomes very much sharper. Thus for  $n = 20$ , using 1.5 for  $\Delta H_r$  and 3.5 for  $\Delta S_r$ ,  $\Delta F_u$  is 2700 for 320°K and zero for 362°K, while for  $n = 100$  the same values are found from 409°K to 416°K, a range of seven degrees as compared to 42 degrees.

The theory gives the probability of formation of  $m$  adjacent hydrogen bonds in a molecule of chain length  $n$  as  $P_m$ , where

$$P_m = [P_0/(n-3-m)] e^{m\Delta F_r/RT} e^{-3\Delta S_r/R} \quad (18)$$

and  $\Delta F_r = \Delta H_r - T\Delta S_r$ .  $P_0$  is the probability of a completely random state. More recent treatments have been given by Zimm and Bragg<sup>33</sup> and by Zimm, Doty, and Iso.<sup>34</sup>

These emerging theories suggest that a combination of physical studies on proteins and nucleic acids together with biological inactivation studies can be very rewarding in determining what is involved in biological inactivation. Thus if we retain the concept of an activated state from which the molecule moves to a "wrong" conformation, both of the above theoretical descriptions suggest that

as the temperature is raised the normal condition of the molecule is being altered. The altered condition may favor the chance attainment of the activated state, not merely by the random acquisition of an energy, but also by the fact that the degree of uncoiling or of swelling aids this acquisition. The presence of both factors—the energy jump and the secondary configurational change—has been known for many years, and they appear in Table VI as enthalpy and entropy values.

If the figures of Eq. (17) are applied to Table VI it is quickly seen that the relative enthalpy and entropy figures do not fit. The reason for this is probably because protein molecules are not simply alpha helices of polypeptide chains but are crosslinked between helices by —S—S— bridges. If the energy to break one of these bridges is included, as suggested by Augenstein<sup>1</sup> then something much closer to the relation suggested by Schellman is found. It seems likely that in the future these figures will be replaced by others which are more definite and in which, for example, parameters such as  $Z_{gm}$ ,  $\epsilon$  and  $n$  receive definite measurement and in which the effect of sulfur bridges is included. One or two possible values are shown in Table VI.

## VI. ENERGY OF THE HYDROGEN BOND

It is clear from all of the foregoing that the actual value of the hydrogen bond energy is important in all the heat effects discussed. A useful spectroscopic study by Frisch and Vidale<sup>5</sup> suggests that the potential energy  $V$ , in ergs per molecule for displacement a distance  $y$  from equilibrium is given by

$$V = 2.5 \times 10^4 y^2 - 1.8 \times 10^{12} y^3 \quad (19)$$

which enables the potential energy curve to be plotted.

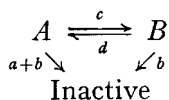
Schellman<sup>28</sup> (see Kauzmann, 1959) has used the breaking of the hydrogen bonds in dimerized urea to estimate a value for the bond energy. He obtains a free energy of  $-400$  cal/mole, and enthalpy of  $1400$  cal/mole and an entropy of  $3.3$  cal/mole/degree. Gibbs and DiMarzio, for the solvated case, use  $\Delta\epsilon = 4140$  cal/mole. Sturtevant, Rice and Geiduschek<sup>30</sup> discuss the numerical significance of a series of denaturation and calorimetric studies.

It is clear that while a hydrogen bond is a very useful idea for the explanation of the internal stability of macromolecules, it is not to

be thought of as having one definite energy like a covalent bond. Thus, as Gibbs and DiMarzio point out, the opening of one or two hydrogen bonds will not permit the free entry of polar water molecules while a whole set of broken bonds will be surrounded by such molecules in varying degrees of orientation. Thus breaking one hydrogen bond may well introduce quite a different energy change from breaking one-third of three bonds. A theoretical discussion of the hydrogen bond has been given by Paoloni.<sup>14</sup>

## VII. LOSS OF INFECTIVITY OF VIRUSES

It was mentioned earlier that many viruses are inactivated by heat in a way which suggests a sensitive and a resistant component. An example of such inactivation was found for T5 bacteriophage by Patch<sup>15</sup> who suggests that there may be inactivation in terms of the action of heat on the tail tip as well as on the nucleic acid. A model for this dual sensitivity was suggested by Woese<sup>31</sup> in terms of there being two forms which a virus could assume, both being viable. The two forms  $A$  and  $B$  are interconvertible and  $B$  is more stable than  $A$ . Two inactivation processes exist, one supposedly like the collapse of DNA and one like chain scission. If only form  $A$  is susceptible to collapse and both  $A$  and  $B$  to scission then if the rate constant for collapse is  $a$ , for scission  $b$  and the inter-conversion rates are  $c$  and  $d$  we have a scheme as drawn



A set of differential equations can be written and solved for this process and they yield a relation for the surviving active virus,  $s$ , as

$$s = \frac{1}{d} \{ c_1 e^{R_1 t} (g + R_1) + C_2 e^{R_2 t} (g + R_2) \} \quad (20)$$

where  $g = a + b + c + d$

$$R_{1,2} = \frac{1}{2} \{ -(g+b) \pm \sqrt{(g-b)^2 - 4ad} \}$$

$$C_1 = \frac{1}{R_1 - R_2} \{ B_0 d - (g-d) + R_2 \} A_0; \quad C_2 = A_0 - C_1$$

$A_0$  and  $B_0$  being the initial amounts of virus. This relation fits some of the data for inactivation of animal viruses quite well and is a

useful model. It explains the puzzling fact, sometimes observed, that the insensitive component appears to be present in amounts which vary with the temperature of inactivation.

It is possible that a rather simpler explanation may hold, which leads out of a more general discussion of the inactivation of viruses by heat. There are certainly two features to the action of heat on viruses: the first, and predominant, the action on the nucleic acid and the second, the action on protein. If we consider the first, one feature to remember is that the nucleic acid is very tightly coiled. Then if we suppose, as suggested by Ginoza and Zimm, that the inactivation process involves both some strand separation and either scission or depurination in the separated part, the center of the coil will not easily undergo strand separation, while the outer coils can do so. Thus the virus will lose activity in the nucleic acid at its periphery. As the virus is heated the protein will swell and the nucleic acid will become more loose so that parts deeper inside can become separated allowing scission to occur. Thus viruses with outer segments rich in adenine and thymine pairs (which are weakly bonded) can be inactivated rather readily at low temperatures while those with guanine and cytosine pairs will resist the action of heat. As the coil loosens the inner turns begin to feel the effect. Thus virus inactivation should be multicomponent. RNA viruses would not show so great an effect as DNA viruses.

The effect of heat on the protein part should also be observable. However, because the protein action is less critical, it will be harder to observe. Studies aimed at observing the effect of heat on specific properties such as attachment, or interference should be very informative in this regard. So far only very few such studies have been made.

Thermal action on viruses can certainly be combined with the action of other agents. There is a definite sensitization of the effect of ionizing radiation when the sample which is being irradiated is held at temperatures close to, but below, the temperature of thermal inactivation. There is also good reason to suppose that heat, in the presence of formalin, causes a greater effect. Since one purpose of the inactivation of viruses is to create an agent which is harmless, but which can still elicit antibodies in a host animal, such combined inactivation may prove to be a very useful technique.<sup>21</sup>

It is very likely that the study of such combined action may be

very informative as to the way in which the nucleic acid is arranged inside the protein coat. Thus, in the case of tobacco mosaic virus, for which it is known that the single stranded RNA is coiled in a definite way in contact with protein and not coiled on itself, there is no combined effect of heat and radiation. Thus future studies of this kind may be quite useful.

### VIII. CONCLUSION

By way of conclusion it can be said that the interpretation of thermal effects on proteins and nucleic acids, in terms of the breaking of hydrogen bonds and hence the passage from an ordered, helical form to a random form, has received experimental support. This fact suggests that several lines of study should be opened up, notably a widening of physical studies on polymers, proteins, and nucleic acids, using physical techniques. In addition purely biological effect studies on enzymes, nucleic acids, and viruses should be conducted in different media, for example in D<sub>2</sub>O solution, in solutions of different osmotic strengths and in the dry state.

Of great value in these studies of biological effects is the observation of several effects at once. For example both the enzyme activity of an enzyme and its ability to combine with antibody should be measured while heat is applied. Virus studies should include mutation, attachment, host killing and so on. The similarity or difference in behavior would be most informative.

As a final word we can make plea that theoretical work be carried one stage farther than is usually done and made to yield expressions which can be directly compared with experiment. One of the reasons for neglect of thermal study has been the feeling that the experimental results would admit no theoretical interpretation. This pessimism is not justified, and yet, at the same time it is not easy for the experimentalist, who has to be competent in biology, to have the ability to reach into theoretical expressions and extract the parameters of significance. A helping hand on the part of the theorist would make a great deal of difference.

### IX. ACKNOWLEDGEMENTS

The author wishes to acknowledge helpful discussions with Dr. W. Ginoza and also the aid of his associates, notably the late

Dr. W. F. Powell, and Jane Setlow, Carl Woese, Marjorie Reaume, and Barbara Ruud.

### General References

The classic work on heat effects is Johnson, F. H., Eyring, H., and Pollisar, M. J., *The Kinetic Basis of Molecular Biology*, Wiley, New York, 1954.

Rate mechanisms are discussed by F. M. Huennekens in *Techniques in Organic Chemistry*, Vol. 8, Interscience, New York, 1953.

Viscosity effects are discussed by Yang in *Advan. Protein Chem.* **16**, 323-400 (1961).

Optical rotation is discussed by Urnes and Doty in *Advan. Protein Chem.* **16**, 402-536 (1961).

Protein denaturation is reviewed by Kauzmann in *Advan. Protein Chem.* **14**, 1-57 (1959).

A most useful discussion of the theory of helix-coil transition is to be found in the article by Katchalski and Steinberg in *Ann. Rev. Phys. Chem.* **12**, 433 (1961).

### References

1. Augenstein, L., in *Information Theory in Biology*, H. Quastler, Ed., University of Illinois Press, Urbana, Illinois, 1953.
2. Doty, P., Marmur, J., and Sueoka, N., *Brookhaven Symposia in Biology* **12**, 1-25 (1959).
3. Doty, P., Marmur, J., Eigner, J., and Schildkraut, C., *Proc. Natl. Acad. Sci. U.S.* **46**, 461-476 (1960).
4. Eigner, J., Boedtker, H., and Michaels, G., *Biochim. Biophys. Acta* **51**, 165-168 (1961).
5. Frisch, H. L., and Vidale, G. L., *J. Chem. Phys.* **25**, 982-986 (1956).
6. Gibbs, J. H., and DiMarzio, E. A., *J. Chem. Phys.* **30**, 271 (1959).
7. Ginoza, W., *Nature* **181**, 958-961 (1958).
8. Ginoza, W., and Zimm, B., *Proc. Natl. Acad. Sci. U.S.* **47**, 639-652 (1961).
9. Greer, S., and Zamenhof, S., *Federation Proc.* **18**, 939 (1959).
10. Guild, W. R., and VanTubergen, R. P., *Science* **125**, 939 (1957).
11. Johnson, F. H., Eyring, H., and Pollisar, M. J., *The Kinetic Basis of Molecular Biology*, Wiley, New York, 1954.
12. Lauffer, M. A., and Price, W. C., *J. Biol. Chem.*, **133**, 1 (1940).
13. Marmur, J., and Lan, D., *Proc. Natl. Acad. Sci. U.S.* **46**, 453-461 (1960).
14. Paoloni, L. J., *J. Chem. Phys.* **30**, 1045-1058 (1959).
15. Patch, C. T., *Arch. Biochem. Biophys.* **81**, 273-278 (1959).
16. Pollard, E., and Reaume, M., *Arch. Biochem. Biophys.* **32**, 278 (1951).
17. Pollard, E., *Am. Scientist* **39**, 106 (1951).
18. Pollard, E., and Dimond, A., reported in *The Physics of Viruses*, by E. Pollard, Academic Press, New York, 1952.
19. Pollard, E., Powell, W. F., and Reaume, S. H., *Proc. Natl. Acad. Sci. U.S.* **38**, 172-180 (1952).
20. Pollard, E., and Setlow, J., *Arch. Biochem. Biophys.* **43**, 136-142 (1953).

21. Pollard, E., *Yale J. Biol. Med.* **11**, 233 (1958).
22. Pollard, E., *Biophysical Society Meeting Abstracts*, 1959.
23. Price, W. C., *Arch. Ges. Virusforsch.* **1**, 373 (1940).
24. Roger, M., and Hotchkiss, R. D., *Proc. Natl. Acad. Sci. U.S.* **47**, 639-652 (1961).
25. Schellman, J. A., *Compt. Rend. Trav. Lab. Carlsberg, Ser. Chim.* **29**, 230 (1955).
26. Schellman, J. A., *J. Phys. Chem.* **62**, 1485 (1958).
27. Schellman, J. A., *Compt. Rend. Trav. Lab. Carlsberg, Ser. Chim.* **30**, 395 (1958).
28. Schellman, J. A. See discussion by Kauzmann in *Advan. Protein. Chem.* **14**, 1-57 (1959).
29. Shack, J., and Thompsett, J. M., *J. Biol. Chem.* **197**, 17-28 (1952).
30. Sturtevant, J. M., Rice, S. A., and Geiduschek, E. D., *Discussions Faraday Soc.* **25**, 138 (1958).
31. Woese, C., *Ann. N.Y. Acad. Sci.* **83**, 741-751 (1960).
32. Zamenhof, S., Alexander, H. E., and Leidy, G., *J. Exptl. Med.* **98**, 373 (1953).
33. Zimm, B. H., and Bragg, J. K., *J. Chem. Phys.* **31**, 526 (1954).
34. Zimm, B. H., Doty, P., and Iso, K., *Proc. Natl. Acad. Sci. U.S.* **45**, 1601-1607 (1959).

## 6

# ADSORPTION OF WATER ON SOLID PROTEINS WITH SPECIAL REFERENCE TO HAEMOGLOBIN

D. D. ELEY and R. B. LESLIE, *University of Nottingham*

## CONTENTS

I. Introduction . . . . .	238
II. Adsorption Isotherms . . . . .	240
III. Hysteresis Effects . . . . .	243
IV. Thermodynamics of Adsorption . . . . .	244
V. The Experimental Kinetics of Adsorption . . . . .	247
VI. Interpretation of the Kinetics . . . . .	249
VII. Conductivity and Adsorbed Water . . . . .	251
A. The Intrinsic Mechanism . . . . .	253
B. The Impurity Mechanism . . . . .	254
References . . . . .	257

## I. INTRODUCTION

Proteins in the living cell may be divided into soluble proteins which are dispersed as molecules, and insoluble proteins which form fibres, membranes and organized structures like mitochondria. In the presence of aqueous solutions the insoluble proteins will adsorb and possibly absorb water molecules, and the physical and chemical properties will depend on this hydration. The present paper reviews the results of physical and physicochemical work on hydration of solid proteins, with emphasis on the work on haemoglobin at the University of Nottingham. Thanks to the brilliant work of Perutz and his colleagues, a clear picture of the structure of this protein is now emerging,<sup>1</sup> making it very suitable for detailed adsorption studies.



The objectives may be summarized briefly. A protein molecule contains one or more polypeptide chains (four in haemoglobin) which are built up of a succession of amino acids,  $-(RCHCONH)_n$ . There are some twenty different side groups, R, including non-polar hydrocarbon and polar  $NH_2$ , OH, and  $-COOH$  groups. This polypeptide chain forms the primary structure, which may further be coiled into an  $\alpha$ -helix in which every  $>C=O$  group is bonded to the  $>N-H$  group three residues along the chain by *intramolecular* hydrogen bonds. Alternatively, in  $\beta$ -proteins the polypeptide chains are stretched out side by side and held laterally by *intermolecular* hydrogen bonds. This forms the secondary structure. Finally, the  $\alpha$ -helices may be coiled up in a characteristic tertiary structure to give a globular molecule. The work of Kendrew on myoglobin established this tertiary structure<sup>2</sup> for the first time for a protein molecule. In the case of enzymes this coiling may cause otherwise widely separated polar side chains to become adjacent, forming an "active site".

The water molecule is spherical, diameter 2.8 Å, with a dipole moment of 1.8 D.<sup>3</sup> Because of its polar character, it will tend to be held to polar groups in the protein, which Sponser, Bath and Ellis<sup>4</sup> classify as backbone groups  $>C=O$  and  $>NH$  and side chain groups  $-COOH$ ,  $-NH_2$  and  $-OH$ . They consider the infrared evidence supports the view that some of the water is held on backbone  $>NH$  groups. Clearly, in the first instance we wish to identify the groups holding the water molecules; we may assume the forces involved are "hydrogen bonds". The first step in this process analyses adsorption isotherms to derive "monolayer coverages", to be compared with numbers of polar groups. The next step involves measuring isotherms at two temperatures so as to derive "entropies of adsorption" which allow one to discriminate between mobile and immobile or ice-like adsorbed water. Such thermodynamic studies still leave the exact chemical nature of the adsorption site in doubt, and here recourse must be made to infrared and possibly also nuclear magnetic resonance spectroscopy. Finally, recent work at Nottingham leads one to investigate possible electron-transfer processes between water and proteins, which may be done by semiconduction methods.<sup>5</sup> Electron transfer to and from proteins may be expected to modify their chemical reactivity and general behaviour in the living cell.

## II. ADSORPTION ISOTHERMS

Interest in this subject was stimulated by Bull's<sup>6</sup> observation that adsorption of water on some eighteen proteins followed the Brunauer–Emmett–Teller or B.E.T. equation, in many cases over the range of relative water vapour pressures 0.05 to 0.5. The isotherm equation is

$$\frac{x}{V(1-x)} = \frac{1}{V_m C} + \frac{(C-1)}{V_m C} x$$

where  $x$  is the relative pressure  $p/p_0$ ,  $V$  is the adsorbed water, expressed here in grams/100 grams protein. By plotting the data according to this equation we may derive values for  $V_m$  and  $C$  from the slope and intercept. Here  $V_m$  is the quantity of adsorbed water corresponding to the monolayer, and  $C$  a constant related to the heat of adsorption. Further data will be found in the review by McLaren and Rowen.<sup>7</sup> In Fig. 1 we give some examples of adsorption isotherms for haemoglobin taken from Cardew and Eley<sup>8</sup> and in Fig. 2 the isotherms are replotted according to the B.E.T. equation. By multiplying the number of molecules in the B.E.T. monolayer by the cross-sectional area of the water molecule, taken as  $10.6 \text{ \AA}^2$ ,<sup>2</sup> a value may be derived for the hydrophilic surface area of the protein crystals. Bull found this to be about one-quarter of the area of the protein monolayer spread on a Langmuir-Adam trough. Shaw<sup>10</sup> found the superficial area of egg albumin crystals to be  $2.42 \text{ m}^2/\text{g}$  measured with nitrogen gas, while the water monolayer value was  $225 \text{ m}^2/\text{g}$ . Palmer's<sup>11</sup> model attributes two intermolecular and one intramolecular polar surface, totalling  $225 \text{ m}^2/\text{g}$  to the egg albumin molecule. Pauling<sup>12</sup> reconsidered Bull's data, pointing out that the small water adsorption by nylon suggested that the peptide links were inactive in water uptake, possibly due to interchain  $\text{C}=\text{O}\cdots\text{HN}$  hydrogen bonding. He found an approximate correspondence between the B.E.T. monolayer water uptake and the number of polar side chains. However, the agreement was only really good for silk, a particularly simple  $\beta$ -protein, and it would seem that the paper does not exclude a certain amount of water adsorption on peptide groups for the more complex structures, involving  $\alpha$ -helices. There is some definite evidence for peptide link adsorption for diglycylglycine,<sup>13</sup> polyglycine<sup>14</sup> and, of course, the early infrared

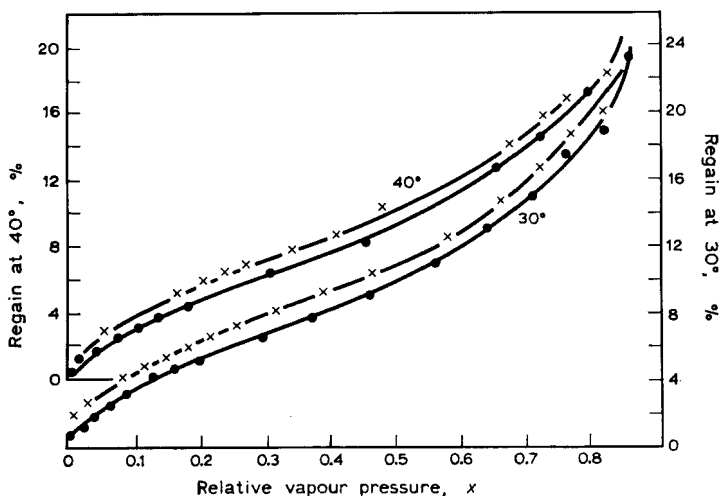


Fig. 1. Adsorption (●) and desorption (×) isotherms for water on freeze-dried haemoglobin. (After Cardew and Eley.<sup>8</sup>)

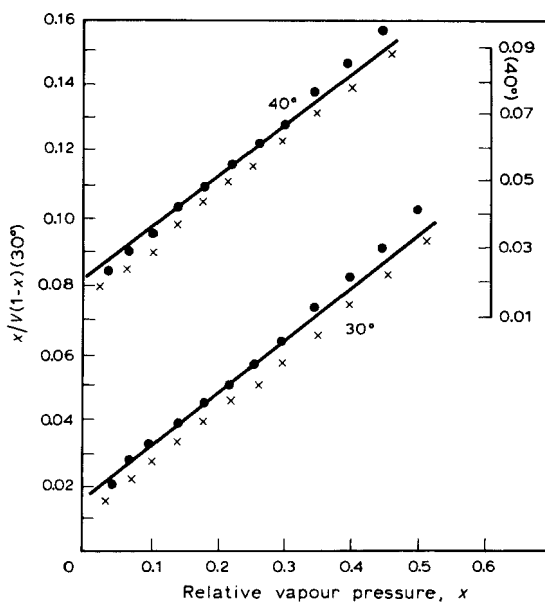


Fig. 2. The adsorption branch of the above isotherm plotted according to the B.E.T. equation. (After Cardew and Eley.<sup>8</sup>)

evidence for gelatin.<sup>4</sup> Peptide groups in casein are responsible for 45% of the total water vapour adsorption, in zein 70% of the water adsorption, at 60% relative humidity.<sup>14</sup> Pauling refers in a footnote to a referee's comment that the failure of water to penetrate the nylon structure may be due to the very compact chain structure of this polymer. Benson and co-workers<sup>15, 16</sup> confirmed that non-polar gases measure the relatively small external area of protein crystals, while polar gases,<sup>17, 18</sup> like water, penetrate the crystals to become adsorbed on polar groups. The state of subdivision of the protein crystals did not effect the amount of adsorbed water.

McLaren and Rowen<sup>7</sup> attempted to reconcile the above views by suggesting that the polar hydrophilic side chains are largely concentrated in the molecular surface of proteins. There is some evidence for this in haemoglobin, since when a crystal swells in water the X-ray spacings characteristic of the molecule itself do not change, but only the intermolecular distances.<sup>19</sup> On complete drying of the crystal as in adsorption work, however, there is evidence for molecular shrinkage, so presumably the first adsorbed water is held intramolecularly. Cardew and Eley<sup>8</sup> studied the water adsorption on ox haemoglobin in freeze-dried and denatured states, the data on the former being already given in Figs. 1 and 2. They derived monolayer values for both samples which were essentially unchanged by a temperature rise from 30° to 40°C, the values being 319 moles H<sub>2</sub>O/10<sup>5</sup> g protein for freeze-dried and 306 moles/10<sup>5</sup> g for denatured haemoglobin. The effect of denaturation is small and may be due to a replacement of some polar by non-polar groups in the molecular surfaces. Haemoglobin<sup>20</sup> contains 435.1 moles polar groups/10<sup>5</sup> g protein. Using an early model of haemoglobin<sup>21</sup> as a spheroidal molecule 45 Å × 45 Å × 65 Å, a close-packed layer of water molecules all over the molecular surfaces would equal 1160 moles water/10<sup>5</sup> g. From this it would seem that the water molecules adsorb on polar groups occupying perhaps a quarter of the molecular surface, and that these surface polar groups are a fraction 0.73 (319/435.1) of the total polar side chains present. Some of these polar groups may well be peptide groups, of course. The recent model of the haemoglobin molecule<sup>1</sup> gives it as a spheroid 64 × 55 × 50 Å, which would further increase the discrepancy between molecular area and water coverage. Photographs of the model would suggest that some water molecules should be able to penetrate into its

interior, and eventually it should prove possible to enumerate the accessible sites. The X-ray crystallographic studies certainly justify the pressing home of detailed studies on haemoglobin hydration. The above ratio may be compared with that of Amberg<sup>22</sup> for bovine serum albumin of 0.84 moles water per polar group.

Although, so far, we have not definitely identified any water bound especially strongly in haemoglobin, we should expect this for water held within the molecule. This raises the vexed question as to how to define the "absolutely dry" state of a protein, with the secondary problem as to whether the dry protein is denatured. Bull dried the protein by holding it for twenty-four hours at 105°C *in vacuo*. Benson and Ellis<sup>15</sup> pumped the sample at room temperature until the steady pressure was less than  $10^{-4}$  mm Hg. Cardew and Eley dried their haemoglobin specimens for three days in air at 110°C, a similar result being given by drying over  $P_2P_5$  *in vacuo* at room temperature. The present authors pumped the specimens at room temperature to constant weight, obtaining isotherms and B.E.T. monolayer values closely similar to those observed by Cardew and Eley for haemoglobin. After drying even under Cardew and Eley's conditions, natural haemoglobin is not denatured in the sense that it is still soluble, but disorder is apparent in the dry state from X-ray measurements.<sup>19</sup> In agreement with these observations, Low and Richards<sup>23</sup> found that temperature of outgassing had little effect on the extent of dehydration of human serum mercaptalbumin. An accurate assessment of this problem will ultimately depend on rate measurements.

### III. HYSTERESIS EFFECTS

The difference between adsorption and desorption curves shown in Fig. 1 is found for all proteins, however long they are left to reach equilibrium. Presumably, therefore, the two curves relate to two states of metastable equilibrium separated by an energy barrier very much greater than  $kT$ , possibly determined by structural changes resulting from complete drying of the protein. The effect is little changed by alcohol denaturation of the protein,<sup>8</sup> so any structural cause must be independent of the disorder related to this denaturation. Further insight may result from kinetic studies such as those described later. Seehof *et al.*<sup>24</sup> found the hysteresis to be

constant down to extremely low relative pressures of water vapour, and almost independent of temperature. They suggested the polar side chains  $\text{NH}_2$ ,  $\text{SH}$  and  $\text{S—S}$  are the strongest water binders, and found a near equality between the number of these groups and the maximum hysteresis, in each case expressed as millimoles per gram of protein. This correlation, however, does not extend to the results on haemoglobin,<sup>8</sup> hysteresis 0.5 millimoles/gram and polar side chains 1.4 millimoles/gram, or  $\beta$ -lactoglobulin,<sup>25</sup> hysteresis 0.7 millimoles/gram and polar side chains 1.32 millimoles/gram.

Seehof *et al.*<sup>22</sup> suggest that hysteresis is related to the cooperative binding of one water molecule by two adjacent polar groups. It would seem that if such a molecule is removed in a very hard vacuum, two adjacent chains may approach each other, to be held by hydrogen bonds between these polar groups, so that the site now becomes virtually inaccessible.

#### IV. THERMODYNAMICS OF ADSORPTION

The evaluation of heats and entropies of adsorption of water on proteins was carried out by Bull,<sup>6</sup> Dole and McLaren,<sup>26</sup> and Davis and McLaren.<sup>27</sup> The methods used were subsequently labelled as solution thermodynamics by T. L. Hill.<sup>28</sup> At low coverages the strongly negative entropies of adsorption on many proteins indicated a localization of water molecules on polar groups, as required by B.E.T. theory and the Pauling model. In some cases the entropy of adsorption was greater than the entropy of freezing of liquid water,  $-5.4 \text{ cal deg}^{-1} \text{ mole}^{-1}$  at  $30^\circ\text{C}$ . Positive entropies of adsorption at low coverages were observed for crystalline egg albumin and lyophilized lactoglobulin and attributed to configurational changes induced in the protein chains, the effect being much less for coagulated egg albumin. The subject of "adsorption thermodynamics" has been developed particularly by Hill<sup>29, 30</sup> who has rigorously derived molar differential heats and entropies and molar integral heats and entropies of adsorption. He has applied his methods to the practical case of nitrogen on graphon,<sup>31</sup> and Cardew and Eley have applied it to their water on haemoglobin data.<sup>8</sup> If  $\Gamma$  is the ratio of moles adsorbed water ( $N_s$ ) to moles adsorbent ( $N_a$ ), and  $x$  is the relative pressure of the water over the adsorbent, the

molar differential heat content  $\bar{H}_s$  and entropy  $\bar{S}_s$  for the adsorbed water is

$$\left(\frac{\partial \ln x}{\partial T}\right)_T = \frac{H_L - \bar{H}_s}{RT^2} = \frac{S_L - \bar{S}_s}{RT} - \frac{\ln x}{T}$$

where  $H_L$  is the molar heat content and  $S_L$  the molar entropy of liquid water. The integral values,  $H_s$  and  $S_s$ , are given by

$$\left(\frac{\partial \ln x}{\partial T}\right)_\phi = \frac{H_L - H_s}{RT^2} = \frac{S_L - S_s}{RT} - \frac{\ln x}{T}$$

The integral values are more difficult to derive, since accurate isotherm data down to very low relative pressure are needed to evaluate the spreading pressure  $\phi$  by

$$\phi = \frac{RT}{N_a} \int_0^x \frac{N_s}{x} dx$$

The data for the entropy of adsorption of water on haemoglobin, the more useful function, are shown in Fig. 3. It may be seen that the

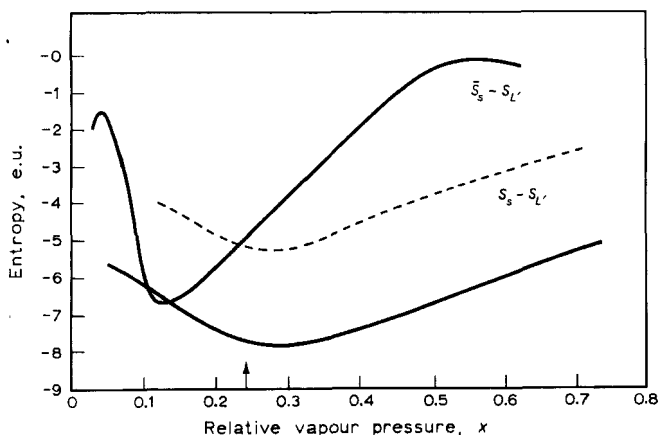


Fig. 3. Molar integral and molar differential entropies of adsorption of water on freeze-dried haemoglobin. (After Cardew and Eley.<sup>8</sup>)

molar integral entropy decreases with surface coverage to a minimum value at the B.E.T. monolayer. According to Hill, Emmett and Joyner<sup>31</sup> this is diagnostic of localized adsorption,

where the configurational entropy term decreases as the coverage approaches that of a monolayer. A discrepancy is apparent when the integral and differential entropies are compared. It is easily shown<sup>31</sup> that the differential entropy curve should cut the integral entropy curve at the minimum in the integral entropy curve. It was therefore suggested that the integral entropy curve should be raised by  $3.5 \text{ cal deg}^{-1} \text{ mole}^{-1}$  to the dotted line.<sup>8</sup> Such a discrepancy might possibly arise (a) from the hysteresis effect and (b) from the lack of sufficient points at very low pressures needed to evaluate  $\phi$

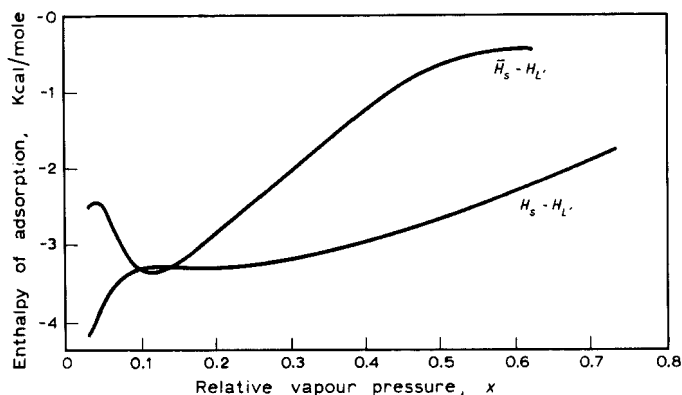


Fig. 4. Molar integral and molar differential heats of adsorption of water on freeze-dried haemoglobin. (After Cardew and Eley.<sup>8</sup>)

with accuracy. If this change is made, the entropy of adsorption barely reaches the  $-5.4 \text{ cal deg}^{-1} \text{ mole}^{-1}$  associated with ice formation in the monolayer. Nevertheless, the values observed would correspond to a strong localization of the water molecules on polar groups. Foss and Reyerson<sup>32</sup> have found similar results for the molar differential entropy of water on ribonuclease.

It is interesting to compare the minimum in the differential entropy with the B.E.T. monolayer value. This is about 50% for both haemoglobin and ribonuclease, whereas for nitrogen on graphon it is 18%<sup>31</sup> and argon on rutile it is 20%.<sup>33</sup> This may reflect the effect of water molecules in perturbing the protein substrate.

Figure 4 shows the differential and integral molar heats of adsorption for haemoglobin and it is seen that the integral heat



decreases fairly abruptly over the first 10 to 40% of the B.E.T. monolayer. It is not clear whether the first 0–10% water is not held even more strongly. The decrease in heat observed, which is about 0.8 kcal/mole, is of the right order to be explained by a repulsive interaction energy between water molecules of dipole 1.8 D at a spacing of 6.2 Å. An interaction energy may also be invoked to explain the kinetics and conductivity changes observed during water sorption.

## V. THE EXPERIMENTAL KINETICS OF ADSORPTION

The tentative model emerging from the previous discussion is that water molecules adsorb onto polar groups, not excluding peptide bonds in the molecular surface. Some penetration of the haemoglobin molecule by water molecules at very low relative pressures is also probable. The total water adsorption at the B.E.T. monolayer corresponds to perhaps only 25% of the molecular surface and 73% of the total polar side chains in the molecule. This is not a very detailed picture, but it does seem definite that the water molecules are localized on definite groups. It is possible that more careful thermodynamic work will yield a more precise picture, but for the moment we turn to the new field of kinetic investigations. We have studied the uptake of water by several proteins, including haemoglobin, in a vacuum microbalance. Under these conditions the heat of adsorption causes a sharp initial rise in the temperature of the protein, but there are reasons for ignoring the effect of this on the initial rate; this is equivalent to assuming a small value for the initial activation energy for adsorption, i.e.  $E_0$  below. Details will be published elsewhere, but the main result is that the adsorption-time curves, similar to those shown in Fig. 5, have been found to follow the Roginsky–Zeldovich equation<sup>34</sup> (or Elovich equation) in a slightly modified form. The derivation of this equation assumes that the rate of adsorption  $dm/dt$  possesses an activation energy which increases linearly with the amount of adsorbed gas  $m$ ,

$$\frac{dm}{dt} = K_0 f(p) \exp - \frac{(E_0 + \alpha m)}{RT} = K^1 \exp - (\alpha m/RT)$$

$K_0$ ,  $E_0$ ,  $\alpha$  are constants, and  $f(p)$  some function of the pressure in

the system. This is integrated to give the equation for the dependence of  $m$  on  $t$ , viz.,

$$m = \frac{RT}{\alpha} \ln \left( t + \frac{RT}{\alpha K'} \right) - \frac{RT}{\alpha} \ln \frac{RT}{\alpha K'}$$

i.e. 
$$m = \frac{RT}{\alpha} \ln(t + t_0) + C$$

This equation predicts that if  $t_0$  is chosen by empirical methods,<sup>35</sup> a plot of  $m$  vs.  $\ln(t + t_0)$  should be a straight line, and that for a range

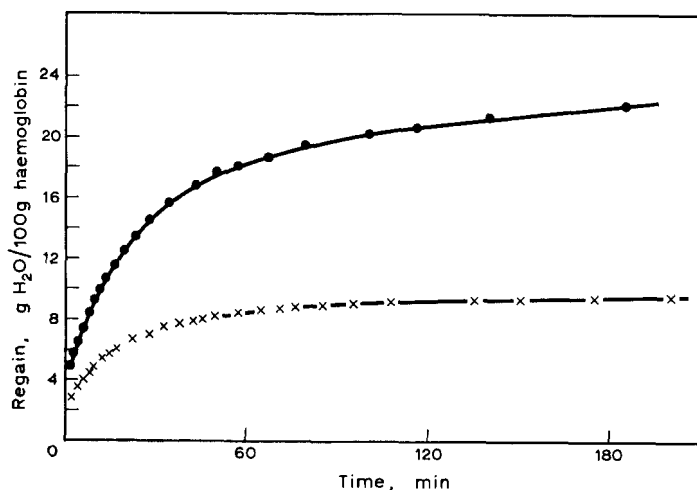


Fig. 5. Integral rate of adsorption of water on haemoglobin (25°C). (●) Relative vapour pressure  $\sim 0.9$ ; (x) Relative vapour pressure  $\sim 0.5$ .

of pressures of adsorbate gas we should obtain a series of parallel straight lines, each pressure giving a different  $t_0$  value but the same slope  $RT/\alpha$  (cf. oxygen on cuprous oxide<sup>36</sup>). Roginsky-Zeldovich plots for the data of Fig. 5 are shown in Fig. 6. However, we have found in a detailed study of bovine plasma albumin (to be published) that the slope of the logarithmic plot is proportional to the pressure of the water vapour so that  $\alpha = \alpha'/p$ . Similarly, it is found that  $K' \propto p^{0.6}$ , so that the basic rate equation becomes:

$$\frac{dm}{dt} = Kp^{0.6} \exp - \left( \frac{E_0 + \alpha' m/p}{RT} \right)$$

We shall now interpret this equation in terms of interaction occurring between adsorbed water molecules. In this way the kinetics may be correlated with the already mentioned fall in integral heat of adsorption of water on haemoglobin, for the first 40% of the B.E.T. monolayer.<sup>8</sup> Finally, we shall indicate how the same idea may underlie the observed relationship between electrical conductivity and adsorbed water content.

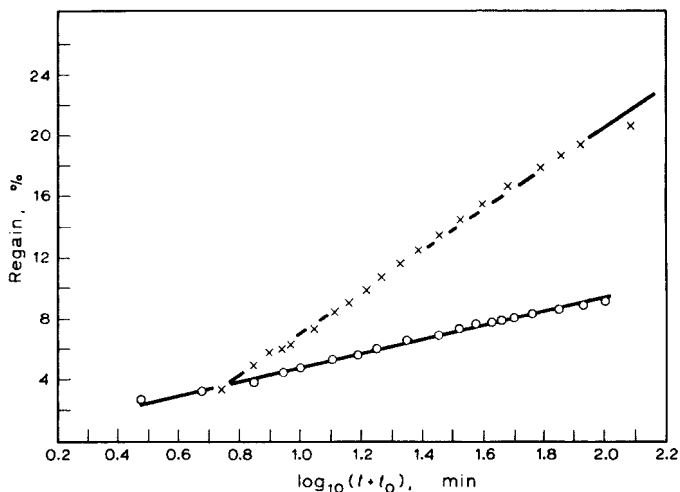


Fig. 6. The data of Fig. 5, plotted according to the Roginsky-Zeldovich equation.

## VI. INTERPRETATION OF THE KINETICS

There are a number of different treatments of the Roginsky-Zeldovich equation, some of which are summarized in a review by Stone.<sup>37</sup> For the present purpose we adapt a simple potential curve model.<sup>38,39</sup> We shall assume a two-stage process, involving first a rapid reversible stage, followed by a rate-determining transition over an energy barrier to the final stage of adsorption.

*Stage 1:* This is probably best described as mobile van der Waals' (V.W.) adsorption on the surface of the protein crystals. The potential curve for this stage is shown on the left in Fig. 7. As the surface concentration of water molecules increases we should expect

its pressure dependence to fall from  $p^1$  to  $p^0$ . Assuming a uniform occupation of adsorbed water molecules, whatever this is, there will be a repulsive interaction between dipoles which will raise the potential energy curve for Stage 1 at higher concentrations, i.e. higher pressures  $p$ .

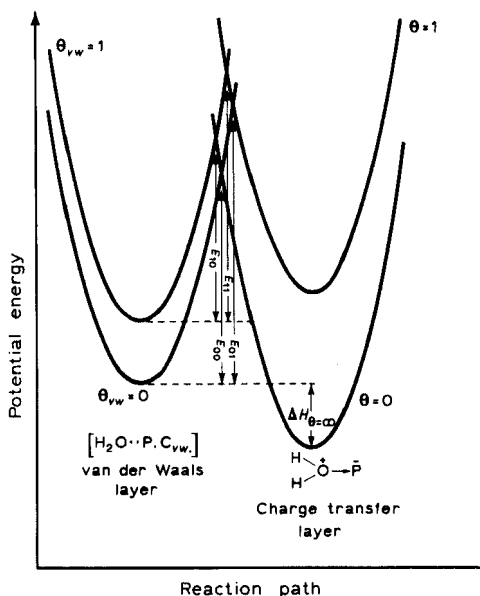
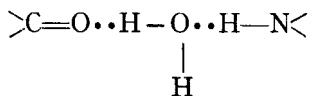


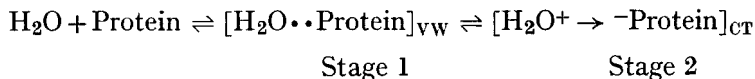
Fig. 7. Potential energies curves for water adsorbed in van der Waals' and charge-transfer states in haemoglobin, explaining the Roginsky-Zeldovich plots.

*Stage 2:* This is the final state, on the right of Fig. 7 corresponding to localized adsorption on polar groups, including most probably  $>C=O$  and  $H-N<$  groups. Hydrogen bridges, e.g.



may even occur. The electrical behaviour (next section) suggests that a definite charge-transfer (CT) bond occurs, resulting in the formation of a dipolar or even ionic double layer. As before, we

expect the energy of this state to rise with surface concentration,  $m$ . Here  $m$  is the moles water/100 g protein in the final equilibrium state. That is:



In passing from Stage 1 to Stage 2, a water molecule will have to pass over the energy barrier  $E$  formed by the intersection of the two potential curves. When the surface coverage in both stages tends to zero, we have  $E_{00}$ , as it rises in the first stage, with increased pressure  $p$ , so the barrier decreases to  $E_{10}$ . As the surface coverage in the second stage rises, with increased  $m$ , so the barrier rises to  $E_{01}$ . To express the effect quantitatively, we need to evaluate the interaction energy and decide what effect it has on the energy barrier. For the present purpose we shall assume the simplest linear law, namely:

$$E = E_{00} + \alpha m/p$$

To this approximation the rate should be

$$\frac{dm}{dt} = A p \exp - \left( \frac{E_{00} + \alpha m/p}{RT} \right)$$

The fact that the experimental pre-exponential term contains  $p^{0.6}$  rather than  $p$ , may reflect (a) non-ideal behaviour of water vapour and (b) a surface coverage in the van der Waals' layer approaching 0.6, therefore beyond the linear Henry's law region.

## VII. CONDUCTIVITY AND ADSORBED WATER

The earlier work in this field concentrated on textiles, see Baxter<sup>40</sup> and Hearle.<sup>41</sup> For the present discussions, we shall start from observations on keratin,<sup>42</sup> and haemoglobin,<sup>43</sup> which suggest at lower water contents ( $m$ ) the relationship

$$\log_{10} \kappa = \alpha m + \text{const.}$$

Here  $\kappa$  is the specific conductance, the relationship holding over six or more powers of 10 of  $\kappa$ , and eventually curving off to a saturation value of  $\kappa$  at very high water contents. Rosenberg<sup>44</sup> has recently

confirmed this relationship for haemoglobin, and his data, converted to specific conductances using an estimated factor, have been shown in Fig. 8. We have repeated this investigation, equilibrating two samples of haemoglobin with water vapour at one and the

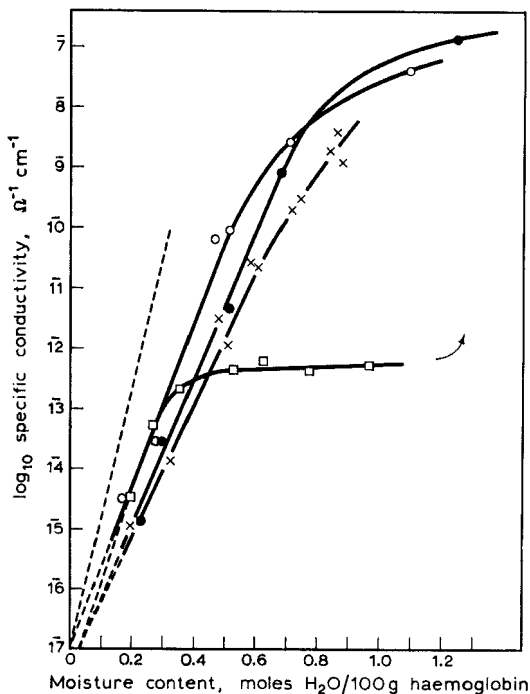


Fig. 8. The logarithmic plot for the effect of adsorbed water, in moles/100 g protein, on the specific conductivity  $\kappa$  of haemoglobin. ● natural haemoglobin; ○ denatured haemoglobin; × denatured globin; dotted line, haemoglobin (Rosenberg).

same time in the same sorption apparatus. The first sample was in a conductivity cell and the second sample was weighed for water uptake on a sensitive microbalance. As a result the three curves for natural and denatured haemoglobin, and denatured globin were obtained, as shown in Fig. 8. The simple logarithmic law is clearly a good fit, and there is a general agreement between Rosenberg's and our data. We have not now been able to find a saturation value (or rather step) in the curve at the monolayer value.

The current carriers in wet proteins have been variously considered to be electrons<sup>45, 46</sup> and ions, more specifically protons.<sup>42, 47</sup> There seems no doubt that the carriers are protons in keratin containing 15% water, since an electrochemical equivalent of hydrogen is evolved.<sup>48</sup> On the other hand, it seems equally definite that the carriers are electrons in haemoglobin containing 7.5% water. A continuous passage of electricity showed no decrease in current value, but if electrolysis had been occurring with loss of water content, there should have been found a ten-fold diminution in current.<sup>46</sup> In addition, we shall later describe evidence for electron transfer from water to *p*-type protein complexes.<sup>49</sup> The various facts may be coordinated if we specify two regions.

(1) At low moisture contents, up to the B.E.T. monolayer (or even beyond) conduction is by electrons by either (a) an intrinsic mechanism or (b) an impurity, or electron transfer mechanism.

(2) At higher moisture contents, e.g. above 2 B.E.T. monolayers, where the water molecules can form chains of neighbours on the surface of the protein, then a Grotthuss proton conduction becomes possible, as visualized by Riehl.<sup>50</sup> Also, if water molecules act as plasticizers, assisting peptide chain rotation, then proton transfer may be possible between C=O and NH, or NH and NH groups on neighbouring peptide chains, as in polyamides.<sup>51</sup>

To further define these regions will require experiments on such topics as Hall coefficients, and electrolytic evolution of hydrogen. Experiments with high-frequency A.C. may also serve to distinguish proton from electron conduction. For the present we shall outline the two approaches to the electronic mechanism.

### A. The Intrinsic Mechanism

In his very interesting paper, Rosenberg<sup>44</sup> has shown that the main effect of adsorbed water on the conductivity of haemoglobin is to lower the energy gap without effecting  $\kappa_0$ ; i.e. if  $m$  is the water content

$$\kappa = \kappa_0 \exp - \frac{(\Delta\epsilon_0 - \alpha m)}{2kT}$$

which, of course, leads to the observed relationship between  $\log_{10} \kappa$  and  $m$ , since  $\Delta\epsilon_0$  is a constant. This extends the earlier observation,

that adsorbed water lowers the energy gap for bovine plasma albumin.<sup>52</sup> Rosenberg's view is that haemoglobin is an intrinsic semiconductor in both dry and wet states, the current carriers being electrons and positive holes. The effect of water is simply to raise the dielectric constant and stabilize the current carriers. Riehl<sup>53</sup> (Lyons<sup>54</sup>) gives for the energy gap

$$\Delta\epsilon = I - E - 2P$$

where  $I$  is the ionization potential,  $E$  the electron affinity of the protein molecule, and  $2P$  is the polarization energy of the separated ions. Rosenberg writes the difference in polarization energy in wet (dielectric constant  $K'$ ) and dry ( $K$ ) states as

$$P' - P = \frac{e}{R} \left( \frac{1}{K} - \frac{1}{K'} \right)$$

He then shows that the experimental  $\Delta\epsilon/m$  relationship leads to a  $K'/m$  relation in agreement with that observed by King and Medley for keratin.<sup>42</sup> A saturation value of the conductivity will be reached at high water contents when  $1/K' = 0$ , and since  $K = 4$  this leads to a value of  $R = 2.8 \times 10^{-8}$  cm, which is reasonable for the radius of polarization.

### B. The Impurity Mechanism

Chemically speaking, in the formation of coordinate links, water behaves as an electron donor. It appears to function in this respect in the adsorbed state, in reducing the  $p$ -type photoconduction in anthracene,<sup>55</sup> and in lowering the energy gap in (presumably  $n$ -type) methylene blue.<sup>56</sup> Davis *et al.*<sup>57</sup> were able to considerably enhance dark semiconduction in bovine plasma albumin by forming a protein-chloranil complex. Since chloranil is a strong electron acceptor, presumably the result is a  $p$ -type protein complex. On admission of water vapour to this  $p$ -type protein-chloranil complex there occurred a decrease in electrical conductivity, so one may assume the water is acting as a donor-type impurity in the complex. One may, therefore, assume that this is a general behaviour for water molecules in proteins. It is very probable that the water molecules directly interact with the  $\text{C}=\text{O} \cdots \text{HN}$  bond system between peptide chains that has been held responsible for the energy bands in



proteins. If this is so, how far can an impurity mechanism account for the observed  $\log \kappa$  vs. water content relationship?

If  $n_D$  is the number of donors per cc, then the conductivity is given by<sup>58</sup>

$$\kappa = e\mu(2n_D)^{1/2} \frac{(2\pi mkT)^{3/4}}{h^{3/2}} \exp(-E_D/2kT)$$

where  $E_D$  is the ionization energy of the donors,  $e$  the electronic charge and  $\mu$  the mobility.  $n_D$  is, of course, proportional to  $m$ , the moles water adsorbed per 100 g protein.

The only way this relationship can lead to the observed relation is if the energy gap  $E_D$  decreases with moisture content according to

$$E_D = E_{D0} - \alpha n_D$$

A relationship of this kind could arise from an interaction between the impurity centres, i.e. water molecules. There is already evidence for an interaction energy, from the heat of adsorption and Roginsky-Zeldovich kinetics. According to Mott and Gurney<sup>58</sup> the variation of activation energy with increasing concentration of impurity is a common phenomenon with semiconductors. Thus, Fritsch<sup>59</sup> has shown, for example, that increase in the excess zinc in zinc oxide results in a decrease in  $E_D$  from 0.6 eV down to 0.01 eV,  $\kappa_0$  varying very little. Here we have a direct parallel with the results on haemoglobin, in a case where the impurity mechanism is quite certain. Pearson and Bardeen<sup>60</sup> found for boron in silicon,

$$E_D = E_{D0} - \alpha n_D^{1/3}$$

the  $n_D^{1/3}$  relation being simply derived on the basis that the interaction energy between impurity atoms is inversely proportional to the average distance between these atoms. The matter has been further discussed by Castellan and Seitz.<sup>61</sup> Extending this simple argument, if the impurity centres are distributed over the surface of spheroidal haemoglobin molecules, we should expect

$$E_D = E_{D0} - \alpha n_D^{1/2}$$

In general, therefore, the impurity mechanism might lead to a result

$$\kappa = e\mu(2n_D)^{1/2} \frac{(2\pi mkT)^{3/4}}{h^{3/2}} \exp - \frac{(E_{D0} - \alpha n_D^x)}{2kT}$$

i.e.  $\log_{10} \kappa = \text{const.} + \log_{10} m^{1/2} + \beta m^x$

where  $x$  will depend on the spatial distribution and law of force between the impurities, being  $\frac{1}{3}$  in certain inorganic cases. We have replotted the haemoglobin data in Fig. 9 as  $\log_{10} \kappa$  vs.  $m^{1/3}$

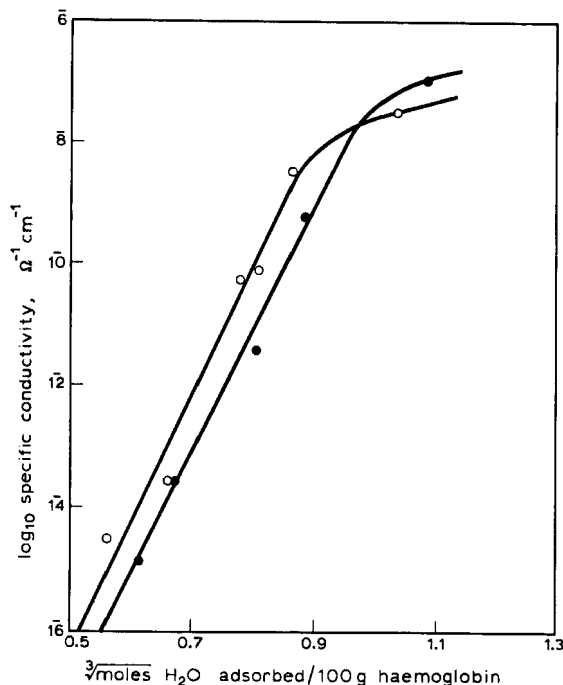


Fig. 9. A  $\log_{10} \kappa$  vs.  $m^{1/3}$  plot for data on haemoglobin from Fig. 8.

(neglecting the  $\log_{10} m^{1/2}$  term) and the result is practically as good as the earlier plot.

We may conclude that if we allow for an interaction between adsorbed water molecules, acting as impurity centres in proteins, we may account for the general form of the relations observed between conductivity and concentration, as well as for heat of adsorption and Roginsky-Zeldovich kinetics. Further progress in this field should be based on a more exact correlation of these three quantities.

The authors express their gratitude to the D.S.I.R. for financial support for this work.

## References

1. Cullis, A. F., Muirhead, H., Perutz, M. F., and Rossman, M. G., *Proc. Roy. Soc. (London)* **A265**, 161 (1962).
2. Kendrew, J. C., Dickenson, R. E., Strandberg, B. E., Hart, R. G., Davies, D. R., Phillips, D. C., and Shore, V. C., *Nature* **185**, 422 (1960).
3. Bernal, J. D., and Fowler, R. H., *J. Chem. Phys.* **1**, 515 (1933).
4. Sponsler, O. L., Bath, J. D., and Ellis, J. W., *J. Phys. Chem.* **44**, 996 (1940).
5. Eley, D. D., and Spivey, D. I., *Nature* **188**, 724 (1960).
6. Bull, H. B., *J. Am. Chem. Soc.* **66**, 1499 (1944).
7. McLaren, A. D., and Rowen, J. W., *J. Polymer Sci.* **1**, 289 (1951).
8. Cardew, M. H., and Eley, D. D., *Fundamental Aspects of the Dehydration of Foodstuffs*, Soc. Chem. Ind., London, 1958, p. 24.
9. Livingston, H. K., *J. Am. Chem. Soc.* **66**, 569 (1944).
10. Shaw, T. M., *J. Chem. Phys.* **12**, 391 (1944).
11. Palmer, K. J., *J. Phys. Chem.* **48**, 12 (1944).
12. Pauling, L., *J. Am. Chem. Soc.* **67**, 555 (1945).
13. Frey, H. J., and Moore, W. J., *J. Am. Chem. Soc.* **70**, 3644 (1948).
14. Mellon, E. F., Korn, A. H., and Hoover, S. R., *J. Am. Chem. Soc.* **70**, 3040 (1948).
15. Benson, S. W., and Ellis, D. A., *J. Am. Chem. Soc.* **70**, 3563 (1948).
16. Benson, S. W., and Ellis, D. A., *J. Am. Chem. Soc.* **72**, 2095 (1950).
17. Benson, S. W., Ellis, D. A., and Zwanzig, R. W., *J. Am. Chem. Soc.* **72**, 2102 (1950).
18. Benson, S. W., and Seehof, J. M., *J. Am. Chem. Soc.* **73**, 5053 (1951).
19. Boyes-Watson, J., Davidson, E., and Perutz, M. F., *Proc. Roy. Soc. (London)* **191**, 83 (1947).
20. Tristram, G. R., *Advan. Protein Chem.* **1**, 83 (1949).
21. Bragg, L., Howells, E. R., and Perutz, M. F., *Proc. Roy. Soc. (London)* **A222**, 33 (1954).
22. Amberg, C. H., *J. Am. Chem. Soc.* **79**, 3980 (1957).
23. Low, B. W., and Richards, F. M., *J. Am. Chem. Soc.* **76**, 2511 (1954).
24. Seehof, J. M., Keilin, B., and Benson, S. W., *J. Am. Chem. Soc.* **75**, 2428 (1953).
25. Reyerson, L. H., and Hnojewy, W. S., *J. Phys. Chem.* **64**, 811 (1960).
26. Dole, M., and McLaren, A. D., *J. Am. Chem. Soc.* **69**, 651 (1947).
27. Davis, S., and McLaren, A. D., *J. Polymer Sci.* **3**, 16 (1948).
28. Hill, T. L., *Advan. Catalysis* **4**, 211 (1952).
29. Hill, T. L., *J. Chem. Phys.* **17**, 520 (1949).
30. Hill, T. L., *J. Chem. Phys.* **18**, 246 (1950).
31. Hill, T. L., Emmett, P. H., and Joyner, L. G., *J. Am. Chem. Soc.* **73**, 5102 (1951).
32. Foss, J. G., and Reyerson, L. H., *J. Phys. Chem.* **62**, 1214 (1958).
33. Drain, L. E., and Morrison, J. A., *Trans. Faraday Soc.* **48**, 840 (1952).
34. Roginsky, S. Z., and Zeldovich, J., *Acta Physicochemica U.S.S.R.* **1**, 449 (1934).

35. Taylor, H. A., and Thon, N., *J. Am. Chem. Soc.* **74**, 4169 (1952).
36. Jennings, T. J., and Stone, F. S., *Advan. Catalysis* **9**, 441 (1955).
37. Stone, F. S., in *Chemistry of the Solid State*, W. E. Garner, Ed., Butterworths, London, 1955, p. 367.
38. Eley, D. D., *Trans. Faraday Soc.* **49**, 643 (1953).
39. Higuchi, I., Ree, T., and Eyring, H., *J. Am. Chem. Soc.* **77**, 4969 (1955).
40. Baxter, S., *Trans. Faraday Soc.* **34**, 207 (1943).
41. Hearle, J. W. S., in *Moisture in Textiles*, J. W. S. Hearle and R. H. Peters, Eds., Butterworths, London, 1960, p. 123.
42. King, G., and Medley, J. A., *J. Coll. Sci.* **4**, 9 (1949).
43. Spivey, D. I., in C. P. S. Taylor, *Discussions Faraday Soc.* **27**, 239 (1959).
44. Rosenberg, B., *J. Chem. Phys.* **36**, 816 (1962).
45. Eley, D. D., and Spivey, D. I., *Nature* **188**, 725 (1960).
46. Rosenberg, B., *Nature* **193**, 364 (1962).
47. Taylor, C. P. S., *Nature* **189**, 388 (1961).
48. King, G., and Medley, J. A., *J. Colloid Sci.* **4**, 1 (1949).
49. Davis, K. M. C., Eley, D. D., and Snart, R. S., *Nature* **188**, 724 (1960).
50. Riehl, N. V., *J. Phys. Chem. (U.S.S.R.)* **29**, 1537 (1955).
51. Eley, D. D., and Spivey, D. I., *Trans. Faraday Soc.* **58**, 2280 (1961).
52. Eley, D. D., Parfitt, G. D., Perry, M. J., and Taysum, D. H., *Trans. Faraday Soc.* **49**, 79 (1953).
53. Riehl, N. V., *J. Phys. Chem. (U.S.S.R.)* **29**, 1152 (1955).
54. Lyons, L. E., *J. Chem. Soc.* 5001 (1957).
55. Schneider, W. G., and Waddington, T. C., *J. Chem. Phys.* **25**, 358 (1956).
56. Vartanian, A. T., *J. Phys. Chem. (U.S.S.R.)* **31**, 1792 (1957).
57. Davis, K. M. C., Eley, D. D., and Snart, R. S., *Nature* **188**, 724 (1960).
58. Mott, N. F., and Gurney, R. W., *Electronic Processes in Ionic Crystals*, 2nd Edition, Oxford, 1948, p. 165.
59. Fritsch, O., *Ann. Physik* **22**, 375 (1935).
60. Pearson, G. L., and Bardeen, J., *Phys. Rev.* **75**, 865 (1959).
61. Castellán, G. W., and Seitz, F., in *Semiconducting Materials*, H. K. Henisch, Ed., Butterworths, London, 1951, p. 8.

## 7

# THE EFFECTS OF IONIZING RADIATIONS ON SOME FIBROUS PROTEINS

R. BRAAMS and G. VAN HERPEN, *Department of Radiobiophysics  
Physics Laboratory, University of Utrecht, Utrecht, Netherlands*

## CONTENTS

I. Introduction . . . . .	259
A. Ionizing Radiation(s) . . . . .	259
B. Proteins . . . . .	261
C. Radiation Effects on Proteins . . . . .	262
II. Studies on Fibrous Proteins . . . . .	264
A. Silk . . . . .	264
(1) Experimental Results . . . . .	264
(2) Discussion . . . . .	265
B. Keratins . . . . .	265
(1) Experimental Results . . . . .	266
(2) Discussion . . . . .	269
C. Collagen . . . . .	270
(1) Experimental Results . . . . .	271
(2) Discussion . . . . .	274
D. Myosin . . . . .	274
(1) Experimental Results . . . . .	275
(2) Discussion . . . . .	276
III. General Conclusions . . . . .	277
IV. Acknowledgements . . . . .	278
References . . . . .	279

## I. INTRODUCTION

### A. Ionizing Radiation(s)

Since the discovery of X-rays in 1895 and radioactivity in 1896 the study of the biological effects of ionizing radiations has received much attention. Research has been carried out at many different levels of organization of the biosystems under investigation. The highest levels of organization and complexity investigated are the somatic and genetic changes in man after exposure to radiation. At

the other extreme, one could place the studies of the smallest inorganic and organic molecules, such as water and amino acids, which are of importance in biological systems. In between these extremes one finds a broad spectrum of objects in radiation research, ranging from small molecules to macromolecules, enzyme systems, viruses and micro-organisms to mammalian or human cells and organs.

Apart from the familiar, practical medical implications, the main reason why the influence of radiation on living systems has attracted so much attention is undoubtedly the fact that a relatively small amount of absorbed radiation energy can lead to large effects that can not be found when the same quantity of energy is given in the form of heat or electromagnetic radiation of wavelengths longer than  $200\text{ m}\mu$ . A dose of ionizing radiation sufficient to cause 50% lethality in primates does not contain enough energy to raise the temperature of the irradiated object by more than  $0.002^\circ\text{C}$ .

When a fast moving charged particle traverses matter, the electric field of the moving particle interacts with electrons of the atoms of which the matter is composed. Electrons may be either excited to states of greater energy or removed from their parent atoms, ions being left behind. These primary electrons will in turn collide with the electrons of other atoms, and may eject them as secondary electrons, etc. The chain of processes that is thus triggered off includes the production of ions and excitations, dissociations, radicals, chemical changes and heat.

Electromagnetic radiations such as X-rays and gamma-rays are absorbed by matter through processes that result in the transfer of a large amount of the initial radiation energy to fast moving electrons. Fast neutrons lose their energy in organic matter chiefly in collisions with hydrogen nuclei thus producing fast moving protons. The interactions of electromagnetic radiations or fast neutrons with matter, therefore, result likewise in the formation of fast charged particles and, as a consequence, cause the same types of processes as those initiated by beams of fast moving charged particles.

The average amount of energy that is lost in an interaction of a fast charged particle with matter is of the order of  $70\text{--}90\text{ eV}$  ( $1\text{ eV} = 1.6 \times 10^{-12}\text{ erg}$ ). The electrons liberated by these interactions are, therefore, predominantly of low energy compared to the

original particle, which may have an energy in the MeV-range. Consequently, these electrons do not travel far, but lose their energy in the immediate vicinity of the initial interaction. Packages of energy are in this way deposited along the track of a fast charged particle. The absorption of energy is measured in *rads*, 1 rad being equivalent to 100 ergs absorbed per gram. Before the rad was introduced the roentgen (r) was employed. In biological material the roentgen is equivalent to 83 ergs per gram.

A dose of 1000 rads, lethal to most mammals, adds only  $2.4 \times 10^{-3}$  calories to a gram of tissue. A dose of  $10^6$  rads (1 Mrad) to a sample of molecular weight 100,000, would add 2.4 calories per gram, or an average of 10 eV per molecule. Not every molecule receives initially 10 eV since, as stated above, the energy is dissipated in quantities of on the average 70–90 eV. Thus only one in every 7–9 molecules takes part in the primary interaction. In radiation chemistry it is common practice to express the amount of chemical change by the number of molecules that have been altered or produced per 100 eV absorbed energy. This number is called the *G-value*.

Two mechanisms may be distinguished by which the radiation energy leads to a chemical effect in the molecule under study: viz., (1) an *indirect action*, through the surrounding medium, secondarily affecting the molecule, and (2) a *direct action* on the molecule itself. In biology the surrounding medium is generally water. Irradiation of water leads to the formation of free radicals, which are chemically extremely reactive and may react with the molecule to produce the chemical radiation effect. If a pure material is irradiated when dry, the radiation action is considered to be direct. On a material dissolved in water both mechanisms will act simultaneously.

The presence of *oxygen* generally *increases* the effect of radiation. A *decrease* in effect, on the other hand, is afforded by some substances, especially sulphur-containing compounds such as cysteine or cysteamine. Such substances are called *chemical protectors* and are thought to compete for free radicals with the target molecule.

## B. Proteins

In this chapter we shall be concerned with the action of ionizing radiations on a special group of biologically important macromolecules, the *proteins*. Proteins are found in all living organisms

and perform a wide variety of functions. They are composed of amino acids that are bound by peptide bonds and form long peptide chains. The peptide chains can be stretched or coiled into typical configurations that are stabilized by intramolecular hydrogen bonds. The coiled or stretched chains may be folded into a structure that can be stabilized by covalent bonds, mainly disulphide links, and by numerous hydrogen bonds between oxygen and nitrogen atoms in the main chain or in side groups. The maintenance of a specific configuration is often essential for the conservation of the specific function of a specific protein, e.g. an enzyme, a hormone, a toxin.

Depending on the shape of the molecule, proteins are classified as *globular* or *fibrous* proteins. The globular proteins have as a first approximation a spherical or ellipsoidal envelope as can be demonstrated with physicochemical methods such as ultra-sedimentation or viscosity measurements. They are often easily soluble in aqueous solutions and perform their typical biological function while in solution or surrounded by water. The fibrous proteins are a group of long, approximately linear, molecules that easily form insoluble fibres. In mammals such proteins are important in connective tissue, tendon, muscle, skin, hair and horn. In these fibres, regions can be found where the long thin molecules are arranged in an orderly manner, leading to birefringence or to small-angle X-ray diffraction patterns. In the ordered regions intermolecular hydrogen bonding provides the stability that is characteristic of protein fibres, as for example in keratin, collagen and in silk. In silk the hydrogen bonding between fibroin molecules in natural fibres is so strong that the fibre can only be dissolved in special reagents.

### C. Radiation Effects on Proteins

Studies on the effects of the action of ionizing radiations on protein have been mainly concerned with *globular proteins*, especially enzymes. The biological function of enzymes is the catalysis of specific chemical reactions. Most globular proteins are, moreover, antigenic, that is to say, they can, when introduced into the animal organism, stimulate the production of antibodies. These react specifically with the corresponding antigen, e.g. in the form of



a precipitation reaction. Thus, with the aid of biochemical or serological techniques, the changes in functional activity of these globular proteins may be investigated.<sup>43, 27</sup> Estimates were, in this way, made of the number of molecules changed by the irradiation. A quantitative analysis in terms of target theory was often possible, giving information on the order of magnitude of the dimensions of the protein molecule under investigation, even under conditions of great chemical impurity such as exist *in vivo* or in the dehydrated whole organism.<sup>43, 57, 75</sup>

More recently, detailed chemical analysis of the irradiated material became possible<sup>20</sup> and some understanding of the chemical and physicochemical alterations has been obtained. However, since, for the globular proteins, the relation between structure and biological function is not yet well understood a satisfactory explanation of the observed facts in terms of physical and chemical processes has not yet been given. In order to bridge existing gaps in knowledge, speculative mechanisms were invoked (energy-transfer, Alexander *et al.*,<sup>4</sup> semiconduction, Blumenfeld *et al.*<sup>12</sup>).

The reason why globular (soluble) proteins have received so much attention is undoubtedly because of their importance in metabolism and because of the effects that ionizing radiation could have on metabolic processes through action on enzymes and enzyme systems.

Relatively few experiments have been reported on *fibrous proteins*. Research in this field could, however, offer certain advantages over work on globular proteins. In several cases knowledge exists about the relation between structure and observed function. Fibrous proteins are often found in ordered biological structures. These structures can be dry (keratin in hair, feather, horn, nail; fibroin in silk fibres) or hydrated (collagen in tendon or in fibrils in skin, myosin in muscle, elastin in connective tissue). The water content of hair is dependent on environmental conditions and varies usually between 5–30%. In collagen fibres the water content is about 55% and in muscle approximately 80%. A large fraction of this water is bound to the surface of the protein molecules.

In the following sections the data available on the action of ionizing radiations on fibrous proteins will be surveyed and analysed. The possible value of the findings for the interpretation of radiation studies of other proteins will be discussed.

## II. STUDIES ON FIBROUS PROTEINS

### A. Silk

Silk is a fibrous material produced by insects or spiders. The most common form of silk fibroin is excreted by the silkworm (*Bombyx mori*). This material has been extensively investigated with X-ray diffraction methods, and models for the structure were proposed by Pauling and Corey<sup>51</sup> and later by Marsh, Corey and Pauling.<sup>47</sup> According to these authors silk is composed of extended polypeptide chains ( $\beta$  configuration) that are arranged in antiparallel-chain pleated sheets. This model is now widely accepted and accounts for such properties of silk as its insolubility in water or weak acids, anisotropy in its infrared absorption spectrum, high tensile strength and lack of extensibility.

Silk can be dissolved in aqueous cupri-ethylene-diamine or in LiBr.<sup>19, 25</sup> Depending on its origin and the methods of preparing the solutions, molecular weights are found between 30,000–150,000.<sup>37</sup> The amino acid composition is typical, 43% of its residues are glycine, 29% alanine and 12% serine.<sup>37</sup>

#### (1) *Experimental Results*

Only a few and sometimes conflicting observations on radiation effects in silk have come to our attention. Little<sup>46</sup> has investigated the X-ray diffraction diagrams of natural fibres after exposure to fast electrons. He reports that collagen has a much lower radiation resistance than either silk or keratin. The silk fibre in its turn loses strength at lower doses than fibres of nylon-66. Alexander and Charlesby<sup>3</sup> found that silk fibres are weakened much more readily than wool fibres. Teszler and Rutherford<sup>72</sup> report that silk has less mechanical stability than wool when exposed to thermal neutrons. Satlow<sup>69</sup> reports a decrease in tensile strength by 42% in natural silk after exposure to  $0.2 \times 10^{17}$  n/cm<sup>2</sup> thermal neutrons. The extension at breakage was reduced by 54%.

Gordy and Shields<sup>31, 32, 33</sup> have made extensive studies of the radical that can be detected by electron spin resonance spectroscopy (ESR) in silk irradiated and observed in a vacuum at room temperature. The observed signal is a doublet, apparently resulting from the interaction of the unpaired electron with one proton. The

observed splitting depends on the orientation of the fibre in the magnetic field. If the axes of the fibres are perpendicular to the magnetic field lines, the splitting is 13 gauss. The splitting increases to 26 gauss when fibre and field are parallel. The doublet resonance was similar to the resonance in glycylglycine and in (glycyl)<sub>2</sub>-glycine. The resonance in glycylglycine remained unchanged after treatment of this peptide with D<sub>2</sub>O and therefore it was concluded that the interaction of the unpaired electron is with a hydrogen atom bonded to a carbon atom.<sup>49</sup> The unpaired spin is in the  $p_x$  orbital perpendicular to the —NCH plane.

## (2) Discussion

No evaluation can be made of the remarks by Little<sup>46</sup> and by Alexander and Charlesby<sup>3</sup> because no experimental data were provided by these authors. For thermal neutron irradiation there is agreement between the observations by Teszler and Rutherford<sup>72</sup> and the data of Satlow<sup>69</sup> on the greater sensitivity of silk compared to wool (for changes in tensile strength). In Parts B (1) and C (1) of this section it is reported that in wool and in collagen the prior chemical introduction of cross-links leads to smaller changes in mechanical strength after irradiation. The absence of covalent cross-links between the fibroin molecules in silk explains a greater sensitivity of silk in comparison to wool.

The work of Gordy and Shields<sup>33</sup> shows that when knowledge is available on the detailed structure of a specific protein, methods of qualitative ESR spectroscopy can lead to an explanation of the structure of the radicals observed after irradiation. It is to be regretted that no further studies of the physical and chemical aspects of radiation effects on silk are available. It is not yet possible to relate the observed radicals to other radiation effects.

## B. Keratins

Keratins are found in insoluble organelles as hair, nail, horn and feather. In keratin the peptide chains contain a great number of amino acids with active side chains (Alexander and Hudson,<sup>2</sup> Mercer,<sup>48</sup> Peters and Woods<sup>53</sup>) that can interact and thus play an important role in giving keratin fibres some of their characteristic

properties. The presence of a number of cysteine residues leads to the formation of cross-links through disulphide bonds, rendering the material insoluble in water.

Keratin fibres have been extensively investigated with X-ray diffraction methods (Astbury<sup>7,8</sup>) and typical fibre diagrams were obtained. It has been shown that in keratin fibres the main protein constituent often exists in one of two modifications: the coiled  $\alpha$  form or the stretched  $\beta$  form.

Full details on keratins can be found in textbooks on wool or keratin or in journals on textile research.

### (1) *Experimental Results*

The first effects of ionizing radiation on keratin were reported by Astbury in 1933. He noticed that some properties of hair had changed after extensive X-ray analysis.<sup>7</sup> It was reported that both "supercontraction"\* and "set"† were accelerated after prolonged exposure to X-rays. The irradiated material also showed increased longitudinal swelling.

The effects of exposure to reactor radiation on wool were investigated by Kirby and Rutherford<sup>40</sup> in 1955, and by Teszler and Rutherford in 1958.<sup>72</sup> An increase in alkaline solubility and changes in stress-strain properties after doses of  $10^{16}$  nvt (total thermal neutrons per square cm) were reported. The cystine content and acid-binding capacity were found to decrease, but total sulphur and nitrogen remained the same. The shape of the stress-strain curve of the exposed fibre was identical with that of the unexposed fibre.

O'Connell and Walden<sup>50</sup> measured some effects of X-rays, <sup>60</sup>Co gamma-rays, electrons and ultraviolet light on wool fibres. The modulus of elasticity and the stress for a 30% extension were found to decrease with increasing dose for wet and for dry fibres. Wool dyed with Rhodamine B showed significantly more resistance to irradiation. Supercontraction tests were performed in hot sodium bisulphite.

In a number of publications Satlow,<sup>67,68,69</sup> Zahn,<sup>67,74</sup> and

\* "Supercontraction" is a contraction in length of a wool fibre with subsequent fixation at its reduced length, after certain treatments.

† "Set" is the elongation remaining after a keratin fibre has been steamed while stretched.<sup>17</sup>

associates<sup>36</sup> describe their investigations on the effects of gamma-radiation (at 20°C) and thermal neutrons (at 75°–80°C) on properties of different kinds of treated and untreated wool.

Some of their experimental findings are summarized here:

- (a) gamma-radiation and neutrons are about equally effective in changing properties of wool when measured in units of absorbed energy,<sup>28</sup>
- (b) the tensile strength of the wet fibres is reduced to about one half by a dose of about  $10^{17}$  n/cm<sup>2</sup>,<sup>69</sup>
- (c) the rate of loss of tryptophan with dose is 10 times the rate of loss for tyrosine and for cystine,<sup>36</sup>
- (d) the presence of air during irradiation increases the amount of change in cystine content,<sup>36</sup>
- (e) certain pretreatments of wool can reduce the radiation effects,<sup>28</sup>
- (f) gamma-rays cause a greater loss in tensile strength in camel hair than in sheep wool,<sup>69</sup>
- (g) the alkaline solubility increases with increasing radiation dose.<sup>36</sup>

From their physical and chemical data they reach the conclusion that mainly *covalent bonds* in the peptide chain and in cystine bridges are broken.<sup>36, 69</sup>

Allen and Alexander in 1961 measured the degree of supercontraction in saturated LiBr solutions of irradiated wool fibres after exposure to 5–200 Mrad of electron-radiation.<sup>6</sup> Irradiation increases the supercontraction produced by LiBr and renders it irreversible. The increase of supercontraction of irradiated fibres in sodium bisulphite solutions (breakage of —S—S— bonds) was less pronounced. The authors conclude that the action of radiation is mainly on the *hydrogen bonds* in fibrils in the micelles, and that radio-chemical changes involving covalent bonds are not principally responsible.

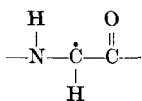
In 1955, Gordy, Ard and Shields<sup>30</sup> revealed with ESR spectroscopy the presence of stable radicals in a number of irradiated proteins including hair, horn and feather. The spectra in these keratins showed similarity with the spectra obtained from irradiated cystine. These results were believed to suggest that the

cystine residues in sulphur-containing proteins act as a preferential site for radiation damage.

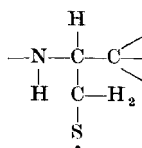
In further work Gordy and Shields,<sup>31</sup> reported a field dependence of the ESR pattern in irradiated hair and nail. The spectrum in irradiated feather quill appeared to be composed of a proton doublet and a cystine-like resonance. The doublet was found to be dependent on the orientation of the fibre in the magnetic field. The cystine-like component showed no orientation dependence. After a discussion of their results, the authors write that it seems probable "that most amino acid residues in the proteins can transmit to other residues any electron vacancy which they receive".<sup>31</sup>

In surveys of the then available results (1960, 1961), the same authors<sup>32,33</sup> discuss investigations on the spectrum of single crystals of irradiated cystine. This spectrum appeared to be highly orientation-dependent in contrast to that of polycrystalline cystine. In fibrous proteins no orientation dependence of the cystine-like spectrum could be found; the pattern was similar to that of polycrystalline cystine. It was concluded that in hair and in feather quill the C—S or S—S bonds must be polyoriented.

The observed signals were believed to be caused by a radical of type (I) for the orientation-dependent doublet and a radical of type (II) for the cystine-like pattern.



(I)



(II)

In 1959, Rajewski, Redhardt and Froese<sup>60</sup> confirmed the early (1955) results by Gordy *et al.*<sup>30</sup> In irradiated cow hair they found immediately after irradiation a spectrum composed of a single line and a cystine-like pattern. The single line disappeared in a few hours, leaving only the cystine pattern. Pohlit, Rajewski and Redhardt<sup>56</sup> investigated the stability of the single-line component in irradiated cow-tail hair under different conditions and compared the behaviour of the hair spectrum with that of mechanical and molecular mixtures of amino acids, similar in gross composition to total cow hair.

Rajewski and Redhardt<sup>61, 62</sup> found after irradiation of dried keratins a slow increase in the intensity of parts of the ESR spectrum. They think it probable that a radical state migrates to the cystine part of the keratin.

## (2) Discussion

There is general agreement among different authors that in wool fibres doses of ionizing radiation of about 10 Mrad cause considerable changes in such properties as strength, alkaline solubility and supercontraction. However, there is difference of opinion concerning the principal points of attack.

Alexander<sup>6</sup> concludes that the main attack is on the *hydrogen bonds* in the fibrous sub-units of the wool fibre (Lincoln wool). These units, the micelles, are responsible for the reversible supercontraction of wool in saturated solutions of LiBr.<sup>1</sup> In support of his conclusion Alexander cites two facts, viz (a) "a lack of loss in dry tensile strength after exposure to ionizing radiation", and (b) "the breakage of 5% of all the peptide bonds by acid treatment is needed before supercontraction in LiBr is changed; such a treatment would also alter the tensile properties and this does not occur".

Concerning the first point it is of importance to note that Satlow and Zahn<sup>67</sup> showed a decrease of 18% in dry tensile strength of untreated wool after approximately 9 Mrad of gamma-radiation. From this work it would appear that a dose of 50 Mrad would cause a reduction in tensile strength to less than 40% of the original value.\*

With regard to the second point it should be noted that according to Elöd, Nowotny and Zahn,<sup>26</sup> a reduction in tensile strength of the dry fibre to about 40% could be brought about by acid hydrolysis of about 5% of the peptide bonds. Furthermore, wool is not a homogeneous material.<sup>2, 29, 48, 65, 69</sup> Cortical cells can be differentiated in basophilic (orthocortex) and acidophilic (paracortex) cells.<sup>45</sup> The

\* Allen and Alexander<sup>6</sup> write that according to Zahn, Fritze, Pfanmuller and Satlow<sup>74</sup> in wool fibres after irradiation with  $50 \times 10^6$  rads the mechanical properties are affected to only a very small extent. In the paper by Zahn *et al.* only radiation effects of gamma-rays are mentioned for a dose of  $10^7$  r ( $9 \times 10^6$  rad). The wool that showed no decrease in tensile strength after irradiation with about  $10^7$  r of  $^{60}\text{Co}$   $\gamma$ -rays had been *cross-linked* with quinone or with difluor-dinitrobenzol before radiation exposure.

paracortex swells faster in acid than in base. The orthocortex contains relatively less cystine. Rogers reports that Lincoln wool fibres contain cortical cells of both types.<sup>65</sup> Therefore the action of acid on the behaviour of the whole fibre would not necessarily parallel the action of ionizing radiation.

More work taking into account the complex architecture of the wool fibre is clearly needed before a full description and explanation can be given of the radiation effects in wool. At present it seems that the explanation offered by Satlow,<sup>69</sup> who suggests that the breakage of peptide bonds is responsible to a large degree for the observed changes in the properties of gamma-irradiated wool, should be favoured. Such a conclusion also seems to be in agreement with results obtained by other workers after investigating irradiated collagen and myosin (Parts C (1) and D (1) of this section).

The important observation by Zahn and Satlow<sup>28, 74</sup> that wool can be protected against radiation-induced reduction of the tensile strength by prior treatment with cross-linking agents is in agreement with similar observations on formaldehyde-treated collagen.<sup>16</sup>

### C. Collagen

Collagen is one of the main protein constituents of tendon, bone, connective tissue, sclera and the corium of the skin. It can be isolated from tendon or skin and dissolved in weak acids. From physicochemical studies of collagen solutions and from X-ray diffraction work on the non-dissolved fibres it has been concluded that the molecule has a molecular weight of approximately 360,000, a length of 2800 Å and a diameter of 14 Å.<sup>70</sup> According to Rich and Crick<sup>63</sup> it is composed of three intertwined helices. Characteristic of collagens is the high content of hydroxyproline and proline. In mammals these two amino acids account for approximately 27% of the total amino content. In fish collagen the pyrrolidine fraction is lower, e.g. 16.6% in cod skin.<sup>34</sup>

Collagen has received much attention because of its importance in the leather industry, gelatin and glue production and as a well-defined material for fundamental protein research. Extensive information about collagen can be found in several books and surveys dealing almost exclusively with collagen and related materials.<sup>11, 34, 35, 39, 59, 64, 70, 71</sup>



### (1) *Experimental Results*

Observations on radiation effects in collagen were nearly all reported within the last 5 years. Only the work of Perron and Wright<sup>52</sup> and the observation by Little<sup>46</sup> (see Part B (1) of this section) are of an earlier date. Perron and Wright observed a marked decrease in intensity of the X-ray diffraction pattern of collagen fibres after exposure to doses of electron-radiation of a few Mrads. For equal electron doses, fibres irradiated in the dry state and subsequently soaked and dried showed a greater loss in intensity of the diffraction pattern than samples that were irradiated while containing the normal amount (approximately 55%) of water.

Cassel (in 1959) irradiated collagen in kangaroo-tail tendon and in purified steerhide powder.<sup>18</sup> He observed a decrease of the shrinkage temperature of irradiated fibres. The shrinkage temperature was measured for different doses and the measured shrinkage temperature plotted against the radiation dose. The curves were found to be independent of the water content and the author concludes that free radicals formed in irradiated water have no effect on the shrinkage temperature. The water-soluble fraction in highly purified steerhide powder after irradiation increases with increasing radiation dose. The amino acid losses showed similarity with those caused by thermal degradation in air. The percentages of amino acid losses for 90, 160 and 220 Mrad of radiation were 4%, 12% and 27%, respectively, representing *G*-values of 4.5, 7 and 12, respectively.

Bowes, Moss and Raistrick<sup>13</sup> irradiated ground oxhide collagen with 50 Mrads of gamma-radiation. An overall loss of 10–15% of the amino acid residues was reported. This would indicate a *G*-value of about 20–30. The increased solubility of irradiated dry collagen (5% moisture content) and the presence of a large proportion of low molecular weight material indicated a degradation of the molecular structure and a decrease in chain length. During irradiation of collagen containing 80% moisture, the formation of cross-links occurred, leading to stabilization of the molecule.

Braams<sup>15</sup> reported in 1961 a marked decrease in tensile strength in collagen fibres after irradiation in the dry and in the wet state. The reduction in tensile strength was most pronounced in the dry irradiated fibre. Irrespective of the conditions of irradiation the

measurements of tensile strength were always carried out on the wet fibre. From these measurements it was concluded that the direct radiation effect and the indirect radiation effect in this system are not additive.

Bowes and Moss in 1962 gave a detailed report of the chemical changes in oxhide collagen after irradiation in oxygen and in nitrogen.<sup>14</sup> They found that after a dose of 50 Mrad about 10% of the amino acids were lost in the dry irradiated material and 20% in the wet irradiated samples. Losses of tyrosine and hydroxyproline were greater in oxygen; those of aspartic acid and proline, were greater in nitrogen. The solubility increased less in the wet irradiated hide powder. The amino acids that showed the greatest sensitivity were the acidic and basic amino acids and those with a ring structure. From a determination of N-terminal residues after irradiation it was concluded that relatively little hydrolysis of peptide bonds had occurred.

Formation of carbonyl compounds took place, but with low frequency. The authors think that the increase in amide nitrogen and the formation of carbonyl groups indicate some breakage of  $\text{—N—C—}$  bonds by the mechanism suggested by Jayko and Garrison.<sup>38</sup>

Bailey, Bendall and Rhodes<sup>9</sup> investigated the effect of irradiation on the shrinkage temperature of rat-tail tendon exposed in saline to doses up to 40 Mrad. They found a decrease of the shrinkage temperature by 20°C after a radiation dose of 10 Mrad. They also observed an increased extensibility that could be partly explained by the small amount of kinking that was found to occur even after doses of less than 5 Mrad. The presence of radical scavengers did not change the relation between shrinkage temperature and radiation dose. When irradiation took place at  $-196^{\circ}\text{C}$  the lowering of the shrinkage temperature was only one-half of that after irradiation at room temperature. Irradiation of the heat-shrunken fibre led to the formation of cross-links with a  $G$ -value of 1.7, as determined from measurements of the stress-strain behaviour. The authors interpret the drop in shrinkage temperature as being due to an irreversible disruption of the secondary structure, with or without an actual chain scission, resulting from an ionizing event according to the mechanism proposed by Platzman and Franck.<sup>58</sup>

In an abstract, Kuntze and White<sup>41</sup> report on experiments with

films of reconstituted collagen. They found that collagen irradiated in the dry state showed an excess of chain breaks over cross-links as measured by stress-strain analysis. Collagen irradiated in the wet state demonstrated a progressive net increase in cross-links for doses between 2.5 and 10 Mrads. A two-peak electron resonance was found after radiation in the dry state. This signal disappeared after wetting.

In 1958 Gordy and Shields<sup>31</sup> reported the detection with ESR techniques of a symmetrical doublet in irradiated chicken bone and attributed this signal to collagen in the bone.

In 1961 the same authors<sup>33</sup> discussed more fully the orientation-dependent resonance observed in irradiated collagen. They think it probable that the principal constituent of the ESR pattern in collagen is a glycy radical similar to a radical of the type proposed for silk. In rat-tail tendon and in fish-fin bone there are indications of a small contribution by a radical of the alanyl type. No agreement could be found with the spectra observed in irradiated proline or hydroxyproline although collagen contains about 27% of these amino acids.

In a second paper on radiation effects in collagen, Braams (1963) reports on the extent of changes in mechanical properties of tendons when irradiated at different conditions.<sup>16</sup> Cross-linking with formaldehyde diminished the reduction in tensile strength after irradiation. Hydration of the dry irradiated fibre amplified the effect of radiation on the tensile strength. The presence of glycine and cysteine during irradiation of the hydrated tendon led to a greater reduction in tensile strength than did the presence of urea or water only. A lower temperature during irradiation reduced the sensitivity. The damage also depended on the treatment after irradiation. If the dry irradiated fibre was hydrated at 0°C and dried again under tension very little reduction in tensile strength could be detected after a dose of 40 Mrad. If, however, the hydration was carried out at 50°C, allowing the irradiated part of the fibre to shrink, and the fibre was then dried under tension, the damage was great, 15 Mrad being sufficient to reduce the tensile strength to half the value of the unirradiated controls.

These results were seen as an indication that the reduction in tensile strength was a result of the decreased order in the irradiated fibre. The decrease in order was seen as a consequence of the

breakage of a considerable number of hydrogen bonds, after main chain breaks were produced by the interaction of the ionizing radiation.

## (2) Discussion

Radiation doses of about 5 Mrad cause considerable changes in the tensile strength and the shrinkage temperature of collagen fibres. The intensity of the low-angle X-ray diffraction diagram is markedly changed. The chemical destruction is large as seen from the high *G*-values for loss of amino acids reported by Cassel<sup>18</sup> and by Bowes and Moss.<sup>14</sup> The increase in solubility<sup>9</sup> together with the high *G*-value for amino acid loss indicates extensive breakage of the peptide chains. The observed disorder appears to be a secondary effect, resulting from the increased mobility of fractured chains under thermal agitation. In the presence of covalent cross-links the disorder caused by thermal action is reduced.

Although after irradiation in the wet state the loss of amino acid residues (Bowes and Moss<sup>14</sup>) is twice that after irradiation in the dry state, the change in shrinkage temperature is independent of water content during radiation exposure (Cassel,<sup>18</sup> Bailey<sup>9,10</sup>) and the change in tensile strength is greater after irradiation in the dry state. The suggestion<sup>18</sup> that the shrinkage temperature is lowered by disruption of hydrogen bonds between peptide chains and by main-chain scission seems fully acceptable in the light of the collective experimental evidence. From measurements on tanned collagen<sup>34</sup> it is known that the shrinkage temperature is increased by the presence of newly introduced cross-links, e.g. in formaldehyde tanning. Cross-linking *prior* to irradiation also has an effect on the radiation sensitivity for changes in tensile strength both in collagen and in wool. Therefore it seems possible that the formation of cross-links *during* irradiation in the wet state could partly counteract a decrease of the shrinkage temperature and of the tensile strength after scission of peptide chains.

## D. Myosin

It is not our intention to report here the literature on histological and physiological changes in muscle after irradiation with ionizing radiations, nor the research that deals with food technology. Only

the work giving information on radiation damage at the molecular level will be dealt with. In this field, however, very few publications are available and little progress has been made. Hardly any attempt has been made to explain the observed physiological changes in irradiated muscle in terms of damage to component molecules. The great complexity of the muscle fibre compared to the collagen fibre and even the keratin fibre will certainly demand much more research in this field.

### (1) *Experimental Results*

In 1944 Lea *et al.*<sup>42</sup> irradiated dried myosin powder with 40 kV X-rays and tested the myosin for ATPase activity. The activity decreased exponentially with the dose. The dose necessary to reduce the activity to 37% of its initial value was  $5.5 \times 10^6$  r.

In 1957 Eidus, Kalamkarova and Otarova<sup>21</sup> reported the presence of a thermo-labile fraction in myosin irradiated in solution. The damage to the myosin was estimated from the remaining ATPase activity. If irradiated myosin is complexed with actin, part of the activity is restored. When the actin is separated from the irradiated myosin, no thermal after-effect can be found in the irradiated myosin. In 1958 Eidus *et al.*<sup>22</sup> reported that in de-aerated solutions of myosin the ATPase activity is unaffected by 50 kr ionizing radiation, but upon admission of oxygen inactivation to a level dependent on the radiation dose occurs. In 1959 Eidus and Ganassi<sup>23</sup> described experiments on the thermal inactivation of the heat-labile fraction in irradiated myosin solutions. The energy of activation of the after-effect reaction was lower than for the native protein and its independence of the dose was seen by the authors as an indication that the damage to all the thermo-labile molecules was the same. They concluded that after irradiation a number of molecules were transformed into some form of a "persistent excited state". With this assumption they attempted to explain the oxygen effect and the repair effect found after complexing irradiated myosin with actin.

In 1960 Eidus and Kayushin<sup>24</sup> reported the presence of long-living radicals in ground myosin powder after the myosin had been irradiated in solution. They attributed the observed ESR signals to radicals that were produced by the ionizing radiation and were

conserved in solution and during the subsequent drying and grinding.

Pinset-Harström and Fritsch<sup>54</sup> irradiated solutions of myosin-B (approximately equivalent to actomyosin) with doses of about 10, 20 and 40 kr of <sup>60</sup>Co gamma-radiation. After exposure to radiation the appearance of agglomerates could be observed. The sedimentation constant of the aggregates increased proportionally with radiation dose, indicating an increased molecular weight through polymerization. With ATP the sediment could be brought into solution again. The depolymerizing effect by ATP was thus unaffected. In a solution of D<sub>2</sub>O the polymerization was already marked with the lowest dose and almost complete with the medium dose. These effects were compared with those of thermal treatment of the protein in H<sub>2</sub>O and D<sub>2</sub>O at temperatures from 37 to 45°C and a marked parallel was found. Such a moderate rise in temperature could only be expected to lead to the breakage of weak bonds, in this instance hydrogen bonds. This seemed to indicate the rupture by radiation of a number of hydrogen bonds and agreed with the model of radiation damage of biological macromolecules of Platzman and Franck.<sup>58</sup> More recently, however, Pinset-Harström, Foissac and Coelho<sup>55</sup> reported that, although with sedimentation analysis after depolymerization with ATP, urea, or sodium pyrophosphate, the products of depolymerization of irradiated myosin-B solutions were not distinguishable from the products derived from intact myosin-B; light-scattering differences were found suggesting that some breakage of covalent bonds had occurred.

## (2) *Discussion*

The work by Eidus and associates<sup>21-24</sup> demonstrates in myosin the presence of partly damaged molecules after irradiation. These results are in agreement with those of Leone, Landmann and Fricke<sup>44</sup> who found in irradiated egg albumin several different heat-labile fractions that had partly retained their antigenic properties. Pinset-Harström and associates<sup>54, 55</sup> confirmed the presence of partly damaged molecules in irradiated myosin-B solutions and their analysis in terms of broken hydrogen bonds seems to lie more within the general framework of thinking in this field than the

hypothesis of a "persistent excited electronic state" as proposed by Eidus.<sup>22, 23</sup>

The results of experiments on the oxygen-effect and on the persistent radicals in irradiated myosin solutions cannot yet be fully evaluated. The presence of an oxygen-effect in the damaged protein fraction could indicate an increased reactivity of the damaged protein to oxygen as reported by Alexander and Hamilton.<sup>5</sup> A fruitful discussion of ESR experiments on myosin can not be attempted until more extensive qualitative and quantitative data become available. The possibility that radicals were introduced in the process of grinding the dried myosin film should not be overlooked, as indicated by the recent work of Ulbert<sup>73</sup> who reported that after filing keratin strong ESR signals are observed in keratin powder.

### III. GENERAL CONCLUSIONS

Protection against changes in some mechanical properties in wool and tendon can be obtained by cross-linking the parallel fibres. In wool the cross-linking was achieved with aromatic reagents, in tendon formaldehyde was used. In tendon, in the presence of water, cross-links are formed during exposure to ionizing radiation, resulting in a smaller impairment of tensile strength. There is no proof that the aromatic rings are the necessary condition to prevent damage to the wool fibres. The fact that the chains are cross-linked seems to be of more importance. This would give support to the explanation that, as the result of the action of ionizing radiation, disorder is introduced in ordered assemblies of fibrillar proteins. Certain properties that depend critically on order (a state of low entropy) will then show marked changes after the action of ionizing radiation. If by the introduction of cross-links (prior to or during irradiation) the disordering effect of ionizing radiation can be reduced, a certain degree of protection can be achieved. Available data indicate that the disorder is the result of the thermal disruption of a number of hydrogen bonds after covalent bonds have been broken. There seems to be no need to invoke the concept of energy transfer for explaining the observed effects.

If the primary reason for the disruption of the hydrogen bonds is the prior breakage of covalent bonds, a possible contribution of the Platzman and Franck mechanism of disruption of hydrogen bonds

would be masked. The present data would seem to indicate that the Platzman and Franck mechanism is not a preponderant process.

In tendon it was found that for certain changes in properties the contributions of the direct and of the indirect effect are not additive. This fact was explained by demonstrating the formation of cross-links during exposure to radiation in the presence of water. Such a mechanism could also exist in globular proteins when irradiated in solution or *in vivo*, and prevent the unfolding of the protein molecule after the interaction with the ionizing radiation. The radiation-induced changes might not be sufficient to inactivate the molecule. Where this occurs the direct effect in the dry state would be different from the direct effect in the wet state, a possibility that appears to have been overlooked by most authors.

The qualitative work on electron spin resonance spectroscopy of irradiated fibrous proteins has proved to be of great interest, especially when a dependence of the observed signal on the orientation of the specimen relative to the direction of the magnetic field could be demonstrated. The work of Gordy and his associates has shown that the interpretation of the observed radicals, e.g. in the case of irradiated silk, can be in agreement with the present information on protein structure.

The importance of quantitative microwave spectroscopy has been stressed by Zimmer.<sup>76, 77</sup> In order to explain the part played by radicals in the mechanism of radiation damage in protein, the need for reliable yield measurements and for the correlation of these yields with results of radio-chemical analysis is clearly indicated. However, sufficient data are still lacking at present. Until ESR work has moved from the descriptive stage into the analytical stage, conclusions should be accepted only with great caution.

The ESR data available on keratin, silk and collagen are mostly of a qualitative nature; in our opinion, therefore, definite conclusions concerning the nature of the radiation damage in fibrillar proteins, would be premature.

#### IV. ACKNOWLEDGEMENTS

The authors wish to thank Professor K. G. Zimmer for his suggestion to undertake this work and for critically reading the manuscript and Dr. R. L. Platzman for his helpful remarks.



Part of this chapter was completed while one of us (R.B.) was a guest in the Institut für Strahlenbiologie, Kernforschungszentrum, Karlsruhe. He is grateful for the hospitality and financial support received.

### References

1. Alexander, P., *Ann. N. Y. Acad. Sci.* **53**, 653 (1951).
2. Alexander, P., and Hudson, R. F., *Wool*, Reinhold, New York, 1954.
3. Alexander, P., and Charlesby, A., quoted in Z. M. Bacq and P. Alexander, Eds., *Fundamentals of Radiobiology*, 1st Ed., Butterworths, London, 1955, p. 135.
4. Alexander, P., Fox, M., Stacey, K. A., and Rosen, D., *Nature* **178**, 846 (1956).
5. Alexander, P., and Hamilton, L. D. G., *Radiation Res.* **15**, 193 (1961).
6. Allen, E., and Alexander, P., *Radiation Res.* **15**, 390 (1961).
7. Astbury, W. T., and Woods, H. J., *Phil. Trans. Roy. Soc. (London)*, Ser. **A 232**, 333 (1933).
8. Astbury, W. T., and Bell, F. O., *Tabulae Biologicae* **17**, 90 (1939).
9. Bailey, A. J., Bendall, J. R., and Rhodes, D. N., *Intern. J. Appl. Radiation Isotopes* **13**, 131 (1962).
10. Bailey, A. J., and Rhodes, D. N., *Proc. 2nd Intern. Congr. Radiation Res., 1962*, North-Holland Publishing Co., Amsterdam, 1963.
11. Bear, R. S., *Advan. Protein Chem.* **7**, 69 (1952).
12. Blumenfeld, L. A., and Kalmanson, A. E., *Biofizika* **3**, 87 (1958).
13. Bowes, J. H., Moss, J. A., and Raistrick, A. S., *Biochem. J.* **76**, 21, (1960).
14. Bowes, J. H., and Moss, J. A., *Radiation Res.* **16**, 211 (1962).
15. Braams, R., *Intern. J. Radiation Biol.* **4**, 27 (1961).
16. Braams, R., *Intern. J. Radiation Biol.* (in press).
17. Brown, A. E., and Beauregard, L. G., in *Sulphur in Proteins*, Academic Press, 1959, p. 59.
18. Cassel, J., *J. Am. Leather Chemists' Assoc.* **54**, 432 (1959).
19. Coleman, P., and Howitt, F. O., *Proc. Roy. Soc. (London)*, **A190**, 145 (1947).
20. Drake, M. P., Giffe, J. W., Johnson, D. A., and Koenig, V. L., *J. Am. Chem. Soc.* **79**, 1395 (1957).
21. Eidus, L. Kh., Kalamkarova, M. B., and Otarova, G. K., *Biofizika* **2**, 573 (1957).
22. Eidus, L. Kh., Kondakova, N. V., and Otarova, G. K., *Biofizika* **3**, 215 (1958).
23. Eidus, L. Kh. and Ganassi, E. E., *Biofizika* **4**, 215 (1959).
24. Eidus, L. Kh. and Kayushin, L. P., *Dokl. Akad. Nauk SSSR* **135**, 1525 (1960).
25. Elliot, A., and Malcolm, B. R., *Biochim. Biophys. Acta* **21**, 466 (1956).
26. Elöd, E., Nowotny H., and Zahn, H., *Kolloid-Z.*, **100**, 283 (1942).
27. Fricke, H., *J. Phys. Chem.* **56**, 789 (1952).
28. Fritze, E. R., Pfanmüller H., and Zahn, H., *Angew. Chem.* **69**, 302 (1957).

29. Gillespie, J. M., and Simmonds, D. H., *Biochim. Biophys. Acta* **39**, 538 (1960).
30. Gordy, W., Ard, W. B., and Shields, H., *Proc. Natl. Acad. Sci. U.S.* **41**, 983 (1955).
31. Gordy, W., and Shields, H., *Radiation Res.* **9**, 611 (1958).
32. Gordy, W. and Shields, H., *Proc. Natl. Acad. Sci. U.S.* **46**, 1124 (1960).
33. Gordy, W., and Shields, H., *Koninkl. Acad. Belg.* **33**, 191 (1961).
34. Gustavson, K. H., *The Chemistry and Reactivity of Collagen*, Academic Press, New York, 1956.
35. Harrington, W. F., and von Hippel, P. H., *Advan. Protein Chem.* **16**, 1 (1961).
36. Hildebrand, D., and Wurcz, H., *Melliand Textilber.* **41**, 1229 (1960).
37. Howitt, F. O., *Textile Res. J.* **25**, 242 (1955).
38. Jayko, M. E., and Garrison, W. M., *Nature* **181**, 413 (1958).
39. Kendrew, J. C., and Perutz, M. F., *Ann. Rev. Biochem.* **26**, 342 (1957).
40. Kirby, R. D., and Rutherford, H. A., *Textile Res. J.* **25**, 569 (1955).
41. Kuntz, E., and White, E., *Federation Proc.* **20**, 376 (1961).
42. Lea, D., Smith, K. M., Holmes B., and Markham, R., *Parasitology* **36**, 110 (1944).
43. Lea, D., *Actions of Radiations on Living Cells*, Cambridge University Press, Cambridge, 1946.
44. Leone, C. A., Landmann, W., and Fricke, H., *Progress in Nuclear Energy Series VI, Biological Sciences*, Vol. 2, Pergamon, 1959, p. 124.
45. Leveau, M., Varney-Cebe, N., and Parosot, A., *Proc. Intern. Wool Text. Res. Conf.*, 1955, Vol. D, 211 (1956).
46. Little, K., *Proc. Intern. Conf. Electron Microscopy*, 3rd, London, 1954, 165 (1956).
47. Marsh, R. E., Corey, R. B., and Pauling, L., *Biochim. Biophys. Acta* **16**, 1 (1955).
48. Mercer, E. H., *Keratin and Keratinization*, Pergamon Press, 1961.
49. Miyagawa, I., and Gordy, W., *J. Am. Chem. Soc.* **83**, 1036 (1961).
50. O'Connell, R. A., and Walden, M. K., *Textile Res. J.* **27**, 516 (1957).
51. Pauling, L., and Corey, R. B., *Proc. Natl. Acad. Sci. U.S.* **37**, 729 (1951).
52. Perron, R. R., and Wright, B. A., *Nature* **166**, 863 (1950).
53. Peters, L., and Woods, H. J., in *The Mechanical Properties of Textile Fibres*, R. Meredith, Ed., North-Holland Publishing Company, Amsterdam, 1956.
54. Pinset-Harström, I., and Fritsch, A., *Intern. J. Radiation Biol.* **4**, 343 (1962).
55. Pinset, I., Foissac, L., and Coelho, R., *Abstr. 2nd Intern. Congr. Radiation Res.*, 1962, North-Holland Publishing Co., Amsterdam, 1963.
56. Pohlit, H., Rajewski, B., and Redhardt, A., *Free Radicals in Biological Systems*, Academic Press, 1961, p. 367.
57. Pollard, E., in *Biophysical Science, A Study Program*, J. L. Oncley, Ed., Wiley, New York, 1959, p. 273.
58. Platzman, R. L., and Franck, J. A., *Symposium on Information Theory in Biology*, Pergamon Press, 1958.

59. Randall, J. T. (Ed.), *Nature and Structure of Collagen*, Butterworths, London, 1953.
60. Rajewski, B., Redhardt A., and Froese, G., *Z. Naturforsch.* **14b**, 740 (1959).
61. Rajewski, B., and Redhardt, A., *Nature* **193**, 365 (1962).
62. Rajewski, B., and Redhardt, A., *Nature* **195**, 492 (1962).
63. Rich, A., and Crick, F. H. C., in *Recent Advances in Gelatin and Glue Research*, G. Stainsby, Ed., Pergamon, London, 1958, pp. 20-24.
64. Rich, A., and Green, D. W., *Ann. Rev. Biochem.* **30**, 97 (1961).
65. Rogers, G. E., *Ann. N.Y. Acad. Sci.* **83**, 378 (1959); *Ann. N.Y. Acad. Sci.* **83**, 408 (1959).
66. Rogers, G. E., *J. Ultrastruct. Res.* **2**, 309 (1959).
67. Satlow, G., and Zahn, H., *Textil Praxis* **12**, 419 (1957).
68. Satlow, G., *Z. Ges. Textil-Ind.* **59**, 349 (1957).
69. Satlow, G., *Melliand Textilber.* **41**, 1525 (1960).
70. Schmitt, F. O., in *Biophysical Science, A Study Program*, J. L. Oncley, Ed., Wiley, New York, 1959, p. 349.
71. Stainsby, G., Ed., *Recent Advances in Gelatin and Glue Research*, Pergamon Press, London, 1958.
72. Teszler, O., and Rutherford, H. A., *Proc. 2nd Intern. Conf. Peaceful Uses Atomic Energy* **29**, 228 (1959).
73. Ulbert, K., *Nature* **195**, 175 (1962).
74. Zahn, H., Fritze, E. R., Pfanmüller H., and Satlow, G., *Proc. 2nd Intern. Conf. Peaceful Uses Atomic Energy* **29**, 233 (1959).
75. Zimmer, K. G., *Quantitative Radiation Biology*, Oliver & Boyd, Edinburgh, 1961.
76. Zimmer, K. G., Ehrenberg, L., and Ehrenberg, A., *Strahlentherapie* **103**, 3 (1957).
77. Zimmer, K. G., *Radiation Res. Suppl.* **1**, 519 (1959).

## 8

# ELECTRONIC CONDUCTION IN ORGANIC MOLECULAR SOLIDS

DAVID R. KEARNS,\* *Department of Biology and Research  
 Laboratory of Electronics,†  
 Massachusetts Institute of Technology,  
 Cambridge, Massachusetts*

## CONTENTS

I. Introduction . . . . .	284
II. Preliminary Theoretical Considerations . . . . .	285
A. Energetics of Charge Carrier Formation . . . . .	285
(1) Donor-Acceptor Theory . . . . .	286
(2) Singlet State Theory . . . . .	287
(3) Triplet State Theory . . . . .	287
(4) Combined Singlet-Triplet Theory . . . . .	287
B. Thermal Generation of Carriers . . . . .	288
C. Photogeneration of Carriers . . . . .	288
(1) Donor-Acceptor Theory . . . . .	288
(2) Singlet State Theory . . . . .	289
(3) Triplet State Theory . . . . .	289
III. Mobilities . . . . .	290
A. Experimental Results . . . . .	290
(1) Pulsed Photoconductivity . . . . .	290
(2) Space-Charge-Limited Currents . . . . .	292
(3) Diffusion Techniques . . . . .	293
B. Theoretical Calculations . . . . .	293
(1) Band Theory Calculations . . . . .	293
(2) Tunnelling Calculation . . . . .	295
(3) Evaluation of $V_{ns}$ . . . . .	295
C. Comparison of Experiment and Theory . . . . .	296
(1) Temperature Dependence . . . . .	296
(2) Anisotropy . . . . .	297
(3) Pressure Dependence . . . . .	297

\* NAS-NRC Postdoctoral Fellow, 1961-1962. Permanent address: Department of Chemistry, University of California, Riverside, California.

† The work of this laboratory is supported in part by the U.S. Army Signal Corps, the Air Force Office of Scientific Research, and the Office of Naval Research.

IV. Solid State Ionization Potentials and Electron Affinities . . . . .	298
A. Ionization Potentials . . . . .	298
B. Electron Affinities . . . . .	302
C. Energy of Charge Carrier Formation . . . . .	303
V. Dark Electrical Conductivity of Pure Aromatic Molecular Solids . . . . .	303
A. Temperature Dependence . . . . .	304
(1) Electrode Effects . . . . .	306
(2) Non-ohmic Behavior . . . . .	306
(3) Impurity Effects . . . . .	307
B. The Pre-exponential Factor in the Conductivity Expression . . . . .	308
VI. Photoconduction in Pure Aromatic Molecular Solids . . . . .	310
A. Sign of the Majority Carrier . . . . .	311
B. Spectral Dependence . . . . .	311
(1) Surface Cell . . . . .	311
(2) Sandwich Cells . . . . .	312
C. Non-ohmic Currents . . . . .	313
D. Temperature Dependence . . . . .	316
E. Intensity Dependence . . . . .	317
F. Impurity Effects . . . . .	318
G. Additional Measurements . . . . .	319
VII. Neutral Free Radicals . . . . .	319
VIII. Donor-Acceptor Complexes . . . . .	320
A. Homogeneous Complexes . . . . .	321
(1) Electrical Properties . . . . .	321
(a) Aromatic-Halogen Complexes . . . . .	321
(b) Aromatic Amine-Quinone Complexes . . . . .	321
(c) Salts . . . . .	323
(2) Magnetic Properties . . . . .	323
(3) Interpretation of Electrical and Magnetic Properties . . . . .	324
B. Lamellar Complexes . . . . .	326
(1) Electrical Properties . . . . .	327
(a) Liquid Electrode Cell. . . . .	327
(b) Condenser Cell . . . . .	327
(c) Surface Cells . . . . .	327
(2) Polarization Measurements . . . . .	329
(3) Electron Spin Resonance Measurements . . . . .	330
(4) Absorption Spectra. . . . .	331
IX. Summary Comparison of Experiment and Theory . . . . .	331
A. Singlet State Theory . . . . .	331
B. Triplet State Theory . . . . .	332
C. Combined Singlet-Triplet State Theory . . . . .	333
D. Donor-Acceptor Theory . . . . .	333
X. Acknowledgment . . . . .	335
References . . . . .	335

## I. INTRODUCTION

Interest in the electrical properties of organic aromatic solids has grown steadily since what might be called the rebirth of the organic semiconductor field in the 1950's. This has included studies of pure aromatic molecular solids, neutral free radicals, electron donor-acceptor complexes, ionic organic salts, synthetic polymers, wools, proteins and even mixtures of cell components extracted from biological systems. Virtually every organic solid, and some liquids, to which a pair of electrodes could be attached seems to have been studied at one time or another. In this article we shall limit our discussion to the first three types of systems because they have been the most thoroughly studied, because it appears that a somewhat unified interpretation can be given to their electrical properties, and finally because of the prejudices and interests of the author.

The early studies of the organic semiconductors can generally be classified as exploratory rather than definitive, but they were useful in determining what generalizations could be made about the electrical properties of the organic solids. These generalizations in turn have led to several different rudimentary theories of the photo- and semiconduction process in organic solids. Although certain of these theories or perhaps more correctly, hypotheses, have already been criticized as theoretically unsound,<sup>20, 22</sup> one of the purposes of our discussion of the electrical properties of organic solids will be to use the existing experimental results to provide tests of these theories.

Our overall purpose here will be several-fold. Very broadly we will be interested in discussing two aspects of the electrical properties of organic molecular solids, namely the mechanism and energetics of the formation of charge carriers, and the migration of carriers in an applied field after their formation.

First, we will present some of the current hypotheses of the mechanism and energetics of carrier formation. Some of the recent measurements and theoretical calculations of carrier mobilities will then be discussed. Because molecular and solid state ionization potentials and electron affinities appear as important parameters in some of the theoretical considerations, some of the recent measurements of these quantities will be presented. With this material as a background we will then discuss the electrical properties of pure

aromatic molecular solids, neutral free radicals and, finally, donor-acceptor complexes. The current interpretations of the results will be discussed and where possible these data will be used to test the various theories of charge carrier formation. When it is important to the interpretation of the electrical properties the results of other types of measurements, such as magnetic properties and optical absorption data, will also be presented. At the end we will summarize the present status of the theoretical interpretations of the electrical properties of organic molecular solids.

Several review articles,<sup>22,32</sup> one excellent collection of recent research papers,<sup>41</sup> and one bibliography,<sup>96</sup> have recently been published so that there will be little attempt to review work preceding 1960 or to discuss in detail experimental techniques. However, within the scope of the topics outlined above, an attempt has been made to point out the important developments which have been made in the last few years.

## II. PRELIMINARY THEORETICAL CONSIDERATIONS

We know from a variety of different measurements that the molecules in an aromatic molecular crystal interact only weakly. For example heats of vaporization are low, melting points are low, and the spectra of the crystals are in most cases quite similar to the spectra of the individual molecules in the gas phase.<sup>32</sup> Recent treatments of crystal spectra are in fact predicated on the assumption that intermolecular interaction is small.<sup>10</sup> We therefore justifiably expect to be able to discuss the properties of a molecular crystal in terms of the properties of the isolated molecule. Although this seems to have been quite generally realized there is a divergence of opinion as to specifically how the properties of the crystal are related to the isolated molecule properties. Since it is possible to determine the isolated molecule properties it is in principle possible to test the different theories.

### A. Energetics of Charge Carrier Formation

Three or, perhaps, four different proposals have been made regarding the relation between the energy required to form charge carriers in a molecular crystal and the isolated molecule properties.

(1) *Donor-Acceptor Theory*

The first theory, which might be called a donor-acceptor theory, stresses the donor-acceptor aspects of the charge carrier formation process and is essentially due to Lyons.<sup>59</sup> It is assumed that in order to have electronic conduction in an initially neutral aromatic molecular solid it is necessary to remove an electron from one molecule in the crystal and take the electron to a point in the crystal sufficiently far from the positive ion such that the Coulombic attraction will be small with respect to  $kT$ . Positive charge (holes) may then migrate through the solid by transfer of electrons from neutral neighbor molecules to the positive ion molecules; negative charge (electrons) may migrate simply by transfer of electrons from negative ions to neutral neighbor molecules. The net energy,  $E$ , required for the formation of charge carriers is

$$E = I_c - A_c$$

where  $I_c$  is the ionization potential of the crystal and  $A_c$  is the electron affinity of the crystal. From essentially classical considerations the crystal ionization potential should be related to the gaseous ionization potential,  $I_g$ , of the molecule which is to be ionized (the electron donor) as follows

$$I_c = I_g - P_+$$

where  $P_+$  is the polarization energy which arises from the fact that a unit positive charge in the crystal will polarize the molecules around it. Similarly the crystal electron affinity is related to the gaseous electron affinity,  $A_g$ , of the molecule which is to accept an electron (acceptor):

$$A_c = A_g - P_-$$

where now  $P_-$  is the polarization energy associated with the presence of a negative charge in a polarizable crystal. Lyons assumed that  $P_+ = P_- = P$  since to a good first approximation the polarization energy depends only on the magnitude of the charge and not the sign. Thus, for a pure molecular crystal, the minimum energy required to form charge carriers is

$$E = I_g - A_g - 2P$$

By assigning an average polarizability to each molecule and summing over the crystal, Lyons was able to obtain a theoretical



estimate for  $P$ , and in this way reduced the problem to the evaluation of isolated molecule properties. As will be seen in Section IV, the Lyons<sup>59</sup> predictions have been reasonably well verified.

### (2) *Singlet State Theory*

It has been suggested<sup>14</sup> that the energy required to form charge carriers should be identified with the energy of the lowest excited singlet state of the isolated molecule,  ${}^1E_1$ . This conclusion appears to be based on the assumption that an electron promoted to the lowest unfilled orbital of one neutral molecule in the crystal will have sufficient energy to tunnel through the intermolecular barrier to the corresponding vacant orbitals of neighbors, thus creating positive and negative ions. This picture naturally led to the prediction that neutral free radicals would be good conductors since the highest filled orbital in the ground state is only partially filled and therefore transfer of electrons from one molecule to the next could be accomplished with essentially no expenditure of energy. Experiments on this point will be discussed in Section VII. These initial considerations were later modified<sup>16</sup> to say that the energy required to overcome the Coulombic attraction energy in the charge separation process (which has been initially neglected) is compensated for by the polarization energy associated with the creation of the two ions. Thus, the equation of  $E$  with  ${}^1E_1$  was reduced to an assumed cancellation of Coulomb energy by polarization energy.

### (3) *Triplet State Theory*

Several authors<sup>87,97</sup> have proposed that the lowest excited triplet state of a molecule is an intermediate in the formation of charge carriers and that the activation energy for this process will be the triplet state energy,  ${}^3E_1$ . Why the triplet state should necessarily be involved as an intermediate is not clear, but as a postulate it is subject to testing.

### (4) *Combined Singlet-Triplet Theory*

This theory, which is to some degree a combination of the singlet and the triplet state theories, suggests that formation of charge carriers takes place via the formation of either excited singlet or

triplet states, which are then ionized by the applied electric field.<sup>75</sup> Singlet states are presumed to be more susceptible to field ionization than are triplet states and therefore the effective activation energy for formation of charge carriers will depend upon the relative population of singlet and triplet states.

### B. Thermal Generation of Carriers

If the concentrations of positive carriers (holes) and negative carriers (electrons) are assumed to be in equilibrium with respect to recombination, the conductivity,  $\sigma$ , of a molecular solid should vary with temperature according to the formula

$$\sigma = \sigma_0 \exp(-E/2kT)$$

where  $E$  is the energy required to form the charge carriers. If carrier mobilities are only slightly temperature dependent  $\log \sigma$  should vary linearly with  $1/T$  with a slope of  $-E/2k$ . Theoretically there is little that can be said about the detailed mechanism of the thermal ionization process. According to the donor-acceptor theory it presumably involves the formation of nearest-neighbor ion pairs, which are subsequently dissociated into next nearest-neighbor ion pairs and so forth until complete charge separation takes place, with the concentration of free carriers varying with temperature as indicated above. According to the singlet or triplet state theories charge carrier formation first involves thermal generation of either the excited singlet or triplet state, followed by their dissociation into carriers under the influence of the applied field or local internal fields.

### C. Photogeneration of Carriers

#### (1) *Donor-Acceptor Theory*

Lyons<sup>59</sup> has calculated the transition probability for the optical generation of nearest-neighbor ion pairs. He predicts an oscillator strength of  $f \simeq 10^{-5} - 10^{-6}$  for the process, and concludes that this transition is essentially forbidden. On this basis it was concluded that it probably would not be possible to observe absorption in crystals due to such transitions. The probability for photogeneration of widely separated positive and negative ions would be con-

siderably smaller since it would involve overlap between non-adjacent molecules. As Lyons has pointed out, however, light which is absorbed in a transition to a neutral, non-conducting singlet state could lead to ion pair formation (*a*) directly, because the neutral state has a small probability of being ionized, or (*b*) indirectly, if a radiationless transition occurs to an ionized state of lower energy. The complete dissociation of the ion pair must occur in order to have conductivity. It is likely that this will require a certain amount of thermal excitation and therefore the quantum yield for the production of carriers might be temperature dependent for this reason. The energy required for dissociation of a nearest-neighbor ion pair was calculated by Lyons to be in the range of 0 to about 1 eV for anthracene and naphthalene. If the direct optical generation of carriers is highly forbidden as the Lyons' calculations suggest, then the indirect process will dominate and the threshold for photoconduction will not coincide with the minimum energy required for the formation of charge carriers.

### (2) *Singlet State Theory*

According to this theory the energy of the first excited singlet state is to be identified with the energy of the conducting state. Therefore the threshold for photoconduction (also the threshold for absorption by the crystal) will give the true energy of carrier formation.<sup>15</sup> If it were postulated that the actual ionization of a molecule in its excited singlet state required a small thermal excitation as well, then the activation energy for the semiconduction would be correspondingly higher than the energy of the lowest excited singlet state.

### (3) *Triplet State Theory*

In this theory the triplet state is postulated to be a necessary intermediate in the photogeneration of charge carriers.<sup>87</sup> Since singlet-triplet transitions are very weak, a higher triplet state population can in general be achieved by excitation to a singlet state, which will be followed by a radiationless transition to the lower lying triplet state. Consequently, it is expected that the threshold for photoconduction will correspond to the threshold for absorption of light by the sample. In order to account for the

observed temperature dependence of the photoconductivity in most organic systems, Rosenberg<sup>87</sup> assumed that the quantum yield for the production of the triplet state by excitation of a molecule to its lowest excited singlet state is temperature dependent for the following reason. He assumed that the triplet state potential curve crosses the excited singlet state potential curve somewhere within one, two or three vibrational levels of the lowest vibrational state of the lowest *excited* singlet state. Under steady state conditions the population of these vibrationally excited states would depend exponentially upon the temperature. If intersystem crossing to the triplet state depends upon the crossing of the singlet and triplet state potential curves, then according to this suggestion the quantum yield for the production of triplet states would vary exponentially with temperature. This prediction is of course subject to testing.

Before considering the experimental data on the semi- and photoconductivity of organic molecular solids to test these various theories, we wish to make a brief departure to discuss some of the theoretical and experimental aspects of carrier mobilities and also to present some discussion of measurements of solid state ionization potentials and electron affinities.

### III. MOBILITIES

From a fundamental standpoint, some of the most important advances in the study of the electrical properties of organic molecular solids have been in the experimental determination of carrier mobilities,  $\mu$ , and the development of a theory of carrier mobilities.

#### A. Experimental Results

Several different experimental techniques have been used to measure mobilities and when applied to the same system they give results which are in reasonable agreement.

##### (1) *Pulsed Photoconductivity*

The pulsed photoconductivity technique is probably the most elegant of those which have been used. In this technique, the

sample is sandwiched between, but insulated from, two semi-transparent electrodes (see condenser cell in Fig. 1). With a voltage applied across them, one of the electrodes is illuminated with a high intensity, short duration pulse of light which is strongly absorbed by the sample. This creates, virtually instantaneously, a high concentration of charge carriers of both signs at one surface. Due to the potential across the sample the carriers of one sign will be pulled

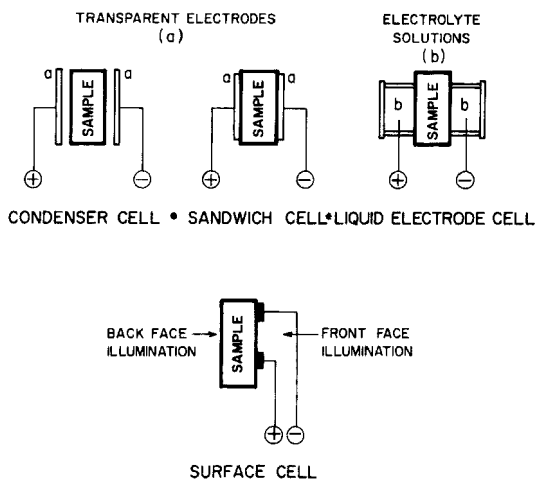


Fig. 1. Schematic cross-sectional views of the various sample cells used for studying the electrical properties of organic molecular solids.

through the crystal (e.g. holes if the positive electrode is illuminated and electrons if the negative electrode is illuminated) and a current will flow in the external circuit until the drifting carriers reach the other side of the crystal. With this arrangement the time required for carriers to traverse a crystal of known thickness with a known applied voltage can be measured. Kepler<sup>50</sup> has used this technique to measure the electron and hole mobilities in anthracene crystals, their anisotropies in different crystal directions, temperature dependences and pressure dependences. Some of these results are shown in Table I. Subsequently, LeBlanc<sup>57</sup> also measured carrier mobilities in anthracene and his results are also given in Table I.

TABLE I. Electron and Hole Mobilities in Organic Solids

Material	Electron mobility, cm <sup>2</sup> /V-sec	Hole mobility, cm <sup>2</sup> /V-sec	Measuring technique	Ref.
Anthracene, crystal	2.0 ( <i>a-b</i> plane)	1.3 ( <i>a-b</i> plane)	Pulsed photo-conductivity	50
	0.3 ( $\perp$ to <i>a-b</i> plane)	0.4 ( $\perp$ to <i>a-b</i> plane)	Pulsed photo-conductivity	50
	0.6 ( $\perp$ to <i>a-b</i> plane)	1.0 ( $\perp$ to <i>a-b</i> plane)	Pulsed photo-conductivity	57
<i>p</i> -Terphenyl, crystal	—	0.03	Space-charge-limited current	66
Metal-free phthalocyanine, amorphous film	—	$4 \times 10^{-3}$	Diffusion	47

(2) *Space-Charge-Limited Currents*

The amount of charge which a crystal can accommodate depends upon the dielectric constant of the material and the voltage applied across the sample. If an electrode can be found which can supply an unlimited number of carriers for injection into the crystal (i.e. form an ohmic contact) then the current flow through the crystal will be limited by the total amount of charge which can be accommodated in the crystal. That is, the current will be space-charge-limited, and under these conditions the current-voltage relation is

$$i = (9/8)\mu\xi V^2/d^3$$

where  $\xi$  is the dielectric constant,  $d$  is the thickness of the crystal and  $V$  is the applied voltage. Under ideal conditions one can obtain from the slope of a current,  $i$ , vs.  $V^2$  plot the mobility of the injected carriers. In practice, the presence of carrier traps complicates the analysis, but it is still possible to derive mobility values from the measurements. Mark and Helfrich<sup>66</sup> have shown that a saturated solution of iodine in 1.0 M NaI forms an ohmic contact with anthracene, *p*-terphenyl and *p*-quatraphenyl. The results of their determinations of hole mobilities for *p*-terphenyl are also given in Table I.

### (3) *Diffusion Techniques*

For order-of-magnitude determinations of mobility, the following technique has been used.<sup>47</sup> Electrodes were placed on one face of a surface cell (see Fig. 1) and the back face was illuminated with a pulse of strongly absorbed light. It has been shown that when the sample is thick enough, the carriers created by illumination of the back face must diffuse to the front surface before the conductivity of the cell is effected. By measuring the delay between the photo-generation of carriers and their time of arrival in a region where they increase the conductivity, the diffusion coefficient,  $D$ , can be determined. Through the use of the Einstein diffusivity-mobility relation  $\mu = De/kT$  the mobility of the majority carrier can be determined. Some disadvantages of the method are that as it was initially used the analysis involved the assumption that the concentration was small enough that Coulombic interaction could be neglected and, secondly, only the effective mobility of both carriers is determined. The measurements were carried out on amorphous films of phthalocyanine and led to a mobility of  $4 \times 10^{-3} \text{ cm}^2/\text{V-sec}$ . In view of the fact that electrons generally appear to be trapped much more effectively than holes, the above mobility is that of the holes. In retrospect, this is quite a reasonable value for hole mobilities in an amorphous film and suggests that the method may be of further utility.

## B. Theoretical Calculations

### (1) *Band Theory Calculations*

LeBlanc<sup>58</sup> has used the tight binding approximation to calculate the one-electron band structure appropriate to excess electrons or holes in an otherwise neutral anthracene crystal. In this calculation one-electron wave functions  $\Psi_{\mathbf{k}}(\mathbf{r})$  with the proper crystal symmetry were constructed from linear combinations of one-electron molecular functions,  $\phi_n$ ,

$$\Psi_{\mathbf{k}}(\mathbf{r}) = \sum_{n=1}^N \exp(i\mathbf{k} \cdot \mathbf{r}) \phi_n(\mathbf{r} - \mathbf{r}_n)$$

where  $\mathbf{r}_n$  locates the center of molecule  $n$  and the sum is over the  $N$  molecules in the crystal. The one-electron wave function,  $\phi_n$ , for hole conduction corresponds to the highest energy bonding orbital

of a neutral anthracene molecule, while for electron conduction  $\phi_n$  corresponds to the lowest anti-bonding anthracene molecular orbital. The  $\phi_n$  are assumed to be oriented in the crystal in the same way as molecule  $n$ , but other than that  $\phi_n$  is the same for all  $n$ .

The velocity  $v(\mathbf{k})$  associated with the function  $\Psi_{\mathbf{k}}(\mathbf{r})$  is given by

$$v(\mathbf{k}) = (1/\hbar) [\partial E(\mathbf{k})/\partial \mathbf{k}]$$

where 
$$[\partial E(\mathbf{k})/\partial \mathbf{k}] = -2 \sum'_s \mathbf{r}_s V_{ns} \sin(\mathbf{k} \cdot \mathbf{r})$$

$$V_{ns} = \langle \phi_{n+s} | V_s | \phi_n \rangle$$

where  $V_s$  expresses the potential energy of an electron in the field of a molecule at the position  $(n+s)$ , which is positively charged in the case of hole conduction, but neutral in the case of electron conduction. For the case of constant free time,  $\tau_0$ , the components of the mobility tensor,  $\mu_{ij}$ , are

$$\mu_{ij} = e\tau_0 \langle v_i v_j \rangle / kT$$

or for a constant free path,  $\lambda$ ,

$$\mu_{ij} = e\lambda \langle v_i v_j / |v(\mathbf{k})| \rangle / kT$$

where the brackets denote averages over  $\mathbf{k}$ .

In his treatment LeBlanc<sup>58</sup> used a sum of Goppert-Mayer and Sklar neutral carbon atom Hartree potentials to express  $V_s$ . The results of his calculations are given in Table II for the case of constant free time. The relative anisotropies found for constant free

TABLE II. Calculated Relative<sup>a</sup> Electron and Hole Mobilities in Anthracene

	Crystal direction		
	<i>a</i> -axis	<i>b</i> -axis	⊥ to <i>a</i> - <i>b</i> plane
Electron mobility	2.1	1.9	(0.008)
Hole mobility	1.0	1.9	0.25

<sup>a</sup> Taken from LeBlanc's<sup>58</sup> results; assuming constant free time and normalizing to the value of 1 for the hole mobility in *a*-direction.



path were virtually identical and in good agreement with the measured values. Using Kepler's<sup>50</sup> values for the mobilities with his calculations LeBlanc found  $\tau_0 = 10^{-12}$  sec or  $\lambda \simeq 30$  Å. With his measurements<sup>57</sup> he found  $\tau_0 = 2 \times 10^{-12}$  or  $\lambda \simeq 80$  Å. These results indicate that on the average the carriers travel several lattice distances before being scattered, and are therefore consistent with the band structure description of conduction.

These calculations have recently been extended<sup>98</sup> to naphthalene, tetracene and pentacene, and if scattering parameters remain about as they are in anthracene, the carrier mobilities in these other systems are expected to be comparable to those found in anthracene.

### (2) *Tunnelling Calculation*

In this calculation,<sup>44</sup> the time,  $\tau$ , required for a hole or an electron, initially localized on one molecule, to tunnel to an adjacent, identical molecule is evaluated using the equation

$$1/\tau = (4/h) V_{ns}$$

where  $V_{ns}$  is the same quantity which appeared in the band theory calculations. The tunnelling calculations were first carried out for a pair of molecules oriented as they would be along some particular direction in the crystal. Then it was assumed that transfer rates calculated on the basis of the dimer model could be used to calculate the rate at which carriers would diffuse through a crystal assuming that there is scattering after each transfer. This allowed the diffusivity to be calculated; using the Einstein diffusivity-mobility relation the mobility could be calculated. The mobilities predicted by this method were all about a factor of five lower than those measured.

### (3) *Evaluation of $V_{ns}$*

Although the tunnelling model is in a sense internally inconsistent (a dimer calculation is carried out and then results are used to discuss electron transfer involving many molecules) the method which was used to evaluate the  $V_{ns}$  which appears in both the band calculations and the tunnelling model calculations leads to an interesting simplification. As in the band calculations the

intermolecular interaction was expressed as a sum of potentials due to carbon atoms that are formally neutral in the case of electron conduction, or bear a small positive charge in the case of hole conduction. It was then assumed that the potential due to a neutral carbon atom is given by a Fermi-Thomas potential. This potential can be expressed as  $Z(r)/r$ , where  $r$  is the distance from the carbon nucleus and  $Z(r)$  is some effective nuclear charge such that at the position  $r$ ,  $Z(r)/r$  is the same as that given by the Fermi-Thomas calculation. Since the quantity  $\langle \phi_{n+s} | V_s | \phi_n \rangle$  will be large only in the region where  $\phi_{n+s}$  and  $\phi_n$  overlap strongly, we may set  $Z(r)$  equal to the value it would have at the position of maximum overlap. If the molecular orbitals are taken to be Hückel molecular orbitals expressed as sums of Slater atomic orbitals, the interaction integral reduces to a sum of integrals involving atomic orbitals. These can be evaluated using integral tables. By direct comparison of the interaction integral  $V_{ns}$  with the overlap integral  $S_{ns}$  between two molecular wave functions it is found that  $V_{ns} = 0.35S_{ns}$  a.u. for the range of internuclear distances of interest to us. Murrell<sup>73</sup> has recently calculated molecular overlap integrals for various crystallographic directions in anthracene and does indeed find that the anisotropy is essentially the same as that found by LeBlanc<sup>58</sup> for the interaction integrals.

## C. Comparison of Experiment and Theory

### (1) *Temperature Dependence*

Contrary to expectations based on the observation that photocurrents increased with temperature, the Kepler<sup>50</sup> and LeBlanc<sup>57</sup> measurements demonstrated that the trap-free mobility of both electrons and holes decreased as the temperature increased. If the scattering of carriers is assumed to be temperature independent, then theory predicts that the mobility of both the electrons should vary as  $1/T$ . Although this accounts for most of the observed temperature variation of the mobilities, it is clear that there are marked deviations from  $1/T$  relation and that scattering of carriers is temperature dependent. The situation seems ripe for some theoretical investigations of the scattering of carriers in molecular crystals since the experimental data are nearly at hand.

## (2) *Anisotropy*

An important aspect of the theoretical predictions is that they give quite a good account of the measured anisotropy of the electron and hole mobilities. The lower mobilities in anthracene along the  $C'$  axis can be very simply interpreted in terms of the small overlap between molecules which are oriented virtually end to end.

## (3) *Pressure Dependence*

From the variation of the intermolecular interaction energy or overlap integral with the intermolecular distance it should in principle be possible to predict the pressure dependence of the mobilities. It was found experimentally that pressure did in fact produce a significant increase in the mobilities of holes in the  $C'$  direction (perpendicular to the cleavage plane) but not in the electron mobility. For electron migration in this particular direction integral involves the difference between two large two-center atomic integrals of about the same magnitude. This cancellation is expected to remain fairly good over a moderate range of intermolecular distance and this may be the reason why the electron mobility in this direction is so pressure insensitive.

The mobility measurements have demonstrated several things:

(a) Mobilities in single crystals are actually rather large (order of unity).

(b) Electron and hole mobilities are comparable in magnitude.

(c) The trap-free mobilities vary approximately inversely with temperature.

(d) Mobilities may be highly anisotropic.

We conclude that as far as they have been carried, the theoretical calculations seem to be in reasonable agreement with the experimental measurements. Because of the similarity in the crystal structure of aromatic molecular crystals and the small range in heats of sublimation, it is clear that intermolecular interaction will not vary significantly from crystal to crystal.\* Consequently, with the exception of special crystallographic directions where there is

\* When the heats of sublimation are normalized to a per  $\pi$  electron basis they are identical.

cancellation similar to that found in anthracene, the trap-free mobilities of both electrons and holes are expected to be close to unity. These deductions are supported by the calculations on naphthalene, naphthacene, and pentacene.<sup>98</sup>

#### IV. SOLID STATE IONIZATION POTENTIALS AND ELECTRON AFFINITIES

Two quantities of particular interest in the discussion of the electrical properties of organic solids are the solid state ionization potential and electron affinity. Although the external photoelectric<sup>79, 81</sup> effect had been observed with an organic solid at the turn of the century, and was used thirty years ago to determine the threshold energy for ionization of several dyes,<sup>27</sup> it was only in the last two years that these measurements were again used to determine the ionization potentials of organic molecular solids.<sup>48, 63</sup>

##### A. Ionization Potentials

In the photoelectric effect measurements, a low intensity beam of monochromatic light is allowed to strike the surface of a sample and any electrons which are ejected are collected on a grid maintained at a small positive potential with respect to the sample. The current which flows in the external circuit as a result of the electron emission is measured and from the spectral dependence of the emission of electrons the threshold for photo-ionization has to be determined. Both Lyons and Morris,<sup>63</sup> and Kearns and Calvin<sup>48</sup> found significant long wavelength tails on the photoelectric emission curves which somewhat complicated the determination of the threshold ionization potential. Lyons and Morris<sup>63</sup> simply chose to call the threshold the wavelength at which the quantum yield for the emission of electrons fell to about  $10^{-6}$  of the maximum yield. Their results are shown in Table III. Kearns and Calvin<sup>48</sup> have determined thresholds in a different manner. The following possible interpretations of the tail were considered by these authors:

(a) The tail is due to the ionization of thermally excited molecules. This was ruled out since such an effect would lead to a much smaller tail than that observed.

(b) The sample may contain impurities which have ionization

TABLE III. Solid State Ionization Potentials of Aromatic Molecular Solids

Molecule	$I_{\text{gas}}$	$I_{\text{surface}}$	Form: x = crystal, F = film	$P = (I_g - I_s)$	$P_{\text{calc}}^{62}$	$P_{\text{solid}} = \frac{1}{0.7}(I_g - I_s)$	Ref.
Naphthalene	8.12 <sup>a</sup>	6.76	x	1.36	1.28	1.9	64
Anthracene	7.38 <sup>b</sup>	5.65	x	1.73	1.74	2.4	64
Naphthacene	6.88 <sup>b</sup>	5.26	x	1.62	1.58	2.3	64
	6.63 <sup>c</sup>	5.38	F	1.26		1.8	48
Phenanthrene	8.0 <sup>d</sup>	6.45	x	1.55		2.2	64
Pyrene		5.81	x				64
Chrysene		5.73	x				64
1,2:5,6-Dibenzanthracene		5.69	x				64
1,2-Benazanthracene		5.68	x				64
Perylene	6.82 <sup>c</sup>	5.39	F	1.43		2.0	48
Pentacene	6.23 <sup>c</sup>	5.08	F	1.15		1.6	48
Decacycene	6.76 <sup>c</sup>	5.40	F	1.36		1.9	48
Violanthrene	6.40 <sup>e</sup>	5.20	F	1.20		1.7	48
Metal-free phthalocyanine		5.15	F				48
		6.0					101
Ni phthalocyanine		4.95	F				48
Fe <sup>3+</sup>		4.95	F				48
Zn		6.0					101
Etioporphyrin		5.29	F				48

<sup>a</sup> Watanabe, K., *Preliminary Table of Ionization Potentials*, University of Hawaii, 1957.<sup>b</sup> Ref. 101.<sup>c</sup> Ref. 23.<sup>d</sup> Wacks, M. E. and Dibeler, V. H., *J. Chem. Phys.*, **31**, 1557 (1959).

potentials lower than that of the host material. From their data there is no way of estimating the importance of this effect.

(c) There will be a variety of molecular sites for the surface molecules in a sublimed film and this will give rise to a distribution of ionization potentials. Figure 2 is a schematic representation of a cross-sectional view of an amorphous film. The type A molecules are surrounded on three sides by other polarizable molecules and as indicated in the diagram this is expected to be the most probable environment. Type B molecules are almost completely surrounded by other molecules and hence have ionization potentials very nearly

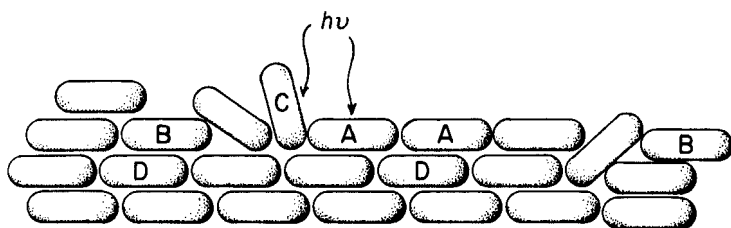


Fig. 2. Schematic side-view representation of an amorphous film of an organic solid.

that of molecules located in the bulk of the layer (type D molecules). Type C molecules on the other hand will have ionization potentials very nearly equal to that of a molecule in the gas phase. It was assumed,<sup>48</sup> therefore, that the number of molecules,  $N(I)$ , which have ionization potentials,  $I$ , which differ from the most probable surface value,  $I_{\text{surface}}$ , by an amount  $\Delta I = (I_{\text{surface}} - I)$  is given by the distribution function

$$N(I) \propto \exp(-h\Delta I^2)$$

where  $h$  is a constant which determines the distribution of ionization potentials about the most probable value. The more uniform the surface the larger the value of  $h$ . With the proper choice of  $h$ , it was possible to fit the observed photoelectric curves for all of the compounds and determine the most probable surface state ionization potential. An interesting aspect of this analysis was that of the ten compounds studied, eight yielded the same value for  $h$ , 30. These results are also presented in Table III.

The interpretation of the ionization tail in terms of a distribution of environments is supported by a comparison of the Lyons and Morris<sup>63</sup> results with those of Kearns and Calvin.<sup>48</sup> As would be predicted according to this interpretation the measurements on single crystals produced photoelectric current curves which had a much more well-defined threshold than did the curves obtained by Kearns and Calvin<sup>48</sup> using sublimed films. While these results are consistent with the interpretation, they cannot be regarded as a proof of it. Tetracene is the only molecule which was studied by both groups, and there seems to be reasonable agreement on the value of the surface ionization potential. Lyons and Morris give 5.26 eV, whereas Kearns and Calvin give 5.38 eV.

If the above interpretation of the tail is in fact correct it raises the question as to what energy is required to ionize a molecule which is located within the crystal. Clearly the polarization energy associated with the ionization of a molecule located on the surface of the sample will be less than the polarization energy associated with a molecule in the bulk of the sample, but by how much? If we assume that the polarization energy associated with the ionization of surface molecule is about 0.7 of that associated with the ionization of a bulk molecule then the following values are obtained for the "true" solid state ionization potential (see Table III).

Vilessov<sup>101, 102</sup> has also measured thresholds for the external photoelectric effect in organic solids. The phthalocyanines offer the only case where his results can be compared with those of others. He obtained a value of 6.0 eV for both metal-free and metal phthalocyanine, whereas Kearns and Calvin obtained a value of 5.15. In view of the fact that the gaseous ionization potential of pentacene (a molecule which is a poorer electron donor than phthalocyanine) is only 6.23 eV, a solid state ionization potential of 6.0 eV is unreasonable for a molecule like phthalocyanine. Perhaps the discrepancy lies in the method which Vilessov used to determine thresholds, or perhaps it was just a matter of sensitivity.

According to the discussion of Section II the difference between the gaseous and solid state ionization potential is the polarization energy,  $P$ , and these values determined from surface ionization potentials are given in Table III. In certain cases where the gaseous ionization potentials are unknown they were calculated using a formula proposed by Hedges and Matsen.<sup>23</sup> In an early paper

Lyons<sup>59</sup> calculated  $P$  for naphthalene and anthracene using the formula  $P = \alpha e^2 / 2R^4$  with a value of  $15 \text{ \AA}^3$  for  $\alpha$ . He summed over the nearest 18 neighbors and obtained values of  $-0.18 \pm 0.3$  and  $-1.0 \pm 0.3$  for naphthalene and anthracene respectively. In very recent work he<sup>62</sup> has included the interaction of the induced dipoles and obtains the values of  $P$  shown in column 6 of Table III. The agreement between the calculated and measured values of  $P$  is indeed encouraging.

### B. Electron Affinities

We have very little direct information about the values of the solid state electron affinities. In some cases it is possible to infer the values and in other cases they can be calculated. The following experiment provides some information on the electron affinity of solid *ortho*-chloranil. Kearns and Calvin<sup>48</sup> found that the threshold for ionization of a film of pure *ortho*-chloranil was somewhat greater than 5.5 eV. However, when this material was supported on a layer of some strong electron donor such as metal-free phthalocyanine, violanthrene or phenothiazine it was possible to observe photoemission of electrons with quanta as low as 4.8 eV, although the most probable value for the threshold (found assuming a distribution of sites as in the measurements on the pure films) was  $5.33 \text{ eV} \pm 0.05 \text{ eV}$  in every case. The interpretation of this result is that the large aromatic molecules are able to inject electrons into the *ortho*-chloranil and that the observed photoelectron currents are actually due to the ionization of *ortho*-chloranil *negative ions*. If this is correct, then these measurements give the solid state electron affinity of the *ortho*-chloranil.

The polarization energy should be the same for either a positive or a negative charge in a crystal and therefore a polarization energy derived from solid state ionization potential measurements can be used with gaseous values of electron affinities to calculate solid state electron affinities. In the Table IV the solid state electron affinities calculated in this manner by Lyons<sup>62</sup> are presented. We have also included in this table the value for *ortho*-chloranil and for I atoms in an  $\text{I}_2$  crystal calculated using the Lyons estimate for the polarization energy of a unit charge in an  $\text{I}_2$  crystal along with the gaseous electron affinity of I atoms.



TABLE IV. Solid State Electron Affinities,  $A_e$ 

Material	$A_e$	Ref.
Naphthalene	2.1 eV	62
Anthracene	3.1	62
Tetracene	3.3	62
Phenanthrene	2.23	62
<i>ortho</i> -Chloranil	5.3	48
I (in I <sub>2</sub> )	6.0	62, 38

### C. Energy of Charge Carrier Formation

The solid state electron affinity and ionization potentials may be used to predict the energy,  $E$ , required to form charge carriers in a pure crystal, and these values are presented below.

Compound	$E$
Naphthalene	4.65 eV
Anthracene	2.55
Phenanthrene	4.2
Tetracene	1.95

If we accept the Kearns-Calvin interpretation of the photoelectric measurements the above  $E$  values should be somewhat reduced.

## V. DARK ELECTRICAL CONDUCTIVITY OF PURE AROMATIC MOLECULAR SOLIDS

It has been fashionable to classify pure organic aromatic molecular solids as semiconductors, and inasmuch as their electrical conductivity is generally intermediate between that of an insulator and of a metal, this is perhaps legitimate. It has also been fashionable to adopt the inorganic semiconductor terminology and formulae to describe the electrical properties of the organics. Although there are similarities between the behavior of the

organic and the inorganic materials, the great differences between the binding energies in a molecular crystal and those in inorganic semiconductors like silicon and germanium suggest that such adoption of terms should be done with great caution. Therefore, we shall avoid using terms which have specific connotations in the theory of inorganic semiconductors, but which may not be applicable to a discussion of electronic conduction in organic molecular solids.

### A. Temperature Dependence

It is found that the specific conductivity,  $\sigma$ , of virtually all organic aromatic molecular solids when properly purified increases with temperature in the following manner

$$\sigma = \sigma_0 \exp(-E/2kT) = \sigma_0 \exp(-E'/kT)$$

where  $E = 2E'$ , a convention which we shall adopt throughout. In Table V, a compilation of  $E$  values derived from measurements of the temperature dependence of the conductivity are given for a variety of molecules. Although it is found that the measured value of the specific conductivity depends to some degree upon the form of the material and the nature of the sample cell (i.e. film or single crystal, surface cell or sandwich cell) the  $E$  values derived from these measurements are virtually the same when carried out by the same investigator.<sup>34</sup> There is not always agreement between different workers on the  $E$  value for a particular compound.

The interpretation of the significance of these  $E$  values, which range from 3 eV down to 0.2 eV, has concerned a number of workers. Logically the first step would be to establish the nature of the carriers, i.e. whether the current carriers are ions or electrons and holes. In general the dark currents are found to be stationary with time and this would tend to support the notion that the conductivity is electronic. The measurement of the temperature dependence of carrier mobilities in anthracene crystals<sup>50,57</sup> certainly proves that in this specific case the conductivity is electronic. If the conductivity were ionic the mobility would have increased with temperature instead of decreasing as observed. The agreement between the calculated and observed anisotropies adds further support to the interpretation that the conductivity is electronic.<sup>58</sup>

TABLE V. Electrical Properties of Some Aromatic Organic Molecular Solids

Compound	$E$ , eV	First excited single state energy, $^1E_1$ , eV	Triplet state energy, $^3E_1$ , eV	$\rho_0$ , $\Omega$ -cm	$\nu$ , $\text{cm}^2/\text{V-sec}$	Form: x = crystal F = film p = powder	Ref.
Naphthalene	2.25	4.0	2.64				103
	3.7			$10^{-13}$	$10^{11}$	x	80
	1.4					x	85
Anthracene	1.94	3.30	1.88				103
	1.93			50		F	75
	1.50					x	85
	2.7			$10^{-2}$	$10^{-1}$	x	30
	1.65			0.5	$10^{-2}$	x	71
Tetracene				30	$10^{-4}$	p	
	1.69	2.61	1.34				103
	1.70			2		F	75
Pentacene	1.5	2.13	1.0				103
	1.5			10		F	75
Pyrene	2.01	3.32	2.02				103
	2.02			1	$10^{-3}$	F	75
	2.40			$10^{-3}$	1		30
Chrysene	2.19	3.42	2.50				103
	2.20			2	$5 \times 10^{-4}$	F	75
Anthranthrene	1.60	2.85	1.32	$10^4$	$10^{-7}$	F	75
	1.67			$3 \times 10^4$	$10^{-7}$	p	28
Coronene	2.05	2.86	2.37				103
	1.7			$4 \times 10^2$	$10^{-5}$	p	32
	2.2			0.2	$10^{-2}$	p	32
Phenanthrene	2.24	3.50	2.70				103
Triphenylene	2.27	3.60	2.86				102
Perylene	1.95	2.85	2.02	1	$10^{-3}$	F	75
	2.0			10	$10^{-4}$	p	32
Metal-free phthalocyanine	1.46			$10^{-1}$	$10^2$	p	14
	1.71			$3 \times 10^{-2}$	$3 \times 10^{-2}$		18
	1.73			3	$3 \times 10^{-4}$		42

Another test of electronic conductivity is to pass a larger amount of charge through the sample than would be allowed by Faraday's law, without a decrease in the conductivity. For a sample with a room

temperature resistivity of about  $10^{15}$  ohm-cm with an applied field of  $10^4$  V/cm it would be necessary to pass current for  $10^{13}$  sec ( $\sim 10^3$  years) in order to satisfy this criterion. In spite of a lack of conclusive evidence on this point in most cases, it is generally assumed, and we shall also assume, that the conductivity is electronic and not ionic.

$E$ , in the conductivity expression, is generally supposed to be identified with the energy required to form charge carriers. As we pointed out in Section II, different authors variously suggested that  $E$  should be identified with (1) the energy of the lowest excited singlet state,  $^1E_1$ , above the ground state;<sup>14</sup> (2) the energy of the lowest triplet state,  $^3E_1$ ;<sup>87,88</sup> (3) an energy intermediate between the excited singlet and triplet state energies;<sup>75</sup> (4) the difference between the solid state ionization potential of the electron donating molecule and the electron affinity of the electron acceptor.<sup>59</sup>

The experimental results are distressing in that for a given compound different workers usually find different  $E$  values, and this makes it difficult to use the  $E$  values to test most of the above theories.

There are a number of factors which might conceivably be responsible for the variance in the  $E$  values.

### (1) *Electrode Effects*

As we shall see in Section VIII it is possible to find electrodes which considerably alter the observed activation energies, so that one might be concerned about the role which various metal electrodes play in the determination of  $E$ . This question has been partially answered by Reucroft<sup>84</sup> who found that the use of metals with a variety of work functions (2.2–4.6 eV) had no effect on the activation energy  $E$  of anthracene.

### (2) *Non-ohmic Behavior*

Another phenomenon which is almost universally observed with the organic solids is that they become non-ohmic at rather low field strengths.<sup>81,99</sup> At present it is unclear what the effect of the non-ohmic behavior will be on the temperature dependence of the conductivity. The discussion of the origin of the non-ohmic behavior will be deferred until Section VI.

(3) *Impurity Effects*

Impurities of known and unknown origin can definitely have an effect on the measured activation energy.<sup>8,75,87</sup> Some of the potentially most illuminating experiments on this matter have been carried out by Northrop and Simpson.<sup>75</sup> In their experiments known concentrations of an impurity were co-sublimed with some host material to form sandwich cells. With the doped material the conductivity in the low temperature region (below or around room temperature) was higher than the pure material and the activation energy corresponded to the triplet state energy of the impurity. In the high temperature region the conductivity corresponded to that found for the pure material both in magnitude and temperature dependence. The results are presented in Table VI and to a remarkable degree there is a strong correlation between the triplet state

TABLE VI. Impurity Activation Energies

Solute \ Solvent	<i>E</i> for impurity activated conductivity			<i>E</i> , pure solute	<sup>3</sup> <i>E</i> <sub>1</sub> solute
	Anthracene	Pyrene	Chrysene		
Naphthacene	1.23	1.25	1.26	1.5–1.7	1.34
Pentacene	0.95	1.03	1.02	1.5–1.7	1.00
Perylene	1.58	1.61	1.57	1.95	1.57
Anthranthrene	1.12	1.16	1.16	1.6–1.7	1.32

energy of the impurity and the measured activation energy, regardless of the host. This is a surprising result in that it suggests that less energy is required to form charge carriers in the two-component system than in either of the pure components. If we applied the energetic considerations of Lyons<sup>59</sup> we would have expected to find the activation energy in the two-component systems to be intermediate between the activation energy of either of the components. On the other hand if we accept the suggestion that the

triplet state of the impurity is involved in the conduction of the doped samples then the question arises as to why the activation energy for conduction in the pure material no longer corresponds to the triplet state energy. Northrop and Simpson<sup>75</sup> suggested that in the pure samples both the excited singlet and triplet levels contributed to charge carrier formation in such a manner that the observed activation energy was intermediate between that of these two levels. However, if this were true then the activation energy should correspond to the triplet state energy at the low temperatures and to the singlet state energy at high temperatures. The fact that the conductivity of the pure material can quite accurately be characterized by a single activation energy over a wide temperature range would seem to rule out this hypothesis.

It should be pointed out that the choice of solvents is unfortunate in that the total spread in their solid state ionization potentials appears to be less than 0.15 eV (see Section IV-A).

We conclude that none of the theories advanced so far accounts for the results which Northrop and Simpson<sup>75</sup> obtained with the pure material and the doped samples. Taken alone, however, the doping studies clearly implicate the participation of the triplet state of the impurity in the charge carrier formation process. These experiments are quite important and should be repeated using additional solvents and impurities.

## B. The Pre-exponential Factor in the Conductivity Expression

If it is assumed that carriers of one sign have greater mobility than carriers of the opposite sign, then the conductivity can be expressed as  $\sigma = e\mu n$ , where  $n$  is the concentration of the more mobile carrier. Furthermore, if the temperature dependence of the conductivity is entirely ascribed to the temperature dependence of the carrier concentration, we may write

$$\sigma = e\mu N_0 \exp(-E/2kT) = \sigma_0 \exp(-E'/kT)$$

where  $E$  is the thermal activation energy for the generation of carriers,  $N_0$  is the effective density of states in the conducting level of the crystal and  $\sigma_0$  is the pre-exponential factor in the expression for the temperature dependence of the conductivity. The appropriate value which should be used for  $N_0$  has been discussed by

Many, Harnik and Gerlich,<sup>65</sup> who concluded that within an order of magnitude  $N_0 \simeq 10^{21}/\text{cm}^3$ . The density of states in a weakly bound molecular crystal should correspond to the density of molecules in the crystal, about  $10^{23}$ , but in a covalently bound crystal, like Ge,  $N_0$  might be as small as  $10^{20}$ . Within these limits it is possible to calculate mobilities of carriers from  $\sigma_0$ . Neglecting the value for naphthalene it was found that the mobilities calculated in this manner varied from a high of  $10^2 \text{ cm}^2/\text{V-sec}$  down to the impossibly low value of  $10^{-12} \text{ cm}^2/\text{V-sec}$  (see Table V). On the basis of what we know about the trap-free mobilities and their expected values in different molecular crystals these results strongly suggest that (1) the majority carriers are being strongly trapped or (2) the conductivity is impurity activated and therefore a value of  $N$  somewhat smaller than  $10^{21}$  should be used, or perhaps both. With respect to this second point, there are definite examples where impurities are at least partly responsible for the low values of mobilities derived from specific conductivity measurements.<sup>49</sup> Violanthrene, for example, has been found to undergo some reaction in air which not only increases the conductivity, but also leads to the formation of unpaired electrons. The degree to which the calculated mobility approaches the true mobility will depend upon the absence of both of these effects. It is interesting to note in this connection that, with one exception, the maximum value of the mobility calculated in this manner was not above  $1 \text{ cm}^2/\text{V-sec}$ , or nearly the maximum value which we expect to find for the true mobility in a molecular crystal. We would like to suggest that mobilities calculated from the pre-exponential factor may be used as one criterion to determine whether or not impurity effects are present or there is trapping of majority carriers. Thus, we would weight the 2.4 eV activation energy for pyrene more strongly than the 2.02 eV value. By this criterion, the measurements on phthalocyanine by Fielding and Gutman<sup>18</sup> also appear to be quite good. It is interesting to note that measurements of pressed powders of phthalocyanine lead to an activation energy virtually identical to that found for the single crystals, but that the pre-exponential factor was a factor of 100 lower for the powders. Perhaps this gives some indication of the effect of non-crystallinity in reducing the mobility of carriers. These results are also consistent with the determination of carrier mobilities from diffusivity measurements<sup>47</sup>

in amorphous phthalocyanine films which gave a value of  $4 \times 10^{-3}$  cm<sup>2</sup>/V-sec. One final aspect of the powder measurements is that the experimental points for the conductivity fell quite accurately on a straight line when plotted as log conductivity vs.  $1/T$  (see Fig. 3).

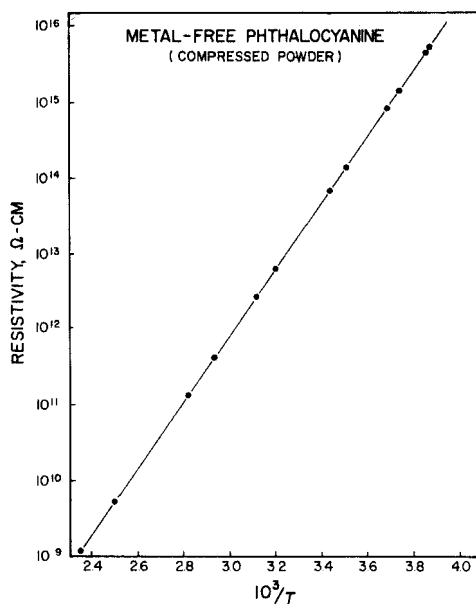


Fig. 3. Temperature dependence of the electrical conductivity of a compressed powder sample of metal-free phthalocyanine.

## VI. PHOTOCONDUCTION IN PURE AROMATIC MOLECULAR SOLIDS

A great number of organic solids have been examined and found to be photoconductive. In order to determine the nature of the process involved in photoconduction a variety of different measurements have been carried out including measurements of spectral dependence, current-voltage relation, temperature dependence, intensity dependence and of impurity effects. In this section we shall examine some of the general results, discuss their interpretation and, where possible, use the photoconductivity data to test the various theories of charge carrier formation.



### A. Sign of the Majority Carrier

Measurements with sandwich cells are particularly useful in determining the sign of the majority carriers. In this type of experiment the magnitude of the photocurrent by illumination of the positive electrode is compared with that produced by illumination of the negative electrode. For cells of anthracene, pyrene, chrysene, and anthranthrene the currents were largest when the positive electrode is illuminated, and this is taken as evidence that the majority carriers are holes.<sup>8, 76</sup> Since the trap-free mobilities of electrons and holes are expected to be comparable, these results indicate that either the electrons are more strongly trapped than are the holes, or that the quantum yield for the production of free holes is greater than that for electrons. The opposite results are reported for perylene, coronene, ovalene, pentacene, violanthrene, and hexacene.<sup>76</sup>

### B. Spectral Dependence

Lyons and Mackie<sup>61</sup> have recently shown that space-charge and trapped charge play an important role in determining the spectral dependence of the photoconductivity and the current-voltage relation of both the semi- and photoconduction of anthracene. Since the spectral dependence of the photoconductivity also varies with the geometry of the cell the results for sandwich cells and surface cells will be discussed separately. The following results refer principally to anthracene.

#### (1) *Surface Cell*

When the front face of a surface cell is illuminated the spectral dependence,  $I-\nu$ , usually resembles the absorption curve,  $\epsilon-\nu$ .<sup>8, 60, 61</sup> This resemblance has been interpreted as a surface effect due possibly to (a) higher carrier mobilities in the surface layer and (b) to a higher quantum yield for the production of carriers at the surface as compared to the bulk. It was found,<sup>61</sup> however, that when the geometry of the electrodes was such that the crystal experienced a non-uniform field, the  $I-\nu$  curve lost its similarity to the absorption curve and the magnitude of the photocurrent was decreased. This suggested that space-charge or trapped charges,

which also would lead to non-uniform fields, could in fact be responsible for dissimilarities between the  $I-\nu$  and  $\epsilon-\nu$  curves occasionally observed. Lyons and Mackie<sup>61</sup> in a very nice series of experiments have verified that this is the case. They showed that the  $I-\nu$  curve most nearly resembled the  $\epsilon-\nu$  curve when the sample was simultaneously illuminated with infrared light which was effective in freeing trapped carriers. The essential conclusion from these experiments is that when space-charge effects are absent, the threshold for photoconductivity corresponds to the threshold for light absorption by the crystal, or namely the absorption due to lowest energy singlet $\rightarrow$ singlet transition.

## (2) *Sandwich Cells*

There have been many observations of the occurrence of trapped charge in sandwich cell arrangements<sup>8,40,64</sup> and Lyons and Mackie<sup>61</sup> have found that this has a pronounced effect on the spectral dependence. Kommandeur and Schneider<sup>53</sup> found that the minima in the absorption spectra corresponded to the maxima in the photocurrent response curve. Lyons and Mackie suggested that this was due to the fact that as the extinction coefficient increases, charge carriers and trapped charge carriers are created in a smaller volume, the space-charge effect increases and so the photocurrent is smaller than that produced by more weakly absorbed light. Of course, at sufficiently long wavelengths where the light is not at all absorbed, the photocurrent falls to zero. This interpretation is supported by the long time constant of the photocurrent decay and the polarization effects which are associated with strongly absorbed light, but which are absent when weakly absorbed light is used. Finally it was found that simultaneous illumination of a sandwich cell with infrared light and ultraviolet light gave rise to photocurrents in which polarization effects were absent. Entirely similar results have been obtained by Bree and Schneider with 9,10-dichloroanthracene.<sup>5</sup> They found that the photosensitivity in the long wavelength of the main singlet-singlet absorption could be attributed to trapped carriers produced by previous illumination in the short wavelength region. Thus, the observations that under certain conditions the photocurrent spectral dependence extends to considerably longer wavelengths than do the singlet-singlet transi-

tions appear to be due to the presence of trapped charge and not due to singlet→triplet transitions as might be predicted on the basis of the triplet state theory.<sup>87</sup>

### C. Non-ohmic Currents

For most organic aromatic molecular solids both the dark and the photoconductivity cease to be ohmic when the field strengths exceed about 1000 V/cm.<sup>22, 32</sup> It has been suggested that this is due to a direct influence of the electric field on the probability of formation of charge carriers.<sup>75</sup> If we consider the formation of charge carriers as analogous to the dissociation of a weak electrolyte then we may use results derived by Onsager<sup>77</sup> for the effect of an electrical field on the dissociation process. According to his results the current-voltage relation is

$$i = i_0 \left[ 1 + \frac{9.6}{2} V / (T^2 \xi) \right] V$$

where  $V$  is the field strength,  $\xi$  the dielectric constant and  $T$  the absolute temperature. If we use the dielectric constant of, say, benzene ( $\xi = 2.3$ ) then at room temperature  $9.6/2.3T^2 \simeq 0.5 \times 10^{-4}$ , or the conductivity is predicted to become non-ohmic at about  $10^4$  V/cm. The fact that there are cases<sup>8</sup> in which the current is non-ohmic as low as 60 V/cm would certainly argue against the importance of this effect. However, a crucial test of the importance of the direct field effect is to determine how the field strength at which the current becomes non-ohmic varies with temperature. According to the Onsager theory as the temperature is increased the current should remain ohmic to higher field strengths. Experimentally, the opposite is found to be true.<sup>30</sup>

There is another test of the direct field effect on the formation of charge carriers. Compton, Schneider and Waddington<sup>8</sup> found that the application of a field perpendicular to the surface cell increased the conductivity when the front face was toward the negative transverse electrode, but decreased the conductivity when the polarity was reversed. Again this would argue against a direct field effect on carrier formation.

The above results apparently rule out the Northrop and Simpson<sup>75</sup> assumption that there is a direct field effect on the ionization of excited singlet and triplet state molecules.

It now appears that trapped charges are responsible for the non-ohmic behavior of the organic solids. The effect of inhomogeneous fields and of IR illumination on the photocurrent spectral dependence curves demonstrated the presence of trapped charge which certainly must have influenced the current-voltage relation. Furthermore, it was found<sup>61</sup> that at low voltages photocurrents were ohmic, at higher voltages the current increased faster than the voltage, but at still higher voltages became ohmic again. These results are consistent with the notion that space-charge is responsible for the non-ohmic behavior. The interpretation is as follows: At low voltages the current is ohmic simply because the polarization or number of trapped charges is proportional to the field.<sup>40, 72</sup> The increase in currents at higher fields ( $> 10^3$  V/cm) is associated with the decreasing importance of space-charge, while at the very high fields space-charge is unimportant and the current becomes ohmic. In the high field ohmic region the photocurrent in a sandwich cell is predicted to be independent of the wavelength of the light in the region where the crystal absorbs light, since carriers produced at various depths should all be equally effective in increasing the current.<sup>64</sup> Such an effect has recently been found by Lyons and Mackie.<sup>61</sup> This is to be expected only if the effects of trapped charge and carrier recombination are not important. The effect of temperature on the field at which the current becomes non-ohmic is interpreted as being due to the diminishing importance of space-charge at higher temperatures.

The results of the following experiments with metal-free phthalocyanine add further support to the interpretation of the non-ohmic currents in terms of space-charge. The dark current-voltage curves for a pure phthalocyanine surface cell are given in Fig. 4, and the current is found to become non-ohmic at about  $10^3$  V/cm. When a thin layer of the very strong electron acceptor *ortho*-chloranil was applied to the *back* face of this same cell the dark current increased markedly (by  $10^4$  in this particular experiment) and was ohmic up to the highest field strength used. A detailed interpretation of the effect of *ortho*-chloranil on the conductivity of organic solids will be given in Section VIII. Suffice it to say here that the principal effect of the *ortho*-chloranil was to inject a high concentration of holes into the phthalocyanine layer. The evidence from rectification measurements of the photocurrent is that electrons are the trapped carriers

responsible for the space-charge and therefore when a high concentration of mobile holes is injected into the phthalocyanine layer the trapped electrons are annihilated, the space-charge is eliminated and the current becomes ohmic.

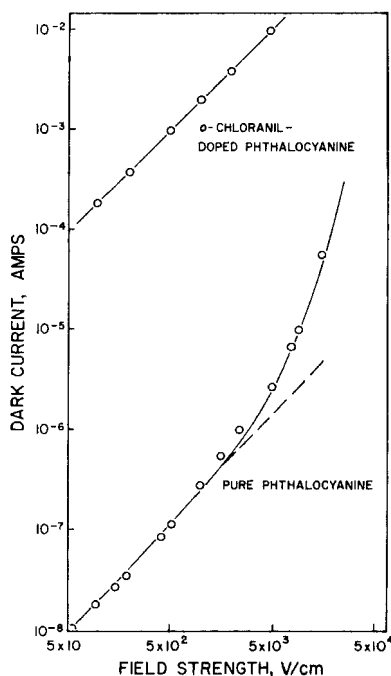


Fig. 4. Current-voltage relation for surface cells of pure metal-free phthalocyanine and *ortho*-chloranil-doped phthalocyanine.

The above experiments strongly suggest that the non-ohmic dark and photocurrents observed with anthracene are due to trapped charge. Although most of the experiments described above pertain to anthracene, the widespread occurrence of non-ohmic currents, polarization effects and similar  $I \sim V$ ;  $\epsilon \sim V$  relations in a variety of systems leads us to conclude that the same interpretation is quite generally applicable.

At present we have no information on just how important the space-charge effects are in influencing the temperature dependence of the dark and photoconductivity.

### D. Temperature Dependence

With few exceptions ( $\beta$ -carotene)<sup>89</sup> photocurrents in organic solids are found to increase with an increase in temperature according to the relation  $i_{ph} = i_{0ph} \exp(-E'/kT)$ . Values of  $E'$  are typically about 0.2–0.4 eV. It was initially suggested that the temperature dependence of the photoconductivity was due to a temperature dependence of carrier mobilities.<sup>8</sup> The measurements of the carrier mobilities demonstrated that the trap-free mobilities decreases with an increase in temperature, but that the quantum yield for the production of carriers increases somewhat with temperature.<sup>50,57</sup> It still seems possible that the temperature dependence of the photoconductivity could in part be due to the liberation of trapped carriers.

Rosenberg<sup>87</sup> has postulated that the temperature dependence of the photoconductivity was due to a temperature dependence of the quantum yield for the photogeneration of the triplet state. He accounted for this by assuming that intersystem crossing from an excited singlet state to a lower lying triplet state resulted from the crossing of the triplet state potential curve and the singlet state curve in the region of the lower vibrational levels of the excited singlet state, but not necessarily *the* lowest vibrational level. The population of the vibrationally excited singlet states would vary according to a Boltzmann distribution and, therefore, Rosenberg<sup>87</sup> concluded, the quantum yield for the production of triplet states should be temperature dependent and so should the photoconductivity derived from these triplet states. This proposal is readily subject to test. If the activation energy for the production of triplet states from excited singlet states were 0.1 eV, then in going from room temperature down to liquid helium temperatures the yield of triplet states would be reduced by a factor of  $10^{130}$ , or at 70°K the yield would be down by a factor of  $\sim 10^7$ . Experimentally this does not appear to be true. Low temperatures are actually employed to study molecules in their triplet state. For example, Sponer *et al.*<sup>95</sup> have observed phosphorescence from benzene and toluene at 4.2°K with a quantum yield apparently as high if not higher than that observed at liquid nitrogen temperatures. We conclude that the temperature dependence of the photoconductivity is *not* due to the temperature dependence of the quantum yield for intersystem

crossing from an excited singlet state to a triplet state. If we still wished to retain the assumption that the triplet state is involved in the formation of charge carriers then it would be necessary to further assume that there is an activation energy involved in the ionization of triplet state molecule, but not in the formation of the triplet state. A second possibility is that the triplet leads to the formation of a nearest-neighbor ion pair which then requires additional energy to be completely ionized. In either case, if the concentration of carriers is in equilibrium with respect to recombination we would expect the conductivity to vary as  $\exp(-E/2kT)$ .

It is also possible that ion-pair formation takes place directly from the singlet state and in this way the temperature dependence of the photoconductivity could be accounted for without ever having to invoke the triplet state as an intermediate. Accurate measurements of the quantum yield for the photogeneration of carriers will be required to ultimately settle this problem. The Kepler technique<sup>50</sup> looks very promising in this respect.

In summary, we conclude that the temperature dependence of the photoconductivity is due neither to

(1) a temperature dependence of the trap-free carrier mobilities, or

(2) a temperature dependence for the quantum yield for the photogeneration of triplet state molecules, but rather to

(1) a temperature dependence in the quantum yield for the ionization of excited state molecules (singlet state, triplet state, or nearest-neighbor ion pair), or

(2) a temperature-dependent ratio of free and trapped charge carriers.

### E. Intensity Dependence

The intensity dependence, like the spectral dependence of the photoconductivity, also appears to be complicated by space-charge effects. Depending upon the type of cell used (sandwich or surface cell) different workers have variously found photocurrents which varied linearly with the light intensity,<sup>35</sup> the square root,<sup>8</sup> or some lower power of the light intensity.<sup>99</sup> Photocurrents which vary with the square root of the light intensity are usually interpreted as

recombination limited<sup>8</sup> whereas linear dependence on the light intensity is presumed to indicate either that the conductivity is not recombination limited and may, as in the case of surface cells, be limited by the rate of diffusion of carriers to the electrode surface of the cell.<sup>8</sup> The effect of space-charge on the intensity dependence of the photoconductivity does not seem to have been as thoroughly investigated as its effect on the spectral response curves. In view of this it is difficult to be sure that the above explanations for the different intensity dependences are actually correct. It would be helpful to investigate the effect of infrared illumination and the variation of voltage on the intensity dependence of the photoconductivity.

### F. Impurity Effects

Several groups have investigated the effect of tetracene as an impurity on the photoconductivity of anthracene. Carswell and Lyons<sup>6</sup> reported that tetracene enhanced the photoconductivity of anthracene in the short wavelength region, and suggested that this increase was consistent with the fact that tetracene itself is a better photoconductor than anthracene. Seemingly opposite results have been obtained by several other workers,<sup>9,76,87</sup> who found that the introduction of small amounts of tetracene into anthracene quenched the photoconductivity. Northrop and Simpson<sup>76</sup> also studied the effect of ovalene and coronene on the anthracene photoconductivity and fluorescence as well. They found that the quenching constant for the reduction of the photoconductivity was identical to the fluorescence quenching, proving that tetracene and the other impurities were not reducing the photocurrent by reducing the carrier lifetime, but rather by acting as "sinks" for the anthracene excitation energy. What is a little surprising about these results is that according to the studies on the dark conductivity of the two component systems the impurities play an important role in increasing the conductivity of the sample.<sup>75</sup> If this is so, one might have expected that funneling the photoexcitation into the impurity would enhance the photoconductivity. Apparently the efficiency with which the impurities produce charge carriers is insufficient to compensate for the lowering of the probability of carrier generation by the solvent molecules.



### G. Additional Measurements

There is an additional measurement, the results of which strongly imply that the triplet state is not involved in the formation of charge carriers. McGlynn<sup>69</sup> examined a series of closely related aromatic solids and found that under similar experimental conditions the quantum yield for phosphorescence was inversely correlated with the magnitude of the photoconductivity.

There is another test of the participation of the triplet state in photoconduction and semiconductor which might be carried out. Suppose a compound which phosphoresces strongly is illuminated with a light intensity such that the photoconductivity and the dark conductivity are of the same order of magnitude. If the triplet state is an intermediate in both dark and photoconduction and if it is possible to observe phosphorescence under the above conditions of illumination it should also be possible to observe thermally generated phosphorescence.

## VII. NEUTRAL FREE RADICALS

The stable neutral organic free radicals are unique molecules and it is reasonable that they were among some of the first compounds whose electrical properties were studied. Eley<sup>14</sup> had suggested that for molecules in which the highest filled orbital is only half-filled the activation energy required to form charge carriers should be quite small. Assuming that the carriers have mobilities near unity, as found for other aromatics, these molecules would be expected on this basis to be quite good conductors. The experimental data obtained by Eley<sup>15</sup> are presented below.

Radical	$E$ , eV	$\rho_0$	$\rho_{25^\circ\text{C}}$	$\mu^a$
DPPH	0.16–0.36	$10^6$ – $10^8$	$\sim 10^9$	$10^{-10}$
Coppinger's radical	1.45	$10^1$	$\sim 10^8$	$10^{-4}$
Banfield and Kenyon's radical	2.31	$10^{-5}$	$\sim 10^{15}$	$10^{+2}$

<sup>a</sup>  $\mu$  calculated from  $\rho_0$ .

The author's own data provide strong evidence that these expectations are incorrect. The presence of unpaired electrons is clearly not a sufficient condition to impart high conductivity to these compounds. The reason for this is that the energy required to ionize a neutral radical molecule (a necessary step in order to have conduction),  $E = I_G - A_A$ , is still rather high. The fact that there are unpaired electrons in the molecule is insufficient to remove these energy requirements. It is quite likely that the low activation energy observed for  $\alpha, \alpha'$ -diphenyl- $\beta$ -picrylhydrazyl (DPPH) is due to some impurity, a possibility which Eley also suggested.<sup>15</sup> This seems reasonable in view of the fact that the mobility derived from the pre-exponential factor using the Many<sup>65</sup> assumptions is  $10^{-10}$  cm<sup>2</sup>/V-sec, a totally unreasonable value. The difficulty is probably in the assumption that the density of states is as high as  $10^{21}$ /cm<sup>3</sup>, i.e. that the conductivity is intrinsic, rather than impurity activated.

### VIII. DONOR-ACCEPTOR COMPLEXES

We now wish to consider the electrical properties of complexes and mixtures of molecules which are strong electron donors with strong electron acceptors. From the standpoint of their electrical properties and their possible relevance to biological systems these complexes are perhaps the most interesting of the organic solids. For example, certain solid complexes have resistivities as low as  $10^{-2}$   $\Omega$ -cm<sup>51</sup> and other two-component systems have been found to exhibit interesting photoelectric properties.<sup>36, 46</sup> In biological systems there are numerous complexes in some sort of aggregated state as well as many interfaces which separate different types of material, i.e. lipid from protein. It is for this reason that the electrical properties of complexes and more specifically of the layered systems may be of more than passing interest to the biologist.

The donor-acceptor complexes have been studied either in the form of homogeneous solid complexes prepared by precipitation from a solution containing the two components or in the form of two distinct layers which are allowed to interact at some common interface. The first type we shall call a *homogeneous* complex, whereas the second type we shall refer to as a *lamellar* complex.

The results of the studies of the homogeneous complexes will first be reviewed and then an interpretation of these results based on the donor-acceptor theory outlined in Section II will be given. We will then show how this interpretation is applicable to a discussion of the electrical, magnetic and optical properties of the lamellar donor-acceptor systems.

## A. Homogeneous Complexes

### (1) *Electrical Properties*

(a) *Aromatic-Halogen Complexes.* Akamatu<sup>2,3</sup> appears to be the first to make a detailed study of the electrical aromatic-halogen complexes. His remarkable observation was that although the electrical resistivity of the pure component materials was about  $10^{12}$ – $10^{14}$   $\Omega$ -cm, the complexes had resistivities as low as 5  $\Omega$ -cm. He also found that the temperature dependence of the conductivity was small, and through the use of Faraday's law demonstrated that the conductivity was electronic. The highest conductivity material was found to have about 1–2 halogen molecules per aromatic molecule, but there was only a factor of five difference in the conductivity of complexes in which the ratio varied from a low of 0.5 up to 3.5 halogen molecules per aromatic donor.

Since these pioneering studies of Akamatu there have been many subsequent studies of the effect of halogen molecules on the electrical properties of the aromatic hydrocarbons.<sup>1,46,54</sup> Kommandeur<sup>54</sup> found that with the highly conductive complexes the electrode contact resistance caused great difficulties in the usual two-probe measurements and therefore he used a four-probe arrangement to determine conductivities. He correspondingly found lower activation energies for conduction than did Akamatu who used the two-probe technique. The results of both the Akamatu and Kommandeur studies are collected in Table VII.

(b) *Aromatic Amine-Quinone Complexes.* The electrical properties of a number of aromatic amine-quinone complexes have been studied and some of these results are listed in Table VIII.<sup>1,16,55,56</sup> In general, it is found that these systems are poor conductors compared to the aromatic-halogen complexes and the activation energies are fairly large. Typically the room temperature

TABLE VII. Electrical Properties of Some Aromatic-Halogen Complexes

Complex	Mole ratio	$\rho_{15^\circ\text{C}}$ , $\Omega\text{-cm}$	$E$ , eV	Spin population per hydrocarbon molecule	Ref.
Perylene-bromine	1:2	7.8	0.13		1
-iodine	2:3	8	0.038		54
,,	2:3	10	0.060	0.06	1
,,	1:3	10	0.06	0.05	1, 92
,,	1:3	2			
Pyranthrene-iodine	1:2	17	0.090	0.090	1
Pyrene-iodine	1:2	75	0.38		54
Violanthrene-bromine	1:2	66	0.20		1
-iodine	1:2	45	0.15	0.14	1
Coronene-iodine		$2 \times 10^8$	0.50		92

TABLE VIII. Electrical Properties of Some Aromatic Amine-Quinone Complexes

Complex	Mole ratio	$\rho_{15^\circ\text{C}}$	$E$	Spin population per donor molecule	Ref.
<i>N,N'</i> -Dimethyl aniline					
-chloranil	1:1	$10^9$	0.47	0.0001	1, 16
-bromanil	1:1	$2 \times 10^9$	0.45	0.05	1, 16
-iodanil	1:1	$2 \times 10^8$	0.43	0.17	1, 16
Tetramethyl- <i>p</i> -phenylene diamine					
-chloranil	3:2-5:3	$5 \times 10^5$	0.57	—	56
,,	3:5	$6 \times 10^6$	0.57	0.01	56
,,	1:1	$2 \times 10^4$	0.53	0.05	1
-bromanil	1:1	$1.6 \times 10^5$	0.56	0.07	56
-iodanil	1:1	$1.8 \times 10^6$	0.59	0.10	56
3,8-Diaminopyrene					
-chloranil	1:1	$4 \times 10^3$	0.15	0.004	56
-bromanil	1:1	$10^3$	0.12-0.15	0.01	56
-iodanil	1:1	$2 \times 10^6$	0.40	0	56
3,10-Diaminopyrene					
-chloranil	3:1	$1 \times 10^7$	0.39	0.20	56

resistivities are in the range of  $10^4$ – $10^9 \Omega\text{-cm}$  when phenylene diamine is used as the electron donor, but they may be as low as  $10^3 \Omega\text{-cm}$  when diaminopyrene is the donor. A complication which must be kept in mind when trying to interpret the behavior of the amine systems is that they are chemically unstable.<sup>11–13</sup> In addition to this it does not seem to have been demonstrated that the conductivity is in fact electronic.

(c) *Salts*. Recently salts of the anion radical formed by the addition of an electron acceptor to tetracyanoquinodimethane (TCNQ) have been prepared<sup>51</sup> using various cations. It was found that the conductivity of the quinolinium salt ( $\rho = 10^{-2} \Omega\text{-cm}$ ,  $E \ll 0.01 \text{ eV}$ ) was the highest yet obtained for an organic solid.

Preliminary crystallographic studies indicate that the TCNQ molecules are arranged in infinite face-to-face stacks with the highest conductivity lying in the direction of these stacks and approximately normal to the TCNQ molecules.

In the triethyl ammonium salt the electrical conductivity was also highly anisotropic, with room temperature values of 4.0, 0.05, and  $0.001 \Omega^{-1}\text{-cm}^{-1}$  in the three principal crystal directions, and varied exponentially with temperature with an activation energy of 0.14 eV.

In these systems there is apparently complete electron transfer from the donors to the TCNQ molecules, and the thermoelectric power measurements indicate that electrons are the majority carriers. Both of the salts mentioned above contained two TCNQ molecules per donor. When a salt was prepared in which the acceptor–donor ratio was 1:1 the conductivity was significantly lower (by a factor of  $10^4$ ) than the 2:1 complex. The possible significance of this dependence of the conductivity on composition will be discussed shortly.

## (2) *Magnetic Properties*

Before attempting to interpret the behavior of the electrical properties of the donor–acceptor complexes the magnetic properties of these systems should also be discussed, since they appear to be related to the electrical properties. In some preliminary studies of the magnetic susceptibility of the aromatic–halogen complexes Matsunaga<sup>67</sup> found that the diamagnetism of the two-component

systems was lower than would be predicted from the sum of the diamagnetisms of the components. He suggested that this might be due to the presence of paramagnetism in the two-component system, and this was subsequently verified<sup>68</sup> by electron spin resonance (ESR) measurements. From these measurements it was possible to estimate the number of unpaired electrons in the samples and these results are shown in Tables VII and VIII for a number of the complexes. In general, it appears that all of the highly conductive donor-acceptor systems contain reasonably large concentrations of unpaired electrons. The spin concentrations are all somewhat less than 100% though.

Some of the strongest evidence that the unpaired spin concentration in the donor-acceptor systems is related to their high conductivity has been provided by the studies of Singer and Kommandeur.<sup>93</sup> They found that the temperature dependence of the unpaired electron spin concentration in single crystals of 2Perylene:3I<sub>2</sub> and Pyrene:2I<sub>2</sub> was the same as that found for the electrical conductivity of these same systems,<sup>54</sup> indicating that the two phenomena have a common origin. The lack of any hyperfine structure prevented identification of the radicals at that time; however in later experiments Kommandeur<sup>52</sup> dissolved perylene in molten iodine and observed an ESR signal with the well-defined hyperfine structure characteristic of the perylene positive ion radical.

### (3) *Interpretation of Electrical and Magnetic Properties*

We now wish to suggest an interpretation of the electrical and magnetic properties of this diverse group of donor-acceptor systems which is based on the ideas Lyons<sup>59</sup> presented in discussing the electrical properties of the pure hydrocarbons. This interpretation has already been adopted in various forms by a number of authors.<sup>37, 46, 54, 83</sup>

The total energy,  $E$ , required for the separation of charge in a donor-acceptor system is given by the following expression

$$E = I_d - A_a - P_+ - P_- - Q$$

where  $I_d$  is the gaseous ionization potential of the molecule which is to lose an electron and  $A_a$  is the gaseous electron affinity of the molecule which is to gain an electron in the charge separation

process;  $P_+$  and  $P_-$  are the gain in energy due to the polarization of the solid by a positive and negative charge respectively and  $Q$  is the remaining Coulombic attraction between the positive and negative ions formed. Under the condition that  $I_d$  is small and  $A_a$ ,  $P_+$  and  $P_-$  are large,  $E$  may become vanishingly small and charge separation may occur spontaneously without need for thermal activation. The solid state ionization potentials of molecules like perylene, violanthrene and pyrene are indeed low; the electron affinity of I atoms and perhaps  $I_2$  molecules is large so that  $E$  is expected to be small for complexes of these donors and acceptors. Due to problems connected with the interpretation of the solid state ionization potential measurements it is difficult to be more quantitative at present about the magnitude of  $E$ .

The extremely high conductivities and the low activation energy for conduction found for the aromatic-halogen complexes is interpreted as being due to the complete transfer of electrons from a certain fraction of aromatic donor molecules to the halogen acceptors with essentially no energy being required in the process. Under these conditions there will be a *mixture* of donor positive ions and neutral donor molecules which will allow positive charges to move through the crystal via electron transfer from neighboring neutral molecules. If every donor molecule were converted to a positive ion then hole conduction could not take place without the formation of doubly positive and neutral donor molecules. Similarly, negative charge may migrate through the crystal via electron transfer from a negative acceptor ion to a neutral acceptor molecule if there is a *mixture* of ions and neutral molecules. The measurements<sup>51</sup> on the TCNQ salts seem to support two important aspects of the above proposal. First the conductivity in the two highly conducting TCNQ salts is greatest in the direction of the face-to-face stacks of acceptor molecules and the conductivity is primarily by electrons. This is consistent with the notion that electron migration takes place essentially through the acceptor molecules whereas hole conduction involves the donor molecules. The fact that the conduction appears to be by electrons rather than holes is consistent with the proposal that ionization of all the donor molecules destroys hole conductivity. Secondly, the conductivity of the 1:1 donor-acceptor salt of TCNQ was a factor of  $10^4$  smaller than that of the 1:2 salts, again consistent with the proposal that high

conductivity requires a *mixture* of positive ion and neutral donor molecules or of negative ion and neutral acceptor molecules. Apparently in the 1:1 TCNQ salts virtually all of the TCNQ molecules have become negative ions and, consequently, the conductivity is reduced. On this basis we would expect the conductivity of the 1:1 samples to be very sensitive to conditions or preparation.

This interpretation of the electrical conductivity of the donor-acceptor complexes is also consistent with the observation of the high concentration of unpaired electrons in the highly conducting materials. The experiments on the temperature dependence of the unpaired electron spin concentration of iodine complexes with pyrene and perylene add strong support for the proposed common origin of the high conductivity and the unpaired electrons. It is not necessary, however, that the ESR and the conductivity have the same temperature dependence in order to have a common origin since the temperature dependence of the conductivity could be simply due to the mobility, whereas spin pairing might cause deviations from an apparent one-to-one relation between the ESR signal and the conductivity.<sup>12</sup> In some complexes where the conductivity is small and the activation energy is large the concentration of unpaired electrons has been found to be temperature independent.<sup>26</sup> This perhaps may be due to the fact that some chemical reaction has taken place which has produced free radicals but not the ion radicals which are necessary for conduction.

Finally, it should be pointed out that with the exception of perhaps the TCNQ salts,<sup>51</sup> the concentration of unpaired electrons falls far short of 100% electron transfer. It appears that within a given complex that a number of donor molecules are engaged in stabilizing the positive ion and acceptor molecules in stabilizing the negative ions.<sup>46, 54</sup> The recent work of Eastman<sup>12</sup> strongly implicates such a cooperative effect. Perhaps this is due, as Kommandeur<sup>54</sup> has suggested, to the increase in the energy of the charge separation process due to the presence of carriers already present.

### B. Lamellar Complexes

We now want to examine some of the properties of lamellar complexes which by virtue of their special geometry provide additional experimental verification of the ideas just presented.



### (1) *Electrical Properties*

(a) *Liquid Electrode Cell.* This variation of the sandwich cell has been used by Kallmann and Pope<sup>36,39</sup> to study the effect of various electrolyte solutions on the electrical conductivity of anthracene crystals. Both NaCl and NaI solutions were used as electrolytes and it was found that if  $I_2$  was added to the positive half of the cell the dark conductivity was increased by perhaps a factor of 10. However, the conductivity was enhanced by a factor of  $3 \times 10^3$  when the  $I_2$  solution was irradiated through the anthracene crystal with light which was not absorbed by the crystal. When the  $I_2$  was contained in the negative half of the cell there was virtually no enhancement of either the dark conductivity or the photoconductivity. The inclusion of  $Ce^{4+}$  ion in the positive electrode solution produced an enhancement of the dark current by a factor of  $10^5$ .<sup>39</sup> The enhancement of the anthracene conductivity by the  $I_2$  solutions can be interpreted as due to abstraction of electrons from the anthracene crystals by I atoms present in the dark, or formed by photodissociation of  $I_2$ . This, of course, is the explanation originally proposed by Kallmann and Pope.<sup>37</sup> They have considered the energetics of the hole injection process and conclude that they are favorable in the case of anthracene but not for naphthalene, in agreement with their experimental findings. Similar considerations apply to the injection of holes into anthracene by the  $Ce^{4+}$  ion.

(b) *Condenser Cell.* Hoesterey<sup>25</sup> has recently used a condenser cell to measure the quantum yield for the photogeneration of electrons and holes in anthracene crystals to which various electron acceptors had been added in the form of a layer on one surface. All of the materials which were used can be classed as electron acceptors relative to anthracene and in general they enhanced the hole injection into the anthracene crystal, but reduced the injection of electrons into the crystal.

(c) *Surface Cells.* Lamellar systems in a surface cell arrangement have also been studied. With crystals, a pair of electrodes are attached to one face and then a second component can be applied to the surface of the crystal between the two electrodes. It has been found<sup>9,91</sup> that both the dark and the photoconductivity of such surface cells are enhanced by electron acceptors such as  $O_2$ ,  $Cl_2$ ,  $NO_2$  and  $Br_2$ . The interpretation of these results is somewhat

complicated in that the increase in conductivity could be due to a change in the double-layer properties at the surface of the crystal, or it could be due to an injection phenomenon similar to that found by Kallmann and Pope.

Recently a number of experiments with lamellar surface cells have been carried out in which the electrodes were placed on the front surface of one layer (generally the electron donor) and the second component (the electron acceptor) was added to the *back* of the first layer.<sup>43, 46, 49</sup> With this geometry the second component is separated from the measuring electrodes by the entire thickness (typically about  $5 \times 10^{-4}$  cm) of the first layer. A variety of electron donors (tetracene, pentacene, phthalocyanine, perylene, violanthrene) along with the three electron acceptors *ortho*-chloranil,  $I_2$  and tetracyanoethylene have been studied with this arrangement, and qualitatively the results were all quite similar.<sup>46</sup> The conductivity in the donor layer was increased to varying degrees (factor of 10 up to a factor of  $10^7$ ) by the addition of any one of the electron acceptors and this was interpreted as being due to the injection of free positive charge (holes) into the donor layer and negative charge (electrons) into the acceptor layer. In agreement with this the conductivity of a layer of *ortho*-chloranil was increased by  $10^8$  by the addition of a layer of phthalocyanine to it.<sup>42</sup> The conductivity of these lamellar two-component systems increased exponentially with temperature with an activation energy that typically was about 0.2 eV.

It has been suggested alternatively that the high conductivity of these lamellar surface cells is due to the formation of a metallic-like region at the interface between the donor layer and the acceptor layer.<sup>21</sup> This can be ruled out by the following calculation. If no alteration of the bulk conductivity of the donor layer occurred, then the resistance of a cell which had metallic conductivity along the back surface of the donor layer, but in which carriers had to migrate through the thickness of the donor layer in order to reach the electrodes, is calculated for a typical surface cell to be a factor of  $10^7$  greater than that observed.\* The correct conclusion is that the *bulk* conductivity of the donor layer is actually increased by the addition of the acceptor layer to one surface of the donor layer.

\*  $\rho = 10^{15} \Omega\text{-cm}$ ; electrode area  $\cong 1 \text{ cm}^2$ ; thickness =  $5 \times 10^{-4} \text{ cm}$ ;  $R_{\text{calc}} = 5 \times 10^{11} \Omega$ ;  $R_{\text{obs}} = 10^4 \Omega$ .

The two-component lamellar systems were also found to be photoconductive,<sup>43, 46, 49</sup> and we may make the following summary comments about the photoconductivity of these systems.

(1) The photoconductivity of the two-component systems was greater than that of the pure donor layer, by as much as  $10^6$  in some cases.

(2) For back-face illumination of the cell the spectral dependence of the photoconductivity corresponded to the absorption spectrum of the donor layer. (See Fig. 1 for a diagram of the surface cell.)

(3) In the layered systems the photocurrents were largest when the back face was illuminated with light that was strongly absorbed by the donor layer, whereas the reverse was true for the pure donor layer, i.e. larger photocurrents were obtained with the front face illuminated.

(4) The photocurrents varied linearly with the light intensity and the decay of the photocurrent following illumination was exponential.

These results indicate that the addition of the electron acceptor layer increased the quantum yield for the photogeneration holes in the donor layer and electrons in the acceptor layer (item 1) that the important interaction was that of an excited donor molecule with an acceptor molecule at the donor-acceptor interface (items 2 and 3), and that there was a high concentration of carriers already present in the dark (item 4) which caused the photocurrent to decay with pseudo-unimolecular kinetics, and vary linearly with the light intensity.

Due to the electron transfer which takes place in the dark the donor and acceptor layers are charged with respect to each other. Therefore, the photo-enhancement of the conductivity must have involved hole injection into the donor layer *against an existing electrical field*, and perhaps this is why the enhancement of the photoconductivity was less than the enhancement of the dark conductivity. The measurements of the photo-polarization and photo-ESR support this interpretation.

## (2) Polarization Measurements

The charge in the donor and acceptor layers produced by electron transfer between the two was measured by placing a layered cell

between two plates of a condenser (see Fig. 1).<sup>49</sup> When a phthalocyanine-*ortho*-chloranil layer cell was placed in the condenser cell, the voltage induced on the two plates indicated that the phthalocyanine layer was positively charged with respect to the *ortho*-chloranil layer. When *either* the front or the back face of the layered system was illuminated (very thin layers were used in this experiment) the polarization of the two layers increased. The spectral dependence of the photo-induced polarization and the decay following illumination was the same as that found for the photoconductivity in this same system. These observations demonstrate that there is photoinjection of holes into the donor layer.

### (3) *Electron Spin Resonance Measurements*

We<sup>46</sup> have carried out electron spin resonance studies of a number of donor-acceptor systems and observed that generally there was a parallel increase in the spin concentration and the conductivity in the donor layer produced by the addition of an electron acceptor layer. This suggested that the ESR and the high conductivity in the two-component systems have a common origin. The fact that there were instances when the conductivity and the ESR had different temperature dependences on the other hand suggested that perhaps they do not.<sup>49</sup> The results of the effect of light on the unpaired spin concentration provides definite evidence that the ESR and the high conductivity do have a common origin.<sup>46</sup> It was found that light produced a reversible change in the ESR of the lamellar systems with the same spectral dependence, decay kinetics and time constant and same temperature dependence of the decay constant as the photoconductivity. These results clearly link the unpaired spin concentration with the conductivity.

An unexpected result of the photo-ESR measurements was that in complexes in which the dark ESR signal was low, light produced an increase in the unpaired spin concentration, but that in complexes in which the dark ESR signal was high, light produced a *decrease* in unpaired spin concentration. While this latter result still remains to be fully explained it is perhaps due to the fact that much of the charge in the two layers may tend to accumulate near the donor-acceptor interface. This would favor the formation of doubly ionized non-paramagnetic species and spin coupling. Under such

circumstances an increase in the charge concentration in the interfacial region might actually lead to, and obviously does lead to, a reduction in the concentration of unpaired spins.

#### (4) *Absorption Spectra*

Further evidence for the formation of ion radicals has been reported recently by Kearns and Calvin<sup>46</sup> who studied the optical absorption spectra of pure violanthrene films and films to which a layer of some electron acceptor had been added. The three electron acceptors iodine, *ortho*-chloranil and  $\text{BF}_3$  were used and it was found that the addition of any one of these to the violanthrene film produced a new absorption band at 7200 Å, on the long wavelength side of the normal violanthrene absorption. This band has been assigned to the absorption by the violanthrene positive ion. Blomgren and Kommandeur<sup>4</sup> have obtained similar spectroscopic evidence for the formation of positive ions of anthracene, pyrene and perylene in the solid state when any one of these are combined with the strong electron acceptor  $\text{SbCl}_5$ . As expected, these complexes also had high conductivity and the concentration of ion radicals calculated from the absorption spectra measurements agreed well with that measured by ESR. It was interesting to note that Bloemgren and Kommandeur<sup>4</sup> also suggested that their results indicated there might be significant formation of doubly charged species or spin coupling.

### IX. SUMMARY COMPARISON OF EXPERIMENT AND THEORY

In this section we wish to make a final comparison of the experimental results and the predictions given by the various theories. Out of this comparison it will also be clear what features are essential to a description of electronic conduction processes in organic molecular solids.

#### A. Singlet State Theory

The singlet state theory makes essentially only two predictions: (1) the activation energy for the formation of charge carriers in a neutral crystal of diamagnetic molecules should correspond to the

energy of the lowest excited singlet states of the isolated molecules, and (2) the activation energy for the formation of charge carriers in a solid free radical should be very small and, therefore, these compounds should be good conductors. Experimentally it is found that the activation energy, as determined from the temperature dependence of the dark electrical conductivity, is never as large as the energy of the lowest excited singlet state and typically is found to be about an electron volt smaller (see Table V). Secondly, the three solid free radicals which have been studied are all found to be poor conductors and two of these have large activation energies for conduction (see Section VII). The fact that the threshold for photoconduction invariably corresponds to the energy of the lowest energy singlet $\rightarrow$ singlet transition cannot be considered as support for the singlet state theory since this is a feature common to all the theories. In view of the lack of agreement between theory and experiment, coupled with the fact that the theory is actually based on an assumed cancellation of Coulomb attraction energy by polarization energy the singlet state theory would appear to be unsupportable.

### B. Triplet State Theory

The triplet state theory, like the singlet state theory, is essentially a postulate that the formation of a non-conducting excited electronic state (the triplet state in this case) is necessary for the formation of charge carriers. Experimentally it is found that, while the activation energy for conduction is often close to the energy of the triplet state, there are a number of cases where it differs by as much as  $\pm 0.5$  eV from the triplet state energy (see Table V). The inverse relation between the photoconductivity and phosphorescence quantum yield which McGlynn<sup>69</sup> observed for a series of related compounds strongly suggests that the triplet state is not even a necessary intermediate in the photogeneration of charge carriers. The very small activation energies for conduction (0.1–0.2 eV) demonstrate that in the two-component donor–acceptor systems the triplet states of the donor and the acceptor molecules are *not* involved in the thermal generation of carriers. In order to account for the temperature dependence of the photoconductivity, Rosenberg<sup>87,88</sup> incorporated into his formulation of the triplet state

theory the assumption that the quantum yield for the photo-generation of triplet states is temperature dependent, increasing exponentially with temperature. This feature of the theory is definitely not correct, and it is necessary to account for the temperature dependence of the photoconductivity in a different manner (see Section VI-D). With the exception of the Northrop and Simpson<sup>75</sup> experiments on mixed crystals (see Section V-A) we conclude that there is no experimental evidence that the triplet state is a necessary intermediate in either the thermal or photo-generation of charge carriers.

### C. Combined Singlet-Triplet State Theory

The evidence for and against the participation of either the excited singlet or triplet states as intermediates in the thermal generation of charge carriers has been discussed above. The fact that the temperature dependence of the conductivity in pure molecular solids can be characterized by a single activation energy is certainly clear evidence against the postulate that *both* the excited singlet and triplet states are participating in the thermal generation of charge carriers. The fact that the excited singlet state is an intermediate in the photogeneration of carriers is of course well established.<sup>76</sup> In order to account for the non-ohmic behavior of the dark conductivity and the photoconductivity Northrop and Simpson<sup>75</sup> proposed that there was a direct field effect on the probability for ionization of an excited state molecule. This proposal has now been shown to be incorrect (see Section VI-C) and the proper explanation appears to involve trapping of carriers. Finally, we note that the combined singlet-triplet state theory cannot account for the properties of the highly conductive donor-acceptor systems.

### D. Donor-Acceptor Theory

It seems to be generally recognized<sup>19,20, 22, 37, 46,54,59, 75,82,83</sup> that the donor-acceptor theory must in principle be correct. The question is what constraints, in addition to those already included in the theory, must be added (e.g. a special selection rule which forbids the thermal generation of ion pairs). It was found that this

theory was generally able to account for the electrical properties of the pure aromatic solids, the neutral free radicals and the two-component donor-acceptor systems. There were many details for which this theory provided an explanation without requiring additional *ad hoc* assumptions (e.g. preferential trapping of electrons in most of the "pure" aromatic molecular solids, prediction that photogeneration of carriers would proceed by an indirect process in the aromatic molecular solids, the compositional dependence of the conductivity of donor-acceptor salts and the fact that the conductivity was by electrons rather than holes, and the temperature dependence of the photoconductivity). The observed activation energies for the pure molecular crystals, the neutral free radicals and the donor-acceptor systems seem to be in qualitative agreement with the theoretical predictions; however accurate values for

TABLE IX. Comparison of Experimental Results and the Predictions of the Theories of Conductivity

Experimental measurement	Singlet state theory	Triplet state theory	Combined singlet- triplet theory	Donor- acceptor theory
Dark electrical conductivity				
<i>E</i> -values				
Doping experiments	—	+	?	—
Photoconduction				
Sign of majority carrier	x	x	x	(+)
Spectral dependence	+	c	c	c
Non-ohmic currents	c	c	—	c
Temperature dependence	x	—	c	c
Impurity effects	c	c	c	c
Phosphorescence-photo- conductivity relation	c	—	c	c
Neutral free radicals	—	x	x	+
Donor-acceptor complexes	x	x	x	+

+ = Experimental results support the theory on a crucial point.

c = Experimental results consistent with theory but not considered to be crucial to the theory.

— = Experimental results contrary to theoretical predictions.

x = No prediction by the theory.



solid state ionization potentials and electron affinities will be required for a quantitative check of the theory.

The only evidence against the donor-acceptor theory are the results of the mixed crystal studies carried out by Northrop and Simpson.<sup>75</sup> Because of their direct relevance to both the donor-acceptor theory and the triplet state theory, these experiments are well worth repeating and extending to other systems.

In Table IX a summary comparison of the predictions of the four theories with experimental results has been given.

The theory of electronic conduction in organic molecular solids is still quite rudimentary, however, as more critical experiments are carried out we may expect important advances in the development of our understanding of processes by which charge carriers are formed and migrate in the organic systems.

## X. ACKNOWLEDGMENT

The support of the National Academy of Sciences-National Research Council and the Air Force Research and Development Command is most gratefully acknowledged.

## References

1. Akamatu, H., and Inokuchi, H., in H. Kallmann and M. Silver, Eds., *Symposium on Electrical Conductivity in Organic Solids*, Interscience, New York, 1962, p. 277.
2. Akamatu, H., Inokuchi, H., and Matsunaga, Y., *Nature* **173**, 168 (1954).
3. Akamatu, H., Inokuchi, H., and Matsunaga, Y., *Bull. Chem. Soc. Japan* **29**, 213 (1956).
4. Blomgren, G. E., and Kommandeur, J., *J. Chem. Phys.* **35**, 1636 (1961).
5. Bree, A., and Schneider, W. G., *J. Chem. Phys.* **34**, 1453 (1961).
6. Carswell, D. J., and Lyons, L. E., *J. Chem. Soc.*, 1743 (1957).
7. Carswell, D. J., and Iredale, T., *Australian J. Appl. Sci.* **4**, 329 (1953).
8. Compton, D. M. J., Schneider, W. G., and Waddington, T. C., *J. Chem. Phys.* **27**, 160 (1957).
9. Compton, D. M. J., and Waddington, T. C., *J. Chem. Phys.* **25**, 1075 (1955).
10. Davydov, A. S., *Zh. Eksperim. i Teor. Fiz.* **18**, 210 (1948), in English translation.
11. Eastman, J., *Thesis*, University of California, Berkeley. University of California Radiation Laboratory Rept. UCRL-8910.
12. Eastman, J. W., Andros, G. W., and Calvin, M., *J. Chem. Phys.* **36**, 1197 (1962).

13. Eastman, J. W., Engelsma G., and Calvin, M., *J. Am. Chem. Soc.* **84**, 1339 (1962).
14. Eley, D. D., and Parfitt, G. D., *Trans. Faraday Soc.* **51**, 1529 (1955).
15. Eley D. D., and Willis, M. R., in H. Kallmann and M. Silver, Eds., *Symposium on Electrical Conductivity in Organic Solids*, Interscience, New York, 1962, p. 257.
16. Eley, D. D., Inokuchi, H., and Willis, M. R., *Discussions Faraday Soc.* **28**, 54 (1959).
17. Eley, D. D., Parfitt, G. D., Perry, M. J., and Taysum, D. H., *Trans. Faraday Soc.* **49**, 79 (1953).
18. Fielding, P. E., and Gutman, F., *J. Chem. Phys.* **26**, 411 (1957).
19. Fox, D., *Phys. Chem. Solids* **8**, 439 (1959).
20. Fox, D., in H. Kallmann and M. Silver, Eds., *Symposium on Electrical Conductivity in Organic Solids*, Interscience, New York, 1962.
21. Franck, J., International Conference on Luminescence, New York, October, 1961.
22. Garrett, C. G. B., in N. B. Hannay, Ed., *Semiconductors*, Reinhold, New York, 1959, p. 634.
23. Hedges, R. M., and Matsen, F. A., *J. Chem. Phys.* **28**, 950 (1958).
24. Helfrich, W., and Mark, P., *Z. Physik* **166**, 370 (1962).
25. Hoesterey, D., *J. Chem. Phys.* **36**, 557 (1962).
26. Huggins, C. M., and LeBlanc, O. H., *Nature* **186**, 522 (1960).
27. Hughes, A. L., and DuBridge, L. A., *Photoelectric Phenomena*, 1st Ed., McGraw-Hill, New York, 1932.
28. Inokuchi, H., *Bull. Chem. Soc. Japan* **24**, 222 (1951).
29. Inokuchi, H., *Bull. Chem. Soc. Japan* **25**, 28 (1952).
30. Inokuchi, H., *Bull. Chem. Soc. Japan* **29**, 131 (1956).
31. Inokuchi, H., and Akamatu, H., *Bull. Chem. Soc. Japan* **35**, 1622 (1960).
32. Inokuchi, H., and Akamatu, H., *Advan. Solid State Phys.* **12**, 93 (1961).
33. Inokuchi, H., Ikeda, K., and Akamatu, H., *Bull. Chem. Soc. Japan* **33**, 1622 (1960).
34. Inokuchi, H., Kuroda, H., and Akamatu, H., *Bull. Chem. Soc. Japan* **36**, 749 (1961).
35. Inokuchi, H., Maruma, Y., and Akamatu, H., in H. Kallmann and M. Silver, Eds., *Symposium on Electrical Conductivity in Organic Solids*, Interscience, New York, 1962, p. 69.
36. Kallmann, H., and Pope, M., *Rev. Sci. Instr.* **30**, 44 (1959).
37. Kallmann, H., and Pope, M., *Nature* **186**, 31 (1960).
38. Kallmann, H., and Pope, M., in H. Kallmann and M. Silver, Eds., *Symposium on Electrical Conductivity in Organic Solids*, Interscience, New York, 1962, p. 1.
39. Kallmann, H., and Pope, M., *J. Chem. Phys.* **36**, 2482 (1962).
40. Kallmann, H., and Rosenberg, B., *Phys. Rev.* **97**, 1596 (1955).
41. Kallmann, H., and Silver, M., Eds., *Symposium on Electrical Conductivity in Organic Solids*, Interscience, New York, 1962.

42. Kearns, D. R., *Thesis*, University of California, Berkeley. University of California Radiation Laboratory Rept. UCRL-9120.
43. Kearns, D. R., *Radiation Res. Suppl.* **2**, 407 (1960).
44. Kearns, D. R., *J. Chem. Phys.* **35**, 2269 (1961).
45. Kearns, D. R., and Calvin, M., *J. Chem. Phys.* **29**, 950 (1958).
46. Kearns, D. R., and Calvin, M., *J. Am. Chem. Soc.* **83**, 2110 (1961).
47. Kearns, D. R., and Calvin, M., *J. Chem. Phys.* **34**, 2022 (1961).
48. Kearns, D. R., and Calvin, M., *J. Chem. Phys.* **34**, 2026 (1961).
49. Kearns, D. R., Tollin, G., and Calvin, M., *J. Chem. Phys.* **32**, 1020 (1960).
50. Kepler, R. G., *Phys. Rev.* **119**, 1226 (1960), and private communication.
51. Kepler, R. G., Bierstedt, P. E., and Merrifield, R. E., *Phys. Rev. Letters* **5**, 503 (1960).
52. Kommandeur, J., *Mol. Phys.* **4**, 509 (1961).
53. Kommandeur, J., and Schneider, W. G., *J. Chem. Phys.* **29**, 1108 (1958).
54. Kommandeur, J., and Hall, F. R., *J. Chem. Phys.* **34**, 129 (1961).
55. Labes, M. M., Rudy, O. N., and Kronick, P. L., *J. Am. Chem. Soc.* **84**, 499 (1962).
56. Labes, M. M., Sehr, R., and Bose, M., *J. Chem. Phys.* **32**, 1570 (1960).
57. LeBlanc, O. H., *J. Chem. Phys.* **33**, 626 (1960).
58. LeBlanc, O. H., *J. Chem. Phys.* **35**, 1275 (1961), and *errata*, **36**, 1082 (1962).
59. Lyons, L. E., *J. Chem. Soc.* 5001 (1957).
60. Lyons, L. E., in H. Kallmann and M. Silver, Eds., *Symposium on Electrical Conductivity in Organic Solids*, Interscience, 1962, p. 193.
61. Lyons, L. E., and Mackie, J. C., *J. Chem. Soc.* 5186 (1960).
62. Lyons, L. E., and Mackie, J. C., *Proc. Chem. Soc.* 71 (1962).
63. Lyons, L. E., and Morris, G. C., *Proc. Phys. Soc.* **69**, 1162 (1956).
64. Lyons, L. E., and Morris, G. C., *J. Chem. Soc.* 5192 (1960).
65. Many, A., Harnik, E., and Gerlich, D., *J. Chem. Phys.* **23**, 1733 (1955).
66. Mark, P., and Helfrich, W., *J. Appl. Phys.* **33**, 205 (1962).
67. Matsunaga, Y., *Bull. Chem. Soc. Japan* **28**, 457 (1955).
68. Matsunaga, Y., *J. Chem. Phys.* **30**, 855 (1959).
69. McGlynn, S. P., International Conference on Luminescence, New York, October, 1961.
70. Meir, H., *Z. Physik. Chem. Leipzig* **208**, 325 (1958).
71. Mette, H., and Pick, H., *Z. Physik* **134**, 566 (1953).
72. Moore, W., and Silver, M., *J. Chem. Phys.* **33**, 1671 (1960).
73. Murrell, J. N., *Mol. Phys.* **4**, 205 (1961).
74. Northrop, D. C., and Simpson, O., *Proc. Phys. Soc.* **65B**, 974 (1955).
75. Northrop, D. C., and Simpson, O., *Proc. Roy. Soc. (London)* **A234**, 324 (1956).
76. Northrop, D. C., and Simpson, O., *Proc. Roy. Soc. (London)* **A244**, 377 (1958).
77. Onsager, L., *J. Chem. Phys.* **2**, 599 (1934).
78. Pastor, R. C., and Turkevich, J., *J. Chem. Phys.* **23**, 1731 (1955).
79. Pauli, W., *Ann. Physik* **40**, 677 (1913).
80. Pick, H., and Wissman, G., *Z. Physik* **138**, 436 (1954).

81. Pochettino, *Atti Accad. Nazl. Lincei* **No. 1**, 355; **No. 2**, 17 (1906).
82. Pope, M., and Kallmann, H., in H. Kallmann and M. Silver, Eds., *Symposium on Electrical Conductivity in Organic Solids*, Interscience, New York, 1962, p. 83.
83. Pope, M., Kallmann, H., Chen, A., and Gordon, P., *J. Chem. Phys.* **36**, 2486 (1962).
84. Reucroft, P. J., *J. Chem. Phys.* **36**, 114 (1962).
85. Riehl, N., *Ann. Physik* **20**, 93 (1957).
86. Riehl, N., in H. Kallmann and M. Silver, Eds., *Symposium on Electrical Conductivity in Organic Solids*, Interscience, New York, 1962, p. 61.
87. Rosenberg, B., *J. Chem. Phys.* **29**, 1108 (1958).
88. Rosenberg, B., *J. Chem. Phys.* **31**, 238 (1959).
89. Rosenberg, B., in H. Kallmann and M. Silver, Eds., *Symposium on Electrical Conductivity in Organic Solids*, Interscience, New York, 1962, p. 291.
90. Rosenberg, B., and Camiscoli, J. F., *J. Chem. Phys.* **35**, 982 (1961).
91. Schneider, W. G., and Waddington, T. C., *J. Chem. Phys.* **25**, 358 (1956).
92. Sehr, R., Labes, M. M., Bose, M., Ur, H., and Wilhelm, F., in H. Kallmann and M. Silver, Eds., *Symposium on Electrical Conductivity in Organic Solids*, Interscience, New York, 1962, p. 309.
93. Singer, L. S., and Kommandeur, J., *J. Chem. Phys.* **34**, 133 (1961).
94. Slough, W., and Ubbelohde, A. R., *J. Chem. Soc.* 911, 918, 982 (1957) and references contained therein.
95. Sponer, H., Kanda, Y., and Blackwell, L., *Spectrochim. Acta* **16**, 1135 (1960).
96. Switzer, D. I., *Organic Semiconductors: Properties and Applications*, Literature Search No. 341. Jet Propulsion Laboratory—C.I.T., 1961.
97. Terenin, A. in H. Kallmann and M. Silver, Eds., *Symposium on Electrical Conductivity in Organic Solids*, Interscience, New York, 1962, p. 39.
98. Thaxton, G. D., Jarnagin, R. C., and Silver, M., Conference on Reversible Photochemical Processes, Duke University, April 1962.
99. Tollin, G., Kearns, D. R., and Calvin, M., *J. Chem. Phys.* **32**, 1013 (1960).
100. Vartanian, A. T., and Karpovich, I. A., *Dokl. Akad. Nauk SSSR* **111**, 561 (1956).
101. Vilesov, F. I., *Dokl. Akad. Nauk SSSR* **132**, 632 (1960).
102. Vilesov, F. I., *Dokl. Akad. Nauk SSSR* **133**, 1060 (1960).
103. Wilk, M., *Z. Elektrochem.* **64**, 930 (1960).

## 9

# THE ELECTRONIC PROPERTIES OF DEOXYRIBONUCLEIC ACID

PIERRE DOUZOU and CHARLES SADRON,  
*Laboratoire de Biophysique du Muséum National d'Histoire  
 Naturelle, Paris*

## CONTENTS

I. Introduction . . . . .	339
II. The Molecular Structure of Deoxyribonucleic Acid . . . . .	341
III. The Study of the Electronic Properties of DNA . . . . .	346
A. Theoretical Aspects of the Problem of the Interaction of Heterocyclic Bases . . . . .	346
B. Comparison of the Electronic Properties of DNA and Its Components . . . . .	347
(1) Studies with Optical Methods . . . . .	347
(2) Studies with Magnetic Methods . . . . .	350
(3) Direct Research on Supramolecular Electronic Properties . . . . .	354
IV. Conclusion . . . . .	357
References . . . . .	357

## I. INTRODUCTION

The study of the electronic (quantum) behavior of nucleic acids is chronologically related to the development of optical and Hertzian techniques. It also results from the hypothesis developed by Szent-Györgyi,<sup>27</sup> that quantum properties similar to those resulting from the crystallization of ions and inorganic molecules might possibly result from the aggregate state of living matter and explain certain characteristics of its behavior. It was an exciting hypothesis for biochemists trying to explain the chemical energy transfers affecting proteins and for physiologists endeavoring to reconstruct the series of mechanisms which enable living matter to convert energy into such varied forms that it is often difficult to find any logical link between them. Techniques of solid-state physics helped

to strengthen the idea of a similarity between the quantum mechanics of inorganic compounds associated in the crystalline state and of polymerized organic compounds.

In spite of the warnings of more discerning authors, most workers coming to biophysics from different fields insisted on "carrying out their own experiments". Very few specified the reasons underlying their plan of action and their experimental attitude toward biological compounds. In fact, most of the time these biophysicists, urged by chemists to study biological compounds, wished to investigate whether, in the solid state, these molecular structures possessed extraordinary physical properties corresponding to their structural perfection and complexity.

In the first phase of the study of the electronic properties of biological compounds, there was doubtless much naivety in the physicist's and biochemist's attitude. They were not sufficiently familiar with each other's discipline to achieve their proposed aims. Thus, the unfavorable conditions under which the first experiments were performed meant that the properties were formulated in terms which disconcerted most writers, irritated some and aroused others. The attention given to these biochemical reactions is indicative of the interest of scientists in the fundamental mechanisms operating in living matter, which physical chemists cannot yet explain or reproduce.

Following the publication of the pioneer works of, among others, Duchesne and Monfils<sup>13</sup> in 1955, the situation began to look more encouraging. In their studies of biological compounds, Blumenfeld and his colleagues discovered certain magnetic properties<sup>4,5</sup> and Sadron *et al.* reported properties reminiscent of those of ferroelectric compounds.<sup>11,25</sup> This impulse stimulated further work along the same lines including the reports of Duchesne,<sup>14</sup> Blois and Maling,<sup>3</sup> Shulman *et al.*<sup>29</sup> and, more recently, of Eley.<sup>17</sup> These results apparently indicated that certain properties similar to those manifested in solid-state physics by some inorganic compounds characterize biological compounds, but some of the properties were so anomalous as to provide grounds for controversy about the analysis.

Consequently, a critical study of our knowledge, especially in the case of the nucleic acids, appears necessary. This article is devoted to such a reappraisal. We will confine our attention to deoxyribonucleic acid since much more is known about its structure than that

of ribonucleic acid. Perhaps it is because of its more orderly structure that deoxyribonucleic acid has attracted more attention. Up to the present time, the previously mentioned properties reminiscent of those assigned by solid-state physics have been demonstrated in deoxyribonucleic acid.

## II. THE MOLECULAR STRUCTURE OF DEOXYRIBONUCLEIC ACID

Deoxyribonucleic acid (DNA), according to the Watson and Crick model, is composed of two polynucleotide chains wound around each other in a double helix. Each chain is composed of a sequence of nucleotide units, as shown in Fig. 1. The bases which

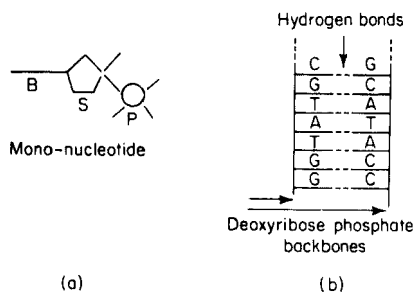


Fig. 1. Diagrammatic representation of the physicochemical structure of DNA. (a) Mononucleotide, where B = base, S = deoxyribose sugar, P = phosphate; (b) Polynucleotide, with the bases: A = adenine, G = guanine (purines); T = thymine, C = cytosine (pyrimidines).

we find in nucleotides, except in a few cases, are the purines, adenine and guanine, and the pyrimidines, thymine and cytosine.

In native DNA the two chains are linked by hydrogen bonds between facing bases. Experiments have shown, however, that adenine is bound only to thymine and cytosine only to guanine. Consequently, in the double helix, the proportion of adenine (A) to thymine (T) is equal to that of cytosine (C) to guanine (G). On the other hand, the  $(A + T)/(C + G)$  ratio depends essentially on the biological background of the sample and it probably varies from one macromolecular particle to another in the same sample.

The morphology of the double strand depends upon the water content of the sample and the nature and concentration of the associated ions. X-ray studies show that for fibers with greater than 40% water content, in the presence of NaCl, the double helix takes the form shown in Fig. 2. In this case, the pairs of bases form parallel plates which are perpendicular to the axis of the double helix, the distance between them being about 3.4 Å. Thus, the molar mass of DNA is about 20,000 for a 100 Å length. The diameter of the double helix is 20 Å.

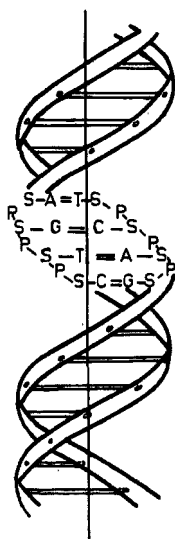
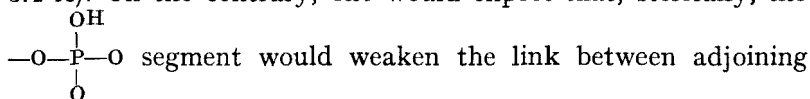


Fig. 2. Watson and Crick's double-stranded model of DNA.

It is now important to find out the origin of the cohesion forces maintaining the arrangement of the parallel plates in the Watson and Crick model. The cohesion does not have its origin in the phosphodiester links of the successive plates (their total length is over 3.4 Å). On the contrary, one would expect that, sterically, the



segment would weaken the link between adjoining plates rather than strengthen it, and this could explain the angular displacement of the axes in the successive plates.



Physicists quite naturally assumed that this stacking of molecular groups, rich in double conjugated bonds or in hydrogen bonds, would allow electronic migration or energy transfers from plate to plate to occur. At the same time, the hypothesis was made that supramolecular phenomena were propagated along the double strand line. Hence, it was natural to think that in such a structure cooperative phenomena would take place and influence certain parts of DNA.

Before proceeding further, we must point out that the molecule cannot be reduced to a model as schematic as Watson and Crick's. We have already said that the structure shown in Fig. 2 exists only in the presence of water and a halogenated electrolyte such as sodium chloride. The DNA molecule tested must, under these conditions, be considered as a "core" consisting of the two polynucleotide strands, probably sheathed in a layer of adsorbed water and covered with negative charges carried by the ionized phosphoric groups, which in turn are surrounded with positive gegenions (generally  $\text{Na}^+$  since sodium deoxyribonucleate occurs with the preparation) in the presence of an excess of  $\text{Na}^+$  and  $\text{Cl}^-$  ions from the electrolyte, and to a lesser extent  $\text{H}^+$  and  $\text{OH}^-$  from the water.

Obviously, the ionic environment and the "core" of the particle are in close interaction. From experiments we know that on being heated the couplings between the plates can be broken and the double helix destroyed, becoming a tangled pellet. This phenomenon is easy to detect by spectral absorption measurements around 2600 Å. The actual temperature at which it takes place depends on the concentration and the nature of the ions introduced into the DNA solution; it takes place at room temperature in DNA-sodium chloride solutions when the NaCl concentration falls below a few thousandths molar.

We must therefore consider the double-helix complex, the adsorbed water and the ionic environment all to be involved in the physicochemical experiments made with "native" DNA. Even if only one of these parts, say the non-ionic "core", is selectively excited in a suitable way (e.g. by an electromagnetic field of sufficiently high frequency), the phenomenon observed will depend *a priori* not only on the chemical composition of the "core", but also on its ionic environment, since there is close interaction

between them. Thus, the experimenter will have to establish carefully the conditions under which the sample is studied. These are as simple as possible when the DNA is highly diluted in the chosen solvent (ionic solution). In this case, the DNA can be considered as if it were alone in an infinite volume of liquid. Unfortunately, we are far from being certain that this assumption is valid. All research work on infinitely dilute DNA solutions induces us to think that the individual particle is not a single cylindrical element, a sort of small stick, but rather a group of such sticks, probably making zigzag

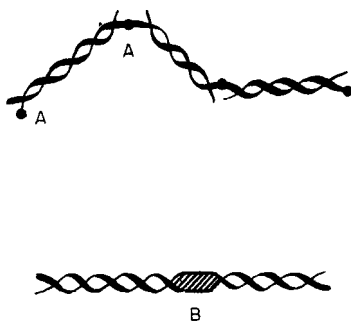


Fig. 3. Configuration pattern of one chain of DNA with points of lesser mechanical or chemical resistance (points A) than with a polypeptidic fragment (B).

configurations (Fig. 3). These various elements, each of the complex structure described, interact with each other making the interpretation of the phenomena observed still more difficult.

Moreover, it must be emphasized that in most cases, with physico-chemical techniques, experimenters do not use dilute solutions but rather fibers or gels, and their preparation (water and salt content) is not always very precise. With such samples, X-ray studies show that the two strands extend lengthwise (model of Wilkins) parallel to one another, according to certain conditions for the arrangement of water layers and the ion distribution. In such a system, the response to a physical reagent doubtless depends on the whole structure of the complex. With this in mind, it would be quite a serious mistake to use the classical double-strand model to interpret the phenomenon observed.

Finally, we must point out that the samples tested, however

carefully they are extracted from their original medium, still possess "impurities", such as protein residues and heavy ions which may be introduced during the preparation of the sample. In the present state of studies we are not sure whether *in vivo* these non-nucleotide components are associated with the elementary particle in the form of complexes, their presence being necessary for the biological activity of DNA. In connection with this, a good example of the difficulties met with can be found in the discussions of the interpretation of the ESR signals reported by Blumenfeld which many writers attribute to the presence of iron cations forming colloidal agglomerates.<sup>25</sup>

There is, we know, a wide gap between the theoretical view of polynucleotides arranged in a double helix and the compound actually tested, "deoxyribonucleic acid". If we consider the double helix only, the scheme is precise and geometrical: each atom is strictly localized, with bonds of known length and direction, and known intermolecular distances. All chemical binding forces are represented in this model; electromagnetic waves, from Schuman's region to the Hertzian domain, should have the opportunity to act upon it. In this connection, nucleic acids give us a remarkable summing up of the types of structures found in nature, experimental material for all physical and chemical sciences.

Unfortunately, the previous picture becomes less clear when we consider a macroscopic sample. Still undefined forces act on the molecular structures and govern their individual and collective behavior. To discuss the physical responses of real samples, first of all, one must question whether they are intrinsic or extrinsic in origin, and whether the experiment has been performed objectively. This will be our aim when we analyze the electrical, magnetic and optical properties conferred on DNA. Taking this opportunity we shall make a provisional statement about the electronic studies made, and at the same time show how they raise new problems and how they prompt us to begin similar studies on the components of nucleic acids.

It is necessary to emphasize the fact that physical chemists have worked at two different levels; some were concerned with possible supramolecular properties and adopted techniques and concepts specific to the quantum physics of crystals; others limited their experiments to the study of molecular and submolecular electronic

properties. This latter work will be referred to when a discussion of the experiments made at the supramolecular level leads us to compare the two approaches. We shall find that physical chemists cannot ignore information obtained in this field if they are seeking an accurate picture of the supramolecular behavior of nucleic acids.

### III. THE STUDY OF THE ELECTRONIC PROPERTIES OF DNA

#### A. Theoretical Aspects of the Problem of the Interaction of Heterocyclic Bases

The composition and configuration of the purine and pyrimidine bases in DNA are fairly well known. More precise determinations are being made by theoretical chemists of the "submolecular outline" of bases.<sup>1,23</sup>

Blumenfeld located the origin of ESR signals at the level of the purine-pyrimidine molecular pairs, assimilated to the charge transfer complexes (CTC) with one unpaired electron.<sup>8</sup> At the same time, he considered the possible action of the piling of these molecular pairs, basing his work, from a magnetic standpoint, on the few theoretical data we now possess. Blumenfeld was able, in the case of synthetic polymers, to show that 5 to 10 flat unsaturated molecules, placed one on top of the other, allow a convenient delocalization of bond electrons.

Until now, the hypochromic effect characterizing the absorption spectra constituted the only test of interaction. Kasha and his co-workers used molecular electronic spectroscopy, which is more explicit than the classical absorption method.<sup>20</sup>

Biophysicists looking for various physical manifestations of the supramolecular behavior of nucleic acids possess only fragmentary data. Their fundamental approach is not based on sufficient elementary information such as the hypochromic effect resulting from the interactions of complementary bases and of the pairs they constitute.

Basic concepts and techniques of solid-state physics offer unsatisfactory ways of avoiding the necessary hard work preliminary to these studies. It is most tempting to look for new criteria which at least would give a suggestive interpretation of processes described by the classical techniques such as hyperchromy. The physical

interpretation of DNA in the solid state represents a necessary step toward the understanding of the quantum dynamics of biological high polymers, at least this was the optimistic view of the biophysicists who did this preliminary work. But are the results obtained really characteristic of the composition, structure and cohesion of the double strand? It is doubtful when we think of the difficulties met with in experiments on macroscopic samples. Let us now analyze these experiments in the optical, magnetic and electrical fields.

## **B. Comparison of the Electronic Properties of DNA and Its Components**

### *(1) Studies with Optical Methods*

The most systematic studies have been made in the optical field. The approach is parallel to that of specialists in molecular spectroscopy when attempts are made to discover differences between the absorption spectra of nucleic acids, polynucleotides and their components. This point of view is classic now and has become mere routine. It is "descriptive". Some authors, Kasha for example, tried to adapt techniques based on more elaborate quantum concepts such as the  $n \rightarrow \pi^*$  transitions, the "excitons", and energy transfers.<sup>19</sup>

In the present case, the comparison considered was relative to the characteristics of the long life-time emission of polynucleotides and their components. As well as wishing to follow strictly the logic of absorption spectroscopy, it was hoped to establish the origin and nature of the emission induced in nucleotides by radiation near the visible, and to verify whether this emission is specific of polymerization or whether it is influenced by it. Finally, we wished to compare the emission characteristics (frequencies, decay-time, temperature effects, dilution, etc.) of polynucleotides and their components, with a view to finding out if essential differences exist between these compounds, in the same way as there exists in the case of simple atoms and molecules in their association in the solid state.

We now turn to the luminescence of nucleic acids. The purine and pyrimidine bases in nucleic acids can be electronically excited

by ultraviolet radiation centered on 2600 Å, and their absorption spectrum gives evidence of this.

In nucleic acids, using the techniques of solid-state physics, it was normal to use the emission of luminescence resulting from the absorption to try and determine the possible transfer of optically

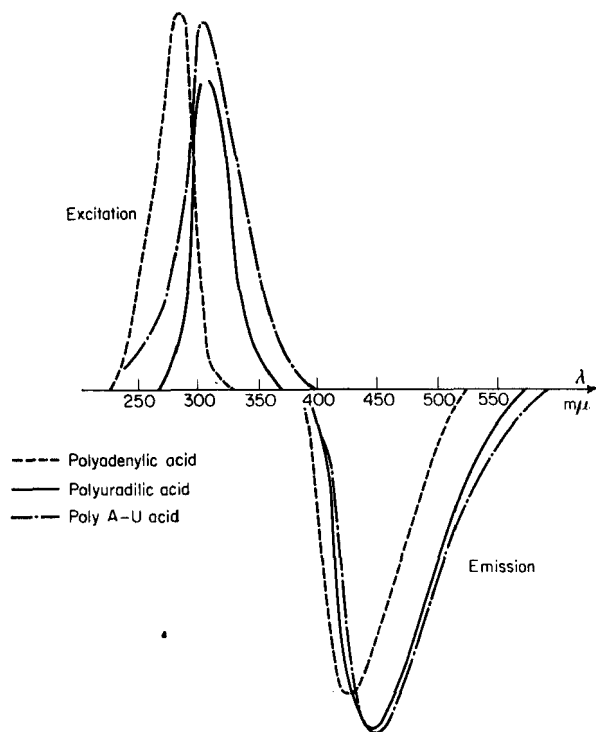


Fig. 4. Excitation and emission spectra of polynucleotides at 77°K.

excited electrons. This approach was based upon the fact that nucleic acids become electronically excited by radiation which is not exactly centered at the maximum of the absorption band, as is the case when the 3600 Å line of an Hg arc is used. Debye and Edwards,<sup>9</sup> followed by Szent-Györgyi,<sup>27</sup> pointed out that these radiations produced an after-glow emission at liquid nitrogen temperatures. Such emission could have been providential for anyone wishing to know about the interaction between nucleotides and their electron

dynamics. Numerous experiments on the photo-conductivity of proteins and nucleic acids have been made in the last few years,<sup>10,16,30</sup> but there was no agreement as to the precise significance of the results, which were usually positive, but disturbed

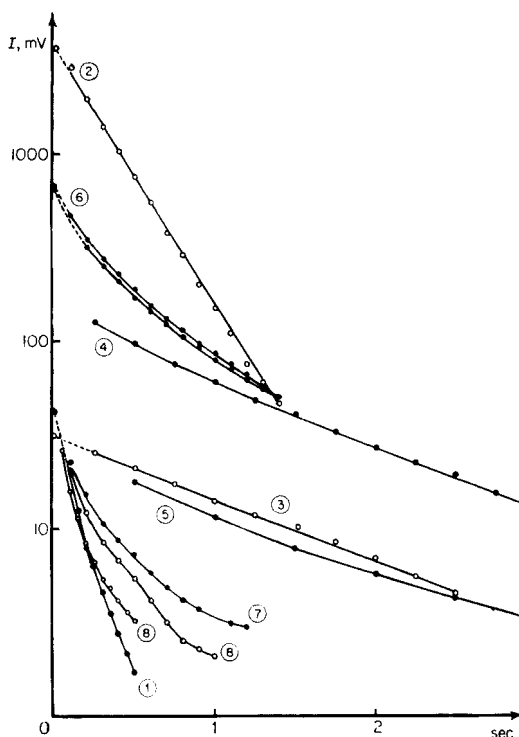


Fig. 5. Decay of deferred luminescence excited by a radiation of 2537 Å. Measured decay,—; extrapolated decay,.....; (1) cytidylic acid; (2) thymine; (3) deoxyadenosine; (4) adenylic acid; (5) guanine; (6) deoxyguanosine; (7) guanylic acid; (8) deoxyribonucleic acid.

by an important ionic component. The stereochemical configuration of nucleic acids should make the migration of electronically excited electrons difficult. In this respect, the molecular view seems more justified than the solid-state view, as has been confirmed experimentally. Not only the polynucleotides but also the nucleotides and the purine and pyrimidine bases, when isolated

from each other, emit an after-glow after optical excitation at low temperatures.<sup>12</sup> Figure 4 shows the excitation and emission phosphorescence spectra of some of the above-mentioned compounds.

Because of these data it was possible to record emission decays following optical excitation. A comparative study of the kinetics of the decay in purines and pyrimidines confirm that the former behave as energy "donors" in the presence of the latter. The polymerization of nucleotides results in an appreciable extinction of their after-glow and the decay-time increases significantly (Fig. 5).

If we study radiative decay kinetics as a function of temperature, we are tempted to conclude that the optical excitation has no part in conduction phenomena, but this would be only a tentative conclusion. The use of more elaborate equipment will perhaps lead to a revision of this conclusion, but it would be surprising if the conductivity of nucleic acids corresponded to expectation. As stated earlier, the atomic vibrations, defects and traps should prevent the migration of free carriers. The possibility of exciton transmission remains, but here again, the structure and the heteroatomic composition of nucleotides are not likely to facilitate this process. On the other hand, optical experimentation shows that each photon absorbed at the level of the bases is partially dissipated, probably as heat. Internal conversion can explain the reversible modifications and the irreversible damage that optically excited nucleic acids undergo. They behave like molecules and not like perfect periodic lattices.

## (2) *Studies with Magnetic Methods*

The systematic comparative study of nucleic acids and components using magnetic methods was made after Blumenfeld's first studies. The most complete attempt we know was made by Blois and Maling.<sup>3</sup> It answers the questions raised by numerous observers on the exact origin of magnetic properties that are generally accepted as far as their existence is concerned. Blois and Maling tried to detect ESR signals in compressed heterocyclic bases. They obtained a positive result and carefully analyzed the heavy-ion content in order to discern whether the magnetism was intrinsic or extrinsic. We shall return to the conclusions of these workers after considering the salient results obtained by such authors as Blumenfeld, Shulman, Ptak, and their collaborators.



In 1958 Blumenfeld and his co-workers at the Institute of Physics and Chemistry in Moscow first published their studies on magnetic properties of DNA, RNA, and their association products with proteins.<sup>4, 5</sup> These complexes are characterized by very wide ESR signals (over 1000 gauss); they are very intense (equivalent to concentrations of about  $10^{20}$ ,  $10^{21}$  spins/gram of substance). Since then, these results have been confirmed by many other workers.<sup>3, 12, 25, 29</sup> An example is given of the ESR curve obtained by Ptak working in our laboratory (Fig. 6).

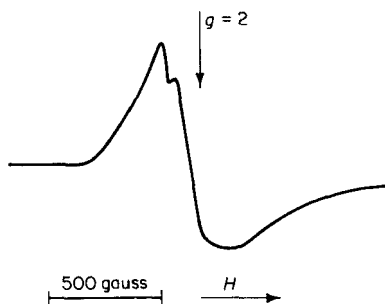


Fig. 6. Electron spin resonance signal of DNA sample.

From the beginning of their experiments, Blumenfeld and his collaborators were trying to relate the structure of nucleic acids to their magnetic characteristics. In treating them at various pH's, temperatures, and ionic concentrations (of sodium chloride), they noticed variations in the intensity and form of ESR signals, corresponding to the different treatments. The same workers have also established the temperature-dependence of these signals.<sup>26, 28</sup> At the same time, the abnormal character of the magnetic properties was observed; some characteristics were similar to those observed in anti-ferromagnetic crystals. On the other hand, measurements of the static magnetic susceptibility showed that magnetic properties were different from those of the ferromagnetic compounds. In fact, no residual moment could be observed after suppression of the magnetic field. Blumenfeld eliminated the possible action of ions of paramagnetic transitions and looked to the very structure of nucleic acids for an explanation of this "pseudo-ferromagnetism". To succeed in this attempt he compiled all theoretical and experimental

data to arrive at a possible explanation of how chemically saturated nucleotides could spontaneously produce free electrons during their polymerization. Considering the intensity of the ESR signals observed, there should be 0.5 to 5 unpaired electrons for each polymerized nucleotide. The range in the number of electrons is related to the "organization" of the nucleic acid; in the native state they produce signals of maximum intensity which decrease with the level of disorganization resulting from the introduction of physical agents of classical use in biochemistry. Similar phenomena have been observed with synthetic polymers.<sup>6,7</sup> According to Blumenfeld, a system of double-bonded hetero-atoms within a polymer chain and the regular and lamellar "lattice" of flat molecules would be necessary for the manifestation of the pseudo-magnetism.

The first thing to be explained is how free electrons are spontaneously produced by organic structures with paired electrons while, normally, such a result can only be reached through optical excitation in the ultraviolet. Blumenfeld worked particularly on the dimerization process of purines and pyrimidines and on the corresponding charge transfer between donor and acceptor molecules. In a charge-transfer complex (CTC) ( $D^+A^-$  configuration) each component has an unpaired electron. In the fundamental electronic state, the formation of a CTC is possible under the condition that

$$I_p - E_A < E_0 \simeq e^2/r_0$$

where  $I_p$  is the ionization potential of donor D,  $E_A$  is the electro-affinity of acceptor A, and  $r_0$  is the distance separating D and A.

The exchange integral of unpaired electrons has been neglected in this formula but it might have an important part in the CTC properties. It is also to be noted that the stability of a CTC is different according to whether it is operated in solution or in the solid state.

Using as a basis the results obtained with synthetic polymers, Blumenfeld estimated that 5 to 10 molecules regularly organized in parallel layers can produce unpaired electrons. He considered the particular case of nucleic acids and critically discussed whether the structural conditions played a part in the existence of unpaired electrons resulting from the interaction of heterocyclic bases.<sup>8</sup>

On this basis, he tried to demonstrate the possibility of the existence of a new class of compounds with electric and magnetic properties specific to the polymer state, its composition, structure and organization. He and his collaborators were not concerned exclusively with DNA but also with synthetic polymers whose properties would not only be mechanical and plastic. On the other hand, the Russian school stands for a technique which consists of a magnetic "test" of the *in situ* activity of nucleic acids.<sup>8</sup>

Discrepancies soon appeared in the interpretation of the magnetic behavior of nucleic acids and scientists noticed differences in this behavior depending on the nature and the preparation of the sample, and the mode of experimentation. Some wondered whether these abnormal magnetic properties were not due to the presence of heavy ions, iron in particular. This is Walsh and Shulman's thesis<sup>29</sup> and it is also Isenberg's.<sup>18</sup>

Blois and Maling<sup>3</sup> were, as far as we know, the first to enumerate the heavy ions present in nucleic acids. These authors worked on purines and pyrimidines subjected to various compression rates and obtained ESR signals for which heavy ions alone can hardly be considered responsible. In these experiments there would occur an exchange between the higher occupied orbital of D and the lower free orbital of A, and the possibility of charge transfer would depend upon the value of

$$S_{D,A} = \int \Psi_D \Psi_A dv$$

where  $\Psi_D$  and  $\Psi_A$  are the wave functions of the orbitals of the donor and acceptor.

At present two interpretations of the magnetism of nucleic acids are proposed: an extrinsic magnetism resulting from iron atoms associated with samples of nucleic acid and intrinsic magnetism linked to the charge-transfer processes at the level of the base plates in the highly organized polymer "domains". In connection with this, Ptak, our collaborator, performed experiments the detailed results and theoretical comments of which will soon be published. He followed the changes of ESR signals in relation to the ageing of DNA and obtained the results shown in Fig. 7. It is to be noted that the factor  $g$  varies between 3 and 2 and that a disymmetry with two peaks only appears after a few days. The integral surface of the curves decreases simultaneously up to a hundredth of its

initial value. Ptak noted that this change was similar to that observed with iron colloids. This analogy gives further support to the fact that the magnetism involved is largely of an extrinsic nature.

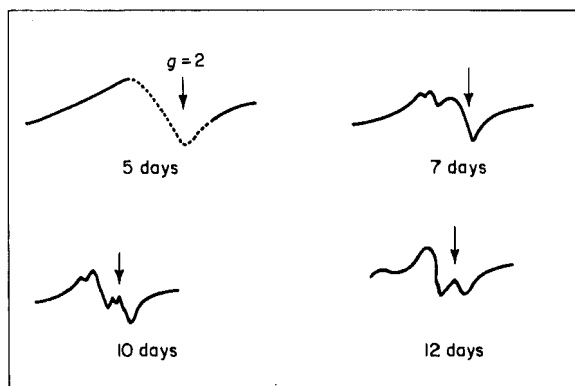


Fig. 7. ESR signals evolution of DNA as a function of time.

### (3) *Direct Research on Supramolecular Electronic Properties*

One of the main approaches is concerned with the dielectric behavior of solid DNA. As already mentioned, Duchesne and Monfils showed that solid samples of DNA behave like piezo-electric compounds.<sup>13</sup> In 1960, Sadron *et al.* noted that DNA did not behave like a normal dielectric substance; the unexpected value of the dielectric constant of solid films, their electric hysteresis and the temperature-dependence of these characteristics could be compared to the behavior of ferroelectric substances. However, scientists hesitated in ascribing these properties to macromolecules<sup>21</sup> and after demonstrating that they were a function of the "degree of crystallinity", they did not eliminate the possibility that processes more common than ferroelectricity were responsible.<sup>11</sup>

One of our collaborators, M. F. Hanss, has been concentrating his efforts during the past few years on electric experimentation. In 1961, he was able to satisfactorily standardize the conditions required for experimentation<sup>12</sup> and arrived at the following conclusions. Electric hysteresis can be produced by interfacial polarization due to the accumulation of ions associated with DNA, thus

explaining why this phenomenon only occurs at low frequencies ( $< 1$  KHz). On the other hand, it is difficult to understand why this non-linearity of ionic origin disappears at around  $60^{\circ}\text{C}$ .

In order to avoid a possible "breakdown" of the DNA film, voltages used are of a few millivolts and experimentation over a wide range of frequencies (50 Hz–25 MHz) makes it possible to eliminate the polarization processes at the electrodes. Under the experimental conditions adopted, the dehydrated DNA resistance, measured in direct current, is about  $10^{12}$  ohms-cm, whereas hydrated DNA (water content of 40% or even 60%) has an abnormally high dielectric constant (see Fig. 8a). Figures 8b and 8c show the values of the dielectric constant of DNA films dehydrated by silica-gel or by primary vacuum. The value of the real part is estimated to be about 5 at  $20^{\circ}\text{C}$ . What is worth noting in Figs. 8b and 8c is the change in slope of the curves  $\log C = F(1/T)$ . It appears that this slope break is due to a "structural transition" affecting DNA molecules; a possible explanation for the sudden change of the dielectric constant beyond the transition point may be found in one of the three following mechanisms:

(1) an anomaly in the thermal expansion coefficient of DNA. Only measurements by micro-dilatometer could possibly confirm this view;

(2) the disappearance of "bound" water or structural water of the DNA. In the absence of data which could be supplied by the thermogravimetric analysis of DNA, it is difficult to take a firm position on this point;

(3) a "steric" transition, corresponding to the disappearance of a highly polarizable structure of macromolecules. We have no evidence of any "spontaneous" DNA polarization and it does not seem probable that such is the case. A sudden variation in the rotatory strength as measured by ultraviolet radiation could perhaps be detected, but even a positive result would not give us any formal evidence of the existence of two different electric structures.

It is known that when the specific heat is measured in terms of temperature in typical ferroelectric compounds, an exothermal "accident" is noted around the Curie point.<sup>15</sup> The only cases in which this behavior is not observed have been shown to depend upon a sudden release of adsorbed water.

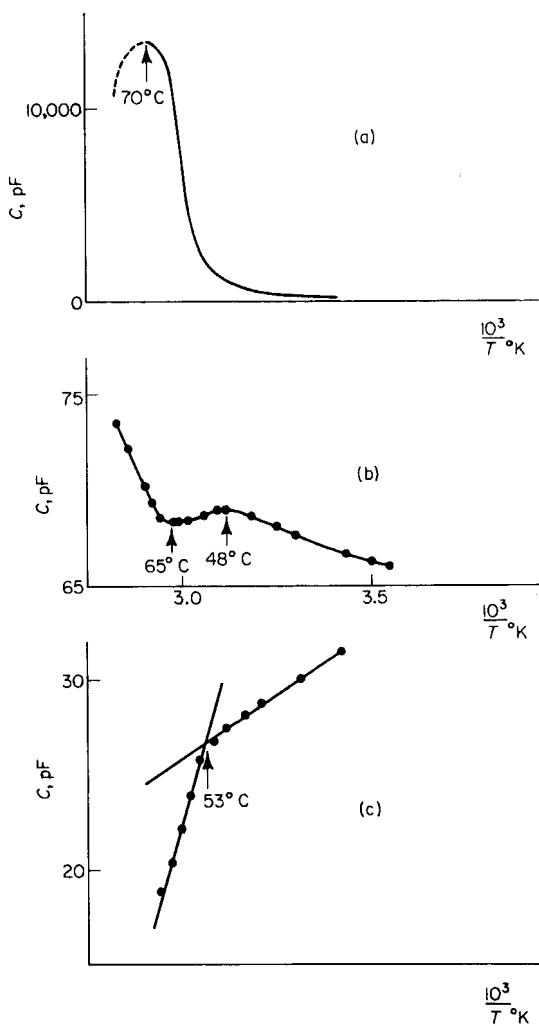


Fig. 8. (a) Capacity variation as a function of temperature; DNA sample of about 40% water-content; (b) sample in equilibrium under silicagel; (c) sample in primary vacuum.

It is to be expected that differential thermal analysis would be a means of studying the eventual transition in DNA in the temperature range where a change in its dielectric properties is observed. But this raises serious difficulties, such as the uncontrolled amount of water in the samples, the subsequent contraction of the test cells, and the heterogeneity of the materials studied.

#### IV. CONCLUSION

The investigation of biological high polymers by techniques which served to study crystalline solids presents serious difficulties on account of the complexity of the systems involved.

Thus, all the isolated components have to be considered first and only after that can the detailed analysis of the nucleic acids, viewed as high polymers, be undertaken successfully. It is certainly the only way to understand how a "submolecular" process can manifest itself in the "supramolecular" level. The study of the physical behavior of nucleic acids is a means of discovering mechanisms explaining the biological properties of these compounds. These mechanisms would be typical of the bonds of all kinds and the forces which characterize the structure.

In this perspective, the analogy between the properties of nucleic acids and those of simple mineral and organic systems will continue to be very profitable for the solution of some of the important problems which have been considered here.

#### References

1. Baudet, P., Berthier, G., and Pullman, B., *Compt. Rend.* **254**, 764 (1962).
2. Blois, M. S., *Free Radicals in Biological Systems*, Academic Press, New York, 1961.
3. Blois, M. S., and Maling, J. E., *Biochem. Biophys. Res. Commun.* **4**, 252 (1961).
4. Blumenfeld, L. A., *Biophysics (USSR)* **4**, 515 (1959).
5. Blumenfeld, L. A., Kalmanson, A. E., and Shen Pei Gen, *Dokl. Akad. Nauk SSSR* **124**, 1147 (1959).
6. Blumenfeld, L. A., Berlin, A. A., Matveeva, N. G., and Kalmanson, A. E., *Vysokomolekul. Soedin.* **1**, 4647 (1959).
7. Blumenfeld, L. A., Berlin, A. A., Glinkin, A. A., and Kalmanson, A. E., *Zh. Strukt. Khim.* **1**, 103 (1960).
8. Blumenfeld, L. A., *Acad. Roy. Belg. Classe Sci. Mem.* **33**, 193 (1961).
9. Debye, P., and Edwards, J. O., *Science* **116**, 143 (1942).

10. Douzou, P., and Thuillier, J. M., *J. Chim. Phys.* **57**, 96 (1960).
11. Douzou, P., Francq, J. C., Polonsky, J., and Sadron, C., *Compt. Rend.* **251**, 976 (1960).
12. Douzou, P., Francq, J. C., Hanss, M., and Ptak, M., *J. Chim. Phys.* **58**, 926 (1961).
13. Duchesne, J., and Monfils, A., *Compt. Rend.* **241**, 749 (1955); Duchesne, J., in *Horizons in Biochemistry*, Academic Press, New York, 1962, p. 335; Read, M., and Duchesne, J., *Compt. Rend.* **257**, 1724 (1963).
14. Duchesne, J., Depireux, J., Bertinchamps, A., Cornet, N., and Van der Kaa, J., *Nature* **188**, 405 (1960).
15. Eisinger, J., Shulman, R. G., and Szymanski, B. M., *J. Chem. Phys.* **36**, 1721 (1962).
16. Eley, D. D., Parfitt, G. D., Perry, M. J., and Taysum, D. H., *Trans. Faraday Soc.* **49**, 79 (1953).
17. Eley, D. D., and Spivey, D. I., *Trans. Faraday Soc.* **58**, 411 (1962).
18. Isenberg, I., *Biochem. Biophys. Res. Commun.* **4**, 252, (1961).
19. Kasha, M., and El Bayoumi, M. A., *J. Chim. Phys.* **58**, 916 (1961).
20. McGlynn, S. P., *Radiation Res. Suppl.* **2**, 300 (1960).
21. Polonsky, J., Douzou, P., and Sadron, C., *Compt. Rend.* **250**, 3414 (1960).
22. Ptak, M., Ropars, C., and Douzou, P., *J. Chim. Phys.* **59**, 659 (1962).
23. Pullman, A., and Pullman, B., *J. Chim. Phys.* **58**, 904 (1961).
24. Robinson, G. W., in *A Symposium on Light and Life*, McElroy and Glass, Eds., Johns Hopkins Press, Baltimore, 1961.
25. Sadron, C., Les propriétés physiques de l'acide désoxyribonucléique en solution, Congrès Solvay, Bruxelles, 1959.
26. Sehn Pei Gen, Blumenfeld, L. A., and Kalmanson, A. E., *Biophysics (USSR)* **5**, 645 (1960).
27. Szent-Györgyi, A., *Bioenergetics*, Academic Press, New York, 1957.
28. Vozvyshaeva, L. V., and Blumenfeld, L. A., *Biophysics (USSR)* **5**, 579 (1960).
29. Walsh, W. M., Jr., Shulman, R. G., and Heidenreich, R. D., *Nature* **192**, 1041 (1961).
30. For a general discussion of energy transfer with special reference to biological systems see *Discussions Faraday Soc.* **27** (1960).



## 10

# THE PROPERTIES OF METAL-PORPHYRIN AND SIMILAR COMPLEXES

P. S. BRATERMAN, R. C. DAVIES, and R. J. P. WILLIAMS,  
*Inorganic Chemistry Laboratory, Oxford University, Oxford, England*

## CONTENTS

I. Introduction . . . . .	360
II. Properties of Metal Complexes . . . . .	360
A. The Metal (Octahedral Field) . . . . .	360
B. Ligand-Field Transitions and the Spectrochemical Series . . . . .	363
C. The Nephelauxetic Series . . . . .	364
D. Change of Spin State . . . . .	365
E. Thermodynamic Factors . . . . .	366
F. Kinetic Effects . . . . .	367
G. Charge Transfer Spectra . . . . .	368
III. The Complexes of Dimethylglyoximate, DMG . . . . .	369
A. Crystal Structure of DMG Complexes . . . . .	369
B. Spectra of Complexes of DMG . . . . .	371
C. Thermodynamic Effects . . . . .	374
D. High and Low Spin States in Equilibrium . . . . .	375
IV. The Reactivity of Ligands . . . . .	376
A. Conjugation with Metals . . . . .	376
B. The Action of Light . . . . .	379
C. Summary of Reactivity . . . . .	379
V. Energy Levels of Ligands . . . . .	380
A. Spectra of Conjugated Organic Ligands . . . . .	380
B. The Effect of Substitution in Pyrrole Rings . . . . .	385
C. Metal Substituents in Phthalocyanines . . . . .	387
D. Metal Substituents in Porphyrins . . . . .	389
E. Spectra of Haemin Derivatives—Effects of <i>z</i> -Axis Ligands . . . . .	394
F. Restrictions upon Ring Conjugation . . . . .	397
G. The Spectra of Conjugated Chains . . . . .	398
H. The Corrins . . . . .	399
VI. Chemical Reactions . . . . .	402
A. Chemical Reactivity of Ring Chelates . . . . .	402
B. Reactions of Some Biologically Important Complexes . . . . .	404
C. Photochemistry of Porphyrin-Like Compounds . . . . .	404
References . . . . .	405

## I. INTRODUCTION

The purpose of this article is to describe recent work, mainly our own measurements, on complex ions which contain a central metal ion, copper or iron for example, a group of four ligands in a plane, such as is provided by a porphyrin or phthalocyanine molecule, and one or two other ligands which are placed above and below the plane so as to complete a rough octahedron around the metal. The article is to be read as an extension of views previously expressed by us.<sup>38, 39</sup> The compounds of this kind of most notable biological importance contain magnesium (the chlorophylls), iron (the haem compounds), and cobalt (the cobalamins), but it may well be that some copper- and vanadium-containing systems are not very different from these in stereochemistry. Rather than to tackle immediately the problem of the biological molecules themselves we have tended first to study related series of molecules containing the same metals but much simpler ligands. In this way we have avoided some difficulties attending the study of metal porphyrins, for example the low solubility, the polymerization, and the difficulty of observing parameters of the metal electrons (ligand field and charge transfer absorption bands) in the presence of the bands of the ligands themselves. The main ligand which has been used by us is dimethylglyoxime. In order to appreciate this work and its relationship to biological problems we shall build slowly from the properties of simple model systems to a discussion of naturally occurring molecules. First we shall concentrate upon the properties of the *metal ions* in complexes, then we shall look at the properties of the *ligands* found in biological systems or ligands very similar to them and finally we shall study the combination of these ligands with metals, firstly in *model compounds* and secondly in *biologically important molecules*.

## II. PROPERTIES OF METAL COMPLEXES

### A. The Metal (Octahedral Field)<sup>26</sup>

The essential electron orbitals of metals in which we are interested are  $3s$  or  $4s$ ,  $3p$  or  $4p$ , and  $3d$ . In a complex of octahedral ligands the three directions,  $x$ ,  $y$ ,  $z$  are equivalent so that the three  $p$  orbitals are degenerate. The electron affinities of the  $s$  and  $p$  orbitals of elements

at the beginning of transition series are low but this is by no means the case towards the end of the series. Thus an ionic model may serve well for Ca(II) or even perhaps Mg(II) complexes but will not suffice for the discussion of the properties of ions such as Co(III), Fe(II) or Fe(III). Again the  $3d$  orbitals are of low electron affinity in ions early in the periodic table, e.g. Mg(II), so that bonding through them is of little interest, but these same orbitals contract and become of high electron affinity and correspondingly greater importance in the chemistry of metals such as Fe and Co. In octahedral symmetry the  $d$  orbitals are split into a group of two,  $e_g$ , and a group of three,  $t_{2g}$  (Fig. 1). The separation between the two sets of orbitals implies a polarisation of the ground state of the central ion. This polarisation gives a stabilization energy to the ground state and gives rise to a set of low lying excited states. Optical transitions, so-called  $d-d$ , between the ground and excited states generate a set of ligand field splitting parameters,  $\Delta$ , specific to a complex. We wish to use the parameters as an aid to the study of chemical bonding. The polarisation energies of the central cation, to which they are related, are a function of the field of the ligands, but unfortunately this field is in turn very sensitive to the polarisation of the ligand by the cation. Thus we are in a dilemma: we wish to divide the properties of a complex into ligand and cation dependencies while in reality these properties are not independent. The approach adopted is therefore empirical—making observations and seeing how they are accounted for by a particular model for the interaction. The molecular orbital model for a ligand field has proved the most satisfactory. It is described in detail in an earlier chapter of this volume. In Figs. 1 and 2 we show how the orbitals of the ligand interact with the orbitals of the cation. The resulting set of energy levels is now to be filled by ligand and cation electrons, making no distinction between them, so as to give the observed number of unpaired electrons. The study of magnetic properties shows how many this is. We can subsequently examine the absorption spectrum of the complex. The intensity and position of bands allow us to relate most spectroscopic bands of transition metals to certain configurational changes between the states in the figures. There are two main types of spectroscopic change possible. The first is a transition from molecular orbitals originating from one set of  $d$  orbitals,  $t_{2g}$ , to orbitals originating from a second set  $e_g$  and is as such

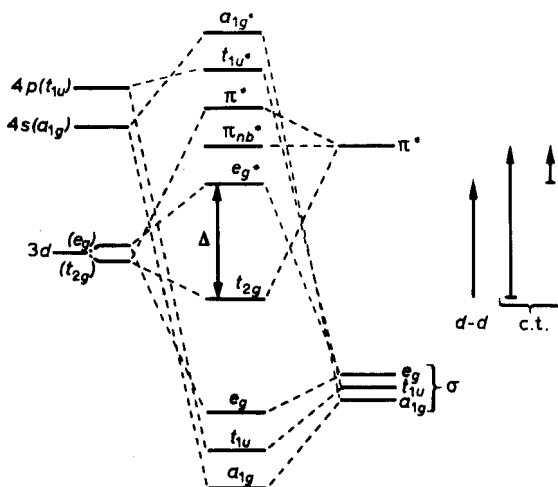


Fig. 1. Energy level diagram for an octahedral complex. The labellings are conventional starting with the isolated cation levels on the left and the isolated ligand levels on the right. Second from left crystal field splitting is introduced and third from left the levels in molecular orbital theory are developed. The interesting transitions for this, the case of an unsaturated ligand, are shown on the extreme right.

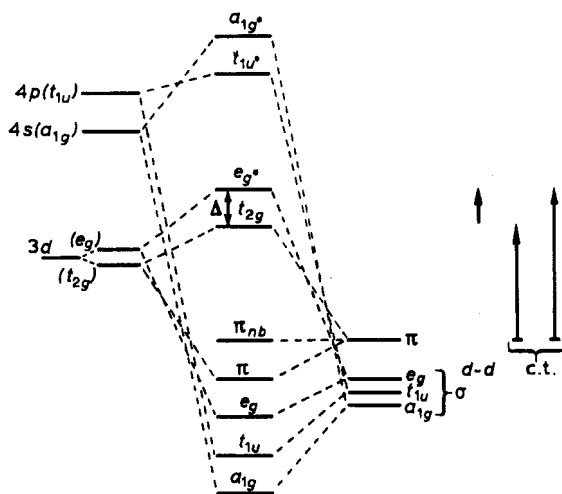
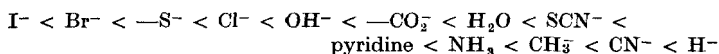


Fig. 2. The figure is similar to Fig. 1, but is the level diagram for saturated ligands.

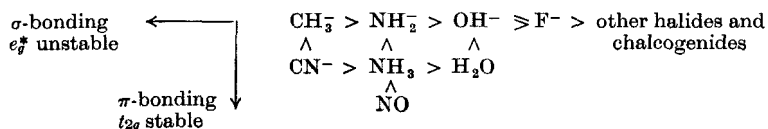
forbidden by the selection rules of atomic spectroscopy. Mixing of the orbitals with ligand orbitals on coupling with vibrations does permit the transitions as would certain deviations from a centre of inversion. We shall describe these  $d-d$  transitions and information related to them first. The second set of transitions is generally termed charge transfer, c.t., and involves the transfer of an electron from an orbital which was closely related to a ligand or a metal level to an orbital which originated from an orbital belonging predominately to the other partner (Fig. 1). There are two possibilities here, charge transfer from and to a ligand, and both are well recognised (see below). The distinction between the two types of transition,  $d-d$  and charge transfer, is only clear cut in ideal circumstances but nearly always provides a basis for classification.

### B. Ligand-Field Transitions and the Spectrochemical Series

These transitions are important as their relative energies are characteristic of particular ligands. Their order of energy,  $\Delta$ , is to a first approximation independent of cation. This order, of increasing energy of the first spectroscopic transition, is roughly



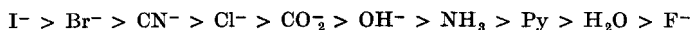
(The excitation is indicated by  $\Delta$  in Figs. 1 and 2.) This series, the spectrochemical series, is not a simple one. It tells us something about the ligands through their effect upon electronic states of cations. The extreme members on the left are  $\pi$ -donors to the  $t_{2g}$  orbitals while the extreme members on the right are either  $\pi$ -acceptors or strong  $\sigma$ -donors or both. The spectroscopic parameter,  $\Delta$ , represents either a transition from  $t_{2g}$  bonding orbitals to  $e_g$  anti-bonding orbitals for unsaturated ligands (Fig. 1) or from  $t_{2g}$  anti-bonding orbitals to  $e_g$  anti-bonding orbitals for saturated ligands (Fig. 2). It is hardly surprising then that the spectrochemical series can be re-arranged in terms of the periodic table



Ligands such as sulphide fall low in the series. The excited state is relatively more stable the better the  $\pi$ -donor character of the ligand and the worse its  $\sigma$ -donor properties while the reverse is true of the ground state. The spectrochemical series thus measures a complicated difference between one electron configuration and another, and is not specifically related to any single characteristic of the ligand. Ligands high in the spectrochemical series either strongly stabilize  $t_{2g}$  electrons (CO) or strongly destabilize  $e_g$  electrons ( $H^-$ ). We must use our general knowledge of the nature of the ligands to decide which effect is most powerful. We are helped in this by a second spectroscopic series—the nephelauxetic series.

### C. The Nephelauxetic Series<sup>20</sup>

In cations which have many  $d$  electrons, and even in a pure octahedral field, there is more than one transition possible between the set of  $t_{2g}$  orbitals and the set of  $e_g$  orbitals. Of considerable interest are two transitions to states which do not differ in spin or in any respect other than the electron repulsion terms of the cation, i.e. they have the same ligand field splitting energy. The differences in energy between the two transitions can then be described in terms of Racah parameters which have known values in the free ions. This term-term splitting causes the spectrum observed for the free gas ions of transition metals. It arises from electron-electron repulsion in the ions and naturally enough the bigger this repulsion the bigger the splitting between different configurations. In the free ion there is a relationship between these electron-electron repulsion energies and another electron-electron repulsion, that opposing spin pairing (see below), which may also be described in terms of Racah parameters. The terms in the free ion may be usefully related to terms in the complexes but it is found that the Racah parameters in complexes have smaller values than in the free gas ions. Ligands may now be arranged in the order, the nephelauxetic series, in which they reduce the Racah parameters. The order is very roughly

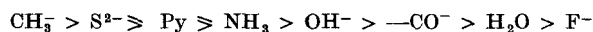


Again this is not a simple series. We see that highly polarisable groups are now at the beginning of the series giving the greatest reduction in electron-electron repulsion although these ligands

produced relatively little ligand field splitting. We cannot deal with the significance of the Racah parameter reduction here but we shall take it that it measures, somewhat roughly, the polarisability of the ligand. A readily polarisable ligand will adjust itself to the electronic states of the cation, readily giving or taking electron density as required. Thus ligands high in the nephelauxetic series but relatively low in the spectrochemical series may well bring about stabilization of excited electronic configurations, e.g. spin paired states. We shall consider spin pairing next.

#### D. Change of Spin State

The energy difference between spin states of a cation, i.e. whether or not  $t_{2g}$  orbitals are doubly occupied before  $e_g$  orbitals are singly occupied, can also be represented in terms of Racah parameters and a function of the field. In order for a ligand to force a change of spin state it must either considerably reduce internal electron-electron repulsion (nephelauxetic effect) or produce a large field (spectrochemical effect). The order in which ligands are effective in promoting changes in spin state in simple complexes, which is independent of cation (roughly), would appear to be

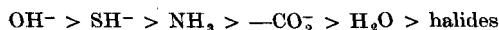


Not unexpectedly this further series of ligands is neither the same as that found for ligand field splitting nor as that for reducing electron-electron repulsion, but is some combination of them. So far, then, we have three ligand series which are observed to control certain properties of cations but which cannot be clearly understood without reference to polarisation,  $\sigma$ -bonds,  $\pi$ -bonds and electrostatic field effects.

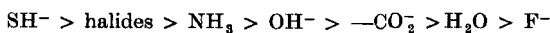
In many systems, especially those of biological importance, the difference in stability between spin states is similar to  $kT$  with the result that complexes are equilibrium mixtures of spin states.<sup>2, 39</sup> The situation is particularly common in iron (both Fe(II) and Fe(III)) and cobaltous complexes but is virtually unknown in cobaltic complexes. We have discussed the magnetic moments of iron complexes in detail elsewhere.<sup>39</sup> A different approach to the problem is given by Schoffa in this volume.

### E. Thermodynamic Factors<sup>40</sup>

There is also a wealth of thermodynamic data about the ligands. For instance the basicity of most simple *saturated* coordinating groups which are likely to be present in biological systems is known. The basicity order for some groups is



We also know the change in stability of complexes of a fixed ligand from an A-metal, e.g. Sr(II), to a B-metal cation, e.g. Hg(II), of approximately the same size. Roughly it is



(Unsaturated ligands such as cyanide are not included in this series as they form considerably more stable complexes with transition metal cations than with either of the A- or B-subgroup ions). The two series of saturated ligands differ from one another much as the spectrochemical series differed from the nephelauxetic series. We can explain this rough parallel with very simple arguments. The sequence of acid dissociation constants is probably quite a good guide to the  $\sigma$ -bond strength of an unperturbed ligand, though naturally the heat of this reaction would be a still better guide. The sequence of stability constant differences between A- and B-subgroup metals is not similar since it contains a term more strongly dependent upon the polarisation of the ligand by the cations. The most polarisable anions are those of the heavier elements. Polarisation also increases as charge on a ligand increases and the earlier the element is in any row of the periodic table. Differences in behaviour between A- and B-subgroup elements then arise largely from the greater polarising power of the B-subgroup element. The order of stability for A-subgroup complexes is more like that of the proton.

Unsaturated ligands such as cyanide differ again in thermodynamic properties from the ligands already mentioned as can readily be seen from Figs. 1 and 2. The term "unsaturation" is used here in a slightly generalized sense;  $\text{SR}_2$  and  $\text{PR}_3$  have low lying empty  $3d$ -orbitals which function in the same way as the ligand  $\pi^*$ -states of Fig. 1 and are therefore included by this term. The stability of a metal-ligand complex can be understood



from this diagram partly in terms of the number of bonding and anti-bonding electrons. In the later transition metal cyanides, the  $t_{2g}$  metal orbitals are full and rather exposed to the empty ligand  $\pi^*$  states. These states will then stabilize the electrons in  $t_{2g}$  orbitals. As the number of the electrons increases along the transition series so the electrons tend to disappear into the core of the cation. After the end of the transition series the  $d$  states can no longer interact strongly with the ligand  $\pi^*$  states. Thus the  $t_{2g}$  electrons are stabilized by unsaturated ligands in the transition series but not very much outside it. On the other hand anionic ligands which are saturated will tend to destabilize the same  $t_{2g}$  metal electrons and, especially in the first transition series, these anions (halides) are not strongly bound.

### F. Kinetic Effects<sup>3</sup>

A final ligand series of importance is that which gives the labilizing power of ligands  $X$  on groups  $Y$  placed *trans* to  $X$ . The series is



This series is of importance in the cobalamins (see later). It is once more a confusion of the nephelauxetic and spectrochemical series. The series is only important in low spin complexes as the rates of replacement of ligands around a high spin ion are very fast. Apart from substitution reactions there are electron transfer reactions of these complexes in which the central cation changes its oxidation state without gain or loss of ligands. Ligands which are polarisable or unsaturated are more effective bridge groups for electron transfer than ligands such as water or fluoride.

From all this empirical information, backed by the qualitative reasoning of molecular orbital theory, we can see that there are three features of a ligand which we need to appreciate in order to understand its interaction with a metal. They are (1) its permanent dipole, polarity, (2) its polarisability and (3) its unsaturation. We use acid dissociation constant values as a guide to (1); the nephelauxetic series and general stability data for B-metals as compared with protons is used as a guide to (2), and a combination of these series with the spectrochemical series as a guide to (3). Of course a great deal is known from organic chemistry about the ligands also. At the same time we note that the importance of the three terms

depends somewhat on the metal with which the ligand is combined. Most of the metals with which we are concerned are strong  $\sigma$ -acceptors, strongly polarising, and are  $\pi$ -donors. However, the ferric ion, in particular is exceptional as we shall show later (Section III-B).

We have refrained from a discussion of magnetic parameters in these compounds since these are to be discussed in other chapters in this volume (see Schoffa and Kotani).

### G. Charge Transfer Spectra<sup>20, 41</sup>

Apart from the transitions of the  $d$  electrons there are also transitions of the ligands themselves (see next section) and transitions which can only be described in terms of orbitals of both ligand and metal. The most important of the latter are the so-called charge transfer transitions (Figs. 1 and 2). The theory of these transitions has been reviewed recently.<sup>41</sup> For the purposes of this article the two important cases are charge transfer from a ligand to a metal ion and charge transfer to a ligand from a metal ion. Both of these transitions are described in Figs. 1 and 2. We draw special attention to the transitions  $e_g^* \rightarrow [\pi_L^*]_{n.b.}$ ,  $t_{2g} \rightarrow [\pi_L^*]_{n.b.}$  to the ligand, and  $[\pi_L]_{n.b.} \rightarrow t_{2g}$ ,  $[\pi_L]_{n.b.} \rightarrow e_g^*$ ,  $[\pi_L] \rightarrow t_{2g}$ ,  $[\pi_L] \rightarrow e_g^*$  to the cation. The energy of charge transfer to a ligand will be smaller the greater the acceptor power of  $\pi_L^*$  (smaller the greater the oxidising power of the ligand in general) and the higher the  $t_{2g}$  levels.  $t_{2g}$  orbitals are raised in energy in *low spin states* and in metal ions of low charge. Not surprisingly we find charge transfer spectra of greatest interest to us in low spin Fe(II) and in Cu(I) complexes. The reverse charge transfer requires a hole in the  $t_{2g}$  or  $e_g$  states and that these states should be good acceptors. Unlike the previous case the metal should be a good oxidising agent. Such a combination is given by the ferric ion (high or low spin) with such ligands as phenolates.

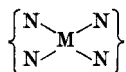
One last example of charge transfer will concern us. In the molecule  $\text{BeCl}_2(\text{dipy})$  an absorption band is observed in the near ultra-violet which is not recognisably that of the ligand.<sup>7</sup> It has been suggested that it is a charge transfer of the electrons associated with the chloride anion to the ligand. This type of electron transfer could be exceedingly important in biologically interesting complex ions, e.g. chlorophyll.

We have now considered all the major parameters of interest obtainable from the chemistry, and especially the spectra, of simple complex ions. We shall next use these parameters in a treatment of the complexes of a "simple" ligand, dimethylglyoximate, DMG, before going on to consider biologically interesting molecules. We shall begin with a description of the structure of some DMG molecules indicating their relevance to our problems.

### III. THE COMPLEXES OF DIMETHYLGLYOXIMATE, DMG

#### A. Crystal Structure of DMG Complexes

The crystal structure of the complexes of nickel, palladium, platinum and cupric dimethylglyoxime have been established. The complexes, but for the last, are planar. The central group is



which has an obvious similarity to the structure of the central atoms of metal porphyrins and phthalocyanines. Moreover, the ligands carry one negative charge each. Working from this structural similarity we have used the molecules of ferrous oximes combined with further ligands along the *z*-axis (Fig. 3) as models for the haem-complexes. Of particular interest is the full structure determination of  $\text{Fe}(\text{nioxime})_2(\text{imidazole})_2 \cdot 2\text{H}_2\text{O}$  for it shows the preferred orientation of the imidazole groups in the absence of a protein.<sup>29</sup> The imidazoles are coordinated so that the plane containing them cuts the plane of the ferrous nioxime at an angle of about  $40^\circ$  to the  $\text{N}-\text{Fe}-\text{N}$  bonds. The water molecules in the compound form hydrogen bonds with the nitrogens not bound to the metal. The structure suggests that the most stable arrangement of the imidazoles is at about  $45^\circ$  to the  $\text{N}-\text{Fe}-\text{N}$  bonds. The benzimidazole of vitamin  $\text{B}_{12}$  subtends about the same angle, but the imidazole of myoglobin is oriented at a presumably unfavourable and much smaller angle. There could be two causes for this disposition—steric hindrance with the protein and strong hydrogen bonding of the imidazole to further protein groups. The metal–nitrogen distances in the above structure (low spin iron) are all very close to 2.00 Å, about 0.1 Å shorter than the distances in high spin ferrous

complexes but very close to those in ferric complexes.<sup>42</sup> This brings out the general problem in proteins—the difficulty of matching the steric requirements of the metal and the protein simultaneously. The steric hindrance is dependent on the spin state of the cation.<sup>18</sup>

A comparison between metal-free, nickel, and platinum phthalocyanines, which have very similar structures,<sup>30</sup> shows that not only are the metal to ligand bond distances variable but also that the non-metal–non-metal distances in the ligand change with the coordinated metal atom. This observation is in keeping with the

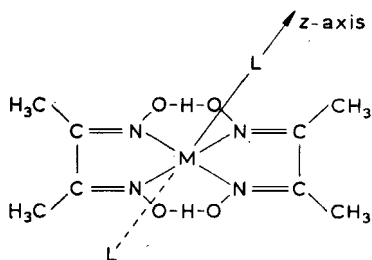


Fig. 3. The structure of iron dimethylglyoximate complexes.

general thesis of this article that metal atoms considerably modify the properties of the ligands to which they are bound.

Apart from the molecular unit of such molecules as a metal dimethylglyoximate we are also concerned with the way in which they pack in a crystal and interact with molecules along the *z*-axis. A simple example demonstrates the importance of this packing. In the crystal of cupric dimethylglyoximate the metal atoms of one molecular unit bind to the oxygen atoms of ligands belonging to a second unit. The cupric cation clearly has considerable electron affinity perpendicular to the plane of the molecule. In the nickel compound the binding between molecules is due to metal–metal interaction. The electron affinity perpendicular to the plane is greater in cupric. This is a general observation—five coordination is observed more frequently in cupric and low spin cobaltous complexes than in low spin nickel complexes. In this respect the binding of copper to an acetylacetonate derivative is interesting.<sup>16</sup> An interaction perpendicular to the plane of the molecule with an adjacent molecule has been observed. The cupric ion in this case

binds weakly to the methene bridge carbon of the next molecule. *Presumably this carbon atom must be polarised in a negative sense in the crystal.* The interaction with acetylacetonate is taken a stage further in the trimethyl-platinum complex where a direct metal to carbon bond is formed. A series of complexes where intermolecular bonding is obviously of similar importance is the metal phthalocyanines. The crystal structures show that each metal binds to the bridge "methene" nitrogen of the next molecule.<sup>30</sup> Fortunately in the phthalocyanines many different metals can be studied in crystals of a fixed geometry so that out of plane bonding can be compared and its effects on some simple physical properties studied.

Having established the relevance of the structures of dimethylglyoximate complexes to the problem of square co-planar complexes in biological systems in general we shall pursue their physical properties further.

### B. Spectra of Complexes of DMG<sup>9</sup>

The weakly tetragonal cobaltic complexes of dimethylglyoximate,  $\text{Co}(\text{DMG})_2\text{X}_2$ , have their first ligand field absorption bands, extinction coefficients 100–150, below 500 m $\mu$  (20,000  $\text{cm}^{-1}$ ), where  $\text{X}$  is any one of the groups ammonia, imidazole, cyanide, aromatic amines or hydroxide. The transitions are  $^1A_{1g} \rightarrow ^1T_{1g}$ , where we use octahedral labellings still, despite the effectively tetragonal field. When  $\text{X}$  is chloride (more strongly tetragonal) there is a band at 610 m $\mu$ ,  $\epsilon_{\text{max}} = 200$ . Presumably this is the first forbidden  $d-d$  transition of this tetragonal complex. The  $d-d$  splitting effect of DMG can now be estimated from a comparison between the  $\text{Co}(\text{DMG})_2\text{Cl}_2$  and the  $\text{Co}(\text{en})_2\text{Cl}_2$  complexes. The order of splitting (spectrochemical series) is  $\text{CN}^- > \text{DMG}^- > \text{en}$ . There is also a very weak band in all the  $\text{Co}(\text{III})$  complexes at about 750 m $\mu$  ( $\epsilon = 1$ ) which we take to be the spin forbidden  $d-d$  transition  $^1A_{1g} \rightarrow ^3T_{1g}$ . The effect of  $z$ -axis ligands on the  $d-d$  transitions in dimethylglyoximates can also be demonstrated from the spectra of the cupric complexes.<sup>25</sup> The first  $d-d$  transition is at 400 m $\mu$  (25,000  $\text{cm}^{-1}$ ). On forming the complex  $\text{Cu}(\text{DMG})_2\text{X}$ , where  $\text{X}$  is  $\text{OH}^-$ ,  $\text{NH}_3$ , Py, the first band moves into the visible. Now the spectrum of the cobaltic complex,  $d^6$  and low spin, arises from the transitions from the  $t_{2g}$  to the  $e_g$  levels. The cupric transitions (very strongly

tetragonal) can be either of this kind or from one  $e_g$  level to another, i.e.  $d_{z^2} \rightarrow d_{x^2-y^2}$ . The second transition will be very sensitive to the  $z$ -ligand and will be expected to move to longer wavelengths the greater the field in the  $z$ -direction, the weaker the tetragonality. This is observed. The actual order is not that of the spectrochemical series. It is, for example,  $\text{H}_2\text{O} < \text{OH}^- < \text{NH}_3$ , as expected.

The ferric complexes,  $[\text{Fe(III)(DMG)}_2\text{X}_2]$ ,  $d^5$ , are largely low spin—a further indication of the strength of the field of this ligand. Their spectra are remarkably different from those of the cobaltic

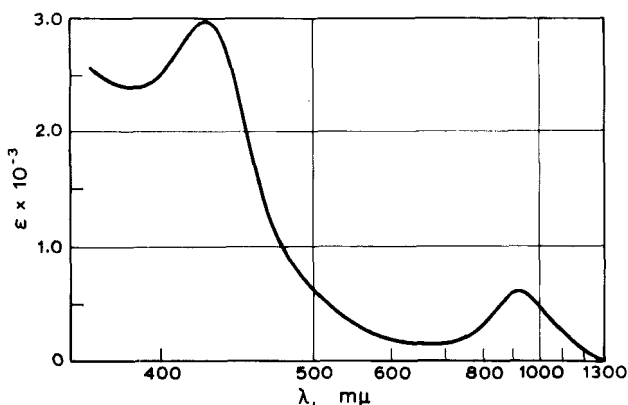
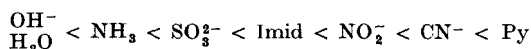


Fig. 4. The spectrum of a typical ferric dimethylglyoximate complex.

complexes. There is an intense band  $\epsilon_{\max} = 3 \times 10^3$  at about 410  $m\mu$  ( $24,500 \text{ cm}^{-1}$ ), which can hardly be a  $d-d$  transition. There is also a second weaker band,  $\epsilon_{\max} = 600$ , at about 700–1100  $m\mu$  ( $9000\text{--}14,000 \text{ cm}^{-1}$ ). See Fig. 4. We attribute both these bands to charge transfer from the ligand to the hole in the  $t_{2g}$  orbitals for the following reasons: (1) The ligand  $\text{DMG}^-$  is strongly reducing. More weakly reducing ligands such as dipyriddy give with ferric (low spin) a first charge transfer band at 600  $m\mu$  ( $17,000 \text{ cm}^{-1}$ ). The intensity of the long wave bands is about  $10^3$  in both cases. (2) The only other transition feasible is a  $t_{2g}(xz, yz) \rightarrow t_{2g}(xy)$ . Now this transition will only be at such short wavelengths ( $\sim 10,000 \text{ cm}^{-1}$ ) if the tetragonal field strength is considerable. The cobaltic spectra allow an estimate of this field tetragonality as approximately  $1000\text{--}2000 \text{ cm}^{-1}$ .<sup>9</sup> There is thus relatively little splitting of the  $t_{2g}$  levels.<sup>3</sup> The band

positions of the longer wavelength charge transfer peaks follow the order of the *z*-axis ligands of the ferric complexes.



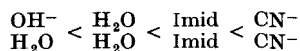
This order is that which could be expected to facilitate charge transfer to the metal. It can be compared with the opposite order of

TABLE I. Band Positions (mμ) in Ferric Dimethylglyoximate Complexes

Compound <sup>a</sup>	Acid form		Alkaline form	
	$\lambda_{\text{max}}$	$\lambda_{\text{max}}$	$\lambda_{\text{max}}$	$\lambda_{\text{max}}$
Fe(DMG) <sub>2</sub> (CN <sup>-</sup> ) <sub>2</sub>	400	950	423	1075
Fe(DMG) <sub>2</sub> (Imid)(HPO <sub>3</sub> <sup>2-</sup> )	405	950	—	—
Fe(DMG) <sub>2</sub> (Imid)(NO <sub>2</sub> <sup>-</sup> )	—	940	—	960
Fe(DMG) <sub>2</sub> (Imid)(CN <sup>-</sup> )	418	930	420	970
Fe(DMG) <sub>2</sub> (Imid) <sub>2</sub>	385–410	920	400	1025
Fe(DMG) <sub>2</sub> (Imid)(SO <sub>3</sub> <sup>2-</sup> )	435	870	—	—
Fe(DMG) <sub>2</sub> (NH <sub>3</sub> ) <sub>2</sub>	395	850	405	950
Fe(DMG) <sub>2</sub> (H <sub>2</sub> O)(OH <sup>-</sup> )	464	685	—	—

<sup>a</sup> Imid is imidazole. A similar table can be drawn up for nioxime complexes.

effect of *z*-axis ligands in charge transfer from Fe(II) to DMG in Fe(II)(DMG)<sub>2</sub>X<sub>2</sub> which is NH<sub>3</sub> ≧ Imid > Py > CN<sup>-</sup>.<sup>19</sup> This example of opposed charge transfer shifts is to be compared with that in other series of iron complexes.<sup>36</sup> Charge transfer in the ferric complex is easier in alkaline solution where the ligand is further ionized, and its intensity is also increased. A similar charge transfer spectrum is observed in the complex Fe(bis-salicylaldehyde ethylenedi-imine)XY, another tetragonal low spin ferric complex. The position of the charge transfer band is at longer wavelengths for different XY:



i.e. the order of ligand effects is much as before.<sup>9</sup> We shall observe the same band order in ferric-haemoproteins. It should be noted

that a di-anion of a porphyrin would be expected to be a better reducing agent than dipyridyl.

### C. Thermodynamic Effects<sup>1,9</sup>

The most obvious thermodynamic property of interest to us is the stability of ligands bound on the *z*-axis to a metal complex planar group. This stability is not just dependent upon the metal and its valence state, but is also dependent on whether the groups above and below the plane interact strongly with one another (the *trans* effect) or interact strongly with the planar ligand itself (the *cis* effect). In previous articles we have stressed that all these effects can be observed in the simple dimethylglyoximates. We shall not concern ourselves further here with these observations nor with studies of the relative stability of the oxidation states of a given

TABLE II. Acid Dissociation Constants,  $pK_a$ , of Oxime Complexes<sup>a</sup>

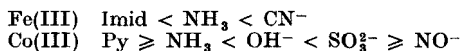
Compound <sup>b</sup>	$pK_a$	Solvent
Fe(Niox) <sub>2</sub> (Imid) <sub>2</sub>	9.15	25% dioxan/water
Fe(DMG) <sub>2</sub> (Imid) <sub>2</sub>	9.6	
Fe(DMG) <sub>2</sub> (NH <sub>3</sub> ) <sub>2</sub>	10.2	
Fe(Niox) <sub>2</sub> (Imid) <sub>2</sub>	8.6	water
Fe(Niox) <sub>2</sub> (Imid)(CN <sup>-</sup> )	9.65	
Fe(Niox) <sub>2</sub> (H <sub>2</sub> O)(OH <sup>-</sup> )	> 11.0	
Fe(Niox) <sub>2</sub> (CN <sup>-</sup> ) <sub>2</sub>	> 11.0	
Co(DMG) <sub>2</sub> (NH <sub>3</sub> ) <sub>2</sub>	10.4	water
Co(DMG) <sub>2</sub> (Py)(Cl <sup>-</sup> )	10.5	
Co(DMG) <sub>2</sub> (Imid)(Cl <sup>-</sup> )	> 10.5	
Co(DMG) <sub>2</sub> (OH) <sub>2</sub>	> 11.0	

<sup>a</sup> For further observations see Ref. 1.

<sup>b</sup> Niox is nioxime; DMG, dimethylglyoxime; Imid, imidazole; Py, pyridine.



metal as affected by changes in the  $z$ -axis ligands. Instead we shall concentrate attention upon the stability of the planar ligand itself, asking what thermodynamic properties of it we can measure and how these properties are altered by changes in the cation or the  $z$ -axis ligands. The simplest thermodynamic property which we can measure is an acid dissociation constant. In  $\text{Fe(III)(DMG)}_2\text{X}_2$  or  $\text{Co(III)(DMG)}_2\text{X}_2$  the acid dissociation of the  $\text{N—OHO—N}$  can be studied. We have found the range of  $\text{p}K_a$  values (Table II),



These orders will be discussed again in relation to the dissociation constants of vitamin  $\text{B}_{12}$  derivatives. The  $\text{p}K_a$  value for  $\text{Fe(II)}$  complexes is very high,  $> 12.0$ . Thus the  $\text{p}K_a$  depends on the charge on the cation and on the  $z$ -axis ligands. The lower the central charge the more difficult is the ionization; and the greater the electron donor power of the  $z$ -axis ligand at fixed charge the higher the  $\text{p}K_a$  (see the spectrochemical and nephelauxetic series).

#### D. High and Low Spin States in Equilibrium 2, 22, 23, 38, 39

So far we have discussed each cation as if it had a single set of parameters which could be used to understand its properties in all circumstances. We have used as parameters size, electronegativity, ionization potential, and have referred to the electron configuration. Now transition metal cations have a duplicity of nature—they are typical schizophrenics. In certain situations, for example, the ferrous ion in aqueous solution has the following properties: (1) 4 unpaired electrons; (2) rapid exchange of ligands; (3) paramagnetic; (4) weakly coloured; (5) radius = 0.75 Å. The ion is described as of “high” spin. In other circumstances, when bound to six imine nitrogen atoms for example, the electrons of the core all pair. The properties of the ferrous ion are now: (1) no unpaired electrons; (2) slow ligand exchange; (3) diamagnetic; (4) strongly coloured; (5) radius = 0.65 Å. The ion is described as of “low” spin.

The low spin state has a considerably greater electronegativity than the high spin state, e.g. it binds nitrogen ligands more strongly. In the types of molecule we are considering, DMG complexes, it is the  $z$ -axis ligand which controls the spin state to a very large degree.<sup>39</sup> The balance in haem-proteins too is very finely adjusted

so that there are many examples of thermal equilibria between spin states which are dependent on  $z$ -axis ligands.

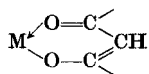
Once again we observe that the effect of the  $z$ -axis ligand on either the spectroscopic or the thermodynamic properties of the planar DMG molecule is not in an order which is related to any single parameter we have obtained from observations on octahedral compounds. We have as yet little understanding of the exact interaction between a planar group and a perpendicular ligand, the *cis* effect. We may hope to improve this situation by comparing the physical parameters of further models with those of biologically important molecules. Before we do this we draw attention to the general reactivity of planar ligands attached to central cations.

## IV. THE REACTIVITY OF LIGANDS

### A. Conjugation with Metals

Kinetic effects differ from effects upon ionization equilibria in that we must consider further the influence of excited states. Probably the most important states for the reactivity of the systems discussed here are the charge transfer states although states of much altered stereochemistry may not be far above the ground state. We consider substitution reactions in the ligand here but we shall not deal with the exchange of ligands bound to a central cation.

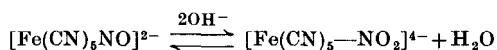
Collman and co-workers have examined a great number of electrophilic substitution reactions in acetylacetonate bound to Co(III), Cr(III) and Rh(III).<sup>8</sup> The attack is apparently by electrophilic reagents on the methene bridge of the six-membered ring



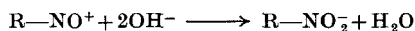
Presumably the methene carbon atom carries negative charge as the  $t_{2g}$  electrons are anti-bonding with the  $\pi$  electrons of the ligand (Fig. 2). The same type of substitution reaction occurs between cupric oxinate or ferrous phenanthroline and a diazonium cation. (Some reactions of ferrocene also fall into this class.) Both Cu(II) and Fe(II) are strong  $\pi$ -donor metals. A similar reactivity has been observed in the copper complex of glycylglycine, which readily undergoes a condensation with aldehydes at the methylene bridge.

Perhaps the simplest case of reactivity induced by a metal cation is the oxidation of an oxime, bound directly to a metal, to a nitroso compound. This reaction has been studied in the cases of Cu(II), Ni(II) and Fe(II). The iron complex  $\text{Fe}(\text{DMG})_2(\text{imidazole})_2$  can be oxidised in a four equivalent step. A similar series of oxidations has been reported by Krumholtz with di-imine ligands.<sup>21</sup> The compound  $\text{Fe}(\text{Niox})_2(\text{imidazole})_2$  undergoes an alternative oxidation in which the cyclohexane ring is attacked. This type of oxidation presumably goes via a nucleophilic attack on the carbon system conjugated to the electrophilic *ferric* ion. Other oxidations of this kind are those of ferric acetylacetonates and *ortho*-phenanthroline complexes. The nucleophilic mechanism of the reaction is suggested by the attack of hydroxide, not water, on ferric trisphenanthroline to yield hydroxyl radicals. Similar reactions are shown by Os(III) and Ru(III).

A further complex which is of interest is  $[\text{Fe}(\text{CN})_5\text{NO}]^{2-}$ . The complex undergoes a reversible reaction with alkali

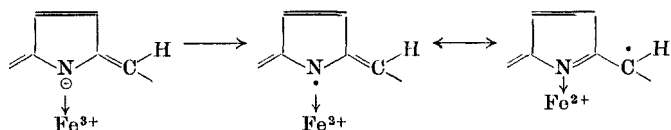


With  $\text{R—S}^-$  groups it yields the  $[\text{N} \begin{smallmatrix} \text{O} \\ \text{SR} \end{smallmatrix}]$  group and the complex also reacts with  $\text{SO}_3^{2-}$  and with reactive methylene groups. None of these reactions occurs as readily with the free NO ligand but perhaps could be expected for  $\text{NO}^+$ . Magnetic data show that the complex is not  $[\text{Fe}(\text{III}) \leftarrow \text{NO}]$  but is  $[\text{Fe}(\text{II}) \leftarrow \text{NO}^+]$  so that in this extreme case the charge-transferred state is the *ground* state. It seems likely that NO groups in other ligands, perhaps in oxime complexes, where the group is written  $\text{—NO}^-$ , behave in a similar manner and undergo similar reactions. For example, we have observed that ferric oximes react with sulphur-containing molecules in a manner not unlike the reactions of  $[\text{Fe}(\text{CN})_5\text{NO}]^{2-}$ .<sup>9, 25</sup> Thus with  $\text{HS}^-$  an intense charge transfer band is observed in the visible at  $640 \text{ m}\mu$  ( $15,500 \text{ cm}^{-1}$ ). There is also a reaction with alkali which may be of the kind

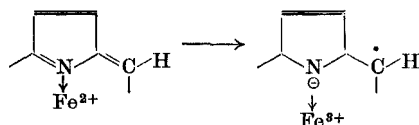


The cytochromes are concerned in very similar reactions to those demonstrated with the  $\text{Fe—NO}$  group. For example they catalyse the reactions of  $\text{NO}_2^-$ ,  $\text{SO}_3^{2-}$ ,  $\text{HS}^-$  and  $\text{O}_2\text{H}^-$ . We suggest that in

these cases reactivity arises from the ability of the complex to be excited, rather easily, into a charge-transferred state not unlike that of  $\text{Fe} \leftarrow \text{NO}^+$ .

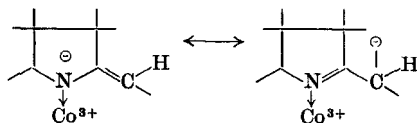


The excited state radical is considered to be electrophilic. Excitation of this kind will occur when the central cation is  $\text{Fe(III)}$  but when it is  $\text{Co(III)}$  or  $\text{Fe(II)}$  we expect the opposed charge transfer to occur.



The excited state radical is considered to be nucleophilic. Perhaps the most nearly related naturally occurring compound to these nitroso-models is not a cytochrome but the recently described ferrous nitrosophenolate, feroverdin.<sup>6</sup>

In all these systems we suspect that the metal acts so as to generate either (1) a negative centre in the ligand, as does  $\text{Co(III)}$  or  $\text{Fe(II)}$ , which is open to attack by electrophiles such as the proton, diazonium cations, carbonyl cations, or (2) a positive centre in the ligand, as does  $\text{Fe(III)}$ , which is open to nucleophilic attack by hydroxide, sulphide, cyanide, hydride. The difference between the cations is that the ferric ion has a hole in the  $t_{2g}$  states. Active centres may be generated at quite a number of different places but one we consider to be of particular importance is the methene bridge. The production of radical excited states must not be confused with the more usual mesomeric shifts which lead to the stabilization of carbonium cations or carbanions and may be induced by cations or anions generally. A particularly important case of the latter may be that of  $\text{B}_{12}$  co-enzymes (Section V-H).



### B. The Action of Light

The action of light may be to decompose a complex, e.g. a carbonyl, or to generate radicals, e.g. the photolysis of ferric oxalate. It is uncertain which of these particular processes will occur in a given complex. The difference between the two possible reactions appears to be just a difference in the type of electronic transition which initiates the process. Thus light absorbed in the charge transfer band of the ferrous cysteinate dicarbonyl leads to the loss of carbon monoxide from the complex. Light absorbed in the charge transfer band of ferric oxalate leads to photo-decomposition of the oxalate anion through a free-radical mechanism. The allowed charge transfer in the ferrous cysteine complex is from the  $t_{2g}$  orbitals to the sulphur ligand. But these  $t_{2g}$  electrons are just the ones which bind CO in the complex. It is not surprising that their excitation leads to carbon monoxide evolution. In the case of ferric oxalate the optical excitation is from the ligand to the ferric  $t_{2g}$  or  $e_g$  orbitals. This one-electron shift can obviously lead directly to the formation of oxalate radicals and subsequent ligand decomposition. We shall see that both types of processes are also observed in biological systems and there have been advocates of both steps as the initial steps of photosynthetic reactions.

### C. Summary of Reactivity

All the evidence we have reviewed concerning model complexes leads us to believe that metals attached to organic ligands, particularly conjugated ligands, act much like substituents in unsaturated organic compounds such as benzene. Some metal ions are electron donors, particularly those with filled  $t_{2g}$  levels, while others are electron acceptors, those with empty or partly filled  $t_{2g}$  levels. The interaction of the metal substituent with the ligand will be especially strong in those cases where charge-transferred states are not much higher in energy than the ground state of the system. We have mentioned several cases where these transitions have been observed spectroscopically at low energies. A metal bound to an organic ligand may also be considerably modified by the other ligands bound to the cation. The metal is not only modified in conventional ways by the change in other groups attached to it, but its spin state may also be

altered. High and low spin states of the same cation may be almost unrecognisably different in their effects on organic ligands. Again charge transfer may be from  $z$ -axis to in-plane ligands. The change in reactivity of the ligands on coordination to the metal may be most noticeable either at the coordinating group, e.g. the N of NO in  $[\text{Fe}(\text{CN})_5\text{NO}]^{2-}$ , or at an atom rather remote from the actual coordination centre, e.g. at a methene bridge of acetylacetonate.

## V. ENERGY LEVELS OF LIGANDS

### A. Spectra of Conjugated Organic Ligands<sup>15, 27</sup>

There are two main classes of ligands which are of interest to us: first, the ring ligands such as porphyrin and, second, the chain ligands such as tetrapyrroles. Addition of a group to a methene bridge of a porphyrin effectively converts it into a chain molecule. On the other hand it might be argued that coordination of such a system to a metal cation more or less permits a continuation of conjugation as a completed ring. We must consider whether such a system (e.g. corrins) should be treated as a ring or not. On a simple ring there will be two low lying transitions which, on the one-electron approximation, are of equal energy. On a conjugated chain these two transitions find their equivalents in two distinct transitions to different excited states. (The situation in the ring problem is further modified by configurational interaction which will split the degenerate transition into a pair of closely related bands. We examine this splitting below.) The difference between these two states will be expected to be more than is found between the first two excited states on a ring (see Tables III and IV). In both chain and ring systems further complications arise from the inclusion of hetero-atoms or from charge. All the species we shall consider carry negatively charged hetero-atoms. In the most stable of the interesting states it will be expected that this charge will reside more or less on the electronegative nitrogen atoms but in excited states it may move away from them.<sup>38</sup> We shall now see how these crude theoretical impressions can be made more exact, first referring to ring molecules and then to chains.

The spectra of the ligands of the porphyrin kind in which we are interested, i.e. metal porphyrins, chlorins and phthalocyanines, all consist of two main groups of bands. In the visible there are the

TABLE III. Spectra of Porphyrins and Some Related Compounds

Compound	Band position, m $\mu$			Intensity
	I	III	Soret ( $\gamma$ )	
Porphin	614	518	392	$\epsilon_\gamma \gg \epsilon_I$
Tetrabenzporphyrin	666	610		
Aetioporphyrin II	622	528	398	$\epsilon_\gamma \gg \epsilon_I$
Di-imido aetioporphyrin II	620	545	373	$\epsilon_\gamma \ll \epsilon_I$
Coproporphyrin II	623	530	398	$\epsilon_\gamma \ll \epsilon_I$
Di-imido coproporphyrin II	619	543	375	$\epsilon_\gamma \gg \epsilon_I$
Tetra-imido porphyrin XV	617	545	333	$\epsilon_I > \epsilon_\gamma$
Phthalocyanine	695	630	350	$\epsilon_\gamma \ll \epsilon_I$
Chlorin <i>f</i>	665	610	400	$\epsilon_\gamma > \epsilon_I$
Rhodoporphyrin XV	635	542	407	$\epsilon_I \ll \epsilon_\gamma$

closely related  $\alpha$ - and  $\beta$ -bands (500–700 m $\mu$ ) and in the near UV there is a further band, the Soret band (350–450 m $\mu$ ). See Fig. 5.

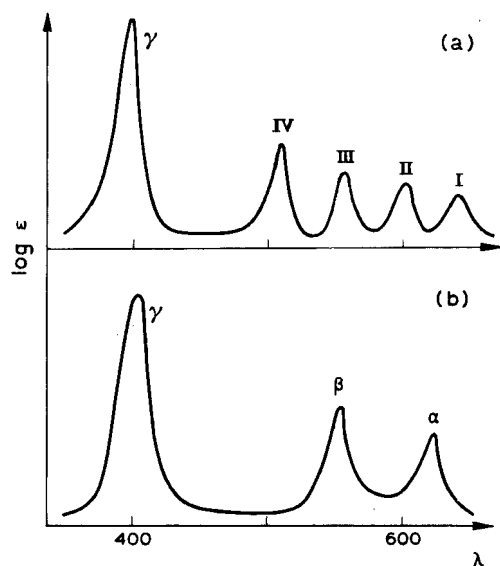


Fig. 5. The spectra of (a) a metal-free porphyrin, and (b) a metal porphyrin showing the labelling of absorption bands.

The Soret band is not split although the envelope of the absorption peak may well hide two transitions. The pair of bands in the visible may be associated with the first two vibrational excitations, 0–0 for the  $\alpha$ -band and 0–1 for the  $\beta$ -band, which belong to the same electronic transition (see next section) although the energy gap between  $\alpha$  and  $\beta$ ,  $1000\text{ cm}^{-1}$ , seems rather large to be consistent with the interpretation.<sup>27</sup> On replacing the metal by two hydrogen atoms in a porphyrin there is a further splitting of the  $\alpha$ - and  $\beta$ -bands to a four-band spectrum in the visible (Fig. 5). The change is thought to be the result of a change of symmetry and it is on first sight surprising that the effect of it is not seen in the Soret region. Vibrational structure is absent in this region too, even at low temperatures. In keeping with the vibrational assignments it is observed that whereas the intensity of the  $\beta$  and the Soret bands are rather little affected by changes of metal and even of substituent in the complexes the  $\alpha$ -band is very sensitive indeed to such changes. Substituents would be expected to affect the transition probability of a forbidden electronic transition uncoupled with vibrational changes, e.g. the postulated 0–0 transition, but not to affect too greatly that of a 0–1 transition. We shall now consider the nature of the electronic excitations.

For an eighteen-atom square-planar ring the single electron wave-function approximation leads to two fairly low energy, fully permitted transitions from the ground state which are of the  $\pi$  to  $\pi^*$  type. The transitions are from the two full levels  $a_{1u}$  and  $a_{2u}$  to the first empty level  $e_g$ . For ligand orbitals we use the labels appropriate to the actual  $D_{4h}$  symmetry of the ligand. The difference between the two ground state electron wave functions lies only in the electron distribution with respect to the atoms in the ring. The two possible levels are labelled  $L$  and  $M$  in Fig. 6, while the empty level is, as in Fig. 6,  $e_g$ . We shall seek information about the spectroscopic labelling of the ground states below. Both excitations move electron density maxima from the centre of the molecule towards the periphery. The periphery refers to any atom on the outside, e.g. to pyrrole carbons and the methene bridges. Clearly the change  $L \rightarrow e_g$  differs from  $M \rightarrow e_g$  in that the former causes a greater shift from the atoms in the centre. The excitation  $M \rightarrow e_g$  actually causes an increase in electron density on those atoms. Assuming that there is no other difference between  $L$  and  $M$  then both transitions



would still be of similar energy. Two factors radically modify this situation. In the first place the ring systems which interest us are not rings of carbon atoms but have nitrogens in the four central positions and in the case of the phthalocyanines have four nitrogens at the "methene bridge" positions also. As nitrogen has a greater electron affinity than carbon the stability of  $L$  is now rather greater than  $M$ . The difference between their stabilities should increase as the number of nitrogens in the porphyrin increases. The positions of

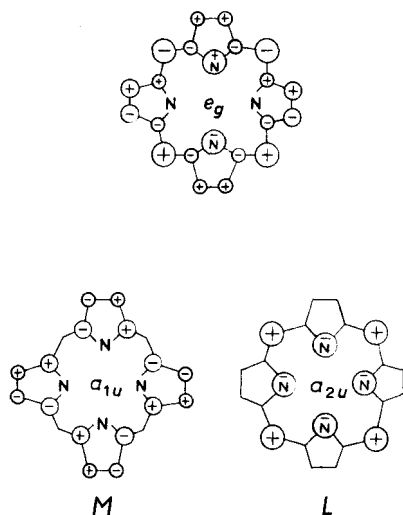


Fig. 6. The size and sign of the wave functions in porphyrins

the first two bands are shown in Table III for imino substitution. It would appear at this stage that  $a_{2u} \rightarrow e_g$  can be definitely identified as the transition from the orbital concentrated on the nitrogen atoms,  $L \rightarrow e_g$ , i.e. the Soret band. This transition becomes less intense and of higher energy as the number of nitrogen atoms is increased while the other transition ( $M = a_{1u}$ )  $\rightarrow e_g$  becomes somewhat stronger and of lower energy. The two transitions in phthalocyanines are of roughly equal probability, the long-wave band being somewhat the more intense (Table III), in keeping with two transitions which are equally allowed.

The above particular assignment has many virtues in the case of the phthalocyanines where the two intense transitions, the Soret and

the group of  $\alpha$ - and  $\beta$ -bands respectively, lie far apart. However, in porphyrins the two excitations are observed to be much closer together and are of very different intensity (Table III). We must now consider configurational interaction.<sup>15</sup> When a molecule of the kind we are discussing closely approaches a ring in its properties, rather than a square, the levels  $a_{1u}$ ,  $a_{2u}$  tend together and interact to produce new levels ( $l = 4$ ) of angular momentum  $\pm 4$  round the  $z$ -axis. In the ground state the orbitals are equally filled and the resultant angular momentum  $L$  is zero. The empty orbitals correspond to  $l = 5$ , and the transitions  $a_{1u} \rightarrow e_g$ ,  $a_{2u} \rightarrow e_g$  interact and are replaced by transitions:  $B[(L = 0) \rightarrow (L = 1)]$ , and  $Q[(L = 0) \rightarrow (L = 9)]$  corresponding to  $(l = +4) \rightarrow (l = 5)$ , and  $(l = -4) \rightarrow (l = 5)$  respectively. Thus the lower state will differ from the ground state by 9 angular momentum units while the higher state will differ from it by 1 unit. (Hund's rules tell us that states of high angular momentum are of high stability.) Furthermore, whereas there were two equally permitted transitions in the simple one-electron model, configurational interaction makes for one permitted transition, that of higher energy (as the allowed jump ( $\Delta L = \pm 1$ ) is to the state of lower angular momentum) and one transition which is strongly forbidden but which is of lower energy ( $\Delta L = \pm 9$ ). The assignment of  $B$  and  $Q$  in porphyrins can now be made on the basis of the intensities of the transitions when we find that the Soret band  $\epsilon_{\max} = 10^5$  is  $B$  and the  $\alpha$ - and  $\beta$ -bands ( $\epsilon \leq 10^4$ ) are  $Q$ . In terms of the original levels  $a_{1u}$  and  $a_{2u}$  we cannot define the system. Both transitions will now share the energy characteristics of the two single-electron transitions originally used (see Fig. 6). All we can safely say is that in both excitations electron density is moved from the central nitrogen atoms towards the periphery, where "periphery" includes both the methene bridge carbon atoms and the exposed carbon atoms of the pyrrole rings. The situation is best understood in terms of the interaction diagram, Fig. 7.

Whatever the merits of the two extreme approaches, with and without configurational interaction, they both indicate that the parameters of the porphyrin spectra which we should study are the intensity of the bands, the gap between the  $\alpha$ - and  $\beta$ -bands and the Soret band, and the effect of substituents upon these bands. We can make four types of substitution: (1) the conjugated ring can be

substituted by replacing carbon by nitrogen, or by replacing the hydrogen atoms on the methene bridges; (2) the pyrrole carbons can be substituted; (3) metals may be placed in the centre of the ring system; (4) substituents may be placed on the metal by its  $z$ -axis coordination. In the discussion of the last two types of substitution

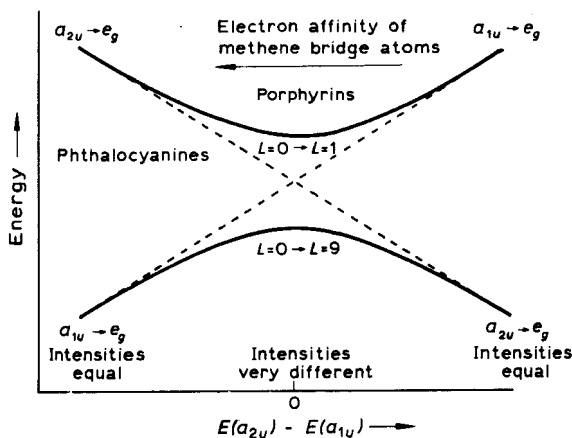


Fig. 7. The configurational interaction diagram.

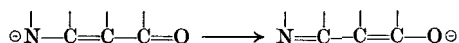
we shall find the ligand field approach as outlined by Kotani and Schoffa in this volume and Sections II-A to II-D of this chapter to be most helpful.

### B. The Effect of Substitution in Pyrrole Rings

This problem has been considered in detail by Platt<sup>27</sup> for the porphyrins. He has suggested that a substituent be given a weighting factor which takes into account both the symmetry of the substitution and its electron attracting or withdrawing character. It is observed that groups such as methyl and methoxy, electron donors, have but a small effect upon the spectrum, always in the direction of moving the groups of bands to shorter wavelengths. On the other hand, unsaturated substituents increase the separation between the bands slightly and at the same time move all the bands to longer wavelengths. Simultaneously, the unsaturated substituents increase the intensity of the long wavelength band

considerably. We can perhaps say that unsaturated substituents move the ring system towards that in the phthalocyanines and away from that in simple porphyrins (Fig. 7), though it is always difficult to understand the effects of asymmetrical substitution.

A further spectral change introduced by the electron attracting groups is a marked increase in the intensity of the  $\alpha$ - relative to the  $\beta$ -band.<sup>27</sup> A number of naturally occurring porphyrins have these carbonyl group substituents, e.g. chlorocruorin and cytochrome *a*, while a number have not, e.g. protoporphyrin and mesoporphyrin. The increased intensity of the 0-0 transition is perhaps to be associated with an increased polarity change from ground to excited state created by the resonance interaction of the pyrrole rings with the unsaturated rhodofying carbonyl group, and with the partial loss of symmetry associated with this interaction, weakening the physical basis of the selection rules. The transition may be thought of partly in terms of the valence bond structures



In keeping with this conclusion the rhodofying groups move the whole band system to longer wavelengths indicating a stabilization of the excited  $e_g$  orbital rather than of either the  $a_{1u}$  or  $a_{2u}$  levels separately (see Fig. 6).

Apart from the introduction of nitrogen atoms (see above) the ring conjugation can be modified by partly saturating one ring (e.g. in chlorins) or even by omitting a methene bridge (e.g. in corrins) and perhaps continuing the ring conjugation through the metal. In such systems the ring model with configurational interaction has lost much of its validity and we should expect either one or another extreme end of the interaction diagram or else a chain model to provide a better approach. This is observed, for in both the corrins and the chlorins the intensities of the bands,  $\alpha$  and  $\beta$  on the one hand and  $\gamma$ -bands on the other, are more nearly equal than in the porphyrins. Moreover, the separation between the band systems has increased so that the spectra are much more nearly akin to those of the phthalocyanines. There are conjugated systems which are intermediate in structure between the chlorins and the porphyrins, e.g. the cytochromes *a* and *a*<sub>2</sub> and they have an intermediate spectrum. In many ways the phthalocyanine spectra should be the easiest of

all to understand for the differentiation between the  $a_{1u}$  and  $a_{2u}$  bands in terms of single-electron density functions is here most realistic.

### C. Metal Substituents in Phthalocyanines<sup>38</sup>

As the two transitions in the phthalocyanines are far apart and of equal intensity the one-electron approximation should be the most useful theoretical approach. The bands at 650–700 m $\mu$  (15,400–14,300 cm<sup>-1</sup>) are then  $a_{1u} \rightarrow e_g$  and the bands at 350 m $\mu$  (28,500 cm<sup>-1</sup>) are  $a_{2u} \rightarrow e_g$ . Table IV shows the effect of different metal ions (note the spin states which are given) on the phthalocyanine spectrum in pyridine and chloronaphthalene. In pyridine the bands are rather insensitive to divalent metal ions in the series of increasing wavelength ( $\alpha$ - and  $\beta$ -bands) Fe < Co  $\leq$  Ni < Cu < Zn. The best  $\pi$ -donor metal, here ferrous, has the greatest effect in increasing the energy of  $a_{1u} \rightarrow e_g$  transition. A  $\pi$ -donor metal will convert the ligand  $e_g$  into  $\pi^*$  anti-bonding (Fig. 1) and so destabilize the levels as well as push them out more to the periphery. It is not surprising that Mn(II), high spin, has quite the opposite effect on the spectrum from Fe(II), low spin. It is a  $\pi$ -acceptor which stabilizes  $e_g$  somewhat and  $a_{2u}$  particularly as compared with  $a_{1u}$ . The band system moves to longer wavelengths and splitting is increased. The ferric ion (high spin) acts rather like the Mn(II) ion but all the bands are also moved to shorter wavelength because of the change.

Apart from these features of the spectrum of the metal phthalocyanines there are specific bands in the different metal complexes. In the ferrous complex in pyridine (low spin) there is a new band at about 400 m $\mu$ . In *ortho*-dichlorobenzene [high spin Fe(II)] the band is absent. We take this to be a charge transfer band, metal to ligand (Section III-B). The ferric phthalocyanine in 1-chloronaphthalene (high spin) has a charge transfer band, ligand to metal, at 845 m $\mu$  (11,820 cm<sup>-1</sup>). The band disappears in the low spin system in pyridine. There would not appear to be a charge transfer band of ferric ion in the low spin phthalocyanines or porphyrins and we can only account for the absence of this band by putting the hole in the  $t_{2g}$  orbitals in plane (i.e.  $d_{xy}$ ). Low spin ferric complexes with other ligands, e.g. *o*-phenanthroline and dimethylglyoximate, do show charge transfer bands (Section III-B). Zinc phthalocyanine in

TABLE IV. The Absorption Spectra of the Phthalocyanines (Main Bands Only)<sup>32, 37</sup>

Phthalocyanine	Solvent <sup>a</sup>	Spin state	Absorption bands, mμ							
Metal-free										
Cupric	c		350	554	602	638	665	698		
	c		350		611		678			
Nickel	p				600		658			
	c	low	351		603		671			
	p	low			590		664			
Cobalt (II)	c	low	348		606		672			
	p	low	330		597		660			
	c	high	340		650		693			
Ferrous	p	low	330	412	594		652			
	c	mixed	(< 325)	(410) weak	598		657		845	
Ferric	c	high	358	(521)	656		730		850, 1090, 1340	
Manganic	p	mixed		(472)	600		664		845, 890, 1080	
Manganous	c				615		675			
Zinc	p		348		607		672		830	
	c		350	(430 broad)	645		720			
Lead	p		328	(412 broad)	652		704			

<sup>a</sup> c is 1-chloronaphthalene and p is pyridine.

pyridine, but not in 1-chloronaphthalene, has a band at  $820\text{ m}\mu$  of low intensity. This band could be a forbidden charge transfer from the  $\pi$ -non-bonding orbitals of the pyridine. The Mn(II) spectrum in pyridine shows a similar band but the limited solubility of other metal phthalocyanines prevents the detection of the same bands of other cation complexes, if there are any. Finally, manganese phthalocyanine, high spin, shows a series of three very sharp bands at  $850$ ,  $890$ , and  $1080\text{ m}\mu$  in *o*-dichlorobenzene. The bands may well be triplets perturbed by the manganous ion.

#### D. Metal Substituents in Porphyrins<sup>13, 38</sup>

When we come to the porphyrin series we can no longer use the two one-electron orbitals without configurational interaction. The bands are best described as *Q* at  $550\text{ m}\mu$  ( $18,200\text{ cm}^{-1}$ ) and *B* at  $400\text{ m}\mu$  ( $25,000\text{ cm}^{-1}$ ). The spectra in benzene show that both bands are now sensitive to change of metal, and almost equally so. In detail the separation between the bands is reduced as the wavelength of the bands is reduced (Table V). Moreover, the splitting is

TABLE V. The Spectra of Some Metal<sup>a</sup> Protoporphyrin Complexes,  $\text{m}\mu$ <sup>13</sup>

	Fe(Py) <sub>2</sub>	Fe(H <sub>2</sub> O) <sub>2</sub>	Co	Ni	Cu	Zn	Cd
Band $\alpha$ $\lambda_{\text{max}}$	558	> 575	562	561	573	579	588
Band $\gamma$ $\lambda_{\text{max}}$	420	415	403	403	409	412	414
Difference	138	> 160	159	158	164	167	174

<sup>a</sup> All the cations are in the divalent state.

larger and the bands are at longer wavelengths for high spin as opposed to low spin cations. This suggests that the splitting is dependent upon the  $\pi$ -donor as well as the  $\sigma$ -acceptor properties of the metals. As with the phthalocyanines a good  $\pi$ -donor (low spin ferrous) forces the bands to shortest wavelengths. The fact that the greatest influence is felt on the  $\alpha$ - and  $\beta$ -band positions suggests that these bands have maintained a greater  $a_{1u}$  character. However, it is clear that both bands behave rather similarly, and whereas the

lead spectrum in the phthalocyanines differs more from that of other cations in the visible, it differs most in the porphyrin series in the ultraviolet region.

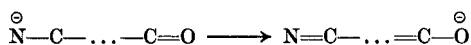
Just as there were additional bands depending specifically on metal in the phthalocyanines so there are metal-dependent bands in the metal porphyrins. The ferrous (low spin) porphyrins have an additional band in the  $450 \text{ m}\mu$  ( $22,000 \text{ cm}^{-1}$ ) region which may well be the charge transfer to the ligand. The ferric spectrum (high spin) is completely anomalous and before we discuss it we shall consider the effect of other metal ions upon the intensity of the ligand transitions.

The most noticeable intensity changes in a series of metal porphyrins are in the  $\alpha$ -bands. The more effective the metal as a  $\pi$ -donor the higher the intensity of the  $\alpha$ - as opposed to the  $\beta$ -band. This is shown in Table VI.<sup>38</sup> Thus  $\pi$ -donor metal ions act in the same

TABLE VI. Extinction Coefficients of  $\alpha$ - and  $\beta$ -Bands of Mesoporphyrins<sup>33, 38</sup>

Cation	$\alpha$ -Band $\epsilon_{\text{max}}$ $\times 10^{-4}$	$\beta$ -Band $\epsilon_{\text{max}}$ $\times 10^{-4}$	Spin state
Zn	2.0	1.8	
Cu	2.6	1.4	
Ni	3.5	1.2	Low
Co	2.4	1.1	Low
$\text{Fe}(\text{H}_2\text{O})_2$	0.5	1.5	High
$\text{Fe}(\text{NH}_3)_2$	3.4	1.5	Low
$\text{Fe}(\text{Py})_2$	3.2	1.6	Low
$\text{Fe}(\text{CO})(\text{Py})$	1.5	1.5	Low
$\text{Fe}(\text{CN}^-)_2$	1.1	1.4	Low
$\text{Fe}(\text{III})(\text{NH}_3)_2$	0.7	1.4	Low (ferric)

way on the intensity as  $\pi$ -acceptor substituents in the pyrrole rings. The effect of both the substituents and the metals is then in the sense that they increase polarity (transfer to the periphery) in the excited state, i.e. they act cooperatively in creating a large dipole moment change to the excited state.





We shall see later how ligands attached to the metal ion affect this polarity also. Writing part of the transition in the above way implies transfer of electron density from the centre to the periphery.

In high spin ferric phthalocyanine we noted two charge transfer bands to the iron at about  $420\text{ m}\mu$  ( $23,080\text{ cm}^{-1}$ ) and  $845\text{ m}\mu$  ( $12,000\text{ cm}^{-1}$ ). The second band was of low intensity,  $\leq 10^3$ . At the same time we found that the Soret band was split away considerably from the longer wavelength bands. In high spin ferric porphyrins it is easy to find the Soret band at  $390\text{--}400\text{ m}\mu$  and to find the long wavelength forbidden charge transfer band at about  $800\text{--}1000\text{ m}\mu$  (Fig. 8). It is

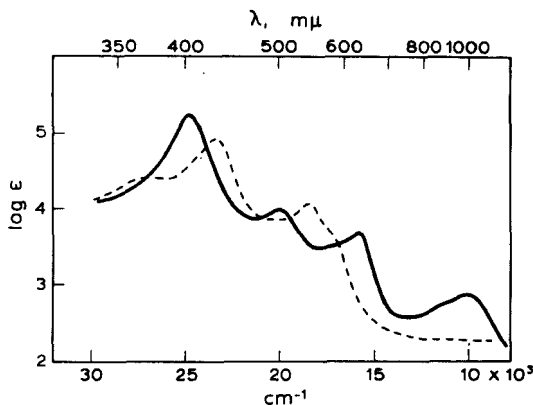


Fig. 8. The spectra of high spin (full line) and low spin (broken line) ferric porphyrins.

very difficult to find the bands corresponding to the  $\alpha$ - and  $\beta$ -bands of the usual metal porphyrins. From what we have said about intensity we should not expect the  $\alpha$ -band intensity to be very appreciable, and it is not surprising that it is difficult to find. It is also difficult to assign the second charge transfer band which should be in the  $500\text{ m}\mu$  region. In place of the apparently missing charge transfer and  $\beta$ -bands we have two new bands at  $500\text{ m}\mu$  ( $20,000\text{ cm}^{-1}$ ) and at  $625\text{ m}\mu$  ( $16,000\text{ cm}^{-1}$ ) respectively. We suspect that these two bands are related to the  $\alpha$  and  $\beta$  and charge transfer bands in the following way. The excited states  $E_u$  mix with charge transfer to the  $d_{xz, yz}$  orbitals to give four excited states (Fig. 9). The transition to the highest energy of these will correspond closely to the Soret band, but it is difficult to conclude anything very precise about the

other three except that we expect the lowest energy transition should be at longer wavelengths than the normal  $\alpha$ - and  $\beta$ -bands. The three bands are charge transfer and three ligand bands at the same time. (Their  $z$ -axis ligand dependence supports this, see below.) In the spectrum of Fe(III) cytochrome *a* where one charge transfer band is at  $\sim 650$  m $\mu$  the so-called  $\alpha$ -band (now more intense) is at 600

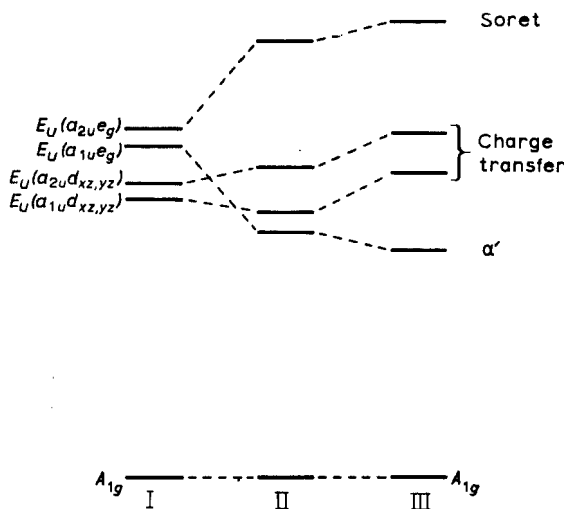


Fig. 9. The ground,  $A_{1g}$ , and excited states in high spin ferric porphyrins. (I) The energies ignoring both electron-electron repulsion and mixing of ligand excitations with charge transfer. (II) The effect of electron-electron repulsion. (III) The effect of mixing.

m $\mu$  which is at longer wavelengths than the Fe(II) band.<sup>22</sup> We suspect that these bands are really due to mixed transitions too and that the position of the third band is at about 525 m $\mu$ . Thus in the visible region of the spectrum the ligand absorption of haem *a* has undergone less modification through interaction with the iron transitions than was the case in the protohaem ferric complexes. (Compare Table VII and Table VIII.) In the near infrared the long wave charge transfer band due to ferric is at much shorter wavelengths in haem *a* than in protohaem complexes (Table IX). It seems reasonable to suppose that all the charge transfer bands of haem *a* ferric complexes will be at shorter wavelengths too, for an *a* type porphyrin is a

poorer electron donor than a protoporphyrin. Perhaps this accounts for the observation that it is the Soret band positions which are rather anomalous in the ferric haem *a* derivatives. As the second charge transfer band moves to shorter wavelengths it will interact more with the Soret transition than with the  $\alpha$  and  $\beta$  transitions (Fig. 9). We have already seen a rather similar effect in the phthalocyanines, for a ligand which is a poorer electron donor than porphyrin.

Low spin ferric porphyrin complexes are like low spin cobaltic complexes and have exactly the same type of spectrum as all low spin complexes. On the other hand high spin Mn(III) porphyrins have an anomalous spectrum with bands at 475 m $\mu$  and 570 m $\mu$ . Thus it would appear that one hole in the  $t_{2g}$  orbitals [Fe(III)] has the same effect as no holes [Co(III)] but three holes [Mn(III)] behave very differently. The same effect was observed in the phthalocyanines. We again conclude that the hole in the  $t_{2g}$  orbitals of the Fe(III) low spin ion is in the  $xy$  plane where it will not interact with the  $\pi$ -electron transitions of the ligand. We see no charge transfer band in ferric low spin porphyrin complexes.

TABLE VII. The Spectra of Protohaem Complexes, Ferrous and Ferric<sup>38</sup>

<i>z</i> -Axis ligand	Absorption maxima, mμ		Spin state
<hr/>			
Fe(II)			
Water	575	415	high
Pyridine	557	426	low
Ammonia	553	422	
Cyanide	569	430	
Carbon monoxide	573	413	
Haemoglobin	590	435	high
Cytochrome <i>b</i>	564	425	
Fe(III)			
Water	622	402	high
Pyridine	558	417	low

TABLE VIII. The Spectra of Haem *a* Complexes, Ferrous and Ferric<sup>22</sup>

<i>z</i> -Axis ligand	Absorption maxima, mμ		Spin state
<hr/>			
Fe(II)			
Water	600	410	largely high
Pyridine	587	430	largely low
Ammonia	592	435	
4-Methylimidazole	594	441	
Cyanide	598	446	
Carbon monoxide	605	426	
Cytochrome <i>a</i>	604	445	mixed
Fe(III)			
Water and hydroxide	635	400	largely high
4-Methylimidazole	597	434	largely low
Cytochrome <i>a</i>	597	419	mixed

### E. Spectra of Haemin Derivatives—Effects of *z*-Axis Ligands<sup>31, 36, 38</sup>

In Table VII we see how ligands perpendicular to the plane of the porphyrin ring affect the separation between the  $\alpha$ - and  $\beta$ - and the Soret bands. In the high spin complexes the separation is much greater than in the low spin compounds. This is an indirect effect of the ligand. Going from a high spin to a low spin situation does in fact move the two bands in opposite directions. The  $a_{2u}$ , more electron density on the nitrogen, which corresponds more nearly to the state from which the electron jumps for the Soret transition, becomes destabilized. While the  $a_{1u}$  state is not much affected, the  $e_g$  states are also destabilized. While high spin states are relatively good  $\pi$ -acceptors for the electrons of the porphyrin, low spin states are  $\pi$ -electron ( $t_{2g}$ ) donors (see Figs. 1 and 2).

The effect of CO on the ferrous spectrum is to split the bands apart, moving them in opposite directions. CO removes electron density from the porphyrin ring nitrogens by stabilizing the  $t_{2g}$

electrons in its own  $\pi$  orbitals and in this way makes the  $a_{2u}$  and  $e_g$  levels more stable but the  $a_{2u}$  level is less affected.

The intensity changes in the 0-0 transition of porphyrins have been described by Platt in terms of substituent factors. In effect, as in the benzene compounds, substituents which have a strong *meta*-directing influence have a strong effect on the intensity of the transition. This suggests (see above) that the excited electronic state is the more polar with negative charge migrating to the substituent. It has been pointed out that the effect of different metals is in keeping with this suggestion as the series of  $\alpha$ -band intensities is  $\text{Fe(II)} (\text{low spin}) > \text{Co(II)} \cong \text{Ni(II)} > \text{Zn} > \text{Mg} > \text{Fe(II)} (\text{high spin}) > \text{three valent ions (low spin)}$ . This order is very much that of the  $\pi$ -donor character of the metals.  $\pi$ -Donation from the central metal will act cooperatively with  $\pi$ -acceptance by peripheral groups. Moreover, the effect of substituent ligands in the  $z$  direction on the intensity is that  $\pi$ -acceptor ligands reduce the intensity of the  $\alpha$ -band, while  $\pi$ -donors increase this intensity. The fact that the band at about  $600 \text{ m}\mu$  ( $17,000 \text{ cm}^{-1}$ ) in the ferric complexes varies in intensity with ligands bound to the cation in the same manner as the  $\alpha$ -band in ferrous porphyrins strongly suggests that this band is related to the  $\alpha$ -band in more usual porphyrins, while the band at  $500 \text{ m}\mu$  ( $20,000 \text{ cm}^{-1}$ ) is more akin to a simple charge transfer transition.

The main transitions of high spin ferric protoporphyrin complexes, no matter what the ligands on the  $z$ -axis, are at about  $400 \text{ m}\mu$ ,  $500 \text{ m}\mu$ ,  $625 \text{ m}\mu$ , and  $900 \text{ m}\mu$ . The band at  $400 \text{ m}\mu$  is recognisably the Soret band. We presume that the bands at  $500$  and  $625 \text{ m}\mu$  are the mixed transitions referred to earlier and that there is a further band in this region at around  $550 \text{ m}\mu$ . In Fig. 10 we show that the relationship between the  $500 \text{ m}\mu$  and the  $625 \text{ m}\mu$  bands is that expected if they had very similar characteristics. A very similar parallel has been reported by us in the spectra of the derivatives of myoglobin and haemoglobin. It appears to be general to the high spin complexes of catalase and peroxidase too.

The further long wavelength band at  $900 \text{ m}\mu$  we take to be a forbidden charge transfer from the ligand to the cation. It could be a spin forbidden transition or a mixture of charge transfer and ligand triplet. The possibility of such transitions was described earlier by us in a discussion of the  $625 \text{ m}\mu$  band. The intensity of the band

at  $625\text{ m}\mu$  can be as high as  $10^4$ , while that of the  $1000\text{ m}\mu$  band does not exceed  $10^3$ . A theory of spin-forbidden transitions coupled with charge transfer has been given by Mulliken and by Murrell.<sup>24</sup> That the bands could be spin-forbidden is based on the argument that: (1) They only appear in high spin Fe(III) complexes—they cannot therefore be  $d-d$  transitions except of a spin-forbidden kind. (2) We have already noted that the  $d^5$  system Mn(II) phthalocyanine

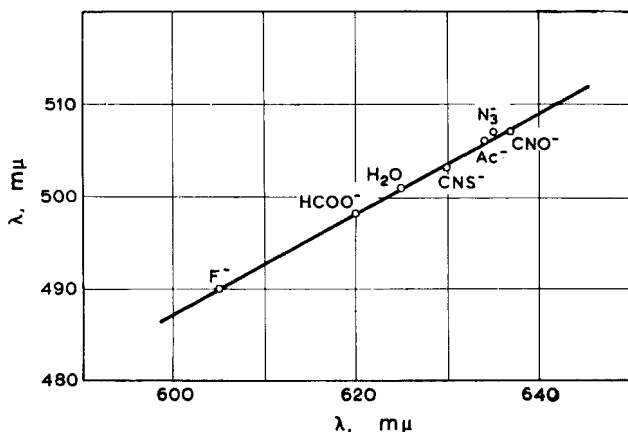


Fig. 10. The relationship between two of the absorption bands of ferric myoglobin.

shows a similar set of bands at  $1000\text{ m}\mu$  ( $\epsilon = 500$ ). (3) Mn(II) and Fe(III) are very unlikely to have similar charge transfer spectra. (4) The band is not a usual ligand band as only Fe(III) compounds (high spin) have the band. (5) The band could be a spin-forbidden ligand band but cannot have the observed intensity without mixing with charge transfer. (6) Charge transfer mixing is implicated as the band position moves with  $z$ -axis ligand in the sequence shown in Fig. 10 which is very similar to that given in Section III-B for the bands of Fe(III) (DMG)<sub>2</sub>X<sub>2</sub> complexes, where the assignment was more positive. The very long wavelength of the band suggests a triplet as a possible origin too. The band has much structure, possibly through coupling with the vibrations of the peripheral groups. The long wavelength band decreases in intensity as the concentration of high spin ferric ion decreases, being virtually absent in

dicyanides. The band is found in biologically important molecules too (Table IX). The band position ( $m\mu$ ) for a given porphyrin,

TABLE IX. The Absorption Spectra of Haemin Derivatives<sup>a</sup>

Ligand		H <sub>2</sub> O	SCN <sup>-</sup>	Ac <sup>-</sup>	HCOO <sup>-</sup>	CNO <sup>-</sup>	N <sub>3</sub> <sup>-</sup>	F <sup>-</sup>	NO <sub>2</sub> <sup>-</sup>	OH <sup>-</sup>
Haemin	$\lambda_{\max}$	975	975	940	925	925	920	820		
	$\epsilon_{\max}$	850	850	700	850	650	660	850		
Myoglobin (pH 7.55)	$\lambda_{\max}$	1000	1000	1000	920	940		850	960	820
	$\epsilon_{\max}$	865	830	850	1050	1020		1300	810	740
Peroxidase	$\lambda_{\max}$	1000						870		
	$\epsilon_{\max}$	560						930		
Catalase <sup>4</sup>	$\lambda_{\max}$	865								
	$\epsilon_{\max}$	860								
Cytochrome <i>c</i> (acid soln.)	$\lambda_{\max}$	980								
	$\epsilon_{\max}$	785								
Cytochrome oxidase	$\lambda_{\max}$	830								
	$\epsilon_{\max}$	1000								

here protoporphyrin, follows the sequence catalase < met-myoglobin < peroxidase, which is in keeping with the probable *z*-axis ligands carboxylate, imidazole, ammine respectively. The intensity of the band increases in the order of the paramagnetic moments in all series of complexes, e.g. in the series described by Schoffa in this volume, which, since we are dealing with magnetic mixtures, is the order of the concentration of the high spin form once again.

### F. Restrictions upon Ring Conjugation

Important examples of the effect of restrictions on the ring conjugation are supplied by compounds in which one of the methene bridge carbons is bound by a double bond to oxygen, sulphur or another carbon. The absorption spectra of all these molecules show considerable separation between the  $\alpha$ - and  $\beta$ -band system and the Soret band. Moreover, the intensities of the bands in the visible and near ultraviolet are roughly the same. An extreme case of the restriction of conjugation is the actual opening of the ring

to give a chain of four pyrrole rings. This structure is found in the purpurins, which have two main absorption bands of equal intensity—one at  $700\text{ m}\mu$  ( $14,000\text{ cm}^{-1}$ ) and one at  $400\text{ m}\mu$  ( $25,000\text{ cm}^{-1}$ ). Further restrictions in the conjugation of this chain system bring about a systematic fall in the wavelengths of the absorption bands, and in the dipyrromethenes the main bands are at  $450\text{ m}\mu$  and  $320\text{ m}\mu$ , the long-wave absorption being the stronger. Any ring model for the wave functions in these molecules is quite inapplicable of course, but we can adopt instead the "electron on a chain" treatment.

### G. The Spectra of Conjugated Chains<sup>23</sup>

A conjugated linear chain gives rise to two readily described absorption bands. The first transition, I, which has been likened to the first unoccupied mode of a vibrating string, is quantum mechanically allowed, while the second, which should be of just over twice the energy for it is the transition to the second mode, is symmetry forbidden. For a kinked molecule such as a carotene with one central *cis* double bond—all the rest being *trans*—the second mode also becomes more or less allowed, this transition having a transition moment perpendicular to the longest axis of the molecule.

TABLE X. The Absorption Spectra of Bile Pigments

Pigment	Bands		Conjugated bonds
	$\lambda_{\text{max}}, \text{m}\mu$	$\epsilon_{\text{max}} \times 10^{-3}$	
Biliverdin	640	10.4	10
	392	25.0	
Mesobiliviolin	607	21.0	8
Bilirubin	450	50.0	5
	300	very low	
Mesobilene	452	25.1	5
	330	3.6	
Pyrrole	below $300\text{ m}\mu$		2
Porphyrin	620	10.0	9
	410	100.0	



In most systems of this kind the second band remains less intense than the first. The splitting between bands I and II is greater than that between the two first transitions on a ring. The poly-pyrroles are a conjugated chain series. Their spectra are given in Table X. The first members, mesobilene and bilirubin, have the spectra expected, band I intense and band II weak, though the ratio of the band energies is less than expected. In the second member, mesobiliviolin, the intensities of the two bands are more nearly equal, while for the third, biliverdin, the second band is the more intense. The metal complexes of these compounds, where known, have very similar spectra to those of the free ligand. The high intensity of band II in the larger molecules suggests that the molecules are not linear but that they are rather like the kinked carotenes. The very high transition moment of these bands is attributable to their highly polar ends.

#### H. The Corrins<sup>17, 28</sup>

The corrin ring system has a conjugated path of six double bonds. On the chain model we should expect an absorption spectrum of one intense long-wave band at about 500  $m\mu$  (see Table X) and a weak second-order transition in the region of 250  $m\mu$  much as is observed in the spectrum of carotene. The wavelength ratio for the two peaks should be about 2:1. In heterocyclics of the pyrrole type the absorption bands are at rather longer wavelengths than in the carotenes for a similar number of double bonds. The actual spectrum of vitamin B<sub>12</sub> (Fig. 11) has the predicted intense band at 550  $m\mu$  but in addition it has an even more intense band at 360  $m\mu$ . The total result is that the spectrum looks rather like that of a porphyrin, i.e. it resembles the spectrum expected from a ring rather than a chain conjugated system, though the bands are rather far apart. We could suppose that conjugation is continued through the metal atom but we should then find it difficult to explain why other metals do not greatly alter the relative intensity of bands I and II of say tetrapyrroles. Moreover, the absorption spectra of the tetrapyrroles themselves consist of a very similar band structure (Table X). We suggest instead that the chain model is valid for the corrins and that band II has such a high intensity because the wrapping of the double-bond system about the metal leads to a high negative charge

on the terminal nitrogens (A and D rings) in the ground state. The second transition leads as we have seen to a shift of this electron density towards the carbon atoms in the centre of the chain. The transition will have a high dipole moment. These conclusions are readily tested by observing the effects of ligands on the metal ( $z$ -axis) upon the absorption spectrum of the compound. The first

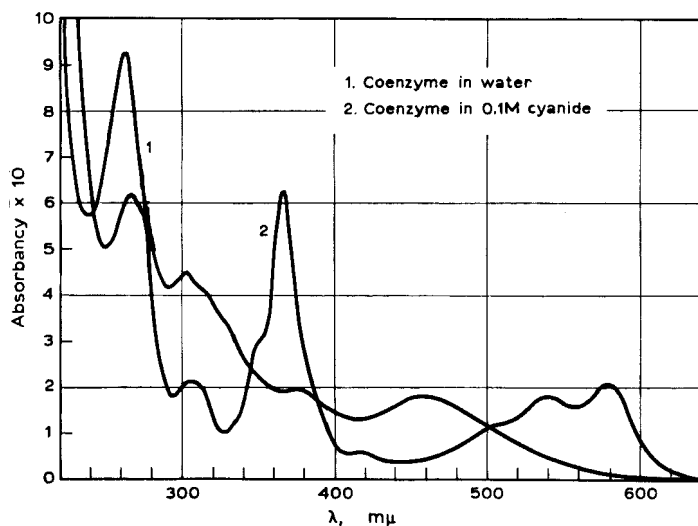
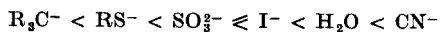


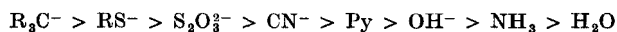
Fig. 11. The spectra of a red (dicyanide) and a yellow cobalamin.

transition should be but little affected in intensity by such changes, as the dipole moment for the transition is from one end of the chain to the other, but the second transition should be grossly altered in intensity and position as its transition moment is from the ends to the middle of the system. The order of intensity of band II is



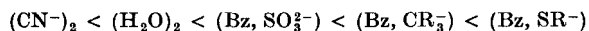
which is rather like the order of decreasing polarisability of the ligand. (It is not unlike the nephelauxetic series.) The  $z$ -axis ligands which donate charge to the metal will naturally prevent the build up of charge on the terminal nitrogens of the chain in the ground state and so they would be expected to reduce the transition dipole. Moreover, the ligands which reduce the intensity of the band II also

move the bands closer together, shifting band I but slightly, but band II to much longer wavelengths, in the extended series



This series is again rather like the nephelauxetic series, an order based on polarisability. We should expect that charge donated to the cobalt by the *z*-axis ligands would destabilize the ground state relative to the excited state much as is observed.

Certain reagents attack cobalamins to give yellow compounds with weak absorption bands in the ultraviolet and yet appreciable bands at 400–460 m $\mu$ . These complexes we take to contain one less double bond than the vitamin B<sub>12</sub> derivatives. Such molecules would still be expected to show an intense band on the edge of the visible (5 double bonds) but the second transition would be weaker because the series of double bonds is more nearly linear and contains one less nitrogen group. Band II is observed at 310 m $\mu$  and is of low extinction coefficient. The fact that B<sub>12</sub> derivatives behave as bases picking up protons and going from red to yellow forms further suggests that the protons are taken up by the conjugated system. Whether they are taken up by carbon or nitrogen is a little difficult to settle but we favour the reaction site as being one of the methene bridges as these groups have a demonstrated reactivity in the models which we have discussed earlier. The functional significance of the *z*-axis carbon anion in the B<sub>12</sub> co-enzymes is then just the activation of the corrin ring system to nucleophilic attack. In a series of cobalamin derivatives we have shown that the ease of proton uptake increases in the ligand sequence



where Bz is benzimidazole and the ligands listed occupy the *z*-axis positions. This sequence of ligands is neither that of the nephelauxetic or spectrochemical series nor is it quite the same as what we have observed for the acid dissociation constants of dimethylglyoximate complexes (Section III-C). However the series is very like that of the effect of ligands on the intensity and position of band II of the red corrins. Strongly polarisable donors have a powerful effect upon the properties of the ring. It would appear that they exert a similar effect on the porphyrin complexes.

We have now completed our account of the spectrophotometric and thermodynamic properties of the ring chelates. In many respects these properties can be understood from our earlier discussion of the properties of much simpler chelates but there are also many highly specific properties of the biologically important chelates. We can illustrate these further in the next section on the reactivity, which is to be compared with Section IV-C on model systems.

## VI. CHEMICAL REACTIONS

### A. Chemical Reactivity of Ring Chelates

Much as all these physical properties are of interest, greater interest centres on the reactivities of the molecules. Calvin and Polanyi observed in 1936 that phthalocyanine could act as a homogeneous hydrogenation catalyst.<sup>5</sup> Elvidge<sup>12</sup> showed that manganous phthalocyanine could act as an oxygen carrier and Terenin showed that very many phthalocyanines could act as electron transporting agents in the solid state. We have been re-investigating this last property of the metal phthalocyanines in recent years. A typical photo-response current for a metal phthalocyanine is shown in Fig. 12.<sup>10,32,35</sup> There is a strong photocurrent not only in the region where strong absorption occurs in the single molecules in solution but also in the longer wavelength regions. In the case of the manganous compound, the only case where we have observed what we take to be the triplet excitation directly (see above), we find a very high photocurrent directly in the region of the supposed triplet excitation (Fig. 12). It should be noted that of all the cations studied by us only the manganous ion is in a high spin state in the solid and therefore only it has holes in the  $t_{2g}$  states. These states interact strongly with the triplet of the ligand.

From these observations we conclude that the phthalocyanine ring system is readily activated by metal ions but that the activation is highly cation specific. Many chemical reactions carried out by Elvidge would seem to confirm these observations. We have noticed, too, that the photocurrents in the metal phthalocyanine compounds are extremely sensitive to adsorbed gases and that in many cases the gases are not readily removed. In some cases the removal of the gas is not achieved except under illumination. Now the gas molecules, oxygen and water in particular, are very

probably bound to the metal atoms on the surface. Thus light absorbed by the ligand (all the absorption processes we observe are basically ligand transitions) is causing the breaking of bonds perpendicular to the ligand plane. This is a photochemical *cis*-effect (Section IV-B) which has been frequently studied in the field of metal porphyrin chemistry, e.g. the photochemical decomposition

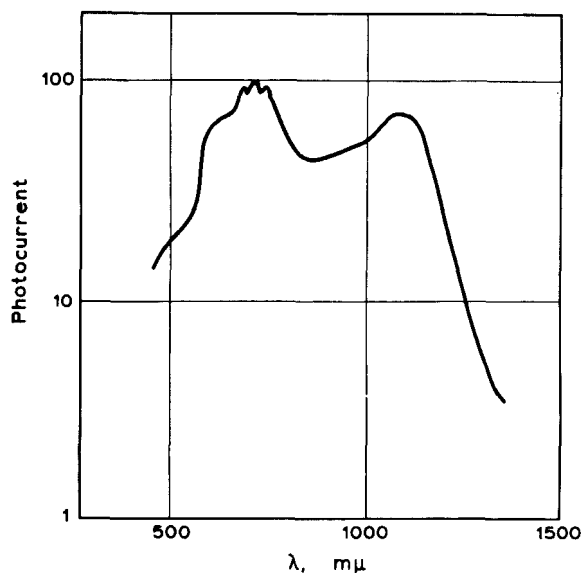


Fig. 12. A typical photo-response curve of a metal phthalocyanine.

of carbonyl haemoglobin. We see that the unit, metal planar-organic ligand (*xy*-plane) and its *z*-axis ligands, acts as one large molecule.

The metal phthalocyanines show a number of oxidation-reduction reactions of possible interest. Thus the copper phthalocyanine was shown by Taube and Cahill to undergo a one electron oxidation which radically modified the spectrum of the ring system.<sup>34</sup> The reaction was further studied by George *et al.*<sup>14</sup> It appears that many metal phthalocyanines will undergo reactions of this kind. As Dwyer and we have stressed, it could be a mistake to differentiate too closely between reactivity of the ligand and the metal in these systems.<sup>11, 39</sup>

### B. Reactions of Some Biologically Important Complexes

While discussing the spectra of the ring and chain poly-pyrrole compounds, we mentioned that the effect of a break in conjugation was to separate the bands in a porphyrin by pushing the Soret band to shorter wavelengths and the  $\alpha$ - and  $\beta$ -bands to longer wavelengths. Thus an attack on the conjugated system by any reagent should be immediately recognised. In a number of reactions of catalase, peroxidase, myoglobin, haemoglobin and RHP cytochrome oxidase exactly this change is observed. In these cases we believe that the methene bridge carbon atoms have suffered attack. In the corrin system, which is best thought of as a chain of pyrrole-like pigments, attack on the conjugated system is expected to produce a shift of all the bands to shorter wavelengths and a great diminution in strength of the (II) bands. We have observed just these spectroscopic changes in a number of reactions of the vitamin B<sub>12</sub> co-enzymes and have therefore postulated that there is attack on the methene bridge of cobalamins. Interestingly the spectrum of the yellow form of cobalamins is very like that of dipyrromethene. In the case of the oxidised iron porphyrins the attack is by nucleophilic groups on a positively charged carbon methene bridge (ferric form) while in the case of cobalamin and reduced iron porphyrins it is of electrophilic groups on the negatively charged methene bridge. The relevance of Section IV-C on comparable model systems is obvious. It is particularly interesting that the groups which attacked the models were oxygen and sulphur anion ligands. Exactly these groups may well attack cytochromes. Such a process could initiate phosphate uptake.

### C. Photochemistry of Porphyrin-like Compounds<sup>35</sup>

As we have mentioned under the discussion of model systems there are two types of photochemical reaction of interest to us. The one generates radicals from a ligand; the other releases a co-ordinately bound group. Examples of both photolyses are known in porphyrin chemistry. In the second group are the dissociations of the carbon monoxide, cyanide, nitric oxide, methyl isocyanide and oxygen complexes of myoglobin and haemoglobin. The action spectrum is exactly that of the metal-porphyrin complex so that light absorbed in either the Soret or the longer wavelength bands is

equally effective. The quantum yield is high,  $\sim 1.0$ . The mechanism of the photolysis may be considered as an excitation of the ligand  $\pi$  electrons transferring them towards the periphery of the molecule. This electron shift makes the porphyrin into a better electron acceptor and it is able to steal electron density from the  $t_{2g}$  bonding orbital which interacts with the small unsaturated ligand on the  $z$ -axis. It is this electron density which helps to stabilize the metal-ligand bond so that the excitation of the porphyrin is equivalent to a weakening of a metal-ligand bond in the  $z$  direction.

The alternative reaction is found in the photolysis of the cobalamin co-enzymes. In this case radicals are thought to be produced. The excitation in this case is very similar to that already described above. In order that radicals may be produced we must presume that subsequent to the excitation an electron of the  $\sigma$ -orbital of the M—C bond is transferred to the porphyrin ring. This type of charge transfer is identical with that mentioned in Section II-G (see also V-H), the charge transfer in beryllium dipyrityl dialkyl, or indeed with that we have described as being responsible for photoconduction in the metal phthalocyanines. It could also be the initial step in the action of light on chlorophyll in photosynthesis. A further interesting possibility is that the light energy absorbed by chlorophyll is transferred to the charge transfer band at longest wavelength of a ferrihaemoprotein. A possible protein would be a cytochrome of mixed spin state such as cytochrome *f*.

In this article we have outlined an approach to the problem of understanding the function of metal ions combined with unsaturated ligands in biological systems. Nearly all the major problems in the work are as yet unsolved. It is for this reason that we are attempting to use a very wide variety of methods in order to obtain new information about complex ions. We have deliberately stressed our current attitudes at the expense of a more general survey, for at the moment it is hard to say which particular line of attack will prove the most fruitful.

### References

1. Ablov, A. B., and Filippov, M. P., *Russ. J. Inorg. Chem. (English Transl.)* **5**, 1311 (1960).
2. Beetlestone, J., George, P., and Griffith, J. S., in J. E. Falk, R. Lemberg, and R. K. Morton, Eds., *Haematin Enzymes*, Pergamon, London, 1961, p. 105.

3. Basolo, F., and Pearson, R. G., *Mechanism of Inorganic Reactions*, Wiley, New York, 1958, p. 177.
4. Brill, A. S., personal communication.
5. Calvin, M., Cockbain, E. G., and Polyani, M., *Trans. Faraday Soc.* **32**, 1436 and 1443 (1936).
6. Chain, E. B., Ballio, A., Berthold, H., and Vittorio, D. V., *Nature* **194**, 769 (1962).
7. Coates, G. E., and Green, S. I. E., *Proc. Chem. Soc.* **376** (1961).
8. Collman, J. P., and Kittleman, E. J., *J. Am. Chem. Soc.* **83**, 3529 (1961).
9. Davies, R. C., and Williams, R. J. P., unpublished observations.
10. Day, P., and Williams, R. J. P., *J. Chem. Phys.* **37**, 563 (1962).
11. Dwyer, F. P., in J. E. Falk, R. Lemberg, and R. K. Morton, Eds., *Haematin Enzymes*, Pergamon, London, 1961, p. 19.
12. Elvidge, J. A., and Lever, A. B. P., *Proc. Chem. Soc.* 195 (1959).
13. Falk, J. E., and Perrin, D. D., in J. E. Falk, R. Lemberg, and R. K. Morton, Eds., *Haematin Enzymes*, Pergamon, London, 1961, p. 56.
14. George, P., Ingram, D. J., and Bennett, J. E., *J. Am. Chem. Soc.* **79**, 1870 (1957).
15. Gouterman, M., *J. Chem. Phys.* **30**, 1139 (1959).
16. Hall, D., Rae, A. D., and Waters, T. N., *Proc. Chem. Soc.* 143 (1962).
17. Hill, J. A., Pratt, J. M., and Williams, R. J. P., *J. Theoret. Biol.* **3**, 423 (1962).
18. James, B. R., Lyons, J. R., and Williams, R. J. P., *Biochemistry* **1**, 379 (1962); James, B. R., Parris, M., and Williams, R. J. P., *J. Chem. Soc.* 4630 (1961).
19. Jillot, B. A., and Williams, R. J. P., *J. Chem. Soc.* 462 (1958).
20. Jorgensen, C. K., *Absorption Spectra and Chemical Bonding in Complexes*, Pergamon, London, 1962, pp. 134-173.
21. Krumholtz, P., in *Abstracts of the Seventh International Conference Coordination Chemistry*, Stockholm, 1962, p. 290.
22. Lemberg, R., Morell, D. B., and O'Hagan, J. E., *Proc. Roy. Soc. (London)* **B155**, 339 (1961).
23. Maccoll, A., *Quart. Rev. London* **1**, 16 (1947).
24. Murrell, J. N., *J. Am. Chem. Soc.* **81**, 5037 (1959); Tsubomura, H., and Mulliken, R. S., *J. Am. Chem. Soc.* **82**, 5966 (1960).
25. Morpurgo, G., Morpurgo, L., and Williams, R. J. P., unpublished observations.
26. Orgel, L. E., *An Introduction to Transition-Metal Chemistry*, Methuen, London, 1960; Griffith, J. S., *The Theory of Transition-Metal Ions*, Cambridge University Press, 1961.
27. Platt, J. R., *Radiation Biology*, Vol. 3, McGraw-Hill, New York, 1956, p. 101.
28. Pratt, J. M., and Williams, R. J. P., *Biochem. Biophys. Acta* **46**, 191 (1961).
29. Prout, K. C., and Wiseman, T. J., unpublished observations.
30. Robertson, J. M., *J. Chem. Soc.* 1195 (1936).
31. Scheler, W., Schoffa, G., and Jung, F., *Biochem. Z.* **329**, 232 (1957).
32. Day, P., Scregg, G., and Williams, R. J. P., *Nature* **197**, 589 (1962).



33. Stern, A., and Dezelic, M., *Z. Physik. Chem.* **A180**, 131 (1937).
34. Taube, H., and Cahill, A. E., *J. Am. Chem. Soc.* **73**, 2847 (1951).
35. Terenin, A., Putzeiko, E., and Akimov, I., *Discussions Faraday Soc.* **27**, 83 (1959).
36. Tomkinson, J., and Williams, R. J. P., *J. Chem. Soc.* 1153 and 2010 (1958).
37. Whalley, M., *J. Chem. Soc.* 866 (1961).
38. Williams, R. J. P., in P. D. Boyer, H. Lardy, and K. Myrback, Eds., *The Enzymes*, Vol. I, Academic Press, New York, 1959, p. 391; Williams, R. J. P., *Chem. Rev.* **56**, 299 (1956).
39. Williams, R. J. P., in J. E. Falk, R. Lemberg, and R. K. Morton, Eds., *Haematin Enzymes*, Pergamon, London, 1961, p. 41.
40. Williams, R. J. P., *Ann. Rept. Chem. Soc. London*, 1960, 87.
41. Williams, R. J. P., *J. Chem. Soc.*, 137 (1955).
42. Williams, R. J. P., *Federation Proc.* **20**, 5 (1961).

*Notes added in proof:*

1. New data on manganese phthalocyanine absorption spectra have been published by Engelsman, G., Yamamoto, A., Merkbam, E., and Calvin, M., *J. Phys. Chem.* **66**, 2517 (1962). Table IV has been modified in the light of this publication and our own observations.
2. Data on manganese porphyrins published by Loach, P. A., and Calvin, M., *Biochemistry* **2**, 361 (1963), show that in the Mn(III) compound the charge transfer interaction splits the Soret band and that this compound too has a long-wave absorption band (770 m $\mu$ ).
3. The reactions of zinc porphyrin, Closs, G. L., and Closs, L. E., *J. Am. Chem. Soc.* **85**, 818 (1963), have clearly demonstrated the reactivity of the methene bridge carbons as discussed in this article.
4. The exchange rate of the methene bridge hydrogen in chlorophyll has been found to be relatively fast, but slower than that of a hydrogen of a tertiary carbon. Katz, J. J., *J. Am. Chem. Soc.* **85**, 4049 (1963).
5. The spectrum of a porphyrin-like pigment with the methene bridge carbon saturated as in the postulated intermediates in catalase has been described and discussed by Gouterman, M., and Wagnière, G. H., *J. Mol. Spectry.* **11**, 108 (1963).

## 11

# PROSPECTS FOR THE USE OF INFRARED SPECTROSCOPY IN BIOLOGY

J. LECOMTE, *Laboratoire des Recherches Physiques de la  
Sorbonne, Paris*

## CONTENTS

I. Introduction . . . . .	408
II. Experimental Technique . . . . .	409
A. Detection of Infrared Radiations . . . . .	409
B. Sample Preparation . . . . .	410
III. Some Applications of Infrared . . . . .	412
A. Identifying Substances by Their Infrared Absorption Spectrum . . . . .	413
B. Demonstrating Small Structural Differences Between Very Similar Compounds or Isomers . . . . .	416
C. Attempts at Determining the Structures of Biological Substances . . . . .	418
D. Detecting Inter- or Intramolecular Bonds . . . . .	423
IV. Prospect for the Use of Infrared Spectrometry (or Global Infrared) in Biology . . . . .	427
A. Experimental Technique . . . . .	427
B. Problems Requiring Study . . . . .	429
C. Use of Undispersed Infrared Radiations . . . . .	432
D. Miscellaneous Applications . . . . .	432
V. Conclusion . . . . .	434

## I. INTRODUCTION

The object of these few pages is not to give a summary of the applications of infrared spectroscopy to biology (or to medicine), but to express a few personal ideas. To begin with is a discussion of the reasons why biological problems have only been considered recently from the infrared point of view and how recent improvements in technique now make possible an everyday application of infrared spectroscopy to a great many biological (or medical) questions (Section II). This will be followed by a few examples of results obtained in biology (Section III), concluding with an outline of future uses of infrared spectroscopy in this field (Section IV).

## II. EXPERIMENTAL TECHNIQUE

### A. Detection of Infrared Radiations

Although the infrared spectrum was discovered more than 150 years ago, until 1945 its use by non-specialists was absolutely impossible because of the many difficulties in experimental technique. Nowadays, mass-produced spectrographs are equipped with an accurate detector combining good reproducibility with fast response and high sensitivity. They provide by means of a pen recorder (or, less often, on the screen of an oscilloscope) a curve giving the intensities of infrared radiations as a function of different wavelengths. Excellent prism, or grating, spectrographs make it possible to investigate without difficulty the spectral range extending from the visible to wavelengths of approximately  $20\mu$ . However, access to longer wavelengths remains difficult. Microspectrographs are particularly valuable to biologists; they make it possible to perform a spectral analysis with quantities not larger than a microgram. Also of value are fast spectrographs, which enable the researcher to follow a reaction occurring within a fraction of a second. Nowadays to obtain the absorption spectrum or the reflection spectrum of a biological compound, it is no longer necessary to consult an infrared specialist but, rather, a careful and skilled technician.

Not only the lack of practical instruments, but also the deplorable use which was made of those existing has often prevented infrared spectroscopy from being introduced into biology. Even now, in certain misinformed research centres, spectrographs continue to be used without taking their dispersion sufficiently into account. As we have pointed out many times in the past quarter of a century, *it is absolutely necessary to choose a correct dispersion if one wishes to get interpretable results; the closer one gets to the visible spectrum, the larger this must be.* A given spectrograph can be used only in a fixed and limited spectral range. It is infinitely better to record infrared spectra in a sometimes very restricted but well-chosen range than to attempt to use a given instrument incorrectly. Failure to observe these rules resulted in a somewhat hasty judgment of the usefulness of the technique, and even now ignorance of these rules still hinders general application in this field. If one merely wishes to examine substances in the infrared region, without spectral

decomposition, the image converter enables one to "see" a wavelength up to  $1.2\ \mu$ . In the same range, photography with sensitized emulsions easily gives excellent results. It is unfortunate that up to the present these two techniques have practically been unused for everyday examination of biological compounds, especially in conjunction with a microscope.

### B. Sample Preparation

Until recently, because of the presence of water, biological compounds, and even more so aqueous solutions, were regarded as excluded from the scope of infrared studies because of the very strong absorption of water, and because of the difficulty of finding insoluble windows for the cells containing the products. The first problem has been solved by adopting differential techniques or through enlarging the scale (a weak transmission, of 5 to 10% for example, is used instead of the usual 100%) and the second by the introduction of new synthetic materials which are insoluble in water, such as sapphire, barium fluoride, thallium bromiodide, and silver chloride. These have widened the previously restricted range (quartz, calcium fluoride, etc.). Thus the technical obstacles to the use of the infrared method in biology were eliminated. Let us also note with interest the substitution of heavy water for ordinary water because of the former's less intense absorption with a less awkward spectral position of absorption bands.

If it is possible to carry out an examination of dry products, we would point out that we have shown, by handling thousands of substances for the last twenty years or so, that powders give excellent spectra. The technique has been improved by using a Nujol paste, for instance, which reduces diffusion. This powder method thus makes it possible to extend the infrared technique to a very large number of compounds which are available only in powder form, and which are almost insoluble and non-melting (or which decompose upon heating).

Ingenuous methods have been introduced, such as that of built-in standard or of compensated extinctions. However, quantitative measurements still involve great difficulties because the loss by diffusion cannot easily be distinguished from the loss by absorption. The usefulness of the pellet method is well known. In this method,

by almost completely avoiding scattering of the powder, quantitative determinations are possible. A 1% mixture of the powder in a metal halide (potassium or caesium bromide or chloride) is used; however, high pressures must be exerted on the mixture, and experience shows that these high pressures fairly often modify the molecular structure of the powder. Changing the halide frequently produces a shift of the absorption maxima as do variations in experimental conditions (particle size, powder moisture, etc.).

If one uses the above-mentioned techniques in preparing the samples, the greatest care must be taken to prevent the modification of the original structure of the biological substance. The same

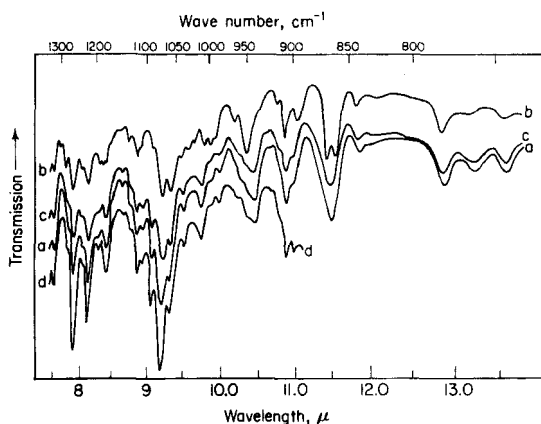


Fig. 1. Variation of the spectrum of deoxycorticosterone with the method of sample preparation; (a) melted film, (b) mineral oil mull, (c) deposited film from chloroform, (d) carbon disulphide solution. (After H. Rosenkrantz and L. Zablów.)

applies to other techniques, such as evaporation *in vacuo*, deposition on a transparent plate after evaporation of a volatile solvent, suspension in a liquid medium or merely dissolution in a suitable solvent or preparation by fusion on a solid layer. If structural modifications take place, they will be immediately manifested in modifications in the infrared spectrum. Figure 1 shows these variations and demonstrates the necessity of using controls, i.e., comparing the results of samples prepared by several different techniques.

It should be noted that even with microspectrographs, it will be

possible to examine crystals by polarized light. For the microspectrographs, small silver chloride cylinders are used as cells. Along their axes they have a hole, a few tenths of a millimetre in diameter (to hold the liquid or the solution) and they lie directly on the plate of the mirror microscope. Mirror microspectrographs have a remarkable depth of field for the examination of samples.

It may thus be concluded that the infrared technique represents an ideal tool which can be used routinely without particular difficulties by biologists.

### III. SOME APPLICATIONS OF INFRARED

All biological compounds have a large number of bands (sometimes several dozen) between the visible and wavelengths of 20 or 25  $\mu$ , that is, in a fairly accessible region, which makes it possible to characterize compounds fairly surely. In the region which extends up to 15  $\mu$ , and which is easily accessible with sodium chloride optics, a spectrum is observed which is generally so characteristic that it has been called the "finger-prints" of a substance.

For a biologist, it is known that the use of the infrared has many valuable advantages:

(1) Spectra may be obtained using a very small quantity of the substance (as little as a microgram).

(2) Compounds may be studied precisely in the state in which they are found (powder or aqueous solution for instance).

(3) Spectral measurements can be made without fear of a change of structure, and even black or fluorescent compounds may be used.

The experimenter's attention has to be drawn to some difficulties arising particularly with biological compounds. Their structural complexity is manifested by the existence of such a large number of bands that in many cases the present state of the technique does not make it possible to separate them. In practice, absorption maxima will be observed which have possibly resulted from the merging of several neighbouring maxima. Hence the appearance of the spectrum and the number of individual bands will depend upon the dispersion of the spectrograph. For it to be possible to make a satisfactory comparison between two spectra obtained with two different instruments, full account must be taken of their respective dispersions. We think that these difficulties can be eliminated, at

least partly, in analogous cases by determining, for example, not only the positions and the *relative intensities of the absorption bands*, but also their *absolute intensities*. The latter represent constants which are independent of the dispersion of the spectrograph (especially of the slit width), and their measurements should be generalized. Unfortunately, they are not as easy to measure as wavelengths or transmission percentages.

Let us now briefly review some of the uses to which a biologist may put the infrared method:

(A) for identifying substances, pure or in mixture, without having to make assumptions about their structure;

(B) for demonstrating structural differences between similar compounds or isomers;

(C) for attempting to make the structural determination of biological substances;

(D) for investigating inter- or intramolecular bonds, which play a part in biology probably essential but as yet underestimated.

#### **A. Identifying Substances by Their Infrared Absorption Spectrum**

These identifications are made without any assumption about the structure of the substance, whether in the pure state or in a mixture; it is also possible to make a comparison of two mixtures by simply considering the position and the intensity of the absorption bands, again without having to make any hypotheses about the structure of the compounds. This operation merely requires a comparison spectrum of a pure compound or a mixture.

Here are some *qualitative applications*:

(1) the identification of steroids in physiological liquids; generally speaking the infrared is the method to be preferred;

(2) the study of modifications in the structure of steroids induced by radioactive radiations;

(3) the verification of the structure of products obtained through microbial action;

(4) the identification of monoglycerides formed in the intestine from the reaction between milk fat and glycerine;

(5) the investigation into the changes in the composition of gall stones over a period of time (the work of our group);

(6) the study of the modifications in the structure of muscle,

brought about by excitation (work published by us in collaboration with Dubuisson and Monnier since 1942);

(7) the comparison of the peritoneal fat of the normal rat and of the castrated rat (work in collaboration with Verne and Wegman);

(8) the comparison of cerebral samples from various species;

(9) the attempted classification of viruses according to their infrared spectrum; the study, as a function of time, of the differences in extracts of tubercular bacilli taken from different species.

A simple comparison of infrared spectra has led to the identification of Karrer's pseudoyohimbine and Hahn's yohimène (Janot), as well as miropinic acid and isodextropimaric acid, etc. It should be noted that in the case of complicated substances or mixtures having a very dense spectrum, the identification of compounds becomes more rapid and more accurate through the use of electronic computers. Mere visual comparison of the spectra is no longer sufficient, especially if it is a question of detecting traces of a constituent compound. Computers have even been used to predict the infrared spectrum of a substance from its chemical formula.

Moreover, it is possible to make *quantitative applications*. For a long time now, methods have been in use which make it possible to determine the quantities of each constituent element in a mixture, provided that one knows a characteristic band for each, called the "key band". Until recently, in order to make the calculation, the maximum absorption coefficient of each substance in the mixture was given for each key band. Nowadays, it has been recognized that it varies with the dispersion of the spectrograph (especially with the slit width) and that it is better to determine and to use the absolute key band intensities, even at the cost of a few extra difficulties.

For semiquantitative determinations, the differential method gives good results if applied skilfully. A double-beam spectrograph is used, and on the reference beam is put a cell containing the pure compound to be identified. In the spectrum given by the cell filled with the mixture and placed on the measure beam, the absorption maxima of the selected compound will not appear, or if compensation is not complete they will be markedly reduced. Of course the same method may be applied to a mixture placed on the reference beam; then the measure beam will give a spectrum diminished by that of the mixture.



It is to be noted that biological problems are generally concerned with mixtures which are of an extremely complex nature and certain constituent elements are present only as minute traces. As the number of constituent elements grows larger, so does the number of absorption peaks, which can no longer be separated, and the infrared spectra are no longer useful. On the other hand a component's characteristic absorption bands may be masked by those of other components, if it is present in only minute amounts, or if its bands coincide with the stronger bands of other components. Therefore, all applications of infrared to biological compounds should begin with as thorough a separation as possible of the components of the mixture by physical methods (fractional distillation, solidification, and dissolution, paper or column chromatography in the gas phase, counter-flow distribution, etc.) or by chemical methods, to avoid handling mixtures containing more than three or four main components.

It may be convenient to prepare precipitates each containing only a very limited number of constituent elements, and to study them separately. In other cases, it will be necessary to break down the studied compound, in the case of polymers for example, or to break the carbon chains if these contain more than 8 to 10 atoms. Experience shows that infrared spectra appear to be very similar when small variations take place in a long carbon chain, whereas small chains show considerable differences in their spectra. Of course, each time a chemical treatment is made, there is the risk of altering the original product. Caution is necessary, but one should not persist in studying a compound as it is, for this may give results which are impossible to interpret. In principle, the sensitivity of the infrared method is rarely less than 1 or 2%, so that it is essential to concentrate a component if only a trace is present.

*It is not sufficient to place before the slit of an infrared spectrograph any mixture of biological compounds, as has been done too often so far.* Let us recall that in the case of other complex mixtures (for example hydrocarbons in automobile or aeroplane fuel or in lubricating oils), the infrared method leads to interesting results only if applied to suitably separated fractions.

In any case, it is possible to measure quantitatively by infrared absorption traces of water (of the order of a microgram); androsterone in isoandrosterone; androsterone in etiocholane-3 $\alpha$ -ol-

17-one; cholesterol, phenacetin, aspirin and caffeine; aldrine and dieldrine, piperine, nicotine, hydrastine, piperidine, strychnine; the sodium salts of different pencillins; cinchonine, cinchonidine; quinidine and quinine; leucine, norleucine, and isoleucine, etc.

### **B. Demonstrating Small Structural Differences Between Very Similar Compounds or Isomers**

We shall briefly mention the possibility of distinguishing between isomers differing in the form of the carbon chain, isomers corresponding to substitutions at different positions of a ring (the case of carcinogenic and non-carcinogenic hydrocarbons seems rather characteristic), and stereoisomers (for example etiocholane-3 $\alpha$ -ol-17-one, androsterone-3 $\alpha$ -ol-17-one, androsterone-3 $\beta$ -ol-17-one and etiocholane-3 $\beta$ -ol-17-one). In the case of polymorphous forms, the infrared spectrum often varies considerably when passing from one to the other (1-monostearine, Fig. 2) or allopregnane-3 $\alpha$ -ol-20-one.

Similarly, it is easy to distinguish between the infrared spectra of theobromine of the theophylline and of caffeine, which are compounds of very similar structure.

In our research we have shown the possibility of distinguishing the various forms of calcium oxalate from plants and the different crystallographic structures of calcium carbonate extracted from animal tissue.

The use of infrared spectroscopy also leads to interesting results in connection with distinguishing between or determining the proportions of tautomeric forms, such as nitriles and carbylamines, *syn* and *anti* forms, ketone-enol isomerism, tautomeric forms of oximes, etc. We emphasize the fact that our technique cannot cause a modification in the equilibrium state.

*Rotational isomers* are generally less familiar to biologists. A quarter of a century ago, we showed the impossibility of interpreting many infrared spectra without assuming the existence of more than one molecular form. In order to reach this conclusion, it was necessary to abandon the principle of a free rotation around a single bond (C—C, C—O, C—N, etc.) and to admit the possibility of discrete rotations around these single bonds, which would give rise to a new isomerism. It is not possible to separate the isomers which derive one from the other by rotations around the single bonds since the forms are in equilibrium at a given temperature, dilution, etc.

If one of them is isolated, it is formed again at the expense of the others in the proportion required to restore the equilibrium. The case of a free rotation around a single bond is not to be excluded but it is rather rare, whereas it used to be considered an absolute generality.

This notion of rotational isomers seems to us particularly important in biology and probably due to experimental difficulties it has not been possible to give it a precise meaning in a large number of

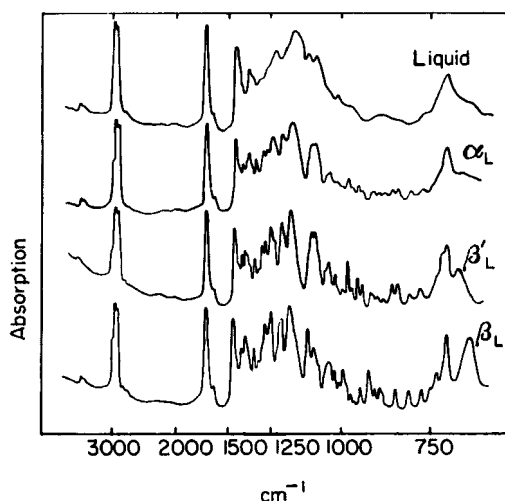


Fig. 2. Polymorphous forms of 1-monostearine. (After D. Chapman.)

cases. As long as one deals with molecules of relatively simple molecular structure there exist only two or at most three rotational isomers. But with compounds of biological interest, their number must be much larger. It would appear that deoxyribonucleic or ribonucleic acids occur in a great number of forms which are transformed from one to the other as a result of relatively weak changes inside the cell (variations in pH, in electric charges, in pressure, in molecular association, and so on).

Spectroscopically speaking, the properties of rotational isomers differ from one another and it has already been shown in a certain number of cases that chemical properties, in particular reactivity, depend on the molecular configurations. In certain of them reacting groups are removed from one another; in others steric hindrances

are produced with the possibility of the further steric hindrances arising or disappearing, the latter favouring the reaction. It would not seem unsuitable to transpose these conclusions to biology.

Mere counting of bands does not always give an idea of the increase or the decrease in the number of forms present. As we have shown in the case of saturated aliphatic acids, an increase in number of forms, in the liquid state, leads to a simplification of the spectrum in comparison to the solid state, where probably only one form exists. It is in fact impossible, in view of the dispersion of present-day spectrographs, to separate the very numerous bands of the liquid state (which merge into wide maximums), whereas the less numerous bands of the solid state remain separate. It arises from the foregoing, and we must emphasize this, that very marked modifications in the infrared absorption spectra are to be expected when the experimental conditions are modified. In biology, the *in vivo* environment of the substances to be studied must be reproduced as exactly as possible, for we shall see further on that other phenomena, such as intermolecular associations, also are involved in producing structural modifications.

It must be concluded that *the infrared spectrum is one of the best methods for bringing to light slight or very slight modifications in molecular structure*. The obstacle, which we have noted already, arises from the complexity of spectra of biological substances, so that the diagnosis regarding possible changes cannot be so easily applied.

### C. Attempts at Determining the Structures of Biological Substances

So far, we have not established any correlation between the structure of molecules represented in a very approximate fashion by the usual formulae and infrared absorption spectra. It has long been recognized that there is a clear relationship between the presence of certain absorption maxima and the existence of given groups. Vibrations such as CH (or CH<sub>2</sub> or CH<sub>3</sub>), NH (or NH<sub>2</sub>), OH, CO, etc. in organic chemistry, CO<sub>3</sub>, SO<sub>4</sub>, NO<sub>2</sub> and so on in inorganic chemistry resonate and use energy from the incident wave, giving rise to absorption bands. These may correspond not only to fundamental vibrations, but also to overtones or to combination vibrations, from which arise the complexity of the infrared spectrum.

Tables of correlation have therefore been established, extending over an important infrared field (from the visible to about  $25\ \mu$ ) and including more or less important groups of structures. These tables have been very useful and still are, but they must be used correctly. In the first place, there exists a certain number of vibrations, characteristic of the structure of the entire molecule; these cannot therefore appear in the tables described. Moreover, they represent only a first approximation. All chemists know that the different parts of a molecule influence one another, and that it would be quite

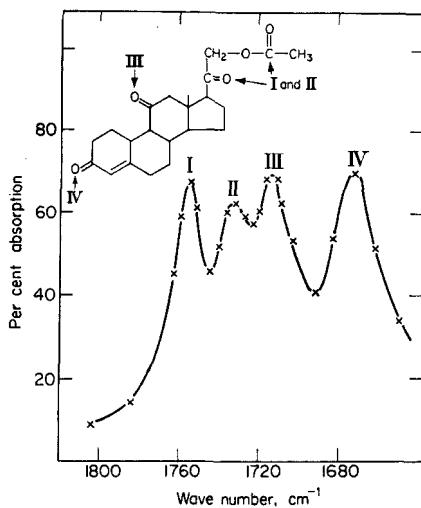


Fig. 3. Transmission of deoxycorticosterone acetate dissolved in carbon disulphide. (After R. N. Jones and K. Dobriner.)

incorrect to consider them separately. We must therefore exercise the greatest caution regarding conclusions based on a division of molecules into parts in order to find bands characteristic of these parts. The abuse of these more or less automatic methods for the interpretation of infrared spectra has led to such errors that if this continued our method might be discredited as a result. We may consider, for instance, dehydrocorticosterone acetate (Fig. 3), where four carbonyl C=O bonds are to be seen, the spectrum presenting four distinct bands of the C=O bond. This example, chosen from many, shows that the vibrations of each group are influenced by their position in the molecule, and also by their

environment. In particular, the structure in the spectrum of the bands relating to  $C=O$  depends on the number of atoms in the cycle on which this group is placed. It was shown by our group some thirty years ago that maxima corresponding to vibrations between carbon and hydrogen are influenced by the presence of "double" or "triple" bonds in the molecule. Halogens generally increase the vibrational frequencies of neighbouring groups, whereas the conjugation of two double bonds decreases them; these two effects may in fact exist together.

The study of absorption bands whose exact position corresponds to that of the above-mentioned correlation tables is justified only as a first approximation. But the increasing precision of measurement and the more exact knowledge of spectra make possible the opening up of a most fertile new line of research, i.e. *the study of variations in position and intensity of bands characterizing a group around its average position, following the structure of the material examined*. The best results of this method have been in the case of steroid classification, and it has become possible to obtain information about the structure of a new steroid without resorting to chemical analysis.

Following the way initiated by Jean Cabannes, the study of symmetries as a means of interpreting spectra has been shown to be most profitable, and conversely it is possible to arrive at the symmetry of the molecule (or the crystal) by consulting the spectroscopic data. Thus, in simple metallic oxalates we have shown in collaboration with Cl. Duval that the  $(COO)_2^-$  ion probably possesses a centre of symmetry which disappears with complex oxalates. In the same way, our research on metallic tartrates shows that the structure is staggered as shown in Fig. 4 and has only a plane of symmetry for the dextro and the laevo compound (one being the mirror image of the other), but has a centre of symmetry for the meso form. Unfortunately, many biological substances have a complex structure of low symmetry, or even none at all, so that rules relating to the studies of symmetries are of less interest.

Infrared methods have to their credit many successes in the determination of molecular structure. The late H. Lenormant showed long ago that absorption maxima corresponding to those of amides monosubstituted on nitrogen could be identified in pure

proteins. The use of our method should be very fruitful in the study of the difficult problem of the structure of polypeptides, especially for the identification of folded up  $\alpha$  or extended  $\beta$  chains, or of the well-known helicoidal form or of a structure proposed by Cannon. Recourse to polarized radiation has been shown to be particularly promising, especially in the case of natural or synthetic fibres.

The case of amino acids seems to us especially interesting. By the infrared method it can be seen at once whether there is a *true acid* structure  $\text{H}_2\text{N}-\text{R}-\text{COOH}$  or an *ionized structure*  $^+\text{H}_3\text{N}-\text{R}-\text{COO}^-$ . Conversion of one to the other depends on physical conditions (solid, alkaline or acid solution) and is of direct interest to biology.

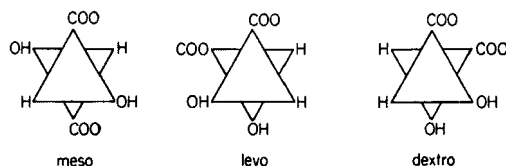


Fig. 4. Symbolic representation of the tartrate ion. (After Cl. Duval and J. Lecomte.)

Thanks to the study of a narrow region, between  $5.5$  and  $7\ \mu$ , it was possible to choose without ambiguity among three formulae put forward for penicillin: an oxazolone structure, a tricyclic structure, or a  $\beta$  lactam. X-rays, in particular, have confirmed the choice of the last, in spite of the complexity of the problem.

Working on alkaloids, the numerous studies undertaken by Dr. Janot and his students produced immediate results. Here again very complicated structures were involved. Thus, for sempervirine the absence of a band at  $3\ \mu$  eliminates all formulae containing the  $\text{NH}$  group. A chain of atoms, hitherto unknown in the plant kingdom,  $\text{CH}_3-\text{O}-\text{C}=\text{C}-\text{O}-\text{CH}_3$ , was distinguished by two maxima neighbouring  $6\ \mu$  ( $5.9$  and  $6.2\ \mu$ ). Each time these appear, the formula must contain this group. This applies to aricine, corynantheine, dihydrocorynantheine, corynoxine, marycumbine, dihydrocorynoxime, alstonine, tetrahydroalstonine, and  $\delta$ -yohambine; but, unexpectedly, these two maxima are not observed in yohambine, *allo*-yohambine, pseudoyohambine, coryanthine,  $\alpha$ -yohambine or  $\beta$ -yohambine. In spite of their relationship

to the foregoing substances, they should be written without the characteristic group described above.

In the case of tricyclic carbon compounds obtained by treating "scareol oxide", the nature of the third cycle could be established through the use of infrared. In collaboration with Y. R. Naves, using our method, we followed the complete structure of ionones and irones, in spite of the existence of several position isomers and stereoisomers.

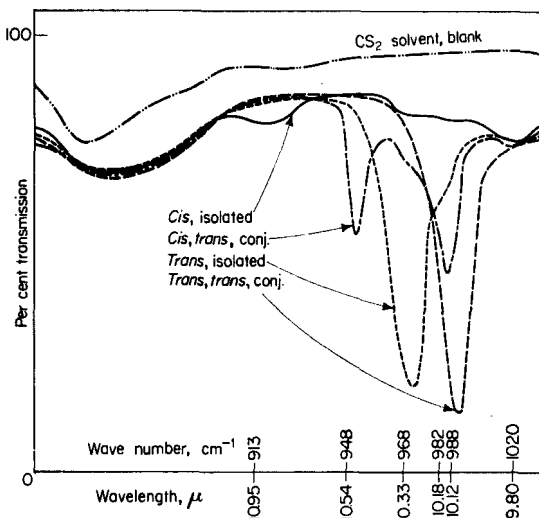


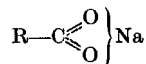
Fig. 5. Distinction of different stereoisomers of methyl linoleate dissolved in carbon disulphide. (After J. E. Jackson, R. F. Paschke, W. Tolberg, H. M. Boyd and D. H. Wheeler.)

The characterization of the *cis-trans* isomerism by absorption bands, other than those of the double bond, as we showed long ago, provides important data for the interpretation of the structure of antibiotics such as mycomicine and isomycomicine or of esters of non-saturated acids (methyl linoleates, Fig. 5).

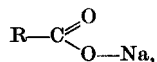
Variation in the position of bands, attributed in a first approximation to the same bond, indicates the existence of different bond forces between the same atoms. The present chemical formulae do not take this into account, as we know. For biological compounds, it seems to us worthwhile to get new information in this way, and



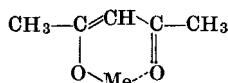
this can be done without difficulty. These ideas could be applied to combinations between organic products and metals, a problem which has as yet been somewhat neglected from the spectroscopic point of view but which is obviously important from the point of view of the part played by metals in the organism. In this way we showed, with Cl. Duval about twenty years ago, that the metal salts of an aliphatic acid should be written



for instance, and not

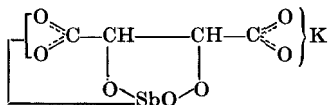


as is found in the early textbooks. Resonance takes place between the two bonds which connect the carbon atom with the two oxygen atoms. In the same way, our spectra of metal acetylacetonates lead one to visualize a series of intermediary bonds between a "single" and "double" bond. The classical formula written as:



takes no account of the real state of the bonds which appears from the shift of the infrared bands.

Similar conclusions emerge from our determinations of bismuth and antimony tartrates (in collaboration with M. Girard). In the case of emetic, one of the ionized carboxyl groups appears to be identical to those of metal salts of carboxylic acids, whereas the former is perturbed by the presence of the SbO radical; the formulae (shown below) in their present form show this very imperfectly.



#### D. Detecting Inter- or Intramolecular Bonds

These bonds probably play a much more important part than is attributed to them at the present time. It is easy to conceive that in living systems bonds more labile than true chemical bonds

may be formed. As we have already pointed out, the nature and number of rotational isomers depend essentially on intermolecular bonds. A thorough study of these biological complexes would certainly give rise to new outlooks.

We believe that the extraordinary syntheses which take place in the plant and animal kingdoms are accompanied by ever evolving associations of molecules. Langmuir remarked that an ocean corresponds to a single molecule if one were to consider the associations made between water molecules; it is even possible to imagine, in certain limited areas, the existence of a pseudocrystalline structure. The degree of vital activity can be measured at least roughly by the rate of syntheses within the organism, and we believe that intermolecular bonds to quite a large extent determine whether or not such syntheses are possible.

Now infrared is one of the best methods of demonstrating these bonds; it is possible to detect them and measure their intensity, without affecting them in any way. Whenever certain groups such as OH (or OD), NH (or ND),  $\text{NH}_2$  (or  $\text{ND}_2$ ), etc. can no longer vibrate freely, for instance as a result of a hydrogen bridge, the corresponding absorption band shifts, often considerably, towards greater wavelengths. The shift is a measure of the strength of the association, and is related to the distance separating the two atoms bound by the hydrogen bridge. Also, bands corresponding to free-molecule vibrations are seen to be narrow and deep; those of associated molecules appear wide. Intermolecular associations are more or less completely broken by dissolving in an inactive solvent, or by raising of the temperature, it is possible to deduce for free molecules and associated molecules the extent of association, and various thermodynamic constants from the respective intensities of the two bands. Consequently, the use of infrared has the great advantage that intermolecular bonds can be immediately classified. One can arrive at a clear picture of their stability; and with these figures available the probability of formation can be determined as well. Associations between molecules of the same type may also be broken by the formation of associations with different molecules, for instance with an active solvent. Where there is only a weak spectral displacement between bands characterizing two types of molecules, associated or non-associated, the method of mixed solvents (used by Prof. M. L. Josien) can successfully be employed.

This method consists of dissolving a certain concentration of a substance in a given solvent, then diluting various concentrations of this solution in another solvent.

Steric hindrance is an important factor in the formation of intermolecular associations. Our group was able to show, twenty years ago or so, that xylidine isomers have intermolecular association ratios which vary according to the isomer. Whenever the  $\text{NH}_2$  group was found on the aromatic nucleus close to the two  $\text{CH}_3$  groups (or *a fortiori* between these), the association of the corresponding isomer molecules was lessened. This was established by measuring the variation in the intensity of NH bands during dissolution in a neutral solvent. The absence of variation corresponded to the absence of association between xylidine molecules, with all the association levels for different variations. The same was recorded with phenols, *ortho*-substituted with a hindering group, such as *t*-butyl or *t*-amyl; their presence precludes the possibility of associations between neighbouring molecules.

Using the Kirkwood-Bauer-Magat line, the points which fall outside this correspond to solvents forming molecular associations with the substance under study. On the abscissa, the relative displacements  $\Delta\nu$  of the chosen characteristic band are plotted, starting from the position occupied for the compound in the vapour state, and on the ordinate is plotted the ratio  $(D-1)/(2D+1)$  where  $D$  is the dielectric constant of the solvent (Fig. 6).

These considerations show that the physical state of the substance studied must be fully taken into account and that one must try to obtain the frequency vibrations of free molecules (low concentrations in a neutral solvent or in vapour state) as these are characteristic rather than the frequency-vibrations of associated molecules. But in biology, it would seem to us certain that there exist other factors which make intermolecular associations more or less likely: certain atoms (halogens in particular) or groups of atoms in molecules have a dissociating power and certain configurations lead to a hindrance which renders associations impossible. In a tissue or in a cell, the production of specific substances will prevent or break up intermolecular associations. But more important, the permeability of certain cell membranes, which had probably been lowered in the presence of certain associated molecules, becomes higher when these molecules are no longer associated.

Certain conditions of pH show themselves to be necessary for the formation and persistence of complexes, as has already been recognized; but we do not believe that the indirect action of electric fields has hitherto been explored deeply enough for all cells are subject to their influence. In our opinion a thrilling chapter remains to be written, embracing the whole of biology and treating the existence of intermolecular associations, the complexity and

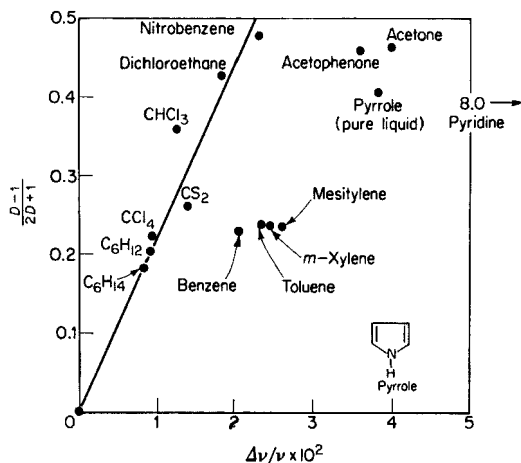
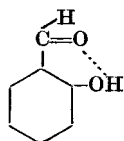


Fig. 6. Relative shift of the NH stretching vibration frequency of pyrrole (diluted solution or pure liquid) as a function of the dielectric constant of the solvent. (After M. L. Josien and N. Fuson.)

variety of which appear to be on the scale of so-called vital phenomena, although still entirely unsuspected.

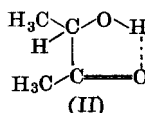
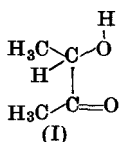
Alongside intermolecular associations must be placed intramolecular associations (chelation phenomena). The best known example is found in certain benzene derivatives ortho-substituted with a hydroxyl group. Thus, with salicylic aldehyde the formula presents an internal hydrogen bridge which modifies at the same



time the vibration frequency of both C=O and of OH. The latter

is displaced to such an extent, in comparison with its position in the case of free or associated OH groups, that it was for a long time thought that chelation was expressed by the suppression of the OH vibrations (fundamental and overtones). The essential difference between association and chelation is that the latter cannot be broken up through dissolution or through an increase in temperature.

Acetyl-methyl-carbinol, studied in our laboratory, provides a particularly interesting example of what can be learned from a study of infrared spectra. This compound exists in two forms, one chelated (II), the other non-chelated, but producing intermolecular associations (I). They are in equilibrium and change from one to



the other depending upon the conditions of the experiment. The dissociation energy of the OH oscillator and its variations when going from form (I) to form (II) can thus be determined by means of calculations and simple experiments, as can the equilibrium constant between these two forms, association heat, entropy and enthalpy and so on.

#### IV. PROSPECT FOR THE USE OF INFRARED SPECTROMETRY (OR GLOBAL INFRARED) IN BIOLOGY

We will examine this from various points of view.

##### A. Experimental Technique

In spite of the perfecting of spectrograph construction, the best results are not obtained by simply pressing buttons, as is too often done. For each problem the choice of a recording speed and a programme for the slit width are required, and this the manufacturer cannot indicate in advance. Similarly, the method chosen for the preparation of samples to be examined (whether in the solid state as powders or pellets, in solution or in the vapour state and the temperature range, etc.) will influence considerably the conclusions to be drawn from infrared examination. In addition, in spite of noteworthy progress in the last fifteen years, the infrared technique

as far as biological applications are concerned still needs to be improved.

The objective to be aimed at is to experiment directly on the cell and its constituent elements, as the area covered by mirror microscopes is still much too large. On account of optical difficulties, we do not think that it is possible to increase sufficiently the magnifying power of these microscopes, so that other solutions must be sought. The advantages of wave guides in the ultra-hertzian region are known; perhaps it might be possible to have recourse to a similar technique, and to operate with infrared radiations of a few dozen microns, instead of restricting the wavelength to 20 or 25  $\mu$ .

It is probable that the frequent use of spectrographs of much bigger dispersion (with echelette grating) or the introduction of interference systems would make it possible to split wide bands into their elements. It would seem to us that the success of these improvements is uncertain, on account of the extreme complexity of many biological products, and also on account of all kinds of intermolecular associations which probably occur. If these associations are not broken (by dissolution in active or non-active solvents, or by increasing the temperature) the chances of success will remain slight.

On the other hand, we foresee a great future in the continuation of studies towards longer wavelengths. In our laboratory, and that of A. Hadni at Nancy, which is derived from ours, wavelengths of several hundred microns can now be reached for current use. Thus there appears a vast, almost unexplored, field which should be very valuable for the study of macromolecules.

It should be said, even though these past few years have shown the possibility of carrying out measurements in aqueous solutions, the technique still has to contend with important difficulties, principally that of compensating for the water absorption. This problem proves to be great largely on account of intermolecular associations of water; systematic though delicate studies aimed at operating with water in a less associated condition would be very worthwhile. In this respect, the use of heavy water results in an immediately noteworthy improvement. It also becomes possible to use a method of total reflection (Fahrenfore).

Finally the great obstacle to the application of infrared to biology stems from the complexity of the mixtures and the minute

percentage of certain constituents. Along with perfecting methods to separate constituent elements, increased precision in measurements should also be sought. Due attention must be paid to apparatus (scale expansion, increase in amplification) and to the preparation of samples made after careful separation of mixtures.

### **B. Problems Requiring Study**

It must be recalled that the growing success of infrared technique as a means of completing chemical analysis derives mainly from an increase in systematic studies. In this way, data needed for comparison become available. But unfortunately, owing to the rather limited number of studies performed on substances of biological interest, we have insufficient information to make comparisons. This is clear when one considers what a great number of substances there are which are biologically important.

It is not intended to enumerate the biological problems in which the use of infrared would probably be profitable. The examples given in this chapter will suggest the ideas needed, especially as we have in each case tried to indicate circumstances favourable and others unfavourable to such studies.

Nevertheless we would like to draw attention to the problem of water in biology, as infrared is able to give information not obtainable by any other method. In the first place the shift of its absorption bands due to intermolecular bonds immediately indicates its degree of bonding, and this is not easy to determine otherwise. Also, hygroscopic water or water of crystallization can be distinguished from constitutive water. In the first case, the infrared spectrum shows all absorption bands proper to water (with the positions corresponding to its degree of bonding and the intensities inherent in the water content). These bands can be made to disappear by dehydrating the substance, and a significant modification of the water spectrum is generally observed when definite intermediate compounds are formed. The preparation is made with a thermobalance in a very simple way, following the technique well-established by Duval, for instance. In the second case, it is impossible to eliminate the water without destroying the substance, for a certain number of water molecules are found bound to the structure of the compound itself. These must be written into the formula itself, and not outside it, as is too often done. In these

conditions, the presence of water will act on the *whole* of the spectrum and not on the regions of the bands characteristic of water. We have many times drawn attention to the remarkable possibility of distinguishing different types of water by means of the infrared spectrum, and we believe this to be of primary importance in biology. Thus, for instance, with deoxyribonucleic acid, protamine sulphate, etc., Miss de Lozé has brought to light important spectral modifications outside regions characteristic of water (or heavy water) showing that it forms part of the structure.

The fact, for certain substances, of compensating rotary power exerted on polarized light by a mixture of left and right constituents. As we have pointed out, it can be known at once if it is a case of simple optical compensation (*d*-pinene, *l*-pinene) or of the formation of a new substance (*d*-tartrate, *l*-tartrate, or racemic compound). In the first case, the infrared spectrum is not modified, whereas the spectrum of the racemic compound happens to be rather different from the spectrum of the dextro or the laevo compound (admitted to be identical) and also of the meso compound. Taking into account the special function exercised in nature by optically active rather than racemic substances, we believe it would be especially worthwhile to apply our method to this problem.

The importance of radioactive substances in biology is well known, and we will indicate under which conditions recourse to isotopes is of value in molecular spectroscopy. Up to the present, it is generally still impossible to bring to light spectral differences when going from one isotope to another, unless the element possesses a sufficiently low atomic number (boron, nitrogen, carbon). However, excellent results can be obtained by replacing hydrogen by deuterium at least partially, and we believe that this line still remains to be exploited more fully. Moreover, from the theoretical point of view, as far as the interpretation of spectra is concerned, the difference in atomic weight between hydrogen and deuterium leads one to expect corresponding displacements of certain bands.

There remains the important question of products of high molecular weight. Where polymers are concerned, one is confronted with a pattern which is repeated many times, and usually the infrared spectrum shows up the presence of this pattern, without giving an account of its repetition. It is not excluded however that the long wavelength range may reveal more information. But it is



not without interest to be able to show how polymerization has taken place and often the infrared gives indications of this where a chain with double bonds is concerned, *cis-trans* isomerism, or in the case of substitutions on an aromatic ring.

Although this is not a general case, if the spectrum of the monomer is different from that of the polymer, the infrared method is exceptionally useful for resolving the difficult problem of the number of monomers in the polymer. One thing is certain at present, and that is the possibility of making use of the infrared method to show the degree of order or disorder in which the groups of molecules under consideration are found. As regards polythene, for instance, our method very easily permits the measurement of crystallinity and this is also possible in certain other cases. The use of polarized radiations is of definite use. It is quite easy to see, by the infrared method, whether the solidification of a substance has produced an edifice without symmetry (like a glass) or a definite crystalline structure.

We would recall also that in very complex molecules whose spectra would not appear immediately interpretable, we have already drawn attention to the possibility of examining parts of these molecules, and we have noted the precautions to be taken.

An important step remains to be taken in order to experiment "in vivo" in correct experimental conditions. In fact we fear that in spite of the care taken to ensure the success of experiments, they do not present a degree of certainty sufficient to enable one to come to valid conclusions.

Very interesting experiments have been performed with infrared spectra comparing cancerous tissue with normal tissue. Preparation of tissues may have an influence on conclusions deduced from an extraordinarily complex group of constituents. Diffusion of infrared radiations also plays an unfortunate part; it is less than that of visible light because the wavelengths of infrared are much longer than those of visible radiations.

Although "labelled" elements have played an important part in biological sciences, attempts to find deuterated compounds again in normal saline solution and to note transformations by the organism are still in an early stage. Thus the injection of allopregnane-5-5d<sub>2</sub>-3-ol-( $\beta$ )-20-one acetate made possible the collecting of substances in the urine and faeces of the patient; in certain cases the presence of

deuterated products was indicated by their C-D bands whereas in the case of others deuteration did not appear.

### C. Use of Undispersed Infrared Radiations

In the foregoing, we have supposed that use was made of dispersed radiations, that is to say appreciably monochromatic throughout the range studied. We would also like to suggest the possibility of using infrared radiations coming *en bloc* from a well-selected source.

*For diagnosis*, "infrared vision" should be automatically applied along with the usual techniques using the visible for macroscopic examination of organs, microscopic examination of bacteria, chromosomes and so on, by means of an image converter or an emulsion sensitive to infrared. Similarly, the showing-up of the superficial venous circulation by the same methods should also produce useful information. The examination of the bottom of the eye by infrared makes possible an examination through the opaque crystalline lens and beyond the retina.

*As regards medical applications*, a certain number of diseases are known for which infrared irradiations give good results without any danger, for the patient always notifies the technician if the dose given is too strong. The rules to be followed in choosing the most suitable complex of invisible rays are now known. Occupational hazards of using infrared radiations, such as cataracts of glass-makers or blacksmiths, are extremely rare. It may be noted in passing that the infrared does not penetrate tissues more than a fraction of a millimetre on account of water absorption, but that action in depth can be observed nonetheless. In surgery, the technique of operations under infrared is not general but it possesses definite advantages, especially in operations of long duration.

### D. Miscellaneous Applications

Many of these are worth mentioning. Gas analysers, sensitized to dose given gases, function without failure in industry. These have already been made use of in biology for dosing, continuously and quantitatively, certain gases during a reaction (e.g. carbon anhydride evolution in the course of fermentation, noxious vapours during manufacture of chemicals). Certain anaesthetics, which have

a characteristic absorption spectrum, may also be submitted to infrared control.

We have always thought that it should be possible to proceed to a selective attenuation of viruses or bacteria by exposing them not to a massive dose of infrared (as for sterilization, for instance) but rather to adequate doses of selected infrared radiations. If we suppose, as would seem probable, that all bacteria or all viruses do not possess the same infrared absorption spectra, it should be possible to selectively inactivate a given bacterium or virus by irradiation with a sufficient dose of radiations for which they are tuned. They will absorb these radiations much more strongly and be inactivated rather than those bacteria or viruses which have no absorption in these characteristic regions. The technique which we are proposing could be compared to the delicate plucking of a stringed instrument in contrast to the playing of chords on a piano.

A problem which has never been resolved and which we would have willingly undertaken long ago had we had the means is the study of infrared rays coming from the sun in various longitudes, latitudes, and climates. It is certain that the infrared bath in which we are plunged must have different effects, depending on the spectral composition. We can state in advance that leaden and cloudy skies correspond to a different emission with longer wavelength than that of clear skies when the rays of the sun act directly with a well-known spectral distribution.

It has long been known that infrared has no effect upon vitamins (except to decompose them) but that it enhances the action of hormones. The action of hormonal treatment on plants can thus be explained at once; the solar rays to which they are exposed contain in fact a great deal of near infrared radiation. It would not seem unreasonable to suppose that action of the same kind occurs where human beings and animals are concerned. As confirmation of this hypothesis certain authors indicate that the Ashiem-Zondek reaction time (injection of a mouse before puberty, or of a doe rabbit, with urine from a pregnant woman) was considerably reduced by infrared irradiation of the hormones contained in the urine or irradiation of the animal.

This short survey shows that undispersed infrared radiations, which can be applied much more easily than dispersed radiations, also possess a quite varied range of applications. In order to be

able to use these scientifically, it is indispensable to know at least approximately the composition of infrared rays on the one hand, and their all-over intensity on the other. If one wishes to arrive at reproducible results it is not sufficient to perform an irradiation from any source or at any distance or for an inaccurately determined period.

## V. CONCLUSION

We have endeavoured in the above to show:

(1) that improvements of all kinds in experimental infrared techniques make possible their routine application in biology on a large scale;

(2) that the introduction of infrared in biology could assist in solving certain problems, and could probably lead to new solutions in a very large number of cases.

On the other hand we cannot emphasize enough the need for the correct use of infrared spectrometry. We have indicated several times the conditions which are to be observed; if they are not, then the results are incoherent and cannot be interpreted.

It should be possible to make use of infrared, dispersed or non-dispersed, in a routine way. For example, as a complement to chemical analysis, with a view to quantitating substances in a mixture, to detecting given elements, or at a more advanced stage, to determining of the constitution of biological substances.

Consequently, at least for the near future, it is desirable that the technique be applied to biological problems by research workers or technicians who are experienced in the use of infrared. Inversely, it would be unexpected for spectroscopists, even established ones, to approach these problems by intuition alone. Collaboration between biologists (or doctors) seems absolutely indispensable to ensure results which will be both correct and of scientific value. Consequently, spectroscopists should be incorporated into teams of biologists, or biologists should be added to teams of spectroscopists. The latter solution would appear to us to present only the temporary advantage of trying to recognize the usefulness of infrared for a given problem. The first solution, however, which in a wider conception would lead to the creation of important departments for the application of physical methods to biology and medicine within biological institutes, would seem to us to offer the greatest chances of success.

## 12

# INFRARED SPECTRA OF NUCLEIC ACIDS AND RELATED COMPOUNDS

TAKEHIKO SHIMANOUCHI, *Department of Chemistry,  
Faculty of Science, University of Tokyo, Bunkyo-ku,  
Tokyo, Japan*

MASAMICHI TSUBOI and YOSHIMASA KYOGOKU,  
*Faculty of Pharmaceutical Sciences, University of  
Tokyo, Bunkyo-ku, Tokyo, Japan*

## CONTENTS

I. Infrared Spectra of Nucleic Acids . . . . .	436
A. Introduction . . . . .	436
B. General Scope of the Spectra . . . . .	436
II. Absorption Bands due to the Base Residues . . . . .	440
A. Nucleosides . . . . .	440
(1) Cytidine . . . . .	441
(2) Adenosine . . . . .	445
(3) Uridine . . . . .	447
(4) Guanosine . . . . .	449
(5) Inosine . . . . .	451
B. Mixed Products of Nucleosides . . . . .	452
C. Synthetic Polyribonucleotides . . . . .	454
(1) Polycytidylic Acid . . . . .	455
(2) Polyadenylic Acid . . . . .	456
(3) Polyuridylic Acid and Polyinosinic Acid . . . . .	459
(4) Complexes of Polynucleotides . . . . .	460
D. Nucleic Acids . . . . .	460
(1) On the 1710 cm <sup>-1</sup> Band of Undeuterated Film . . . . .	460
(2) On the 1685 cm <sup>-1</sup> Band of Deuterated Nucleic Acid . . . . .	463
(3) Infrared Dichroism of Deoxyribonucleate . . . . .	467
III. Absorption Bands due to the Phosphate Groups . . . . .	467
A. General Considerations . . . . .	467
B. Phosphite Anion . . . . .	469
C. Monoalkyl Phosphate Anions . . . . .	476
D. Mononucleotides . . . . .	477
E. Hypophosphite Anion . . . . .	478
F. Dialkylphosphate Anions . . . . .	484

G. Deoxyribonucleate . . . . .	489
H. Ribonucleates . . . . .	492
IV. Absorption Bands due to the Sugar Groups . . . . .	494
References . . . . .	496

## I. INFRARED SPECTRA OF NUCLEIC ACIDS

### A. Introduction

Infrared spectra and X-ray diffraction are the two useful means by which the structure of high-molecular-weight compounds may be studied. The former give information about the amorphous parts of samples as well as the crystalline parts, while the latter gives mainly the details of the structure of crystalline parts.

The double-helix configuration of the crystalline salts of deoxyribonucleic acid (DNA) has now been well established.<sup>29,68</sup> However, as to the secondary structure of DNA in aqueous solutions and that of ribonucleic acid (RNA) in amorphous solids and in solutions there seems to remain much to be studied. Toward this end a series of studies is being carried out in our laboratories on the infrared spectra of nucleic acids and related compounds and on their correlation with the secondary structures of DNA and RNA.<sup>24-27, 50, 59-65</sup> This article will summarize the results which have so far been obtained in this work.

### B. General Scope of the Spectra

Infrared spectra of nucleic acids were first reported by Blout and Fields<sup>4</sup> and were further investigated by Fraser and Fraser,<sup>16</sup> Blout and Lenormant,<sup>5</sup> Lenormant and Lozé,<sup>31,32</sup> Sutherland and Tsuboi,<sup>54</sup> Wilkinson, Price and Bradbury<sup>71</sup> and Bradbury, Price and Wilkinson.<sup>7</sup> These results and those obtained in our laboratories show that the spectra have several groups of strong absorption bands (as shown in Fig. 1).

Nucleic acids have complex chemical structures (I and II) and the groups of infrared bands can be assigned to the vibrations of individual chemical groups. The correspondence is shown in Fig. 2, where the spectra of nucleic acids are compared with those of their component compounds. These figures show that the broad bands at about  $3400\text{ cm}^{-1}$  are assigned mainly to the OH stretching vibrations of adsorbed water molecules; the groups of bands in the

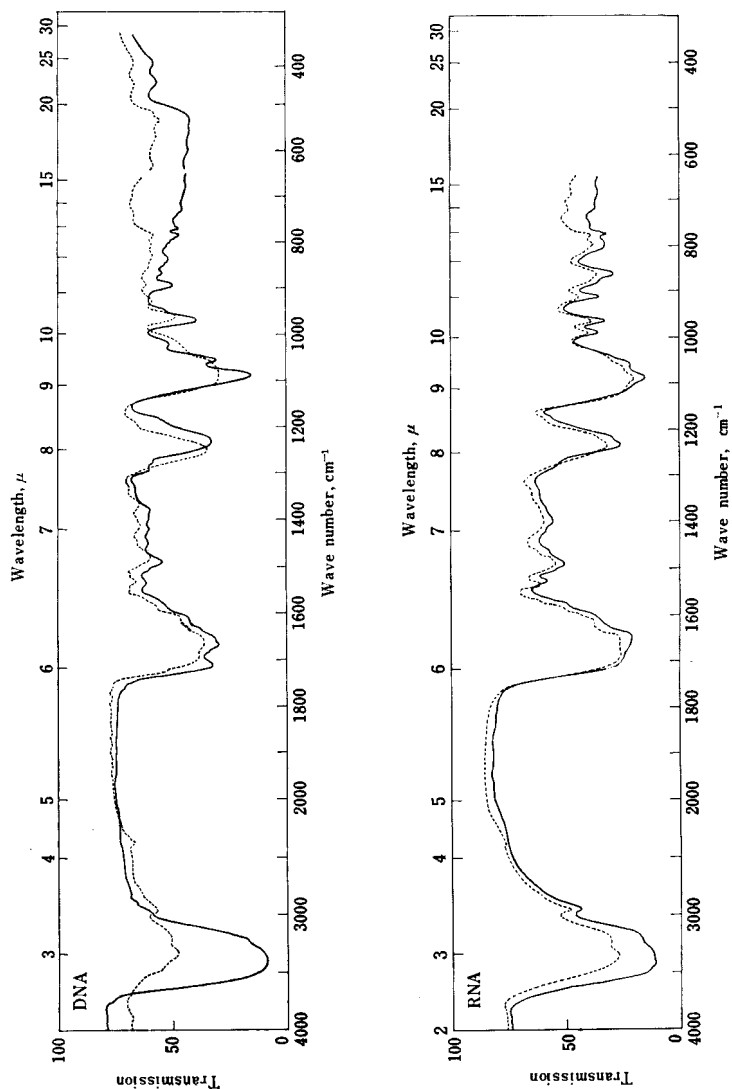
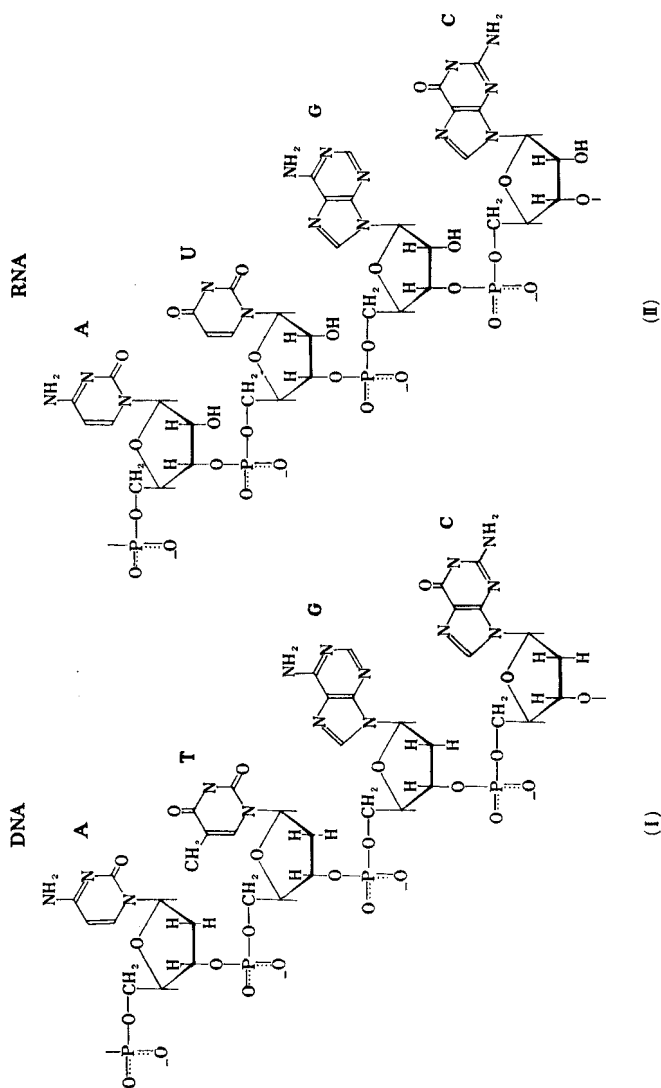


Fig. 1. Infrared spectra of films of sodium deoxyribonucleate from calf thymus and ribonucleate from rat liver observed at 75% relative humidity (—) and at 0% relative humidity (-----).





1800–1500  $\text{cm}^{-1}$  region are assigned to the  $\text{C}=\text{O}$  stretching, skeletal stretching and  $\text{NH}$  bending vibrations of the base residues; a strong band at 1220  $\text{cm}^{-1}$  is assigned to the  $\text{P}=\text{O}^-$  stretching vibration of the

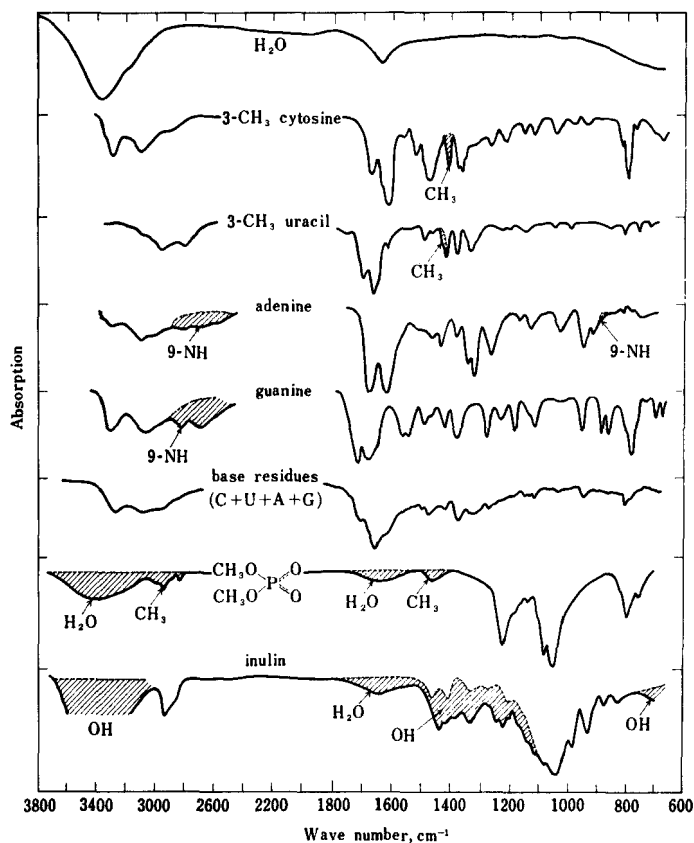


Fig. 2. Infrared spectra of the compounds constituting nucleic acids. The sixth curve is obtained by adding the four above it.

phosphate group; and the groups of strong bands in the 1100–1000  $\text{cm}^{-1}$  region are assigned to the  $\text{P}=\text{O}^-$  stretching vibration of the phosphate group and the  $\text{C}-\text{O}$  stretching vibrations of ribose and deoxyribose. There are some bands with medium or weak intensities in the region between 1000  $\text{cm}^{-1}$  and 700  $\text{cm}^{-1}$ . These bands are

assigned to the P—O stretching, C—O stretching and NH out-of-plane bending vibrations. The bands in the 600–300  $\text{cm}^{-1}$  region are mainly due to the ring deformation vibrations of base residues and the skeletal deformation vibrations of the sugar-phosphate chain. In the following chapters details of the assignments and the behavior of these bands will be described.

## II. ABSORPTION BANDS DUE TO THE BASE RESIDUES

As has been mentioned in Section I, the absorption bands in the 1800–1500  $\text{cm}^{-1}$  region can be assigned for the most part to the in-plane vibrations of the base residues with pyrimidine and purine rings. No significant contribution by the phosphate units or by the sugar unit can be expected in this region. In this section, our attention will be concentrated on this spectral region. The discussion will begin with nucleosides rather than the purine and pyrimidine bases themselves.<sup>1, 2, 9, 51, 57</sup> Infrared spectra are considerably affected by the substituent (whether hydrogen or other radicals) at position 3 of the pyrimidine bases and at position 9 of the purine bases and, therefore, the corresponding nucleosides are more suitable than the free bases for the study of the base portions of nucleic acids.

### A. Nucleosides

The infrared spectra of five nucleosides, cytidine, adenosine, uridine, guanosine<sup>61</sup> and inosine,<sup>63</sup> observed in various solid states and deuterium oxide solutions at several pD's are given in Figs. 3–8. The following two points are to be noted about the spectra: First, they show the correlations between the changes in the spectral region 1800–1500  $\text{cm}^{-1}$  and the protonated or deprotonated structures to be expected from the modes of preparations of the samples; it is hoped that these correlations are useful for the interpretation of the spectral changes observed in nucleic acids and nucleoproteins. Secondly, approximate assignments of some of the bands can be made from the deuteration effect observed and from the general background of the present stage of the infrared spectroscopy. The discussions of these points will be given below for each of the five nucleosides separately.

(1) *Cytidine*

*Spectral change due to the pH change:* Levene and Simms<sup>33</sup> reported the pK for cytidine to be 4.2. As would be expected from this value, the infrared spectra at pD's 2.0 and 0.2 were found to be the same. A similar coincidence of spectra was found for pD's 7.0 and 11.0. These latter spectra, however, differed considerably from those obtained in the acid region (see Fig. 3). Likewise, the spectrum

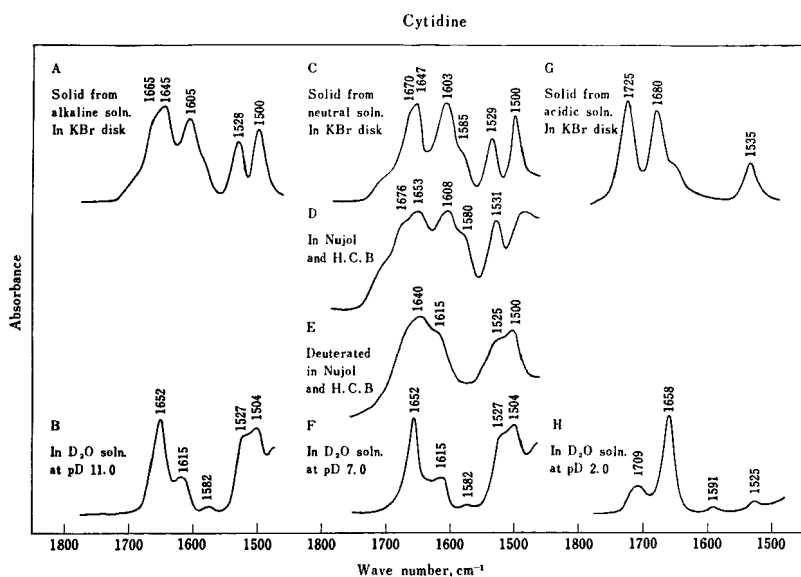


Fig. 3. Infrared spectra (1800—1450 cm<sup>-1</sup> region) of cytidine.

of solid state cytidine obtained from a neutral H<sub>2</sub>O solution (Fig. 3C) is the same as that obtained from an alkaline solution (Fig. 3A), but is different from that obtained from an acidic solution (Fig. 3G).

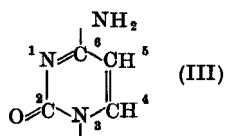
*D<sub>2</sub>O solutions:* In the deuterium oxide solutions, the NH<sub>2</sub> group or NH<sub>3</sub><sup>+</sup> group (if any) of the cytosine molecule should be deuterated and no NH<sub>2</sub> bending or NH<sub>3</sub><sup>+</sup> deformation vibrations are expected. All the absorption bands of the deuterium oxide solutions observed in the 1750–1500 cm<sup>-1</sup> region are attributed to ring vibrations involving C=O, C=N and C=C stretching modes. These bands are

at 1652, 1615, 1582, 1527, and 1504  $\text{cm}^{-1}$  in the neutral form and 1709, 1658, 1591, and 1525  $\text{cm}^{-1}$  in the acidic form. The band at 1709  $\text{cm}^{-1}$  of the acidic form is assigned to the stretching vibration of the C=O group, which has a nearly normal double-bond character. The strong band at 1658  $\text{cm}^{-1}$  of the acidic form of cytidine may be assigned to a ring vibration in which mainly the C=N stretching motion takes place. It is considered that the frequency value of the C=N bond in question shows that it has a normal double-bond character.

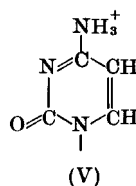
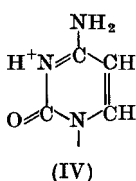
The strong band at 1652  $\text{cm}^{-1}$  and the medium intensity band at 1615  $\text{cm}^{-1}$  of the neutral form of cytidine may be assigned to two ring vibrations in which the C=O and C=N stretching motions are predominant. Because of the relatively low frequencies of these bands, it is suggested that there is an appreciable delocalization of the  $\pi$  electrons in the conjugated C=O, C=N, and C=C system in the neutral form, so that the C=O and C=N bonds show partially single-bond characters.

*NH<sub>2</sub> bending vibration:* For the undeuterated, neutral form of cytidine, there should be, in the 1750–1500  $\text{cm}^{-1}$  region, the NH<sub>2</sub> bending vibration in addition to the ring vibrations mentioned above. As Figs. 3C and D show, there is, in the spectrum of undeuterated cytidine, a strong band at about 1603  $\text{cm}^{-1}$  and a shoulder at about 1670  $\text{cm}^{-1}$  instead of the medium intensity band at 1615  $\text{cm}^{-1}$  in the spectrum of deuterated cytidine (Fig. 3E). The 1670  $\text{cm}^{-1}$  shoulder is mainly due to the NH<sub>2</sub> bending vibration, but this vibration is combined with the ring vibration corresponding to the 1615  $\text{cm}^{-1}$  band of the deuterated cytidine, so that the 1615  $\text{cm}^{-1}$  band is pushed down a little to 1603  $\text{cm}^{-1}$ .

*The protonated form:* The solid state spectrum of the acidic or protonated form of cytidine is shown in Fig. 3G together with that of the neutral form (Fig. 3C) for comparison. The structure of the neutral form, as determined by X-ray diffraction,<sup>20</sup> ultraviolet absorption spectrum<sup>9,36</sup> and infrared spectrum,<sup>1,2,9,51,57</sup> is as follows:



For the structure of the acidic or protonated form there are the following two possibilities:



It is believed, on the basis of the following evidence, that form IV is predominant:

(1) As has been mentioned, the ring stretching vibrations of the acidic form in the deuterium oxide solution appear at higher frequencies than do those of the neutral form. In the solid state spectra, as transition occurs from the neutral form to the acidic form, similar frequency shifts toward higher frequencies are observed for the ring stretching vibrations in the 1750–1500  $\text{cm}^{-1}$  region (see Figs. 3C and G). This fact suggests that a  $\pi$ -electron localization takes place in the acidic form, so that this form then has  $\text{C}=\text{O}$  and  $\text{C}=\text{N}$  bonds with more pronounced double-bond character than those of the neutral form. Such a  $\pi$ -electron localization may be expected in form IV more naturally than in form V.

(2) To test the above idea we observed the infrared spectra of protonated pyridine and protonated aniline. The results are given in Fig. 4. In pyridine the ring stretching vibrations appear at 1597 and 1581  $\text{cm}^{-1}$ , and, when pyridine is protonated, these bands shift toward higher frequencies, namely to 1635 and 1610  $\text{cm}^{-1}$ . When, on the other hand, aniline is protonated, the ring stretching bands at 1601 and 1500  $\text{cm}^{-1}$  do not shift toward higher frequencies. These facts suggest that the protonated form of cytosine is nearer to that of pyridine than to that of aniline.

(3) The strong band at 1276  $\text{cm}^{-1}$  of aniline was reasonably assigned to the  $\text{C}-\text{N}$  stretching vibration.<sup>3, 59</sup> In a similar way, the strong band at 1285  $\text{cm}^{-1}$  of cytosine may be assigned to a vibration in which the bond stretching motion takes place chiefly at the  $\text{C}-\text{N}$  bond connecting the  $\text{NH}_2$  group and the ring carbon,  $\text{C}_6$ . When cytosine is protonated, the position and intensity of this band for cytosine remains almost unchanged. This fact is explained by assuming that the protonated structure has form IV and not form V.

(4) The acidic form of cytidine gives a frequency characteristic of the carbonyl stretching at  $1725\text{ cm}^{-1}$  (in the solid state) or at  $1709\text{ cm}^{-1}$  (in the deuterium oxide solution). This fact is explained

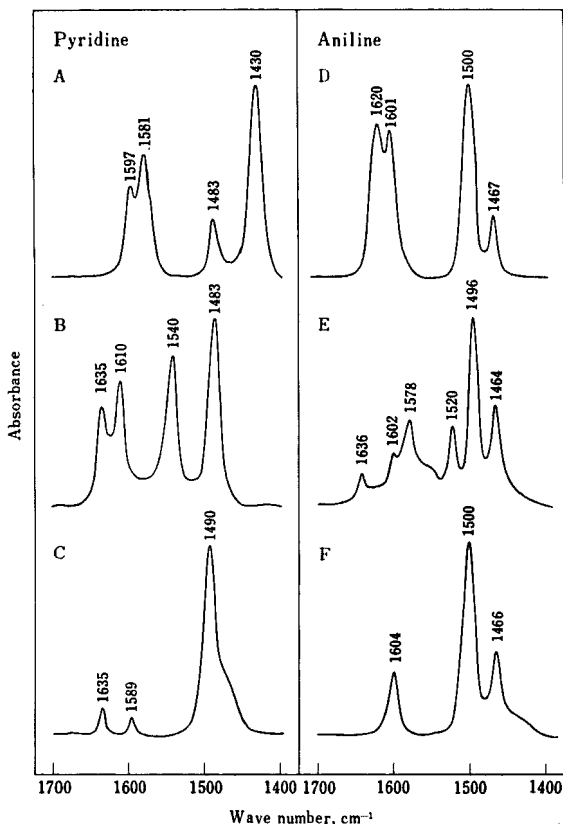


Fig. 4. Infrared spectra of (A) pyridine in the liquid state; (B) pyridine hydrochloride in a chloroform solution; (C) pyridine deuteriochloride ( $\text{C}_5\text{H}_5\text{ND}^+$ ) in  $\text{D}_2\text{O}$  solution; (D) aniline in the liquid state; (E) aniline hydrochloride in Nujol and H.C.B. mull; (F) aniline deuteriochloride ( $\text{C}_6\text{H}_5\text{ND}_3^+$ ) in  $\text{D}_2\text{O}$  solution.

by the protonated form IV rather than by the form V. In the neutral form III, the  $\text{C}=\text{O}$  bond has much of a single-bond nature because of an electron migration from position-1-nitrogen to position-2-carbon, and this may be the main reason for the absence of a band

near  $1700\text{ cm}^{-1}$ . In the form IV, position-1-nitrogen has a positive charge and the electron migration from this nitrogen should not take place. Therefore, form IV should have a carbonyl group which has the ordinary double-bond nature and which gives a band near  $1700\text{ cm}^{-1}$ . On the other hand, form V would not give the  $1700\text{ cm}^{-1}$  band for the same reason that form III does not.

## (2) Adenosine

*Spectral change due to the pH change:* Adenosine has a  $\text{pK}$  of 3.5.<sup>33</sup> As would be expected from this  $\text{pK}$  value, the infrared absorption curve of the deuterium oxide solution of adenosine at  $\text{pD} = 12.6$  is the same as it is at  $\text{pD} = 7.0$ , but is different from that at  $\text{pD} = 2.0$

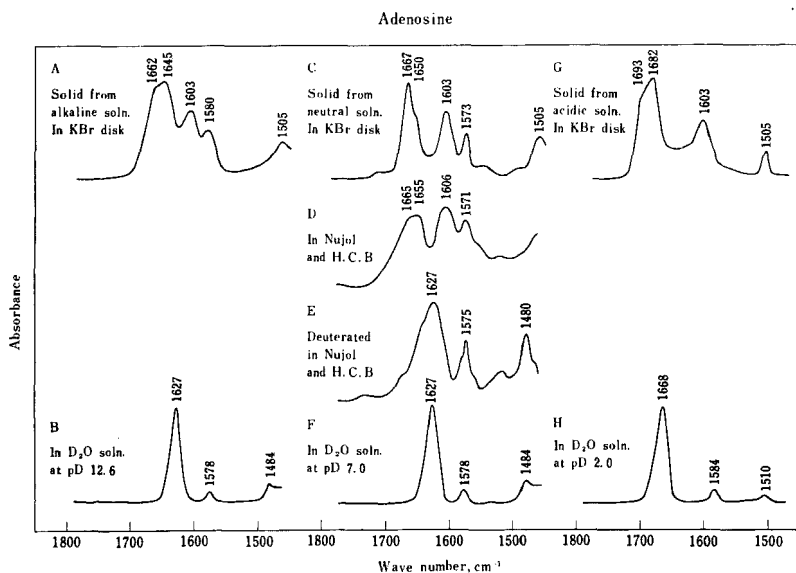


Fig. 5. Infrared spectra of adenosine.

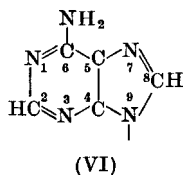
(see Fig. 5). The spectrum of solid state adenosine obtained from a neutral  $\text{H}_2\text{O}$  solution (Fig. 5C) is the same as that obtained from an alkaline solution (Fig. 5A), but is different from that obtained from an acidic solution (Fig. 5G).

*D<sub>2</sub>O solutions:* In the deuterium oxide solution, the neutral form of adenosine shows a strong band at  $1627\text{ cm}^{-1}$  and this may be assigned to a ring vibration in which the  $\text{C}=\text{N}$  stretching motions predominate. During transition from the neutral to the acidic form, this band shifts to the higher frequency  $1668\text{ cm}^{-1}$ . This change may be interpreted as indicating that the double-bond nature of the  $\text{C}=\text{N}$  bonds of adenosine is stronger in its acidic form than it is in its neutral form.

The solid state spectrum of deuterated adenosine may be further explained by postulating that in the normal vibration of deuterated adenosine at  $1627\text{ cm}^{-1}$  there is an appreciable amount of stretching of the  $\text{C}-\text{N}$  bond connecting the position-6-carbon and the  $\text{NH}_2$  group and, in addition, stretching of  $\text{C}=\text{N}$  bonds. There is in adenosine no strong band in the vicinity of  $1280\text{ cm}^{-1}$  which could be assigned to the  $\text{C}-\text{N}$  bond stretching vibration corresponding to the  $1285\text{ cm}^{-1}$  band of cytidine. There is, instead, a strong band at about  $1215\text{ cm}^{-1}$ .

*NH<sub>2</sub> bending vibration:* As is seen from Figs. 5C and E, undeuterated adenosine shows two strong bands at about  $1665\text{ cm}^{-1}$  and  $1605\text{ cm}^{-1}$ , but no band in the vicinity of  $1627\text{ cm}^{-1}$ , where deuterated adenosine shows a ring stretching vibration. This fact shows that in the undeuterated adenosine molecule there is a strong coupling between the  $\text{NH}_2$  bending motion and the ring stretching motion (corresponding to the  $1627\text{ cm}^{-1}$  band of deuterated adenosine). Such a coupling is just what would be expected from the type of the normal vibration at  $1627\text{ cm}^{-1}$  postulated above.

*The protonated form:* The neutral form of adenosine is considered to be as follows<sup>1, 2, 9, 36, 51, 57</sup>



This has five basic nitrogen atoms, and the problem is one of finding which of these five acquires the proton in the protonated form corresponding to the infrared absorptions observed at lower pH's



(or pD's). In connection with this problem, the present experimental results show that the conjugated double-bond system of the adenosine residue should be greatly affected by this protonation. Thus, the ring vibrational frequencies are found at 1627, 1578, and 1484  $\text{cm}^{-1}$  in the neutral and alkaline  $\text{D}_2\text{O}$  solutions, while in the acidic  $\text{D}_2\text{O}$  solution these are found at higher frequencies: 1668, 1584, and 1510  $\text{cm}^{-1}$  (Fig. 5). Similar frequency shifts are observed in the solid state spectra during transition from the neutral form to the acidic form (Figs. 5C and G). On the other hand, a strong band at about 1215  $\text{cm}^{-1}$ , which is assignable to the C—(NH<sub>2</sub>) stretching vibration at position 6, remained in every solid state spectrum examined. It is considered that these facts show that the proton in the acidic form of adenosine is situated on the —N= type nitrogen at position 1, 3, or 7, rather than on the amino group at position 6 or —N— type nitrogen at position 9. From the position of the electron

density maximum determined by an X-ray diffraction study, Cochran<sup>10</sup> concluded that the proton is situated at a point  $1.0 \pm 0.2$  Å from the center of N<sub>1</sub> in the adenosine hydrochloride crystal. This is consistent with our infrared spectroscopic evidence on the possible positions of the proton in the protonated adenosine molecule.

### (3) Uridine

*Spectral change due to the pH change:* For uridine, a pK of 9.2 has been reported.<sup>33</sup> Corresponding to this, the infrared absorption curve of the deuterium oxide solution of uridine at pD = 7.0 is the same as that at pD = 2.0, and that at pD = 11.0 is the same as that at pD = 13.4, but the curve at pD = 7.0 is different from that at pD = 11.0 (see Fig. 6). In the solid state, spectra of uridine given in Fig. 6G are practically the same as C, and these are different from A.

*Double-bond stretching and NH bending vibrations:* As may be seen in Figs. 6C and D, there is, at about 1680  $\text{cm}^{-1}$ , a peak for undeuterated uridine, but not for deuterated uridine. Three other bands at about 1700, 1650, and 1620  $\text{cm}^{-1}$  are observed for both deuterated and undeuterated uridine. The band at 1680  $\text{cm}^{-1}$  of undeuterated uridine may therefore be assigned to the NH bending vibration and the other three bands to three double-bond stretching

vibrations. It is considered that the acidic or neutral form of uridine corresponds to the following structural formula: 9, 46, 51, 57

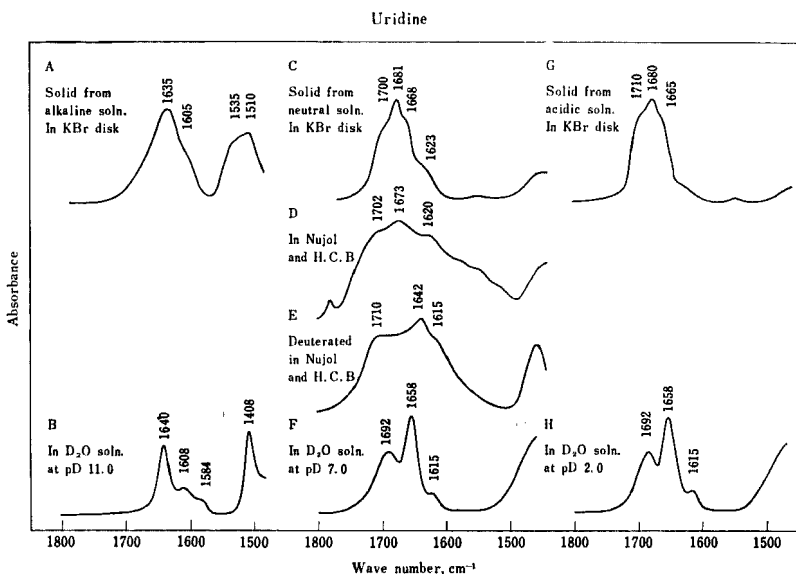
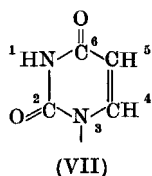
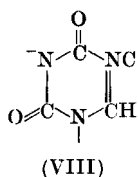


Fig. 6. Infrared spectra of uridine.

The three double-bond stretching frequencies 1700, 1650 and 1620  $\text{cm}^{-1}$  may be assigned to the position-2-carbonyl, position-6-carbonyl, and ring C=C bonds, respectively. The position-2-carbonyl would be close to a normal carbonyl and the position-6-carbonyl would have less double-bond nature because it is conjugated with the C=C bonds.

*The deprotonated form:* It is considered that the acidic or neutral

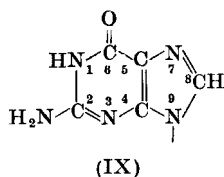
form corresponds to the structural formula VII, and the basic form to



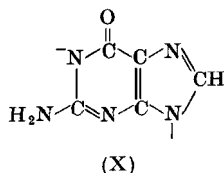
The double-bond stretching vibrations are found at much lower frequencies of the basic form than of the neutral or acidic form (Figs. 4A, C, and G). The deprotonation at position-1-nitrogen would cause an increase of the electron delocalization in the whole conjugated double-bond system. This would result in less of a double-bond nature and therefore in a lower force constant for each carbonyl bond. This explains the observed frequency shifts during transition from the neutral (or acidic) to the basic form.

#### (4) *Guanosine*

For guanosine, two dissociations are known with  $pK = 1.6$  and  $pK = 9.2$ .<sup>33</sup> As is expected from these values of  $pK$ 's, absorption curves A, C, and G in Fig. 7 are all different. The curve C may be correlated to the neutral form:<sup>1, 2, 9, 36, 51, 57</sup>



and the curve A to a basic form:



Because of the low solubility, the spectrum of the neutral form of guanosine could not be observed in the deuterium oxide solution.

At higher and lower pD's, however, the solubilities are sufficient to show the spectra of basic and acidic forms. As is expected, these two spectra are very different (see Fig. 7). In the spectrum obtained at pD = 12.6 in the deuterium oxide solution, no strong band appears in the frequency region higher than 1592 cm<sup>-1</sup>. This fact is well understood if we consider the great degree of delocalization of the

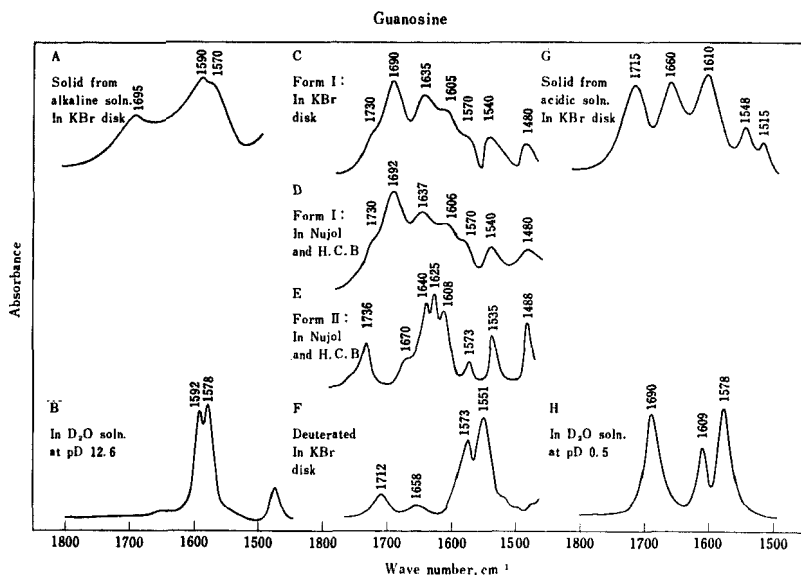
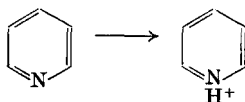


Fig. 7. Infrared spectra of guanosine.

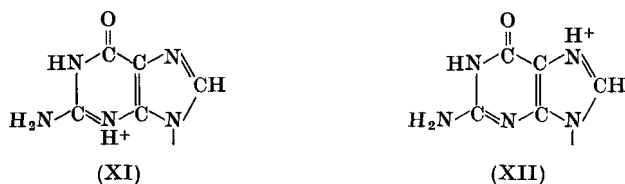
$\pi$  electrons expected in the structure X. In the spectrum obtained at pD = 0.5 in the deuterium oxide solution, strong bands appear at much higher frequencies. This fact shows that, in the acidic form, the C=N and C=O bonds have appreciable double-bond characters. It was found that there are at least two modifications in neutral guanosine which give very different infrared absorptions (Figs. 7D and E). Detailed study of this dimorphism has not yet been made, nor has its rather complicated deuteration effect yet been interpreted.

During the transition from the neutral to the acidic form, there is

a general shift of the bands in the  $1700\text{--}1400\text{ cm}^{-1}$  region toward higher frequencies; this resembles the shift of the bands of pyridine in the same frequency region during the transition



This fact suggests that the protonation in the acidic form of guanosine takes place at the position-3-nitrogen or position-7-nitrogen to form the following structure:

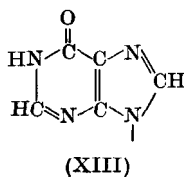


Of these two, structure XII is consistent with the result of an X-ray study made by Broomhead<sup>8</sup> on guanine hydrochloride, because he found that there is a strong intermolecular hydrogen bond between the position-7-nitrogen and oxygen atoms in the guanine hydrochloride crystal.

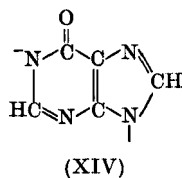
### (5) *Inosine*

For inosine, a  $pK$  of 8.75 has been reported.<sup>34</sup> As is expected from this  $pK$  value, the infrared absorption curve of the deuterium oxide solution of inosine at  $pD = 7.0$  is different from that at  $pD = 14.0$  (Fig. 8).<sup>63</sup>

It is considered that the neutral form corresponds to the structural formula XIII:



and the basic form to



The band at  $1675\text{ cm}^{-1}$  of the neutral solution is assigned to a coupled vibration in which  $\text{C}=\text{O}$  stretching would make the

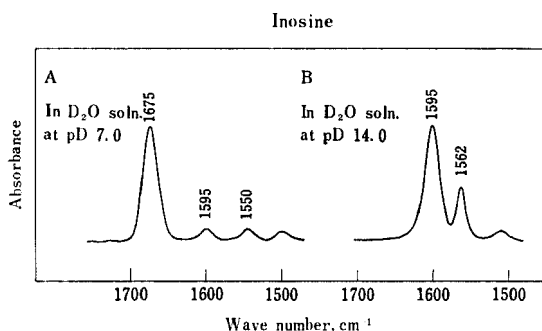


Fig. 8. Infrared spectra of inosine.

greatest contribution. In the spectrum of the solution at  $\text{pD} = 14$ , no strong band appears in the region higher than  $1595\text{ cm}^{-1}$ . This fact may be taken as showing that the deprotonation at position-1-nitrogen causes a delocalization of the  $\pi$  electrons in the conjugated system and results in a lower force constant of the  $\text{C}=\text{O}$  bond.

### B. Mixed Products of Nucleosides

In the secondary structure of native DNA, base residues are considered to be involved in the specific base pairings of adenine to thymine and guanine to cytosine. Therefore, it would be interesting to examine whether the base-base interactions similar to those in these base pairings can be realized with the nucleosides. In aqueous solutions, no interaction can be detected by the infrared method. As may be seen in Fig. 9, a 50%-50% mixture solution of adeno-

sine and uridine gives practically the same infrared absorption curve as that obtained by the graphical summation of the curves of adenosine and uridine solutions. On the other hand, in solid states appreciable intermolecular interactions are observed.<sup>24</sup> With a 50% adenosine–50% uridine mixture, a few different modifications were found.<sup>26</sup> A crystalline product is obtained from an equimolar aqueous mixture of adenosine and uridine after slow evaporation in a desiccator. This gives an infrared absorption spectrum different

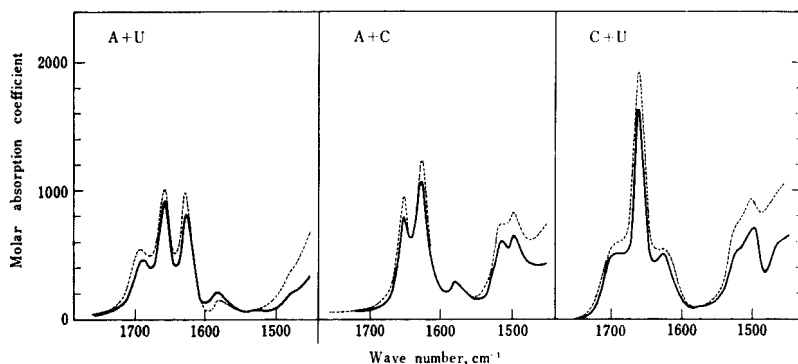


Fig. 9. Infrared spectra of nucleoside mixtures in  $D_2O$  solutions (—), and the sum of the spectra of each nucleoside (----).

from those of the 50%–50% mechanical mixture of adenosine and uridine crystals obtained from a commercial source (Nutritional Biochemicals Corp., Cleveland 28, Ohio, U.S.A.). An amorphous product is obtained from a similar aqueous mixture by quick lyophilization. This gives an infrared absorption spectrum different from the crystalline product and also from mechanical mixtures. As may be seen in Fig. 10, both of these products from the aqueous mixture give absorptions in the  $1710\text{ cm}^{-1}$  region. Especially in the case of an amorphous product this band is much stronger than those of adenosine–uridine mechanical mixtures. These absorptions in the  $1710\text{ cm}^{-1}$  region might be correlated to the  $1710\text{ cm}^{-1}$  band of sodium deoxyribonucleate, which seems to be a characteristic band of the secondary structure (see Section II-D(1)).

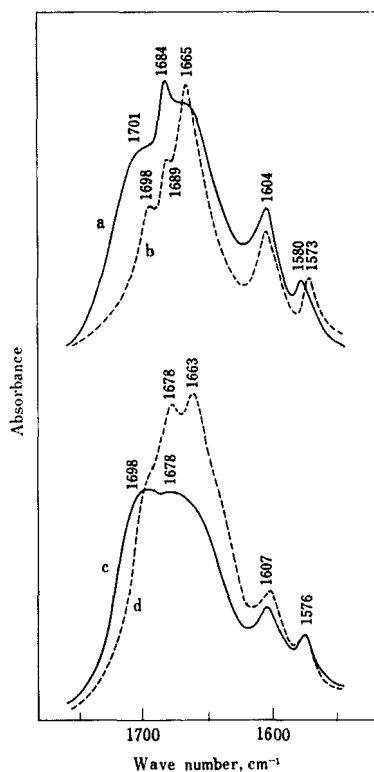


Fig. 10. Infrared spectra of the mixture of adenosine and uridine in the solid state (in Nujol mull). (a) A product obtained from an equimolar aqueous mixture by slow evaporation in a desiccator; (b) an equimolar mechanical mixture of crystalline adenosine and crystalline uridine powder, obtained from a commercial source; (c) a product obtained from an equimolar aqueous mixture by quick lyophilization; (d) an equimolar mechanical mixture of adenosine and uridine powder each of which was obtained by quick lyophilization separately from each aqueous solution.

### C. Synthetic Polyribonucleotides

We are now in a position to discuss the absorptions due to the base residues in polynucleotides. First, we shall consider the 1800–1500 cm<sup>-1</sup> region spectra of a few synthetic homopolymers of ribonucleotides.



## (1) Polycytidylic Acid

Todd Miles<sup>40, 42</sup> observed the infrared absorptions in the 1800–1600  $\text{cm}^{-1}$  region of polycytidylic acid in its neutral  $\text{D}_2\text{O}$  solution. He found a strong band at 1651  $\text{cm}^{-1}$  and a band with medium intensity at 1617  $\text{cm}^{-1}$ . These are very similar, respectively, to the 1652 and 1615  $\text{cm}^{-1}$  bands of cytidine in its neutral  $\text{D}_2\text{O}$  solution (see Fig. 3). Figure 11 shows infrared absorption curves

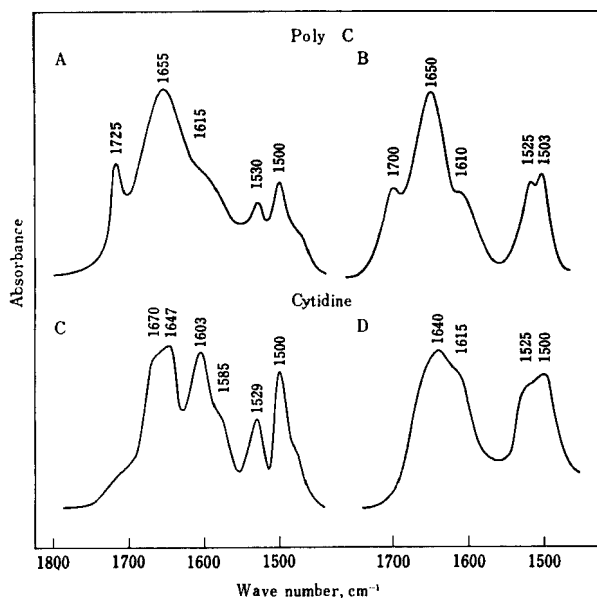


Fig. 11. Infrared spectra of polycytidylic acid film and cytidine. (A) Polycytidylic acid film in the air of 75% relative humidity (r.h.); (B) polycytidylic acid film in the  $\text{D}_2\text{O}$  vapor of 75% r.h.; (C) cytidine in the solid state (in KBr disk); (D) deuterated cytidine in the solid state (in Nujol and H.C.B. mull).

obtained by Tsuboi *et al.*<sup>65</sup> of polycytidylic acid film cast from a slightly acidic ( $\text{pH} = 5.5$ ) aqueous solution. As may be seen in this figure, the spectral features in the 1530–1500  $\text{cm}^{-1}$  region of polycytidylic acid are also very similar to those of cytidine. Thus, the undeuterated film gives a strong band at 1500  $\text{cm}^{-1}$  and a slightly weaker band at 1530  $\text{cm}^{-1}$ ; these are similar to the respective 1500 and 1529  $\text{cm}^{-1}$  bands of undeuterated cytidine. The deuterated film

shows a strong band at  $1503\text{ cm}^{-1}$  and a shoulder at  $1525\text{ cm}^{-1}$ ; these are similar to the respective  $1500$  and  $1525\text{ cm}^{-1}$  bands of deuterated cytidine. These facts show that the molecular structure and vibrational modes of cytosine residue in polycytidylic acid are very similar to that in cytidine. If a more detailed knowledge of the normal vibrations of cytidine is obtained, it must be directly applicable to polycytidylic acid.

In the absorption curve of undeuterated film given in Fig. 11A, there is an additional band observed at  $1725\text{ cm}^{-1}$ . This band is shifted to  $1700\text{ cm}^{-1}$  on deuteration. This is probably assignable to the protonated cytosine residue, which is produced in the slightly acidic solution. As has been described in Section II-A(1), the protonated cytidine gives a band at  $1725\text{ cm}^{-1}$  which is shifted to  $1709\text{ cm}^{-1}$  on deuteration.

## (2) *Polyadenylic Acid*

It is known that there are two forms for this polymer.<sup>18, 19, 67</sup> One of them (acidic form) is obtained in acidic solutions with pH lower than 6 and the other (alkaline form) in neutral and alkaline solutions. The acidic form is considered to have a double-helix structure<sup>17, 48</sup> and the alkaline form is considered to be an almost random coil. Morgan and Blout<sup>45</sup> observed the infrared spectra of acidic and alkaline form polyadenylic acids in the solid state. Todd Miles<sup>38, 39, 41</sup> observed the infrared absorptions in the  $1800\text{--}1600\text{ cm}^{-1}$  region of polyadenylic acid in a neutral  $\text{D}_2\text{O}$  solution. Recently, Tsuboi, Yamamoto, Kyogoku, and Shimanouchi<sup>64</sup> made an additional study of the infrared absorptions of this polymer both in solutions (at various pD's and temperatures) and in the solid state (in the air of controlled humidities). Some of the results obtained by Tsuboi *et al.* are given in Figs. 12 and 13. As may be seen in the figures, polyadenylic acid in deuterium oxide solutions with  $\text{pD} = 8$  shows a strong absorption band at  $1624\text{ cm}^{-1}$  and a weak one at  $1570\text{ cm}^{-1}$ . These are similar respectively to the  $1627$  and  $1578\text{ cm}^{-1}$  bands of adenosine in neutral or alkaline  $\text{D}_2\text{O}$  solution (see Fig. 12). On going to acidic solution a new strong band appears at  $1665\text{ cm}^{-1}$ , which is similar to the  $1668\text{ cm}^{-1}$  band of adenosine in acidic  $\text{D}_2\text{O}$  solution. These facts may be taken as showing that the adenine ring has almost the same electronic and

molecular structure in polyadenylic acid as that in adenosine, and that the protonation takes place at position-1-nitrogen in the former as in the latter. At pD 4.8, besides the strong  $1665\text{ cm}^{-1}$

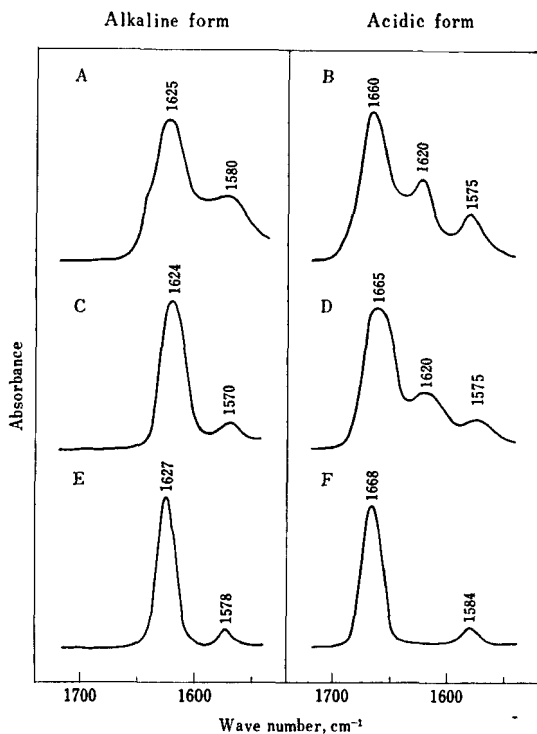


Fig. 12. Infrared spectra of deuterated polyadenylic acid and adenosine: (A) polyadenylic acid film cast from pH 8.0 solution observed in the  $\text{D}_2\text{O}$  vapor of 75% r.h.; (B) polyadenylic acid film cast from pH 4.2 solution observed in the  $\text{D}_2\text{O}$  vapor of 75% r.h.; (C) polyadenylic acid in the  $\text{D}_2\text{O}$  solution at pD 8.0; (D) polyadenylic acid in the  $\text{D}_2\text{O}$  solution at pD 4.8; (E) adenosine in the  $\text{D}_2\text{O}$  solution at pD 7.0; (F) adenosine in the  $\text{D}_2\text{O}$  solution at pD 2.0.

band, the  $1620\text{ cm}^{-1}$  band is still seen, showing that the alkaline form of polyadenylic acid remains at this pD. At pH 4.8, the same polyadenylic acid (undeuterated) shows a steep rise in the optical density ( $252\text{ m}\mu$ ) vs. temperature curve with the "melting temperature" at about  $70^\circ\text{C}$ . Therefore, at this pD, polyadenylic

acid seems to form the double-strand structure, and only a partial protonation seems to be sufficient for the formation of this structure. On heating the  $D_2O$  solution to  $70^\circ C$ , no significant change is observed in the positions and relative intensities of the infrared

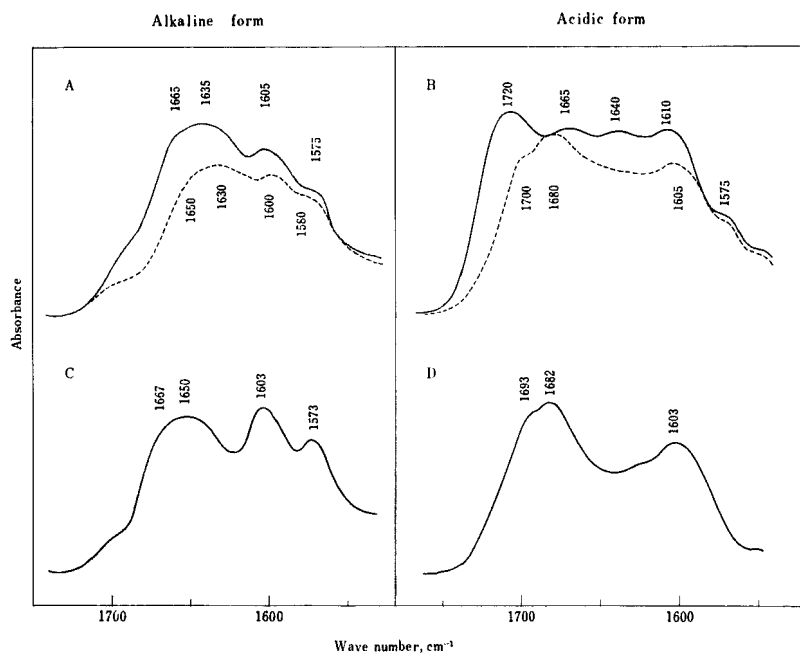


Fig. 13. Infrared spectra of polyadenylic acid and adenosine: (A) polyadenylic acid film cast from pH 8.0 solution observed in the air of 75% r.h. (—) and 0% r.h. (----); (B) polyadenylic acid film cast from pH 4.2 solution observed in the air of 75% r.h. (—) and 0% r.h. (----); (C) adenosine in the solid state obtained from an alkaline solution; (D) adenosine in the solid state obtained from an acidic solution.

bands so far mentioned. Hence the breakdown of the double-helix structure does not seem to cause any change in the force constants and polarity of bonds forming the adenine ring.

In air of 75% relative humidity, deuterated polyadenylic acid film shows a strong band at  $1625\text{ cm}^{-1}$  in the film cast from the  $D_2O$  solution of pD 8, and a strong band at  $1660\text{ cm}^{-1}$  in the film cast from the  $D_2O$  solution of pD 4.2. These are similar to the strong

bands of the  $D_2O$  solutions mentioned above. A weaker band observed at  $1620\text{ cm}^{-1}$  for the film cast at pD 4.2 is probably due to the adenine residues remaining without protonation in the film in which the most adenine residues are protonated at position-1-nitrogen. This band is also seen in the curve obtained by Morgan and Blout<sup>45</sup> for an oriented, deuterated, acidic polyadenylic acid film. This band shows a marked perpendicular dichroism as the  $1660\text{ cm}^{-1}$  band does. This fact means that an adenine residue without protonation, which probably cannot form a pair with another adenine residue, is incorporated in the double-helix structure, so that it is fixed with its plane parallel to other adenine residues. On drying the film, practically no change is observed in the positions and intensities of the bands in question.

Undeuterated film of polyadenylic acid cast at pH 4.5 shows a strong band at  $1720\text{ cm}^{-1}$  in the air of 75% relative humidity. This band is considered to correspond to the  $1693\text{ cm}^{-1}$  band of protonated adenosine (see Section II-A(2)) and to be assigned to a coupled vibration of the  $NH_2$  bending and  $C=N$  and  $C=C$  stretching motions. The fact that this frequency is much higher in polyadenylic acid than that in protonated adenosine may be explained by taking the double-helix structure into account. In this structure, each  $NH_2$  group in one of the two helices is considered to be involved in two strong hydrogen bondings,  $N-H\cdots O$  and  $N-H\cdots N$  respectively, with the  $PO_2^-$  group and with the position-7-nitrogen of a nucleotide residue in the other helix.<sup>48</sup> The  $NH_2$  group in the adenosine crystal would not be involved in such strong hydrogen bondings, as there is no  $PO_2^-$  group. On drying the film, the  $1720\text{ cm}^{-1}$  band is shifted to  $1700\text{ cm}^{-1}$ . This is probably due to breakdown of the double-helix structure and, therefore, of the hydrogen bonds mentioned above. Drying the film also causes a lowering of the intensity of absorptions in the  $1660\text{--}1600\text{ cm}^{-1}$  region. This is explained as due to the removal of the water molecules, whose HOH bending frequency is about  $1640\text{ cm}^{-1}$ .

### (3) *Polyuridylic Acid and Polyinosinic Acid*

Todd Miles observed a band with medium intensity at  $1695\text{ cm}^{-1}$  and a strong band at  $1661\text{ cm}^{-1}$  of polyuridylic acid in its neutral  $D_2O$  solution.<sup>38, 39, 41</sup> He also found a strong band at  $1677\text{ cm}^{-1}$  of

polyinosinic acid in its neutral D<sub>2</sub>O solution.<sup>40, 42</sup> These are all very similar to corresponding bands of uridine and inosine in their D<sub>2</sub>O solutions, which we have described in the preceding section.

#### (4) *Complexes of Polynucleotides*

Polyriboadenylic acid and polyribouridilic acid are known to form a DNA-like double-helix structure (and in certain conditions a triple-helix structure) when they are mixed in solution.<sup>13</sup> A double-helix structure is also formed of polyinosinic acid and polycytidylic acid. Todd Miles<sup>38-42</sup> observed infrared spectra of a few mixtures of these polynucleotides in D<sub>2</sub>O solutions, and found that the absorptions of the base residues in the 1750–1500 cm<sup>-1</sup> region are quite different in these double- (or triple-) helix structures from those in their component simple polynucleotides. This finding would lead to important information of the base–base interactions, and is to be analyzed in detail.

### D. Nucleic Acids

Nucleic acids, both DNA and RNA, give strong absorptions in the 1800–1500 cm<sup>-1</sup> region. There are several peaks observed here, and their positions and relative intensities vary according to whether the nucleic acid is DNA or RNA, dry or wet, deuterated or undeuterated. The absorptions can be assigned mostly to the in-plane vibrations of the base residues, i.e. several complicated vibrations involving the stretching motions of the C=O, and C=C bonds, and partly to the in-plane deformation motions of NH and NH<sub>2</sub> groups and to the deformation vibration of the adsorbed water. At present, a more detailed assignment cannot be made to any of these absorption peaks. However, in the following paragraphs a few interesting features are given.

#### (1) *On the 1710 cm<sup>-1</sup> Band of Undeuterated Film*

Sodium salt of deoxyribonucleic acid from calf thymus placed in air of 75% relative humidity shows a strong band at 1708 cm<sup>-1</sup> (Fig. 14). In dry air, however, a much weaker absorption is observed. This band is either absent or much weaker in the spectra of the film

obtained from aqueous solutions treated with deoxyribonuclease at 37°C for 10 min, heated to 100°C for 10 min, treated with formamide,

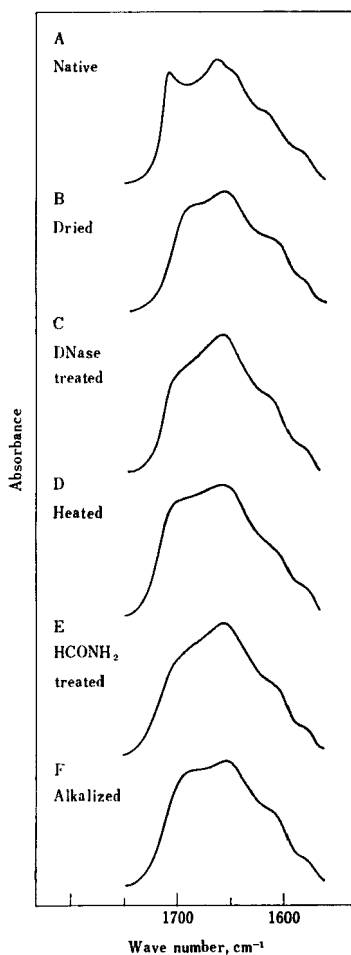


Fig. 14. Infrared spectra of sodium deoxyribonucleate film: (A) native at 75% r.h.; (B) native at 0% r.h.; (C) treated with deoxyribonuclease; (D) heated to 100°C for 10 min; (E) treated with HCONH<sub>2</sub>; (F) alkalized to pH 11. (C, D, E and F were observed at 75% r.h.)

or alkalized to pH 11 and then neutralized (Fig. 14). Hydrodynamical, optical and X-ray examinations show that these

treatments including drying cause a breakdown of the secondary structure of nucleic acids.<sup>11,14,22,35,47</sup> The  $1708\text{ cm}^{-1}$  band may, therefore, be taken as a characteristic band of the secondary structure of NaDNA. As to what scheme of the secondary structure is responsible for this  $1708\text{ cm}^{-1}$  band, however, no conclusive explanation has been established.

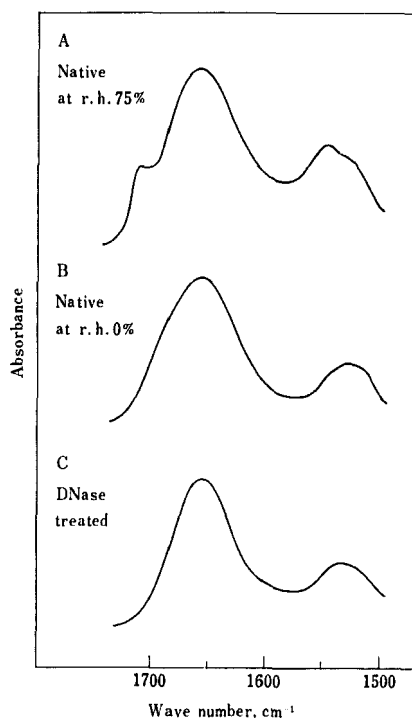


Fig. 15. Infrared spectra of nucleohistone: (A) native at 75% r.h.; (B) native at 0% r.h.; (C) treated with deoxyribonuclease, observed at 75% r.h.

The sodium salt of ribonucleic acid prepared from *E. coli* ribosomes by the phenol method<sup>21</sup> shows a moderately strong band at  $1705\text{ cm}^{-1}$  in wet state. When it is heated at  $100^{\circ}\text{C}$  for 10 min or treated with ribonuclease, the  $1705\text{ cm}^{-1}$  band observed is of much weaker intensity. A strong band is also seen at  $1710\text{ cm}^{-1}$  for the sodium salt of nucleohistone (deoxyribonucleic acid-histone) from calf thymus (Fig. 15). This fact may be interpreted as indicating that



there are numerous base pairings in nucleohistone as in NaDNA. This is in accordance with what has been suggested from X-ray work.<sup>70</sup>

(2) *On the 1685 cm<sup>-1</sup> Band of Deuterated Nucleic Acid*

In the spectra of NaDNA and NaRNA in the deuterium oxide solutions or in the spectra of the films of these nucleates placed in D<sub>2</sub>O vapor, a strong absorption is observed in the 1670–1690 cm<sup>-1</sup> region. This seems to be also characteristic of the secondary structure, and seems to correspond to the absorption in the 1700–1720 cm<sup>-1</sup> region of the undeuterated nucleic acids. Figure 16 shows

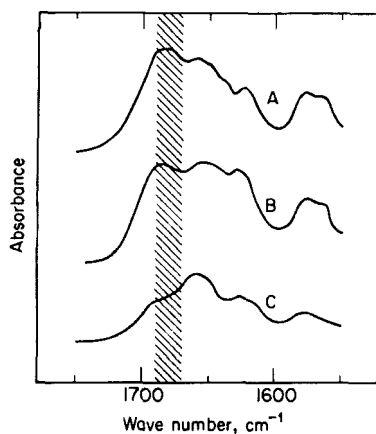


Fig. 16. Infrared spectra of sodium ribonucleate from *E. coli* ribosomes in D<sub>2</sub>O solutions: (A) native; (B) heated to 100°C for 10 min; (C) treated with ribonuclease. (Reproduced from ref. 50 by courtesy of the Elsevier Publishing Company.)

some of the results of our measurements of the infrared spectra of the sodium salt of ribonucleic acid, prepared by the phenol method from ribosomes of *E. coli* in D<sub>2</sub>O solution. A native NaRNA has a strong absorption band at 1685 cm<sup>-1</sup> which is slightly weakened in intensity upon heating at 100°C for 10 min. When the sodium salt of ribonucleic acid is treated with ribonuclease, the 1685 cm<sup>-1</sup> absorption is considerably weakened. Blout and Lenormant<sup>6</sup> found

that the high-polymer sodium salt of deoxyribonucleic acid shows a strong band at  $1685\text{ cm}^{-1}$  in  $\text{D}_2\text{O}$  solution, and that, when the solution is heated, treated with deoxyribonuclease, or treated with alkali, its  $1685\text{ cm}^{-1}$  band is much weakened. They also found that the low-polymer sodium salt of deoxyribonucleic acid does not show

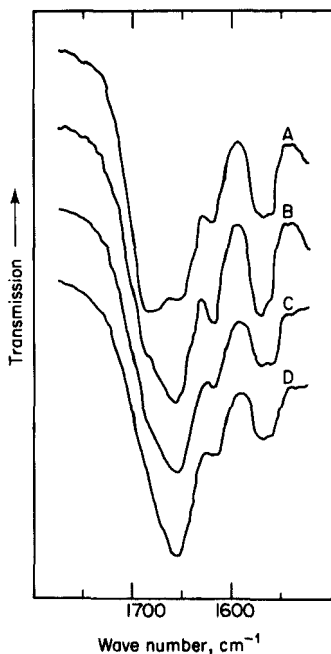


Fig. 17. Infrared spectra of sodium ribonucleate in  $\text{D}_2\text{O}$  solutions: (A) before the  $\text{HCONH}_2$  treatment at  $30^\circ\text{C}$ ; (B) the same, at  $70^\circ\text{C}$ ; (C) after the  $\text{HCONH}_2$  treatment at  $30^\circ\text{C}$ ; (D) the same, at  $70^\circ\text{C}$ . (Reproduced from ref. 25 by courtesy of the Academic Press.)

the strong  $1685\text{ cm}^{-1}$  band. It has also been clearly shown that the absorption at  $1685\text{ cm}^{-1}$  is greatly weakened by the  $\text{HCONH}_2$  treatment (see Fig. 17).

Further information on the nature of this  $1685\text{ cm}^{-1}$  band may be obtained by an examination of the temperature effect. Some of the results of such an examination are shown in Figs. 18 and 19. Here, the samples used are the sodium salt of calf thymus deoxyribonucleic acid and the sodium salt of ribonucleic acid from rat liver

ribosomes. These are dissolved (5–10%) in a deuterium oxide solution which is 0.1 molar in potassium chloride. The deoxyribonucleic acid solution was heated to 93°C, and the ribonucleic acid solution to 70°C. After they were kept at these temperatures for 1–2 min, they were cooled and the spectral changes were examined for reversibility. As is seen in Fig. 18, the most conspicuous spectral change that occurs with the change of temperature of the solution is that of the relative intensity of the 1685  $\text{cm}^{-1}$  band.

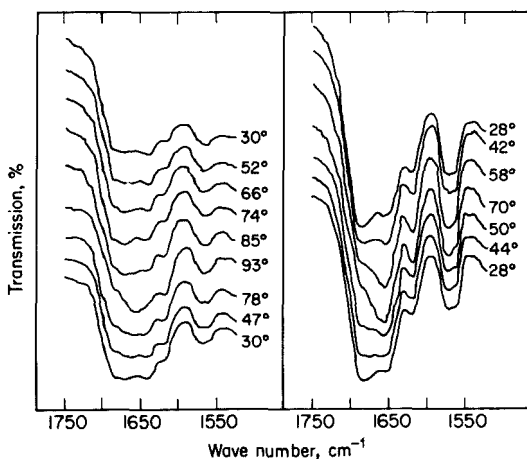


Fig. 18. Infrared spectra of sodium deoxyribonucleate and ribonucleate in  $\text{D}_2\text{O}$  solutions at various temperatures. Left: sodium deoxyribonucleate from calf thymus in 0.1 M potassium chloride  $\text{D}_2\text{O}$  solution, right: sodium ribonucleate from rat liver in 0.1 M potassium chloride  $\text{D}_2\text{O}$  solution. (Reproduced from ref. 24 by courtesy of Macmillan and Company Ltd.)

In Fig. 19, the reciprocal of the intensity of the 1685  $\text{cm}^{-1}$  band relative to that of the 1685  $\text{cm}^{-1}$  band is plotted against the temperature of the solution. In the deoxyribonucleic acid solution there is a sharp change (transition) at about 85°C, while in the ribonucleic acid solution the change occurs gradually from 30°C to 70°C. The "cooling curve" always lies somewhat higher than the "heating curve". This trend is more evident when the maximum temperature reached is higher or when the solution is kept at the maximum temperature for a longer period.

All these features of the curves of reciprocal intensity at  $1685\text{ cm}^{-1}$  vs. temperature of the solution are very similar to those of the corresponding curves of optical density at  $260\text{ m}\mu$  vs. temperature of the solution given by Marmur and Doty<sup>35</sup> and by Doty, Boedtke, Fresco, Haselkorn and Litt.<sup>12</sup> This fact shows again that the  $1685$

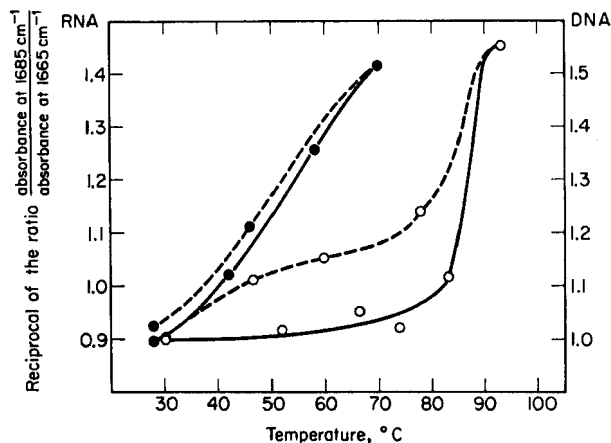


Fig. 19. The variations in the reciprocal of the relative intensity of the  $1685\text{ cm}^{-1}$  band as a function of temperature of the solution: —○—, heating curve of deoxyribonucleate; ---○---, cooling curve of deoxyribonucleate; —●—, heating curve of ribonucleate; ---●---, cooling curve of ribonucleate. (Reproduced from ref. 24 by courtesy of Macmillan and Company Ltd.)

$\text{cm}^{-1}$  band is characteristic of the secondary structure of nucleic acids.

In this connection, it should be pointed out that the temperature effects of the absorptions at  $260\text{ m}\mu$  and in the  $1800\text{--}1500\text{ cm}^{-1}$  region do not always parallel each other. As has been mentioned in Section II-C(2), spectral features in the  $1800\text{--}1500\text{ cm}^{-1}$  region are not affected by heating to  $70^\circ\text{C}$  the  $\text{D}_2\text{O}$  solution of polyriboadenylic acid at pD 4.8, while absorption intensity at  $252\text{ m}\mu$  is greatly increased. Apurinic acid<sup>55</sup> shows a weak band at about  $1630\text{ cm}^{-1}$  in  $\text{D}_2\text{O}$  solution. This band seems to disappear on heating the solution to  $75^\circ\text{C}$  and appears again on cooling. On the other hand the absorption intensity at  $268\text{ m}\mu$  of this acid is not affected by heating the solution to  $90^\circ\text{C}$ . These facts suggest that the  $1800\text{--}1500\text{ cm}^{-1}$

region spectrum reflects a different face of the secondary structure of nucleic acids from that known by the absorption intensity at 260 m $\mu$ .

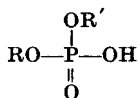
### (3) *Infrared Dichroism of Deoxyribonucleate*

It is found that the absorption bands in the 1750–1600 cm<sup>-1</sup> region of NaDNA and LiDNA are always polarized perpendicular to the orientation direction.<sup>7, 54</sup> As Fraser and Fraser<sup>16</sup> first pointed out, this proves the approximate perpendicularity of the planar bases to the extension direction of the polymer chain. For obtaining further information on the orientation of base residues in the fiber, examination of the deuterated specimen is more effective than that of undeuterated specimen. In the former, the absorptions due to the bending vibration of water and the NH<sub>2</sub> group are removed from the 1750–1600 cm<sup>-1</sup> region, and only the bands due to the ring stretching vibrations, whose transition moments would be practically in the base planes, remain there. The dichroic ratio (perpendicular to parallel) obtained here at 92% relative humidity is always greater than that at 75% relative humidity.<sup>54</sup> This fact is in agreement with what was found by X-ray studies.<sup>14, 15, 69</sup> According to the latter studies, the base planes are almost exactly parallel to the fiber axis at 92% relative humidity (structure B) and are tilted about 20° from a plane perpendicular to the fiber axis at 75% relative humidity (structure A).<sup>28</sup>

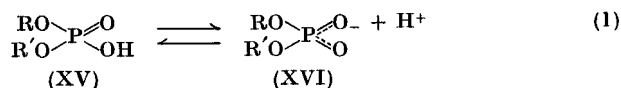
## III. ABSORPTION BANDS DUE TO THE PHOSPHATE GROUPS

### A. General Considerations

The phosphate groups of natural nucleic acids, synthetic polynucleotides, and mononucleotides give a few characteristic strong bands in their infrared spectra. In polynucleotides of biological interest, most phosphorus atoms are involved in the phosphodiester linkages. These are formally written as

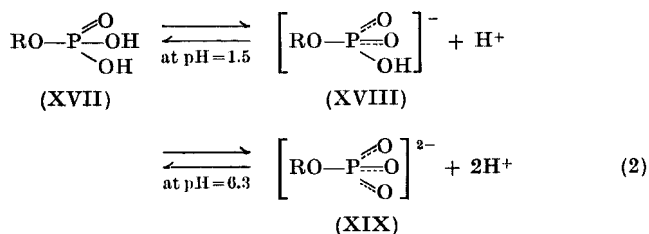


Each of these is a very strong acid, and readily dissociates as



The dissociation constant of this reaction is very high; in other words, the pK of the acid XV is very low. For instance, the pK is about 1.4 for dimethylphosphoric acid,<sup>23</sup> (CH<sub>3</sub>O)<sub>2</sub>PO<sub>2</sub>H. Therefore, in aqueous solutions with pH greater than 3, the phosphodiester linkage is considered to take the form XVI instead of XV. In the form XVI the two P—O bonds are considered to have equal amounts (about one-half) of double-bond character.

Mononucleotides and terminal parts of polynucleotides have the phosphomonoester group, RO—P<sup>OH</sup><sub>2</sub>. This group has two pK's, one at about 1.5 and the other at about 6.3,<sup>23</sup> and it dissociates as follows:



In the form XVIII, the two P—O bonds are considered to have equal amounts (about one-half) of double-bond character; and in the form XIX, the three P—O bonds to have equal amounts (about one-third) of double-bond character.

Based upon what has just been described, we shall concentrate our attention on the infrared absorptions due to the vibrations of the  $\left[ \text{>P} \begin{array}{l} \diagup \text{O} \\ \diagdown \text{O} \end{array} \right]^-$  and  $\left[ \text{—P} \begin{array}{l} \diagup \text{O} \\ \diagdown \text{O} \end{array} \right]^{2-}$  groups. As will be discussed below, it has been concluded that the former group gives two strong bands at about 1230 cm<sup>-1</sup> and 1080 cm<sup>-1</sup>, and the latter group at about 1100 cm<sup>-1</sup> and 980 cm<sup>-1</sup> (see Table I). All of these four bands are so characteristically strong that even in a complex spectrum of a complex compound these bands are relatively easily identified, as far as they have the  $\text{>PO}_2^-$  or  $\text{—PO}_3^{2-}$  groups.

TABLE I. Characteristic Bands of the  $>\text{PO}_2^-$  and  $-\text{PO}_3^{2-}$  Groups

Group	Frequency, $\text{cm}^{-1}$	Description	Assignment
$\left[ \begin{array}{c} \diagup \text{P} \diagdown \\ \diagdown \text{O} \diagup \end{array} \right]^-$	1230 1080	strong strong	$\text{PO}_2^-$ antisymmetric stretching $\text{PO}_2^-$ symmetric stretching
$\left[ \begin{array}{c} \diagup \text{P} \diagdown \\ \diagdown \text{O} \diagup \\ \diagdown \text{O} \diagup \end{array} \right]^{2-}$	1100 980	strong, broad strong, sharp	$\text{PO}_3^{2-}$ degenerate stretching $\text{PO}_3^{2-}$ symmetric stretching

### B. Phosphite Anion

Let us first consider the  $-\text{PO}_3^{2-}$  group. The simplest anion with this group may be the phosphite anion,  $\text{H}-\text{P} \begin{array}{c} \diagup \text{O}^- \\ \diagdown \text{O} \end{array}$ . The Raman spectrum of this anion was observed for an aqueous solution of sodium phosphite,  $\text{Na}_2\text{HPO}_3$ , by Mathieu and Jacques.<sup>37</sup> Infrared spectra of an aqueous solution of potassium phosphite,  $\text{K}_2\text{HPO}_3$ , and of crystalline barium phosphite,  $\text{BaHPO}_3$ , in Nujol were examined by Tsuboi.<sup>58</sup> Recently, Raman and infrared spectra of deuterated phosphite anion,  $\text{DPO}_3^{2-}$ , have also been observed by Kyogoku, Shimanouchi, and Tsuboi.<sup>27</sup> Of the results obtained, those for aqueous solutions are summarized in Figs. 20 and 21. The observed frequencies both for aqueous solutions and solid states are listed in Table II.

Assuming that the  $\text{HPO}_3^{2-}$  ion has  $C_{3v}$  symmetry,<sup>66</sup> we may expect three fundamental frequencies due to totally symmetric vibrations (of the  $A_1$  type) and three fundamental frequencies due to doubly degenerate vibrations (of the E type). As is shown in Table II, six bands are observed in each aqueous solution, of which three split into two components each in the barium salt crystals. Most probably the splitting is due to removal of the degeneracy, and these three bands may be assigned to the degenerate vibrations. The assignment given in the last column of Table II, as well as in Figs. 20 and 21, has been made, not only on the basis of the

observation of the splitting, but also on the basis of the comparison of the frequencies observed for  $\text{HPO}_3^{2-}$  and  $\text{DPO}_3^{2-}$ , of the depolarization degrees of the Raman lines, and of the intensities of the

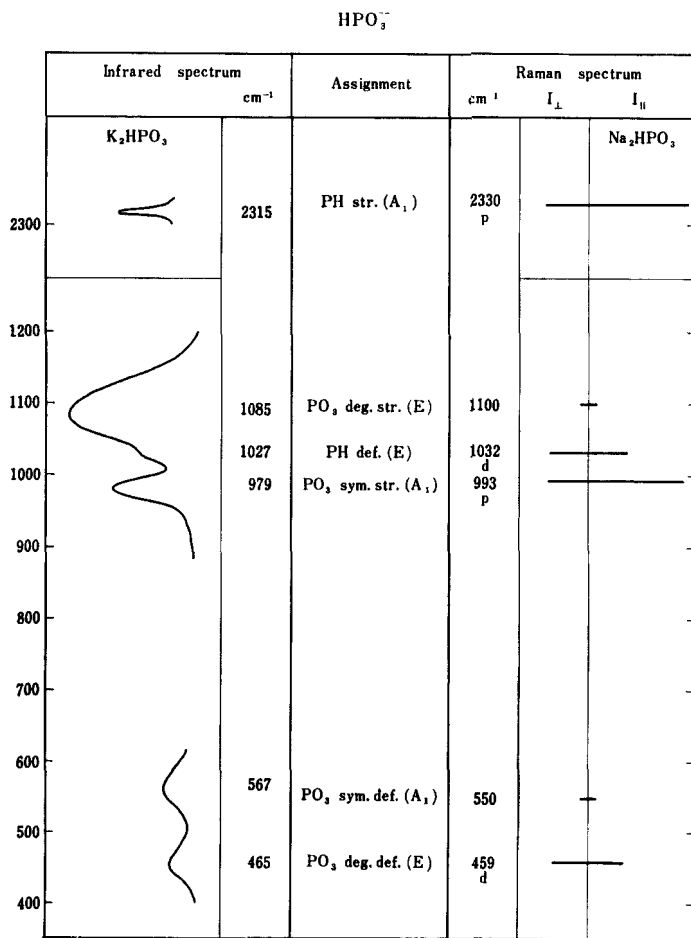


Fig. 20. Infrared and Raman spectra of aqueous solutions of potassium and sodium phosphites.

Raman lines and absorption bands. For instance, the Raman line at  $993\text{ cm}^{-1}$  of  $\text{Na}_2\text{HPO}_3$  is strong and polarized. The corresponding infrared band is very sharp. The position of this line or band remains



almost unchanged on deuteration. Therefore, this is almost undoubtedly due to the symmetric  $\text{PO}_3$  stretching vibration. Of the two degenerate bands at  $1085\text{ cm}^{-1}$  and  $1027\text{ cm}^{-1}$  of  $\text{K}_2\text{HPO}_3$ , the

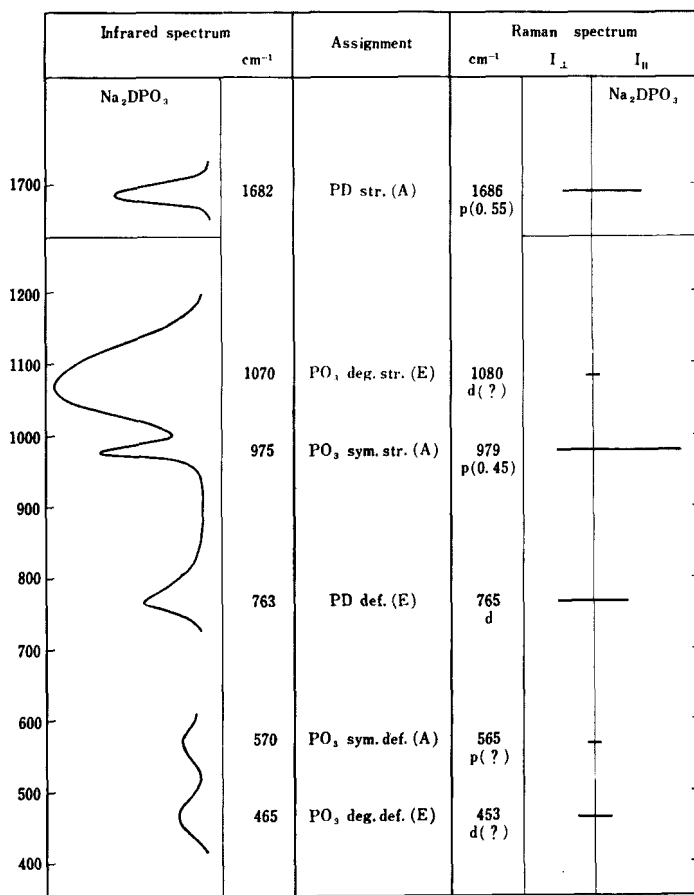


Fig. 21. Infrared and Raman spectra of aqueous solution of sodium deuterated phosphite.

former is very strong and the latter is extremely weak in infrared absorption. On deuteration the former remains at  $1070\text{ cm}^{-1}$ , while the latter is shifted to  $763\text{ cm}^{-1}$ . Therefore, the former is assignable

TABLE II. Vibrational Spectra<sup>a</sup> of Phosphite Anions  $\text{HPO}_3^-$  and  $\text{DPO}_3^-$ 

Raman, $\text{cm}^{-1}$		Infrared, $\text{cm}^{-1}$		Assignment	
$\text{Na}_2\text{HPO}_3$ aq. soln.	$\text{K}_2\text{HPO}_3$ aq. soln.	$\text{BaHPO}_3$ solid in Nujol			
459 m, d	465 m, b	{ 471 m 498 m		E	$\text{PO}_3$ deg. def.
550 vw	567 m	591 m		$\text{A}_1$	$\text{PO}_3$ sym. def.
993 s, p	979 m, sh	977 m, sh		$\text{A}_1$	$\text{PO}_3$ sym. str.
1032 m, d	1027 vw, b	{ 1006 w, sh 1021 w, sh		E	PH def.
1100 vw	1085 vs, b	{ 1083 vs, b 1100 vs, b		E	$\text{PO}_3$ deg. def.
2330 s, p	2315 m, sh	2410 m, sh		$\text{A}_1$	PH str.

$\text{Na}_2\text{DPO}_3$ aq. soln.	$\text{K}_2\text{DPO}_3$ aq. soln.	$\text{Na}_2\text{DPO}_3$ solid in Nujol	$\text{BaDPO}_3$ solid in Nujol		
453 m	465 m, b	470 w	{ 463 m, sh 489 m, sh	E	$\text{PO}_3$ deg. def.
565 w	570 w, b	570 w	584 s	$\text{A}_1$	$\text{PO}_3$ sym. def.
765 m, d	763 m	760 m	{ 747 m, sh 754 m, sh	E	PD def.
979 s, p	975 s, sh	975 s	973 s, sh	$\text{A}_1$	$\text{PO}_3$ sym. str.
1080 w	1070 s, b	1075 s	{ 1075 s 1120 s	E	$\text{PO}_3$ deg. def.
1686 s, p	1682 s	1710 m	1738 s	$\text{A}_1$	PD str.

<sup>a</sup> vs, very strong; s, strong; m, medium; w, weak; vw, very weak; d, depolarized; p, polarized; b, broad; sh, sharp.

to the  $\text{PO}_3$  degenerate stretching and the latter to PH deformation vibrations.

A normal coordinate treatment made by Kyogoku *et al.*<sup>27</sup> gives us further information on the vibrational modes of the phosphite anion. By setting the values of seven force constants as given in Table III, all of the six frequencies of  $\text{HPO}_3^{2-}$  and six frequencies of

TABLE III. Frequencies and Potential Energy Distributions of the Normal Vibrations of Phosphite Anions

Assumptions in the calculation <sup>a</sup>	Calculated frequency, cm <sup>-1</sup> (observed frequency in parentheses)	Potential energy distributions among the symmetry coordinates (Underline indicates greater distributions in each normal vibration.)					
		PH or PD str.	PO <sub>3</sub> sym. str.	PO <sub>3</sub> sym. def.	PO <sub>3</sub> deg. str.	PH or PD def.	PO <sub>3</sub> deg. def.
P—H = 1.50 Å	HPO <sub>3</sub> <sup>2-</sup>	1.01	0	0			
P—O = 1.53 Å	A <sub>1</sub> { 2333 (2315) 977 (979)	0.03	1.03	0.04			
OPH = 109° 28'	568 (567)	0.03	0.01	1.02			
OPO = 109° 28'	E { 1086 (1085) 1012 (1027)				0.78	0.27	0.06
	468 (465)				0.23	0.64	0
					0.02	0.25	1.08
K(P—H) = 2.078 md/Å	DPO <sub>3</sub> <sup>2-</sup>	1.01	0	0			
K(P—O) = 5.756 "	A <sub>1</sub> { 1666 (1682) 977 (975)	0.04	1.03	0.04			
H(OPH) = 0.036 "	566 ( 570)	0.02	0.01	1.02			
H(OPO) = 0.402 "	E { 1074 (1070) 775 (763)				1.00	0.04	0.06
F(O..H) = 0.583 "	451 (453)				0.02	0.72	0.06
F(O..O) = 0.670 "					0.01	0.40	1.03
κ = 0.598 mdÅ							

<sup>a</sup> K, H, F and κ are the stretching, bending, repulsive force constants and the internal tension respectively; md/Å denotes millidyne per Angstrom.

$\text{DPO}_3^{2-}$  are calculated to be very close to the observed frequencies (see Table III). In order to make an accurate assignment, the percentage distributions of vibrational potential energy among each group vibration coordinate are also calculated. The results are

TABLE IV. Normal Vibrations

Assumption in the calculation	Calculated frequency $\text{cm}^{-1}$ (observed fre- quency in parentheses)	$\text{CH}_3$ deg. def.	$\text{CH}_3$ sym. def.	$\text{CH}_3$ rock.
<b>A'</b>				
$\text{P} \cdots \text{O} = 1.53 \text{ \AA}$				
$\text{P}-\text{O} = 1.60 \text{ \AA}$	1483 (1465)	0.79	0	0.19
$\text{O}-\text{C} = 1.47 \text{ \AA}$	1469 (1465)	0	1.05	0
$\text{C}-\text{H} = 1.09 \text{ \AA}$	1174 (1183)	0.19	0	0.69
$\text{O} \cdots \text{P} \cdots \text{O}$	1097 (1115)	0.01	0.01	0.04
$\text{O}-\text{P} \cdots \text{O}$	1056 (1056)	0	0.08	0.01
$\text{H}-\text{C}-\text{O}$	992 (983)	0	0	0
$\text{H}-\text{C}-\text{H}$	751 (750)	0	0	0.05
$\text{C}-\text{O}-\text{P} = 120^\circ$	596 (573)	0	0	0.01
	508 (510)	0	0	0
	396 (393)	0	0	0
	267 (265)	0	0	0.01
$K(\text{P} \cdots \text{O}) = 5.9 \text{ md/\AA}$				
$K(\text{P}-\text{O}) = 2.5$				
$K(\text{O}-\text{C}) = 2.7$				
$K(\text{C}-\text{H}) = 4.3$				
$H(\text{O} \cdots \text{P} \cdots \text{O}) = 0.29$				
$H(\text{O}-\text{P} \cdots \text{O}) = 0.29$				
$H(\text{C}-\text{O}-\text{P}) = 0.5$				
$H(\text{O}-\text{C}-\text{H}) = 0.2$				
$H(\text{H}-\text{C}-\text{H}) = 0.42$				
$F(\text{O} \cdots \text{P} \cdots \text{O}) = 0.67$				
$F(\text{O}-\text{P} \cdots \text{O}) = 0.67$	2985 (2990)	1.00	0	0
$F(\text{C}, \text{P}) = 0.35$	1474 (1465)	0.01	0.81	0.18
$F(\text{O}, \text{H}) = 0.9$	1127 (1140)	0.03	0.19	0.85
$F(\text{H}, \text{H}) = 0.07$	1086 (1090)	0	0	0
$\kappa(\text{PO}_4) = 0.52 \text{ md\AA}$	544 (530)	0	0	0
$\kappa(\text{CH}_3\text{O}) = -0.02$	391 (393)	0	0	0
<b>A''</b>				
		$\text{CH}_3$ anti- sym. str.	$\text{CH}_3$ deg. def.	$\text{CH}_3$ rock.

given in Table III. These values are obtained from  $F_{ii}L_{ik}^2$  for the  $k$ th normal vibration, where  $F_{ii}$  is a diagonal term of the potential energy matrix  $F$ , and  $L_{ik}$  is an element of the  $L$ -matrix, which gives the degree of contribution for each group coordinate to the normal

of the  $\text{CH}_3\text{OPO}_3^{2-}$  Anion

Potential energy distribution							
$\text{PO}_3$ deg. str.	C—O str.	$\text{PO}_3$ sym. str.	P—O str.	$\text{PO}_3$ sym. def.	$\text{PO}_3$ rock.	$\text{PO}_3$ deg. def.	C—O—P bend.
0	0	0	0	0	0	0	0
0	0.01		0	0	0	0	0
0.04	0	0	0.03	0	0.01	0	0.07
0.83	0.11	0	0.01	0	0.06	0.04	0.01
0.13	0.91	0	0.08	0	0.02	0	0.12
0	0	1.02	0.05	0.06	0	0	0
0.01	0.03	0	0.74	0.17	0.04	0	0.12
0.02	0.02	0.01	0	0.46	0.12	0.09	0.17
0.01	0.04	0	0.09	0.33	0.54	0.31	0
0	0.03	0	0.05	0.03	0.28	0.60	0.15
0	0	0	0.02	0.01	0.51	0.03	0.47

$\text{PO}_3$ deg. str.	$\text{PO}_3$ rock.	$\text{PO}_3$ deg. def.
0	0	0
0	0	0
	0	0
1.01	0.04	0.04
0	0.67	0.64
0.02	0.36	0.39

coordinate.<sup>49</sup> The distributions given in Table III also support all of the above-given assignments.

Thus, it has now been established that, in the  $\text{HPO}_3^{2-}$  and  $\text{DPO}_3^{2-}$  anions, a sharp band at  $980\text{ cm}^{-1}$  and a broad band at  $1100\text{ cm}^{-1}$  are respectively due to the  $\text{PO}_3$  symmetric and degenerate stretching motions. An examination will be made below as to whether these two bands may be considered as characteristic of the  $\text{PO}_3^{2-}$  group.

### C. Monoalkylphosphate Anions

As the simplest phosphomonoester, the monomethylphosphate anion  $\text{CH}_3\text{OPO}_3^{2-}$  will be considered next. Raman and infrared spectra<sup>27, 58</sup> of sodium monomethylphosphate are shown in Fig. 22. As may be seen in the figure, monomethylphosphate anion

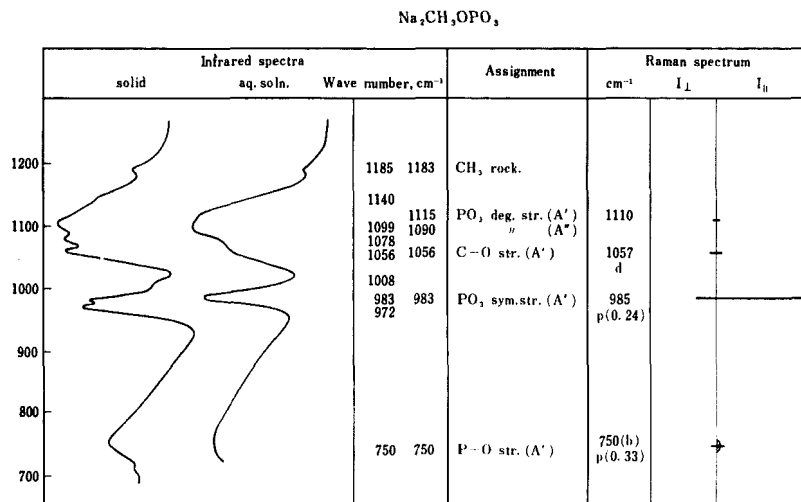


Fig. 22. Infrared and Raman spectra of sodium monomethylphosphate.

shows sixteen frequencies in the  $1500\text{--}250\text{ cm}^{-1}$  region. There are 2

	750	750	$\text{P}-\text{O}$ str. ( $A'$ )	750(h)		
				p(0.33)		

from molecules such as  $\text{HPO}_3^{2-}$ , or by estimating properly from those of similar molecules such as carbonic esters or ethers.<sup>27</sup> All of the observed sixteen frequencies correspond well with the calculated values and can be reasonably assigned (see the second and third columns of Table IV). By this treatment, it was also shown that the sharp absorption band at  $983\text{ cm}^{-1}$  is due to the  $\text{PO}_3$  symmetric stretching and that the two strong bands at  $1115$  and  $1090\text{ cm}^{-1}$  are due to the  $\text{PO}_3$  "degenerate" stretching. Here, the "degeneracy" is of course removed, because the molecule retains only the  $C_s$  symmetry and no longer has a  $C_3$  axis. This removal of the degeneracy seems to cause the frequency splitting of about  $25\text{ cm}^{-1}$ .

In the infrared spectra of sodium monoethylphosphate and barium monobutylphosphate, a similarly sharp band at about  $980\text{ cm}^{-1}$  and a group of strong bands in the vicinity of  $1100\text{ cm}^{-1}$  are observed. These are considered to essentially correspond to the two  $\text{PO}_3$  stretching motions in question, although some ambiguity arises because of the expected superposition of the bands due to the C—O and C—C stretching motions in this frequency region.

#### D. Mononucleotides

As has been mentioned in Section III-A, mononucleotides should take the  $\text{PO}_3$  structure when they are in aqueous solution at pH higher than 8. Infrared absorption spectra<sup>62</sup> of inosine-5'-monophosphate in  $\text{H}_2\text{O}$  solution obtained at various pH's are given in Fig. 23. In the solutions at higher pH, this compound shows a sharp band at  $980\text{ cm}^{-1}$  and a broad and strong band at  $1100\text{ cm}^{-1}$ . Two similar bands were observed<sup>30</sup> for  $\text{D}_2\text{O}$  solutions of adenosine-5'-monophosphate at higher pH's. Sinsheimer, Nutter, and Hopkins<sup>52</sup> observed strong bands at  $975$  and  $1105\text{ cm}^{-1}$  for all of the seven nucleotides which they examined in solutions at high pH (both in  $\text{H}_2\text{O}$  and  $\text{D}_2\text{O}$ ). In the solutions of lower pH these two bands are absent for every nucleotide (for inosine-5'-monophosphate, see Fig. 23). Hence, it is quite clear that these two bands come from the  $\text{PO}_3^{2-}$  group in the nucleotide. In the light of what is known of the  $\text{HPO}_3^{2-}$  and  $\text{CH}_3\text{OPO}_3^{2-}$  anions (see above), these are undoubtedly ascribed to the  $\text{PO}_3$  symmetric ( $980\text{ cm}^{-1}$ ) and degenerate ( $1100\text{ cm}^{-1}$ ) stretching motions.

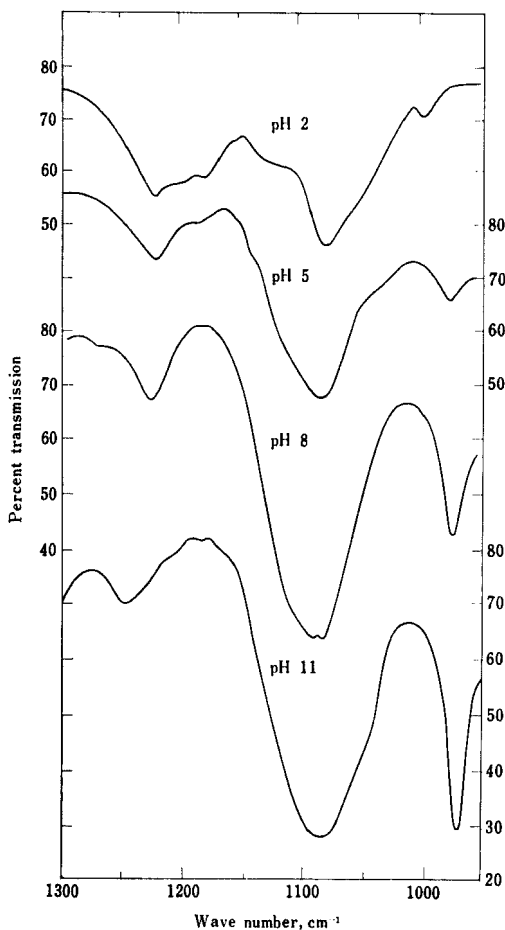


Fig. 23. Infrared spectra of inosine-5'-monophosphate in aqueous solutions of various pH's.

### E. Hypophosphite Anion

Now the  $\text{PO}_2^-$  group will be considered. The simplest system with this group may be the hypophosphite anion,  $\text{H}_2\text{PO}_2^-$ . Infrared and Raman spectra have been observed for all of the three isotopic species of this anion, i.e.  $\text{H}_2\text{PO}_2^-$ ,<sup>58, 73</sup>  $\text{HDPO}_2^-$ ,<sup>27</sup> and  $\text{D}_2\text{PO}_2^-$ .<sup>27, 73</sup> Part of the results are given in Figs. 24, 25, and 26. Based upon



the comparison of these spectra, upon the depolarization degree observed<sup>27, 58, 73</sup> for each of the Raman lines, and upon the infrared

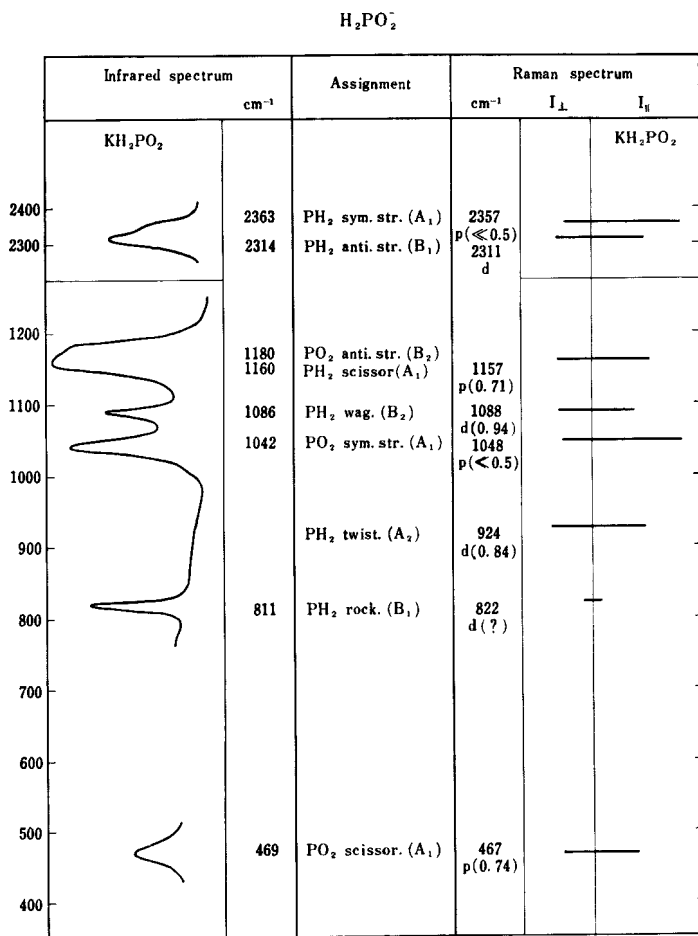


Fig. 24. Infrared and Raman spectra of aqueous solution of potassium hypophosphite.

dichroism observed<sup>58</sup> for the potassium hypophosphite crystal, a practically unequivocal set of assignments of the frequencies has been made (see Figs. 24–26). The two strong infrared absorptions

at about  $1200\text{ cm}^{-1}$  and  $1050\text{ cm}^{-1}$  remain unchanged on deuteration; the Raman line corresponding to the former is weak and

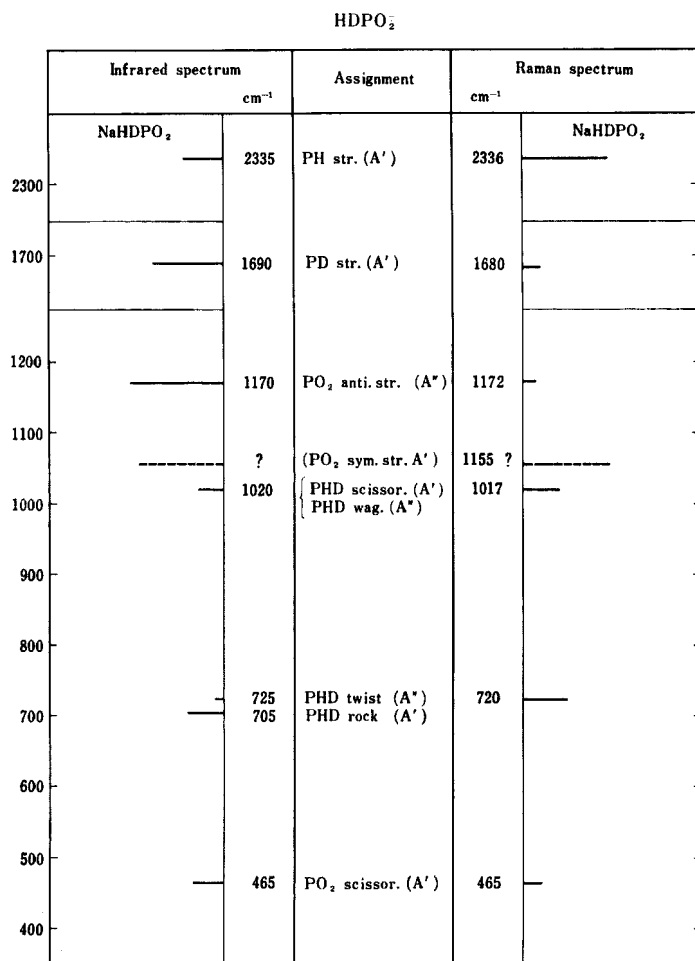


Fig. 25. Infrared and Raman spectra of aqueous solution of sodium hypophosphite- $d$ ,  $\text{NaHDPO}_2$ .

depolarized, while that corresponding to the latter is very strong and markedly polarized. These two are assigned respectively to the  $\text{PO}_2$  antisymmetric stretching and the  $\text{PO}_2$  symmetric stretching

vibrations. Normal coordinate treatments have been made by Kyogoku *et al.*,<sup>27</sup> the result of which is shown in Table V. The force

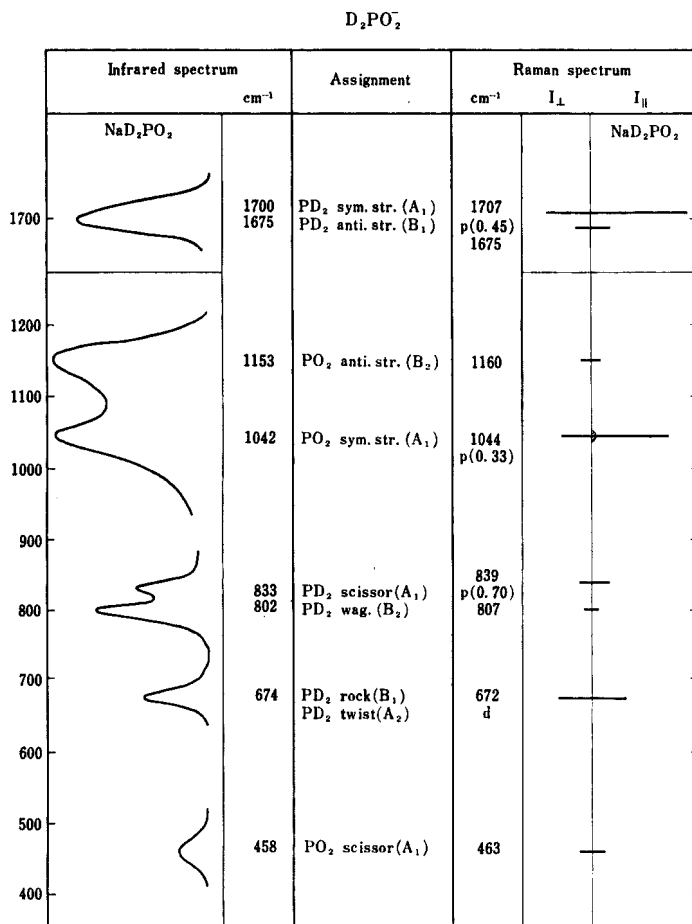


Fig. 26. Infrared and Raman spectra of aqueous solution of sodium hypophosphite- $d_2$ ,  $NaD_2PO_2$ .

constants given in this table were obtained from the observed frequencies by means of the method of least squares. As may be seen in the table, the results of the normal coordinate treatment lend

TABLE V. Frequencies and Potential Energy Distributions of the Normal Vibrations of Hypophosphite Anions

Assumptions in the calculation	Calculated frequency, cm <sup>-1</sup> (observed frequency in the parenteses)	Potential energy distributions among the symmetry coordinates <sup>a</sup> (Underline indicates greater distributions in each normal vibration.)								
		S <sub>1</sub> <sup>b</sup>	S <sub>2</sub>	S <sub>3</sub>	S <sub>4</sub>	S <sub>5</sub>	S <sub>6</sub>	S <sub>7</sub>	S <sub>8</sub>	S <sub>9</sub>
$r(\text{P}-\text{H}) = 1.50 \text{ \AA}$ $r(\text{P}-\text{O}) = 1.51 \text{ \AA}$ $\text{H}-\text{P}-\text{H} = 90^\circ$ $\text{O}-\text{P}-\text{O} = 120^\circ$	$\text{H}_2\text{PO}_2^-$									
	$\left\{ \begin{array}{l} 2377 (2363) \\ 1160 (1160) \end{array} \right\}$	1.00	0	0	0					
	$A_1$	0	0.90	0.05	0.02					
	$\left\{ \begin{array}{l} 1040 (1042) \\ 469 (469) \end{array} \right\}$	0.05	<u>0.04</u>	0.97	0.03					
	$B_1$	0.02	0.19	<u>0.02</u>	<u>0.11</u>					
	$\left\{ \begin{array}{l} 2326 (2314) \\ 806 (811) \end{array} \right\}$					1.00	0			
$K(\text{P}-\text{H}) = 2.275 \text{ md/\AA}$ $K(\text{P}-\text{O}) = 6.749$ " $K(\text{HPH}) = 0.202$ " $H(\text{OPO}) = 0.410$ " $H(\text{OPH}) = 0.049$ " $F(\text{H}\cdots\text{H}) = 0.127$ " $F(\text{O}\cdots\text{O}) = 0.495$ " $F(\text{O}\cdots\text{H}) = 0.681$ " $\kappa = 0.539 \text{ md\AA}$ $\text{I}_{\text{OH}} = -0.047$	$\text{HDPO}_2^-$									
	$\left\{ \begin{array}{l} 2352 (2336) \\ 1679 (1690) \end{array} \right\}$	1.00	0	0	0	0	0			
	$A'$	0	0	0	0	1.01	0			
	$\left\{ \begin{array}{l} 1071 \\ 1014 (1020) \end{array} \right\}$	0	0.57	0.37	0.04	<u>0.01</u>	0.03			
	$\left\{ \begin{array}{l} 705 (705) \\ 464 (465) \end{array} \right\}$	0.04	<u>0.44</u>	<u>0.46</u>	0	0.01	0.07			
	$\left\{ \begin{array}{l} 1165 (1170) \\ 1024 (1020) \end{array} \right\}$	0.02	0	<u>0.07</u>	0.03	0.01	0.96			
	$A''$	0.01	0.02	0.23	<u>1.10</u>	0.01	0			
	$\left\{ \begin{array}{l} 1024 (1020) \\ 717 (720) \end{array} \right\}$							1.03	0.01	0
								<u>0.03</u>	<u>0.79</u>	0.25
								0	<u>0.27</u>	<u>0.74</u>



further support to the above-given assignments. Ziomek *et al.*<sup>73</sup> have also studied the spectra of  $D_2PO_2^-$ . Although their results are somewhat different from ours, the assignments of  $PO_2$  stretching vibrations are in agreement with those referred to above.

### F. Dialkylphosphate Anions

Next, dimethylphosphate anion  $(CH_3O)_2PO_2^-$  is considered. The Raman spectrum of this anion has been observed in an aqueous solution of its sodium salt. The infrared spectra have been observed for solid-state barium dimethylphosphate. The results are given in Fig. 27.

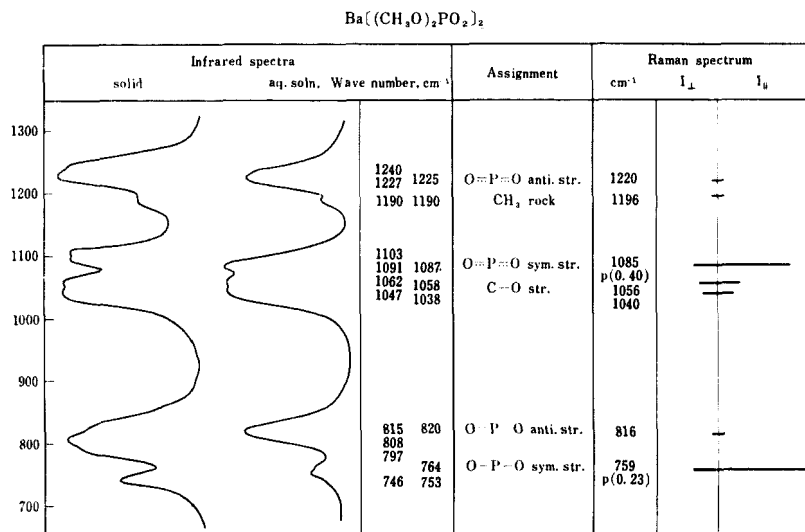


Fig. 27. Infrared and Raman spectra of barium dimethylphosphate.

The dimethylphosphate anion has two axes of internal rotation and the problem of rotational isomerism has to be taken into account. Studies of the structures of simple molecules by spectroscopic and diffraction methods have led to the generalization that only the staggered conformation is stable unless there are special reasons to the contrary.<sup>43</sup> This means that for dimethylphosphate anion only the three conformations shown in Fig. 28 can be

considered stable. In the  $C_{2v}$  conformation, both of the O—CH<sub>3</sub> bonds are *trans* to the P—O bonds, i.e. the azimuthal angle of the O<sup>I</sup>—CH<sub>3</sub> bond in the internal rotation about the O<sup>II</sup>—P axis is nearly 180° from the P<sup>III</sup>—O bond, and the azimuthal angle of the O<sup>IV</sup>—CH<sub>3</sub> bond in the internal rotation about the P<sup>III</sup>—O axis is nearly 180° from the O<sup>II</sup>—P bond. In the  $C_2$  conformation, both of the O—CH<sub>3</sub>

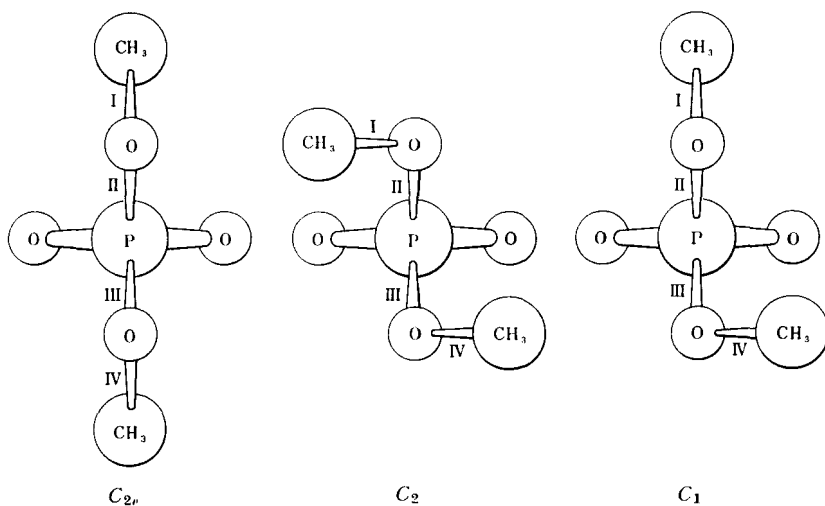


Fig. 28. Three possible conformations of dimethylphosphate anion.

bonds are in the *gauche* positions to the P—O bonds, i.e. the azimuthal angle of the O<sup>I</sup>—CH<sub>3</sub> bond in the internal rotation about the O<sup>II</sup>—P axis is nearly 60° from the P<sup>III</sup>—O bond, and the azimuthal angle of the O<sup>IV</sup>—CH<sub>3</sub> bond in the internal rotation about the P<sup>III</sup>—O axis is nearly 60° from the O<sup>II</sup>—P bond, while in the  $C_1$  conformation one of the two O—CH<sub>3</sub> bonds is in the *trans* and the other in the *gauche* position.

One of the reliable methods of determining the structure of a rotational isomer is to calculate the vibrational frequencies for a given conformation and to compare them with the observed values.<sup>43,44</sup> Kyogoku *et al.*<sup>27</sup> made a calculation of normal

frequencies for these three possible conformations, in the hope that a knowledge of the conformation of this anion might be obtained. In this calculation all the force constants except  $F(\text{O—}, \text{O—})$  are transferred from  $\text{H}_2\text{PO}_2^-$  and  $\text{CH}_3\text{OPO}_3^{2-}$  anions. The value of  $F(\text{O—}, \text{O—})$  is properly estimated from those for similar molecules. The calculated frequencies are given graphically in Fig. 29 along with the observed frequencies. From a comparison of the calculated and observed frequencies, and on the basis of the following considerations, it has been suggested that only the  $C_2$  conformation is involved in the actual barium dimethylphosphate solutions and crystal.

First of all, the calculation shows that the frequencies in the  $900\text{--}300\text{ cm}^{-1}$  region of the dimethylphosphate anion are fairly sensitive to its conformation, and may be used for its structure determination. From the fact that the number of the observed frequencies of aqueous solutions of barium dimethylphosphate is just what is expected for one conformation and is not greater than that, it was suggested that in the solution only *one* conformation is involved. In addition, all the frequencies observed in solution are in close agreement with those observed in the crystal, and hence, the *one* conformation in solution would be the same as that in the crystal. In the  $750\text{--}850\text{ cm}^{-1}$  region two normal vibrations are expected in one of which the stretching motions of the two  $\text{P—O}$  single bonds take place in phase and in the other with  $180^\circ$  phase difference. In the  $C_{2v}$  conformation the in-phase  $\text{P—O}$  stretching should have higher frequency than the out-of-phase  $\text{P—O}$  stretching; in the  $C_1$  conformation the two vibrations give almost the same frequency, and in the  $C_2$  conformation, the former should have lower frequency than the latter. Actually, there are two frequencies observed in this spectral region for the aqueous solution of barium dimethylphosphate. It was found that the higher frequency component is stronger in the infrared absorption while the lower frequency component is stronger in the Raman spectrum. Moreover, the Raman line with the lower frequency is strongly polarized. Therefore, it is almost certain that the higher frequency is due to the  $\text{P} \begin{smallmatrix} \text{O} \\ \diagup \end{smallmatrix} \text{O}$  antisymmetric stretching and the lower frequency to the  $\text{P} \begin{smallmatrix} \text{O} \\ \diagup \end{smallmatrix} \text{O}$  symmetric stretching. Accordingly, the conformation actually involved in the solution and crystal would not be that of  $C_{2v}$ . The case of  $C_1$  is also unfavorable. The calculated frequencies of the  $C_2$



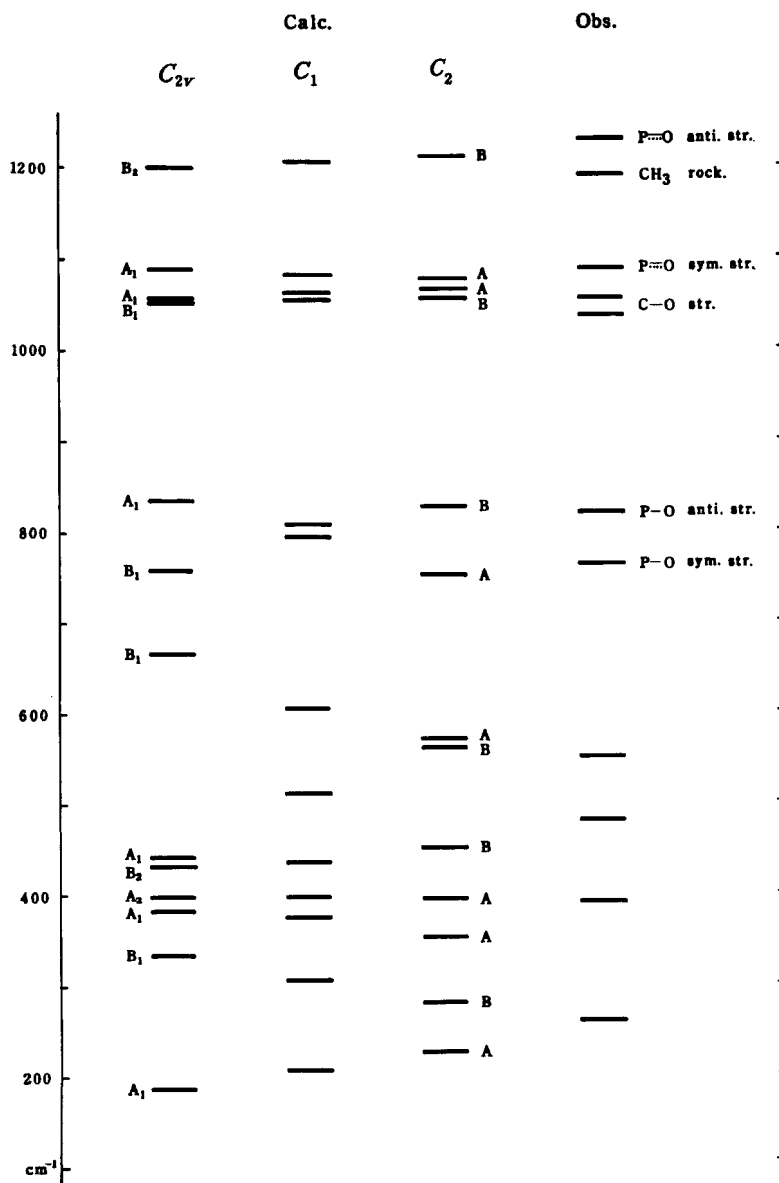


Fig. 29. Calculated and observed frequencies of dimethylphosphate anion.

conformation are generally in good agreement with the observed frequencies. Therefore, this is the most probable conformation of the dimethylphosphate anion.

The dimethylphosphate anion gives strong infrared absorption bands at  $1220\text{ cm}^{-1}$  and  $1085\text{ cm}^{-1}$ . The Raman line corresponding to the latter is very strong and strongly polarized. The former is assignable to the  $\text{PO}_2$  antisymmetric stretching and the latter to

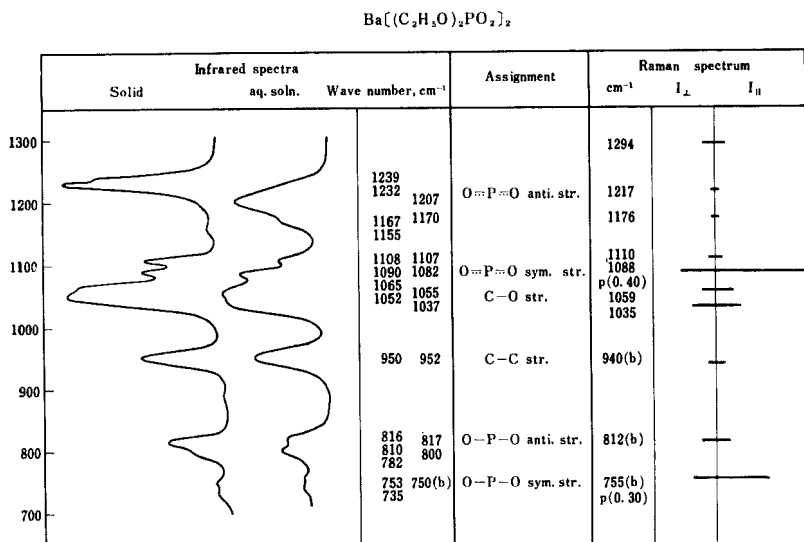


Fig. 30. Infrared and Raman spectra of barium diethylphosphate.

the  $\text{PO}_2$  symmetric stretching vibrations of the  $\text{P}(\text{O})\text{O}^-$  group. The calculation of the normal vibrations shows that these two frequencies are not sensitive to the conformation.

Barium diethylphosphate in its aqueous solution shows a strong absorption band at  $1207\text{ cm}^{-1}$  and a band with medium intensity at  $1082\text{ cm}^{-1}$  (see Fig. 30). The Raman line corresponding to the latter is strong and polarized. These two frequencies are assignable to the  $\text{PO}_2$  antisymmetric and  $\text{PO}_2$  symmetric stretching vibrations, respectively. A band at  $810\text{ cm}^{-1}$  is assignable to the antisymmetric  $\text{P}(\text{O})\text{O}^-$  stretching vibration. The Raman line corresponding to the latter is strong and polarized.

For any of the hypophosphite anions and dialkylphosphate anions, the  $\text{PO}_2$  antisymmetric stretching frequency of the  $\text{P}\begin{smallmatrix} \text{O}^- \\ \diagup \diagdown \\ \text{O} \end{smallmatrix}$  group is  $10\text{--}50\text{ cm}^{-1}$  higher in the solid state than in the aqueous solution. This may be due to hydrogen bonding in aqueous solution between the  $\text{O}\text{--}\text{H}$  of water and the  $\text{O}$  of the  $\text{P}\begin{smallmatrix} \text{O}^- \\ \diagup \diagdown \\ \text{O} \end{smallmatrix}$  group.

### G. Deoxyribonucleate

In the infrared spectrum of sodium deoxyribonucleate (NaDNA) film,<sup>54</sup> there is an isolated, strong band with its maximum near  $1230\text{ cm}^{-1}$  (see Figs. 1 and 31). This is assigned to the antisymmetric stretching motion of the  $\text{P}\begin{smallmatrix} \text{O}^- \\ \diagup \diagdown \\ \text{O} \end{smallmatrix}$  group in NaDNA, for the following reasons:

(1) As may be seen from Fig. 1 (Section I), it is unlikely that a strong band near  $1230\text{ cm}^{-1}$  could arise from the base or the sugar residues in NaDNA.

(2) This band remains unchanged on deuteration, except for the superposition of the  $\text{D}_2\text{O}$  band at  $1225\text{ cm}^{-1}$ .<sup>54</sup>

(3) As has been shown above, the hypophosphite anion and alkylphosphate anion have a strong band in the  $1180$  to  $1240\text{ cm}^{-1}$  region, which can be assigned to the  $\text{PO}_2^-$  antisymmetric stretching vibration.

(4) As has been mentioned, the band in the anions is found at about  $1230\text{ cm}^{-1}$  in the solid state, but in aqueous solution it shifts toward lower frequency (probably due to hydrogen-bonding between the water molecule and the  $\text{PO}_2$  group). Similar behavior is observed for the NaDNA band in question, i.e. in the dry state the band is at  $1240\text{ cm}^{-1}$ , but when the film adsorbs  $\text{H}_2\text{O}$  (or  $\text{D}_2\text{O}$ ), the band peak shifts down to  $1220\text{ cm}^{-1}$ .

(5) In the spectrum of NaDNA, the band due to the  $\text{PO}_2^-$  group at  $1240\text{ cm}^{-1}$  has an intensity comparable to that of the strong complex of bands near  $1660\text{ cm}^{-1}$ . This is just what is expected. Thus, a 1 mole to 1 mole mixture of barium dimethylphosphate and uracil shows a  $1230\text{ cm}^{-1}$  band with an intensity comparable to the strong band at about  $1660\text{ cm}^{-1}$ .

When NaDNA film acquires high crystallinity at higher humidity, the band in question splits into two. The separation is about  $9\text{ cm}^{-1}$  at 75% relative humidity and about  $6\text{ cm}^{-1}$  at 92%

relative humidity.<sup>7</sup> The higher component shows perpendicular dichroism, while the lower one shows parallel dichroism. This would seem to indicate that the antisymmetric stretching motion of each

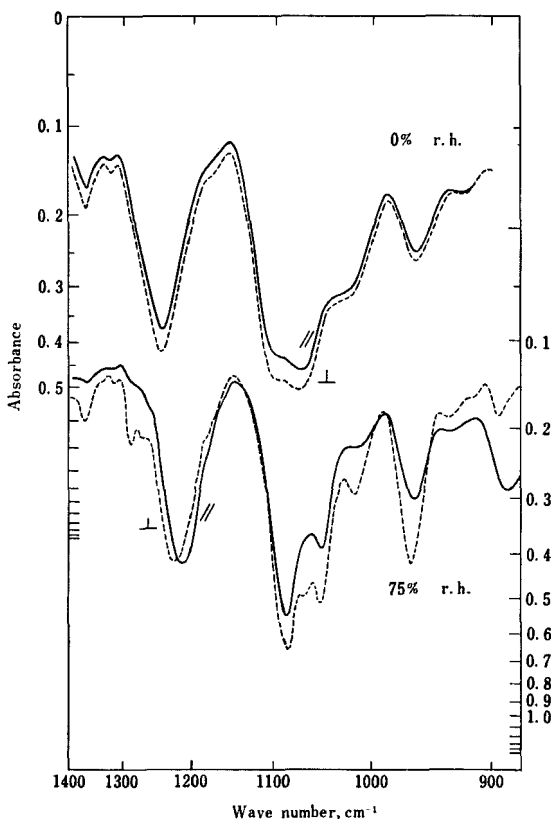


Fig. 31. Infrared spectra of an oriented film of sodium deoxyribonucleate placed in dry air and in air of 75% relative humidity: (—) electric vector parallel to the fiber axis; (.....) electric vector perpendicular to the fiber axis.

$\text{PO}_2^-$  group does not take place independently, but that adjacent  $\text{PO}_2^-$  groups interact with each other appreciably, resulting in a number of complicated vibrations extending over the whole chain. The lower frequency component with parallel dichroism must be due to the mode in which the  $\text{PO}_2^-$  vibrations take place in phase,

and the higher frequency component with perpendicular dichroism must be due to the mode in which the  $\text{PO}_2^-$  vibrations take place with  $2\pi/n$  phase difference, where  $n$  is the number of nucleotide residues in one turn of the helix of NaDNA.

In the X-ray analysis of the NaDNA structure,<sup>15, 69</sup> it has been shown that there are two crystal forms, A and B; A is obtained at 75% relative humidity and B at 92% relative humidity. Both of these have double-helix conformations, but their detailed structures are somewhat different from each other. For instance, each helix of form A has a pitch of 28 Å, a diameter of 18 Å, and involves 11 residues per turn, while each helix of form B has a pitch of 34 Å, a diameter of 17 Å, and involves 10 residues per turn. Bradbury *et al.*<sup>7</sup> made a plot of the frequencies of the two components of the band due to the antisymmetric stretching vibration of the  $\text{PO}_2^-$  group of NaDNA against the water content of the specimen. In this plot they found a double plateau, which shows that the frequency of the perpendicular component is constant over the ranges of humidity where form A and form B are observed. Another interesting fact which their plot seems to show is that the frequency separation of the two components is appreciably greater in form A ( $\sim 9 \text{ cm}^{-1}$ )<sup>41</sup> than that in form B ( $\sim 6 \text{ cm}^{-1}$ ). In the vibration corresponding to the perpendicular component, the  $\text{PO}_2^-$  antisymmetric stretching motions of two adjacent nucleotide residues along the helix take place with  $360/11 = 32.7^\circ$  phase difference in form A, but with  $360/10 = 36^\circ$  phase difference in form B. Therefore, if the interaction between the two adjacent  $\text{PO}_2^-$  groups were of the same order in form A as in form B, the frequency separation would be greater in form B than in form A. Actually, however, the reverse relation has been observed. This means probably that a potential constant expressing the interaction between the  $\text{PO}_2^-$  antisymmetric motions of adjacent nucleotides is much greater in form A than in form B.

In the  $1050\text{--}1100 \text{ cm}^{-1}$  region we may expect a strong band due to the  $\text{PO}_2$  symmetric stretching vibration of the  $\text{P}(\text{O})\text{O}^-$  group in NaDNA. Sutherland and Tsuboi<sup>54</sup> assigned the band at  $1050 \text{ cm}^{-1}$  of NaDNA to this vibration, and Bradbury *et al.*<sup>7</sup> also adopted this assignment. However, on the basis of the results of the study of dialkylphosphate anions, the  $1088 \text{ cm}^{-1}$  band of NaDNA is more probable than the  $1050 \text{ cm}^{-1}$  band to be assigned to the  $\text{PO}_2$  symmetric stretching vibration. Thus, barium dimethylphosphate

shows a strong and polarized Raman line at  $1085\text{ cm}^{-1}$  in its aqueous solution, and barium diethylphosphate shows a similarly strong and polarized Raman line at  $1088\text{ cm}^{-1}$ . The corresponding infrared bands are as strong as the  $1220\text{ cm}^{-1}$  band, and on going from aqueous solutions to the solid state the frequencies shift slightly (by  $3\text{--}8\text{ cm}^{-1}$ ) to higher frequencies and the intensities are slightly lowered. Likewise, the  $1088\text{ cm}^{-1}$  band of NaDNA is as strong as the  $1220\text{ cm}^{-1}$  band, and on drying it shifts to  $1096\text{ cm}^{-1}$  and becomes a little weaker.

The  $\text{PO}_2$  antisymmetric stretching vibration would have its transition moment nearly along the direction of the  $\text{O}\cdots\text{O}$  line of the  $\text{P}\begin{smallmatrix} \text{O}^- \\ \diagup \\ \text{O} \end{smallmatrix}$  group; and the  $\text{PO}_2$  symmetric stretching vibration is nearly along the bisector of the angle  $\text{OPO}$ . Therefore, the dichroism of these two bands (see Fig. 31) must be related to the orientations of the  $\text{P}\begin{smallmatrix} \text{O}^- \\ \diagup \\ \text{O} \end{smallmatrix}$  group in NaDNA. As may be seen in Fig. 31, the parallel and perpendicular components of the  $1220\text{ cm}^{-1}$  band have the same intensity. This fact suggests that the  $\text{O}\cdots\text{O}$  line lies very close to  $55^\circ$  to the helix axis. The  $1084\text{ cm}^{-1}$  band, on the other hand, shows a strong perpendicular dichroism ( $\parallel/\perp = 1/1.5$ ). Therefore the  $\text{OPO}$  bisector must be inclined more than  $60^\circ$  to the helix axis (probably about  $65^\circ$ ). These conclusions on the orientation of the  $\text{PO}_2$  group must hold good for NaDNA both at 75% and at 92% relative humidity. The orientation of the  $\text{P}\begin{smallmatrix} \text{O}^- \\ \diagup \\ \text{O} \end{smallmatrix}$  group of NaDNA was first suggested by Sutherland and Tsuboi.<sup>54</sup> This suggestion was taken into consideration by Langridge *et al.*<sup>29</sup> in their X-ray study of DNA. Unfortunately, however, there was some misunderstanding. They took the absence of dichroism in the  $1220\text{ cm}^{-1}$  band as indicating that the  $\text{O}\cdots\text{O}$  direction and the bisector of the  $\text{OPO}$  angle both lie at about  $55^\circ$  to the helix axis.

## H. Ribonucleates

Sodium ribonucleates, both natural and synthetic, show an isolated strong band at about  $1230\text{ cm}^{-1}$  (see Fig. 32) and a strong band at about  $1090\text{ cm}^{-1}$ . These are assigned respectively to the antisymmetric and symmetric stretching vibrations of the  $\text{P}\begin{smallmatrix} \text{O}^- \\ \diagup \\ \text{O} \end{smallmatrix}$  group. The  $1230\text{ cm}^{-1}$  band of polyadenylic acid is a doublet with two peaks about  $15\text{ cm}^{-1}$  apart. According to an observation made

by Morgan and Blout<sup>45</sup> with polarized radiation, both of these peaks show perpendicular dichroism. One possible explanation is that there are two different states of  $\text{PO}_2^-$  groups in polyadenylic acid; in one of them, the  $\text{PO}_2^-$  group is involved in a stronger hydrogen bond than in the other. In connection with this, it is interesting to note that some of the adenine residues are protonated and some are not

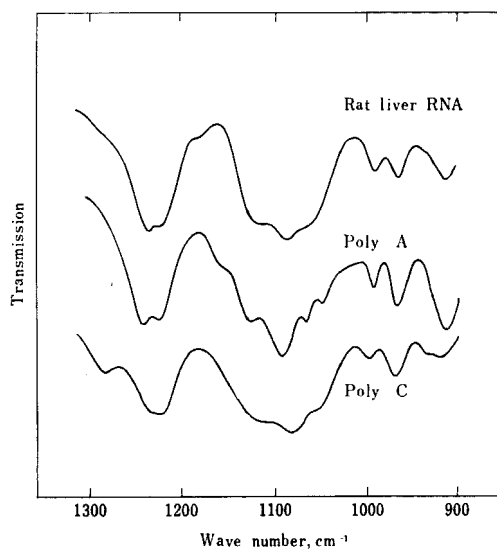


Fig. 32. Infrared spectra of sodium salts of ribonucleic acid from rat liver ribosomes, polyadenylic acid (cast at pH 4.2) and polycytidylic acid (cast at pH 5.5).

in the double-helix conformation of polyadenylic acid (see Section II-C(2)).

The spectral feature of ribonucleate is greatly different from that of deoxyribonucleate especially in the spectral region of  $1000\text{--}700\text{ cm}^{-1}$  (see Fig. 1). The differences may be attributed mainly to the difference in the chain conformations of these two nucleates. As has been illustrated by the normal coordinate treatment of dimethylphosphate anion (see Section III-F), frequencies in the spectral region in question may be very sensitive to the chain conformation of the polynucleotide chain with the  $\text{C—O—PO}_2^-\text{—O—C}$  group. The differences may partly be due to the different sugar residues (see Section IV).

#### IV. ABSORPTION BANDS DUE TO THE SUGAR GROUPS

Unfortunately, only a limited amount of information has thus far been obtained from the infrared spectra of the ribose part of nucleic acids. The ribofuranose ring has one ether and one alcohol group. In

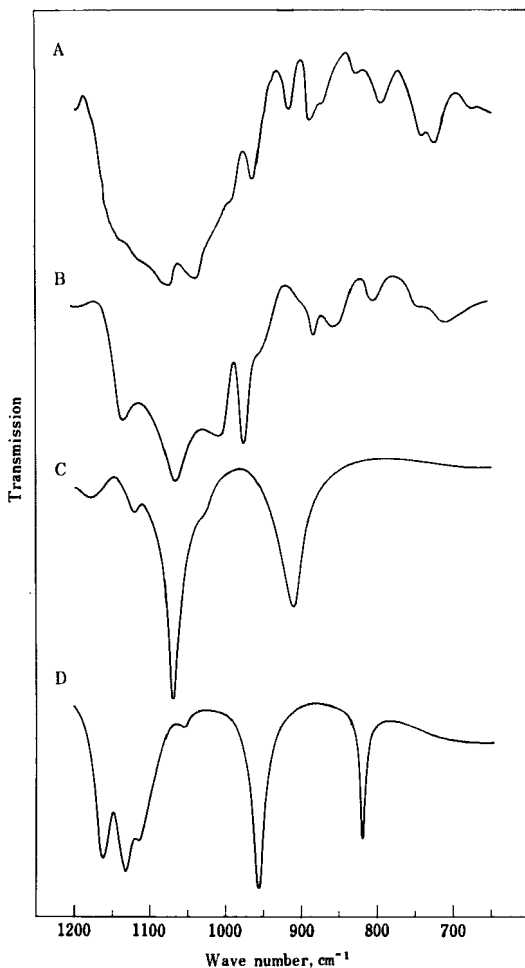


Fig. 33. Infrared spectra of ribose and related compounds. (A) D-Ribose; (B) 2'-deoxy-D-ribose; (C) tetrahydrofuran; (D) isopropyl alcohol.



Fig. 33 the spectra of D-ribose and 2'-deoxy-D-ribose are shown as compared with those of related compounds.

The assignments of absorption bands for isopropyl alcohol have been made by Tanaka<sup>56</sup> and are given in Table VI together with

TABLE VI. Assignments of Main Bands for Tetrahydrofuran and Isopropyl Alcohol

	Wave number	Assignments
$\begin{array}{c} \text{H}_2\text{C} \quad \text{CH}_2 \\   \quad \quad   \\ \text{H}_2\text{C} \quad \text{O} \quad \text{CH}_2 \end{array}$	— 2970	Antisymmetric $\text{CH}_2$ stretching vibration
	— 2860	Symmetric $\text{CH}_2$ stretching vibration
	1464	$\text{CH}_2$ scissoring vibration
	1072	Skeletal stretching vibration in which mainly two C—O bonds move out of phase
	910	Skeletal stretching vibration in which mainly two C—O bonds move in phase
$\begin{array}{c} \text{H}_3\text{C}-\text{CH}-\text{CH}_3 \\   \\ \text{OH} \end{array}$	3345	OH stretching vibration
	2978, 2938, 2894	CH stretching vibrations
	1470	$\text{CH}_3$ degenerate deformation vibration
	1382, 1372	$\text{CH}_3$ symmetric deformation vibrations
	1342	CH bending vibration ( $\text{A}''$ )
	1412, 1311	Coupled vibrations between CH bending and OH in-plane bending motions ( $\text{A}'$ )
	1165, 953	Coupled vibrations between $\text{CH}_3$ rocking and skeletal II motions ( $\text{A}'$ )
	1130	Skeletal III vibration ( $\text{A}''$ )
	1113	$\text{CH}_3$ rocking vibration coupled with OH in-plane bending vibration ( $\text{A}'$ )
	818	Skeletal I vibration ( $\text{A}'$ )

$\text{A}'$ : vibration symmetric to the HC—OH plane.

$\text{A}''$ : vibration antisymmetric to the HC—OH plane.

Skeletal I vibration: vibration corresponding approximately to the symmetry coordinate  $(\Delta\text{CC} + \Delta\text{CC} + \Delta\text{CO})/\sqrt{3}$ .

Skeletal II vibration: vibration corresponding approximately to the symmetry coordinate  $(2\Delta\text{CO} - \Delta\text{CC} - \Delta\text{CC})/\sqrt{6}$ .

Skeletal III vibration: vibration corresponding approximately to the antisymmetric CC stretching coordinate.

those for tetrahydrofuran. A study of the spectra of similar compounds shows that in the case of ethers and alcohols almost all the strong bands appearing in the region between 1200–800  $\text{cm}^{-1}$  can be assigned to the C—O stretching vibrations which are in many cases coupled with C—C stretching or other vibrations.

The situation seems to be similar for ribose and deoxyribose. The symmetric  $\begin{array}{c} \text{C}-\text{C}-\text{C} \\ | \\ \text{O} \end{array}$  stretching vibrations are expected to appear with medium or weak intensities in the region 900–800  $\text{cm}^{-1}$ . The approximately degenerate  $\begin{array}{c} \text{C}-\text{C}-\text{C} \\ | \\ \text{O} \end{array}$  stretching vibrations are expected to appear with strong intensities in the region 1200–950  $\text{cm}^{-1}$ . The bands appearing at 890 and 860  $\text{cm}^{-1}$  are assigned to the former vibrations and those at 1130, 1065, 1010 and 975  $\text{cm}^{-1}$  are assigned to the latter for deoxyribose. In the case of ribose only the latter group of bands appears definitely.

In the spectra of sodium ribonucleates (Fig. 32), there is a strong band observed at 1120  $\text{cm}^{-1}$ . This is absent from the spectrum of sodium deoxyribonucleate (Fig. 1A). This may be explained by assigning the 1120  $\text{cm}^{-1}$  band to the “degenerate” type  $\begin{array}{c} \text{C}-\overset{2'}{\text{C}}-\text{C} \\ | \\ \text{O} \end{array}$  stretching vibration around the 2'—OH group, which is involved in ribonucleates but not in deoxyribonucleates.

A strong band at 1050  $\text{cm}^{-1}$  appears both in ribonucleates and deoxyribonucleates. This may be due to a ring vibration of furanose or a C—O stretching vibration of the ester linkages.

There is a sharp band with medium intensity at 975  $\text{cm}^{-1}$  for deoxyribonucleates. This band cannot be observed for ribonucleates. This situation looks similar to the cases of ribose and deoxyribose. However, the assignment of this band is not yet clear. It is also possible that the phosphate group is responsible for this band.

Weak bands expected to appear in the region between 950 and 800  $\text{cm}^{-1}$  are sensitive to the configuration or conformation. However, they are too weak and overlap the bands due to the phosphate group.

### References

1. Angell, C. L., *J. Chem. Soc.* 504 (1961).
2. Angell, C. L., and Werner, R. L., *J. Chem. Soc.* 2911 (1952).

3. Bellamy, L. J., *The Infrared Spectra of Complex Molecules*, 2nd Ed., Methuen, London, 1959.
4. Blout, E. R., and Fields, M., *J. Biol. Chem.* **178**, 335 (1949).
5. Blout, E. R., and Lenormant, H., *Biochim. Biophys. Acta* **15**, 303 (1954).
6. Blout, E. R., and Lenormant, H., *Biochim. Biophys. Acta* **17**, 325 (1955).
7. Bradbury, E. M., Price, W. C., and Wilkinson, G. R., *J. Mol. Biol.* **3**, 301 (1961).
8. Broomhead, J. M., *Acta Cryst.* **4**, 92 (1951).
9. Brown, D. J., and Short, L. N., *J. Chem. Soc.* 168 (1952).
10. Cockran, W., *Acta Cryst.* **4**, 81 (1951).
11. Creeth, J. M., Gulland, J. M., and Jordan, D. O., *J. Chem. Soc.* 1141 (1947).
12. Doty, P., Boedtker, H., Fresco, J. R., Haselkorn, R., and Litt, M., *Proc. Natl. Acad. Sci. U.S.* **45**, 482 (1958).
13. Felsenfeld, G., and Rich, A., *Biochim. Biophys. Acta* **26**, 457 (1957).
14. Franklin, R. E., and Gosling, R. G., *Acta Cryst.* **6**, 673 (1953).
15. Franklin, R. E., and Gosling, R. G., *Nature* **172**, 156 (1953).
16. Fraser, M. J., and Fraser, R. D. B., *Nature* **167**, 759 (1951).
17. Fresco, J. R., *J. Mol. Biol.* **1**, 106 (1959).
18. Fresco, J. R., and Doty, P., *J. Am. Chem. Soc.* **79**, 3928 (1957).
19. Fresco, J. R., and Klemperer, E., *Ann. N.Y. Acad. Sci.* **81**, 730 (1959).
20. Furberg, S., *Acta Cryst.* **3**, 325 (1950).
21. Gierer, A., and Schramm, G., *Z. Naturforsch.* **116**, 138 (1956).
22. Helmkamp, G. K., and Ts'o, P. O. P., *J. Am. Chem. Soc.* **83**, 138 (1961).
23. Kumler, W. D., and Eiler, J. J., *J. Am. Chem. Soc.* **65**, 2355 (1943).
24. Kyogoku, Y., Tsuboi, M., Shimanouchi, T., and Watanabe, I., *Nature* **189**, 120 (1961).
25. Kyogoku, Y., Tsuboi, M., Shimanouchi, T., and Watanabe, I., *J. Mol. Biol.* **3**, 741 (1961).
26. Kyogoku, Y., Tsuboi, M., Shimanouchi, T., and Watanabe, I., *Nature* **195**, 459 (1962).
27. Kyogoku, Y., Shimanouchi, T., and Tsuboi, M., to be published.
28. Langridge, R., Wilson, H. R., Hooper, C. W., Wilkins, M. H. F., and Hamilton, L. D., *J. Mol. Biol.* **2**, 19 (1960).
29. Langridge, R., Marvin, D. A., Seeds, W. E., Wilson, H. R., Hooper, C. W., Wilkins, M. H. F., and Hamilton, L. D., *J. Mol. Biol.* **2**, 38 (1960).
30. Lenormant, H., and Blout, E. R., *Compt. Rend.* **239**, 1281 (1954).
31. Lenormant, H., and Lozé, C., *Compt. Rend.* **240**, 1327 (1955).
32. Lenormant, H., and Lozé, C., *Bull. Soc. Chim. France* 1501 (1955).
33. Levene, P. A., and Simms, H. S., *J. Biol. Chem.* **65**, 519 (1925).
34. Levene, P. A., Simms, H. S., and Bass, L. W., *J. Biol. Chem.* **70**, 243 (1925).
35. Marmur, J., and Doty, P., *Nature* **183**, 1427 (1959).
36. Marshall, J. R., and Walker, J., *J. Chem. Soc.* 1004 (1951).
37. Mathieu, J. P., and Jacques, J., *Compt. Rend.* **215**, 346 (1942).
38. Miles, H. T., *Chem. Ind. (London)* 591 (1958).
39. Miles, H. T., *Biochim. Biophys. Acta* **30**, 324 (1958).
40. Miles, H. T., *Biochim. Biophys. Acta* **35**, 274 (1959).
41. Miles, H. T., *Biochim. Biophys. Acta* **45**, 196 (1960).

42. Miles, H. T., *Proc. Natl. Acad. Sci. U.S.* **47**, 791 (1961).
43. Mizushima, S., *Structure of Molecules and Internal Rotation*, Academic Press, New York, 1954.
44. Mizushima, S., Shimanouchi, T., Nakagawa, I., and Miyake, A., *J. Chem. Phys.* **21**, 215 (1953).
45. Morgan, R. S., and Blout, E. R., *J. Am. Chem. Soc.* **81**, 4625 (1959).
46. Pauling, L., and Corey, R. B., *Arch. Biochem. Biophys.* **65**, 164 (1956).
47. Rice, S. A., and Doty, P., *J. Am. Chem. Soc.* **79**, 3937 (1957).
48. Rich, A., Davies, D. R., Crick, F. H. C., and Watson, J. D., *J. Mol. Biol.* **3**, 71 (1961).
49. Shimanouchi, T., and Suzuki, I., *J. Mol. Spectry.* **6**, 277 (1961).
50. Shimanouchi, T., Tsuboi, M., Kyogoku, Y., and Watanabe, I., *Biochim. Biophys. Acta* **45**, 195 (1960).
51. Short, L. N., and Thompson, H. W., *J. Chem. Soc.* 168 (1952).
52. Sinsheimer, R. L., Nutter, R. L., and Hopkins, G. R., *Biochim. Biophys. Acta* **18**, 13 (1955).
53. Souda, R., *Bull. Chem. Soc. Japan* **30**, 499 (1957).
54. Sutherland, G. B. B. M., and Tsuboi, M., *Proc. Roy. Soc. (London)* **A239**, 446 (1957).
55. Tamm, C., Hodes, M. E., and Chargaff, E., *J. Biol. Chem.* **195**, 49 (1952).
56. Tanaka, C., *Nippon Kagaku Zasshi* **83**, 521 (1962).
57. Tanner, E. M., *Spectrochim. Acta* **8**, 9 (1956).
58. Tsuboi, M., *J. Am. Chem. Soc.* **79**, 1351 (1957).
59. Tsuboi, M., *Spectrochim. Acta* **16**, 505 (1960).
60. Tsuboi, M., *Progr. Theoret. Phys. (Kyoto), Suppl.* **17**, 99 (1961).
61. Tsuboi, M., Kyogoku, Y., and Shimanouchi, T., *Biochim. Biophys. Acta* **55**, 1 (1962).
62. Tsuboi, M., and Matsuo, K., unpublished data.
63. Tsuboi, M., Takenishi, T., and Muramatsu, N., unpublished data.
64. Tsuboi, M., Yamamoto, H., Kyogoku, Y., and Shimanouchi, T., unpublished data.
65. Tsuboi, M., Yamaguchi, Y., Shiobara, K., and Egami, F., unpublished data.
66. Van Wazer, J. R., *Encyclopedia of Chemical Technology*, Vol. X, Kirk, R. C., and Othmer, D. F., eds., Interscience, New York, 1953, p. 470.
67. Warner, R. C., *J. Biol. Chem.* **229**, 711 (1957).
68. Watson, J. D., and Crick, F. H. C., *Nature* **171**, 737 (1953).
69. Wilkins, M. H. F., Seeds, W. E., Stokes, A. R., and Wilson, H. R., *Nature* **172**, 759 (1953).
70. Wilkins, M. H. F., Zubay, G., and Wilson, R. H., *J. Mol. Biol.* **1**, 179 (1959).
71. Wilkinson, G. R., Price, W. C., and Bradbury, E. M., *Spectrochim. Acta* **14**, 284 (1959).
72. Zahariasen, W. M., and Mooney, R. C. L., *J. Chem. Phys.* **2**, 34 (1934).
73. Ziomek, J. S., Ferraro, J. R., and Peppard, D. F., *J. Mol. Spectry.* **8**, 212 (1962).

## 13

# THE STUDY OF SPECIFIC MOLECULAR INTERACTIONS BY NUCLEAR MAGNETIC RELAXATION MEASUREMENTS

OLEG JARDETZKY, *Department of Pharmacology,  
 Harvard Medical School, Boston, Massachusetts*

## CONTENTS

I.	Introduction . . . . .	499
II.	Theoretical Foundations . . . . .	501
	A. Basic Definitions . . . . .	501
	B. The Interpretation of Relaxation Times ( $T_1$ and $T_2$ ) in Terms of Molecular Events . . . . .	505
	C. Simplifications of the Theory Applicable to High Resolution Proton Magnetic Resonance . . . . .	511
	D. Interpretation of Relaxation Measurements in Terms of Molecular Interactions . . . . .	515
III.	Experimental . . . . .	518
	A. Interactions between Small Molecules . . . . .	518
	B. The Binding of Small Molecules to Macromolecules . . . . .	523
	References . . . . .	531

## I. INTRODUCTION

The proposition that biological specificity ultimately rests on subtle variations in the electronic structure of molecules is as easy to defend as it is difficult to establish. The reason for this lies on one hand in the still recent success of physical methods in elucidating molecular structure and, on the other, in the fact that the core of structural chemistry consists of information derived from the study of the gaseous and the solid states. This information is neither immediately applicable nor, in most instances, sufficient to define with any precision the structure and properties of molecules in the solutions to which biological processes are confined. The less ambiguous methods, such as X-ray crystallography or atomic and molecular spectroscopy, become comparatively uninformative when applied to liquids. On the other hand, the readily applicable

chemical and physical techniques—spectrophotometry, electrochemistry, kinetics, etc.—rest for the most part on alterations of molecular properties too large to reflect the relevant structural information in significant detail.

Among the few physical methods which do not suffer from this limitation are nuclear and electron spin resonance spectroscopy. In either case the energy changes involved are sufficiently small to make the appearance of the spectra dependent on slight variations in the electronic configuration. However, the usefulness of electron spin resonance is confined to the study of free radicals and paramagnetic ions, inasmuch as the phenomenon can only be observed on substances containing unpaired electrons. Since the overwhelming majority of biologically active substances do not fall into this category, nuclear magnetic resonance (NMR) is by far more generally applicable to the study of their structure and properties in solution.

The interpretation of NMR spectra is based on three sets of parameters which characterize the absorption of radiofrequency radiation by atomic nuclei placed in a magnetic field: (1) the frequencies of the absorbed radiation, expressed as the *chemical shifts* relative to an arbitrary standard absorption line; (2) the multiplicity of the lines originating from a given group of nuclei, determined by the coupling between neighboring nuclei and described by the appropriate *coupling constants*; and (3) the decay times characterizing the return of the nuclei excited by the absorption of radiation to a lower energy state referred to as the *relaxation times*.

Most of the existing chemical correlations take into account the information obtained from the measurement of chemical shifts and coupling constants. In contrast, relaxation studies have received comparatively little attention, despite the well-established fact that relaxation processes are extremely sensitive to variations in the molecular environment and therefore provide the potentially most informative measurements for the study of molecular interactions.

The limited use of relaxation measurements to obtain information of chemical interest can be attributed to two major difficulties: (1) the comparatively intricate underlying physical theory which has made meaningful interpretation contingent on an extensive

investigation of numerous experimental parameters, and (2) the comparatively low sensitivity of the NMR method, which has made such measurements technically difficult in the lower concentration range, effectively limiting experimentation to solutions of the order 0.1 M or higher. In view of the well-known dependence of the relaxation times on even minor changes in the molecular environment, this limitation has made the generality of conclusions drawn from measurements on pure liquids or concentrated solutions somewhat uncertain.

The work described in this chapter has shown that information on the nature of interactions between comparatively large molecules (M.W. 100–800) can be obtained from relaxation measurements. The procedures used, their theoretical foundations and some of the results are discussed below. A general introduction to the basic concepts of magnetic resonance is omitted because of space limitations, but has recently been given elsewhere.<sup>10,11</sup> A more extensive exposition of the theory is also to be found in a recent treatise by Abragam.<sup>1</sup>

## II. THEORETICAL FOUNDATIONS

### A. Basic Definitions

For purposes of the relaxation experiments to be described here, a high resolution proton magnetic resonance spectrum can be thought to represent as many *spin systems* as there are lines in the spectrum. In this definition a *spin system* is an assembly of nuclei characterized by *two* energy levels (denoted as  $\alpha$  for the lower and  $\beta$  the upper level, and expressed in angular frequency units so that  $\hbar\alpha = E$ , where  $\hbar = h/2\pi$ ,  $h$  being the Planck constant and  $E$  the energy of the level), which can be calculated from the chemical shift and spin coupling constants of the protons (e.g. CH, —CH<sub>2</sub>, —CH<sub>3</sub>) or system of protons\* (AB<sub>2</sub>, ABC, etc.) from which the line originates.† When attention is focused on a given spin system, all

\* In the terminology of high resolution spectroscopy, also called a “spin system”, a meaning not to be confused with that given here.

† This formulation applies only to the experimental situation, in which a single well-defined line is exposed to the radiofrequency radiation. If other transitions involving the same energy levels are allowed to occur simultaneously, a more general formulation must be applied (see Chapter VIII of ref. 1). In complicated spectra such transitions must always be considered in

other nuclei and electrons in the sample are collectively referred to as the *lattice*.

At equilibrium the nuclei comprising a given spin system are distributed between the two energy levels and the ratio of the *populations* of each level (i.e. the number of spins at each level) is given by the Boltzmann factor

$$\frac{N_\beta}{N_\alpha} = \exp(-\hbar\omega_{\alpha\beta}/kT) \quad (1)$$

where  $N_\beta$  and  $N_\alpha$  are the populations of the lower and the upper state respectively,  $\hbar\omega_{\alpha\beta} = \Delta E$  the energy difference between the two states,  $k$  the Boltzmann constant and  $T$  the absolute temperature. In the presence of electromagnetic radiation of the frequency

$$\omega_{\alpha\beta} = \alpha - \beta \quad (2)$$

the spin system absorbs energy from the radiation field, with a consequent increase in the population of the upper state and a corresponding decrease in the population of the lower state. If the amount of energy absorbed by the spin system is sufficient to equalize the populations of the two states, the system is said to have undergone *saturation*.

The return of an either completely or partially saturated system to equilibrium consists of two simultaneously occurring processes: (1) a redistribution of the absorbed energy within the spin system, in which every transition of a nucleus from a higher to a lower state is accompanied by a transition of another equivalent nucleus from the lower to the higher state, a process referred to as *spin-spin relaxation*, and (2) a loss of energy to the lattice resulting from transitions of nuclei from the upper to the lower state induced by the motion of magnetic (or electric) fields in the lattice, called *spin-lattice relaxation*. The two processes may or may not occur at the

† (cont.)

detail since relaxation transitions from other accessible levels will occur simultaneously with the relaxation of the excited line. The present formulation should therefore be regarded only as a first approximation, which is useful because it readily allows an interpretation in terms of molecular parameters. The limits of its validity are determined by the possibility of finding lines or combinations of lines in the spectrum for which redistribution of nuclei between levels can be neglected.



same rate and can be observed separately on a given absorption line.

Macroscopically the state of a spin system can be described by its magnetization vector  $M$ , which is the vectorial sum of all nuclear magnetic moments comprising the system (see p. 254 of ref. 10). At equilibrium the magnetization vector is aligned with the external magnetic field (i.e. has no components in the plane perpendicular to the field) and has a value proportional to the equilibrium population of the lower energy state. In a partially saturated system the population of the lower state is less than the equilibrium population and the magnitude of the longitudinal component of the magnetization vector (i.e. the component in the direction of the external field) is correspondingly smaller. In addition, a component of magnetization appears in the plane perpendicular to the external magnetic field (the transverse component) owing to the alignment of nuclei with the magnetic vector of the radiation field, which is rotating in the plane.

A redistribution of nuclei within the spin system will not involve a loss of absorbed energy from the spin system and hence will not affect the magnitude of the longitudinal component. It will, on the other hand, affect the transverse component, since two nuclei reorienting each other's moments with respect to the stationary field lose their phase coherence with the magnetic vector of the radiation. The phenomenon of spin-spin relaxation is therefore equally properly described by the term *transverse relaxation*.

In contrast, the transfer of absorbed energy from the spin system to the lattice involves a change in the relative populations of the upper and the lower state and hence a change in the magnitude of the longitudinal component of magnetization. The equilibrium distribution of populations is therefore reestablished by *longitudinal* or *spin-lattice* relaxation.

For a spin system, as defined here, characterized by two energy levels, the changes of both longitudinal and transverse components are single exponential functions of time and can be described by characteristic time constants, the *longitudinal* or *spin-lattice* relaxation time  $T_1$ , and the *transverse* or *spin-spin* relaxation time  $T_2$ . The measurement of relaxation times is illustrated in Figs. 1 and 2 respectively. The intensity  $A_i$  of the signal (periodically traversed at low levels of the radiofrequency radiation) (see Fig. 1)

is proportional to the longitudinal component of magnetization and increases according to the equation

$$A_t = A_\infty(1 - e^{-t/T_1}) \quad (3)$$

where  $A_\infty$  is the equilibrium intensity.  $T_1$  can be obtained from a semi-logarithmic plot of  $(A_\infty - A_t)/A_\infty$  vs. time and using Eq. (3).

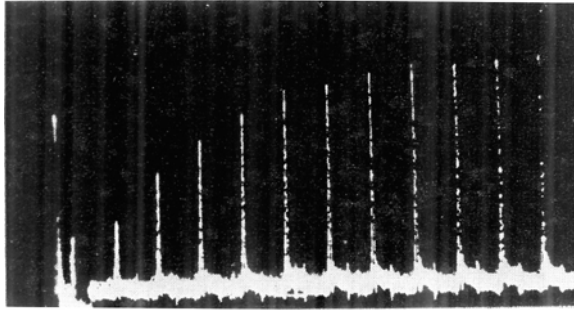


Fig. 1. Oscilloscope trace showing the recovery of the amplitude of a single nuclear magnetic resonance line following complete saturation at time  $t = 0$ .

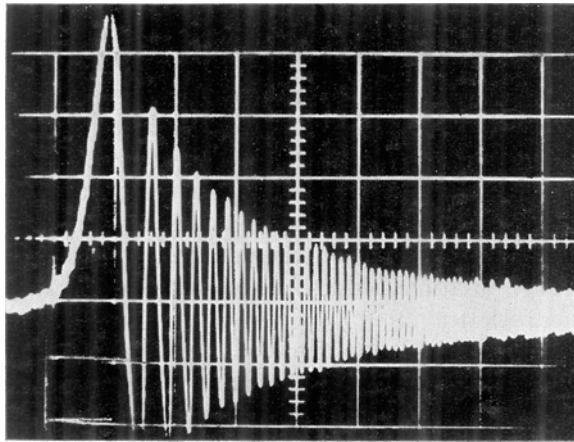


Fig. 2. Oscilloscope trace of a rapidly traversed single nuclear magnetic resonance line. The exponential decay of the transverse component of magnetization can be followed by the decay of the amplitude of the beats between the magnetization vector and the oscillating radiation field (the "wiggles").

The relaxation time  $T_2$  can be calculated from the half-time of the wiggle decay  $T_{1/2}$  (Fig. 2) obtained from a semi-logarithmic plot of amplitude vs. time, using the relationship

$$T_2 = 0.693/T_{1/2} \quad (4)$$

An alternative measurement of  $T_2$  (and indirectly of  $T_1$ , if it is known that  $T_1 = T_2$ ) is from the line width in a high resolution spectrum, owing to the relationship (see p. 273 of ref. 10)

$$\Delta\nu_{1/2} = 1/\pi T_2 \quad (5)$$

where  $\Delta\nu_{1/2}$  is the width at half height.

### B. The Interpretation of Relaxation Times ( $T_1$ and $T_2$ ) in Terms of Molecular Events

The principal mechanism of relaxation involves the interaction of the nuclear magnetic moment with a magnetic field periodically varying at a frequency  $\omega_{\alpha\beta}$ . In the case of spin-spin relaxation this field originates from other nuclei in the spin system. In the case of spin-lattice relaxation the field may originate from any of the following sources:

- (1) magnetic moments of other nuclei (of the same, as well as of other spin systems);
- (2) magnetic moments of unpaired electrons;
- (3) asymmetric distributions of electronic charges, giving rise to diamagnetic anisotropy.

The local fields arising from other magnetic particles may be of two kinds: (a) those representing direct coupling of magnetic dipoles, and (b) those representing indirect (scalar, electron transmitted) coupling. In addition, nuclei possessing an electric quadrupole moment (see p. 333 of ref. 10) can be relaxed by periodically varying inhomogeneous electric fields, such as are found in the asymmetric distribution of electronic charge in most molecules. Since protons have no quadrupole moment, this mechanism is of importance in proton resonance spectroscopy only because of the possibility of scalar coupling (see below) of a proton to another nucleus, such as  $^{14}\text{N}$ , which is undergoing quadrupolar relaxation.

The periodic variation of the fields arising from nuclei in the *same* spin system results from the precession of their magnetic moments

in the external field. On the other hand, the periodic variation of the *lattice* fields arises from the random motion of the relaxing nucleus and the source of the field relative to each other through either rotational or translational diffusion, internal rotation of the molecules, or collisions involving chemical exchange.

The mathematical problem of calculating the relaxation time in terms of the time-dependent local fields consists of (1) relating the relaxation time to the probability of the transition  $\beta \rightarrow \alpha$  produced by the local fields and (2) expressing the transition probability in terms of the intensity of the component of the local field which varies with frequency  $\omega_{\alpha\beta}$ , since this is the only component which can produce the transition  $\beta \rightarrow \alpha$ . In detail the calculation is based on the following series of arguments:

(1) The relaxation rate,  $1/T$ , of a spin system undergoing excitation from a given energy level  $\alpha$  is taken as the sum of the transition probabilities  $W_{\alpha\beta}$  between  $\alpha$  and any other energy level  $\beta$ .<sup>1, 2, 3</sup> For a two-level spin system we thus have

$$1/T_1 = W_{\alpha\beta} \quad (6)$$

where  $W_{\alpha\beta}$  is the transition probability (number of transitions  $\beta \rightarrow \alpha$  per unit time) between the two levels  $\alpha$  and  $\beta$ , defined with respect to the stationary field  $H$ .

(2) The transition probability  $W_{\alpha\beta}$  is calculated by the methods of radiation theory<sup>1, 4</sup> from the time-dependent Hamiltonian expressing the interaction of the spin system with the varying local fields, using the relation

$$W_{\alpha\beta} = |(\beta|\mathcal{H}(t)|\alpha)|^2 \quad (7)$$

In the theory of relaxation as applied to liquids—the only case under discussion here—the motion giving rise to relaxation processes is rotational and translational diffusion (often referred to as Brownian motion), which has a random character. The time-dependent Hamiltonian is therefore taken to be a random function of time. It is usually possible to separate the Hamiltonian into an *operator* part  $\mathcal{H}'$  (containing the appropriate atomic constants and spin operators) and a time dependent part expressing the random changes of coordinates in time. This is expressed by setting

$$\mathcal{H}(t) = \mathcal{H}' F(t) \quad (8)$$

where  $F(t)$  is a *random* function of time.

The spectral density of such a random function, which is proportional to the intensity of the randomly varying field, is given, according to the Wiener-Khinchin theorem, by the Fourier transform of the correlation function  $g(\tau)$  of the random function, where

$$g(\tau) = \overline{F(t)F^*(t+\tau)} \quad (9)$$

the average being taken over all possible values of  $F(t)$ . The intensity of the component varying with frequency  $\omega_{\alpha\beta}$  is therefore given by

$$J(\omega_{\alpha\beta}) = \int_{-\infty}^{\infty} g(\tau) \exp(-i\omega_{\alpha\beta}\tau) d\tau \quad (10)$$

And the transition probability  $W_{\alpha\beta}$  can be expressed as

$$W_{\alpha\beta} = (\alpha|\mathcal{H}'|\beta)^2 J(\omega_{\alpha\beta}) \quad (11)$$

In the calculations it is generally assumed that the correlation function of  $F(t)$  is exponential, with a characteristic time constant, the "correlation time"  $\tau_c$ ,\* i.e.

$$g(\tau) = \overline{F(t)F^*(t)} \exp(-t/\tau_c) \quad (12)$$

This form of the correlation function takes into account the principal property of the random processes involved, i.e. the probability of finding the system in a state close to its initial state (at an arbitrarily chosen instant) decreases as the time interval following that instant increases. The correlation time  $\tau_c$  can then be understood as a crude measure of the time interval during which any two spins in the system maintain a given orientation with respect to each other.

A plot of the spectral density  $J(\omega)$  as a function of the correlation time is shown in Fig. 3.

(3) The interaction Hamiltonian  $\mathcal{H}_i$  for any spin  $i$  in the system with the surrounding local fields is given by

$$\mathcal{H}_i(t) = \mathcal{H}_i^D(t) + \mathcal{H}_i^S(t) + \mathcal{H}_i^A(t) \quad (13)$$

$$\text{with} \quad \mathcal{H}_i^D = \sum_j \frac{\hbar}{r_{ij}^3} \gamma_i \gamma_j \left[ \mathbf{I}_i \cdot \mathbf{I}_j - 3 \frac{(\mathbf{I}_i \cdot \mathbf{r}_{ij})(\mathbf{I}_j \cdot \mathbf{r}_{ij})}{r_{ij}^2} \right] \quad (14a)$$

\* In the case of diffusion this form of the correlation function arises from the assumption that the molecular motion can be described by the diffusion equation.

being the Hamiltonian for the direct dipolar interaction

$$\mathcal{H}_i^S = \sum_j J_{ji} \mathbf{I}_i \cdot \mathbf{I} \quad (14b)$$

the Hamiltonian for indirect scalar spin coupling and

$$\mathcal{H}_i^A = -\gamma_i \mathbf{H} \cdot \mathcal{A} \cdot \mathbf{I}_i \quad (14c)$$

the Hamiltonian for anisotropic chemical shifts.  $\gamma_i$  is the gyro-

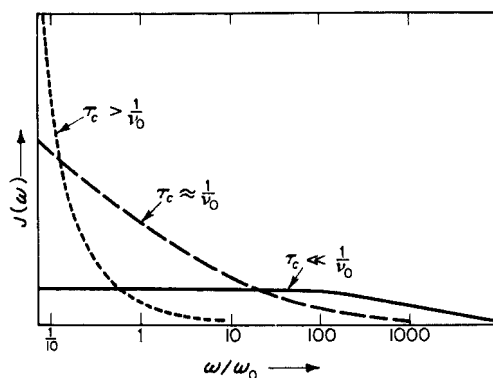


Fig. 3. The frequency spectrum  $J(\omega)$  as a function of the correlation time. Abscissa: frequency; ordinate: intensity of the Fourier component of frequency  $\omega$ . It is apparent that the intensity is high for frequencies  $\nu > 1/\tau_c$ , and low for  $\nu' < 1/\tau_c$  so that correlation times long compared with the Larmor frequency are more efficient in producing relaxation.

magnetic ratio of spin  $i$ ,  $\gamma_j$  that of (either nuclear or electronic) spin  $j$ ,  $r_{ij}$  the distance between spins,  $\mathbf{I}_i$  and  $\mathbf{I}_j$  their respective spin vectors,  $J_{ij}$  the spin coupling constant,  $\mathcal{A}$  the anisotropy tensor and  $\mathbf{H}$  the external magnetic field.

All coordinates are understood to be random functions of time, so that the operator and time-dependent parts of the dipolar Hamiltonian can be written respectively as:

$$\mathcal{H}^{(0)} = -\frac{3}{2}\gamma_i\gamma_j\hbar\left\{-\frac{2}{3}I_{iz}I_{jz} + \frac{1}{6}(I_{i+}I_{j-} + I_{i-}I_{j+})\right\}$$

$$\mathcal{H}^{(1)} = -\frac{3}{2}\gamma_i\gamma_j\hbar\{I_{iz}I_{j+} + I_{i+}I_{jz}\}$$

$$\mathcal{H}^{(2)} = -\frac{3}{4}\gamma_i\gamma_j\hbar I_{i+}I_{j+}$$

and

$$F^{(0)} = \frac{1 - 3 \cos^2 \theta_{ij}}{r_{ij}^3}$$

$$F^{(1)} = \frac{\sin \theta_{ij} \cos \theta_{ij} \exp(-i\varphi_{ij})}{r_{ij}^3}$$

$$F^{(2)} = \frac{\sin^2 \theta_{ij} \exp(-2i\varphi_{ij})}{r_{ij}^3}$$

where  $I_{\pm} = I_x \pm iI_y$ , the subscripts  $x, y, z$  denoting the Cartesian components of the spin vectors in a coordinate system in which the  $z$  axis is defined by the direction of the stationary magnetic field.  $\theta_{ij}$ ,  $\varphi_{ij}$  and  $r_{ij}$  are the spherical polar coordinates of nucleus  $j$  relative to nucleus  $i$ .

A similar separation is made for expressions (14b) and (14c). Inasmuch as the present discussion is confined to proton resonance in liquids, additional terms in the total Hamiltonian, accounting for interaction with (a) external magnetic fields, (b) the magnetic field resulting from molecular rotation, and (c) quadrupolar interaction, can be omitted.

For purposes of detailed calculation it is convenient to distinguish individual terms in the Hamiltonian Eq. (14a) by the origin of the time dependent fields. Thus the dipolar Hamiltonian can be separated into terms representing interactions with (a) nuclei of the same chemical species and (b) nuclei of other chemical species or unpaired electrons. Similarly, the scalar Hamiltonian (14b) can be considered in two parts, corresponding to a time dependence of the coupling constant (scalar relaxation of the first kind) or of the spin  $I_j$  (scalar relaxation of the second kind).

Two additional assumptions are usually made in the calculation of relaxation times:

(1) That the relative motion of any particle in the spin system and any other particle (or source of field, such as a magnetically anisotropic molecule) is entirely uncorrelated. This assumption is not strictly valid for any two particles on the same molecule, since their motions are correlated in so far as the molecule behaves as a rigid body. Calculations for three- and four-spins whose motions are correlated, carried out by Hubbard,<sup>9</sup> lead to a system of equations in which the relaxation process can no longer be described by a

single exponential. However, the deviation from a single exponential is sufficiently small (of the order of  $< 1\%$ ), so that the assumption of completely uncorrelated random motion adequately describes the processes occurring in the liquid state; and

(2) That the relaxation processes occur over a time very long compared to the Larmor period  $\omega_{\alpha\beta}$ . This condition is satisfied in all the cases to be discussed here (relaxation times of the order of 0.1–10 sec, Larmor periods  $10^{-8}$  sec).

Term-by-term calculation of the transition probabilities yields the following set of equations for the relaxation rates of a given nucleus by *any one other individual nucleus, electron or field*.

$$\begin{aligned}\left(\frac{1}{T_1}\right)_i &= \left(\frac{1}{T_1}\right)_{DL} + \left(\frac{1}{T_1}\right)_{DU} + \left(\frac{1}{T_1}\right)_S + \left(\frac{1}{T_1}\right)_\sigma \\ \left(\frac{1}{T_2}\right)_i &= \left(\frac{1}{T_2}\right)_{DL} + \left(\frac{1}{T_2}\right)_{DU} + \left(\frac{1}{T_2}\right)_S + \left(\frac{1}{T_2}\right)_\sigma\end{aligned}\quad (15)$$

where

$$\begin{aligned}\left(\frac{1}{T_1}\right)_{DL} &= \frac{3}{2}\gamma_i^4 \hbar^2 I_i(I_i+1) \{J^{(1)}(\omega_i) + J^{(2)}(2\omega_i)\} \\ \left(\frac{1}{T_1}\right)_{DU} &= \gamma_i^2 \gamma_j^2 \hbar^2 I_j(I_j+1) \left\{ \frac{1}{12} J^{(0)}(\omega_i - \omega_j) + \frac{3}{2} J^{(1)}(\omega_i) \right. \\ &\quad \left. + \frac{3}{4} J^{(2)}(\omega_i + \omega_j) \right\} \\ \left(\frac{1}{T_1}\right)_S &= \frac{1}{3} J_{ij}^2 I_j(I_j+1) J(\omega_i - \omega_j) \\ \left(\frac{1}{T_1}\right)_\sigma &= \frac{6}{45} \gamma_i^2 H^2 \delta_z^2 \left(1 + \frac{\eta^2}{3}\right) J(\omega_i) \\ \left(\frac{1}{T_2}\right)_{DL} &= \gamma_i^4 \hbar^2 I_i(I_i+1) \left\{ \frac{3}{8} J^{(0)}(0) + \frac{1}{4} J^{(1)}(\omega_i) + \frac{3}{8} J^{(2)}(2\omega_i) \right\} \\ \left(\frac{1}{T_2}\right)_{DU} &= \gamma_i^2 \gamma_j^2 \hbar^2 I_j(I_j+1) \left\{ \frac{1}{6} J^{(0)}(0) + \frac{1}{24} J^{(0)}(\omega_i - \omega_j) + \frac{3}{4} J^{(1)}(\omega_i) \right. \\ &\quad \left. + \frac{3}{2} J^{(1)}(\omega_j) + \frac{3}{8} J^{(2)}(\omega_i + \omega_j) \right\} \\ \left(\frac{1}{T_2}\right)_S &= \frac{1}{6} J_{ij}^2 I_j(I_j+1) \{J(0) + J(\omega_i - \omega_j)\} \\ \left(\frac{1}{T_2}\right)_\sigma &= \frac{1}{45} \gamma_i^2 H^2 \delta_z^2 \left(1 + \frac{\eta^2}{3}\right) \{4J(0) + 3J(\omega_i)\}\end{aligned}$$



and

$$J(\omega) = \frac{2\tau_c}{1 + \omega^2 \tau_c^2}$$

$$J^k(\omega) = |F^{(k)}|^2 \frac{2\tau_c}{1 + \omega^2 \tau_c^2}$$

with  $k = 0, 1, 2$ . The subscripts denote the individual contributions, as follows:  $DL$ , dipolar contribution of like nuclei;  $DU$ , dipolar contribution of unlike nuclei or electrons;  $S$ , scalar coupling contribution;  $\sigma$ , contribution of fields arising from the magnetic anisotropy of the molecule,  $\delta_z$  being the anisotropy shift and  $\eta$  a geometrical parameter;  $\omega = \omega_i = \omega_{\alpha\beta}$ ,  $\omega_i \pm \omega_j$ , or  $2\omega_i$ , as the case may be.

### C. Simplifications of the Theory Applicable to High Resolution Proton Magnetic Resonance

If attention is confined to relaxation processes as they occur under the conditions of conventional high resolution proton magnetic resonance spectroscopy (30–100 Mc, fields of 7000–24,000 gauss), Eq. (15) and the interpretation of the corresponding experiments is considerably simplified by several additional considerations:

(1) The “extreme narrowing approximation”, i.e.  $\tau_c \ll 1/\omega_{\alpha\beta}$  is applicable under most circumstances for dipole–dipole interactions. This becomes apparent if one calculates the line widths predicted from Eqs. (5) and (15), which are of the order of 100 cps (using correlation times  $\tau_c \approx 10^{-8}$  sec) and considerably greater than is consistent with a high resolution spectrum with shifts of the order of 10–100 cps.

(2) The contribution of the scalar coupling terms to  $T_1$  is negligible.

(3) Dipolar relaxation by nuclei other than protons can be neglected, except for single protons directly bonded to  $^{14}\text{N}$ . This becomes apparent by comparing the figures in Table I.

(4) The nonequivalence of protons which is due to chemical shifts can also be neglected, so that proton–proton relaxation may be treated as relaxation by “like spins”.

(5) The contributions of unpaired electrons located on the same molecule need not be taken into account, since the relaxation

TABLE I. The Relative Magnitude of Dipolar Relaxation Terms for Protons Relaxed by Different Nuclei

$$(1/T_1)_p = C(\tau_e/r^6), \tau \text{ in sec, } r \text{ in Angstroms}$$

For protons relaxed by	C
H	$88.5 \times 10^{10}$
D	$1.31 \times 10^{10}$
$^{14}\text{N}$	$0.29 \times 10^{10}$
$^{23}\text{Na}$	$3.91 \times 10^{10}$
$^{31}\text{P}$	$9.18 \times 10^{10}$
$^{35}\text{Cl}$	$0.54 \times 10^{10}$
$^{39}\text{K}$	$0.12 \times 10^{10}$

caused by them would lead to a broadening of the spectrum beyond detection. This is not true, on the other hand, of relaxation by paramagnetic species elsewhere in the solution. In fact, the presence of such species must be carefully eliminated before any interpretation is attempted.

With these simplifications the equations on which the interpretation of relaxation measurements in high resolution proton resonance spectra rests can be written in the following form (taking the sums over all possible interactions)

$$\left(\frac{1}{T_1}\right)_i = \left(\frac{1}{T_1}\right)_{\rho_i} + \left(\frac{1}{T_1}\right)_{D_i} + \left(\frac{1}{T_1}\right)_{E_i} + \left(\frac{1}{T_1}\right)_{\sigma_i} \quad (16)$$

$$\left(\frac{1}{T_2}\right)_i = \left(\frac{1}{T_2}\right)_{\rho_i} + \left(\frac{1}{T_2}\right)_{D_i} + \left(\frac{1}{T_2}\right)_{E_i} + \left(\frac{1}{T_2}\right)_{\sigma_i} + \left(\frac{1}{T_2}\right)_{S_i} + \left(\frac{1}{T_2}\right)_{S'_i} + \frac{\gamma_i}{2\pi} \Delta H$$

where

$$\begin{aligned} \left(\frac{1}{T_1}\right)_{\rho_i} &= \left(\frac{1}{T_2}\right)_{\rho_i} \cong \frac{3}{2} \gamma^4 \hbar^2 \sum_j \frac{\tau_{ij}}{\langle r_{ij} \rangle^6} \\ \left(\frac{1}{T_1}\right)_{D_i} &= \left(\frac{1}{T_2}\right)_{D_i} \cong \frac{1}{5} \pi \gamma^4 \hbar^2 \frac{N_k}{\langle r_{ik} \rangle D_{ik}} \\ \left(\frac{1}{T_1}\right)_{E_i} &= \left(\frac{1}{T_2}\right)_{E_i} \cong 3 \gamma^2 \sum_l \frac{\langle \mu_{\text{eff}} \rangle^2}{\langle r_{il} \rangle^3} N_l \tau_{il} \end{aligned}$$

$$\left(\frac{1}{T_1}\right)_{\sigma_i} \cong \frac{3}{20} \gamma^2 H^2 \delta_z^2 \left(1 + \frac{\eta^2}{3}\right) \tau_\rho$$

$$\left(\frac{1}{T_2}\right)_{\sigma_i} \cong \frac{7}{40} \gamma^2 H^2 \delta_z^2 \left(1 + \frac{\eta^2}{3}\right) \tau_\rho$$

$$\left(\frac{1}{T_2}\right)_{S'_i} \cong \frac{1}{3} \sum_m J_{im} I_m (I_m + 1) \tau_e$$

$$\text{and} \quad \left(\frac{1}{T_2}\right)_{S''_i} \cong \frac{1}{3} \sum_n J_{in} I_n (I_n + 1) \tau_{in}$$

The individual terms are denoted by subscripts as follows:  $\rho$  intramolecular contribution, resulting from rotational diffusion;  $D$ , intermolecular contribution, resulting from the translational diffusion of two molecules with respect to each other, with a diffusion coefficient  $D_{ik}$ ;  $E$ , contribution of paramagnetic species in solution;  $\sigma$  and  $S$  as above [Eq. (15)], distinguishing between scalar relaxation of the first ( $S'$ ) and second kind ( $S''$ ).  $\gamma$  is the gyromagnetic ratio of protons,  $\langle r_{ij} \rangle$ ,  $\langle r_{ik} \rangle$ ,  $\langle r_{il} \rangle$  are the time average distances of particles  $i$  and  $j$ ,  $k$  or  $l$  respectively,  $\tau_{ij}$ ,  $\tau_{ik}$ ,  $\tau_{il}$  the corresponding correlation times;  $N_k$  and  $N_l$  are the concentrations of protons  $k$  and paramagnetic particles  $l$  respectively,  $\langle \mu_{\text{eff}} \rangle$  the average effective magnetic moment of the paramagnetic species. The correlation time of proton  $i$  with an anisotropic magnetic field is denoted by  $\tau_\rho$  and the lifetime of an exchanging species  $m$  as  $\tau_e$ .  $\Delta H$  is the inhomogeneity of the applied magnetic field  $H$ , and other symbols are as defined above. Equation (16) is a generalization of the equations proposed by Gutowsky and Woessner<sup>8,13,20</sup> *with the significant difference that different correlation times are assumed for different pairs of nuclei and the internuclear distances are averaged over time.* The generalization is made necessary by the fact that an *a priori* calculation of relaxation rates for non-rigid molecules from a single correlation time (obtained from a  $T_1$  and  $T_2$  measurement on one of the lines in the spectrum) and the known internuclear distances for a single rigid configuration leads to a relatively poor agreement with experimentally measured values. This fact is illustrated by the data in Table II, indicating that in the case of non-rigid molecules rotation of one part of the molecule with respect to another makes a significant contribution to the relaxation process.

TABLE II. Measured and Calculated Relaxation Rates for Non-rigid Molecules<sup>a</sup> (in sec<sup>-1</sup>)

Compound	1/T <sub>1</sub> (obs.)	1/T <sub>1</sub> (calc.)
<i>Mesitylene</i>		
Ring <sup>+</sup>	0.024	0.024
CH <sub>3</sub>	0.094	0.129
<i>Penicillin</i>		
Phenyl	0.63	0.45
H <sub>(10)</sub> H' <sub>(14)</sub> <sup>+</sup>	0.4	0.40
H <sub>(5)</sub>	0.78	0.56
H <sub>(18)</sub>	2.8	0.80
CH <sub>3</sub>	0.6	1.20
<i>Uridylic acid</i>		
H <sub>(4)</sub>	0.3	0.45
H <sub>(5)</sub>	0.4	0.52
H' <sub>(1)</sub> <sup>+</sup>	0.4	0.40
H' <sub>(6)</sub>	0.6	0.65
<i>Polyuridylic acid</i> <sup>b</sup>		
H <sub>(4)</sub>	2.2	450.0
H <sub>(5)</sub>	2.8	520.0
H' <sub>(1)</sub>	2.8	400.0
H' <sub>(6)</sub>	3.0	650.0

<sup>a</sup> The measured values are extrapolated to infinite dilution. The calculated values are for a rigid molecule approximation, using known interatomic distances and a single value of the correlation time obtained from one of the peaks on the spectrum (marked +).

<sup>b</sup> The correlation time for the polyuridylic acid molecule (rigid model) is taken as roughly 10<sup>3</sup> × correlation time for uridylic acid (for a chain of 100 uridylic acid residues).

The use of Eq. (16) allows the analysis of relaxation time measurements in terms of a *selective* change of the correlation time. *Such a selective change will result from the stabilization of one part of a non-rigid molecule by its participation in the formation of a molecular complex, since the motion of the bound part will be restricted to a different extent than will be the motion of the remaining parts of the molecule.* The detailed experimental procedure for obtaining useful information from this type of study depends to a large extent

on the individual problem, but certain general features can be specified, as is done in the following section.

#### D. Interpretation of Relaxation Measurements in Terms of Molecular Interactions

It is apparent from the considerations discussed in the preceding sections that a selective change of correlation times will always manifest itself as a selective change of the rotational contribution to the relaxation times, i.e.  $(T_1)_\rho$  and  $(T_2)_\rho$ . A demonstration of such a *selective change in  $(T_1)_\rho$  or  $(T_2)_\rho$*  can therefore be taken as evidence for a preferential stabilization and hence for the direct participation of a portion of a molecule in the formation of a molecular complex. The interpretation of a selective change in the *measured* relaxation time  $(T_1)$  or  $(T_2)$  in terms of a molecular interaction hinges however on (1) the exclusion of other terms which could potentially contribute to this change, such as  $(T_1)_\sigma$ ,  $(T_2)_E$ , etc., and (2) on the demonstration of the extent (if any) to which changes in the average internuclear distance affect the measurements.

It is apparent from Eq. (16) that a change in  $T_1$  is easier to interpret in terms of a change of  $(T_1)_\rho$  than is a corresponding change in  $T_2$  (although the latter is easier to observe as a broadening of the absorption line), both since the scalar relaxation terms are small and since the inhomogeneity of the external magnetic field does not enter into the measurement. In the experiments to be described in the following section the interpretation has therefore been based mostly on  $T_1$  measurements, although line broadening has been found to be a useful indicator when scanning the spectrum in search of the effect. To obtain an estimate of  $(T_1)_\rho$ , the measured  $T_1$  values must be corrected for intermolecular contributions by extrapolating them to infinite dilution in a deuterated solvent, thus eliminating intermolecular terms arising from solute-solute and solute-solvent interactions respectively (neglecting the small contribution to the proton relaxation by deuterons, cf. Table I). The diamagnetic anisotropy term  $(T_1)_\sigma$  can be evaluated by carrying out relaxation measurements at two different field strengths (e.g. 60 and 15.9 Mc corresponding to *ca.* 14,000 and 3700 gauss for protons). Most difficult to eliminate is the paramagnetic term  $(T_1)_E$  which can give rise to measurable proton relaxation effects even in the absence of

any directly detectable paramagnetism. In most cases, it is possible, however, to make reasonably certain that the system in question is free of paramagnetic impurities, including oxygen, and to rely on the fact that the effects of such impurities on the relaxation times will be non-selective in the absence of specific complex formation involving the paramagnetic species, so that their presence could be detected by a change in the relaxation time of the solvent. The problem of interpreting a given change in  $(T_1)_\rho$  in terms of a change of correlation times or a change of internuclear distances is considerably simplified by the fact that the dominant contribution to the relaxation rate of any given proton arises from its nearest neighbors, as can be readily verified by order of magnitude calculations. It is therefore only in the case of groupings such as  $R_2CH-CHR'_2$  that the proton relaxation time can be varied by a factor of 7 by rotation around the C—C bond from a *cis* to a *trans* orientation of the two protons. In contrast for groups such as  $CH_2$ ,

$CH_3$ ,  $H \text{---} \text{C}_6\text{H}_5$ , with a fixed distance to the nearest neighbor, the effect of changing the distance to the next nearest neighbor on the relaxation time is much smaller. This fact is illustrated in Table III, for the cases of  $R_2CH-CHR'_2$ ,  $R_2CH-CH_2R'$ , and  $R_2CH-CH_3$ . Although an *a priori* calculation of the various contributions to the relaxation rate—and of their variations with changes in conformation—on every molecule under study is essential for interpretation, in many cases it is found that the total contribution of more distant nuclei to the sum of Eq. (16) does not exceed a few percent.

In several of the cases which have been studied it was possible to infer from the unchanged values of shifts and coupling constants after complex formation that no change of conformation, and hence no change of internuclear distances, had occurred. In these cases the relaxation rates before and after complexing for any two groups *A* and *B* can be written

$$\begin{aligned} \left(\frac{1}{T_1}\right)_{\rho A} &= K_A \tau_A & \left(\frac{1}{T_1}\right)_{\rho B} &= K_B \tau_B \\ \left(\frac{1}{T_1}\right)'_{\rho A} &= K_A \tau'_A & \left(\frac{1}{T_1}\right)'_{\rho B} &= K_B \tau'_B \end{aligned} \quad (17)$$

TABLE III. Proton Relaxation Rates as Functions of the Dihedral Angle between the H—C—C and C—C—H Planes

$$\frac{1}{T_1} = \sum_j C \frac{\tau_c}{r_{ij}^6} = C_\phi \tau_c^a$$

$\phi$	$R_2CH-CHR'_2$ $C_\phi \times 10^9$	$R_2CH-CH_2R'$ $C_\phi \times 10^9$	$R_2CH-CH_3$ $C_\phi \times 10^9$
0°	6.91	18.41	29.91
30°	5.85	17.35	28.85
60°	3.88	15.38	26.88
90°	2.41	13.91	25.41
120°	1.58	13.08	24.58
150°	1.21	12.71	24.21
180°	1.10	12.60	24.10

<sup>a</sup> Assuming the same correlation time for all protons.

where  $K_A$  and  $K_B$  are numerical factors including the appropriate internuclear distances, and primes denote the relaxation and correlation times in the complex, as compared to the unprimed free species, so that if

$$\tau'_A/\tau_A > \tau'_B/\tau_B$$

the relaxation time (and in these cases the corresponding line widths) obey the relation

$$(T_{1A}/T'_{1A})/(T'_{1B}/T_{1B}) > 1 \quad (18)$$

and the line originating from the group stabilized by molecular interaction shows selective broadening. Examples of this type are discussed in the following section, but in general it must be borne in mind that the application of the simple relations [Eq. (17)] to derive information on the group stabilized by molecular interactions must be justified by corollary evidence that the contributions of changes in internuclear distances are negligible. If more than a single correlation time determines the relaxation rate of a given group, or if there is a change of interproton distances, Eq. (16) must be solved in detail to obtain the desired information. In principle,

this is possible by making relaxation measurements on a series of deuterium-substituted analogs and thus obtaining the contribution of each individual proton to the relaxation rate of any other proton.

### III. EXPERIMENTAL

#### A. Interactions between Small Molecules

A case which has been studied by this method in detail is the weak complex formed by catecholamines with nucleotides.<sup>18,19</sup> This complex has been thought to be the storage form of catecholamines in the chromaffin granules of the adrenal medulla.<sup>17</sup> Its structure is therefore of biological as well as chemical interest. The simplicity of the multiplet structure and the magnitude of the spin coupling constants in the high resolution spectra of epinephrine and its analogs indicate that there is free rotation about all bonds in the aliphatic side-chain and make it possible to pose the question as to which portion of the molecule is involved in the formation of the complex. The fact that the multiplet structure and the magnitude of coupling constants in the high resolution spectrum of the complex is preserved (Fig. 4) suggests that there is no restriction of internal rotation within the side-chain as a result of complexing. It is therefore permissible to assume, as a first approximation: (1) that the observed decrease in relaxation times reflects a restriction of the motion of the side-chain as a whole, and (2) that there is no change in the internuclear distances in the dominant terms of Eq. (16) so that Eq. (17) will apply. One would therefore expect one of the following results: (a) a relative decrease in the relaxation times of the ring as compared to that of the side-chain, if the ring but not the side-chain took part in the formation of the complex, (b) a relative decrease in the relaxation times of the side-chain, if the reverse were the case, and (c) no selective change if both the ring and the side-chain (or neither) were involved.

The result apparent from Fig. 4 is that there is a more pronounced broadening of the side-chains than of the peaks arising from the aromatic ring, suggesting a larger change of  $T_2$  (perhaps accompanied by a change of  $T_1$ ) in the former. An interpretation of this broadening in terms of molecular events is, however, ambiguous, as may be seen from Eq. (16). For this reason  $T_1$  measurements were carried out, following the procedure outlined at the close of the



preceding section. The measurements were carried out at two field intensities (rf frequencies of 40 Mc and 60 Mc), to evaluate the field-dependent contribution of the diamagnetic anisotropy term  $(1/T_1)_\sigma$ . All measurements were extrapolated to infinite dilution in  $D_2O$  as shown in Fig. 5 for the uncomplexed species, in order to correct

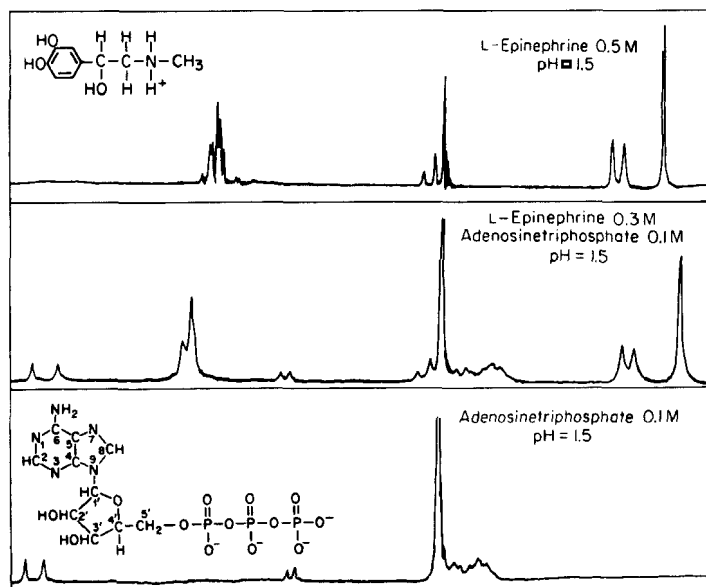


Fig. 4. Proton magnetic resonance spectra of epinephrine, ATP and the 1:1 epinephrine-ATP complex in  $D_2O$ .

for the intermolecular contributions. The extrapolated values, summarized in Table IV, were taken as a crude measure of  $(1/T_1)_p$ , since measurements at two field strengths indicated that there was no measurable contribution of  $(1/T_1)$  and the long relaxation time of the solvent ruled out a contamination with paramagnetic species. From these values it is apparent that: (1) there is a greater decrease in the relaxation times of the side-chain protons than of either the ring or the methyl protons, and (2) that the decrease of  $T_1$  and  $T_2$  is proportional, indicating that the broadening of the  $CH-CH_2$  lines is not to be attributed to a scalar coupling to the  $^{14}N$  nucleus. A mechanism of this type could have given rise to a selective change of  $T_2$  if the electron cloud about the  $^{14}N$  nucleus were appreciably



distorted by the formation of the complex. No evidence for such an effect was found, however, in a double resonance experiment (irradiating the  $^{14}\text{N}$  nucleus while observing the proton spectrum): the proton line width remained unchanged. It therefore appears reasonable to assume that the measured values of  $T_1$  and  $T_2$  reflect primarily a change in the rotational correlation times and thus indicate a greater restriction of motion in the epinephrine side-chain. This can be interpreted to mean that *the side-chain, but not*

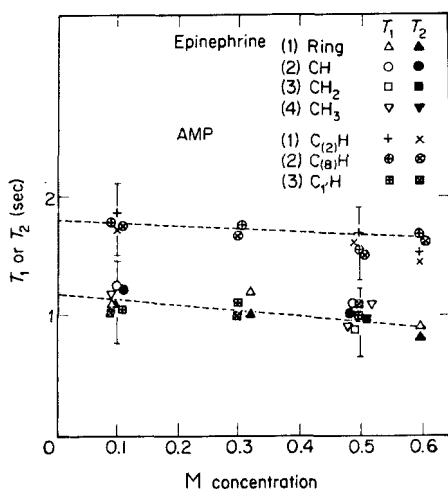


Fig. 5. Extrapolation of relaxation times to infinite dilution in  $\text{D}_2\text{O}$ .

*the ring, is involved in the formation of a complex.* No similar selective change in the relaxation time is found in the proton magnetic resonance spectrum of the nucleotide, as would be expected if the phosphate group alone were involved in the complex. A confirmation of this inference by  $^{31}\text{P}$  resonance would be of great interest.

The relative decrease in the relaxation time of the epinephrine side-chain is a function of the epinephrine to nucleotide ratio in the solution, as shown in Fig. 6. The change is small if epinephrine is in excess and maximal if there is an excess of nucleotide. This finding also indicates that the exchange between the free and complexed species is rapid, so that the observed relaxation times are an average

of the relaxation times for the two forms. In the case of slow exchange one would have expected the sharp peaks of the free species to be superimposed on the broad peaks of the complex (since no shifts were found) and in the intermediate range of exchange rates additional broadening by a  $T_2$  mechanism would have resulted from the exchange process, making  $T_2 \neq T_1$ . This however was not found to be the case.

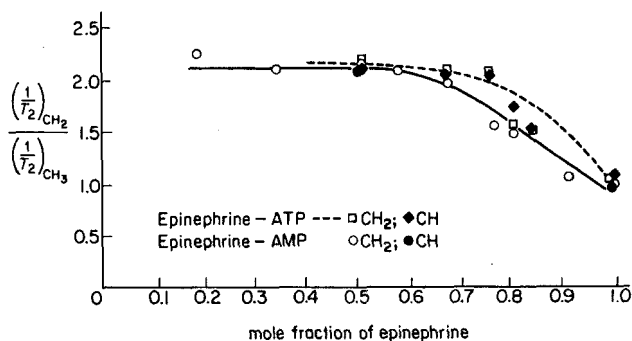


Fig. 6. Plot of the relative increment in relaxation time [Eq. (18)] for the  $CH_2$  and  $CH_3$  groups of epinephrine as functions of the mole fraction of epinephrine in the complex.

The conclusion that the epinephrine-nucleotide complex involves specifically the attachment of the catecholamine side-chain to (probably) the phosphate of the nucleotide is further corroborated by the temperature dependence of the relaxation time, shown in Fig. 7. While the relaxation times of the methyl group, the ring protons of either epinephrine or adenine and of the ribose protons change only slightly with temperature, the relaxation times of the CH and  $CH_2$  protons of the side-chain show a more pronounced change. This, taken together with the fact that the relaxation times of the  $CH_2$  and  $CH_3$  groups are nearly equal at higher temperatures as they are in the free catecholamine, strongly indicates that the complex does not form at higher temperatures.

It may be seen from the preceding example that although experiments of this type are crude at the present stage of development as compared to the theoretically possible refinement, they can yield some interesting information. Especially interesting is the fact that

changes of relaxation times were found in the absence of any shifts or changes of coupling constants, indicating that relaxation processes more readily reflect subtle changes in the state of the molecules. The difficulties encountered at present arise primarily from the inaccuracies of evaluating  $T_1$  or  $T_2$  at low concentrations (0.001 to 0.01 M) and of measuring  $T_1$  of individual lines separated by less than 10 cps. Also, the direct measurement of very short relaxation

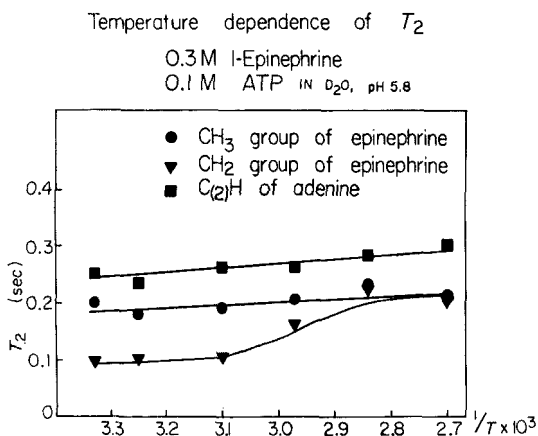


Fig. 7. The temperature dependence of the relaxation times in the epinephrine-ATP complex as functions of temperature.

times ( $< 0.1$  sec) is not readily possible on conventional high-resolution equipment. For these reasons extensive checks on the reproducibility of the measurements are imperative and small differences in the measured values must be accepted with extreme caution.

### B. The Binding of Small Molecules to Macromolecules

The method of relaxation times can also be used to derive some interesting information on the binding of small molecules to macromolecules. In the cases of protein binding investigated so far the protein spectrum consists of four to nine very broad peaks (line widths of 50–80 cps) and forms an uninformative background on

which the high resolution spectrum of the small molecules is superimposed. Differential broadening of one (or more) peak(s) as compared to others gives an indication that the portion of the molecule from which the peak originates is more affected by the interaction with the protein than the remainder of the molecule.

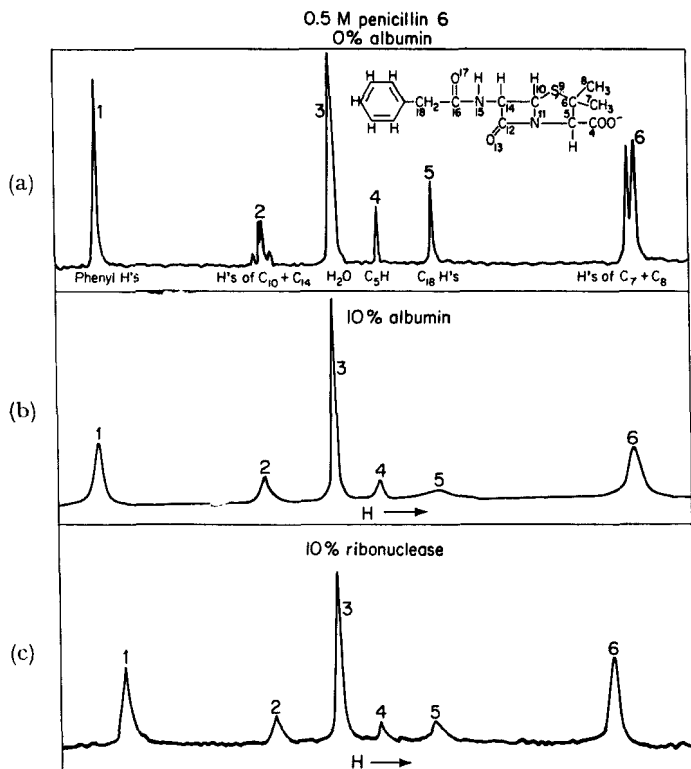


Fig. 8. The spectra of penicillin G (a) in  $D_2O$ , (b) in  $D_2O$  in the presence of 10% BSA, (c) in  $D_2O$  in the presence of 10% ribonuclease.

An effect of this type is shown in Fig. 8 for the system penicillin G-bovine serum albumin (BSA).<sup>5,6,7,13</sup> It is seen that peak number 5, arising from the benzyl methylene group, is broadened more than the remainder of the peaks. At concentrations of  $5 \times 10^{-3}M$  penicillin and  $5 \times 10^{-4}M$  BSA, peak number 5 is broadened beyond detection, although all other peaks remain

clearly defined. The effect is specific for the protein insofar as it is not observed with ribonuclease (Fig. 8c).

To interpret these findings quantitatively in terms of a preferential stabilization of one portion of the penicillin molecule relative to another, it is necessary to compare the relaxation rates of different penicillin peaks in the presence and in the absence of the

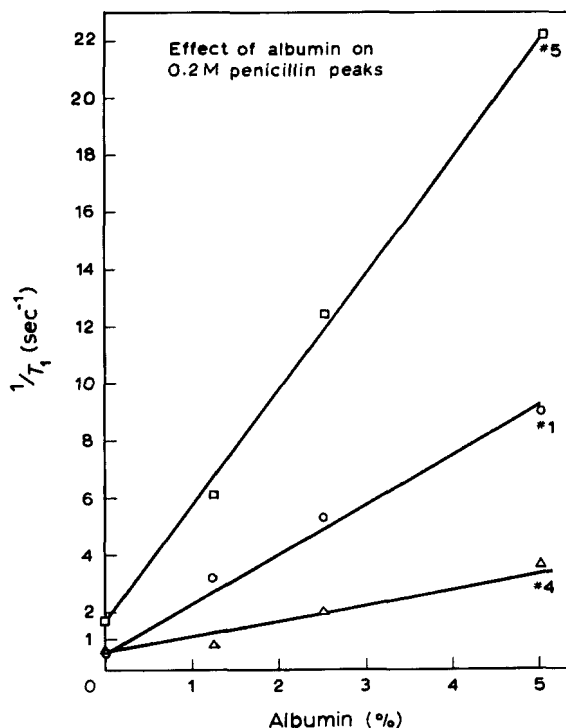


Fig. 9. Relaxation rate of penicillin peaks as a function of albumin concentration.

protein [Eq. (17)]. Such a comparison can be made from the data in Fig. 9 in which  $1/T_1$  for peaks (1), (4) and (5) is plotted for different penicillin/protein ratios. The relaxation rates of the phenyl (1) and methylene (5) peaks are found to increase by factors of about 20 and 10 respectively, whereas those of the remaining peaks increase by a factor of 4 over the same range of protein concentration.

It is known from dialysis experiments that in the concentration range used in this study only a small fraction of the penicillin molecules is in the bound state at any given time. Since only a single peak is observed for each group of protons, the exchange between the free and the bound state must be rapid and the ob-

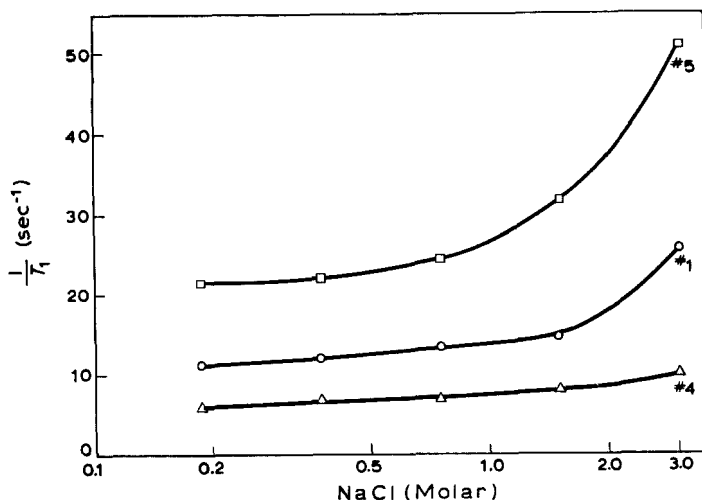


Fig. 10. Effect of increasing ionic strength on the relaxation rate of peaks in 0.1 M penicillin–2.5% albumin.

served relaxation rates must represent an average between the relaxation rates in the two states, i.e.,

$$\left(\frac{1}{T_1}\right)_{\text{obs.}} = (1-p)\left(\frac{1}{T_1}\right) + p\left(\frac{1}{T_1}\right)' \quad (19)$$

where  $p$  is the fraction bound and unprimed and primed rates represent those of the free and the bound species respectively. Inasmuch as  $p$  is the same for all peaks, the differences between the increments of relaxation rates can be understood in terms of Eq. (18) as arising from differences in  $(1/T_1)'$ . The findings thus indicate that the penicillin molecules are attached to the protein through the benzyl residue.



If this interpretation is correct, the probable mode of binding is a hydrophobic interaction of the benzene ring with aromatic residues in the protein, which should be enhanced by increasing the ionic strength of the solvent. That this is indeed the case is illustrated in Fig. 10. At a given penicillin/protein ratio the relaxation rates increase with increasing salt concentration.

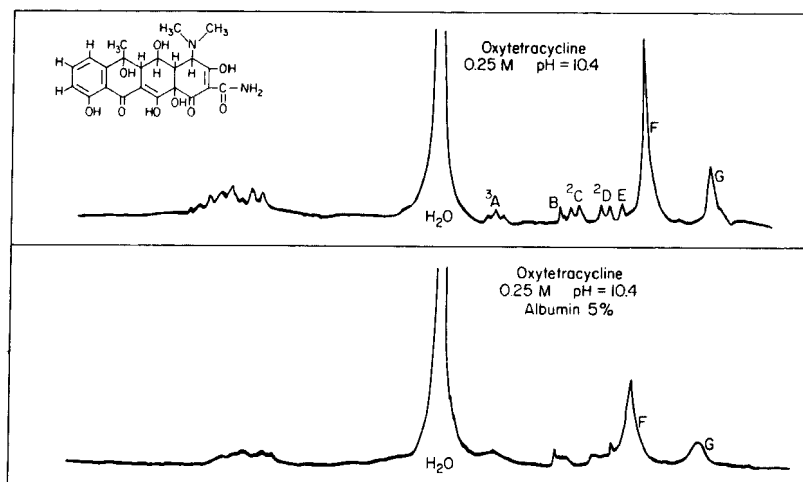


Fig. 11. Proton magnetic resonance spectrum of oxytetracycline in  $D_2O$ .  
(a) 0.25 M, (b) 0.25 M tetracycline in 5% BSA.

Under the simple conditions of Eq. (17) differential broadening will not be observed in the case of rigid molecules. Their motion can be described by a single correlation time both before and after binding since the binding of one part of the molecule leads to a stabilization of the entire molecule. This is well illustrated by the case of oxytetracycline (Figs. 11 and 12) where, with the addition of protein, all line widths increase proportionally as the protein concentration is increased. In principle it is still possible, however, to obtain information on the portion of a rigid molecule which is involved in an interaction, if a change of internuclear distances accompanying the interaction results in a measurable contribution to the relaxation rate. Thus far, such an effect has not been found.

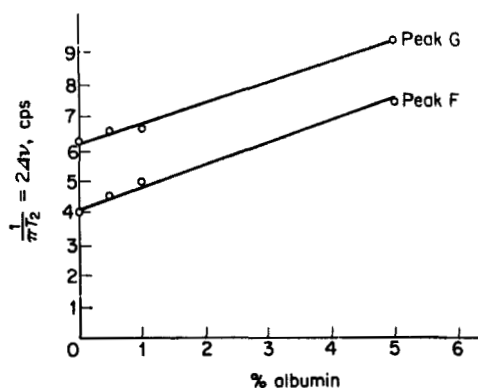


Fig. 12. Line widths of two peaks in the oxytetracycline spectrum as a function of BSA concentration.

In the case of a series of sulfonamides (Fig. 13 and Table V)<sup>15,16</sup> the preferential broadening of the lines originating from the *p*-amino-phenyl moiety (forming an  $A_2B_2$  system) as compared to the lines originating from the substituent ring is readily apparent.

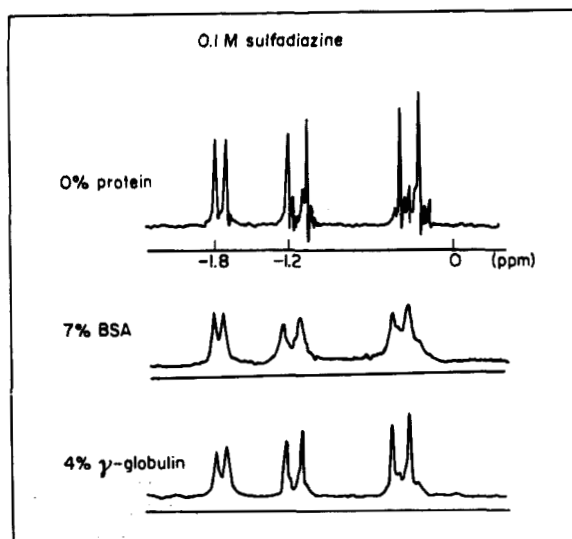


Fig. 13. The spectra of 0.1 M sulfadiazine in  $D_2O$ . (a) Without protein, (b) in 7% BSA, (c) in 4%  $\gamma$ -globulin.

As in the case of the penicillin, the effect is specific for BSA inasmuch as in the presence of other proteins, such as  $\gamma$ -globulin, all lines broaden to a comparable extent. Insofar as direct  $T_1$  measurements have been possible, an agreement with the  $T_2$  measurements has been found, suggesting that, in this case as well, the line broadening reflects a change in the rotational correlation times. The findings thus suggest a binding of the sulfonamide moiety to BSA, leaving

TABLE V. Relative Increments in Line Widths [Eq. (18)] in the Presence of 7% BSA

Drug	Sulfonamide ring protons	Substituent ring protons	
		(1)	(2)
Sulfacetamide	2.0	—	—
Sulfadiazine	$2.5 \pm 0.3$	$1.7 \pm 0.2$	—
Sulfamethazine	2.8	2.0	—
Sulfathiazole	3.1	2.5	—
Sulfadimethoxine	2.5	2.2	—
Sulfisoxazole	2.6	2.6	—
Orisul	$3.5 \pm 0.5$	$1.8 \pm 0.2$	$2.6 \pm 0.2$

the substituent on the amide group relatively free. The only exception to this finding in the series which has been investigated is sulfisoxazole, in which the shortening of relaxation times is the same for the sulfonamide and the substituent ring, suggesting that both rings are involved in the binding. The alternative interpretation, i.e. that neither ring is involved, is less likely since the changes of the relaxation times are comparable to those found for other sulfonamides.

A major difficulty in the use of conventional high resolution NMR spectroscopy for this type of study has been the relatively low sensitivity of the apparatus, which necessitated the use of comparatively high concentrations of material (i.e. of the order of 0.1 M or higher). This difficulty has been overcome only in recent months by the use of an average response computer in line with the spectrometer.<sup>12</sup> By this method it is possible to average the noise on repeated sweeps through the spectrum, while accumulating the

signal from comparatively dilute solution ( $10^{-4}\text{M}$  for single protons). The lower range of concentrations of sulfonamides and penicillins, discussed above, could only be examined by this technique.

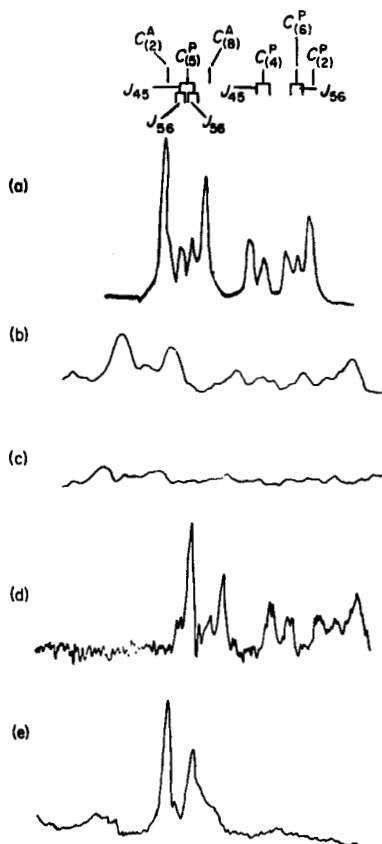


Fig. 14. (a) Nuclear magnetic resonance spectrum, and (b) average response nuclear magnetic resonance spectrum of  $0.1\text{ M}$   $\beta$ -DPN in  $\text{D}_2\text{O}$  (pH 7.2); (c)  $0.0002\text{ M}$   $\beta$ -DPN in the presence of  $0.005\text{ M}$  ADH (pH 7.2); (d)  $0.005\text{ M}$   $\beta$ -DPN, and (e)  $0.005\text{ M}$   $\beta$ -DPN in the presence of  $0.0005\text{ M}$  ADH.

The most interesting possibility opened by making the lower concentration range accessible to high resolution relaxation measurements is that of studying specific interactions in biochemical systems. A study of this type has been initiated on the system DPN-yeast alcohol dehydrogenase which binds four molecules of

DPN per molecule of enzyme.<sup>12</sup> The average response spectra of DPN in the presence and in the absence of the enzyme are shown in Fig. 14. It is apparent that in the presence of stoichiometric (or near stoichiometric) quantities of enzyme the pyridine portion of the DPN spectrum is broadened beyond detection, indicating an interaction of the pyridine ring with the protein under the condition of the experiment. A much more detailed characterization of this interaction by this method has been undertaken.

### References

1. Abragam, A., *The Principles of Nuclear Magnetism*, Clarendon Press, Oxford, 1961.
2. Bloembergen, N., *Nuclear Magnetic Relaxation*, W. A. Benjamin, New York, 1961.
3. Bloembergen, N., Purcell, E. M., and Pound, R. V., *Phys. Rev.* **73**, 679 (1948).
4. Bloch, F., *Phys. Rev.* **102**, 104 (1956).
5. Fischer, J. J., *Studies of the Protein-Binding of Several Penicillins by Nuclear Magnetic Resonance*. Thesis for Honors, 1961, Harvard Medical School.
6. Fischer, J. J., Ph.D. Thesis, Harvard University, 1964.
7. Fischer, J. J., and Jardetzky, O., to be published.
8. Gutowsky, H. S., and Woessner, D. E., *Phys. Rev.* **104**, 843 (1956).
9. Hubbard, P. G., *Phys. Rev.* **109**, 1153 (1958).
10. Jardetzky, O., and Jardetzky, C. D., "Magnetic Resonance Spectroscopy. Methods and Biochemical Applications" in D. Glick, Ed., *Methods of Biochemical Analysis*, Vol. IX, Interscience, New York, 1962, pp. 235-410.
11. Jardetzky, C. D., and Jardetzky, O., "Nuclear Magnetic Resonance" in M. Florkin and E. Stotz, Eds., *Comprehensive Biochemistry*, Vol. 3, Elsevier, Amsterdam, 1962, pp. 209-264.
12. Jardetzky, O., Wade, N. G., and Fischer, J. J., *Nature* **197**, 183 (1963).
13. Jardetzky, O., and Fischer, J. J., *Proc. 4th Intern. Conf. Med. Electronics*, p. 46, 1961.
14. Jardetzky, O., Fischer, J. J., and Pappas, P., *Biochem. Pharmacol.* **8**, 115 (1961).
15. Jardetzky, O., and Seery, V. L., *Pharmacologist* **4**, 156 (1962).
16. Jardetzky, O., and Seery, V. L., to be published.
17. Weiner, N., "The Catecholamines" in G. Pincus, K. V. Thimann and E. B. Astwood, Eds., *The Hormones*, Academic Press, New York (in press).
18. Weiner, N., and Jardetzky, O., *Biochem. Pharmacol.* **8**, 115 (1961).
19. Weiner, N., Pappas P., and Jardetzky, O., *Arch. Exptl. Pathol. Pharmacol.*, in press.
20. Woessner, D. E., *J. Chem. Phys.* **36**, 1 (1962).

## 14

# RECENT ADVANCES IN EPR SPECTROSCOPY\*

BERNARD SMALLER, *Argonne National Laboratory,  
Argonne, Illinois*

## CONTENTS

I. Introduction . . . . .	532
II. Theoretical Aspects of Hyperfine Interaction . . . . .	533
A. Isotropic "Contact" Term . . . . .	534
B. Anisotropic Dipolar Interaction . . . . .	540
III. Free Radicals Produced in Organic Single Crystals . . . . .	541
A. Dicarboxylic Acid and Derivatives . . . . .	541
B. Amino Acid and Derivatives . . . . .	546
C. Glycollic Acid and Derivatives . . . . .	552
IV. Triplet State Studies . . . . .	553
A. Zero-Field Splittings . . . . .	554
(1) Experimental Determinations . . . . .	556
(2) Theoretical Basis . . . . .	559
B. Hyperfine Structure and Line Widths . . . . .	562
C. Lifetime Studies . . . . .	564
D. Energy Transfer Experiments . . . . .	567
E. Triplet State and Photochemical Processes . . . . .	576
References . . . . .	579

## I. INTRODUCTION

The technique of paramagnetic resonance has been exploited vigorously in the past several years in various fields of scientific endeavor. Its contribution in the field of free radicals has been particularly outstanding in the understanding of the nature of these entities. Considerable information concerning the wave functions, i.e. electron orbitals, of the unpaired electron has been derived by studying their interaction with magnetic nuclei present in the given species. Several excellent review articles are available on the

\* Based on work performed under the auspices of the U.S. Atomic Energy Commission.

subject<sup>63, 64, 110, 146</sup> and thus it was the considered opinion of the author that it would perhaps be of greater value to the reader to restrict his attention to a somewhat more limited field. The study of free radicals produced in organic single crystals has been under vigorous study of late because of the wealth of information that is provided of not only the radical but its orientation and distortion in the parent lattice. Although brief reviews of this field are also available<sup>148, 149</sup> we shall attempt to present the material and results derived in more complete form, along with the basic theory involved.

The latter part of the article will be devoted to the subject of studies on the excited triplet state in organic molecules which is only in its nascent stage of attack by electron paramagnetic resonance (EPR). Molecular orbital theory concerning this state is discussed briefly in order to familiarize the reader with the problems involved, and its relation to the results derived by EPR. The results are as yet quite meager especially in regard to energy transfer and photochemical effects. The data quoted are, in the main, results of the author which are as yet unpublished. As such, the ability of the interpretations to withstand the test of time and more complete investigations may be considered questionable. Their value may thus only serve to stimulate further work in this most interesting field. Yet in the final analysis, this can be said to represent the philosophical goal of all science.

## II. THEORETICAL ASPECTS OF HYPERFINE INTERACTION

In order to interpret the results derived from electron paramagnetic experiments it is necessary to discuss briefly the nature of the magnetic interactions involved in the phenomenon. The interaction Hamiltonian for a free radical in terms of its unpaired electron and magnetic nuclei can be described as

$$\mathcal{H} = \mathcal{H}_e + \mathcal{H}_{\text{int}} + \mathcal{H}_n \quad (1)$$

The first term,  $\mathcal{H}_e$ , describes the interaction of the unpaired electron with the external magnetic field:

$$\mathcal{H}_e = \beta S \cdot g \cdot H \quad (2)$$

where  $S$  is the vector spin of the electron,  $\beta$  the Bohr magneton and

$H$  the vector magnetic field. The tensor  $g$  describes the magnitude and direction of the coupling between electron and field. It is more easily evaluated in terms of its principal values  $g_1, g_2, g_3$ , whose directions depend upon the direction of the crystalline field of the parent molecule. The magnitudes are determined by the amount of mixing of higher states of the same symmetry.<sup>94</sup> For organic free radicals it has been found that the magnitude of the  $g$  values is very close to that of the free electron,  $g = 2.0023$ , and the directions of the principal values are close to those of the molecular bonds. Departure from the "free electron" implies incomplete "quenching" of the residual orbital magnetic moment which depends on the energy separation,  $\Delta E$ , to the excited states and the spin-orbit coupling parameter,  $\xi$ , with  $\Delta g \approx 2\xi/\Delta E$ . For the axial symmetric case,  $g_1 \equiv g_{\parallel}$ ;  $g_2 = g_3 \equiv g_{\perp}$ , the departure  $\Delta g_{\perp} > \Delta g_{\parallel}$  because of the relative values of  $\Delta E$  for the two cases. In general, for organic free radicals,  $\Delta g_{\perp} > 0$ , and since its magnitude depends on the atomic species it is often of value in identifying the location of the free spin.

The term  $\mathcal{H}_n$  describing the Zeeman energy of the nuclear dipoles is usually negligible in comparison with  $\mathcal{H}_{\text{int}}$ , and in first approximation can be ignored.

### A. Isotropic "Contact" Term

The interaction term  $\mathcal{H}_{\text{int}}$  is a measure of the coupling of magnetic nuclei to the field produced by the electron and is also expressible in tensor notation

$$\mathcal{H}_{\text{int}} = \mu_N I \cdot A \cdot S \quad (3)$$

The principal values of  $A_{ii} \equiv A_i (i = 1, 2, 3)$  are related in direction to the electron-nucleus bond direction and the symmetry axes of the electron wave function. It is convenient to decompose the  $A$  tensor into the sum of an isotropic component,  $a$ , and an anisotropic term,  $A_d$ , where  $A_d$  represents the contribution due to classical dipole-dipole interaction. The trace of the latter vanishes

$$\sum_{i=1}^3 A_{id} = 0 \quad \text{and} \quad \sum_{i=1}^3 (A_i = A_{id} + a) = 3a \quad (4)$$

The isotropic term is derived from the Fermi-type "contact"<sup>32</sup> interaction that exists because of the penetration of the electron wave function  $\psi$  into the nucleus. The best known example is that of



atomic hydrogen with an electron occupying a 1s orbital about the nucleus of magnetic moment,  $\mu_N$ . We have for the hyperfine interaction,  $a$ , in terms of the electron wave function,  $\psi(r)$ ,

$$a_{1s}(H_0) = \frac{16}{3} \pi g \beta \mu_N \psi_{1s}^2(0) \quad (5)$$

$\beta$  is the Bohr magneton. A convenient energy unit used is that of  $\nu$ , the frequency in megacycles ( $10^6$  cycles) per second. Conversion to c.g.s. units requires multiplication by  $h$ , Planck's constant ( $\times 10^6$ ). For the hydrogenic 1s orbital  $a_{1s}(H_0) = 1420$  Mc/sec, which corresponds thus to an unpaired electron or spin density,  $\rho_{1s}(H_0)$ , equal to unity. Experimental values of the isotropic proton hyperfine constants,  $a(H)$ , can then be interpreted in terms of the corresponding spin density at the hydrogen nucleus or in terms of the partial 1s character of the unpaired electron wave function by means of the relation

$$\rho_{1s}(H) = a(H)/1420 \quad (6)$$

It has been found experimentally, in the study of the isotropic interaction constants for various aliphatic<sup>2, 33, 68, 129</sup> and aromatic<sup>11-14, 16, 17, 65, 102, 136, 137, 141, 145, 147</sup> free radicals, that certain generalizations can be deduced concerning their dependence on the nature of the radical. For the aliphatics (Table I) it appears to be quite independent of the molecular species, while for the aromatics, provided cognizance is taken of the non-localized nature of the unpaired electron, similar conclusions can be derived. The appearance of hyperfine structure indicative of magnetic coupling to the molecular protons is not obvious if it is assumed that the unpaired electron representative of the free radical is in a  $p_z$ ,  $\pi$ -type orbital. The corresponding wave function has a node in the molecular plane containing the carbon and hydrogen nuclei, held in  $\sigma$ -type bands, and  $\psi_{2p}(C) = 0$  at these sites. To account for this anomaly Wiessman<sup>144</sup> suggested that a modification of the ground state wave function must be made, similar to that found necessary by Abragam and Pryce<sup>1</sup> to account for the presence of hyperfine structure in the  $Mn^{2+}$ ,  $^6S_{5/2}$ , state. By introducing a small amount of the excited configuration produced by an unpairing of the  $(ns)^2$  term, i.e. a  $c[ns + (n+1)s]$  term, to the wave function, the unpaired  $s$  orbital could provide the necessary hyperfine interaction. A significant contribution towards a simplification and generalization of the experimental results was achieved by McConnell,<sup>88</sup> who

TABLE I. Isotropic Hyperfine Coupling Constants, Mc/sec

Line	Molecule	Radical	$a(H_\alpha)$	$a(C_\alpha)$	$b(H_\beta)$	Ref.
<i>Experimental Values</i>						
1	CH <sub>3</sub> OH	$\dot{\text{C}}\text{H}_3$	63.0 ± 0.5			a
2	<sup>13</sup> CH <sub>3</sub> I	$\dot{\text{C}}\text{H}_3$		115 ± 10		b
3	C <sub>2</sub> H <sub>2</sub> OH	$\dot{\text{C}}\text{H}_2\text{CH}_3$	61.4		74.8	a
4	C <sub>2</sub> H <sub>6</sub>	$\dot{\text{C}}\text{H}_2\text{CH}_3$	56.0		74.6	c
5	C <sub>2</sub> H <sub>6</sub>	$\dot{\text{C}}\text{H}_2\text{CH}_3$	63		75.9	d
6	C <sub>6</sub> H <sub>6</sub>	$(\dot{\text{C}}_6\text{H}_6)^-$	$\frac{63.1}{6}$			e
<i>Theoretical Calculations</i>						
	Model					
7	Semi-empirical	$\dot{\text{C}}\text{H}$	63			f
8	Valence bond	$\dot{\text{C}}\text{H}_3$	74 ± 14			g
9	Valence bond	$\dot{\text{C}}\text{H}_2\text{CH}_3$			78.5	h
10	Molecular orbital	$\dot{\text{C}}\text{H}_2\text{CH}_3$			77.8 ( $\rho_{12}$ 0.93)	i
					47.4 ( $\rho_{12}$ 0.70)	

<sup>a</sup> Smaller, B., (UV photolysis, unpublished data).

<sup>b</sup> Cole, T., Pritchard, H. O., Davidson, N. R., and McConnell, H. M., *Mol. Phys.* **1**, 406 (1958).

<sup>c</sup> Smaller, B., and Matheson, M. S., *J. Chem. Phys.* **28**, 1169 (1958).

<sup>d</sup> Fessenden, R. W., and Schuler, R. H., *J. Chem. Phys.* **33**, 935 (1960).

<sup>e</sup> Tuttle, T. R., Jr., and Weissman, S. I., *J. Am. Chem. Soc.* **80**, 5342 (1958).

<sup>f</sup> McConnell, H. M., and Chestnut, D. B., *J. Chem. Phys.* **28**, 107 (1958).

<sup>g</sup> Karplus, M., *J. Chem. Phys.* **30**, 15 (1959).

<sup>h</sup> McLachlan, A. D., *Mol. Phys.* **1**, 233 (1958).

<sup>i</sup> Chestnut, D. B., *J. Chem. Phys.* **29**, 43 (1958).

proposed that the indirect hyperfine interaction could be studied in terms of a  $\dot{\text{C}}\text{—H}$  fragment which can by a  $\pi\text{—}\sigma$  atomic exchange mechanism give rise to the spin polarization effect corresponding to a required s orbital contribution. In valence bond nomenclature one

can consider the relative contribution of the excited state formed by a pairing of the  $p_z$  spin with the  $sp^2 (= h)$  bonding orbital. The magnitude of the first-order correction to the ground state wave function and thus the induced polarization depends on the exchange integral  $J_{ph}$  ( $J_{ps}$  is assumed negligible) and the energy separation,  $\Delta E_{21}$ , to the excited level. In molecular orbital terminology one must consider the configuration interaction wherein the two  $\sigma$  bonding molecular orbitals of opposite spin are affected unequally by the  $p_z$  spin state. The concept was extended by McConnell and Chestnut<sup>91</sup> by exploiting the concept of "spin density" introduced by Brovetto and Ferroni<sup>15</sup> to derive a general relation between the proton hyperfine constant,  $a$ , and the spin density,  $\rho$ , at the adjacent carbon site of the  $\pi$  unpaired electron. Designating by  $H_\alpha$  the proton bonded to the carbon containing the unpaired spin ( $C_\alpha$ ),  $a_{1s}(H_\alpha) = Q\rho_{2p}(C_\alpha)$ , where  $Q$  has the empirical value of  $-63$  Mc/sec. This value is used since accurate theoretical values are difficult to derive. For the aliphatic radicals the  $p_z$  electron is localized at the carbon site, since the radical is usually formed by the removal of a hydrogen atom and  $\rho_{2p}(C_\alpha) \approx 1$ . However, for the aromatic radicals formed by electron addition or removal, the unpaired electron is non-localized in a molecular  $\pi$  orbital, i.e.  $\rho$  is proportional to  $C_n^2$ , where  $C_n$  is the coefficient of the component atomic orbital wave function. Thus for the simple case of the benzene negative ion  $\rho = \frac{1}{6}$ . The concept of "spin density" is a valuable one for unlike that of "unpaired electron density" it can take on either positive or negative values. These are associated with the direction of the spin polarization at the nucleus in question which can be either parallel or antiparallel to that of the polarizing  $p_z$  electron. Thus, corresponding to the deduced negative sign of  $Q$  the spin density and polarization at the  $\alpha$  proton is negative with a value for aliphatic radicals

$$\rho_{1s}(H_\alpha) = \frac{a_{1s}(H_\alpha)}{a_{1s}(H_0)} = -63/1420 = -4.4\%$$

Since a polarization effect implies no net gain or loss of spin density there must be a corresponding positive polarization at the carbon nucleus. Verification of its existence and sign have been provided by the use of  $^{13}\text{C}$  substituted radicals.<sup>24, 92, 142</sup> One can thus interpret the observed EPR spectra of the methyl radical (Fig. 1) in terms of

three planar C—H fragments in  $sp^2$ -1s bonding orbitals with the unpaired  $p_z$  electron perpendicular to their plane. The quartet of lines arises from the combinations of alignments of nuclear spins possible, with the separations indicated in Table I. The doublet spectrum of atomic hydrogen is also present, since the radical has in this case been formed by  $\gamma$ -irradiation at low temperature. Verification of this planar configuration deduced from ultraviolet absorption spectra studies<sup>53</sup> was made by Karplus,<sup>69</sup> who studied the expected splitting as a function of angular configuration of the molecule. A non-empirical approach to the problem has also been

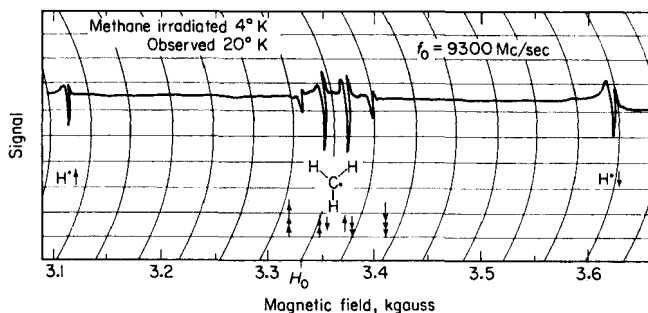


Fig. 1. Electron paramagnetic resonance spectra of  $\gamma$ -irradiated methane at 4°K revealing presence of atomic hydrogen and methyl radical.

made using a molecular orbital treatment, where it was found that it was necessary to include the carbon 3s atomic orbital for good agreement with experiment.<sup>54</sup>

The theoretical interpretation of the ethyl radical EPR spectra requires the introduction of a second type of interaction possible between the unpaired  $\pi$  orbital and the bonding orbitals. The spectra (Fig. 2) can be resolved into a quartet of triplets. The latter are due to the two protons bonded to the  $\alpha$  methylene carbon, while the quartet splitting is attributable to the presence of spin density on the three protons on the  $\beta$  methyl carbon group. McLachlan,<sup>98</sup> using a valence bond approach, derived a value for this isotropic  $\beta$  hyperfine splitting in terms of the exchange integrals involving mainly the exchange between the unpaired  $\alpha$   $p_z$  electron and the  $p$  orbitals on the carbon hybridized tetrahedrally ( $sp^3$ ) to the methyl protons. The interaction is thus of a  $\pi$ - $\pi$  nature and its magnitude depends on the overlap of these orbitals. It will be greatest for that

hybrid whose symmetry axis has its projection on a plane perpendicular to the C—C bond parallel to the unpaired  $p_z$  symmetry axis ( $\theta = 0$ ). The angular dependence of this splitting constant,  $b$ , will depend on the relative orientations of the two symmetry axes and also on the spin density in the  $p_z$  orbital. The most obvious relation is thus

$$b_{1s} = B \cos^2 \theta \rho_{2p}(C_\alpha) \quad (7)$$

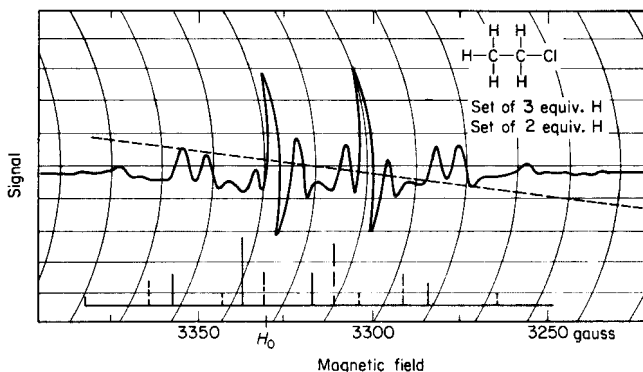


Fig. 2. Electron paramagnetic resonance spectrum of  $\gamma$ -irradiated ethyl chloride revealing presence of ethyl radical.

For a rapidly rotating methyl group, as in the ethyl radical, one must average the angular dependence with  $\cos^2 \theta = \frac{1}{2}$ . The experimental values of  $B$  are given in Table I. Better fit with the data on single crystals is sometimes secured by adding a second parameter,  $B'$ , which corresponds to a finite coupling when the hybrid orbital is in the  $\sigma$  plane ( $\theta = \pi/2$ ), although theoretical justification is not obvious. The mechanism is most easily seen in the valence bond representation as a mixing into the ground state of excited states formed by pairing of the  $p_z$  orbital with one of the hybrid bonding orbitals. The resultant unpaired  $1s$  orbital at the proton can thus constitute the source of the hyperfine interaction. The values derived by McLachlan for each of the protons in the methyl group of the ethyl radical are  $b = 78.5$  Mc/sec and

$$\rho_{1s}(H_\beta) = +5.5\%$$

Since the total polarization of the methyl group must be zero, the corresponding spin density at the  $\beta$  carbon is

$$\rho(C_\beta) = -16\%$$

It is of interest to note that the sign of the  $\beta$  proton splittings is opposite to that of the  $\alpha$  protons.

This isotropic hyperfine interaction has also been treated by Chestnut<sup>18</sup> for simple aliphatic radicals (ethyl, methyl ethyl, and dimethyl ethyl) using a molecular orbital treatment of hyperconjugation similar to that used by Bersohn in methylated semiquinones.<sup>9</sup> He achieved good agreement with experimental results by proper choice of resonance integral. The value for relative overlap integral was found, for best agreement with experiment, to be  $\rho_{12} = 0.93$ , rather than the value  $\rho_{12} = 0.7$  used by Crawford and Coulson<sup>27</sup> for methyl benzene. However, since the treatment is a single-electron M.O. without configuration interaction, the calculated spin densities at the methyl protons are positive. The results showed, as had been found experimentally, that for the aliphatic radicals the total hyperfine splitting is proportional to the number of contributing protons, the spin density at each nucleus being fairly independent of the extent of the substitution. The value of coupling constant for the methyl protons in the ethyl radical was found to be 77.8 Mc/sec (using  $\rho_{12} = 0.93$ ) in good agreement with experiment.

### B. Anisotropic Dipolar Interaction

Where the radicals are not free to rotate, one must consider the effect of the electron dipole-nuclear dipole interaction  $\mathcal{H}_d$  which can be presented as

$$\mathcal{H}_d = \mu_e \mu_N \left[ \frac{(S \cdot I)}{r^3} - \frac{3(S \cdot r)(I \cdot r)}{r^5} \right] \quad (8)$$

between electron of spin  $S$  and magnetic moment  $\mu_e$  and nucleus of spin  $I$ , magnetic moment  $\mu_N$ , separated by a distance  $r$ . In a strong magnetic field which quantizes the spin in its  $z$  direction, the expression simplifies for point dipoles to

$$\mathcal{H}_d = \mu_e \mu_N \frac{(3 \cos^2 \theta - 1)}{r^3} S_z I_z \quad (9)$$

where  $\theta$  is the direction between  $r$  and the magnetic field. Thus there are two apparent principal axes: for  $\theta = 0$ ,  $A_{1d} = A_{\parallel}$ , while for  $\theta = 90^\circ$ ,  $A_{2d} = A_{3d} = A_{\perp} = -\frac{1}{2}A_{\parallel}$ . This cylindrical symmetry will also exist for non-point dipoles when there is rapid rotation about the bond axis. However, in general and for the static case one must

consider the electron density distribution,  $\rho$ , and integrate  $\mathcal{H}_d$  over the prescribed orbital. The theoretical calculations of the anisotropic dipolar interaction between unpaired electron and proton in a  $\dot{\text{C}}\text{—H}$  fragment have been performed by McConnell and Strathdee<sup>95</sup> for both the  $p$  and  $\sigma$  contributions in terms of the spin density. Comparison with experimental results reveals that the  $\sigma$  contribution, the result of the isotropic spin polarization, is apparently negligible and one need only consider the unpaired  $p$  wave function, for  $\rho_{2p} = 1$ . The principal values of dipolar contributions,  $A_{id}$ , are  $A_{1d} = +42$  Mc along the CH bond;  $A_{2d} = -6$  Mc, parallel to the  $p$  orbital symmetry axis; and  $A_{3d} = -40$  Mc in the direction perpendicular to the above axes. The qualitative arguments for the magnitude and sign are given by Ghosh and Whiffen<sup>39</sup> in terms of the conic angle subtended by boundaries  $\theta = 55^\circ$ , where the term  $3\cos^2\theta - 1 = 0$  and the contribution changes sign. The approximation to cylindrical symmetry is obviously poor although the average  $\frac{1}{2}(A_{2d} + A_{3d}) = -23$  Mc is approximately that suggested by the point dipole relationship between  $A_{\parallel}$  and  $A_{\perp}$ . The total principal values (isotropic plus anisotropic) of the coupling parameters are given in Table II. The smallest value corresponds to the direction of the CH bond, the intermediate value to the  $p$  wave functions symmetry axis, and the maximum value to a direction perpendicular to both CH and  $p$  axis. Since the anisotropic contribution is also dependent on the spin density,  $\rho_{2p}$ , at the  $\alpha$  carbon, comparison of theoretical and experimental values of  $A_i$  can also serve to determine the value for  $\rho_{2p}$  for a given free radical. Similarly the anisotropic contribution to the hyperfine coupling of the protons on the  $\beta$  carbon can be calculated. However, since the interaction is proportional to the inverse cube of the separation, in most cases the contribution will be quite small.

### III. FREE RADICALS PRODUCED IN ORGANIC SINGLE CRYSTALS

#### A. Dicarboxylic Acid and Derivatives

*Malonic acid.* Experimental verification of the negative sign of the isotropic component of the hyperfine interaction was provided by the investigation of Cole, Heller and McConnell<sup>23</sup> on irradiated single crystals of malonic acid. The total hyperfine interaction was

determined (both isotropic and anisotropic) for the radical  $\dot{\text{C}}\text{H}(\text{COOH})_2$  and compared with the previously derived theoretical values for the C—H fragment. As shown in Table II, line 3, they are in good agreement with the assumption of the negative sign for  $a$  and substantiate the utility of treatment of the radical in terms of the  $\dot{\text{C}}\text{—H}$  fragment.

A more intensive investigation by McConnell, Heller, Cole, and Fessenden<sup>93</sup> (Table II, line 4) revealed in the spectra also the presence of lines due to the "forbidden transitions". These correspond to  $\Delta m_s = \pm 1$ ,  $\Delta m_I = \pm 1$  transitions, i.e. spin flip of both electron and nucleus, can occur when the external field,  $H$ , at the nucleus becomes comparable in magnitude to that due to the electron,  $H_e$ . The magnetic nucleon cannot then be considered quantized in the direction of  $H_e$ , but possesses a "quantization" axis which depends on the relative magnitude and direction of  $H_e$  and  $H$ . Because of the anisotropic nature of the hyperfine interaction, the intensity of these transitions as well as their resonance field will depend on crystal orientation. Alternatively, one can consider that the nucleon  $| -1 \rangle$  and  $| +1 \rangle$  spin states are mixed since they are no longer quantized in the electron spin framework axis and thus the  $\Delta m_I$  transition probability becomes more allowed.

Further investigations on the "forbidden line" intensities were made by Lin and McDowell<sup>81</sup> using X-irradiated single crystals of potassium hydrogen malonate. The hyperfine constants were substantially in agreement (Table II, line 7) with that of malonic acid. The relative intensities of the forbidden transitions<sup>22</sup> were also in good agreement with theoretical calculations in their dependence on angle of rotation of the crystal with respect to magnetic field.

The magnetic parameters at the carbon nucleus have also been determined using  $^{13}\text{C}$  substituted  $[(\text{HOOC})^{13}\text{CH}_2(\text{COOH})]$  malonic acid crystals<sup>92</sup> where it was found that the data were in agreement with the theoretical prediction of a positive spin density at the carbon nucleus. The hyperfine constants were found by Cole and Heller<sup>21</sup> to be  $A_1(C_\alpha) = 42.2$  Mc/sec,  $A_2(C_\alpha) = 212.7$  Mc/sec,  $A_3(C_\alpha) = 22.8$  Mc/sec,  $a(C_\alpha) = 92.6$  Mc/sec. From the  $^{13}\text{CH}_3$  data of Cole and co-workers<sup>24</sup> and the isotropic splitting constant  $a(C_\alpha) = 115$  Mc/sec, the calculated spin density at the methylene carbon could be determined as  $\rho_{2p}(C_\alpha) = 0.8 \pm 0.08$ . The values for



$A_i$ , the total coupling parameters, are also in fair agreement with this value of spin density.

The magnetic and structural properties of a second, less stable, free radical produced in malonic acid have been determined by Horsfield, Morton, and Whiffen.<sup>56</sup> The species is  $\dot{\text{C}}\text{H}_2(\text{COOH})$  produced by detachment of a (COOH) group. The hyperfine components (Table II, line 6) for both methylene protons indicate that the free radical carbon atom has converted to a planar  $sp^2$  hybridization with an H $\dot{\text{C}}\text{H}$  angle of  $116^\circ \pm 5^\circ$ . Interestingly enough, the data also reveal that the plane of the  $\dot{\text{C}}\text{H}_2$  group is perpendicular to the carboxyl acid group.

A recent determination by Heller<sup>51</sup> has been made of the  $\beta$  coupling parameters  $A_i(H_\beta)$  of the hyperfine interaction between the  $\pi$  electron on the  $\alpha$  carbon and the protons on the  $\beta$  carbon in methyl malonic acid. Two radicals were detectable,  $\text{CH}_3\dot{\text{C}}(\text{COOH})_2$  and  $\text{CH}_3\dot{\text{C}}\text{H}(\text{COOH})$ . A detailed study made of the former revealed a 4-line methyl spectrum due to  $\beta$  coupling. The interaction has only a small anisotropy as expected from the reduced dipolar interaction. The values are indicated in Table II, line 8, and are in agreement with the determination of the  $\beta$  coupling parameter  $b$  derived from the ethyl radical spectrum (Table I, lines 3, 4, and 5). At 4.2°K the methyl group in  $\text{CH}_3\dot{\text{C}}(\text{COOH})_2$  was found to execute nearly free rotation, while for  $\text{CH}_3\dot{\text{C}}\text{H}(\text{COOH})$  hindered rotation was indicated presumably due to the presence of the adjacent  $\dot{\text{C}}\text{H}$  proton.

In the case of irradiated ethyl malonic acid, Rowlands and Whiffen<sup>121</sup> found the resultant radical  $\text{CH}_3\text{CH}_2\dot{\text{C}}(\text{COOH})_2$  revealed a spectrum assignable to the  $\beta$  methylene protons. However, assuming  $sp^2$  hybridization of the methylene group, with fixed orientation and an HCH angle of  $120^\circ$ , the possible values of  $B = 84$  Mc/sec or 254 Mc/sec. It remains unclear why these values are outside the accepted range and the authors suggest that  $B$  may depend on the radical.

*Succinic acid.* The earliest determinations of the " $\pi$ - $\pi$ " (i.e.  $\beta$ ) interaction in single crystals were made by Heller and McConnell<sup>52</sup> on irradiated  $\beta$ -succinic acid (Table II, line 10). The radical  $(\text{COOH})\text{CH}_2\dot{\text{C}}\text{H}(\text{COOH})$  contains a single  $\alpha$  ( $\sigma$ ) proton along with the two  $\beta$  protons that can couple to the  $\pi$  electron. The  $\alpha$  proton

TABLE II. Hyperfine Coupling Constants for Dicarboxylic Acids and Derivatives, Mc/sec

Line	Molecule	Free radical	$A_i(H_\alpha)$			$A_i(H_\beta)$			Ref.	
			$A_1$	$A_2$	$A_3$	$a$	$A_1$	$A_2$		$A_3$
1	Theoretical	$\dot{\text{C}}\text{H}$	-21	-69	-103				a	
2	Theoretical	$\dot{\text{C}}\text{H}$	-20	-68	-102				b	
3	Malonic acid	$\dot{\text{C}}\text{H}(\text{CO}_2\text{H})_2$	30	58	93				b	
4	Malonic acid	$\dot{\text{C}}\text{H}(\text{CO}_2\text{H})_2$	-28.8	58	90.3				c	
5	Malonic acid	$\dot{\text{C}}\text{H}(\text{CO}_2\text{H})_2$	-28	-58	-91	-59			d	
6	Malonic acid	$\dot{\text{C}}\text{H}_2(\text{CO}_2\text{H})$	$\alpha_1$	-30	-55	-91	-62		d	
			$\alpha_2$	-37	-59	-92	-63		d	
7	Potassium hydrogen malonate	$\text{OOC}\dot{\text{C}}\text{HCOO}$	28	53.5	86				e	
8	Methyl malonic acid	$\text{CH}_3\dot{\text{C}}(\text{CO}_2\text{H})_2$					75.4	68.6	68.6	f
9	Ethyl malonic acid	$\text{CH}_3\text{CH}_2\dot{\text{C}}(\text{CO}_2\text{H})_2$					$\beta_1$ 75 $\beta_2$ 62	71 56	64 53	g g

10	Succinic acid	$(\text{CO}_2\text{H})\text{CH}_2\dot{\text{C}}\text{H}(\text{CO}_2\text{H})$						$\beta_1 \approx 98$ $\beta_2 \approx 83$	<sup>a</sup>
11	Succinic acid	$(\text{CO}_2\text{H})\text{CH}_2\dot{\text{C}}\text{H}(\text{CO}_2\text{H})$	-30	-59	-92	-60	$\beta_1$ 108 $\beta_2$ 89	98 79	<sup>b</sup>
12	Glutaric acid	$(\text{CO}_2\text{H})(\text{CH}_2)_2\dot{\text{C}}\text{H}(\text{CO}_2\text{H})$	A -26 B -23	-53 -52	-88 -79	-56 -51	$\beta_1$ $\beta_2$	$\Delta\nu \sim 8$ $\Delta\nu \sim 6$ $\Delta\nu \sim 6$ $\Delta\nu \sim 7$	<sup>c</sup> <sup>d</sup> <sup>e</sup> <sup>f</sup>
13	Adipic acid	$(\text{CO}_2\text{H})(\text{CH}_2)_3\dot{\text{C}}\text{H}(\text{CO}_2\text{H})$	-27.8	-49.6	-93.6		$\beta_1$ $\beta_2$	$\Delta\nu \sim 8$ $\Delta\nu \sim 4$	<sup>g</sup> <sup>h</sup>

<sup>a</sup> McConnell, H. M., and Strathdee, J., *Mol. Phys.* **2**, 285 (1959).

<sup>b</sup> Cole, T., Heller, C., and McConnell, H. M., *Proc. Natl. Acad. Sci. U.S.A.* **45**, 525 (1959).

<sup>c</sup> McConnell, H. M., Heller, C., Cole, T., and Fessenden, R. W., *J. Am. Chem. Soc.* **82**, 766 (1960).

<sup>d</sup> Horsfield, A., Morton, J. R., and Whiffen, D. H., *Mol. Phys.* **4**, 327 (1961).

<sup>e</sup> Lin, W. C., and McDowell, C. A., *Mol. Phys.* **4**, 343 (1961).

<sup>f</sup> Heller, C., *J. Chem. Phys.* **36**, 175 (1962).

<sup>g</sup> Rowlands, J. R., and Whiffen, D. H., *Mol. Phys.* **4**, 349 (1961).

<sup>h</sup> Heller, C., and McConnell, H. M., *J. Chem. Phys.* **32**, 1535 (1960).

<sup>i</sup> Pooley, D., and Whiffen, D. H., *Mol. Phys.* **4**, 81 (1961).

<sup>j</sup> Morton, J. R., and Whiffen, D. H., *Mol. Phys.* **4**, 169 (1961).

<sup>k</sup> Morton, J. R., and Horsfield, A., *Mol. Phys.* **4**, 219 (1961).

hyperfine interaction was found to have the same anisotropy and magnitude as found in malonic acid. The methylene  $\beta$  proton interaction constants were found to be unequal, indicative of a twisting of the HCH angle bisector with respect to the  $\pi$  electron nodal plane. The values of  $B(\theta)$  were found to be in the range 80–100 Mc/sec, the small anisotropy being in the expected range.

The results were confirmed by Pooley and Whiffen, who calculated a value of  $B = 120$  Mc/sec and a twist angle for the methylene group of  $\psi = 5^\circ$ .<sup>115</sup> The derived values of the coupling parameters for the  $\alpha$  proton,  $A_i(H_\alpha)$ , are indicated also in Table II, line 11, along with  $A_i(H_\beta)$ , those of the two  $\beta$  protons. Since the value of  $a(H_\alpha)$  implies a  $\rho_{2p}(C_\alpha) \approx 1$ , the low value of  $B$ , 120 Mc/sec as compared to 150 Mc/sec for ethyl radical, remains unexplained.

*Glutaric acid.* The spectrum of irradiated glutaric acid in the dicarboxylic acid series has also been investigated by Horsfield, Morton, and Whiffen.<sup>57</sup> Two different radical species were found to be trapped in the crystal ( $A$  and  $B$  in Table II, line 12) with different hyperfine coupling constants. The  $\beta$  protons showed unequal  $\pi$  couplings indicative of the twisting of the methylene axis for both  $A$  and  $B$  species of about  $25^\circ$  from the radical plane. The radical in each case is presumably  $(\text{COOH})\text{CH}_2\text{CH}_2\dot{\text{C}}\text{H}(\text{COOH})$ , and while no definite explanation for their difference is apparent, it was assumed that it is due to the lack of a molecular two-fold axis of symmetry. No evidence for a  $\gamma$  coupling to the second methylene group was detected and an upper limit of 9 Mc/sec was placed on this interaction.

*Adipic acid.* The next higher aliphatic ( $n = 4$ ) in the dicarboxylic series, adipic acid, was investigated by Morton and Horsfield<sup>107</sup> to determine if the anomalous behavior of glutaric acid was unique. The values for the  $\alpha$  and  $\beta$  couplings are given in Table II, line 13; no  $\gamma$  coupling was evident. From the directions of both  $\alpha$  and  $\beta$  hyperfine tensors it was concluded that the radical is twisted by an angle  $\psi \approx 10^\circ$  from the original molecular plane.

## B. Amino Acid and Derivatives

*Glycine.* Single crystals of irradiated glycine were first investigated by Uebersfeld and Erb<sup>138</sup> who noted the anisotropy in the hyperfine interaction. A more detailed analysis was conducted by

Ghosh and Whiffen,<sup>39</sup> who were able to derive the magnetic parameters for the  $\alpha$  proton,  $A_i(H)$ , the  $\beta$  protons,  $A_i(H_\beta)$ , and also the  $\beta$  nitrogen,  $A_i(N_\beta)$ . Direct determination of the spin density at the  $\beta$  position can in this case be experimentally determined because of the spin and magnetic moment of the nitrogen nucleus in the radical  $\text{NH}_3^+ - \dot{\text{C}}\text{H} - \text{CO}_2^-$ . As shown in Table III, line 1, the values of  $A_1(H_\alpha)$  are, for reasons unknown, somewhat high. Interpretation of the data is consistent with the theoretical predictions of a negative spin density on the nitrogen nucleus and  $\alpha$  protons, and a positive density for the nitrogen protons. The latter three nuclei have an almost isotropic equivalent coupling constant and hence it is assumed that tunneling or rotation of the  $\text{NH}_3^+$  group is occurring. The approximate spin densities for the various orbitals have been calculated to be

$$\begin{aligned}\rho_{2p}(C_\alpha) &\approx +1, & \rho_{1s}(H_\alpha) &= -0.053, & \rho_{2s}(N_\beta) &= -0.006, \\ \rho_{2p}(N_\beta) &\approx +0.015, & \rho_{1s}(H_\beta) &= +0.037 \text{ each}\end{aligned}$$

The orientation in the crystal of the radical is apparently the same as the parent molecule.

*N-Acetylglycine.* Irradiated *N*-acetylglycine, investigated by Miyagawa,<sup>106</sup> Kurita, and Gordy, demonstrated a doublet hyperfine structure which apparently arises by hydrogen removal from the methylene group. The radical is presumed to be  $\text{RNH}\dot{\text{C}}\text{H}(\text{CO}_2\text{H})$ . From the magnetic parameters (Table III, line 2) it is deduced that the spin density at the carbon site  $\rho_{2p}(C_\alpha) = 0.72$ . The bond axis for the  $\dot{\text{C}}-\text{H}$  fragment is in the molecular plane, the resultant of re-orientation of the methylene group after loss of a hydrogen. The direction of the principal values indicated to the authors that the CH bond approximately bisects the N—C—C angle. From the line broadening, the spin density on the nitrogen was estimated at  $\rho_{2s}(N_\beta) \leq 0.06$ .

*Glycyl glycine.* The spectra of  $\gamma$ -irradiated glycyl glycine was investigated by Katayama and Gordy<sup>71</sup> who concluded that the free radical species was due to removal of a hydrogen from the methylene group adjacent to the  $\text{COO}^-$ . The spectra contained only partially resolved lines from which the  $\alpha$  coupling constants were calculated (Table III, line 3). An estimate of the nitrogen coupling terms was also made and the spin density at the nitrogen nucleus estimated at

TABLE III. Hyperfine Coupling

Line	Molecule	Radical	$A_i(H_\alpha)$			
			$A_1$	$A_2$	$A_3$	$a$
A. Amino Acid						
1	Glycine	$\text{NH}^+\dot{\text{C}}\text{HCO}_2^-$	-36	-80	-109	-75
2	Acetylglycine	$\text{H}_3\text{CCONH}\dot{\text{C}}\text{HCOOH}$	-28	-47	-76	-50
3	Glycyl glycine	$\text{RNH}\dot{\text{C}}\text{HCO}_2^-$	25	53	79	
4	Glycyl glycine	$\text{RNH}\dot{\text{C}}\text{HCO}_2^-$	-24.1	-47.0	-82.7	-51.3
5	Alanine	$\text{CH}_3\dot{\text{C}}\text{HNH}_2(\text{CO}_2\text{H})$	19.6	76	76	-56
6	Alanine	$\text{CH}_3\dot{\text{C}}\text{HNH}_2(\text{CO}_2\text{H})$	-25	-49.8	-89.4	
7	Alanine	$\text{CH}_3\dot{\text{C}}\text{HNH}_2(\text{CO}_2\text{H})$				
8	L-Cystine dihydrochloride	$(\text{CO}_2\text{H})\text{CH}(\text{NH}_2)\dot{\text{C}}\text{HS}$				
9	Methyl urea	$\dot{\text{C}}\text{H}_2\text{NHCO}(\text{NH}_2)$	28	59	67	50
10	Ethyl urea	$(\text{H}_3\text{C})\dot{\text{C}}\text{HNHCO}(\text{NH}_2)$				
11	Aspartic acid	$\text{CH}_3\text{CH}_2\dot{\text{C}}\text{H}_3\text{COOH}$				
12	Isovaline	$\text{CH}_3\text{CH}_2\dot{\text{C}}\text{H}_3\text{COOH}$				
13	Dimethylglyoxime	$\text{R}-\text{C}(\text{CH}_3)_2\dot{\text{N}}^+\text{OH}$				
B. Glycollic						
14	Glycollic acid	$\text{HOCH}(\text{CO}_2\text{H})$	-30	-55	-86	-57
15	Glycollic salt	$\text{HO}\dot{\text{C}}\text{HCO}_2^-$	-23	-50	-80	-57
16	Diglycollic acid hydrate	$(\text{HO}_2\text{C})\text{CH}_2\text{O}\dot{\text{C}}\text{H}(\text{CO}_2\text{H})$	31	53	73	52
17	Thiodiglycollic acid	$(\text{HO}_2\text{C})\text{CH}_2\text{S}\dot{\text{C}}\text{H}(\text{CO}_2\text{H})$	-19	45	64	42

<sup>a</sup> Ghosh, D. K., and Whiffen, D. H., *Mol. Phys.* **2**, 285 (1959).<sup>b</sup> Miyagawa, I., Kurita, Y., and Gordy, W., *J. Chem. Phys.* **33**, 1599 (1960).<sup>c</sup> Katayama, M., and Gordy, W., *J. Chem. Phys.* **35**, 117 (1961).<sup>d</sup> Lin, W. C., and McDowell, C. A., *Mol. Phys.* **4**, 33 (1961).<sup>e</sup> Miyagawa, I., and Gordy, W., *J. Chem. Phys.* **32**, 255 (1960).<sup>f</sup> Morton, J. R., and Horsfield, A., *J. Chem. Phys.* **35**, 1142 (1961).<sup>g</sup> Horsfield, A., Morton, J. R., and Whiffen, D. H., *Mol. Phys.* **4**, 425 (1961).<sup>h</sup> Kurita, Y., and Gordy, W., *J. Chem. Phys.* **34**, 282 (1961).

Constants, Mc/sec

$A_i(H\beta)$				$A_i(N_{\alpha,\beta})$				Ref.
$A_1$	$A_2$	$A_3$	$b$	$A_1$	$A_2$	$A_3$	$b$	
<i>Derivatives</i>								
+41	+50	+64	+53	-59	-11.5	-12.1	-9.8	a
								b
				6	8	11		c
								d
			73					e
$\beta_1 67.0$	} 300°K							
$\beta_2 67.5$			70					f
$\beta_3 76.5$								
$\beta_1 120$	} 77°K							
$\beta_2 76$			70					g
$\beta_3 14$								
		$\begin{cases} b(H_1) \approx 25 \\ b(H_2) \approx 5 \end{cases}$						h
								i
		64						j
		$\begin{cases} b_1(\text{CH}_2) = 116 \\ b_2(\text{CH}_2) = 20 \end{cases}$						k
		$b(\text{CH}_3) = 65$						k
		$b_1(\text{CH}_2) = 22-31$						k
		$b_2(\text{CH}_2) = 106-112$						l
		126		70	70	89		
<i>Acid Derivatives</i>								
-7	+4	+28	+8				$c(H_\gamma)$	m
8	12	18	7					n
							14	o
							15.5	o

<sup>1</sup> Anderson, R. S., and Jaseja, T. S., *Proceedings of the Fifth International Symposium on Free Radicals, July 1961*, Almqvist and Wiksell, Stockholm.

<sup>1</sup> Jaseja, T. S., and Anderson, R. S., *Bull. Am. Phys. Soc.* **6**, 247 (1961).

<sup>k</sup> Jaseja, T. S., and Anderson, R. S., *J. Chem. Phys.* **36**, 1098 (1962).

<sup>1</sup> Miyagawa, I., and Gordy, W., *J. Chem. Phys.* **30**, 1590 (1959).

<sup>m</sup> Atherton, N. M., and Whiffen, D. H., *Mol. Phys.* **3**, 1 (1960).

<sup>n</sup> Atherton, N. M., and Whiffen, D. H., *Mol. Phys.* **3**, 103 (1960).

<sup>o</sup> Kurita, Y., and Gordy, W., *J. Chem. Phys.* **34**, 1285 (1961).

$\rho(N_\beta) < 0.05$ . Similarly, an evaluation of that on the  $\alpha$  carbon is given as  $\rho_{2p}(C_\alpha) \approx 0.75$ . The results were confirmed by Lin and McDowell with values of the coupling constants (Table III, line 4) corresponding to  $\rho_{2p}(C_\alpha) = 0.80$ .<sup>82</sup>

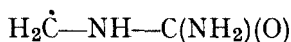
*L-Alanine.* The spectra of alanine was first studied by van Roggen, van Roggen, and Miyagawa and Gordy.<sup>105,120</sup> The radical, on analysis of the data, was found to be a  $\text{CH}_3\dot{\text{C}}\text{HR}$  (R, indicating a group with no detectable coupling). The  $\alpha$  proton hyperfine splitting was analyzed in terms of point dipole coupling with the unpaired electron and hence the indicated constants (Table III, line 5) show, as expected, cylindrical symmetry. The methyl  $\beta$  protons displayed an equivalent isotropic coupling and so it can be assumed that rapid rotation of the group occurs at this temperature. The spectra was complicated by the "forbidden transition" spectra, and detailed analysis of these transitions is given. The spin density at each of the methyl protons is calculated to be  $\rho_{1s}(H_\beta) = 0.05$ . A more complete analysis of the radical was also made by Morton and Horsfield with somewhat different values for the  $\alpha$  proton coupling constants<sup>108</sup> (Table III, line 6) indicating that axial symmetry does not exist for this coupling. The cylindrical symmetry of the methyl protons was verified with the axis of symmetry being the C—CH<sub>3</sub> bond. The work was extended to low temperature investigations of the methyl group by Horsfield, Morton, and Whiffen.<sup>58,59</sup> At 77°K the rotation frequency was found to be less than the hyperfine coupling frequency, for the three methyl protons gave non-equivalent coupling constants. The constants for each proton (Table III, line 7) correspond to a value of  $B = 138$  Mc/sec and an angle of  $\theta = 18^\circ$  for the projection of a CH bond of the methyl group with the perpendicular to the radical plane.

*L-Cystine dihydrochloride.* An interesting effect has been noted in the investigation of the nature of the free radical produced in L-cystine dihydrochloride by Kurita and Gordy<sup>73</sup> who found it necessary to hypothesize a reorientation of the radical to account for the observed effects. The disulfide bond is broken during irradiation and the unpaired electron can be considered to reside on the sulfur site, i.e.  $-\text{CH}_2\dot{\text{S}}$ . A relatively strong  $g$ -anisotropy,  $g_1 = 2.003$ ,  $g_2 = 2.029$ ,  $g_3 = 2.052$ , confirms this hypothesis of a  $\pi$  electron centered on an atom of large spin-orbit coupling,  $\zeta$ . For sulfur,  $\zeta = 382 \text{ cm}^{-1}$  as compared with  $\zeta = 28 \text{ cm}^{-1}$  for carbon. The



hyperfine structure consisting of an isotropic doublet denoted that only one of the methylene protons was in a favorable orientation with respect to the  $3p$  orbital of the sulfur. The authors thus postulated a reorientation of the  $\text{S—H—}(\beta_1)\text{—H}(\beta_1)$  group about the  $\text{C—C}$  bond into a *cis* configuration. The resultant geometry favors coupling to only one of the protons, in agreement with experimental results.

*Urea compounds.* The nature of the radicals formed by irradiation of single crystals of various urea compounds was investigated by Anderson and Jaseja.<sup>3</sup> No resonances were observed in urea or thiourea presumably due to the short lifetime of the radicals. In methyl urea the spectrum was analyzed as due to



with the methylene protons providing the hyperfine structure. The coupling values are indicated in Table III, line 9. The radical produced in ethyl urea,  $\text{H}_3\text{C—}\dot{\text{C}}\text{H—NH—CO(NH}_2\text{)}$ , showed also an isotropic  $\beta$  coupling corresponding to a spin density at each proton of  $\rho_{1s}(H_\beta) = 0.045$ . They calculated a corresponding reduction in  $\alpha$  carbon spin density of  $\rho_{2p}(C_\alpha) = 0.865$ . From the orientation dependence of the  $\alpha$  proton splitting it was deduced that the  $\dot{\text{C}}\text{H}$  bond direction corresponded to a crystal axis. From the line width measurements an upper limit on nitrogen spin density was placed at  $\rho(N_\beta) < 0.002$ .

*DL-Aspartic acid.* Jaseja and Anderson<sup>66</sup> investigated the radical formed from X-irradiated aspartic acid. The radical formed was found to be  $(\text{CO}_2\text{OH})\text{CH}_2\dot{\text{C}}\text{H}(\text{COOH})$  derived from removal of the  $\text{NH}_2$  group. The two methylene  $\beta$  splittings were unequal, 116 Mc and 20 Mc (Table III, line 11), corresponding to a twist of the methylene axis of  $\psi = 31^\circ$ .

*DL-Isovaline.* Similar results were found for isovaline, also investigated by Jaseja and Anderson.<sup>67</sup> Upon  $\gamma$ -irradiation, the  $\text{NH}_2$  group is lost to form the radical indicated in Table III, line 12. The methyl group  $\beta$  interaction was found to be isotropic, indicating free rotation, while the methylene group  $\beta$  interaction shows unequal splittings of each proton along with a small anisotropic contribution. No  $\gamma$  interaction of the end methyl group was detected. Assuming  $B = 112$  Mc/sec as for  $(\text{CH}_3)_2\dot{\text{C}}\text{OH}$  and

$\rho_{2p}(C_\alpha) \approx 1$  the results indicated that the methylene H—C—H group must be twisted  $\psi = 31^\circ$  with respect to the C—C axis, as it is for *dl*-aspartic acid.

*Dimethylglyoxime.* An interesting example of irradiation damage was investigated by Miyagawa and Gordy in the radical produced from dimethylglyoxime.<sup>104</sup> The triplet hyperfine structure was deduced as being due to the nitrogen magnetic moment, thus indicating that instead of a hydrogen removal due to irradiation, only an ionization of a non-bonding electron had taken place. The coupling parameters (Table III, line 13) indicate a cylindrical symmetry and the authors deduce that the free electron is in an  $sp^2$  orbital, whose calculated *s* character is 0.19. The reduction from the expected value of 0.33 is ascribed to possible approximations of their treatment and/or distortion caused by the molecular field. The value for the isotropic coupling, *a*, is between that of NO (30 Mc) and NO<sub>2</sub> (131 Mc).

### C. Glycollic Acid and Derivatives

*Glycollic acid.* Gamma-irradiation of glycollic acid has been shown by Grant, Ward, and Whiffen<sup>44</sup> to give rise to the HO— $\dot{C}H$ —COOH radical. A study by Atherton and Whiffen<sup>4</sup> on single crystals of this molecule gave additional information on the nature of the  $\beta$ -coupling for the hydroxyl proton. While  $\alpha$ -couplings are in agreement with other radicals (Table III, line 13), it is apparent that since the isotropic component, *b*, is only 8 Mc, the hydroxyl proton must lie quite close to the plane of the radical (i.e.  $\cos \theta \ll 1$ ). However, the relatively large values of the anisotropic component indicate a carbon- $\beta$ hydrogen distance of about 1.7 Å. The combination of both factors lends an explanation for the failure to detect OH proton interactions in polycrystalline irradiated alcohols, for the combination of large anisotropic and small isotropic terms would result in a broadened  $H(\alpha)$  spectrum without further resolution. The forbidden  $\Delta m_I = \pm 1$  transitions were also noted in the spectra and discussed briefly. Values of the spin densities are calculated to be

$$\rho_{1s}(H_\alpha) = 0.040, \quad \rho_{1s}(H_\beta) = 0.006$$

The potassium salt was also investigated (Table III, line 14).<sup>5</sup> The values of the  $A_i(H_\alpha)$  isotropic term are somewhat lower in this

case, while the anisotropic values for  $A_i(H_\beta)$  are appreciably different and the sign is undetermined.

*Thiodiglycollic acid.* A study of the substituted glycollic acids, diglycollic acid hydrate and thiodiglycollic acid has been made by Kurita and Gordy<sup>74</sup> to find the effect of an interposed sulfur or oxygen atom. The data indicated that the radical has  $A_i(H_\alpha)$  values (Table III, line 15) in agreement with other determinations. However, the methylene protons which are in  $\gamma$  position with relation to the  $\pi$  electron gave a measurable isotropic hyperfine interaction ( $\equiv c(H_\gamma)$ ). The presence of non-magnetic nuclei in the  $\beta$  position rendered this observation possible. The thiodiglycollic acid was investigated intensively in order to obtain a value for the spin density at the sulfur site. From the relatively large  $g$  shifts,  $g_1 = 2.002$ ,  $g_2 = 2.005$ ,  $g_3 = 2.011$ , the relative probabilities of the structures



were determined as 0.22, 0.60, and 0.16 respectively, corresponding to a spin density distribution  $\rho_{2p}(C_\alpha) = 0.60$ ,  $\rho_{1s}(H_\gamma) = 0.01$ ,  $\rho_{3p}(S) = 0.22$ .

#### IV. TRIPLET STATE STUDIES

One of the most exciting breakthroughs in experimental techniques has been the detection of triplet states by electron paramagnetic resonance. The long-lived phosphorescence properties of many complex organic molecules had been attributed by Lewis, Lipkin, and Magel<sup>80</sup> and Terenin<sup>132</sup> to their being excited into a triplet state. Since the total spin for this state is  $S = 1$ , it should exhibit a photomagnetism and also be detectable by the paramagnetic resonance technique. Early results of Lewis and Calvin<sup>76</sup> on fluorescein in boric acid verified the existence of photo-induced static susceptibility while a more thorough study by Lewis, Calvin, and Kasha<sup>77</sup> gave quantitative agreement with expectations. However, a painstaking search by many laboratories using electron paramagnetic resonance yielded negative results until Hutchison and Mangum,<sup>60, 62</sup> by using single dilute crystals of naphthalene in durene, were able to detect the presence of the triplet state. The

possibilities of the technique were greatly enhanced by the findings of van der Waals and de Groot<sup>46, 139</sup> who showed that the triplet state could also be detected in a polycrystalline or glassy matrix, by observing the forbidden transitions. Utilizing this procedure, the presence and properties of a great many aromatic, substituted aromatic, and heterocyclic compounds have been determined.<sup>125</sup> Studies of energy transfer between triplet states have been made,<sup>126, 127</sup> as well as studies on the possible role of triplet states in sensitizing photo-reactions.<sup>127, 128</sup> The previous failures have been attributed by Weissman<sup>143</sup> and others to the large anisotropy produced by the dipolar coupling of the individual spins comprising the  $S = 1$  state. The static dipolar broadening in randomly oriented molecules would be expected to produce a line width for the case of naphthalene from Hutchison's observations of about 2100 oersteds. Use of a fluid medium to produce "motion narrowing" requires, unfortunately, correlation times which produce strong spin-lattice relaxation and a corresponding excessive line broadening.

### A. Zero-Field Splittings

The theory of paramagnetic resonance spectra in crystals has been derived by Abragam and Pryce wherein effects due to crystal-line electric field, along with spin-orbit and spin-spin interactions, are considered.<sup>1</sup> The results, interpreted in terms of a "Spin Hamiltonian" wherein orbital effects are contained as parameters, have been extremely useful in interpretation of transition group spectra. For the case of spin,  $S = 1$ , in an orthorhombic field, Griffith and Owen have found that the behavior of the energy levels can be described in terms of the Hamiltonian<sup>45</sup>

$$\mathcal{H} = g\beta H \cdot S + DS_z^2 + E(S_x^2 - S_y^2) \quad (10)$$

wherein  $D$  and  $E$  are appropriate constants and  $S_i$  are the components of the spin vector. The energy levels,  $W_i$  in strong<sup>131</sup> fields and  $w_i$  in weak fields, have been shown to have the form given in Table IV in terms of the magnetic quantum number  $S_z$ , 1, 0, -1, and for quantization along the  $x$ ,  $y$ ,  $z$  axes, along which the external magnetic field is directed. Since the  $g$ -values have been found to be quite isotropic, the equations have been simplified accordingly. The

TABLE IV. Energy Levels for  $S = 1$  State in Orthorhombic Crystalline Field for Strong ( $W_i$ ) and Weak ( $w_i$ ) Magnetic Fields

$S_z$	$z$	Axis of quantization $x$	$y$
$\left\{ \begin{array}{l} +1 \end{array} \right\}$	$W_1$	$D + g\beta H + E \tan \theta_z$	$\frac{1}{2}(D - E) + g\beta H + \frac{1}{2}(D - E) \tan \theta_y$
	$w_1$	$D + [E^2 + (g\beta H)^2]^{\frac{1}{2}}$	$\frac{1}{2}(D - E) + \left[ \left( \frac{D - E}{2} \right)^2 + (g\beta H)^2 \right]^{\frac{1}{2}}$
$\left\{ \begin{array}{l} 0 \end{array} \right\}$	$W_2$	0	$\frac{D + E}{D + E}$
	$w_2$	0	$\frac{D + E}{D + E}$
$\left\{ \begin{array}{l} -1 \end{array} \right\}$	$W_3$	$D - g\beta H - E \tan \theta_z$	$\frac{1}{2}(D - E) - g\beta H - \frac{1}{2}(D - E) \tan \theta_y$
	$w_3$	$D - [E^2 + (g\beta H)^2]^{\frac{1}{2}}$	$\frac{1}{2}(D - E) - \left[ \left( \frac{D - E}{2} \right)^2 + (g\beta H)^2 \right]^{\frac{1}{2}}$
	$\tan 2\theta_z \equiv E/g\beta H$	$\tan 2\theta_z \equiv -(D + E)/2g\beta H$	$\tan 2\theta_y \equiv (D - E)/2g\beta H$

transition probabilities between states  $i$  and  $j$ ,  $T_{ij}$ , for the field quantized on the  $z$  axis are<sup>45</sup>

$$\begin{aligned} T_{12} &= 1 + \sin 2\theta \cos 2\alpha \\ T_{23} &= 1 - \sin 2\theta \cos 2\alpha \\ T_{13} &= 0 \end{aligned} \quad (11)$$

where  $\alpha$  is the angle between the radio frequency field and the  $x$  axis in the  $xy$  plane. It should be noted, as expected, that the  $\Delta m \pm 2$  transition,  $T_{13}$ , is forbidden for strong fields. The energy difference between the  $W_{12}$  and  $W_{23}$  resonances from Table IV for  $z$  quantization is  $2D$ , giving rise to two lines,  $2D$  apart.

### (1) *Experimental Determinations*

The values of  $D$  and  $E$  derived by Hutchison and Mangum for naphthalene are  $D = +0.1003 \text{ cm}^{-1}$ ,  $E = -0.0137 \text{ cm}^{-1}$ . The assigned sign for the parameters is made on the basis of relative EPR intensity observations at  $4.2^\circ\text{K}$  by Hornig and Hyde.<sup>55</sup> The relation between the spin-spin interaction term (Eq. (8) with  $S \rightarrow S_1$ ,  $I \rightarrow S_2$ ,  $\mu_N \rightarrow \mu_e$ ) and its formalization in terms of the zero-field splitting term,  $D$  (ignoring  $E$ ), can be seen by considering the form of the diagonal part of the matrix, Eq. (9), where it is apparent that for  $S_{1z} = S_{2z} = \pm \frac{1}{2} (S_z = \pm 1)$  the interaction is positive, while for  $S_{1z} = -S_{2z} (S_z = 0)$  it has a negative value. The difference in energy between the states (quantized on the  $z$  axis) is thus  $\pm D$ . The  $E$  term is identically zero for molecules having a three-fold symmetry axis (or higher) and is a measure of the departure from symmetry in the molecular plane. Thus while for benzene, triphenylene, or coronene,  $E = 0$ , one can expect its value to increase as one proceeds down the polyacene series—naphthalene, anthracene, and tetracene.

The determination of the  $D$  values for the various organic phosphors by the single-crystal technique presents a tedious task to the experimenter. Thus the discovery by van der Waals and de Groot<sup>139</sup> of the "forbidden transition" technique of measuring triplet state properties in glassy matrices represents an important development to work in this field. Their papers present a detailed development of the theory for the cases when the radio frequency field,  $H_1$ , is parallel and perpendicular to the static magnetic field  $H$ ,

the latter case corresponding to conventional spectrometers. Transition probabilities are determined as functions of the random orientation of the spin vector with respect to  $H$  and the resultant line shapes are deduced. For the parallel case,  $H_1 \parallel H$ , a two-peak absorption curve is calculated corresponding to values of field defined as  $H_0$  and  $H_{\min}$ , while for  $H_1 \perp H$ , a single peak occurs at  $H_{\min}$ . For the case of  $E \ll D$ , and provided,  $D/h\nu < 3/4$  ( $\nu$  = operating frequency of the spectrometer), the values of  $H_0$  and  $H_{\min}$  are given by the relation

$$\frac{g\beta H_{\min}}{h\nu} = \left\{ \frac{1}{4} - \frac{1}{3} \left( \frac{D}{h\nu} \right)^2 \right\}^{1/2} \quad (12)$$

$$\frac{g\beta H_0}{h\nu} = \frac{1}{2} \left\{ 1 - \left( \frac{D}{h\nu} \right)^2 \right\}^{1/2} \quad (13)$$

For  $E$  not negligible, Eq. (12) must be corrected by substituting for  $D$ ,  $D_1 \equiv D(1 + 3E^2/D^2)^{1/2}$ . No simple correction exists for Eq. (13). For  $D/h\nu \ll 1$ , the latter relation is easily derivable also from Table IV. The zero-field splittings  $D_1$  (in  $\text{cm}^{-1}$ ) for several phosphors are calculated by de Groot and van der Waals<sup>46</sup> to be for triphenylene, 0.134; coronene, 0.096; 1,3,5-triphenylbenzene, 0.111; naphthalene, 0.1048.

The technique has been exploited by the author<sup>125</sup> to determine  $D_1$  for a great many organic phosphors. The results are given in Table V for a series of aromatics, substituted aromatics and heterocyclics. Unfortunately, the  $E$  value cannot be determined and it may assume importance in those molecules having reduced symmetry properties. Qualitative conclusions on the variation of  $D_1$  in homologous series or compounds are apparent. The polyacene series, benzene, naphthalene, and anthracene, shows decreasing values of  $D_1$  with increasing molecular size or "space" for the unpaired electrons to separate. Similarly for the benzene, diphenyl, terphenyl series. The effect of substitution of nitrogen for carbon has little effect as is apparent from comparison of naphthalene, quinoline, fluorene, and carbazole. The five-membered rings show appreciably higher coupling than do the six-membered rings, e.g., indole vs. quinoline or naphthalene and fluorene vs. anthracene.

While calculations of the dipolar interaction would appear to be beset with difficulties because of the  $R^{-3}$  dependence, McConnell<sup>89</sup> has shown that the Pauli exclusion principle confines the two

TABLE V. Zero-Field Splittings and Line Widths for Forbidden Transitions of Various Phosphors

	$\frac{D_1 \times 10^3 \text{ cm}^{-1} \text{ }^a}{(\text{P.E.} \pm 0.15)}$	$\frac{\Delta H}{\text{oersteds}} \frac{\text{ }^a}{(\text{P.E.} \pm 0.7)}$
Benzene	15.93	18.1
Naphthalene	10.49	11.2
Anthracene	7.70	11.9
Diphenyl	11.30	12.6
Terphenyl	9.61	9.1
Triphenylene	13.53	7.9
Phenanthrene	13.35	12.2
Chrysene	10.52	10.1
Coronene	9.71	7.0
Pyrene	9.29	11.5
3,4-Benzpyrene	7.58	10.2
Fluorene	10.96	13.7
Benzoic acid	13.85	15.8
Hydroquinone <sup>b</sup>	13.21	11.5
Aniline <sup>b</sup>	13.17	45.0
Diphenylamine	9.94	21.8
Indole	12.77	16.5
Quinoline	10.68	14.9
Carbazole	10.44	11.1

<sup>a</sup>  $D_1 = [D^2 + 3E^2]^{1/2}$ . Although the parameter  $E \neq 0$  for molecules of lower than three-fold symmetry, it has been assumed negligible except as indicated in the text.

<sup>b</sup> Spectra complex.

electrons of parallel spins to orbitals antisymmetric in the space variables and thus the calculations should be fairly reliable. A theoretical evaluation of the parameters has been made by Gouterman and Moffitt<sup>43</sup> in terms of a prototype ethylene triplet molecule. The results were then applied by Gouterman<sup>42</sup> to various aromatics.



(It should be noted that in his paper the derived parameters are  $D'$  and  $E$  where  $D' = \frac{1}{3}D$ .)

## (2) *Theoretical Basis*

The theoretical calculations are based on a nomenclature of molecular spectra developed by Platt in terms of a "free-electron orbital" model.<sup>103</sup> The orbitals are those of a quantized plane rotator of energy

$$E_q = q^2 h^2 / 2ml^2 \quad (14)$$

where  $q$  is a running integer,  $h$  Planck's constant,  $m$  the electron mass, and  $l$  the perimeter of the orbital. The levels are doubly degenerate since clockwise or counterwise rotation is permitted (along with a double degeneracy due to spin). The orbital quantum number,  $q$ , of each electron adds algebraically to form the total ring quantum number,  $Q$ . In a cata-condensed system of  $n$  rings, each of the  $2(n+1)$  carbons contributes one  $\pi$  electron which will fill successive shells. The highest filled shell with  $q = n$  has four electrons designated as  $f$  electrons; the next highest (empty) shell with  $q = n+1$  is the  $g$  shell. In an optical transition of an  $f$  electron to a  $g$  shell,  $Q = (n+1) \pm n$ , since the quantum numbers may add or subtract, corresponding to an excited state of  $Q = 1$  or  $(2n+1)$ . The state designation for  $Q$  values of 0, 1, 2, are  $A$ ,  $B$ ,  $C$ , and for  $Q = 2n$ ,  $2n+1$ ,  $2n+2 \dots$  are  $K$ ,  $L$ ,  $M \dots$ . Thus the excited state designations are, for an  $f^3g$  configuration, of eight types,

$$1, {}^3B_{a,b}, \quad 1, {}^3L_{a,b}$$

The superscripts correspond to the spin configuration and the sub-letters correspond to the possible degeneracy in angular momentum. The former degeneracy is removed by spin-orbit coupling and the latter by introduction of periodic potentials and cross links. In a standing-wave representation of the degeneracy, represented by the  $a$  and  $b$  subscripts, each set will have  $2Q$  nodal points along the perimeter and will be orthogonal to the other. The relation between the above designation and group theory notation is given by Platt<sup>103</sup> and will not be repeated here. The correlation of this classification with experimental data is provided also in later papers.<sup>72, 103, 114</sup>

The treatment has been extended to include electronic interaction by Ham and Ruedenberg and the transition energies,

intensities, and polarizations carried out for the main UV transitions.<sup>48, 49</sup> The transitions considered are from the two-fold-degenerate ground-state free-electron orbitals (in a cylindrical potential)

$$b_1 \sim \cos M\theta \quad b_2 \sim \sin M\theta,$$

$M$  being a running number, and  $\theta$  the angle around the axis perpendicular to the molecular plane, going through the center of the molecule. The excited states conform to the lowest degenerate unfilled orbitals

$$c_1 \sim \cos (M+1)\theta \quad c_2 \sim \sin (M+1)\theta$$

A correct representation of the excitation state requires thus a 2-electron function and determines the symmetry property of the state. The four triplet states  ${}^3L_a$ ,  ${}^3L_b$ ,  ${}^3B_a$ ,  ${}^3B_b$  correspond to a different state function  ${}^s\Phi_s$  which can be represented in general in terms of the excitation wave functions  ${}^s\phi(b_ic_j)$  by

$${}^s\Phi_s = \sum_{j=1}^2 \sum_{i=1}^2 {}^sk_{ij} {}^s\phi(b_ic_j) \quad (15)$$

where the superscript  $s$  is the multiplicity ( $= 3$  for triplet states). For molecules with at least one plane of symmetry only two excitation functions are necessary, which on normalization permit the coefficients  ${}^sk_{ij}$  to be expressed as trigonometric functions of an angle,  $\gamma$ . A table of these coefficients is contained in the original paper as well as the transition energies for the theoretically possible states of many organic molecules.<sup>49</sup>

For the treatment of the ethylene triplet state zero-field splitting, the perturbation energy to be evaluated is  $\int \psi_T \mathcal{H}_s \psi_T d\tau$  with  $\psi = [a(1)b(2) - b(1)a(2)]$ . Corresponding to  $a$  and  $b$  are the  $p_x$  orbitals of the two carbon atoms having a bond axis in the  $z$  direction. The parameters  $D$  and  $E$  are expressible in terms of the expectation values, respectively

$$\langle r_{12}^{-5} [3z_{12}^2 - r_{12}^2] \rangle$$

and

$$\langle r_{12}^{-5} [3x_{12}^2 - 3y_{12}^2] \rangle$$

The zero-field splitting is thus the result of first-order anisotropies in the electronic correlations. Similarly, the spin interaction  $\mathcal{H}_s$  of the

other excitation functions for the aromatics are built up from orbitals of an ethylene-like molecule. The integrals are evaluated both in terms of cyclic polyene and Hückel molecular orbitals. To Gouterman, the choice of coefficients is  $\theta$  and  $\phi$  in place of Ham and Ruedenberg's  $\gamma_b$  and  $\gamma_a$  with  $\phi = (\pi/2) - \gamma_a$ . The best fit with the naphthalene data required for the  ${}^3L_a$  state  $\phi = 38.5^\circ$  instead of the expected value<sup>48</sup> of  $80.7^\circ$ . (A later calculation corrects this value to  $58^\circ$ .) In any case the theoretical state assignment appears correct.

Theoretical comparison with experiment by the author for the other polyacenes were found to be in good agreement with the data for the  ${}^3L_a$  state provided  $\phi \approx 45^\circ$  for benzene as well as naphthalene and anthracene. For benzene, theory predicts this value of  $45^\circ$  from symmetry considerations. The difference in calculated  $\phi$  values for naphthalene is probably due to the insensitivity of the calculated  $D$  to  $\phi$  and because  $E$ , which must also fit the same  $\phi$  value, cannot be derived easily from the forbidden transition data. No agreement with theory for phenanthrene was apparent although Chiu<sup>19</sup> has indicated a calculation yielding somewhat better agreement.

A theoretical determination of the zero-field splitting has also been made by Hamerka<sup>50</sup> for the triplet state of benzene using a straightforward calculation of both spin-spin and spin-orbit perturbation. The wave functions were those used by Goeppert-Mayer and Sklar.<sup>41</sup> His results showed that spin-orbit coupling could be neglected while the spin-spin interaction gave a double-singlet separation of  $D = 0.15 \text{ cm}^{-1}$  for the  ${}^3B_{1u}$  state and  $0.09 \text{ cm}^{-1}$  for the  ${}^3B_{2u}$  state. These correspond in Platt's notation to the  ${}^3L_a$  and  ${}^3L_b$  state respectively and hence the agreement with experimental results confirms the  ${}^3L_a$  state as being the proper lowest triplet state.

McWeeny<sup>101</sup> has developed a general theory for calculating the parameters  $D$  and  $E$  in terms of a "coupling anisotropy function" defined in terms of a two-electron density matrix. Using a series of approximations including replacement of the  $p$  orbital by  $\frac{1}{2}$  point charges at the position of most probable nuclear-electron distances in each lobe, he has derived the values of  $(D + E) = 0.107 \text{ cm}^{-1}$ ,  $(D - E) = 0.066 \text{ cm}^{-1}$ .

Not considered in the above calculations is the contribution to the zero-field splitting of the induced spin densities due to the spin polarization effects. As indicated by McConnell<sup>90</sup> neighboring

carbon atoms will have induced spin densities of opposite sign because of the fact that the  $\pi$ - $\sigma$  interaction produces positive spin density at the carbon nucleus containing the unpaired  $\pi$  electron while the  $\pi$ - $\pi$  interaction will result in negative spin density at the neighboring carbon site. This anti-parallel spin configuration, i.e. positive spin-negative spin at adjacent sites, results in a negative contribution to the total electron dipolar interaction,  $D$ .

McLachlan,<sup>99</sup> by using either an extended Hartree-Fock or a molecular orbital with configurational mixing treatment, demonstrated that the negative spin densities induced by the excited electron and "hole" are nearly the same as found for the radical ions. Indications are, however, that the negative contributions to the zero-field splittings from this effect are not enough to change the sign of  $D$ .

### B. Hyperfine Structure and Line Widths

Hutchison, from his single crystal naphthalene data, has calculated the hyperfine structure due to the  $\pi$ -electron interaction with the neighboring protons. Using Pariser's value for the spin density distribution,  $\rho_{1s}(H_\alpha) = 0.18$ ,  $\rho_{1s}(H_\beta) = 0.07$ ,<sup>111</sup> experimental values for the anisotropic coupling constants were determined to be  $A_2 = 76$  Mc/sec,  $A_3 = 115$  Mc/sec,  $A_1 = -30$  Mc/sec. Conversely, assuming the theoretical values of  $A_i$ , i.e.  $A_2 = 61.5$  Mc/sec,  $A_3 = -92.5$  Mc/sec, they derive a value of  $\rho_{1s}(H_\alpha) = 0.209$ , in good agreement with the value of Carrington, Dravnieks, and Symons of 0.218 for the naphthalene negative ion.<sup>16</sup>

Although the anisotropic hyperfine structure is completely smeared out in observing the  $\Delta m = \pm 2$  transitions, the line width has been shown to be largely determined by the nuclear magnetic interaction. From the analysis of the line shape by de Groot<sup>46</sup> and van der Waals it would appear that second-order anisotropy effects determine the line width and thus its value would be dependent on the magnitude of the zero-field splitting. Table IV, column 3, shows, however, that the experimentally determined line widths are rather constant for most of the molecules. It is only for benzene that any appreciable  $D$  broadening can be ascertained. This reduced line-width effect is due to the asymmetry of the absorption line shape, that of an anisotropically broadened line, which has a sharply

TABLE VI. Effect of Deuteration on Triplet State EPR Line Widths (Oersteds)

Molecule	$\Delta H(\text{H, H})$ (solvent E.P.A.)	$\Delta H(\text{D, H})$	$\Delta H(\text{D, D})$ (solvent $\text{C}_2\text{D}_6\text{OD}$ )	$\frac{\Delta H(\text{H, H})}{\Delta H(\text{D, D})}$
Benzene	18.1	12.2	10.5	1.7
Naphthalene	11.2	4.6	4.2	2.7
Diphenyl	12.6	4.9	4.5	2.8
Phenanthrene	12.2	5.6	3.9	3.1
Anthracene	11.9	5.6	3.6	3.3

rising front at low fields, gradually falling off at high fields. The instrumentation used for signal detection, a dual-modulation system,<sup>130</sup> has an output signal approximately proportional to the second derivative of the absorption curve. This accentuation of the "step" character of the absorption yields line width which may be determined solely by hyperfine interaction. The nature of the line shape for *g*-anisotropically broadened lines has been investigated by Blinder<sup>10</sup> and Cochran and Adrian and Bowers<sup>20</sup> and has been used by McMillan and Smaller<sup>100</sup> to determine the *g*-values and hyperfine constants in cylindrically symmetric systems of silver and copper complexes. The line shape for the allowed  $\Delta m = \pm 1$  transitions has a similar step-type shape in polycrystalline material and the corresponding EPR signals in a glassy matrix have been detected by the author and by others. However, because of the increased line width, the signal intensities are reduced about one hundred-fold from that of the  $\Delta m = \pm 2$  forbidden transition.

Analysis of the line width data in Table V reveals that good correlation of  $\Delta H$  can be secured for most of the compounds with the ratio of hydrogen/carbon in the given molecule. These results were confirmed by comparison with  $\Delta H$  for the deuterated species as shown in Table VI. Using a deuterated solvent results in a further reduction in line width and indicates the extent of the interaction of the triplet orbital with the environment. The theoretical ratio of line widths for light and deuterated systems, if magnetic interaction is the only contribution, is 3.25. As the molecular size increases and the *D* anisotropy decreases the expected ratio is achieved. However,

it is surprising that the  $E$  anisotropy term, which is expected to increase with reduction of molecular symmetry, does not contribute to the line width.

### C. Lifetime Studies

In Lewis'<sup>78</sup> original paper proposing the identity of the phosphorescent state as that of an excited triplet, qualitative measurements of the lifetimes were also given in terms of short, intermediate, or long. Quantitative measurements were subsequently made by McClure,<sup>86</sup> among others who correlated the decay times with the spin-orbit coupling parameter  $\zeta$ . This interaction provides a mechanism for overcoming the zero-order forbiddenness of the  $T \rightleftharpoons S$  transition. Using halogen substituted aromatics with high atomic number and hence large  $\zeta$  a corresponding reduction in decay time was noted. For other substituted compounds, McClure considered a model whereby the excitation can be considered as residing in each component and thus the total decay probability can be considered to be composed of the sum of the probabilities of each component weighted by its relative contribution to the wave function of the compound molecule.

The anomaly still remained on the relatively high probability for the intersystem crossover of excited singlet to excited triplet ( $S_1 \rightarrow T_1$ ), while the corresponding triplet decay to the ground state ( $T_1 \rightarrow S_0$ ) probability remains very low.

Pariser<sup>111</sup> has attempted to resolve this difficulty by the introduction of an additional state designation: plus and minus states. Because of the two-fold degeneracy in state designation of excitation of an electron ( $i \rightarrow j'$ ,  $j \rightarrow i'$ ), the sets of states will be either of plus or minus type with transitions only allowed between plus and minus states. A similar derivation has been given by Pople.<sup>116</sup> Besides predicting a greater number of possible states, Pariser applies the concept to an explanation of the long decay time of the triplet states. It is assumed that the ground state is an  $S_0^-$ , which can excite to an  $S_1^+$  state. The latter can rapidly decay to the lowest singlet ( $k \sim 10^{11} \text{ sec}^{-1}$ ) excited state, which is assumed  $S^-$ . The fluorescence  $S_1^- \rightarrow S_0^-$  is not allowed ( $- \rightarrow -$ ) and so requires a relatively long time ( $k \sim 10^6 \text{ sec}^{-1}$ ). However,  $S_1^-$  will couple to an excited triplet  $T_1^-$  of equal energy and thus provide a relatively efficient mechanism for the  $S \rightarrow T$  conversion. Decay to the lowest

triplet ( $T_1^- \rightarrow T_1^+$ ) is rapid being an allowed transition, while the final decay of triplet to ground state  $T_1^+ \rightarrow S_0$  is spin forbidden and hence long lived. The anomaly is thus circumvented by the  $S_1^- \rightarrow T_1^-$  mechanism.

The work of Wright, Frosch, and Robinson<sup>151</sup> on the triplet lifetime at 4.2°K of light and deuterated benzene (Table VII) in different rare-gas solvents showed the striking effect of intermolecular spin-orbit perturbations on the triplet lifetime, as evidenced by the profound reduction in  $\tau$  with increasing  $Z$  of the solvent. The effect of the spin-orbit properties of the solvent on the spectral properties of phosphorescence was further investigated by Robinson,<sup>119</sup> who postulated the formation of a "complex" between solute and solvent, which then reduces the symmetry properties of the solute. (The term "complex" is used very loosely and may well be considered to be a weakly bonded system derived solely from van der Waals-type forces. The utility of this concept will be amplified in the next section.) The resultant introduction of additional previously forbidden states by this exchange interaction produces an increase in the phosphorescent yield, due to a higher probability of  $S_1 \rightarrow T_1$  intersystem crossover along with a marked reduction in triplet lifetime ( $T_1 \rightarrow S_0$ ). Suppression of this intermolecular mechanism by the use of low  $Z$  solvents permits a second intramolecular radiationless process of "tunneling" to determine the triplet lifetime. It was suggested by Shull<sup>123</sup> and Craig<sup>26</sup> that this intramolecular phosphorescence mechanism is vibrationally induced, and the effect of deuteration is due to the reduction in vibronic overlap between triplet and ground state. The lifetimes thus approach the radiation lifetimes calculated by Gilmore, Gibson, and McClure<sup>40</sup> from measurements on quantum yield for phosphorescence.

Electron paramagnetic measurements of the effect of deuteration on lifetime were made for naphthalene (Table VII), by Hutchison and Mangum,<sup>61</sup> but no apparent effect was noted due to deuteration of the durene matrix. Similar results were noted by de Groot and van der Waals,<sup>47</sup> using deuterated naphthalene in a (light) glassy matrix. The studies have been continued by the author for a series of light and deuterated aromatic phosphors in both light and deuterated matrices. The results, except possibly for anthracene, verify the role of deuteration in reducing the radiationless transition

TABLE VII. Effect of Molecular and Solvent Deuteration on Lifetime of Triplet States

Isotope	Solvent	Phosphor	$\tau$ , sec	Method	Ref.
H	CH <sub>4</sub>	Benzene	16	Phosphorescence	<sup>a</sup>
	Ar		16	Phosphorescence	<sup>a</sup>
	Kr		1	Phosphorescence	<sup>a</sup>
	Xe		0.07	Phosphorescence	<sup>a</sup>
D	CH <sub>4</sub>		22	Phosphorescence	<sup>a</sup>
	Ar		26	Phosphorescence	<sup>a</sup>
	Kr		1	Phosphorescence	<sup>a</sup>
	Xe		0.07	Phosphorescence	<sup>a</sup>
H	EPA	Naphthalene	7.0 $\pm$ 0.7	Phosphorescence	<sup>b</sup>
D	EPA		13.1 $\pm$ 1.0	EPR	<sup>c</sup>
D	EPA		17.1 $\pm$ 0.8	EPR	<sup>c</sup>
H	Durene ( <i>H</i> )		2.1 $\pm$ 0.9	EPR	<sup>d</sup>
D	Durene ( <i>H</i> )		16.9 $\pm$ 0.9	EPR	<sup>d</sup>
D	Durene ( <i>D</i> )		17	EPR	<sup>d</sup>
H	Glass ( <i>H</i> )		2.2	EPR	<sup>e</sup>
D	Glass ( <i>H</i> )		18	EPR	<sup>e</sup>
D	EPA		20.0 $\pm$ 0.5	EPR	<sup>c</sup>
	C <sub>2</sub> D <sub>5</sub> OD		23.1 $\pm$ 0.8	EPR	<sup>c</sup>
H	EPA	Diphenyl	4.4	Phosphorescence	<sup>f</sup>
D	EPA		11.2	EPR	<sup>c</sup>
D	C <sub>2</sub> D <sub>5</sub> OD		12.5	EPR	<sup>g</sup>
H	EPA	Phenanthrene	3.3	Phosphorescence	<sup>b</sup>
D	EPA		13.4	EPR	<sup>c</sup>
D	C <sub>2</sub> D <sub>5</sub> OD		15.5	EPR	<sup>g</sup>
H	EPA		0.09	Quantum yield	<sup>h</sup>
H	EPA		0.02	EPR	<sup>g</sup>
D	EPA		0.15	EPR	<sup>g</sup>
D	C <sub>2</sub> D <sub>5</sub> OD		< 0.2	EPR	<sup>g</sup>

<sup>a</sup> Wright, M. R., Frosch, R. P., and Robinson, G. W., *J. Chem. Phys.* **33**, 934 (1960).

<sup>b</sup> McClure, D. S., *J. Chem. Phys.* **17**, 905 (1949).

<sup>c</sup> Smaller, B., *J. Chem. Phys.* **37**, 1578 (1962).

<sup>d</sup> Hutchison, C. A., Jr., and Mangum, B. W., *J. Chem. Phys.* **32**, 1261 (1960).

<sup>e</sup> de Groot, M. S., and van der Waals, J. H., *Mol. Phys.* **4**, 189 (1961).

<sup>f</sup> Terenin, A., and Ermolaev, V., *Trans. Faraday Soc.* **52**, 1042 (1956).

<sup>g</sup> Smaller, B., unpublished results.

<sup>h</sup> Porter, G., and Windsor, M. W., *J. Chem. Phys.* **21**, 2088 (1953).



process. The effects of solvent deuteration in increasing the lifetime, however, may best be explained in terms of a solvent-solute "complex" previously invoked. The lifetime of the triplet state of anthracene remains short, contrary to expectations. Intensity measurements show, however, that the light anthracene lifetime is considerably shorter than that of the deuterated species, probably close to 20 msec. Thus deuteration may well correspond to a radiation lifetime, unaccountably short.

#### D. Energy Transfer Experiments

The mechanism of transfer of excitation between molecules has held the interest of investigators for many years. An excellent review of the subject has been given by Livingston<sup>85</sup> and by Förster.<sup>34, 35</sup> Excitation transfer in molecular crystals has been treated extensively by Davydov<sup>28</sup> and others.<sup>37, 87, 124, 150</sup> Dexter<sup>29</sup>

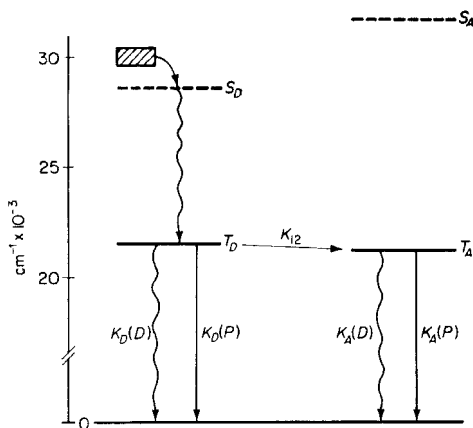


Fig. 3. Energy level scheme demonstrating energy transfer process,  $K_{12}$ , and triplet  $\rightarrow$  singlet phosphorescence,  $K_A(P)$ ,  $K_D(P)$ , and radiationless,  $K_A(D)$ ,  $K_D(D)$ , decay.

and Vavilov<sup>140</sup> have also given independent treatments of this problem. Excitation transfer between triplet states has been the subject of intensive investigation by Terenin and Ermolaev.<sup>30, 133-135</sup> The earlier literature on energy transfer and quenching effects is summarized in Pringsheim's excellent monograph.<sup>118</sup> The energy

transfer process is conventionally described in terms of an energy donor-acceptor system. For triplet-triplet transfer the relation between energy levels is as shown in Fig. 3 wherein the donor triplet level,  $T_{1D} > T_{1A}$ , the acceptor triplet level. In order to avoid obscuring the effect due to excited singlet  $\rightarrow$  triplet transfer ( $S_{1A} \rightarrow T_{1A}$ ) in the acceptor system the species are selected satisfying the condition that the excited singlet level of the donor,  $S_{1D} < S_{1A}$ . Using monochromatic light or suitable filters, the light is restricted to quanta  $h\nu$  such that  $S_{1D} < h\nu < S_{1A}$ , so that the energy transfer is as shown,  $S_{1D} \rightarrow T_{1D}$ ,  $T_{1D} \rightarrow T_{1A}$ . The return to the ground state  $S_0$  for both donor and acceptor may be either by phosphorescent emission  $K(P)$  or radiationless decay rate  $K(D)$ . For purposes of brevity they may be summed as a total decay rate,

$$K_D(P) + K_D(D) = K_D$$

for the donor triplet and similarly for the acceptor. The probability for transfer is indicated by  $K_{12}$ . In order to avoid the possibility of strong complexing effects<sup>31,97</sup> the pure aromatic system phenanthrene-naphthalene was studied by the author to determine the properties of the transfer parameter. Electron paramagnetic resonance, as previously stated, is ideally suited to this type of study since it enables one to determine independently and unambiguously the triplet state concentration of each component. Its value is especially enhanced in cases where the technique of observing the phosphorescence is obscured by overlapping of emission bands or where the decay to the ground state is entirely radiationless.

A typical EPR spectrum revealing the triplet energy transfer phenomenon is shown in Fig. 4. The emission of the exciting light is set by a monochromator to 3400 Å, so that the singlet state of naphthalene is unexcited and thus no triplet state signal appears for pure naphthalene. For pure phenanthrene, however, its triplet state,  $T_{1D}$ , is populated via intersystem crossover from the excited singlet,  $S_{1D}$ , with the resultant indicated EPR signal. Addition of naphthalene now results in the appearance of a naphthalene triplet signal,  $N_A$ , at the expense of the phenanthrene triplet,  $N_D$ . The relative signal intensities as a function of naphthalene concentration,  $C_A$ , is shown in Fig. 5. A convenient parameter describing the dependence of signal height,  $N$ , i.e. relative triplet state

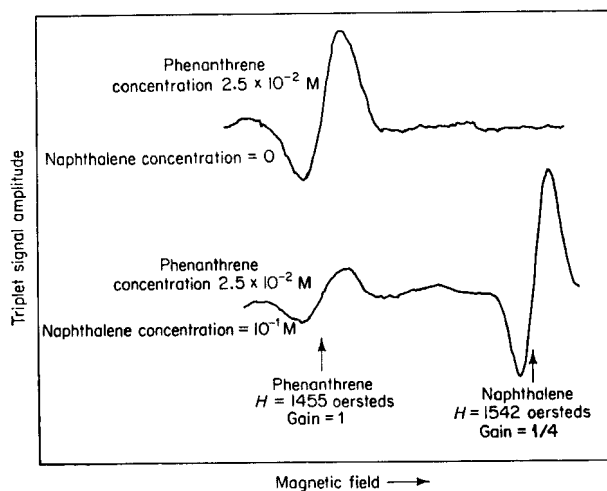


Fig. 4. Electron paramagnetic resonance spectra of phenanthrene triplet state concentration, with and without naphthalene present, and naphthalene triplet state concentration, the result of energy transfer from phenanthrene.

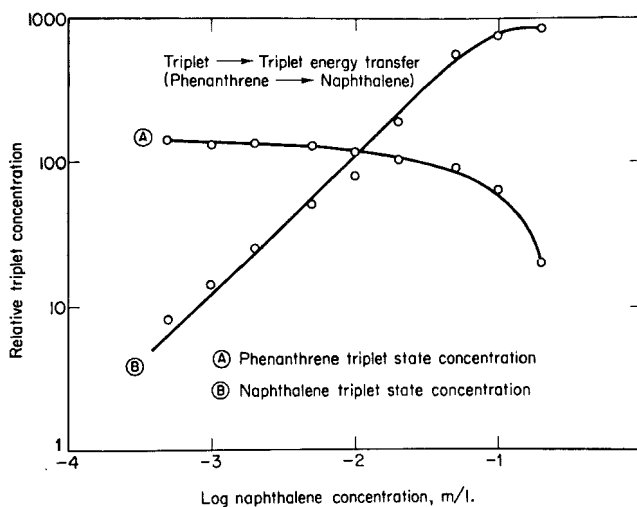


Fig. 5. Phenanthrene and naphthalene relative triplet state concentrations as a function of naphthalene concentrations (signals not normalized to each other).

concentration, on acceptor concentration,  $C_A$ , is that value of concentration,  $C_A(\frac{1}{2})$ , where the donor signal drops to one-half its maximum value. Alternatively this should be equivalent to that concentration where the acceptor triplet concentration is one-half of its maximum value.

The extension of the above energy transfer scheme to a multi-component system can be easily achieved by proper choice of intermediates. As shown in Fig. 6 the author has investigated, among others, the three component system diphenylamine

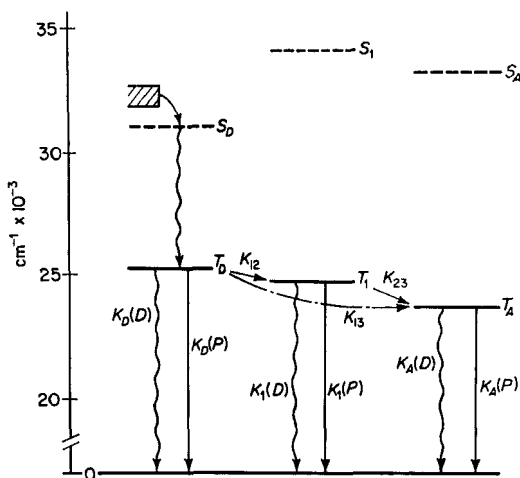


Fig. 6. Energy level scheme demonstrating two-step energy transfer process. Notation same as in Fig. 3.

(donor)  $\rightarrow$  indole (intermediate)  $\rightarrow$  fluorene (acceptor). The requirement on the triplet level of the intermediate,  $T_{1I}$ , is that  $T_{1D} > T_{1I} > T_{1A}$ , while for isolation of effects the singlet level of the intermediate  $S_I$  should obey the relationships  $S_{1D} < S_{1I}$ ,  $S_{1A}$ . Shown in Fig. 7 are the triplet level concentrations for donor and acceptor with and without intermediate and for intermediate, as a function of acceptor concentration. It is of interest to note that the effect of intermediate in relative enhancement of acceptor triplet concentration is greatest at low acceptor concentration and may even, for other acceptors, reverse its effect at high  $C_A$ .

Theoretical treatments of the problem have been both formalistic and mechanistic. A brief summary of the various formulations is presented along with the experimental conclusions. The results are summarized in Table VIII for comparison. As indicated the distinction arises in the dependence of the triplet state concentrations on the parameters, the triplet decay constant, or inverse lifetimes, and the probability of triplet-triplet transfer.

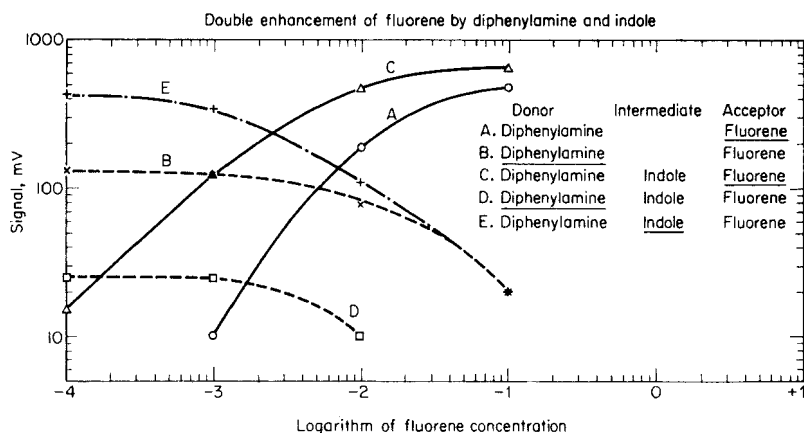


Fig. 7. Relative triplet concentrations of donor, intermediate, and acceptor under single and double enhancement (one-step and two-step energy transfer). Triplet state concentration plotted indicated by underlined molecule.

A comprehensive treatment of resonance transfer was given by Förster<sup>34,35</sup> and has been found applicable in the study of excited singlet states. The interaction depends on the overlap of donor emission spectra and acceptor absorption spectra as well as the separation,  $r$ , between the two entities. For a "strong interaction" the excitation appears delocalized and is best described in terms of a "molecular exciton". For weak interactions, however, as might occur for the forbidden triplet state transitions, the transfer probability,  $K_{12}$ , becomes inversely proportional to the sixth power of the separation,  $R^{-6}$ , i.e. the square of the concentration. Dexter<sup>29</sup> has formulated the necessary restrictions when applying the theory

TABLE VIII. Relationship between Parameters Using Various Models of Energy Transfer

Model	$N_D$	$N_A$	$C_A(\frac{1}{2})$	$\frac{C_A(\frac{1}{2})H}{C_A(\frac{1}{2})D}$	$\tau_D$ (high $C_A$ )
1. Förster-Dexter	$1 - N_A$	$\alpha\alpha C_A + \beta C_A^2 + \dots$	$\left(\frac{K_D}{k_{12}}\right)^{\frac{1}{2}}$	2	$\sim C_A^{-1}$ nonexponential
2. Terenin-Kinetic	$\frac{1}{K_D + k_{12}C_A}$	$\frac{k_{12}C_A}{K_D + k_{12}C_A}$	$\frac{K_D}{k_{12}}$	4	$\sim C_A^{-1}$ nonexponential
3. Terenin-Perrin	$\alpha e^{-\alpha C_A}$	$\alpha(1 - e^{-\alpha C_A})$	$\sim R_0^{-3}$	1	Constant exponential
4. "Complex"	$\frac{1}{1 + K_{12}C_A}$	$\frac{K_{12}C_A}{1 + K_{12}C_A}$	$K_{12}^{-1}$	1	Constant exponential
Experiment		$\alpha C_A$ at low $C_A$		$\leq 1.5$	Constant exponential

to triplet state transfers but the essential relationships, assuming  $K_{12} = k_{12}C_A^2$  ( $k_{12}$  being a constant), are given in Table VIII, line 1. Although it would appear that  $N_D$  and  $N_A$  depend quadratically on the acceptor concentration, it has been shown by Dexter and Galanin<sup>38</sup> that upon space integration of this interaction, a linear dependence ensues, i.e.  $N_D, N_A \sim C_A$  at low acceptor concentrations.

Terenin, whose study of energy transfer in triplet states has extended over many years, originally proposed<sup>134</sup> a transfer scheme whereby, similar to the Förster–Dexter model, the transfer probability is assumed in competition with the normal decay of the donor triplet state,  $K_D$ . As a first approximation, the model, from simple chemical kinetics, assumes  $K_{12} = k_{12}C_A$ , i.e. a linear dependence on  $C_A$ . The dependence of  $N_D$  and  $N_A$  on the parameters is shown for this model in Table VIII, line 2. Although Terenin's<sup>134</sup> original data showed a decrease in donor lifetime at very high acceptor concentrations, quantitative agreement was lacking and the results in general warranted a re-examination of the theoretical model. In order to explain the relative independence of transfer efficiency,  $K_{12}$ , on  $T_D$ , Terenin<sup>135</sup> utilized Perrin's<sup>112</sup> formalism of concentration quenching of fluorescence. The latter assumes that the fluorescence probability  $K_F(r)$  is affected by the presence of a quencher molecule at a distance  $r$ . In the extreme case, a critical radius  $R_0$  is assumed and for separations  $r > R_0$  the fluorescence (or phosphorescence) is normal, while for  $r < R_0$  the donor energy is "instantly" transferred to the acceptor. The ensuing relationships are shown in line 3. Terenin suggests that the critical radius  $R_0$  may well be simply the separation between molecules on contact for the values are of the order of 10 Å.

In this light a more realistic model suggests itself, namely that of a "complex", for while the reality of such an entity in terms of known strongly interacting constituents is open to question it has sufficient merit as a working hypothesis to warrant further study. The nature of complex formation and their interpretation by optical studies are reviewed by McGlynn<sup>96</sup> as well as their possible implications in sensitized phosphorescence. Although strongly complexed aromatic molecules are considered unlikely, theoretical examinations of the benzene self-complex have been made by Mulliken<sup>109</sup> and Shuler.<sup>122</sup> Whether charge-transfer forces or the London dispersion forces studied by Coulson and Davies<sup>25</sup> are the determining factor in the

van der Waals cohesion binding the components remains to be determined. However, if one can assume the existence of a complex formation, the Benesi-Hildebrand<sup>7</sup> equilibrium constant becomes  $K_{BH} = K_{12}$ , i.e. it takes on the role of a transfer probability as shown by line 4 in Table VIII. The energy transfer phenomenon thus both in the Terenin-Perrin and "complex" model is no longer describable as a true transfer process but as a competition between isolated donors and complexed donors (or donors within  $R_0$  of an acceptor) for the incident light. The effect is thus independent of donor triplet lifetime. Two convenient criteria can be selected to test the validity of the above models in their applicability to triplet transfer. Since the first two theories are based on a competition of transfer and normal donor decay, a change of donor lifetime,  $1/K_D \equiv \tau_D$ , by deuteration should result in a corresponding effect on the donor characteristics. The dependence of  $C_A(\frac{1}{2})$  on  $K_D$  and  $K_{12}$  is indicated in column 4 for the various models, while in the adjoining column the expected ratio of  $C_A(\frac{1}{2})$  for light ( $H$ ) and deuterated ( $D$ ) phenanthrene is indicated, assuming  $K_{12}$  is unaffected by deuteration.

The dependence of the donor triplet state lifetime  $\tau_D$  on the transfer rate is also a useful criterion. Using the Förster-Dexter model, Galanin has shown that at low values of  $C_A$ , the effect of transfer is to produce a shortening of  $\tau_D$  of relative magnitude one-half that manifested by the reduction in  $N_D$ . For larger values of  $C_A$ , the transfer process becomes important and a deviation from exponential decay, proportional to  $C_A$ , becomes manifest. Similar qualitative arguments can be given for the second model, while the last two possibilities, since they are not based on a competitive process, predict  $\tau_D$  independent of  $C_A$ . A summary of the results can be made by comparison of the experimental data and the various models with the following correlations and discrepancies.

(1) The effect of deuteration of the donor increases its lifetime four-fold. The Terenin-Kinetic model predicts a corresponding four-fold decrease in the parameter  $C_A(\frac{1}{2})$ , while the Förster-Dexter model predicts a two-fold decrease. Experimentally, as shown in Table VIII, the maximum decrease is 50% and thus neither model appears to conform to the data.

(2) The above models, since they represent the transfer process as being in competition with the normal decay, would predict a



reduction of the net lifetime as the transfer probability increased with increasing  $C_A$ . No such effect is detected experimentally. Measurement of  $T_D$  at  $C_A(\frac{1}{2})$  reveals no reduction from that at  $C_A = 0$  and no apparent deviation from exponential character. The energy level and transfer scheme of Figs. 3 and 6 must then be reinterpreted in terms of relative probability of a donor molecule to become complexed with the acceptor molecule and thus transfer upon excitation via  $K_{12}$ , or to remain uncomplexed and decay normally to the ground state. Consideration may also be given to the possibility that the complexing might be stabilized following triplet excitation because of the alterations in the wave function in the excited state. Comparison can be made between these results and the photo-flash experiments conducted in solution of triplet-triplet transfer by Porter and Wilkinson.<sup>117</sup> Measuring the reduction in donor lifetimes due to the acceptor quenching action they find for the phenanthrene-naphthalene system in hexane that the decay rate doubles at a naphthalene concentration,  $C_A$ , of  $4 \times 10^{-3}M$ . They conclude that, for fluids, the process is diffusion controlled and transfer takes place by a "collision of the second kind" with an exchange transfer mechanism occurring due to orbital overlap at that instant.

The dependence of the parameter  $C_A(\frac{1}{2})$  on deuteration of either donor or acceptor is shown in Table IX. The effect is a small one and

TABLE IX. Effect of Deuteration of Acceptor and Donor on Energy Transfer Parameter,  $C_A(\frac{1}{2})$

$C_A (\times 10^{-3})M/L$

	<i>H</i> -Naphthalene	<i>D</i> -Naphthalene
<i>H</i> -Phenanthrene	7.0	7.1
<i>D</i> -Phenanthrene	5.8	4.6

any explanation at this time would be presumptuous. The "complex" model defines  $C_A(\frac{1}{2}) = K_{12}^{-1}$  and thus the values in the table represent the inverse of the equilibrium constant. Their

magnitude is about ten-fold greater than those determined for the benzene-I<sub>2</sub> complex<sup>7</sup> or naphthalene-picrate.<sup>36</sup> As Terenin has indicated, the energy transfer may not depend on overlap between the spectral properties of donor and acceptor but more correctly should depend on the overlap of the wave functions themselves, since an exchange integral is involved. The spatial extension into the environment of the triplet orbital has been indicated by the line width and lifetime studies and substantiates the above qualitative arguments. A study of the dependence of energy transfer on these overlap properties is being undertaken and may explain why in some instances no transfer is observed between triplets.

### E. Triplet State and Photochemical Processes

A discussion of the field of photochemistry and the possible role of triplet states as intermediates must be, by necessity, treated here in only a cursory fashion. However, the utility of the EPR technique for investigating problems of this nature will be indicated and some results presented. A review of the field has been given by Livingston.<sup>84</sup> The original work of Lewis and co-workers<sup>75, 78, 79, 80</sup> indicated a correlation between triplet state excitation and electron-ejection or bond dissociation. Linschitz, Berry, and Schweitzer<sup>83</sup> observed a luminescence presumably due to a triplet state arising from recombination of radicals or trapped electrons following excitation. The photo-ionization of aromatic hydrocarbons in boric acid glasses has also been reinvestigated more completely by both optical absorption and electron paramagnetic resonance with results similar to those of Lewis, Lipkin, and Linschitz. Backstrom and Sandros<sup>6</sup> studied the hydrogen abstracting properties of excited biacetyl, presumably a triplet state, which could be strongly quenched by collision with polynuclear hydrocarbons whose triplet states lie below that of the biacetyl.

The sensitization of the photolysis of methanol by indole has been investigated by the author<sup>128</sup> in an attempt to determine the role of the excited triplet state of indole in the reaction. The photolysis of pure methanol at 77°K under ultraviolet irradiation results, in the main, in the production of the methyl radical  $\dot{\text{C}}\text{H}_3$ . Although at 4°K this species is stable, at 77°K its lifetime is only several minutes. The stable radicals  $\dot{\text{C}}\text{H}_2\text{OH}$  and  $\dot{\text{C}}\text{HO}$  are also produced but with

greatly reduced yields. Upon addition of indole to the glassy matrix the rate of production of these radicals is greatly enhanced. The equilibrium EPR spectra revealing the presence of the products is shown in Fig. 8. The relative concentration of the  $\dot{\text{C}}\text{H}_2\text{OH}$  radical ( $N_{\text{F.R.}}$ ) as a function of indole concentration is shown in Fig. 9. The relative triplet state concentration,  $N_T$ , of the indole is shown also on the same plot for comparison. The two species, triplet and free radical, appear to correlate well except for the high indole

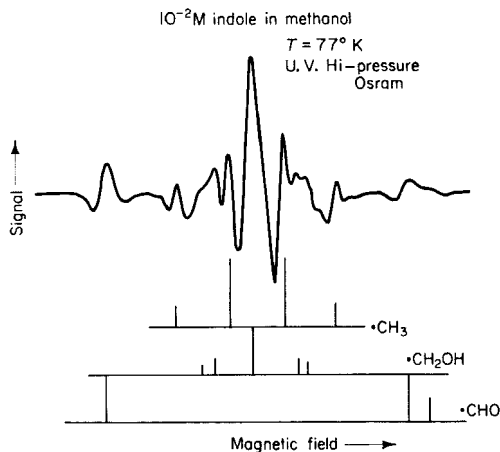


Fig. 8. Electron paramagnetic spectrum of free radicals in methanol. Photoproduction enhanced by addition of  $10^{-2}$  M indole.

concentration region where it can be expected that a competitive concentration quenching reaction might become important.

The relative role played by the excited singlet and triplet state was examined by employing the triplet energy transfer scheme described previously. In this, benzaldehyde was used as donor and the incident excitation confined to photon energies,  $h\nu < 34,000 \text{ cm}^{-1}$ , the first excited singlet level of indole. The indole triplet concentration  $N_T$  along with the free radical production  $N_{\text{F.R.}}$  were found to co-exist under these conditions indicating the non-essentiality of singlet state excitation. However, using intermittent light, a kinetic study of  $N_{\text{F.R.}}$  vs.  $N_T$  revealed an interesting effect. Since  $\tau_T$  for the indole triplet state is 7 seconds, a fairly high although

variable level of  $N_T$  can be attained by adjusting the on-off excitation period to this value. The free radical production rate, however, was found to follow the light excitation rather than  $N_T$ . An alternative precursor to the free radical may be considered, e.g. the higher  $T_i$  states which could be excited, by a two-quanta process. However, replacement of the shutter by an appropriate filter indicated that if such a triplet level existed it must lie higher than  $57,000\text{ cm}^{-1}$  above the ground state.

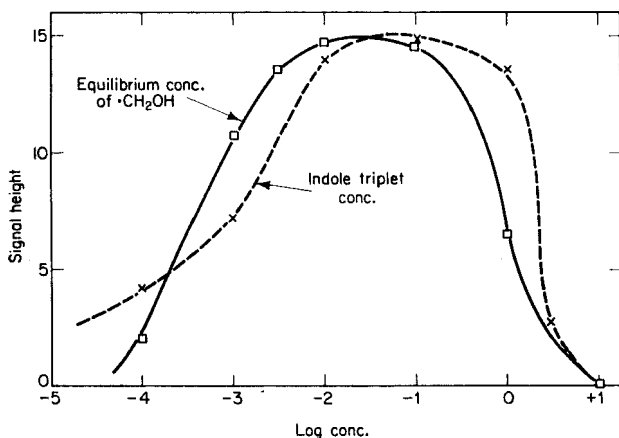


Fig. 9. Relative concentration of indole triplet state and  $\dot{\text{C}}\text{H}_2\text{OH}$  radical as a function of indole concentration.

These negative results can also be explained by assuming the intermediate state is that of an excited complex rather than the triplet and that the excitation of the latter is only through a competitive process to the methanol photolysis. Hydrogen bonding in the indole-methanol system undoubtedly occurs and the complex may well involve this effect. Kasha<sup>70</sup> has discussed the reactivity of excited states and McGlynn<sup>96</sup> has reviewed the importance of complex formation in interpretation of the results. The experimental and theoretical information as well as the arguments can best be attained from the above sources. It is apparent, however, that this field of study, using the techniques described, can well provide a wealth of knowledge on these important problems. The

pertinence of investigations of this nature in the field of radiation biology in regard to the mechanism of radiosensitization is apparent. Tryptophan, contained in tissues in relatively high concentrations, possesses triplet state characteristics and free-radical photosensitization properties similar to indole, mentioned above.

Other problems that may yield to the EPR technique are manifold. For example, the possible role of the triplet state of chlorophyll in the photosynthetic process requires further elucidation. To the investigator eager to bridge the disciplines of sciences lies the reward of nature revealed.

### References

1. Abragam, A., and Pryce, M. H. L., *Proc. Roy. Soc. (London)* **A205**, 135 (1951).
2. Alger, R. S., Anderson, T. H., and Webb, L. A., *J. Chem. Phys.* **30**, 695-706 (1959).
3. Anderson, R. S., and Jaseja, T. S., *Proceedings of Fifth International Symposium on Free Radicals, July, 1961*, Almqvist and Wiksell, Stockholm.
4. Atherton, N. M., and Whiffen, D. H., *Mol. Phys.* **3**, 1 (1960).
5. Atherton, N. M., and Whiffen, D. H., *Mol. Phys.* **3**, 103 (1960).
6. Backstrom, H. L., and Sandros, K., *Chem. Scand.* **12**, 823 (1958).
7. Benesi, H. A., and Hildebrand, J. H., *J. Am. Chem. Soc.* **71**, 2704 (1949).
8. Bennema, P., Hoistine, G. J., Lupinski, J. H., Osterhoff, L. J., Seher, P., and van Voorst, J. D. W., *Mol. Phys.* **2**, 431 (1959).
9. Bersohn, R., *J. Chem. Phys.* **24**, 1066 (1956).
10. Blinder, S. M., *J. Chem. Phys.* **33**, 748 (1960).
11. Boer, E. de, *J. Chem. Phys.* **25**, 190 (1956).
12. Boer, E. de, and Weisman, S. I., *J. Am. Chem. Soc.* **80**, 4549 (1958).
13. Bolton, J. R., and Carrington, A., *Mol. Phys.* **4**, 407 (1961).
14. Bolton, J. R., Carrington, A., and McLachlan, A. D., *Mol., Phys.* **5**, 31 (1962).
15. Brovetto, P., and Ferroni, S., *Nuovo Cimento* **5**, 142 (1957).
16. Carrington, A., Dravnieks, F., and Symons, M. C. R., *J. Chem. Soc.* 947-952 (1959).
17. Carrington, A., and dos Santos-Veiga, J., *Mol. Phys.* **5**, 21 (1962).
18. Chestnut, D. B., *J. Chem. Phys.* **29**, 43 (1958).
19. Chiu, Y. N., private communication.
20. Cochran, E. L., Adrian, F. J., and Bowers, V. A., *J. Chem. Phys.* **34**, 1161 (1961).
21. Cole, T., and Heller, C., *J. Chem. Phys.* **34**, 1085 (1961).
22. Cole, T., Heller, C., and Lambe, J., *J. Chem. Phys.* **34**, 1447 (1961).
23. Cole, T., Heller, C., and McConnell, H. M., *Proc. Natl. Acad. Sci. U.S.* **45**, 525 (1959).

24. Cole, T., Pritchard, H. O., Davidson, N. R., and McConnell, H. M., *Mol. Phys.* **1**, 406 (1958).
25. Coulson, C. A., and Divies, P. L., *Trans. Faraday Soc.* **48**, 777 (1952).
26. Craig, D. P., *J. Chem. Phys.* **18**, 236 (1950).
27. Crawford, V. A., and Coulson, C. A., *J. Chem. Soc.* 2052 (1953).
28. Davydov, A. S., *Theory of Molecular Excitons*, translated by M. Kasha and M. Oppenheimer, Jr., McGraw-Hill, New York, 1962.
29. Dexter, D. L., *J. Chem. Phys.* **21**, 836 (1953).
30. Ermolaev, V., and Terenin, A., *J. Chem. Phys.* **55**, 698 (1958).
31. Farmer, J. B., Gardner, C. L., and McDowell, C. A., *J. Chem. Phys.* **34**, 1058 (1961).
32. Fermi, E., *Z. Physik* **60**, 320 (1930).
33. Fessenden, R. W., and Schuler, R. N., *J. Chem. Phys.* **33**, 935 (1960).
34. Förster, T., *Discussions Faraday Soc.* **27**, 7 (1959).
35. Förster, T., *Excitation Transfer. Comparative Effects of Radiation*, M. Burton, J. S. Kirby-Smith and J. L. Magee, Eds., Chapter 13, Wiley, New York, 1960.
36. Foster, R., *J. Chem. Soc.* 5098 (1957).
37. Fox, D., and Schnepf, O., *J. Chem. Phys.* **23**, 767 (1955).
38. Galanin, M. D., *J. Exptl. Theoret. Phys. U.S.S.R.* **28**, 48 (1955).
39. Ghosh, D. K., and Whiffen, D. H., *Mol. Phys.* **2**, 285 (1959).
40. Gilmore, E. H., Gibson, G. E., and McClure, D. S., *J. Chem. Phys.* **20**, 829 (1952).
41. Goeppert-Mayer, M., and Sklar, A. L., *J. Chem. Phys.* **6**, 645 (1938).
42. Gouterman, M., *J. Chem. Phys.* **30**, 1369 (1959).
43. Gouterman, M., and Moffitt, W., *J. Chem. Phys.* **30**, 1107 (1959).
44. Grant, P. M., Ward, R. B., and Whiffen, D. H., *J. Chem. Soc.* 4635 (1958).
45. Griffiths, J. H. E., and Owen, J., *Proc. Roy. Soc. (London)* **A213**, 459 (1952).
46. Groot, M. S. de, and van der Waals, J. H., *Mol. Phys.* **3**, 190 (1960).
47. Groot, M. S., de and van der Waals, J. H., *Mol. Phys.* **4**, 189 (1961).
48. Ham, N. S., and Ruedenberg, K., *J. Chem. Phys.* **25**, 1 (1956).
49. Ham, N. S., and Ruedenberg, K., *J. Chem. Phys.* **25**, 13 (1956).
50. Hametka, H. F., *J. Chem. Phys.* **31**, 315 (1959).
51. Heller, C., *J. Chem. Phys.* **36**, 175 (1962).
52. Heller, C., and McConnell, H. M., *J. Chem. Phys.* **32**, 1535 (1960).
53. Herzberg, G., and Shoosmith, J., *Can. J. Phys.* **34**, 523 (1956).
54. Higuchi, J., and Aono, S., *J. Chem. Phys.* **32**, 52 (1960).
55. Hornig, A. W., and Hyde, J. S., *Bull. Am. Phys. Soc.* **6**, 445 (1961).
56. Horsfield, A., Morton, J. R., and Whiffen, D. H., *Mol. Phys.* **4**, 327 (1961).
57. Horsfield, A., Morton, J. R., and Whiffen, D. H., *Mol. Phys.* **4**, 169 (1961).
58. Horsfield, A., Morton, J. R., and Whiffen, D. H., *Mol. Phys.* **4**, 425 (1961).
59. Horsfield, A., Morton, J. R., and Whiffen, D. H., *Mol. Phys.* **5**, 115 (1962).

60. Hutchison, C. A., Jr., and Mangum, B. W., *J. Chem. Phys.* **29**, 952 (1958).
61. Hutchison, C. A., Jr., and Mangum, B. W., *J. Chem. Phys.* **32**, 1261 (1960).
62. Hutchison, C. A., Jr., and Mangum, B. W., *J. Chem. Phys.* **34**, 908 (1961).
63. Ingram, D. J. E., *Spectroscopy at Radio and Microwave Frequencies*, Butterworth, London, 1955.
64. Ingram, D. J. E., *Free Radicals as Studied by Electron Spin Resonance*, Academic Press, 1958.
65. Jarrett, H. S., Sloan, G. J., and Vaughan, W. R., *J. Chem. Phys.* **25**, 697 (1956).
66. Jaseja, T. S., and Anderson, R. S., *Bull. Am. Phys. Soc.* **6**, 247 (1961).
67. Jaseja, T. S., and Anderson, R. S., *J. Chem. Phys.* **36**, 1098 (1962).
68. Jen, C. K., Foner, S. N., Cochran, E. L., and Bowers, V. A., *Phys. Rev.* **112**, 1169 (1958).
69. Karplus, M., *J. Chem. Phys.* **30**, 15 (1959).
70. Kasha, M., Ultraviolet Radiation Effects: Molecular Photochemistry. *Comparative Effects of Radiation*, M. Burton, J. S. Kirby-Smith, and J. L. Magee, Eds. Wiley, New York, 1960, p. 72.
71. Katayama, M., and Gordy, W., *J. Chem. Phys.* **35**, 117 (1961).
72. Kleven, H. B., and Platt, J. R., *J. Chem. Phys.* **17**, 470 (1949).
73. Kurita, Y., and Gordy, W., *J. Chem. Phys.* **34**, 282 (1961).
74. Kurita, Y., and Gordy, W., *J. Chem. Phys.* **34**, 1285 (1961).
75. Lewis, G. N., and Bigeleisen, J., *J. Am. Chem. Soc.* **65**, 2419 (1943).
76. Lewis, G. N., and Calvin, M., *J. Am. Chem. Soc.* **67**, 1232 (1945).
77. Lewis, G. N., Calvin, M., and Kasha, M., *J. Chem. Phys.* **17**, 804 (1949).
78. Lewis, G. N., and Kasha, M., *J. Am. Chem. Soc.* **66**, 2100 (1944).
79. Lewis, G. N., and Lipkin, D., *J. Am. Chem. Soc.* **64**, 2801 (1942).
80. Lewis, G. N., Lipkin, D., and Mogel, T. T., *J. Am. Chem. Soc.* **63**, 3005 (1941).
81. Lin, W. C., and McDowell, C. A., *Mol. Phys.* **4**, 343 (1961).
82. Lin, W. C., and McDowell, C. A., *Mol. Phys.* **4**, 33 (1961).
83. Linschitz, H. M., Berry, G., and Schweitzer, D., *J. Am. Chem. Soc.* **76**, 5833 (1954).
84. Livingston, R., *J. Phys. Chem.* **61**, 860 (1957).
85. Livingston, R. Photochemistry. *Radiation Biology*, Vol. VII, A. Hollander, Ed., McGraw-Hill, New York, 1955, pp. 1-40.
86. McClure, D. S., *J. Chem. Phys.* **17**, 905 (1949).
87. McClure, D. S., *Electronic Spectra of Molecules and Ions in Crystals: Part I, Molecular Crystals*, Vol. 8, *Solid State Physics*, Academic Press, New York and London, (1959).
88. McConnell, H. M., *J. Chem. Phys.* **24**, 764 (1954).
89. McConnell, H. M., *Proc. Natl. Acad. Sci. U.S.A.* **45**, 172 (1959).
90. McConnell, H. M., *J. Chem. Phys.* **35**, 1520 (1961).
91. McConnell, H. M., and Chestnut, D. B., *J. Chem. Phys.* **28**, 107 (1958).
92. McConnell, H. M., and Fessenden, R. W., *J. Chem. Phys.* **31**, 1688 (1959).
93. McConnell, H. M., Heller, C., Cole, T., and Fessenden, R. W., *J. Am. Chem. Soc.* **82**, 766 (1960).

94. McConnell, H. M., and Robertson, R. E., *J. Phys. Chem.* **61**, 1018 (1957).
95. McConnell, H. M., and Strathdee, J., *Mol. Phys.* **2**, 285 (1959).
96. McGlynn, S. P., *Chem. Rev.* **58**, 1113 (1958).
97. McGlynn, S. P., Boggus, J. D., and Elder, E., *J. Chem. Phys.* **32**, 357 (1960).
98. McLachlan, A. D., *Mol. Phys.* **1**, 233 (1958).
99. McLachlan, A. D., *Mol. Phys.* **5**, 51 (1962).
100. McMillan, J. A., and Smaller, B., *J. Chem. Phys.* **35**, 1698 (1961); *J. Chem. Phys.* **35**, 763 (1961).
101. McWeeny, R., *J. Chem. Phys.* **34**, 399 (1961).
102. Maki, A. H., and Geske, D. H., *J. Am. Chem. Soc.* **83**, 1852 (1961).
103. Mann, D. E., Platt, J. R., and Klevens, H. B., *J. Chem. Phys.* **17**, 481 (1949).
104. Miyagawa, I., and Gordy, W., *J. Chem. Phys.* **30**, 1590 (1959).
105. Miyagawa, I., and Gordy, W., *J. Chem. Phys.* **32**, 255 (1960).
106. Miyagawa, I., Kurita, Y., and Gordy, W., *J. Chem. Phys.* **33**, 1599 (1960).
107. Morton, J. R., and Horsfield, A., *Mol. Phys.* **4**, 219 (1961).
108. Morton, J. R., and Horsfield, A., *J. Chem. Phys.* **35**, 1142 (1961).
109. Mulliken, R. S., *J. Am. Chem. Soc.* **74**, 811 (1952).
110. Pake, G. E., *Advances in Solid State Physics*, Vol. II, Chapter 1, Academic Press, New York, 1956.
111. Pariser, R., *J. Chem. Phys.* **24**, 250 (1956).
112. Perrin, F., *Compt. Rend.* **178**, 1978 (1924).
113. Platt, J. R., *J. Chem. Phys.* **17**, 484 (1949).
114. Platt, J. R., *J. Chem. Phys.* **22**, 1448 (1954).
115. Pooley, D., and Whiffen, D. H., *Mol. Phys.* **4**, 81 (1961).
116. Pople, J. A., *Proc. Phys. Soc. (London)* **A68**, 81 (1955).
117. Porter, G., and Wilkinson, F., *Proc. Roy. Soc. (London)* **264**, 1 (1961).
118. Pringsheim, P., *Fluorescence and Phosphorescence*, Interscience, New York, 1949.
119. Robinson, G. W., *J. Mol. Spectry.* **6**, 58 (1961).
120. Roggen, A. van, Roggen, L. van, and Gordy, W., *Bull. Am. Phys. Soc.* **1**, 266 (1956).
121. Rowlands, J. R., and Whiffen, D. H., *Mol. Phys.* **4**, 349 (1961).
122. Shuler, K. E., *J. Chem. Phys.* **21**, 765 (1953); *J. Chem. Phys.* **20**, 1865 (1952).
123. Shull, H., *J. Chem. Phys.* **17**, 295 (1949).
124. Simpson, W. T., and Peterson, D. L., *J. Chem. Phys.* **26**, 588 (1957).
125. Smaller, B., *J. Chem. Phys.* **37**, 1578 (1962).
126. Smaller, B., *Bull. Am. Phys. Soc.*, **7**, 397 (1962).
127. Smaller, B., *Radiation Res.* **16**, 599 (1962).
128. Smaller, B., *Nature* **195**, 593 (1962).
129. Smaller, B., and Matheson, M. S., *J. Chem. Phys.* **28**, 1169 (1958).
130. Smaller, B., and Yasaitis, E., *Rev. Sci. Instr.* **24**, 991 (1953).
131. Stevens, K. W. H., *Proc. Roy. Soc. (London)* **A214**, 237 (1952).
132. Terenin, A., *Acta Physicochim. U.S.S.R.* **18**, 210 (1943).
133. Terenin, A., and Ermolaev, V., *Dokl. Akad. Nauk SSSR* **85**, 347 (1952).



134. Terenin, A., and Ermolaev, V., *Trans. Faraday Soc.* **52**, 1042 (1956).
135. Terenin, A., and Ermolaev, V., *Izv. Akad. Nauk SSSR Phys. Ser.* **26**, 121 (1962).
136. Tuttle, T., and Weissman, S., *J. Chem. Phys.* **25**, 189 (1956).
137. Tuttle, T. R., Jr., and Weissman, S. I., *J. Am. Chem. Soc.* **80**, 5342 (1958).
138. Uebersfeld, J., and Erb, E., *Compt. Rend.* **242**, 478 (1950).
139. van der Waals, J. H., and de Groot, J. H., *Mol. Phys.* **2**, 333 (1959).
140. Vavilov, S. I., *J. Phys. U.S.S.R.* **1**, 141 (1943).
141. Vincow, G., and Fraenkel, G. K., *J. Chem. Phys.* **34**, 1333 (1961).
142. Ward, R. L., *J. Chem. Phys.* **32**, 1592 (1960).
143. Weissman, S. I., *J. Chem. Phys.* **29**, 1189 (1958).
144. Weissman, S. I., *J. Chem. Phys.* **22**, 1378 (1954).
145. Weissman, S. I., Tuttle, T. R., Jr., and de Boer, E., *J. Phys. Chem.* **61**, 28 (1957).
146. Wertz, J. E., *Chem. Rev.* **55**, 829 (1955).
147. Wertz, J. E., and Vivo, J. L., *J. Chem. Phys.* **24**, 479 (1956).
148. Whiffen, D. H., Electron Spin Resonance of Oriented Organic Molecules, *Free Radicals in Biological Systems*, Chapter 17, Academic Press, New York, 1961.
149. Whiffen, D. H., Electron Spin Resonance Studies on the Geometry of Trapped Radicals, *Proceedings of Fifth International Symposium on Free Radicals, July 1961*, Almqvist and Wiksell, Stockholm.
150. Wolf, H. C., *The Electronic Spectra of Aromatic Molecular Crystals*, Vol. 9 of *Solid State Physics*, Academic Press, New York and London, 1959.
151. Wright, M. R., Frosch, R. P., and Robinson, G. W., *J. Chem. Phys.* **33**, 934 (1960).

## 15

# PHOTOPROTECTION FROM FAR ULTRAVIOLET EFFECTS IN CELLS

JOHN JAGGER, *Biology Division, Oak Ridge National Laboratory,\*  
Oak Ridge, Tennessee*

## CONTENTS

I. Introduction . . . . .	584
A. Some Definitions . . . . .	585
B. Photoreactivation . . . . .	586
II. Behavior of Photoprotection . . . . .	587
A. Photoprotection in <i>Escherichia coli</i> . . . . .	587
B. Photoprotection in Other Organisms. . . . .	591
C. Attempts to Photoprotect Subcellular Systems . . . . .	593
III. The Chromophore . . . . .	593
IV. The Mechanism . . . . .	595
A. Direct Effects . . . . .	595
(1) Simple Photochemical Alteration . . . . .	595
(2) Utilization of Other Molecules . . . . .	595
B. Enzyme Involvement . . . . .	596
C. Indirect Effects . . . . .	597
(1) Alteration of Enzyme Balance . . . . .	597
(2) Superimposed Damage . . . . .	598
D. Further Experiments . . . . .	599
V. General Remarks . . . . .	600
References . . . . .	600

## I. INTRODUCTION

It has long been known that far ultraviolet radiation (see next section for definition) can produce a wide variety of effects in living cells, and is especially potent for killing and mutation.<sup>13</sup> But only quite recently has it been demonstrated that most of these effects can be partially reversed by *subsequent* irradiation at longer wavelengths (photoreactivation) and that, in a few systems, some of the

\* Operated by Union Carbide Corporation for the U.S. Atomic Energy Commission.

effects can be partially prevented by *prior* irradiation at longer wavelengths (photoprotection\*).

There is good reason to believe that in cells nucleic acid is the most important single absorber of far ultraviolet radiation, both in terms of light absorbed and of biological effects observed. Some of the considerations leading to this belief are the following: (1) Most cells contain of the order of 10% nucleic acid by dry weight, which is generally more than any other component except protein, (2) on a weight basis, nucleic acid is one of the best organic absorbers of far ultraviolet radiation, being an order of magnitude more effective than protein, (3) nucleic acid is the only type of molecule known to contain genetic information, and (4) action spectra for both killing and mutation of cells usually resemble the absorption spectra of nucleic acids, especially as compared to those of proteins. The photochemistry of nucleic acid therefore becomes a subject of great importance to biology. And, in a search for the site of action of treatments that modify the response of a cell to far ultraviolet radiation, the first molecule we suspect is nucleic acid.

In the past ten years, research on the actions of nonionizing radiations on nucleic acids has considerably increased knowledge of the physical properties of these molecules. This research is now moving so rapidly that we may confidently expect to understand within the next five years the nature of the major physical and chemical changes that far ultraviolet radiation produces in nucleic acid. Work on the photoreactivation and photoprotection of cells will contribute to this end. These studies will also tell us something of the physicochemical properties of other important biological compounds, namely, those that absorb the longer-wavelength radiation utilized in photoreactivation and photoprotection. It is for such reasons that a discussion of near ultraviolet photobiology is appropriate to a volume dealing with the physical properties of biochemical compounds.

#### A. Some Definitions

*Far ultraviolet radiation* (UV), usually considered to lie in the 1900–3000 Å range, shall for our purposes mean 2300–3000 Å, a

\* We undertake here no discussion of photoprotection from X-ray effects, recently discovered in *Nocardia* by Clark and Frady.<sup>6</sup> We have been unable to photoprotect from X-ray killing in *E. coli* B. The two types of photoprotection are probably basically different phenomena.

band very effectively absorbed by the conjugated purine and pyrimidine bases of nucleic acids and the aromatic amino acids of proteins. *Near ultraviolet radiation* lies in the range 3000–3800 Å, and at longer wavelengths (3800–7600 Å) is *visible radiation*, or visible light. A *recovery* is a reduction in final effects caused by treatments applied after the beginning of irradiation, and a *protection* is a reduction in final effects caused by treatments applied before the beginning of irradiation. Thus, *photoreactivation* (PR) is a recovery and *photoprotection* (PP) is a protection. A *chromophore* is a molecule, or part thereof, that absorbs the effective radiation in a given process. The *modifiable site* is the crucial molecule, or part thereof, that is normally damaged by far ultraviolet radiation, the damage being subject to modification, thus initiating a chain of events that results in the macroscopically observed modification (recovery or protection). The *dose-reduction factor* is the ratio of the dose producing a given effect in the absence of a modifier to that producing the same effect in its presence. Deoxyribonucleic acid (DNA), ribonucleic acid (RNA), and reduced nicotinamide adenine dinucleotide (NADH), formerly called DPNH, are extremely important and universal biological molecules.

### B. Photoreactivation

This subject has been extensively reviewed.<sup>8,14,26</sup> However, a brief outline here of PR is essential to an understanding of research on PP, since the two effects are operationally so similar and may have something in common at the molecular level.

Photoreactivation has been found in virtually all living systems, including bacteria, fungi, protozoa, plants, invertebrates, and mammals. (In the larger organisms, of course, it is necessarily a surface effect, since UV penetrates only some 5–30 microns in tissue.) It is known that the modifiable site for PR can be in DNA, since bacterial viruses and transforming principles can be photoreactivated in cells or cell extracts. The modifiable site can also be in RNA, since plant viruses, particularly the separated RNA of tobacco mosaic virus, can be photoreactivated in cells. Furthermore, all the known cellular PR effects can be accounted for on the basis of reactivation of either DNA or RNA, while *in vitro* experiments with proteins have been negative. It is clear that nucleic acid, and

probably only nucleic acid, contains the modifiable site(s) for PR. In transforming DNA, the site is known to be a thymine dimer,<sup>29,34</sup> and it is likely that this is the major site in the DNA of cells. The site in RNA is unknown; it may be a uracil dimer.<sup>31</sup>

There is evidence for an enzyme that mediates PR of transforming DNA.<sup>26,27</sup> This enzyme can be extracted from photoreactivable cells. It forms a complex with UV-irradiated DNA. The complex absorbs photoreactivating radiation and dissociates into enzyme and repaired DNA. The enzyme has not been highly purified (it may be a mixture of different enzymes, some perhaps having cofactors). To date we have no certain knowledge of the chemical nature of the chromophore for PR, which presumably is part of the enzyme system.

Because PR is an enzymatic process, it shows a positive temperature coefficient and a dependence upon the dose rate of the reactivating radiation, becoming saturated at high dose rates.

It is not known that the PR enzyme accounts for all PR effects, but, in the presence of PR radiation, it can reverse up to 90% of the UV damage in transforming DNA. Furthermore, temperature-dose rate effects suggest that most PR of cells and of virus-cell complexes is mediated by enzymes. It is almost certain that there is more than one enzyme (Rupert's, for example, does not combine with RNA) and more than one chromophore for PR.

## II. BEHAVIOR OF PHOTOPROTECTION

### A. Photoprotection in *Escherichia coli*

One of the first unequivocal reports of photoprotection was that of Weatherwax,<sup>32</sup> who found a large effect on killing in *E. coli* B, but no effect in *E. coli* B/r (see Fig. 1). Aside from the obvious difference in the time of the modifying treatment relative to the UV irradiation, it was evident, even in this early brief report, that PP was quite different from PR. The fact that it occurred in strain B, but not in B/r, which shows excellent PR, suggested that PP was less widespread than PR. Also, Fig. 1 shows that PP does not cause a constant dose reduction, i.e. the extent to which it reduces the effective UV dose varies greatly with survival level, whereas most PR shows fairly constant dose reduction. At some survival levels, however,

PP is quite as large an effect as PR, yielding dose-reduction factors around 0.3.

At about the same time, Miki<sup>22</sup> got essentially the same results as Weatherwax, and also showed a large PP from killing in the lysogenic *E. coli* K12 ( $\lambda$ ), but no effect with nonlysogenic K12S. Miki's paper, written in Japanese, is discussed by Jagger,<sup>15</sup> who points out

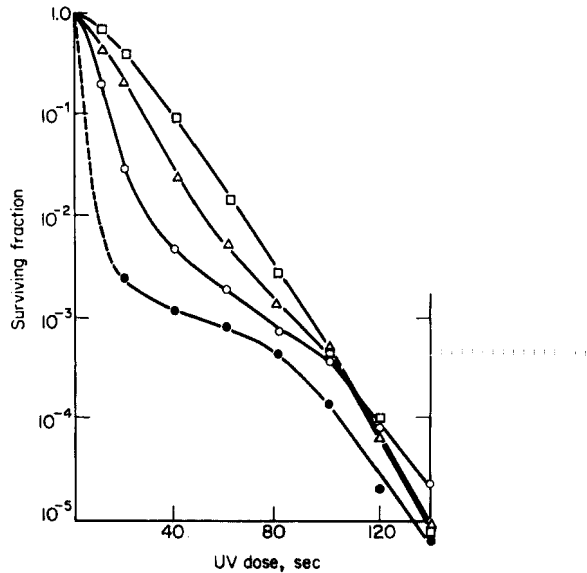


Fig. 1. Ultraviolet survival of *E. coli* B after photoprotection by exposure to 0 (●), 1.5 (○), 2.5 (△), and 4.0 (□) minutes of visible and near ultraviolet radiation.<sup>22</sup>

that it is difficult to decide whether Miki was actually protecting from UV killing, or was simply destroying, with the photoprotecting radiation, the capacity of the lysogenic bacterium to support phage growth. The latter would also lead to a higher survival, since the same UV that kills K12 ( $\lambda$ ) directly also kills it by inducing the development of prophage inside the bacterium. At any rate, Miki did find that PP in K12 ( $\lambda$ ) is a multi-hit process and that it is quite stable, with no loss of PP if the cells are left in broth at 37°C for three hours between the time of PP and UV treatment. (Miki observed no division during this period.)

In recent years, we have attempted in our laboratory to find out more about PP by directing our attention especially to two questions: (1) How widespread is PP in the biological world? and (2) how does PP work? An obvious approach to the second question is to compare PP and PR whenever possible, since we do know a great deal about PR behavior and even something of its mechanism. We began our studies in this way, comparing PR and PP in *E. coli* B,

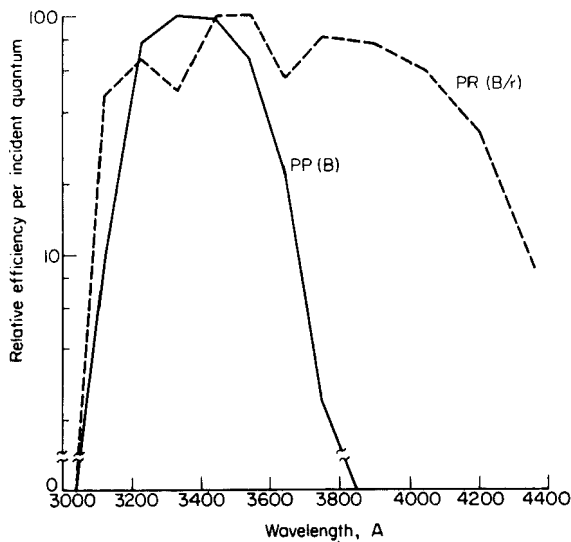


Fig. 2. Action spectra for photoprotection from killing in *E. coli* B (solid line) and for photoreactivation of killing in *E. coli* B/r (broken line).<sup>16</sup>

feeling that it was necessary to characterize the phenomenon before we could conduct a meaningful search for it in other organisms.

In all experiments, we inactivated cells with radiation (2537 Å) from a germicidal lamp. In our early experiments<sup>15</sup> we used a broad band of photoprotecting radiation (3100–6000 Å), since we did not then know what wavelengths were effective. We found that the degree of PP was dependent upon the plating medium. The effect was much greater when the cells were plated on nutrient agar containing 0.8% NaCl, and most subsequent experiments with *E. coli* B were done using this medium. Miki's agar contained 0.5%

NaCl, and our experience strongly suggests that Weatherwax must also have used a salt agar.

In agreement with Miki, we found PP to be very stable, showing only 50% decay in 28 hours for cells kept in phosphate buffer at 23°C between exposure to optimal doses of photoprotecting radiation and exposure to UV. Also in agreement with Miki, we found PP to be a multi-hit phenomenon, in contrast to PR, which is nearly single-hit in many systems. No protection was found from killing with 250 kvp X-rays.

Photoprotection as a function of dose of photoprotecting radiation was found to be practically independent of temperature during PP irradiation ( $Q_{10}$  of 1.05) and independent of dose rate (when changed by a factor of 16) of the photoprotecting radiation. This indicated that limiting thermal reactions were not involved in the early events in PP and, therefore, that these early events very probably did not utilize enzymes. This is in definite contrast to PR, which seems in all systems to use enzymes to some extent.

In later experiments,<sup>16</sup> we investigated the action spectrum for PP in *E. coli* B and found it to be a narrow band, lying entirely in the near ultraviolet, with a single peak at about 3400 Å (see Fig. 2). This finding is also in contrast to the situation with PR, where a much broader band is effective.\* Using a 200-Å band centered at 3341 Å, dose-rate independence for the photoprotecting radiation was confirmed, this time by changing the dose rate by a factor of 64. It was also found that, when using efficient photoprotecting wavelengths, PP is a nearly single-hit effect, similar to PR. Only for the longest wavelengths (around 3650 Å) is PP multi-hit. The radiation used in our earlier work, as well as in all probability that of other investigators, was much richer in these long wavelengths than in the short ones, and this undoubtedly led to the observation of a multi-hit dose response, which is now seen to be atypical.

In general, the amount of radiation needed for PP is considerably greater than for PR. It is difficult to compare the two in this respect since the dose required for maximum PR we found to be nearly a linear function of UV dose, whereas the dose required for maximum PP is nearly independent of UV dose. For a UV survival of 2%, the

\* It should be noted that the spectrum shown for PR applies to *E. coli* B/r, while that for PP applies to *E. coli* B. It is assumed that the PR action spectrum for strain B will not differ greatly from that for strain B/r.



required dose for maximum PP is about three times that required for maximum PR. Even at the most efficient photoprotecting wavelengths, a dose giving maximum PP kills up to 20% of the cells. This seems to be a highly susceptible portion of the population, however, for considerably higher doses cause only slightly more killing.

In some very interesting recent work, Harm and Hillebrandt<sup>11</sup> have obtained a mutant (*phr*<sup>-</sup>) of *E. coli* B that is nonphotoreactivable. They report that PP occurs in both B and B *phr*<sup>-</sup>, presumably to about the same extent. The experiments show that PP can occur in an organism incapable of PR, thus revealing another aspect in which the two phenomena differ.

### B. Photoprotection in Other Organisms

In his first report of photoreactivation, Kelner<sup>20</sup> described attempts to photoprotect *Streptomyces griseus* conidia from UV killing. Although he found no effect, many other workers in PR have been aware of the possibility of PP and have looked for it. Most reports were negative. Some of these earlier results are included in Table I. In our laboratory, having found the optimum conditions for *E. coli* B, we sought PP in several other organisms, including some that had been tested by earlier workers, who did not then know that PP existed. Our results are also shown in Table I. Among other findings, we have confirmed Kelner's report of no PP in *S. griseus*, as well as the reports of Weatherwax and Miki of none in *E. coli* B/r. In some systems we found slight PP, but this was often too small to be sure of, and these have been reported in Table I as being negative. Really striking PP was found only in *E. coli* B and *Pseudomonas aeruginosa*.

Because some cells are very easily killed by the shorter wavelengths in the near ultraviolet, and because the action spectrum may differ in different organisms, we sometimes tried a variety of radiation bands in the range 3000–6000 Å. We always found that cells that did not show PP at 3400 Å did not show it at other wavelengths.

To our knowledge, Table I includes all organisms in which PP has been found.\* These are all either bacteria or protozoa. Attempts to

\* Weatherwax<sup>23</sup> has recently reported PP from both killing and mutation to independence of arginine in *E. coli* 15 T<sup>-</sup>.

TABLE I.<sup>a</sup> Photoprotection from Ultraviolet Damage in Microorganisms

Order	Family	Genus, species, strain	Effect	Photoreactivation	Photoprotection
Pseudomonadales	Pseudomonadaceae	<i>Pseudomonas aeruginosa</i> <i>Photobacterium fischeri</i>	killing killing	+ (Jagger and Stafford, 1962) <sup>16</sup> + (Jagger and Stafford, 1962) <sup>16</sup>	+ (Jagger and Stafford, 1962) <sup>16</sup> - (Jagger and Stafford, 1962) <sup>16</sup>
Eubacteriales	Enterobacteriaceae	<i>Escherichia coli</i> B B phr <sup>-</sup> B/r	killing killing killing	+ (Dulbecco, 1955) <sup>8</sup> - (Harm and Hillebrandt, 1962) <sup>11</sup> + (Kelner, 1949) <sup>21</sup>	+ (Weatherwax, 1956) <sup>32</sup> + (Harm and Hillebrandt, 1962) <sup>11</sup> - (Kelner, 1949) <sup>21</sup>
	Micrococaceae	K12(λ) K12S <i>Staphylococcus aureus</i>	induction killing induction	+ (Monod <i>et al.</i> , 1949) <sup>23</sup> + (Cantelmo, 1951) <sup>5</sup>	Weatherwax, 1956 <sup>32</sup> <sup>b</sup> + (Miki, 1956) <sup>22</sup> - (Miki, 1956) <sup>22</sup> + (Cantelmo, 1951) <sup>5</sup>
Actinomycetales	Brucellaceae	<i>Haemophilus influenzae</i>	killing	- (Rupert <i>et al.</i> , 1958) <sup>27</sup>	- (Jagger and Stafford, 1962) <sup>16</sup>
	Streptomycetaceae	<i>Streptomyces griseus</i>	killing	+ Kelner, 1949) <sup>20</sup>	- (Kelner, 1949) <sup>20</sup> ; Jagger and Stafford, 1962 <sup>16</sup>
Endomycetales	Endomycetaceae	<i>Saccharomyces cerevisiae</i>	killing	+ (Sarachek, 1954) <sup>28</sup>	- (Jagger and Stafford, 1962) <sup>16</sup>
Amoebida	Amoebidae	<i>Amoeba proteus</i>	division delay	+ (Jagger and Stafford, 1962) <sup>16</sup>	± (Jagger and Stafford, 1962) <sup>16</sup>
Holotrichida	Tetrahymenidae	<i>Colpidium colpoda</i>	division delay	+ (Giese <i>et al.</i> , 1954) <sup>10</sup>	+ (Giese <i>et al.</i> , 1954) <sup>10</sup>

+ = large effect; - = little or no effect; ± = effect under some conditions.

<sup>a</sup> Adapted from Jagger and Stafford.<sup>16</sup>

<sup>b</sup> Where two references are indicated, the second is more recent and probably more reliable, since the work was done under conditions that gave a positive result in some other system.

find PP in higher organisms have been made, with negative results.<sup>3,4,24</sup>

It is clear that PP is not nearly so widespread in the biological world as PR. Its distribution is highly random, occurring in widely different orders, yet sometimes in only one of two closely related strains, e.g. in *E. coli* B, but not in B/r. Perhaps when more is known of the mechanism, it will be possible to show PP in organisms that now appear nonphotoprotectable. Our experience with the plating medium for *E. coli* B is a good case in point. The effect is sufficiently small on nutrient agar lacking NaCl that, unless one were operating under optimal conditions, the PP might well go unnoticed.

### C. Attempts to Photoprotect Subcellular Systems

Both viruses and transforming principles can be photoreactivated. It is of obvious interest to see if they also show PP. Bawden and Kleczkowski<sup>2</sup> showed that illumination of plants before infection with UV-inactivated spherical viruses did not protect the viruses from expression of the UV damage. In a similar experiment, Dulbecco<sup>7</sup> illuminated *E. coli* B for long periods up to the moment that UV-inactivated T2 virus was added, but found no effect. Dulbecco's doses of visible light were probably too low, and neither he nor Bawden and Kleczkowski may have used sufficiently short wavelengths. However, experiments in our laboratory<sup>18</sup> show that, under conditions providing good PP of the bacterium, there is no PP of phage T2 after injection of its DNA into *E. coli* B. Thus it appears unlikely that viruses can be photoprotected.

In cooperation with Dr. Jane Setlow, we have attempted to photoprotect purified transforming DNA that can convert cells of the bacterium *Haemophilus influenzae* to streptomycin resistance. During both photoprotecting and UV irradiation, the DNA was in phosphate buffer. No PP was found.

## III. THE CHROMOPHORE

The chromophore for PP has not yet been identified, but some clues exist.

As noted above, the action spectrum for PP in *E. coli* B is a narrow band in the near ultraviolet, with a single peak at about 3400 Å (Fig. 2). We have also obtained an action spectrum for PP in *P.*

*aeruginosa*. Although we used fewer wavelengths, it is clear that the spectrum is very similar to that for *E. coli* B, showing the same maximum, but slightly higher effectiveness, at the extremes of the spectrum. Within experimental error, however the two curves may be considered identical. It is of interest that Giese and co-workers obtained PP in the protozoan *Colpidium colpoda* by exposure to daylight,<sup>10</sup> but not by exposure to blue light,<sup>9</sup> suggesting that this PP was mediated by near ultraviolet radiation.

Thus, in the only organisms for which anything is known of the spectral range of PP, the effective radiation lies entirely in the near ultraviolet. This fact, as well as consideration of the narrowness of the near ultraviolet region (800 Å) and the similarity of the spectra for two bacteria lying in different taxonomic orders, suggests that there is only a single chromophore for PP. This is in contrast to PR, for which different organisms may show quite different action spectra.

If the modifiable site is nucleic acid, and if the initial reaction is purely photochemical, the simplest assumption regarding the chromophore would be that it is also nucleic acid. The effective wavelengths for PP are all in the near ultraviolet and the doses required are high. Nucleic acid absorbs slightly in this region, and it is conceivable that it could serve as the chromophore.

However, if nucleic acid were the chromophore, one would not expect the action spectrum to drop at wavelengths below 3400 Å. There is some killing by the radiation in this region, and one might expect that this is masking the PP. But we have found that, even after correction for killing, the curve still drops in this region.<sup>16</sup> Therefore, if our correction is accurate, nucleic acid is probably not the chromophore.

A more likely candidate for the chromophore is NADH. We have shown that the absorption curve of this compound fits quite well the action spectrum for PP, after the spectrum has been corrected for killing at the shorter wavelengths.<sup>16</sup> Some support for the possibility of such a chromophore comes from experiments of Shugar [see Section IV-C (1)], which show that absorption of near ultraviolet radiation in NADH can alter an associated enzyme, and of Rupert,<sup>26</sup> which show that the dialyzable component of the PR enzyme for *E. coli* B can be replaced by NADH or reduced glutathione. However, NADH is not particularly photolabile, so that, if it were the

chromophore, it would presumably operate only as an intermediate carrier of the photon energy.

Recent work by Kashket and Brodie<sup>19</sup> has shown that quinones that are essential parts of the respiratory mechanism are readily destroyed by near ultraviolet irradiation of *E. coli* W. Similar doses had a small effect on flavin mononucleotide and no effect on flavin adenine dinucleotide or cytochromes. We have found (unpublished data) that doses of radiation at 3400 Å that are sufficient to produce good PP in *E. coli* B cause, in pure solution, no alteration of NADH but destroy (as measured by changes in the entire ultraviolet absorption spectrum) a large fraction of the naphthoquinone, vitamin K<sub>2</sub>.

It now seems very likely that quinones are the chromophores for PP. The absorption spectra of some of them (e.g. vitamin K<sub>2</sub>) fit the action spectrum of PP as well as does NADH.

#### IV. THE MECHANISM

What mechanisms can we postulate for PP? For convenience, these can be divided into two types, *direct effects*, in which the site of action of PP is intimately related to the site of action of the UV, and *indirect effects*, in which the two sites are not closely related to each other.

##### A. Direct Effects

###### (1) *Simple Photochemical Alteration*

The simplest mechanism we can imagine is a direct photochemical alteration of the modifiable site that renders it less sensitive to UV. In favor of this is the independence of temperature and dose rate during PP irradiation, as well as the single-hit reaction kinetics, both suggesting that the early reactions are purely photochemical. However, if the modifiable site is nucleic acid, evidence against this mechanism is our inability to photoprotect either phage DNA inside cells or transforming principle in phosphate buffer, in addition to the action spectrum drop below 3400 Å. Simple photochemical alteration thus seems an unlikely mechanism.

###### (2) *Utilization of Other Molecules*

Other direct effects presumably would involve reaction of the modifiable site with some other molecule. This molecule could be

something quite simple, such as water, or it could be complex, such as a dye or an enzyme. Many possible types of reaction can be envisioned, but we shall not discuss these, partly because evidence bearing on them is scanty, and partly because at the present time direct effects seem less likely mechanisms than indirect effects.

### B. Enzyme Involvement

Both the wavelength range and the shape of the action spectrum make it unlikely that the PP photon is absorbed in unbound nucleic acid or protein, but rather favor a molecule showing better absorption in the near ultraviolet. Some dyes show an affinity for nucleic acids. Most cofactors or prosthetic groups of enzymes absorb well in the near ultraviolet. One can imagine a protein–nucleic acid complex sufficiently strained that it would absorb in the near ultraviolet without the aid of another molecule, but such a strain followed by photochemical reaction would require the protein to be, in effect, an enzyme. The spectral evidence thus tends to favor participation of a dye and/or an enzyme in PP, although the temperature–dose rate evidence is against an early enzymatic reaction.

What indication is there that the PR enzyme might be involved in PP? It is clearly unlikely that the mechanism of PP is similar to that of PR. However, the action spectrum for PR in *E. coli* B/r (Fig. 2) shows three components, and the PP action spectrum may correspond to the lower two of these. (It is possible that the lowest peak is involved in single-hit PP and the higher one in multi-hit PP.) Rupert's discovery of the ability of NADH to enhance PR and our finding of a PP action spectrum resembling NADH absorption is an interesting coincidence, for these results were obtained independently.

Harm and Hillebrandt<sup>11</sup> imply that the *phr*<sup>−</sup> mutant of *E. coli* B lacks the PR enzyme and conclude that it is not involved in PP. However, the mutation possibly involves merely a subtle change in the PR enzyme, perhaps affecting the cofactor known to be required for the *E. coli* system (Rupert *et al.*<sup>27</sup>). This mutation might render the enzyme incapable of the PR reaction, but still permit it to participate in one of the other types of reaction that we have discussed above. If so, one would expect the *phr*<sup>−</sup> strain to possess an enzyme capable of complexing with nucleic acid.

### C. Indirect Effects

The site of action of PP may be only distantly related to what is normally the site of crucial UV damage. In such an event, PP must be considered to be an "indirect effect". One can imagine at least three possible types of indirect effect: (1) alteration of the metabolism of the cell, permitting it to recover from UV damage by normal processes, (2) an action that permits the cell to bypass otherwise critical UV damage, or (3) prevention of a crucial UV damage by blockage of UV-induced poisons. The third mechanism seems unlikely, since there is little evidence that UV acts through the agency of diffusible poisons.<sup>14</sup> The second mode also seems unlikely, since the crucial UV damage is presumably to genetic material, which is usually indispensable. Only the first mechanism seems probable.

Photoprotection therefore probably acts by altering the metabolism of the cell in such a way that it can recover from the UV damage by processes not related to the initial events in PP. This implies that these processes occur normally, and that PP enhances their action, which is presumably repair of UV damage by enzymes. The alteration of metabolism by PP might operate in either of two ways: (1) by altering the enzyme balance of the cell, thus either enhancing the activity of repair enzymes or destroying molecules that interfere with normal repair processes, or (2) by producing a damage itself ("superimposed damage") that slows up the cell, thus providing more time for the operation of normal repair processes.

#### (1) *Alteration of Enzyme Balance*

Shugar<sup>30</sup> has reported that a triose phosphate dehydrogenase, to some fraction of which NADH is bound, could be inactivated by centrifugation and then reactivated by absorption of radiation in the range 3100–3800 Å. The NADH was not oxidized in this process, but merely passed the energy on to some other site, which Shugar tentatively associates with SH groups. This phenomenon, like PP, shows no temperature dependence during irradiation (5–25°C). Thus, it is possible that PP operates by changing the enzyme balance in the cell so it can more effectively cope with later UV irradiation. If this were so, one might expect that anoxic cells would have a

different NADH content and show a different degree of PP. However, a preliminary experiment in our laboratory showed the same PP whether cells were irradiated under a nitrogen or an air atmosphere.

## (2) *Superimposed Damage*

Hollaender,<sup>12</sup> who published some of the first careful studies of the action of near ultraviolet radiation on cells, has shown that near ultraviolet produces a delay in cell division in nutrient broth at sublethal doses. This is consistent with the hypothesis that PP acts by superimposed damage. However, the fact that we have been unable to photoprotect from X-ray damage argues against generalized effects such as those observed by Alper and Gillies<sup>1</sup> to operate with both UV and X-rays.

The recovery obtained by holding cells in liquid medium before plating, reported by Roberts and Aldous,<sup>25</sup> shows curves surprisingly similar to those for PP reported by Weatherwax (Fig. 1). This recovery works for *E. coli* B but not for B/r, and is observed with UV but not with X-rays, in agreement with the behavior of PP. Furthermore, it has been shown<sup>1</sup> that this "liquid-holding recovery" induces a division delay on nutrient agar of UV-irradiated cells that is greater than the division delay produced by UV alone, thus suggesting a similarity to the division delay in broth known to be produced by near UV.<sup>12</sup>

We have conducted experiments with *E. coli* B to investigate these factors.<sup>18</sup> Microscopic observations show that growth delay followed by division delay (i.e., no growth followed by growth without division, or "filament" formation) occurs on nutrient agar after irradiation at 3341 Å. These effects also occur in nutrient broth. The action spectrum for induction of growth delay in nutrient broth is identical to that for PP. Furthermore, the kinetics of this growth-delay induction are similar to those for PP. We conclude that an early step in the mechanism of PP is the induction of a growth delay.

We have also found<sup>18</sup> that liquid-holding recovery shows complete overlap with PP, and the two effects show additivity at suboptimal levels of treatment. We thus conclude that PP and liquid-holding recovery operate on the same UV damage.

Finally, if our hypothesis is correct, that PP operates by inducing



an additional growth delay after UV, then it should be possible to "photoprotect" cells by irradiation with near UV *after* irradiation with far UV. In most systems, this effect would be difficult to observe, since one might not distinguish "post-photoprotection" from photoreactivation. However, the *phr*<sup>-</sup> mutant of Harm permits the crucial experiment. We have found<sup>17</sup> that 4047 Å (a wavelength that should photoreactivate but not photoprotect) has no effect on *E. coli* B *phr*<sup>-</sup>, either before or after UV, thus confirming that this mutant is incapable of photoreactivation. However, 3341 Å produces high and roughly equal recovery whether given immediately before or immediately after UV. The effect in both cases is apparently an expression of the phenomenon that we have been calling "photoprotection" (quite correctly, since this is operationally defined). Thus, part of the normally observed phenomenon of photoreactivation is, in some organisms, a nonenzymatic effect that causes growth delay.

Kashket and Brodie<sup>19</sup> observed effects on respiration caused by irradiation of *E. coli* W with a broad band of near ultraviolet radiation. We have observed immediate effects on respiration caused by irradiation of *E. coli* B with a similar broad band. These results are consistent with the hypothesis that near ultraviolet inactivates quinones that are essential for normal respiration.

The following outlines our current concept of the mechanism of photoprotection. Photoprotecting radiation destroys certain quinones in the cell. These substances are essential for respiration, and their destruction causes a drop in respiration, with consequent induction of growth delay and division delay. This slowing of cellular metabolism (from which the cell recovers as soon as it has replaced the damaged quinones) permits more time for normally occurring processes to repair the UV damage in nucleic acid before the nucleic acid is required to replicate, an action that would probably confirm the damage. Liquid-holding recovery causes a similar slowing of cellular metabolism (by some unknown mechanism), leading to a similar repair of the UV damage.

#### D. Further Experiments

If our hypothetical mechanism of photoprotection is correct, then any treatment that induces a growth delay *in a photoprotectable cell* ought also to effect recovery from UV damage. Investigation of

such treatments should be carried out. The effect of "salt agar" might be explained in this way; one would predict that salt agar would cause the cells to grow and/or divide more rapidly, thus producing lower survival after UV and allowing a larger photoprotection. Similarly, holding recovery should appear larger if the cells are plated on salt agar.

It would be most satisfying and conclusive if we could eliminate the growth delay induced by near ultraviolet by feeding the cells normal quinones. This is not an easy experiment, but it seems well worth attempting.

Finally, it is conceivable that some of the cellular effects of far UV involve other components than nucleic acid. In particular, some of the growth-division effects may result from damage to quinones. Careful action spectra ought to provide the answer.

## V. GENERAL REMARKS

Although it is clear that photoprotection is of less biological importance than photoreactivation, the phenomenon nevertheless remains of great interest to the photobiologist. The very fact that it can happen is both fascinating and unexpected. The unraveling of its mechanism will contribute to our knowledge of the actions of both far and near ultraviolet radiation on cells. In particular, these studies may help illuminate the nature of the great variability in response that cells show to far ultraviolet radiation, as in the classic example of *E. coli* B and B/r.

## References

1. Alper, T., and Gillies, N. E., *J. Gen. Microbiol.* **18**, 461 (1958); **22**, 113 (1960).
2. Bawden, F. C., and Kleczkowski, A., *J. Gen. Microbiol.* **8**, 145 (1953).
3. Blum, H. F., Loos, G. M., and Robinson, J. C., *J. Gen. Physiol.* **34**, 167 (1950).
4. Blum, H. F., and Matthews, M. R., *J. Cellular Comp. Physiol.* **39**, 57 (1952).
5. Cantelmo, P., *Compt. Rend. Soc. Biol.* **145**, 1882 (1951).
6. Clark, J. B., and Frady, J., *J. Bacteriol.* **81**, 524 (1961).
7. Dulbecco, R., *J. Bacteriol.* **59**, 329 (1950).
8. Dulbecco, R., in A. Hollaender (Ed.), *Radiation Biology*, Vol. II, McGraw-Hill, New York, 1955, pp. 455-486.
9. Giese, A. C., Brandt, C. L., Iverson, R., and Wells, P. H., *Biol. Bull.* **103**, 336 (1952).

10. Giese, A. C., Brandt, C. L., Jacobson, C., Shepard, D. C., and Sanders, R. T., *Physiol. Zool.* **27**, 71 (1954).
11. Harm, W., and Hillebrandt, B., *Photochem. Photobiol.* **1**, 271 (1962).
12. Hollaender, A., *J. Bacteriol.* **46**, 531 (1943).
13. Hollaender, A. (Ed.), *Radiation Biology*, Vol. II, McGraw-Hill, New York, 1955.
14. Jagger, J., *Bacteriol. Rev.* **22**, 99 (1958).
15. Jagger, J., *Radiation Res.* **13**, 521 (1960).
16. Jagger, J., and Stafford, R. S., *Photochem. Photobiol.* **1**, 245 (1962).
17. Jagger, J., and Stafford, R. S., *Biophys. J.* (submitted) (1964).
18. Jagger, J., Wise, W. C., and Stafford, R. S., *Photochem. Photobiol.* (in press) (1964).
19. Kashket, E. R., and Brodie, A. F., *J. Bacteriol.* **83**, 1094 (1962).
20. Kelner, A., *Proc. Natl. Acad. Sci. U.S.* **35**, 73 (1949).
21. Kelner, A., *J. Bacteriol.* **58**, 511 (1949).
22. Miki, K., *Japan. J. Bacteriol.* **11**, 803 (1956) (in Japanese).
23. Monod, J., Torriani, A. M., and Jolit, M., *Compt. Rend.* **229**, 557 (1949).
24. Perlitz, M., and Kelner, A., *Science* **118**, 165 (1953).
25. Roberts, R. B., and Aldous, E., *J. Bacteriol.* **57**, 363 (1949).
26. Rupert, C. S., in A. C. Giese (Ed.), *Photophysiology*, Academic Press, New York, 1964.
27. Rupert, C. S., Goodgal, S. H., and Herriott, R. M., *J. Gen. Physiol.* **41**, 451 (1958).
28. Sarachek, A., *Cytologia* **19**, 77 (1954).
29. Setlow, J. K., and Setlow, R. B., *Nature* **197**, 560 (1963).
30. Shugar, D., *Experientia* **7**, 26 (1951).
31. Swenson, P. A., and Setlow, R. B., *Photochem. Photobiol.* **2**, 419 (1963).
32. Weatherwax, R. S., *J. Bacteriol.* **72**, 124 (1956).
33. Weatherwax, R. S., *Bacteriol. Proc.* 99 (1961).
34. Wulff, D. L., and Rupert, C. S., *Biochem. Biophys. Res. Commun.* **7**, 237 (1962).

*Addendum.* It has recently been reported (Witkin, E. M., *Proc. Natl. Acad. Sci. U.S.* **50**, 425, 1963) that *E. coli* B/r, strain WU36, shows PP in the late lag phase of growth. We have since found that our strain of B/r (ORNL) shows excellent PP in the logarithmic phase but none in stationary phase. Apparently, previous unsuccessful attempts to photoprotect B/r were made with stationary cultures. Other microorganisms that have shown no PP in stationary phase should now be tested in logarithmic phase. These and similar tests may, as we have suggested (Section II-B), reveal that PP is more widespread than present data would indicate. This behavior of B/r is consistent with our proposed mechanism of PP, since the inherent division delay of freshly plated stationary cells may, in this strain, be sufficient for full dark recovery and therefore not be aided by additional photo-induced division delay. In agreement with this interpretation is our recent finding that PP in strain B is much larger for logarithmic than for stationary cultures.

## 16

# SOME RECENT DEVELOPMENTS IN THE STUDY OF PARAMAGNETIC SPECIES OF BIOLOGICAL INTEREST

ANDERS EHRENBORG, *Biokemiska Institutionen,  
 Medicinska Nobelinstitutet, Karolinska Institutet, Stockholm, Sweden*

## CONTENTS

I. Introduction . . . . .	602
II. Experimental Techniques . . . . .	603
A. Static Susceptibility . . . . .	603
(1) Gouy Balance . . . . .	603
(2) Rankine Balance . . . . .	605
B. Electron Spin Resonance Spectroscopy . . . . .	605
C. Comparison of Methods . . . . .	607
III. Enzyme Systems and Components . . . . .	607
A. Hemoproteins . . . . .	607
(1) General Considerations . . . . .	607
(2) Temperature Dependence . . . . .	609
(3) Reactions between Ferrihemoproteins and Peroxides. . . . .	612
B. Flavin Free Radicals and Flavoproteins . . . . .	617
C. Multicomponent Systems . . . . .	620
IV. Radiation-Induced Free Radicals . . . . .	621
A. General Considerations . . . . .	621
B. Model Systems . . . . .	622
C. Living Seeds . . . . .	623
V. Concluding Remarks . . . . .	626
References . . . . .	626

## I. INTRODUCTION

The work in the 1930's of Pauling and co-workers on hemoglobin and its derivatives<sup>29</sup> and of Michaelis and his associates on organic free radicals related to enzyme systems<sup>27</sup> was a "catalyst" that started an increasing interest in the magnetic properties of biochemicals. The development and application of more sensitive experimental techniques and more refined theoretical treatments during the last fifteen years have led to a steady increase in the

number of investigations on paramagnetic biological material reported each year.

Informative data on the structure and mode of action of many enzymatically active metalloproteins have been obtained by magnetic methods. Likewise, the appearance of free radicals has been traced during the reactions of several metalloproteins and flavoproteins and in the photosynthetic process. In the last few years the powerful technique of electron spin resonance (ESR) absorption has been applied extensively by research workers in the fields of biochemistry and radiobiology. In the following we will briefly discuss some methods used and outline some current trends and problems in the fields of research mentioned.

## II. EXPERIMENTAL TECHNIQUES

### A. Static Susceptibility

#### (1) *Gouy Balance*

It was possible to study only a limited number of biological substances by the susceptometric techniques used in common physicochemical work. The expenses and the difficulties involved in the preparation of the comparatively large quantities of pure material needed by the conventional techniques created the need for experimental methods more suited for biochemical and biophysical work. The construction by Theorell in 1942<sup>33</sup> of a modification of the well-known Gouy method with a horizontal tube in bifilar suspension was the first successful attempt to decrease the sample volume and still maintain a high sensitivity. It is interesting to note that a modified version of this instrument has also been used by Howland and Calvin<sup>24</sup> in order to determine the magnetic properties of transuranium salts in dilute solutions. The technical problems faced in the research on the physicochemical properties of biological material have much in common with the difficulties met in the study of rare inorganic substances. The principle of Theorell's original instrument was that a deflection of the sample tube itself was a measure of the acting magnetic force. For an improved design, the principle of which is shown in Fig. 1, Theorell and Ehrenberg<sup>34</sup> took advantage of the inherent possibility of this type of instrument, viz. that a decrease in the volume of the sample by shortening the tube and concentrating the sample to the region of maximum

force in the inhomogeneous field should simultaneously increase the sensitivity. Because of the increase of the ratio between the weights of the sample tube and the sample when the length of the tube is decreased, there is an optimum size of the tube that gives the best sensitivity for a given shape and material. It is essential to keep the sample in the region of maximum field inhomogeneity independently of the strength of the acting magnetic force. Therefore the

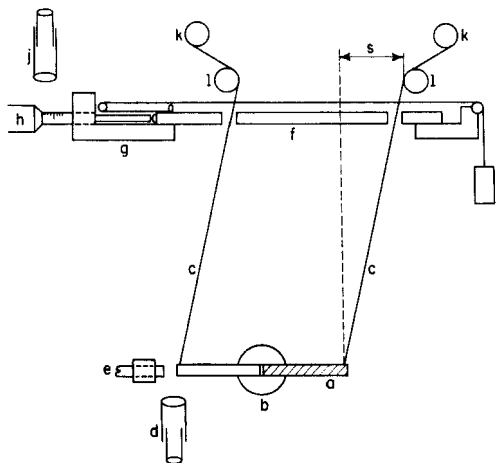


Fig. 1. The main principles of the modified Gouy balance. (a) Sample tube, (b) poles of electromagnet, (c) suspension fibers, (d) microscope, (e) fixed index screw, (f) slide, (g) guide, (h) micrometer, (i) weight, (j) reading telescope, (k) unrolling cylinders, (l) cylinders with guiding core, and (s) displacement.

(From Theorell and Ehrenberg.<sup>34</sup>)

upper fixing points of the thin suspension fibers of the tube are made so that they can be moved on a guide. The necessary displacement to maintain the position of the tube is read on a sensitive micrometer which controls the movement along the guide while the position of the tube itself is checked under a microscope. With the improvements described there was about a ten-fold increase in sensitivity and the whole construction of the instrument was made suitable for quick and easy operation. Later, an adequate temperature control further improved the reproducibility and made it possible to operate the instrument at any temperature within the range from about 5° to about 50°C.<sup>12</sup>

The main drawback of the modified Gouy balance is the poor time

resolution (see Table I). It takes between  $1\frac{1}{2}$  and 2 min after mixing the sample until the first reading can be made. It has nevertheless been possible to obtain reliable data on some intermediates in the important reactions between hemoproteins and peroxides.<sup>11, 36</sup>

### (2) *Rankine Balance*

In order to make it possible to follow the magnetic changes of more rapid reactions and to determine the paramagnetic susceptibility of more short-lived reaction intermediates Brill and co-workers<sup>9</sup> constructed a very sensitive Rankine balance. With this type of instrument, having a stationary sample container and a suspended mobile bar magnet, it was possible to use a flow system and an automatic recording of the susceptibility data. The careful design of this unique susceptometer led to a time resolution of better than 0.05 sec for flow experiments and better than 1 sec for stopped flow experiments. The main difficulties with the present apparatus seem to be the rather large volume required by the flow system (cf. Table I and Reference 7) and great sensitivity to magnetic disturbances from the surroundings, e.g. magnetic storms. As pointed out by Brill<sup>7</sup> the necessary volume of the flow system could possibly be reduced by a factor of about six.

### B. Electron Spin Resonance Spectroscopy

Before the ESR technique could be used with success in biological research some special technical problems had to be solved. Most biochemical experiments have to be carried out in liquid aqueous solutions, but any penetration of the sample into the high frequency electric field of the standing wave of the spectrometer cavity decreases the sensitivity seriously because of the great dielectric loss of the water. However, it was soon realized that the dielectric loss could be abolished to a large extent by a decrease of the sample dimensions by using a capillary with a bore of less than 1 mm or a planar cuvette with a very thin layer of liquid. Because of the positioning of the sample in the region of maximum amplitude of the high frequency magnetic field the effective filling of the cavity is decreased much less than in proportion to the sample volume and a great sensitivity is therefore still maintained.

The combination of the ESR technique with flow experiments has

been achieved in two rather different ways. Yamazaki *et al.*<sup>38</sup> and Nakamura<sup>28</sup> have coupled a mixing chamber immediately before the liquid aqueous sample cuvette. This technique has the advantage that the aqueous solutions are studied at room temperature, so that isotropic hyperfine structures of small substrate molecules will be well resolvable. It is further possible to correlate the ESR data directly to changes in the light absorption.

The other method as developed by Bray<sup>3,5</sup> is based on the principle that the sample after the mixing, via a jet, is thrown into a low temperature coolant so that the sample is very rapidly frozen in small droplets and the reaction is stopped at the moment of freezing. The sample is packed into a quartz tube and is supposed to remain unchanged during the length of time necessary for its detailed examination in the ESR spectrometer at a low temperature. The method has the obvious and great advantage of an increased sensitivity as compared with the measurement on liquid aqueous samples. A drawback is that most hyperfine structures will become unresolvable in the frozen state. Complications might also arise from possible thermal shifts of redox equilibria in complex enzyme systems through electron transfer between the active groups, a mechanism that could well operate even at very low temperatures.

In biochemical and radiobiological work it is often desired to determine the absolute amount or concentration of the free radicals or transition metal ion complexes investigated. Several methods have been developed and a number of calibration agents have been used in order to achieve an absolute calibration of the ESR spectrometer. An absolute calibration cannot at present be considered reliable to better than  $\pm 50\%$ , as has been demonstrated in a recent comparison between calibration data obtained by several research groups, each group applying its own technique.<sup>25</sup> The determination of relative concentrations of paramagnetic centers in samples giving equal or only slightly different dielectric losses is comparatively easy. It is far more difficult to compare samples with greater differences in the dielectric properties, e.g. hydrophilic colloids or living seeds with different water contents. Our method<sup>15</sup> with successively decreasing geometrical dimensions of the samples and an extrapolation to infinitely small samples, seems to have a rather general applicability. Only when the ESR signal strength is weak it is difficult to make a satisfactory extrapolation.



### C. Comparison of Methods

Some data on the performance of the three methods discussed above are collected in Table I. The data chosen for the ESR technique are estimated from the author's own experience and should be considered as approximations. The sensitivity figures are in this case valid for free radical signals with a width of about 10 gauss. A narrower signal corresponds to a greater sensitivity and vice versa. As usual the sensitivity is also dependent on the time resolution chosen, the longer response time corresponding to the higher sensitivity. Only typical data are given in the table.

The two susceptometer methods respond indistinguishably to all magnetic species of the sample and special corrections for diamagnetism are usually necessary in order to obtain the sum of the paramagnetic contributions. One of the great advantages of the ESR spectroscopy is its independence of the diamagnetism and its power to resolve the absorptions from the different paramagnetic species. A serious drawback is, however, that some ESR absorptions are not detectable under normal experimental conditions and that interactions between paramagnetic species in close proximity to each other might distort the absorptions and make them difficult to identify. For these reasons the susceptometric methods and the ESR method are in many cases necessary complements to each other (cf. Section III-C). Also, the two susceptometric techniques described are complementary. From Table I it is seen that in order to achieve the increased time resolution of the Rankine method it is necessary to spend at least 30 times more material than in the Gouy method. Therefore, the Rankine method has so far been applied only to reactions with velocities that really require the high time resolution.

## III. ENZYME SYSTEMS AND COMPONENTS

### A. Hemoproteins

#### (1) *General Considerations*

Theoretical aspects on the magnetic properties of iron porphyrin compounds are found in other chapters of this volume. Here it may be sufficient to make a few remarks for reference in the following sections.

TABLE I. Typical Data of Performance of Three Important Magnetic Methods Applied in Biological Research on Aqueous Solutions

Method	Volume		Sensitivity, "noise level", expressed				Time resolution, sec
	$V_{\text{required}}$	$V_{\text{effective}}$	in detectable susceptibility increment $\Delta\chi$ ,	in detectable number of spins ( $S = \frac{1}{2}$ ) in effective volume,	as relative sample sensitivity $V_{\text{required}} \times \Delta\chi$ ,		
	cm <sup>3</sup>	cm <sup>3</sup>	cgsemu $\times 10^{-11}$	10 <sup>13</sup>	cm <sup>3</sup> $\times$ cgsemu $\times 10^{-11}$		
Gouy <sup>a</sup>	0.3	0.3	5	700	1.5		$\geq 100$
Rankine <sup>b</sup>	{ flow stopped flow	300	0.7	0.5	150		0.05
		300	0.7	0.15	45		$\leq 1$
ESR <sup>c</sup>	{ no flow flow or stopped flow	0.2	0.075	0.15	0.03		$\geq 10$
		10	0.075	1	10		0.1

<sup>a</sup> Theorell, H., and Ehrenberg, A., *Arkiv Fysik* **3**, 299 (1951).<sup>b</sup> Brill, A., den Hartog, H., and Legallais, V., *Rev. Sci. Instr.* **29**, 383 (1958).<sup>c</sup> Sensitivity figures in this case were estimated for free radical signals with a width of 10 gauss.

The effective magnetic moment  $\mu_{\text{eff}}$  of the iron is calculated from the measured paramagnetic susceptibility  $\chi$ , the absolute temperature  $T$  and Curie-Weiss constant  $\Theta$  according to the formula

$$\mu_{\text{eff}} = 2.84\sqrt{\chi(T + \Theta)} \quad (1)$$

When  $\Theta$  is not known it is generally assumed to be zero.

The hemoproteins with ferric or ferrous octahedrally coordinated iron are known to form both high- and low-spin compounds with suitable ligands in the sixth position. Based on theoretical arguments Griffith<sup>23</sup> has suggested that compounds with this property cannot usually be expected to form derivatives also of the intermediate-spin type. Predicted values of the magnetic moment of the iron of heme compounds are shown in Table II.

TABLE II. Predicted  $\mu_{\text{eff}}$  Values of Pure High- and Low-Spin States of Heme Compounds at 20°C with the Iron in Various Oxidation States (from Ehrenberg<sup>13</sup>)

Oxidation state	Number of unpaired electrons	Susceptibility	Predicted $\mu_{\text{eff}}$ value or range Bohr magnetons
Fe <sup>2+</sup>	4	spin + orbital	4.90-5.64
Fe <sup>2+</sup>	0	diamagnetic	0
Fe <sup>3+</sup>	5	spin only	5.92
Fe <sup>3+</sup>	1	spin + orbital	1.73-2.8
Fe <sup>4+</sup>	4	spin only	4.90
Fe <sup>4+</sup>	2	spin + orbital	2.5-3.6
Fe <sup>5+</sup>	3	spin only	3.87

## (2) Temperature Dependence

The possibility of a close balance between two spin states of a compound and an equilibrium between these states as an explanation of intermediate experimental susceptibility values seems to have been considered for the first time by Cambi and Szegoe in the case

of some substituted dithiocarbamate iron complexes.<sup>10</sup> Because hemoglobin hydroxide has a paramagnetic susceptibility intermediate between that of the hydroxide of myoglobin, which is not far from the expected high-spin value, and that of the hydroxide of horse-radish peroxidase, which is close to the expected low-spin value, and because the absorption spectrum of hemoglobin hydroxide in the visible region is strictly intermediate between those of the other two hemoprotein hydroxides, we suggested the possibility that there might be equal portions of high- and low-spin iron in hemoglobin hydroxide.<sup>35</sup> Later theoretical considerations by Griffith<sup>23</sup> have led to the conclusion that intermediate magnetic moments of heme compounds in general should be due to intramolecular thermally balanced equilibria of different spin states. Great caution is necessary, however, when judging the weight of the existing experimental evidence. When the temperature dependence of the paramagnetic susceptibility of the heme compound is studied it must be remembered that two effects are superimposed: the temperature dependence of the susceptibility of the pure spin states according to Curie-Weiss law

$$\chi = C(T + \Theta) \quad (2)$$

and the thermal shift of the equilibrium of the two spin forms. The investigations by Schoffa *et al.*<sup>31</sup> on frozen solutions of several hemoprotein derivatives indicated that the Curie law ( $\Theta = 0$ ) should be valid for most of the compounds studied. A serious difficulty encountered in the interpretation of these data is, however, the unexpectedly but consistently low susceptibilities observed in the frozen solutions. Schoffa *et al.* suggested that the effect could be a result of a proposed magnetic anisotropy of the heme compounds. This explanation seems, however, to be in conflict with the recent observation by McKim<sup>26</sup> that there is no detectable magnetic anisotropy of acid ferrimyoglobin above 200°K, but below this temperature the anisotropy is developed and increases rapidly with falling temperature. Furthermore, the magnetic anisotropy must be expected to be different for different heme derivatives.

The determination of the Weiss constant,  $\Theta$ , for hemoproteins in aqueous solution is quite difficult because the temperature range within which the susceptibility measurements can be achieved is

restricted and because the physically dissolved oxygen must be removed or else corrected for. Sometimes, as in the case of ferri-myoglobin hydroxide and ferrihemoglobin hydroxide, it is also necessary to correct for the thermal shift of an acidic dissociation in which the species under study are involved. Furthermore, we have experienced that the measurements are occasionally complicated by irreversible denaturation processes at the elevated temperature used. Some preliminary results obtained by the author on the temperature dependence of the acidic and alkaline forms of ferri-myoglobin and ferrihemoglobin from horse are given in Table III.

TABLE III. The Temperature Dependence of the Paramagnetic Susceptibility of Some Hemoprotein Derivatives in Aqueous Solutions

Derivative	Temperature range, °C	$\Theta_{app}$ , °K	$\mu_{app}$ , Bohr magnetons
Ferritin	6-43	-93 ( $\pm 17$ )	2.9 ( $\pm 0.2$ )
Ferrimyoglobin	13-37	0 ( $\pm 30$ )	5.8 ( $\pm 0.3$ )
Ferrimyoglobin hydroxide	8-37	70 ( $\pm 60$ )	5.7 ( $\pm 0.6$ )
" "	1-20	1300 <sup>a</sup>	$\geq 6$ <sup>a</sup>
Ferrimyoglobin fluoride	1-20	0 <sup>a</sup>	5.9 <sup>a</sup>
Ferrimyoglobin cyanide	1-20	270 <sup>a</sup>	2.9 <sup>a</sup>
Ferrihemoglobin	13-39	70 ( $\pm 60$ )	6.2 ( $\pm 0.5$ )
Ferrihemoglobin hydroxide	13-39	$\sim \infty$	$\geq 6$

<sup>a</sup> Data calculated from George, P., Beetlestone, J., and Griffith, J. S., in J. E. Falk *et al.*, Eds., *Haematin Enzymes*, Pergamon Press, London, 1961, Part 1, p. 105.

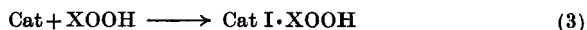
The results are expressed in terms of the Weiss constant  $\Theta$ , and the apparent magnetic moment  $\mu_{app}$  has been calculated by means of  $\Theta$ . Ferritin has also been included in the table since it was used to check the performance of the instrument. The  $\theta$  value of ferritin agrees well with that found by Bayer and Hausser.<sup>2</sup> Some data calculated from susceptibility values reported by George *et al.*<sup>21</sup> are also included. It is seen that with the techniques used, the accuracy of the susceptibility data does not lead to any irrefutable conclusions about equilibria between closely balanced spin states. The high  $\Theta$  values for the hydroxides indicate, however, that such

equilibria are likely to exist in these cases, but for myoglobin hydroxide the data are still somewhat contradictory. More conclusive experimental evidence that these derivatives really represent thermally balanced mixtures of high- and low-spin forms has, however, been obtained by means of light absorption<sup>21</sup> and electron spin resonance absorption.<sup>14</sup> The result from differential light absorption experiments at two temperatures usually must be interpreted with some caution because the results will be influenced by the same complicating factors as discussed above in connection with the corresponding magnetic experiments.

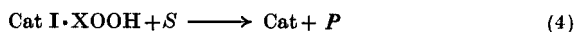
### (3) *Reactions between Ferrihemoproteins and Peroxides*

Among the hemoproteins the hydroperoxidases catalase (Cat) and horse-radish peroxidase (Per) are well known as catalysts for the oxidation of substrates by means of peroxide. With the notation XOOH for hydrogen peroxide or an alkylhydrogen peroxide, *S* for substrate and *P* for product, the widely accepted reaction schemes are as follows.

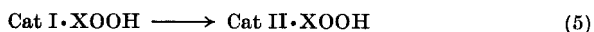
Ferricatalase reacts with peroxide under the formation of a primary compound (I)



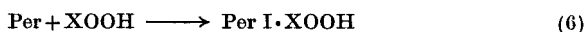
This compound will rapidly oxidize the substrate and reverts into catalase



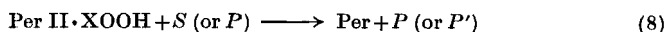
Under certain experimental conditions the primary compound may be transformed into a secondary compound, which is comparatively inactive as an oxidant



Ferriperoxidase also forms a primary compound with peroxide



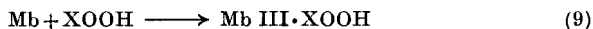
which, however, reacts with the substrate in two steps, with the secondary compound as an intermediate:



Other peroxide compounds of the hydroperoxidases and also of

other hemoproteins are known and classified as type III, IV or V according to their light absorption bands.

Ferrimyoglobin (Mb), which is not a true hydroperoxidase, also combines with peroxide in a reaction where a compound of type III is formed:



The available susceptibility data expressed in  $\mu_{\text{eff}}$  for the ferri-hemoprotein peroxide compounds of formulas (3)–(9) are collected in Table IV. From titration experiments it is known that the primary compounds contain the full oxidative power of the peroxide while the compounds of type II and III retain only one of the original oxidizing equivalents of peroxide. The formal valence of the iron, or of the whole complex, if that terminology is preferred, corresponds to  $\text{Fe}^{\text{V}}$  in the compounds of type I and to  $\text{Fe}^{\text{IV}}$  in those of type II and III. For details see, for examples, the brief review<sup>13</sup> with references.

It might be valuable to briefly discuss here the postulated mechanisms in terms of the magnetic data and their relationship to the splitting parameter  $\Delta$  of the ligand-field theory.  $\Delta$  denotes the energy separation between the three nonbonding  $t_{2g}$  orbitals and the two antibonding  $e_g$  orbitals and determines largely how the available  $3d$  electrons of the iron are distributed among these orbitals. In a high-field compound  $\Delta$  is large, and in a low-field compound  $\Delta$  is small. For details of the ligand-field theory the reader is referred to other chapters of this volume, especially Chapter 3. In the following discussion we will omit the peroxide symbol from the symbols of the hemoprotein derivative but add the assumed valence of iron.

Cat  $\text{Fe}^{\text{III}}$  is a low-field compound with five unpaired electrons. Cat I  $\text{Fe}^{\text{V}}$  has three unpaired electrons, which case does not distinguish between the high- and the low-field alternatives. If we, however, assume an extra stabilizing  $\pi$  bond between the peroxide (or the peroxide rest) and the iron, one of the  $t_{2g}$  orbitals will be used and we are consequently led to assume that Cat I  $\text{Fe}^{\text{V}}$  is a low-field compound. It is reasonable to picture also the activated intermediates of reactions (3) and (4) as low-field catalase compounds, e.g. excited Cat I  $\text{Fe}^{\text{V}}$  without any  $\pi$  bond. Only rather small changes of the orbitals and minor redistribution of the charges are necessary and, as far as the heme iron of catalase is concerned, there is thus only a

TABLE IV. Magnetic Properties of Some Hemoproteins and Their Peroxide Compounds

Compound	$\mu_{\text{eff}}$ , Bohr magnetons <sup>a</sup>	Assumed valence of Fe	Assumed number of unpaired electrons	Ref.
Cat	5.66	3	5 ( $\rightleftharpoons 1$ )	b
Cat I · MeOOH	3.90	5 (3)	3 ( $5 \rightleftharpoons 1$ )	c
Cat II · MeOOH	2.93	4	2	d
Per	5.27	3	$5 \rightleftharpoons 1$	d
Per I · MeOOH	3.99	5 (3)	3 ( $5 \rightleftharpoons 1$ )	d
Per II · MeOOH	3.53	4	(2) $4 \rightleftharpoons 2$	d
Mb	5.73	3	5 ( $\rightleftharpoons 1$ )	e
Mb III · MeOOH	$\begin{cases} 2.76 \\ 2.79 \end{cases}$	4	2	$\begin{cases} d \\ f \end{cases}$
Mb III · HOOH	2.97	4	2	d

When the valence or the number of unpaired electrons is uncertain the alternatives are indicated, the less likely being within parentheses. Assumed equilibria between spin states are indicated with double arrows. When the equilibrium is shifted far to one side, the less important state is written within parentheses.

<sup>a</sup> All  $\mu_{\text{eff}}$  values have been corrected according to Griffith, J. S., *Biochem. Biophys. Acta* **28**, 439 (1958).

<sup>b</sup> Deutsch, H. F., and Ehrenberg, A., *Acta Chem. Scand.* **6**, 1522 (1952).

<sup>c</sup> Brill, A. S., and Williams, R. J. P., *Biochem. J.* **78**, 253 (1961).

<sup>d</sup> Theorell, H., and Ehrenberg, A., *Arch. Biochem. Biophys.* **42**, 442 (1952).

<sup>e</sup> Theorell, H., and Ehrenberg, A., *Acta Chem. Scand.* **5**, 823 (1951).

<sup>f</sup> Brill, A. S., Ehrenberg, A., and den Hartog, H., *Biochim. Biophys. Acta* **40**, 313 (1960).

small contribution to the activation energy. This is in accordance with the high velocity constants of the reactions.

Cat II Fe<sup>IV</sup>, on the other hand, is a low-spin, high-field compound with large  $\Delta$ . The activated intermediates between Cat I Fe<sup>V</sup> and Cat II Fe<sup>IV</sup> and between the latter compound and Cat Fe<sup>III</sup> are likely to be high-spin, high-field compounds of a type represented by, for example, excited Cat Fe<sup>IV</sup>, with four unpaired electrons. Obviously, the contribution to the activation energy from this kind



of electron redistribution at the iron must be considerably larger than in the case discussed in the previous paragraph. This is in good agreement with the comparative sluggishness of reaction (5) and of the peroxidatic action of Cat II  $\text{Fe}^{\text{IV}}$  leading back to Cat  $\text{Fe}^{\text{III}}$ . Similar arguments apply to the formation (reaction (9)) and further reaction of Mb III  $\text{Fe}^{\text{IV}}$ .

From Table IV we see that peroxidase has a much lower  $\mu_{\text{eff}}$  than catalase and myoglobin, which derives from an intermediate susceptibility of peroxidase. Therefore, we have to assume that Per  $\text{Fe}^{\text{III}}$  is a thermal mixture of high- and low-spin forms with a corresponding intermediate value of  $\Delta$  (i.e. medium ligand field) in order to satisfy the requirements of a close balance between the two spin forms. The electronic structure of the heme of Per I  $\text{Fe}^{\text{V}}$  is presumably similar to that of Cat I  $\text{Fe}^{\text{V}}$ . The activated intermediate of reaction (6) and that of the peroxidase analogue of reaction (4) are presumably of the intermediate-field type. Because Per  $\text{Fe}^{\text{III}}$  also has an intermediate field the activation energy of reaction (6) will receive only a small contribution from the heme. However, the contribution to the activation energy of a two-electron transfer reaction similar to reaction (4) will be larger than the corresponding for catalase.

The activated intermediates of the peroxidatic reactions (7) and (8) are presumably also of the intermediate-field type. This means a smaller contribution to the activation energy of reaction (7) leading from Per I  $\text{Fe}^{\text{V}}$  to Per II  $\text{Fe}^{\text{IV}}$  as compared with the corresponding reaction of catalase. If we further assume that Per II  $\text{Fe}^{\text{IV}}$  is an intermediate-field compound, which is in agreement with its magnetic moment (see Table IV), the contribution from the heme iron to the activation energy of reaction (8) must also be comparatively small. Hence, there is agreement between the magnetic data and the reaction velocities in the proposed reaction scheme.

It is not suggested that the above discussion offers an explanation of the enzymatic mechanisms. These are determined by several factors, the most important of which are the iron-protein and iron-peroxide coordination, influences from neighboring groups, and steric factors. Of these effects only those from the iron-protein and iron-peroxide coordination are likely to be reflected in the paramagnetic properties of the compounds involved. Our arguments are merely meant to show that there is no contradiction between the

present interpretation of the magnetic susceptibility data by means of the ligand-field theory and the known reaction mechanisms: a direct transfer of two equivalents in one step in the catalytic reaction of catalase and the successive two-step release of the oxidative equivalents in the peroxidatic reaction of peroxidase.

It is obvious that the primary products of reactions (7) and (8) must be free radicals provided the substrate itself is not a free radical. By means of ESR spectroscopy Yamazaki *et al.*<sup>38</sup> have studied the steady state concentration of the free radicals formed in flow experiments with peroxidase. They found the dependence of the free radical concentration on the concentrations of the reactants to be well compatible with the reaction sequence (6) to (8). As they point out, however, their data are completely inconsistent with a mode of reaction similar to that of catalase (reactions (3) and (4)), followed by free radical formation in a dismutation reaction.

It has been proposed that the second oxidative equivalence of peroxide, which is not present in Mb III, should be released as a free radical in reaction (9). The released radicals would be short lived but could be stabilized by reaction with the protein. The existence of such radicals was discovered by Gibson *et al.*<sup>22</sup> who investigated frozen reaction mixtures in an ESR spectrometer.

In collaboration with Brill and den Hartog the author had the privilege to take part in an investigation of reaction (9) by means of the Rankine balance with its regenerative flow system.<sup>8</sup> The maximum decrease in susceptibility led to a value of the susceptibility of Mb III · MeOOH in excellent agreement with our previous value (see Table IV). The kinetics of the decrease of the paramagnetism and of the changes in light absorption were compared. The directly observed susceptibility change was found to be slightly slower than expected from the curve calculated from the light absorption data. This difference is likely to be due to a piling up of short-lived free radicals during a period of the reaction when they are being formed most rapidly.

Applying the same technique Brill<sup>7</sup> has investigated reactions (3) and (4) with bacterial catalase. In this case also it was found that the change in paramagnetism and in light absorption did not have exactly the same time course. The difference might be due to the formation of free radicals or to a yet unidentified intermediate, but the interpretation is uncertain and it is not yet even clear whether

the transient paramagnetism observed is related to the main reaction or to a side reaction.

As far as the author is aware it has not yet been possible to detect any ESR absorption from the heme iron of the peroxide complexes discussed in this section.

### B. Flavin Free Radicals and Flavoproteins

The reduction or oxidation of flavins is known to take place in two successive one equivalent steps with stable free radicals as intermediates. It is generally considered that these free radicals have importance for the action of the flavoenzymes of the respiratory chain.

When flavin mononucleotide alone is partially reduced the yield of free radicals varies considerably with pH.<sup>12</sup> Only at very low pH values is the yield high enough to make it possible to measure the paramagnetic susceptibility in the modified Gouy balance. Such measurements were used in order to achieve an absolute calibration of the ESR spectrometer for flavin free radicals. The flavin radical has two acid dissociations and the hyperfine structure of the ESR spectrum changes accordingly with pH, as can be seen from Fig. 2. The alkaline form has 14 evenly spaced hyperfine lines, whereas the neutral form has at least 32 lines with uneven spacing. At pH 9 to 10 and in very acid solutions there is a smearing out of the hyperfine structure which is probably due to interaction between the free radicals and the oxidized and reduced forms, respectively.<sup>12</sup>

The observed hyperfine structures have to be explained in terms of interactions between the unpaired electron and the hydrogens and nitrogens of the isoalloxazine framework. Whereas the spectrum of the neutral form is so complicated that no complete explanation is desired at present, that of the alkaline form is comparatively simple and a limited number of schemes of hyperfine interaction can be set up which agree about equally well with the experimentally determined absorption curve. In none of the cases can there be neglected the contribution from the hydrogens and methyl groups of the benzenoid ring or from the nitrogens of the pyrazine-like central ring. Because experiments in alkaline D<sub>2</sub>O give identically the same ESR absorption as in H<sub>2</sub>O, it is concluded that the imino nitrogen of the pyrimidine-like ring does not take part in the

hyperfine splitting. According to Theorell and Nygaard<sup>37</sup> this group is engaged in the binding of the coenzyme to the apoprotein of the flavoenzyme named the "old yellow enzyme". Ehrenberg

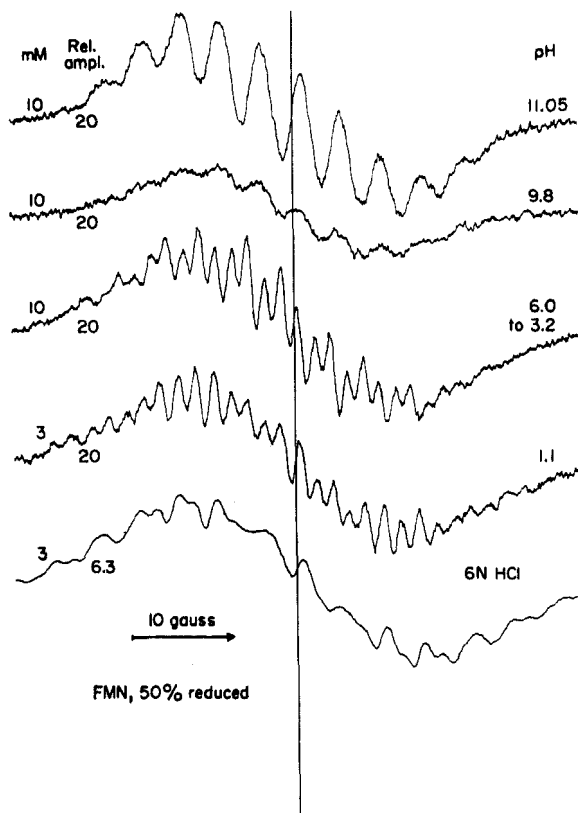


Fig. 2. ESR recordings of FMN free radicals at different pH values. All samples were half-reduced with dithionite. Concentrations and relative amplifications are indicated. A 100 kc peak-to-peak modulation of 0.30 gauss was employed. (From Ehrenberg.<sup>12</sup>)

and Ludwig<sup>18</sup> have shown, by means of ESR absorption, that free radicals are formed in this enzyme when it operates between its specific reductant and oxygen. These findings suggest that there might exist an interesting functional partition within the flavin molecule.

The ESR spectra of the enzyme radicals do not show any of the hyperfine details of the unbound flavin free radicals. This is clearly demonstrated in Fig. 3 from which it is also seen that the absorption of the enzyme radicals covers a much wider range of the field. The reason for this behavior is that the radicals of the flavin

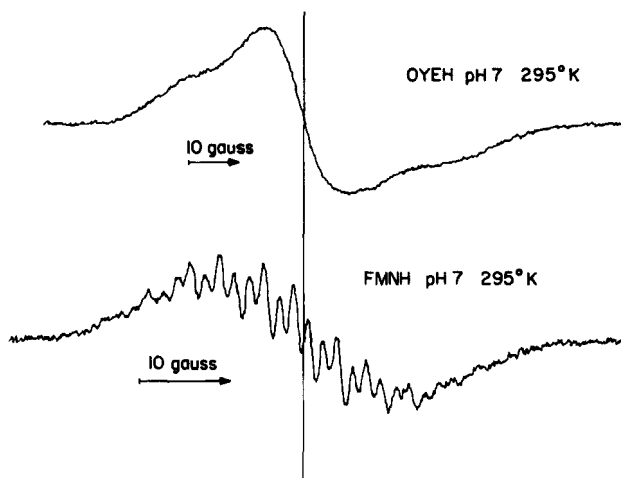


Fig. 3. ESR recordings of OYE (*ca.* 1 mM in FMN) reacted with TPNH (*ca.* 50 mM) in 0.2 M phosphate, and 10 mM FMN half-reduced by dithionite in the same buffer, both at room temperature. Note the different field scales. (From Ehrenberg.<sup>12</sup>)

mononucleotide in the aqueous solution have a thermal rotational relaxation time of about  $10^{-9}$  sec, whereas the much larger protein molecules have a relaxation of the order of  $10^{-7}$  sec. This means that the averaging out of the anisotropic terms of the ESR absorption will be effective up to about 30 gauss for the flavin radicals but only up to a fraction of a gauss for the enzyme radicals. The lack of resolved isotropic hyperfine structure from the radicals of the enzyme system is thus evidence showing that the radicals are really bound to the macromolecules. The same circumstance, however, renders it impossible with the present technique to unequivocally identify the enzyme radicals as belonging to the flavin moiety.

### C. Multicomponent Systems

The two enzymes cytochrome oxidase and xanthine oxidase which contain more than one type of paramagnetic center have been investigated by means of all three methods discussed in Sections II-A to C.

Cytochrome oxidase contains heme *a*, which is considered to be present in the two chemically different forms: cytochrome *a* and cytochrome *a*<sub>3</sub>. All active preparations invariably contain copper, but the amount of copper in proportion to heme *a* seems to differ for different modes of preparation. The enzyme functions as a catalyst for the oxidation of cytochrome *c* by molecular oxygen.

The first magnetic measurements on this complex enzyme were carried out by Yonetani<sup>39</sup> with the Rankine instrument. When reduced cytochrome oxidase in the presence of reductant was oxidized with oxygen in the flow apparatus, a steady state increase in the susceptibility was observed. The increase amounted to  $1850 \times 10^{-6}$  cgs emu calculated per heme *a* (T. Yonetani, recalculated value, personal communication). Later Ehrenberg and Yonetani<sup>19</sup> investigated the same enzyme by means of the modified Gouy balance and in the ESR spectrometer. Our result showed that an increase of  $3200 \times 10^{-6}$  cgs emu would have been expected in Yonetani's experiment if all the copper and heme *a* changed valence. If the copper did not change valence an increase of only  $200 \times 10^{-6}$  cgs emu would have been expected. The actual increase observed by Yonetani might therefore be due to a partial oxidation of the copper or to the formation of free radicals, the presence of which in the reaction considered has been demonstrated by Fridovich and Handler.<sup>20</sup> Our ESR experiments showed that the copper of the cytochrome oxidase preparation used was reduced by dithionite and ascorbate but not by the true substrate ferrocytochrome *c*. In the ESR experiments it was only possible to detect the absorption from the copper, but this absorption showed a hyperfine structure from which it could be concluded that the copper was coordinated to nitrogen atoms of the protein.

From our experimental susceptibility values it was possible to deduce the most likely molecular susceptibilities of the components of cytochrome oxidase. Cytochrome *a* is presumably a low-spin compound in both the oxidized and reduced states. In analogy with

cytochrome *c*, cytochrome *a* would therefore be well suited for electron transport. Cytochrome  $a_3$  is, however, a high-spin compound when reduced. Compounds of this type are known to be more easily oxidized by molecular oxygen than are the low-spin complexes. Oxidized cytochrome  $a_3$ , on the other hand, has more than 50% low-spin character, and hence would readily be reduced by electron transfer. As pointed out by us<sup>13</sup> the magnetic properties of cytochrome  $a_3$  therefore seem to support the hypothesis of its function as a link between molecular oxygen and the electron transporting cytochrome system.

Xanthine oxidase is a complex enzyme promoting the oxidation of xanthine by oxygen. It contains FAD, molybdenum and iron in the approximate molecular ratios of 2:1.5:8. Bray *et al.*<sup>4</sup> have demonstrated that when the oxidized enzyme is reduced anaerobically by the substrate, ESR absorptions from both the flavin and the molybdenum are developed. Extended ESR work combined with susceptibility measurements in the modified Gouy balance<sup>6</sup> led to the conclusion that a fraction of the iron of the resting oxidized enzyme is in the ferric state. There are indications both from the susceptibility data and from the appearance of an unidentified ESR absorption that not only flavin and molybdenum but also iron is reduced by the substrate. Ackerman and Brill,<sup>1</sup> using the Rankine susceptometer, found that the measured susceptibility changes accompanying the enzymatic reaction under certain conditions were greater than could be accounted for by the maximum possible contributions from all flavin, molybdenum and iron of the enzyme. They attributed this large paramagnetic increase to a production of free radicals in the substrate. The formation of these radicals has not yet been confirmed by ESR measurements.

#### IV. RADIATION-INDUCED FREE RADICALS

##### A. General Considerations

When a quantum of high energy electromagnetic radiation is absorbed or fast particles are retarded by a chemical system, practically any chemical change can occur. In general, the primary act or event has to be considered as a kind of excitation extending over a smaller or wider region. Often an electron is expelled from an electron pair or a covalent bond is broken so that free radicals are

formed. These free radicals later react more or less rapidly with each other or with other molecules. If the chemical compound considered is a part of a biological system, this system is usually disturbed by the radiation-induced changes or by the reaction products formed from sequences initiated by the primary alterations. The observed biological effect is thus often the end phase of an extended chain of reactions. The ESR spectroscopy is a useful tool, by means of which we can make detailed studies of the free radical intermediates and their kinetics without seriously interfering with the system. We cannot, however, expect that studies of this kind on complicated living systems can be successful before detailed investigations of different models have been carried out.

### B. Model Systems

The simplest models are low molecular weight compounds of biological importance. The radiation-induced free radicals in polycrystalline samples of such compounds have generally been found to be surprisingly stable, even in the presence of radical-scavenging gaseous molecules. This is presumably due to the slow diffusion of the gas and hindered reactions because of steric effects in the crystal lattices of these compounds. Each compound gives its own characteristic ESR spectrum upon irradiation. That quite small changes of the micro-environment are sufficient to alter the ESR spectrum considerably is exemplified in Fig. 4 for polycrystalline and freeze-dried sucrose.

When we turn to more complex model systems, especially hydrophilic colloids, e.g. starch, proteins and nucleic acids, the situation is much more complicated. In a vacuum or in an inert atmosphere the radicals decay, often rather rapidly. This is probably due to cross-reactions between the radicals which are rendered possible by the residual mobility or by some kind of conduction via the layer of hydration. In the presence of oxygen or nitric oxide the radicals decay very rapidly because the reactive gas molecules can easily diffuse between the macromolecules and react with the radicals.

*A priori* all the low molecular weight components of a polymer would be expected to contribute to the ESR spectrum developed upon exposure to high energy radiation. The relative contributions to the absorptions are, however, often not equal to the relative



abundances of the components in the polymer. An interesting example is offered by our recent finding<sup>17</sup> that the ESR spectrum from  $\gamma$ -irradiated DNA has many similarities with the spectrum from  $\gamma$ -irradiated thymine. Our conclusion that thymine residues

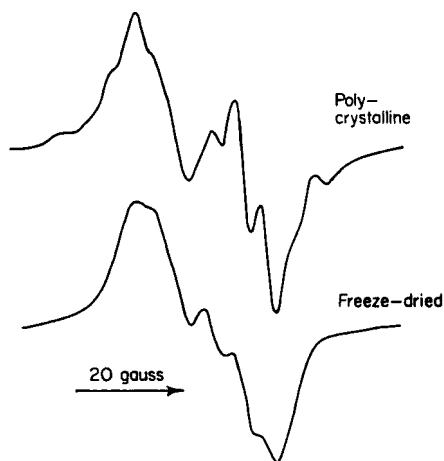


Fig. 4. ESR recordings of radiation-induced free radicals in polycrystalline and freeze-dried sucrose. (From Ehrenberg, A., Ehrenberg, L., and Löfroth G., unpublished.)

are the preferred points where the radicals are stabilized is in agreement with the results by Pullman and Pullman.<sup>30</sup> Based on theoretical considerations they suggested that the pyrimidines should be preferred to the purines as reactive centers for the fixation of radicals.

### C. Living Seeds

In a more complex chemical system, such as living seeds represent, all the ESR spectra of radiation-induced radicals are superimposed on each other and give a resultant spectrum which is practically without any visible hyperfine details. It is indeed with the present technique a rather hopeless task to resolve the components of an ESR recording from a system of this complexity. Furthermore, only a small fraction of the radiation-induced radicals can in a true sense be connected with the biological effect. It is, however, possible to

find correlations between the response of the ESR recordings, or portions of them, to various kinds of treatment and the variation of the observed biological effects caused by the same treatments. The discovery of such correlations has encouraged more detailed investigations. For this type of research we have found that living seeds are a suitable object for investigation since they can tolerate relatively high doses of radiation and the subsequent reactions of the primary radiation-induced free radicals are slow, at least at relatively low water contents.

It is known that in relatively dry seeds an increase of the water content protects against the radiation damage. The protection is greatest at a water content of 12–15%. Ehrenberg and Ehrenberg have found<sup>15</sup> that a portion of the radiation-induced radicals in seeds decay fairly rapidly. The decaying portion of the radicals increases with increasing water content, and there is a strong correlation between the number of radicals remaining at germination and the observed growth inhibition or mutations. Furthermore, Sparrman *et al.*<sup>32</sup> have shown that nitric oxide abolishes all radiation-induced free radicals in dry seeds and simultaneously protects against the ionizing radiation. These results led to the conclusion that part of the radiation-induced free radicals, which we can study by means of ESR spectroscopy, by all probability are links in the chain of reactions leading from the absorption of radiation energy to the biological effect finally manifested.

Oxygen, in contrast to nitric oxide, is known to enhance the radiation damage of seeds. Both gases react with the free radicals, but while nitric oxide forms an inert compound the reaction with oxygen leads to peroxy radicals or peroxides, compounds which are known to be reactive and harmful to the organism. Therefore, in the case of seeds with a low water content a great portion of the damage must be of an "indirect" nature, viz. a radical induced in one part of a molecule leads through further reactions to an eventual damage in another part of the same molecule or in another molecule.

In recent investigations on grass seeds we have shown that two groups of chemically different free radicals are produced in grass seeds by ionizing radiation.<sup>16</sup> This is illustrated in Fig. 5. When the seeds are in equilibrium with air, low doses give only radicals with a narrow ESR absorption. At higher doses also radicals with a broader absorption become stable. Pretreatment with a high

pressure of oxygen, which amplifies the radiation effect, increases the limiting dose below which only the narrow absorption is visible. Furthermore, during storage in air the broader signal decays more rapidly than the narrow one. Hence the radicals giving the broader absorption are of a special chemical type, more sensitive to oxygen

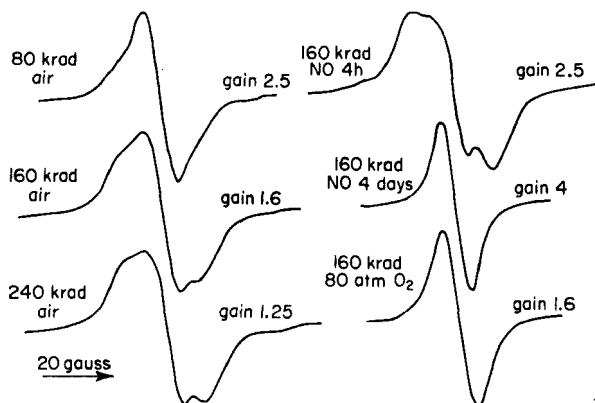


Fig. 5. ESR spectra of seeds irradiated under different conditions. Left, after different doses of  $\gamma$ -radiation on seeds in equilibrium with air. Right, after different pretreatments with the same dose of  $\gamma$ -radiation, from the top: "NO 4 h" means pretreatment with NO for 4 hours, NO removed immediately after irradiation; "NO 4 days" means that NO is not removed until after 4 days' storage at room temperature (this strongly decreases the total concentration of free radicals, cf. the gain used); 80 atm of O<sub>2</sub> were applied 12 h before irradiation (this treatment strongly enhances the radiation effect). The seeds were of *Agrostis stolonifera* and contained 4% H<sub>2</sub>O. (From Ehrenberg *et al.*<sup>16</sup>.)

than the radicals giving the narrow absorption. The broader signal first appears when the intracellular oxygen has been consumed.

The spectra shown in Fig. 5 also demonstrate that nitric oxide removes all the intracellular oxygen so that the ratio between the amplitudes of the broad and the narrow absorptions is increased considerably. During storage in nitric oxide the radicals giving the broad absorption react much faster with nitric oxide than the other radicals and after some time only the narrow signal remains.

It is known that heat treatment of dry seeds before irradiation decreases the observed biological damage. We have observed that

after such treatment, relatively more of the broader absorption is induced by the ionizing radiation.<sup>16</sup> Hence, the protective action of heat treatment might be connected with an expulsion of oxygen.

Preliminary attempts to resolve the two types of ESR spectra indicate that the broader signal is probably a doublet. Its width and shape show resemblances to the absorptions from some carbohydrates.

## V. CONCLUDING REMARKS

Magnetic methods have proved to be of considerable value in biochemical and radiobiological research. The more classical methods for determining magnetic susceptibility have not been replaced by the more recently developed ESR spectroscopy. The information obtained from the two types of methods are in many cases of complementary value. New techniques are under development for applications in the future. Combination techniques of nuclear magnetic resonance and electron spin resonance seem especially promising.

*Acknowledgements.* The work presented has been supported by grants from Statens Naturvetenskapliga Forskningsråd, Statens Råd för Atomforskning, Riksföreningen mot Cancer, Knut och Alice Wallenbergs Stiftelse and by PHS research grant A-5895 from the National Institute of Arthritis and Metabolic Diseases, Public Health Service.

## References

1. Ackerman, E., and Brill, A. S., Biophysical Society Meeting, Pittsburgh, Pa., U.S.A., Feb. 25 (1959).
2. Bayer, E., and Hausser, K. H., *Experientia* **11**, 254 (1955).
3. Bray, R. C., *Biochem. J.* **81**, 189 (1961).
4. Bray, R. C., Malmström, B. G., and Vänngård, T., *Biochem. J.* **73**, 193 (1959).
5. Bray, R. C., and Pettersson, R., *Biochem. J.* **81**, 194 (1961).
6. Bray, R. C., Pettersson, R., and Ehrenberg, A., *Biochem. J.* **81**, 178 (1961).
7. Brill, A., in M. S. Blois *et al.*, Eds., *Free Radicals in Biological Systems*, Academic Press, New York, 1961, p. 53.
8. Brill, A. S., Ehrenberg, A., and den Hartog, H., *Biochim. Biophys. Acta* **40**, 313 (1960).
9. Brill, A., den Hartog, H., and Legallais, V., *Rev. Sci. Instr.* **29**, 383 (1958).
10. Cambi, L., and Szegoe, E. L., *Ber.* **66**, 656 (1933).

11. Dalziel, K., and Ehrenberg, A., *Acta Chem. Scand.* **9**, 727 (1955).
12. Ehrenberg, A., *Arkiv Kemi* **19**, 97 (1962).
13. Ehrenberg, A., *Svensk Kem. Tidskr.* **74**, 103 (1962).
14. Ehrenberg, A., *Arkiv Kemi* **19**, 119 (1962).
15. Ehrenberg, A., and Ehrenberg, L., *Arkiv Fysik* **14**, 133 (1958).
16. Ehrenberg, A., Ehrenberg, L., and Löfroth, G., *Abhandl. Deut. Akad. Wiss. Berlin, Kl. Med.* No. 1, 229 (1962).
17. Ehrenberg, A., Ehrenberg, L., and Löfroth, G., *Nature* **200**, 376 (1963).
18. Ehrenberg, A., and Ludwig, G. D., *Science* **127**, 1177 (1958).
19. Ehrenberg, A., and Yonetani, T., *Acta Chem. Scand.* **15**, 1071 (1961).
20. Fridovich, I., and Handler, P., *J. Biol. Chem.* **236**, 1836 (1961).
21. George, P., Beetlestone, J., and Griffith, J. S., in J. E. Falk *et al.*, Eds., *Haematin Enzymes*, Pergamon Press, London, 1961, Part 1, p. 105.
22. Gibson, J. F., Ingram, D. J. E., and Nicholls, P., *Nature* **181**, 1398 (1958).
23. Griffith, J. S., *Proc. Roy. Soc. (London)* **A235**, 23 (1956).
24. Howland, J. J., and Calvin, M., *J. Chem. Phys.* **18**, 239 (1950).
25. Köhnlein, W., Müller, A., Henriksen, T., Ehrenberg, A., Ehrenberg, L., Löfroth, G., ten Bosch, J. J., Braams, R., Redhardt, A., and Randolph, M. L., *Second International Congress of Radiation Research, Abstracts of Papers, Harrogate, 1962*, p. 22. Cf. Boag, J. W. in M. Ebert and A. Howard, Eds., *Radiation Effects in Physics, Chemistry and Biology*, North-Holland Publishing Co., Amsterdam, 1963, p. 194 and pp. 205-207.
26. McKim, F. R., *Proc. Roy. Soc. (London)* **A262**, 287 (1961).
27. Michaelis, L., in J. B. Sumner, and K. Myrback, Eds., *The Enzymes*, Academic Press, New York, 1951, Vol. 2, Part 1, p. 1.
28. Nakamura, T., in M. S. Blois *et al.*, Eds., *Free Radicals in Biological Systems*, Academic Press, New York, 1961, p. 169.
29. Pauling, L., *Nature of the Chemical Bond*, 3rd Ed., Cornell University Press, Ithaca, 1962.
30. Pullman, B., and Pullman, A., in M. Burton *et al.*, Eds., *Comparative Effects of Radiation*, Wiley, New York, 1961, p. 105.
31. Schoffa, G., Scheler, W., Ristau, O., and Jung, F., *Acta Biol. Med. Germ.* **3**, 65 (1959).
32. Sparrman, B., Ehrenberg, L., and Ehrenberg, A., *Acta Chem. Scand.* **13**, 199 (1959).
33. Theorell, H., *Arkiv Kemi Mineral. Geol.* **16A**, No. 1 (1942).
34. Theorell, H., and Ehrenberg, A., *Arkiv Fysik* **3**, 299 (1951).
35. Theorell, H., and Ehrenberg, A., *Acta Chem. Scand.* **5**, 823 (1951).
36. Theorell, H., and Ehrenberg, A., *Arch. Biochem. Biophys.* **41**, 442 (1952).
37. Theorell, H., and Nygaard, A. P., *Acta Chem. Scand.* **8**, 1649 (1954).
38. Yamazaki, I., Mason, H. S., and Piette, L., *J. Biol. Chem.* **235**, 2444 (1960).
39. Yonetani, T., *Federation Proc.* **19**, 32 (1960).

## 17

# ESR INVESTIGATIONS ON DIFFERENT PLANT SYSTEMS

CLAUDE S. NICOLAU, *Centre of Research of the Ministry of Health,  
and Institute of Petroleum, Gas and Geology, Bucharest, Rumania*

## CONTENTS

I. Introduction . . . . .	628
II. ESR Investigation of the Mechanism of Photosynthesis in Green Plants . . . . .	628
III. Non-photosynthetic Plant Material . . . . .	638
IV. Irradiated Plant Material . . . . .	640
References . . . . .	643

## I. INTRODUCTION

Recent developments of the electron spin resonance (ESR) technique have made it useful for investigations in various fields of biological interest. In this chapter attention will be focused on its use in botany or, perhaps more correctly, plant physiology.

In the study of plants by means of the ESR method, there have been several general areas in which efforts have been directed:

- (1) The mechanism of photosynthesis in green plants using intact organisms and plant parts.
- (2) The occurrence of paramagnetic species in non-photosynthetic plant material.
- (3) The production of free radicals in irradiated plants.

## II. ESR INVESTIGATION OF THE MECHANISM OF PHOTOSYNTHESIS IN GREEN PLANTS

The most important process in the organic world is photosynthesis. Many studies have been devoted to this complex process. Although an immense amount of experimental material concerning photosynthesis has accumulated, the manner in which energy is dissipated and transferred during photosynthesis still requires

elucidation. The ESR method was used in order to obtain information concerning the electronic changes which might occur during this process.

The first attempt to correlate photosynthetic activity with free radical content of plant material was reported by Commoner, Townsend and Pake.<sup>1,2</sup> They found that normal green barley leaves

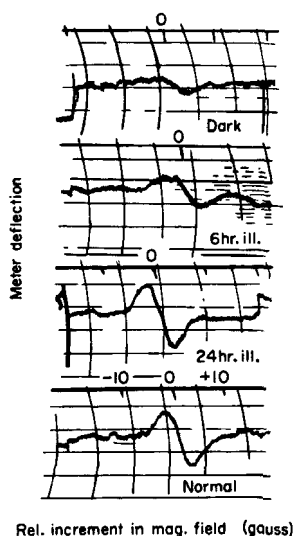


Fig. 1. ESR signal growth under illumination of bleached barley leaves.  
(From Pake, Weissmann, and Townsend.<sup>2</sup>)

exhibit an electron resonance about 5 gauss wide. By the exclusion of sunlight, the leaves are bleached and the signal decays to about 20% of its original intensity. When the bleached leaves are returned to 100 foot-candles of illumination from fluorescent light, after 6 hours of exposure the signal recovers about 50% of its normal intensity. After 24 hours of illumination the intensity of the signal is equal to the original one and the leaves fully recover their green colour. These facts suggested that a certain relationship might exist between photosynthetic activity and the observed ESR signal in green plants.

Commoner, Heise and Townsend<sup>3</sup> discovered an ESR signal in isolated *Nicotiana tabacum* chloroplasts. When chloroplasts were

examined in the dark, a small paramagnetic resonance absorption was detected. By illuminating the chloroplasts inside the resonator cavity a noticeable increase of the signal occurred. The amplitude of this light-induced signal was found to be about 3–6 times that exhibited by chloroplasts in the dark. The  $g$ -factor of the signal was  $2.002 \pm 0.001$ . The half-line width of the signal was of  $\sim 10$  gauss,

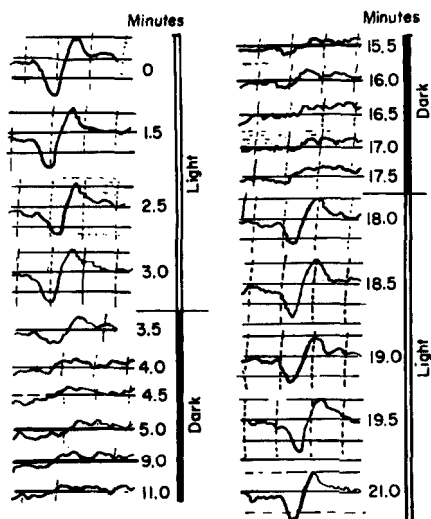


Fig. 2. ESR signals shown by a chloroplast suspension at intervals during successive light, dark, and light periods. The times noted represent minutes elapsed after the first curve (upper left corner) was obtained and refer to the centre point of each absorption curve. (After Commoner, Heise and Townsend.<sup>3</sup>)

similar to other biological preparations. The response of a chloroplast preparation to illumination was found to be rapid and readily reversible. In this investigation the effect of alternate light and dark on the ESR signal yielded by chloroplasts was studied and it was observed that the light-induced radical decayed to its dark value within about one minute after turning off the illumination. The same signal is reported to attain its highest intensity within 30 seconds after the onset of illumination. Figure 2 shows the results of this ESR investigation on chloroplasts.

The same authors also investigated the effect of light intensity



upon the amplitude of the ESR signal of the chloroplasts. It has been observed that the relative number of unpaired electrons increases with light intensity; however, it is found that the paramagnetic resonance absorption of the chloroplasts is subject to light-saturation. Such light-saturation is a feature of the photosynthetic activity of both chloroplasts and intact cells. Commoner *et al.* reported that when irradiated exclusively with wavelengths in the range 400–700 m $\mu$ , chloroplasts show a light-sensitive paramagnetic resonance signal. Based upon these facts, the authors assigned the observed ESR signal to “either or to both an excited state of chlorophyll and oxidation–reduction intermediates”.<sup>3</sup>

Somewhat later, Commoner, Heise, Lippincott, Norberg, Passoneau and Townsend,<sup>4</sup> investigating wet spinach chloroplasts, found two distinctive ESR signals. One signal (I) was centred at  $g = 2.002$  and had a line width of 9 gauss. It appeared only upon illumination of chloroplasts. A second signal (II) appearing in the dark, centred at  $g = 2.005$  and with a width of 25 gauss, exhibited five symmetrical hyperfine peaks<sup>4</sup> (intensity ratio 1:2:3:2:2). The authors concluded that signal II was definitely a free radical with the free electron in the neighbourhood of the equivalent nitrogens. In some preparations they found additional splitting, suggesting that the five resolved peaks may have been only part of a more complex structure.

The effect of onset and of cessation of illumination upon these ESR signals led the authors to the opinion that spectrum (I) was more directly associated with the primary photochemical process and that component (II) was a free radical intermediate in a dark redox process, which was enhanced by electron transfer from species (II).

The unstructured signal (I) was ascribed by these workers to a water-free chlorophyll–lipoprotein complex from which an electron transfer to an organic free radical, responsible for the five-line spectrum, should occur.<sup>4</sup> The chlorophyll–lipoprotein complex was assumed to be in a “light-excited” state, and was viewed by the authors as the product of the primary photochemical process of the photosynthesis.

The interpretations by Commoner *et al.*<sup>3,4</sup> of their experimental data are subject to criticism. In the two above-mentioned papers no study of the temperature dependence of the observed ESR signals

was undertaken and there was no attempt to correlate quantitatively the ESR results with the kinetic and chemical studies of photosynthesis. Further, the assignment of the light-induced ESR signal to a triplet state of chlorophyll is also subject to criticism. Such a triplet state would have a very short lifetime and the observation of such an excitation to the triplet state would be improbable.

This question was answered by Sogo, Pon and Calvin<sup>5</sup> shortly after the publication by Commoner, Heise and Townsend of their first results on chloroplasts. Using both spinach chloroplasts and eucalyptus leaves at different temperatures, Sogo *et al.* obtained the results shown in Table I. The intensity of the observed ESR signals

TABLE I. ESR Observation of Various Samples of Photosynthetic Material<sup>a</sup>

Substance	Light intensity, quanta/sec	Temperature, °C	Signal growth time	Signal decay time
Dried eucalyptus leaves	$10^{15}$	25	min	hr
Dried whole chloroplasts	$10^{15}$	25	min	hr
		60	sec	sec
Wet whole chloroplasts	$10^{15}$	25	sec	1 min
		-140	sec	hr
Wet small chloroplast fragments	$10^{15}$	25	sec	min
Wet large chloroplast fragments	$10^{15}$	25	30 sec	30 sec
	$10^{16}$	25	6 sec	30 sec
	$10^{16}$	-140	10 sec	hr

<sup>a</sup> Taken from Sogo, Pon and Calvin.<sup>5</sup>

indicates that the equilibrium free-electron concentration is about  $10^{16}$  either with light intensities of  $10^{15}$  or  $10^{16}$  quanta/sec set into the cavity. Consequently, the quantum-efficiency for the photo-reproduction of free spins should be of 1-10 quanta per free spin. The ESR curves obtained at room temperature and at  $-140^{\circ}\text{C}$  differ in line width. While the former suggests some form of exchange narrowing, the latter is considerably broader and shows a certain asymmetry (Fig. 3). Freezing at  $-140^{\circ}\text{C}$  does not destroy

the samples in any way. Upon warming to room temperature, their behaviour is the same as that of samples kept continuously at room temperature.

It is very interesting to note that the decay time of the light-induced ESR signal is much longer at  $-140^{\circ}\text{C}$  than at  $25^{\circ}\text{C}$ . This fact seems to rule out the triplet excitation of chlorophyll as a source of the ESR signal. On the other hand, the fact that the growth time of the ESR signal is almost the same at both temperatures, i.e. at  $+25^{\circ}\text{C}$  and at  $-140^{\circ}\text{C}$  indicates that enzymatic reactions may not be regarded as the origin of the observed spectra.

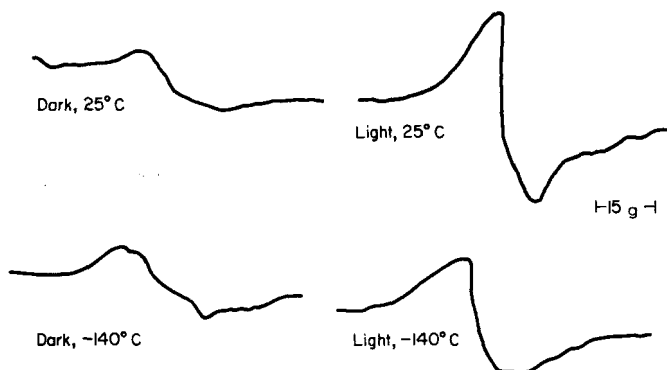


Fig. 3. Electron spin resonance spectra from wet, large chloroplast fragments. (From Sogo *et al.*<sup>5</sup>)

In 1955, Bradley and Calvin<sup>7</sup> advanced a hypothesis concerning the mechanism of conversion of the electromagnetic energy into chemical potential. According to this hypothesis, the absorption of light leads to the first excited singlet state of chlorophyll, which would then be converted to a triplet state. This triplet excitation should be followed by an ionization process leading to an electron and a hole, "these entities being the reducing and oxidizing components which must be simultaneously generated".<sup>5</sup>

The very rapid capture of an electron from water or from a product formed from it would be a part of the process.<sup>7</sup> Such a theory of semiconductor action of chloroplast received experimental support from glow-curve and resistance measurements.<sup>8</sup> The results of the ESR investigations strongly support this view.

Investigations of the luminescence of similar chloroplasts lend further support to the semiconductor theory of photosynthesis.<sup>6</sup> At the moment of cessation of illumination, there will be a certain proportion of trapped electrons, "free" electrons, trapped holes and "free" holes in the chloroplasts.<sup>5</sup> The luminescence observed at this time will then arise from radiative recombination of electrons and holes. Following this, a new emission will be originated by thermal excitation of electrons and holes from the shallowest traps, the time of decay being a function of trap depth and temperature. Since the trap depth is the same, the much longer decay time observed with wet whole chloroplasts and with wet large chloroplast fragments at  $-140^{\circ}\text{C}$  could be accounted for in this way.

Thus, the ESR results, corroborated by luminiscence and resistance measurements, allowed an insight into the process of photosynthesis. Meanwhile, other investigations of certain aspects of the processes yielded results, which although not contradictory to those cited, suggest new interpretations of the observed ESR signals.

Bubnov, Tsepalov and Shlyapintokh<sup>9</sup> investigated by means of the ESR samples of *Hordeum vulgare*. The signal observed upon illumination was a doublet centred at  $g = 2.004$  and with a splitting of 1.8 g. The width of each component was 1.9 g. Sometime later, Bubnov, Krasnovskii, Umrichina, Tsepalov and Shlyapintokh<sup>10</sup> performed new investigations on several plants such as *Triticum vulgare*, *Hordeum vulgare*, *Avena sativa* and *Santheria*. The illuminated leaves of *Santheria* yielded a broad signal with a complex structure. Quite different spectra were obtained with *Triticum vulgare* and with *Hordeum vulgare*; with this material, spectra essentially the same as those previously reported by Bubnov, Tsepalov and Shlyapintokh<sup>9</sup> were obtained. The ESR signal observed belongs to a very active species which disappears immediately after cessation of illumination. At first, the authors believed that the ESR signal was shown by some radicalized form of the chlorophyll. To test this assumption, experiments were carried out with both oxidized and reduced chlorophyll a and b, peophytine a and b, haematoporphyrin and magnesium phthalocyanine. All pigments in the oxidized form yielded negative results. Oxidation with molecular oxygen in pyridine or alcohol solution did not yield an ESR signal either at room or at lower temperatures (as low as  $-60^{\circ}\text{C}$ ).

On the contrary, reduction of all the pigments with ascorbic acid upon illumination produced a paramagnetic species showing an ESR spectrum much the same as those shown by *Hordeum vulgare* and *Triticum vulgare* (Figs. 4 and 5). As can readily be seen in these figures the similarity between ESR spectra of the photoreduced pigments and those of the intact plant material is striking.

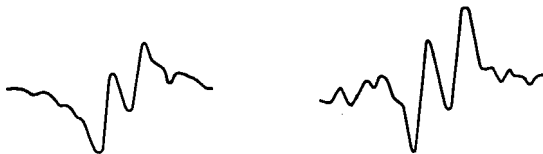


Fig. 4. ESR spectra of illuminated *Triticum vulgare* and *Hordeum vulgare*.<sup>2</sup>  
(From Bubnov *et al.*<sup>10</sup>)

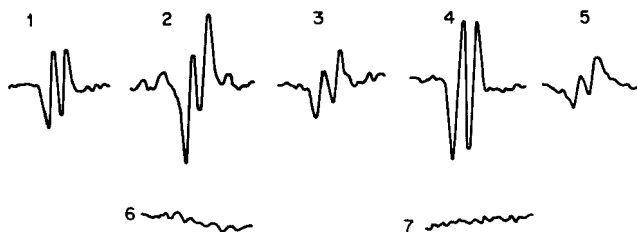


Fig. 5. ESR spectra recorded during photoreduction of pigments with ascorbic acid in pyridine solution. (1) Chlorophyll a; (2) chlorophyll a and b; (3) phorphytine a and b; (4) haematoporphyrin; (5) Mg phthalocyanine; (6) ascorbic acid in pyridine without pigment; (7) chlorophyll in pyridine without ascorbic acid.<sup>10</sup>

In further experiments solutions of ascorbic acid in piperidine were prepared. Upon illumination they yielded the same doublet with the same parameters. The addition of one of the previously used pigments did not alter the shape of the signal. The fact that upon photoreduction with ascorbic acid all the pigment solutions yielded the same spectra clearly indicates that the structure of the pigment is immaterial to the signal recorded. Therefore, it was concluded that the observed ESR spectrum refers to the oxidized radical form of ascorbic acid—probably monodehydroascorbic

acid.<sup>10</sup> Reduction with other hydrogen donors failed to produce any ESR signal, which further supports the hypothesis that monodehydroascorbic acid is responsible for the recorded ESR spectrum.

The authors further state that "the monodehydroascorbic acid in model systems may be formed at the expense of the energy of light absorbed by the pigment or by the direct photoreaction of ascorbic acid bound to a molecule of strong basis".<sup>10</sup> These findings point to an interesting aspect of photosynthesis, namely the possible photoreduction of pigments by ascorbic acid during photosynthesis.

Based upon different features of the ESR experiments in photosynthesis, i.e. the low quantum yield of trapped electrons and free-spin formation, Rabinowitch<sup>11</sup> suggested that they follow only exceptional absorption acts. He further pointed out that effects observed with dried chloroplasts might be due to chlorophyll aggregates formed during the drying process.<sup>11</sup> He added that further experimental evidence is needed to demonstrate the relevance of ESR, photoconductivity and delayed light emission stimulated by heat to the main sequences of photosynthesis, for these phenomena may well be connected with some minor side processes.

It has been well known for almost 30 years that hydroxylamine was a very active poison of photosynthesis.<sup>12</sup> Concentrations of  $2.2 \times 10^{-4}$  M  $\text{H}_2\text{NOH}$  completely inhibit photosynthesis. It was found that concentrations as small as  $10^{-6}$  M of  $\text{H}_2\text{NOH}$  were also active in inhibiting photosynthesis. In order to test the influence of hydroxylamine on the ESR signal, Khalil and Thom<sup>13</sup> and Nicolau<sup>14</sup> performed ESR measurements on plant material previously imbibed with different concentrations of  $\text{H}_2\text{NOH}$ . *Hordeum vulgare* s. Bartex was used and three series of samples were investigated: (1) primary leaves of *H. vulgare*, (2) leaves imbibed with water, and (3) leaves imbibed with aqueous solutions of hydroxylamine in the concentration range  $10^{-10}$  M  $\text{H}_2\text{NOH}$  to  $10^{-2}$  M  $\text{H}_2\text{NOH}$ .

Samples (1) and (2) yielded upon illumination in the resonator cavity an ESR signal with an amplitude indicating a spin concentration of  $10^{13}$ – $10^{14}$ . The very sensitive superheterodyne-ESR spectrometer used permitted measurements on samples containing certain amounts of water.

Sample (3) did not yield any ESR signal upon illumination. The fact that even at concentrations of hydroxylamine as low as  $10^{-10}$  M no signal could be detected, although photosynthesis is not inhibited by this concentration, seems to suggest that the ESR signal observed in samples (1) and (2) is not necessarily directly connected with the main sequences of photosynthesis. Measurements in the Warburg apparatus show that concentrations of  $\text{H}_2\text{NOH}$  ranging from  $10^{-10}$  to  $10^{-6}$  M have no influence on the photosynthetic production of  $\text{O}_2$ .

The fact that correlation of ESR and direct measurement data on photosynthetic activity is not possible at this concentration range of poison may prove to support the suggestion made by Rabinowitch.<sup>11</sup> Further experiments are, of course, required, in order to supplement these facts.

Commoner<sup>4a</sup> recently reported an interesting experiment. Growing *Chlorella* in a highly deuterated medium he obtained an ESR signal similar in shape to that obtained with normal *Chlorella*, but about twice as intense. Studies by Smaller<sup>21</sup> showed that deuterated chlorophyll, upon illumination in solution, shows an ESR signal increased in intensity and reduced in width by a factor of two, and this fact shows that the line width of the resonance signal of illuminated chlorophyll is broadened only by a dipole-dipole interaction of the free electron with the hydrogen nuclei in the chlorophyll molecule. The same reason may account for the increase in intensity of the *Chlorella* ESR signal upon deuteration.

At any rate, ESR investigation of the mechanism of photosynthesis has proved useful since it brought new ideas in connection with the mechanism of energy transfer, while regarding enzymatic reactions which play a part in the process. Although the electron spin resonance method provides a useful instrument for this kind of study, many experimental problems still render the interpretation of the results rather difficult.<sup>15</sup> The loss of sensitivity by ESR spectrometers when aqueous samples are investigated, and the high optical density of chloroplast material which makes the absorption of light possible only at the surface of the sample are only two aspects which have many implications in such investigations. Nevertheless, the results obtained until now permit us to believe that new information about photosynthesis may be obtained in this way.

### III. NON-PHOTOSYNTHETIC PLANT MATERIAL

Some efforts have been recently made in ESR investigation of some non-photosynthetic plant material. Miyagawa, Gordy, Watabe and Wilbur<sup>16</sup> reported that they were able to detect paramagnetic species in several tissues but only when the material was in the presence of oxygen. It was assumed that the ESR signal in biological material arises from trapped molecular oxygen or from peroxide radicals. The fact that pumping out the oxygen leads to the disappearance of the signals seemed to strengthen this view.

Harhash, Brucker and Schoffa<sup>17</sup> undertook some ESR measurements on *Phycomyces* thalli, in order to investigate this assumed effect of oxygen more closely. During all the experiments, the mushroom *Phycomyces blakesleanus*, strain XXXVII H 102 Burgeff was used. The samples were grown 12 days in a Schöpfer medium. The mature mushrooms were then thoroughly washed and samples dried in one of the following ways: (1) at 60° in contact with air, (2) after alcohol fixation, over  $\text{CaCl}_2$ , *in vacuo*, or (3) by lyophilization. In some cases, after air-drying and ESR investigation, the samples were evacuated for 5 hours ( $10^{-2}$  Torr). Also, after ESR measurement, lyophilized samples were exposed to air for 24 hours.

The samples dried in air at 60°C yielded an ESR signal of about 10 gauss line-width and with a  $g$ -factor of 2.003. The intensity of the spectra indicated the presence of some  $10^{17}$  u.s./g. The paramagnetic species was very stable since the signal could be detected for several weeks without amplitude change. The lyophilized samples, on the contrary, did not show any ESR signal. The samples, dried on  $\text{CaCl}_2$ , after alcohol fixation, showed a very weak signal, its intensity calculated to be  $10^{13}$  u.s./g. When the samples dried in air were evacuated for 5 hours and then measured again in the ESR spectrometer, they no longer showed a signal. Admission of oxygen resulted again in the appearance of the strong ESR signal previously described. If the lyophilized samples were exposed to the air for 24 hours, they also yielded an ESR signal with features similar to sample (1), but with a lower intensity.

Cold and hot trichloroacetic acid and alcohol-ether extracts were obtained from the mushroom. In the trichloroacetic acid extracts mainly phosphorus-containing compounds are found, such as



phosphorylated sugars, nucleotides and "energy-rich" phosphates. This extract exhibited an ESR signal, centred at  $g = 2.00$ , with a  $\Delta H_{1/2}$  of 125 gauss. Another strong signal was shown by the alcohol-ether extract. This spectrum had a  $\Delta H_{1/2}$  of 150 gauss. However, the residue of the mushroom yielded an ESR line of 8–10 gauss line width. The first two spectra were ascribed by the authors to paramagnetic ions, which are present in the plant material. The last was attributed to chitine. However, the oxygen dependence of the ESR signal was not accounted for. It was assumed that the conclusion of Miyagawa *et al.* stated above could be extended to this system also.

It is rather striking that whole mushroom yielded the same signals as the residue, while the other fractions exhibited ESR signals thoroughly different in shape and size. A new series of experiments was run by Nicolau<sup>18</sup> and by Brucker, Thom and Nicolau.<sup>19</sup> This time, an ESR signal was obtained also from wet samples. If, however, the mushroom was imbibed with a reducing solution, as for instance ascorbic acid or hydroxylamine in water, no signal could be obtained even after prolonged drying in air or in an oxygen atmosphere.

It is known that the mushroom *Phycomyces* contains appreciable amounts of melanin (Reinhardt<sup>21</sup>). Allen, Ingram and Mason<sup>20</sup> showed that melanin shows a strong, narrow, ESR line ( $\Delta H_{1/2} = 8\text{--}10$  g; intensity  $10^{17}$  u.s./g). The signal was interpreted as being due to a semiquinoid form of melanin, a form attained during oxidation of the polymer. Since only upon oxidation could we detect a narrow, rather intense ESR signal in our mushroom, and since upon reduction it completely disappeared, we believed that the ESR signal was indeed due to this pigment. The amounts of melanin are high enough in *Phycomyces*<sup>21</sup> to give rise to a signal of the intensity reported here.

This finding by no means contradicts the results of Miyagawa, Gordy, Watabe and Wilbur. They show that mere oxidation of a chemical compound like melanin (which may be easily oxidized and reduced) may lead to the result described. We must note, however, that the signal of the mushroom was symmetric so that evidence of trapped oxygen was lacking from the beginning. Similar results might also be obtained with different biological material.

#### IV. IRRADIATED PLANT MATERIAL

Zimmer, Ehrenberg and Ehrenberg,<sup>22</sup> by means of the ESR method, studied the production of free radicals in living cells following irradiation. In the experiment reported they used embryos which were cut from resting barley seeds and subsequently X-rayed. They were able to record an ESR signal, centred at  $g = 2.00$  and exhibiting a line width of 11 gauss. No differences in

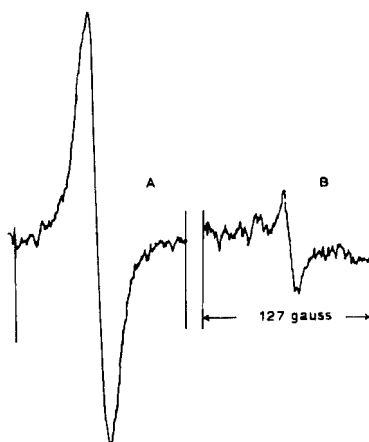


Fig. 6. ESR spectra obtained from *Agrostis stolonifera*:<sup>23</sup> (A) after 160 kr of X-rays; (B) before irradiation.

the shape of the resonance absorption spectrum were found, either for different X-ray doses or for different surrounding gases.<sup>23</sup>

Ehrenberg and Ehrenberg<sup>24</sup> thoroughly investigated the radiation-induced free radicals in *Agrostis stolonifera*. They were able to record two lines, a weak one before irradiation, and a much stronger one after X-ray irradiation (Fig. 6). Both lines were centred at  $g = 2.00$ . Decay was measured in seeds with different water contents and in water-imbibed starch samples. Allowance was made for the growth-inhibiting effect of X-rays upon the seeds. Because of the possibility of errors due to weight differences, all the results were extrapolated for zero-weight. Finally, measurements were performed on the time dependence of the signal amplitude for irradiated seeds of different water content (Fig. 7). As can be seen, the

same number of free radicals is produced by X-rays in seeds of different water content. The radical concentration does not vary in the samples with the lowest water content, but as the water content increases, increasing numbers of free radicals decay. The initial rapid decay stops at a practically constant level; further decay occurs slowly. It was also observed that the growth-inhibiting

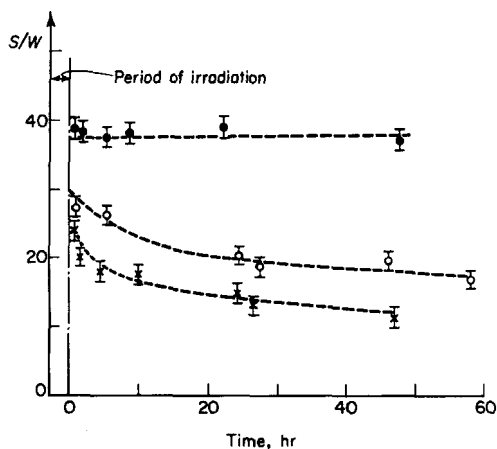


Fig. 7. Time dependence of signal amplitude from X-ray irradiated seeds of different water content.<sup>23</sup>

● 3.1% H<sub>2</sub>O; ○ 8.5% H<sub>2</sub>O; × 9.9% H<sub>2</sub>O.

Abscissa: time in hours.

Ordinate: amplitude of the ESR signal/effective weight.

effect of X-rays on the seeds was proportional to these constant levels.

Sparrman, Ehrenberg and Ehrenberg<sup>26</sup> found that when nitric oxide is added to irradiated seeds, the radical signal decays probably as a result of the reaction  $R_1^{\cdot} + \cdot\text{NO} \rightarrow R_1\text{—NO}$ , where a non-radical is formed. Oxygen does not decrease the number of free radicals. It was assumed that the formation of an equal number of peroxy radicals  $R_1^{\cdot} + \cdot\text{O—O}\cdot \rightarrow R\text{—O—O}$  may account for this observation.<sup>27</sup>

Conger and Randolph<sup>25</sup> investigated the production of free radicals in cereal embryos by ionizing radiation. Barley seeds, barley embryos and wheat embryos were irradiated with X- and

$\gamma$ -rays and subsequently examined for the presence of free radicals. Doses of  $\sim 10$  kr were shown to produce detectable amounts of free radicals but, generally, larger doses were used in order to produce higher concentrations of unpaired spins. The production and the decay of the signal were influenced by environmental conditions of irradiation and storage.<sup>25</sup> Decay was accelerated by moisture and enhanced by oxygen. An initial rapid decay was observed, which continued to a level where it became much slower.

The concentration of free radicals induced by irradiation in dry wheat germ (1.5% water content) is 2 or 3 times higher than that induced under the same conditions in wet wheat germ (8.5% water content).

The wheat germ exhibited an ESR signal with a line-width of 27 gauss. Fractionation of the wheat germ in water-soluble protein fraction, alcohol-soluble protein and residue fraction, yielded signals of different sizes. Signals from barley embryos and from the wheat germ were indistinguishable in shape from those of the whole wheat germ.

No direct relationship between the environmental conditions of storage and irradiation were proposed, but these factors, as well as the presence of oxygen, were seen to have a definite effect on the free radical concentration produced by irradiation of cereal embryos.

These are only a few of the results obtained by means of the ESR method in the investigation of radiation effects on plant material. At present it is, of course, very difficult to assign the observed ESR signals to any paramagnetic species. It may only be stated that the water content of the samples and the irradiation conditions are important in the determination of the radiation-induced free radicals concentration.

The ESR investigation of plant systems has yielded some results which are of importance.<sup>28</sup>

- (1) Ionizing radiations produce free radicals in plant material.
- (2) The concentration of those radicals increases with increasing doses of radiation.
- (3) The decay of the radicals' concentration is comparatively slow, remaining easily measurable for a long period after cessation of the irradiation.
- (4) Comparison of the ESR spectra of various biochemicals and

separate components irradiated in the presence and in the absence of radioprotective agents suggests strong molecular interaction between those compounds and the radioprotectors, both in model experiments and *in vivo*.<sup>29, 30</sup> Further studies are required in order to obtain a more comprehensive picture of this aspect of radiation damage in plants.

It was the aim of this chapter to discuss, based upon the results obtained up to the present, the potentialities of electron spin resonance spectroscopy in the investigation of plants. Rather than presenting a complete bibliographical review of the subject discussed, only the papers thought to be the most relevant for the stated purpose were discussed (the choice was, of course, entirely subjective). Some advances have been made in different fields of biology through the use of the ESR method, and more advances may be expected through the application of this powerful instrument to the study of molecular processes of biological importance.

### References

1. Commoner, B., Townsend, J., and Pake, G. E., *Nature* **174**, 689 (1954).
2. Pake, G. E., Weissmann, S. I., and Townsend, J., *Discussions Faraday Soc.* **19**, 147 (1955).
3. Commoner, B., Heise, J. J., and Townsend, J., *Proc. Natl. Acad. Sci. U.S.* **42**, 710 (1956).
4. Commoner, B., Heise, J. J., Lippincott, B. B., Norberg, R. E., Passoneau, J. U., and Townsend, J., *Science* **126**, 57 (1957).
- 4a. Commoner, B., *Acad. Roy. Belg. Classe Sci. Mem.* **33**, 67 (1961).
5. Sogo, P. B., Pon, N. G., and Calvin, M., *Proc. Natl. Acad. Sci. U.S.* **43**, 387 (1957).
6. Tollin, G., and Calvin, M., *Proc. Natl. Acad. Sci. U.S.* **43**, 895 (1957).
7. Bradley, D. F., and Calvin, M., *Proc. Natl. Acad. Sci. U.S.* **41**, 563 (1955).
8. Arnold, W., and Sherwood, H. K., *Proc. Natl. Acad. Sci. U.S.* **43**, 105 (1957).
9. Bubnov, N. N., Tsepalov, V. F., and Shlypintokh, V. Ya., *Izv. Akad. Nauk SSSR* **10** (1959).
10. Bubnov, N. N., Krasnovskii, A. A., Umrichina, A. V., Tsepalov, V. F., and Shlyapintokh, V. Ya., *Biofizika* **5**, 121 (1960).
11. Rabinowitch, E., *Discussions Faraday Soc.* **27**, 161 (1959).
12. Shibata, K., and Yakushigi, E., *Naturwissenschaften* **21**, 267 (1933).
13. Khalil, M. S. H., and Thom, H. G., *Flora (Jena)* **149**, 323 (1960).
14. Nicolau, Cl., *Arch. Sci. (Geneva)* **13**, 278, 1960, fasc. spéc.
15. Sogo, P. B., Carter, L. A., and Calvin, M., in *Free Radicals in Biological Systems*, M. S. Blois, R. O. Lindblom, H. W. Brown, R. M. Lammon, M. Weissbluth, Eds., Academic Press, New York, 1961, p. 311.

16. Miyagawa, I., Gordy, W., Watabe, M., and Wilbur, K. M., *Proc. Natl. Acad. Sci. U.S.* **44**, 613 (1958).
17. Harhash, A. W., Brucker, W., and Schoffa, G., *Acta. Biol. Med.* **6**, 211 (1961).
18. Nicolau, Cl., *Acad. Roy. Belg. Classe Sci. Mem.* **33**, 215 (1961).
19. Brucker, W., Thom, H. G., and Nicolau, Cl., *Arch. Sci. (Geneva)* **14**, 184 (1961).
20. Allen, B. T., Ingram, D. J. E., and Mason, H. S., *Arch. Biochem. Biophys.* **86**, 225 (1960).
21. Smaller, B., in *Free Radicals in Biological Systems*, Academic Press, New York, 1961, p. 315.
22. Zimmer, K. G., Ehrenberg, L., and Ehrenberg, A., *Strahlentherapie* **103**, 3 (1957).
23. Zimmer, K. G., *Radiation Res. Suppl.* **I**, 519 (1959).
24. Ehrenberg, A., and Ehrenberg, L., *Arkiv Fysik* **14**, 133 (1958).
25. Conger, A., and Randolph, M. L., *Radiation Res.* **11**, 54 (1959).
26. Sparrman, B., Ehrenberg, L., and Ehrenberg, A., *Acta Chem. Scand.* **13**, 199 (1959).
27. Ehrenberg, A., in *Free Radicals in Biological Systems*, Academic Press, New York, 1961, p. 334.
28. Müller, A., and Zimmer, K. G., in *Free Radicals in Biological Systems*, Academic Press, New York, 1961, p. 325.
29. Schröder, E., Thom, H. G., Nicolau, Cl., and Huber, R., *Strahlentherapie* **112**, 457 (1960).
30. Smaller, B., and Avery, E. C., *Nature* **183**, 539 (1959).

## 18

# THE USE OF PRODUCT INHIBITION AND OTHER KINETIC METHODS IN THE DETERMINATION OF MECHANISMS OF ENZYME ACTION

CHARLES WALTER, *Cardiovascular Research Institute, University  
 of California Medical Center, San Francisco, California*

## CONTENTS

I. Preliminary Considerations . . . . .	645
II. Single-Substrate, Single-Product Reactions . . . . .	648
III. More-than-One-Substrate, Single-Product Reactions . . . . .	653
IV. Reactions in Which More than One Product is Formed by One Substrate . . . . .	665
V. Reactions of More than One Substrate to Form More than One Product . . . . .	676
VI. General Comments on the Methods Employed . . . . .	721
References . . . . .	723

## I. PRELIMINARY CONSIDERATIONS

In the consideration of a general chemical reaction which *actually* proceeds according to the equation:



the forward and reverse rates of reaction are given by

$$v_+ = k_r A^a B^b \quad (2)$$

$$v_- = k_{-r} M^m N^n \quad (3)$$

where  $k_r$  and  $k_{-r}$  are forward and reverse rate constants, and a species and its concentration are denoted by the same letter. The quantity,  $v_+ - v_-$ , is said to be the reaction rate or the net forward rate of the reaction. According to the above, the net rate of the reaction described by Eq. (1) must be

$$v_+ - v_- = k_r A^a B^b - k_{-r} M^m N^n \quad (4)$$

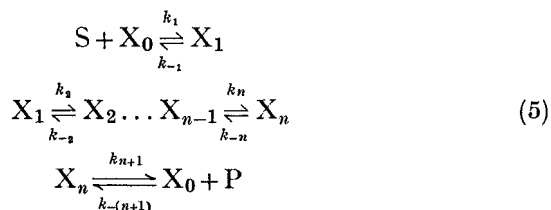
It is apparent from Eq. (4) that the net rate of the reaction depicted in Eq. (1) will depend on the concentrations of all species

contained in Eq. (1) except under a certain circumstance. If the species M and N are not present, then the net rate of the reaction will be equivalent to the rate of the forward reaction and will become independent of  $k_{-r}$ , M, and N. This circumstance would be encountered if the rate of the reaction were measured before it had actually begun. Since it is impossible to measure a rate before it has begun, this circumstance is approximated when the rate of the reaction is extrapolated to zero time. Such rates are commonly referred to as "initial rates". It is emphasized that true initial rates are independent of the species formed during the reaction.

It should be noted that at any finite time the net reaction rate will continue to decrease from the initial reaction rate for two different reasons. The value of  $v_+$  will decrease with time because A and B are used up during the reaction, and the value of  $v_-$  will increase with time since M and N increase until the reaction proceeds to equilibrium. When the two rates,  $v_+$  and  $v_-$ , become equal, the net reaction rate is zero and the reaction is said to be at equilibrium.

It is possible then to think of the reduction in rate of a net reaction in terms of the effects exhibited by the products formed. It is apparent that the degree of reduction of the net rate will depend upon the value of the reverse rate constant,  $k_{-r}$ . If measured quantities of the products are added at zero time, it is possible in principle to obtain information about  $k_{-r}$  using initial rates.

In the case of enzymic reactions, one of the components of the reaction is conserved. If only one species is catalytically converted to a single product the reaction can proceed in only one manner:

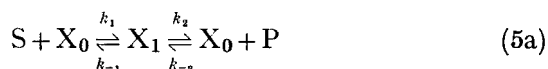


Once again, if initial rates are used, the net reaction will be independent of the product, P. However, if P is added to the system, or the reaction is measured at some time after which the reaction between P and  $\text{X}_0$  is significant, the net rate will be decreased or "inhibited" by P. We may define product inhibition then as a



reaction between an enzyme and a reaction product of the enzymic reaction which reduces the rate of formation of the product per mole of enzyme. This type of enzyme-product interaction may occur not only by the microscopic reversal of the enzymic reaction but also by a specific reaction between the enzyme and the product. Since the products and respective substrates of enzymic reactions often bear structural similarities, it would be expected that most of the product-enzyme interactions are at or near the active site of the enzyme.

The basic equation generally applied to single-substrate and single-product enzyme kinetics was first derived by Henri in 1903<sup>1</sup>



$$v = V_m / \left\{ \frac{K_m}{[S]} \left( 1 + \frac{[P]}{K_i} \right) + 1 \right\} \quad (6)$$

where  $V_m$  is  $k_2[E_0]$ ,  $[S]$  is the initial substrate concentration minus the product concentration,  $[P]$ , which has arisen from  $S$ ,  $X_0$  is the free form of the enzyme,  $X_1$  is the combined form(s) of the enzyme, and  $E_0$  is the total concentrations of active centers. If this equation is based on a steady-state of  $X_1$ , i.e.  $X_1' \sim 0$ , the meaning of  $K_m$  is  $(k_2 + k_1)/k_1$ ;  $K_i$  is  $(k_2 + k_{-1})/k_{-2}$ .

If it is assumed that initial rates are measured, Eq. (6) becomes

$$v_0 = V_m / \left( \frac{K_m}{[S_0]} + 1 \right) \quad (7)$$

provided  $[P]$  is small enough. This form of the rate expression is particularly useful since it is the recommended form to be programmed if electronic computer systems are used.<sup>2</sup> Thus many of the expressions derived in this paper are presented in this form. In the cases where the two parameters,  $V_m$  and  $K_m$ , take on more complicated meanings, they will be denoted as  $V'_m$  and  $K'_m$ .

A useful second form of rate equations which will be presented in this chapter is the linear velocity versus velocity divided by substrate concentration form

$$v_0 = V'_m - K'_m \frac{v_0}{[S_0]} \quad (7a)$$

This form of the rate equation is particularly useful since both the

desired parameters,  $V'_m$  and  $K'_m$ , are immediately obtainable by inspection.

The validity of the use of the steady-state approximation in enzyme kinetics has been discussed by Morales and Goldman<sup>4</sup> and more recently by Hommes.<sup>5</sup> Morales and Goldman point out that the steady-state is actually obtained for only a single instant if at all in the Michaelis–Menten model for enzyme action. However, it is possible that an approximate steady-state of the enzyme–substrate complex is maintained for a considerable time interval.

The effects of product inhibition on rate equations derived from transient-state kinetics are relatively unknown. Naturally, since even the transient-state equations for systems more complicated than the simple Michaelis–Menten mechanism are unknown, it is not possible to predict the effects of inhibitory products on these equations.

Hommes<sup>5</sup> has pointed out that if one assumes a steady-state of the Michaelis–Menten mechanism, it is inconsistent to integrate the resulting rate expression over a large time interval. It can be shown in a straightforward derivation that the steady-state assumption can give only zero-order reactions, i.e. that the term,  $K_m \ln[S_0]/[S]$ , in the integrated Michaelis–Menten equation must be negligible. If, on the other hand, the substrate concentration is of the same order of magnitude as the  $K_m$ , the reaction is no longer zero order and deviations from the steady-state become appreciable. Since the effect of many inhibitors is to increase the apparent Michaelis constant, thereby making it closer to any given larger substrate concentration, it would be expected that deviations from the steady-state may become even more important in the presence of inhibitors.

An analog computer solution for the simple Michaelis–Menten mechanism in the transient state and in which the product competes with the substrate for the free enzyme has been reported by Hommes.<sup>5</sup> The solution was applied to the carboxypeptidase-A catalyzed hydrolysis of chloroacetyl-L-phenylalanine to the inhibitory product, L-phenylalanine.

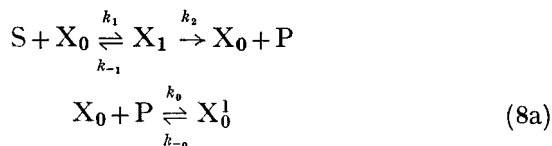
## II. SINGLE-SUBSTRATE, SINGLE-PRODUCT REACTIONS

The equation reported by Henri clearly shows that the product, P, is expected to inhibit the conversion of S to P. If it is assumed that

a significant amount of P is present such that the ratio  $[P]/K_i$  is large but that  $[S]$  is still approximately equal to  $[S_0]$ , the initial substrate concentration, Eq. (6) can be written for the steady-state as

$$v = V_m - K_m \left( 1 + \frac{[P]}{K_i} \right) \frac{v}{[S_0]} \quad (8)$$

The conditions suggested above can readily be attained if sufficient quantities of P are added to the reaction or if  $K_i$  is very small. Equation (8) clearly shows that the inhibition by P will be strictly competitive. Furthermore, Eq. (8) is precisely what one obtains if the reaction mechanism were written in the manner usually done for a competitive inhibitor



where  $K_i$  is now  $k_{-0}/k_0$ .

If the amount of P formed also reduces the amount of substrate so that  $[S_0]$  does not equal  $[S]$  and the reverse reaction becomes significant not only as a reaction tying up free enzyme as an enzyme-product complex, but also for the formation of the enzyme-substrate complex and eventually S, the resulting rate expression will be the one reported by Alberty<sup>6</sup> for the complete steady-state of Eq. (5), where  $K_i = (k_{-1} + k_2)/k_{-2}$ .

$$v = \frac{[E_0] \left( k_2 \frac{[S]}{K_m} - k_{-1} \frac{[P]}{K_i} \right)}{1 + \frac{[S]}{K_m} + \frac{[P]}{K_i}} \quad (9)$$

This equation may be written in the  $v$  versus  $v/[S]$  form as

$$v = V_m \left( 1 - \frac{[P]}{K_{eq}[S]} \right) - K_m \left( 1 + \frac{[P]}{K_i} \right) \frac{v}{[S]} \quad (10)$$

where  $K_{eq} = k_1 k_2 / k_{-1} k_{-2}$ . It can be seen that when the product concentration formed from S becomes large enough that  $(1/K_{eq}) [P]/[S]$  is of the same order of magnitude as 1.0, the inhibition will not be strictly competitive and the  $v$  versus  $v/[S]$  plots will not be linear. The apparent limiting velocity,  $V'_m$ , will decrease as the

concentration of P increases. This result is significantly different from that expected when P acts as a simple competitive inhibitor or when the reverse reaction does not contribute significantly to the net rate. Morales<sup>7</sup> and King<sup>8</sup> have pointed out that the second term in the  $V'_m$  will be negligible as long as the reaction is far from equilibrium. It necessarily follows then that as long as the  $v$  versus  $v/[S]$  plots are linear, this term is negligible and the  $V_m$  is unaffected by the product. However, Alberty<sup>9</sup> has pointed out that this is not a sufficient condition to reduce Eq. (9) to the simple Michaelis-Menten equation, Eq. (7). The third term in the denominator of Eq. (9) can be neglected only if  $[P]/K_i \ll 1$ . Under the conditions when  $[P]/K_i$  is not  $\ll 1$ , but the second term in the  $V'_m$  is negligible, the product will appear as a strictly competitive inhibitor. Alberty points out that the maximum extent of reaction which may be used in determining initial steady-state rates depends in this way on the Michaelis complex for the product. Under the conditions when  $[P]/K_i \ll 1$ , no inhibition by product will be observed.

It is possible then in principle to distinguish between the mechanism in which the product reacts with  $X_0$  as a competitive inhibitor and the mechanism in which it reacts as a substrate for the reverse reaction. In the former case, the limiting velocity will not be affected, and the  $v$  versus  $v/[S]$  plots will always be linear, even at high product concentrations. In the latter case, on the other hand, the  $v$  versus  $v/[S]$  plots will be affected because the  $V'_m$  is affected if the product concentration is made large enough.

For these two mechanisms of product inhibition to be really different, some factor must be absent so that the enzyme-product complex, EP, cannot reform the substrate. It would be expected then from the principle of microscopic reversibility, that if the EP complex formed from P and  $X_0$  is the same as that formed during the production of P, all the ingredients are present for the simple reversal of the reaction. Alberty<sup>9</sup> has suggested that the additional reaction between the inhibitor and free enzyme normally associated with competitive inhibition is unnecessary in many cases of competitive product inhibition if the reverse reaction mechanism is used. This would seem to be especially appropriate in reactions involving only one substrate and one product.

Recently, Peller and Alberty<sup>10</sup> have extended this discussion of single-substrate-single-product enzyme kinetics to include the

cases of Eq. (5a) in which more than a single intermediate is involved. The net result of this treatment has been, among other things, to show that the parameters given in Eq. (9) take on more complicated meanings as the number of enzyme complexes increases. However, it is important to emphasize that all the additional parameters remain independent of the substrate and product concentrations so that the discussion presented for the single intermediate case can be extended to include the cases where more intermediates are involved, provided all the intermediates are in the steady-state.

It has been pointed out that while reaction rates are generally measured when they are far from equilibrium, it is possible in principle to determine rate constants of a reaction from studies conducted close to equilibrium. Thus, the addition of the products of a reversible enzymic reaction affords a convenient approach to study the reaction, especially if the reaction is too rapid to permit the use of mixing methods and subsequent determination of initial velocities. If one starts with reaction mixtures containing ratios of substrate and product which are slightly different from those of the equilibrium mixture, the return to equilibrium is characterized by relaxation times which are related to the rate constants in any particular mechanism.<sup>11</sup> The steady-state relaxation time for the enzymic reaction of a single substrate to a single product has been reported recently by Hammes and Alberty.<sup>12,13</sup> If in Eq. (9) the substrate concentration,  $[S]$ , at any time,  $t$ , is equated to the equilibrium substrate concentration,  $[\bar{S}]$ , plus  $\Delta[S]$  and the product concentration at any time is  $[\bar{P}] - \Delta[S]$ , it is possible to write Eq. (9) as

$$\frac{d\Delta[S]}{dt} = \frac{-\Delta[S]\left(\frac{V_m}{K_m} + \frac{V_p}{K_i}\right)}{1 + \frac{[\bar{S}]}{K_m} + \frac{[\bar{P}]}{K_i} + \Delta[S]\left[\frac{1}{K_i} - \frac{1}{K_m}\right]} \quad (11)$$

where  $V_p$  is  $k_{-1}[E_0]$ .

Since  $\Delta[S] \ll [\bar{S}]$  and  $[\bar{P}]$ ,  $\Delta[S](1/K_i - 1/K_m) \ll 1 + [\bar{S}]/K_m + [\bar{P}]/K_i$ , and integration of Eq. (11) yields

$$\Delta[S] = \Delta[S_0] \exp^{-\frac{t}{1 + [S_0](1 + V_m/V_p)/K_m(1 + K_{eq})} \frac{V_m/K_m + V_p/K_i}} \quad (12)$$

Inspection of Eq. (12) reveals that the denominator of the exponent,  $\tau_{ss}$ , is inversely proportional to  $[E_0]$  and is a linear function of the total substrate concentration,  $[S_0]$ . Thus, from measurements of  $\tau_{ss}$  as a function of  $[S_0]$ , two independent parameters which, when coupled with  $K_{eq}$ , the equilibrium constant for the overall reaction, give three independent relationships between  $K_m$ ,  $K_i$ ,  $V_m$  and  $V_p$ . Therefore, from a knowledge of only one of these parameters from some independent source, the other three can be calculated directly from the steady-state relaxation times.

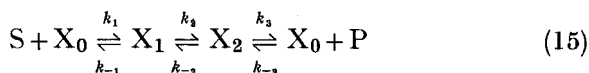
Two relaxation times are obtained from the mechanism described by Eq. (5a).

$$\tau_1 = \{k_1([\tilde{S}] + [\tilde{E}]) + k_{-2}([\tilde{P}] + [\tilde{E}]) + k_{-1} + k_2\}^{-1} \quad (13)$$

$$\tau_2 = \frac{k_1([S] + [E]) + k_{-2}([\tilde{P}] + [\tilde{E}]) + k_{-1} + k_2}{[\tilde{E}] k_1 k_{-2}([\tilde{E}] + [\tilde{P}] + [\tilde{S}]) + k_1 k_2 + k_{-1} k_{-2}} \quad (14)$$

Hammes and Alberty<sup>12</sup> have shown that for this case  $\tau_2 = \tau_{ss}$ .

If it is assumed that there are two intermediates in the enzyme mechanism, Eq. (5a) becomes



The relaxation times derived by Hammes and Alberty<sup>12</sup> are

$$\tau_{ss} = \frac{k_{-1} k_3 + k_{-1} k_{-2} + k_2 k_3 + [\tilde{S}] k_1 (k_2 + k_{-2} + k_3) + [\tilde{P}] k_{-3} (k_{-1} + k_2 + k_{-2})}{[\tilde{E}] \{k_1 k_2 k_3 + k_{-1} k_{-2} k_{-3} + k_1 k_{-3} (k_2 + k_{-2})\} ([\tilde{S}] + [\tilde{P}])} \quad (16)$$

$$\tau_1 = (k_1[\tilde{S}] + k_{-3}[\tilde{P}] + k_{-1} + k_2 + k_{-2} + k_3)^{-1} \quad (17)$$

$$\tau_2 = \frac{k_1[\tilde{S}] + k_{-3}[\tilde{P}] + k_{-1} + k_2 + k_{-2} + k_3}{k_1[\tilde{S}] (k_2 + k_{-2} + k_3) + k_{-3}[\tilde{P}] (k_{-1} + k_2 + k_{-2}) + k_{-1} k_{-2} + k_{-1} k_3 + k_2 k_3} \quad (18)$$

It should be noted that the transition-state relaxation times given by Eqs. (13), (17), and (18) are independent of the enzyme concentration.

An application of this method of determining  $K_i$  and  $V_p$  for the

enzyme fumarase has been reported by Hammes and Alberty.<sup>12</sup> The steady-state relaxation times from Eq. (12) are plotted versus the total substrate concentration. From the slope and intercept of these plots and previously determined values of  $K_{eq}$  and  $K_m$ ,  $K_i$ , and  $V_P/V_m$  were determined at pH 7.70 and 6.75. These results are summarized in Table I taken from the data of Hammes and Alberty.<sup>12</sup> It can be seen from this table that a consistent determination of  $K_i$  was obtained by this method. A less consistent determination was made at pH 6.75 where  $K_i$  and  $K_m$  are more similar.

TABLE I. The Determination of Michaelis Constants for the Products of Simple Enzymic Reactions from Measurements of Relaxation Times (taken from the data of Hammes and Alberty<sup>12</sup>)

pH 7.70;  $K_m = 5.1 \times 10^{-8} \text{ M}$ ;  $K_{eq} = 4.4$

Malate Fumarate	Intercept, <sup>a</sup> sec	Slope <sup>a</sup> $\times 10^{-4}$ , sec/M	$K_i \times$ $10^3 \text{ M}$	$V_P/V_m$
5	51.5	2.09	0.75	0.65
5	49.0	1.94	0.78	0.68
3.5	68.0	2.60	0.83	0.72
3.5	78.0	2.86	0.89	0.78
		Ave.	$0.82 \pm 0.05$	$0.71 \pm 0.04$

<sup>a</sup> From plots of  $\tau_{ss}$  versus total substrate concentration.

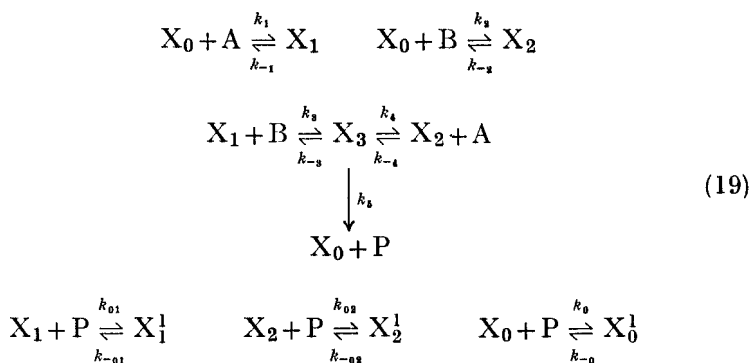
Enzymic reactions in which a single substrate reacts to form a single product are relatively rare. Other examples of this type of reaction would include the isomerases or other reactions in which water is the second substrate or product.

### III. MORE-THAN-ONE-SUBSTRATE, SINGLE-PRODUCT REACTIONS

The rate equations for reactions of this type in a partial steady-state have been reported recently by Walter and Frieden.<sup>14</sup> Since only one product is involved, it can be desorbed from the enzyme-substrate complex in only one way. However, since more than a

single substrate is involved, it is possible that the substrates could react with the enzyme in an ordered sequence or that the reaction could occur randomly. If  $n$  substrates react in an ordered sequence there are  $n!$  possible sequences in which the substrates could react. A comprehensive discussion of the basis and kinetic consequences of the ordered sequence assumption has been given.<sup>2</sup> The primary point to be considered in this regard is that the steady-state rate equations arising from the random addition are extremely complicated and linear plots of  $v$  versus  $v/[S]$  are not possible unless the system is at quasiequilibrium or other conditions are met. On the other hand, the steady-state rate equations arising from the ordered sequence mechanism, while complicated, predict linear plots of  $v$  versus  $v/[S]$  provided the final step in the sequence is essentially "irreversible", that is, provided initial rates are used in the plots.<sup>2</sup>

The following equations describe the reactions involved for reactions of this type when two substrates react randomly with an enzyme to form a single product:



The last three equations define  $K_{01} = k_{01}/k_{-01}$ ,  $K_{02} = k_{02}/k_{-02}$ , and  $K_0 = k_0/k_{-0}$ , the three possible steps in which the product is in equilibrium with the enzyme. It will be observed that all these reactions allow for interactions between a portion of  $P$  and the active center of the enzyme. Thus  $P$  competes with  $B$  for both  $X_0$  and  $X_1$ , and competes with  $A$  for both  $X_0$  and  $X_2$ .

In order to simplify the rate equations obtained from this mechanism it is assumed that each substrate is in equilibrium with the



free form of the enzyme,  $X_0$ , and that the concentration of  $X_3$  is steady. In this case,  $K_1 = k_1/k_{-1}$  and  $K_2 = k_2/k_{-2}$  and  $v = k_5[X_3]$ .

$$v = \frac{k_5[E_0]}{\frac{\phi}{[A][B]} (1 + K_1[A] + K_2[B] + K_0[P] + K_{01}K_0[A][P] + K_{02}K_0[B][P]) + 1} \quad (20)$$

From this equation it can be shown that the parameters,  $V'_m$  and  $K'_m$ , are:

	<i>v</i> with respect to	$V'_m$	Parameter	$K'_m$
A		$\frac{k_5[E_0]}{\frac{\phi K_1(1 + K_{01}[P])}{[B]} + 1}$	$\phi \left\{ \frac{1 + K_0[P]}{[B]} + K_2(1 + K_{02}[P]) \right\}$	$\frac{\phi K_1(1 + K_{01}[P])}{[B]} + 1$
B		$\frac{k_5[E_0]}{\frac{\phi K_2(1 + K_{02}[P])}{[A]} + 1}$	$\phi \left\{ \frac{1 + K_0[P]}{[A]} + K_1(1 + K_{01}[P]) \right\}$	$\frac{\phi K_2(1 + K_{02}[P])}{[A]} + 1$

(21)

where  $\phi = (k_{-3} + k_{-4} + k_5)/(K_1k_3 + K_2k_4)$ .

From Eq. (21) it can be seen that the apparent limiting velocity,  $V'_m$ , can be made to equal  $k_5[E_0]$  and be independent of the product concentration under certain conditions:

(1) If  $K_{01}[P]$  is small; that is, if the reaction between P and  $X_1$  has not occurred to a significant extent either because  $K_{01}$  is small or because  $[P]$  is small the  $V'_m$  with respect to substrate A, but not necessarily B, will be independent of P. On the other hand, if  $K_{02}[P]$  is small, that is, if the reaction between P and  $X_2$  has not occurred to a significant extent either because  $K_{02}$  is small or because  $[P]$  is small, the  $V'_m$  with respect to substrate B, but not necessarily A, will be independent of P. Correspondingly, it is necessary that if  $[P]$  is large enough, both  $K_{02}$  and  $K_{01}$  must be small for both  $V'_m$ 's to be independent of P provided circumstance (2) is not met.

(2) If the non-variable substrate with respect to which the velocity

is *not* being measured is large so that  $[B]/K_1$  in the case of variable A, or  $[A]/K_2$  in the case of variable B, can be made large enough, the  $V'_m$ 's with respect to either substrate may be made independent of P. Since the disappearance of the terms involved depends on the ratios  $K_1\phi(1 + K_{01}[P])/[B]$  and  $K_2\phi(1 + K_{02}[P])/[A]$  respectively, it is possible that the ratios  $[B]/K_1$  or  $[A]/K_2$  cannot *actually* be made large enough so that these terms drop out.

It is also possible to make the  $K'_m$  independent of the product concentration under certain conditions. It should be noted that every condition which will make the  $K'_m$  independent of P will also make  $V'_m$  independent of P except in certain coincidental cases. For instance, if  $(1 + K_0[P])/[B] \gg K_2(1 + K_{02}[P])$ ,  $\phi K_1(1 + K_{01}[P])/[B] \gg 1$ , and  $K_{01} = K_0$ , the  $K'_m$  with respect to substrate A will equal  $1/K_1$  and be independent of the concentration of P whereas  $1/V'_m$  will be a linear function of  $[P]$ . Similarly if

$$(1 + K_0[P])/[A] \gg K_1(1 + K_{01}[P]), \phi K_2(1 + K_{02}[P])/[A] \gg 1$$

and  $K_0 = K_{02}$ , the  $K'_m$  with respect to substrate B will equal  $1/K_2$  and be independent of P, whereas  $1/V'_m$  will be a linear function of the concentration of P. Generally, additional conditions are required to make the respective  $K'_m$ 's independent of P. The conditions which reduce  $K'_m$  with respect to substrate A to  $\phi K_2$  or  $K'_m$  with respect to substrate B to  $\phi K_1$  are:  $K_{02}[P] \ll 1$ . This requires that the reaction between P and  $X_2$  has not occurred to a significant degree. In addition it is necessary that  $K_0[P] \ll 1$  (the reaction between P and  $X_0$  has not occurred to a significant degree) *or* that the other substrate concentration (the non-variable substrate concentration) is large enough that  $(1 + K_0[P])/B \ll K_2$ . This would require that the concentration of substrate B be large enough to saturate the enzyme even in the presence of P. In addition to the above it is also necessary that  $K_{01}[P] \ll 1$  (the reaction between P and  $X_1$  has not occurred to a significant degree) *or* that the non-variable substrate concentration be large enough that

$$\phi(1 + K_{01}[P])/[B]/K_1$$

in the case of  $K'_m$  with respect to A or  $\phi(1 + K_{02}[P])/[A]/K_2$  in the case of  $K'_m$  with respect to B be much less than one. It is possible that the  $K'_m$  will become independent of P and no product inhibition

will be observed with respect to either substrate provided the non-variable substrate concentration is maintained large enough to saturate the enzyme and the  $X_1$  or  $X_2$  product interactions do not occur.

On the other hand, it is possible that inhibition will be observed with respect to one substrate but no inhibition will be observed with respect to the other substrate. Thus, if P actually reacts with  $X_2$ , inhibition must be observed with respect to substrate A. It follows that if P actually reacts with  $X_1$  and  $X_2$ , inhibition must be observed with respect to both substrates.

The conditions for which the ratio,  $K'_m/V'_m$ , is not a function of the product concentration are easily seen from Eq. (21). Any time the product inhibits only by the interaction with  $X_1$  (the step described by  $K_{01}$ ), the ratio of  $K'_m/V'_m$  with respect to substrate A will become independent of P, but the  $V'_m$  will not. Correspondingly, any time the product inhibits only by the interaction with  $X_2$  (the step described by  $K_{02}$ ), the ratio of  $K'_m/V'_m$  with respect to substrate B will become independent of P, but the  $V'_m$  will not. These results are summarized in Table II.

TABLE II. Conditions When the Rate Parameters of the Mechanism Described by Eq. (19) Become Independent of the Concentration of the Product

Parameter that becomes independent of P	With respect to	Condition*
$V'_m$	A	$K_{01}[P] \ll 1$ or $[B] \rightarrow \infty$
$V'_m$	B	$K_{02}[P] \ll 1$ or $[A] \rightarrow \infty$
$K'_m$	A or B	$K_0[P], K_{01}[P], K_{02}[P] \ll 1$ or
$K'_m$	A	$K_{02}[P] \ll 1$ and $[B] \rightarrow \infty$
$K'_m$	B	$K_{01}[P] \ll 1$ and $[A] \rightarrow \infty$
$K'_m/V'_m$	A	$K_0, K_{02} = 0$
$K'_m/V'_m$	B	$K_0, K_{01} = 0$

\* The value of  $\phi$  is defined in Eq. (21).

In summary then, it is possible in this mechanism that both the  $V'_m$  and the  $K'_m$  will depend on the concentration of P. By measuring the rate with respect to both A and B at different levels of P, it is possible, using initial rates, to determine the parameters associated with the interactions between  $X_0$ ,  $X_1$ , and  $X_2$  and the product. Low concentrations of substrate must be used in order to gain information about the  $X_0$  product interaction and high concentrations of either substrate may obscure this interaction by saturating the free enzyme.

If it is assumed that all forms of the enzyme are in equilibrium with each other and with the substrates, two additional equilibrium constants may be defined:  $K_3 = k_3/k_{-3}$ , and  $K_4 = k_4/k_{-4}$ . Equations (21) now become:

<i>v</i> with respect to	$V'_m$	<i>Parameters</i>	$K'_m$
A	$\frac{k_5[E_0]}{\frac{1}{K_3[B]}(1 + K_{01}[P]) + 1}$	$\left(1 + \frac{1}{K_2[B]} + K_{02}[P]\right) \frac{1}{K_4}$	$\frac{1}{\frac{1}{K_3[B]}(1 + K_{01}[P]) + 1}$
(22)			
B	$\frac{k_5[E_0]}{\frac{1}{K_4[A]}(1 + K_{02}[P]) + 1}$	$\left(1 + \frac{1}{K_1[A]} + K_{01}[P]\right) \frac{1}{K_3}$	$\frac{1}{\frac{1}{K_4[A]}(1 + K_{02}[P]) + 1}$

From Eq. (22) it can be seen that the  $V'_m$  can be made independent of P by the same conditions as were required in Eqs. (21) except that in this case the non-variable substrate concentration need only be large enough to make the ratios

$$(1 + [P] K_{01})/K_3[B] \text{ or } (1 + [P] K_{02})/K_4[A]$$

small compared to unity.

Fewer conditions are required in this case to make the  $K'_m$ 's independent of P. It is necessary that  $[P] K_{02} \ll 1$  and that  $[P] K_{01} \ll 1$  or that the concentration of B be large enough to make

$$(1 + K_{01}[P])/k_3[B] \ll 1$$

in order to make  $K'_m$  with respect to substrate A independent of P.

Furthermore, it is necessary only to make  $[P]K_{01} \ll 1$  and  $[P]K_{02} \ll 1$  or that the concentration of A be large enough to make

$$(1 + [P]K_{02})/K_4[A] \ll 1$$

in order to make  $K'_m$  with respect to substrate B independent of P. It should be noted that the last requirement in each case is sufficient to make the corresponding  $V'_m$  independent of P.

In addition, it is possible that the  $K'_m$  with respect to substrate A will be independent of the concentration of P if  $[P]K_{02} \gg 1 + 1/K_2[B]$  and  $[P]K_{01}/K_3[B] \gg 1 + 1/K_3[B]$  or if  $[P]K_{02} \gg 1/K_2[B]$ ,  $[P]K_{01} \gg 1$  and  $K_{02} = K_{01}K_4[A]$ . The  $K'_m$  with respect to substrate B will be independent of the concentration of P if  $[P]K_{01} \gg 1 + 1/K_1[A]$  and  $[P]K_{01}/K_4[A] \gg 1 + 1/K_4[A]$  or if  $[P]K_{01} \gg 1/K_1[A]$ ,  $[P]K_{02} \gg 1$  and  $K_{02} = K_{01}$ . In both these situations the reciprocals of the limiting velocities will be linear functions of the concentration of P.

TABLE III. Conditions When the Rate Parameters of the Mechanism Described by Eqs. (19) at Quasiequilibrium Become Independent of the Concentration of the Product

Parameter that becomes independent of P	With respect to	Condition
$V'_m$	A	$\frac{[P]K_{01}}{K_3[B]} \ll 1$
$V'_m$	B	$\frac{[P]K_{02}}{K_4[A]} \ll 1$
$K'_m$	A	$[P]K_{02} \ll 1 + 1/K_2[B]$ and $\frac{[P]K_{01}}{K_3[B]} \ll 1$
$K'_m$	B	$[P]K_{01} \ll 1 + \frac{1}{K_1[A]}$ and $\frac{[P]K_{02}}{K_4[A]} \ll 1 + \frac{1}{K_4[A]}$
$K'_m/V'_m$	A	$[P]K_{02} \ll 1 + \frac{1}{K_2[B]}$
$K'_m/V'_m$	B	$[P]K_{01} \ll 1 + \frac{1}{K_1[A]}$

The ratio,  $K'_m/V'_m$ , with respect to substrate A will be independent of the concentration of P whenever  $[P]K_{02} \ll 1 + 1/K_2[B]$  and this ratio with respect to the other substrate, B, will be independent of P whenever  $[P]K_{01} \ll 1 + 1/K_1[A]$ . In both these cases the  $V'_m$  will continue to depend upon the concentration of P unless

$$[P]K_{01}/K_3[B] \ll 1 \text{ (substrate A)}$$

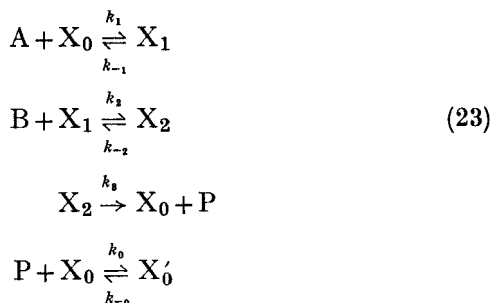
or

$$[P]K_{02}/K_4[A] \ll 1 \text{ (substrate B)}$$

These results are summarized in Table III.

These two mechanisms do not lend themselves to ready differentiation since the only difference exists in the kinetic state of the enzyme complexes. Nevertheless both mechanisms discussed here can be distinguished from the one in which all forms of the enzyme are in the steady-state since in that case the  $v$  versus  $v/[S]$  plots will be non-linear.<sup>15</sup>

If it is assumed that two substrates, A and B, react with the enzyme in an ordered sequence, and that the product, P, reacts only with the free form of the enzyme,  $X_0$ , the rate equations are



It is not intended in the mechanism described by Eqs. (23) and the subsequent mechanisms involving a final uni-directional step that the enzymic conversion of substrate(s) to product(s) cannot occur in the reverse direction. Rather, we are making a mechanistic restriction that at the time that the rates are measured, the interaction of P and  $X_0$  has not reached the stage at which the substrate is being reformed. Furthermore, it should not be assumed that the complete role of P in the fully reversible mechanism is the same as the role of P in the mechanism described by Eqs. (23).

The values of the parameters are:

<i>v</i> with respect to	$V'_m$	Parameters $K'_m$
A	$\frac{[E_0]}{\frac{\phi}{[B]} + \frac{1}{k_3}}$	$\frac{\frac{k_{-1}}{k_1} \left( \frac{1}{k_{-1}} + \frac{\phi}{[B]} \right) (1 + [P] K_0)}{\frac{\phi}{[B]} + \frac{1}{k_3}}$
B	$\frac{[E_0]}{\frac{1}{k_3} + \frac{1 + [P] K_0}{k_1[A]}}$	$\frac{\frac{k_{-1}}{k_1} \left( \frac{\phi}{[A]} \right) (1 + [P] K_0) + \phi}{\frac{1}{k_3} + \frac{1 + [P] K_0}{k_1[A]}}$

(24)

where  $\phi = \frac{1}{k_2} + \frac{k_{-2}}{k_2 k_3}$ .

Equations (24) show that for this ordered sequence mechanism the  $V'_m$  with respect to substrate A will always be independent of the inhibitory product but the  $K'_m$  will always be a linear function of the product concentration. On the other hand, the  $V'_m$  with respect to substrate B may depend upon the product concentration. If the concentration of the non-variable substrate, A, is made high enough so that the ratio  $(1 + [P] K_0)/k_1[A]$  is much less than  $1/k_3$ , the  $V'_m$  will become independent of P. On the other hand, if this ratio is much greater than  $1/k_3$ , the reciprocal of  $V'_m$  will become a linear function of the product concentration. It is not sufficient that only  $(1 + [P] K_0)/k_1[A] \ll 1/k_3$  but also  $k_{-1}(1 + [P] K_0)/k_1[A] \ll 1$  before the  $K'_m$  with respect to substrate B becomes independent of P.

There is one additional circumstance where the  $K'_m$  with respect to substrate B, but not the  $K'_m$  with respect to substrate A, can become independent of the concentration of P. Furthermore, in the following case, the reciprocal of the  $V'_m$  with respect to B will become a linear function of [P]. If  $(1 + [P] K_0)/[A] \gg k_1/k_{-1}$  and  $(1 + [P] K_0)/[A] \gg k_1/k_3$ , the  $K'_m$  will be independent of the concentration of P. Physically this means that if  $k_1$  is a very slow step, the inhibition by P may appear to be strictly uncompetitive with respect to  $S_2$  but competitive with respect to  $S_1$ . These results are summarized in Table IV.

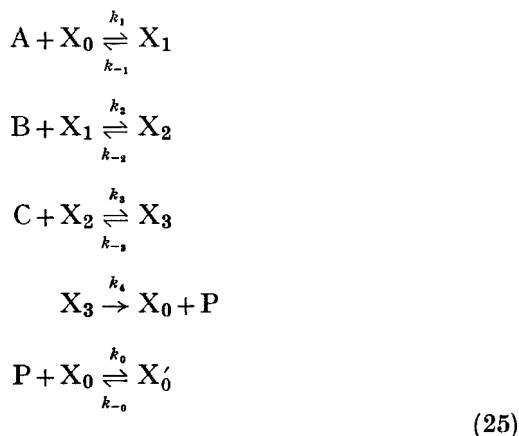
TABLE IV. Conditions When the Rate Parameters of the Mechanism Described by Eqs. (23) Become Independent of the Concentration of the Product

Parameter that is made independent of P	With respect to	Condition
$V'_m$	A	Always
$K'_m$	A	Never if there is inhibition
$V'_m$	B	$\frac{1}{K_1[A]} (1 + [P] K_0) \ll \frac{1}{k_3}$
$K'_m$	B	$\frac{k_{-1} (1 + [P] K_0)}{k_1 [A]} \ll 1$ and $\frac{1}{k_1[A]} (1 + K_0[P]) \ll \frac{1}{k_3}$
$K'_m$	B	$\frac{k_{-1}}{k_1} \frac{1}{[A]} (1 + [P] K_0) \gg 1$ and $\frac{1}{k_1[A]} (1 + [P] K_0) \gg \frac{1}{k_3}$
$K'_m/V'_m$	A	Never if there is inhibition
$K'_m/V'_m$	B	$\frac{k_{-1}}{k_1} \frac{1}{[A]} (1 + [P] K_0) \ll 1$

This mechanism is characterized by several striking features. It is possible to identify which substrate reacts first and which second in the ordered sequence, since the  $V'_m$  with respect to the first substrate, A, will be independent of P and the  $K'_m$  will be a linear function of [P]. The  $V'_m$  with respect to the second substrate can be made to depend upon P, especially at low concentrations of the first substrate and the  $K'_m$  will probably not be a linear function of the concentration of P. Also, this mechanism is easily distinguishable from the random addition mechanism since in that case the  $V'_m$ 's of both substrates depend upon P.



If it is assumed that three substrates, A, B, and C, react with the enzyme in an ordered sequence, and that the product, P, reacts only with the free form of the enzyme,  $X_0$ , the rate equations are



*v* with  
respect to      *Parameters*

---

A	$V'_m$	$\frac{[E_0]}{\frac{1}{[B]}\left(\frac{1}{k_2} + \frac{\phi}{[C]}\right) + \frac{1}{[C]}\left(\frac{1}{k_3} + \frac{k_{-3}}{k_3 k_4}\right) + \frac{1}{k_4}}$
	$K'_m$	$\frac{\frac{k_{-1}}{k_1}\left(\frac{1}{k_{-1}} + \frac{1}{[B]}\right)\left(\frac{1}{k_2} + \frac{\phi}{[C]}\right)(1 + [P]K_0)}{\frac{1}{[B]}\left(\frac{1}{k_2} + \frac{\phi}{[C]}\right) + \frac{1}{[C]}\left(\frac{1}{k_3} + \frac{k_{-3}}{k_3 k_4}\right) + \frac{1}{k_4}}$
B	$V'_m$	$\frac{[E_0]}{\frac{1 + [P]K_0}{k_1[A]} + \frac{1}{[C]}\left(\frac{1}{k_3} + \frac{k_{-3}}{k_3 k_4}\right) + \frac{1}{k_4}}$
	$K'_m$	$\frac{\frac{k_{-1}}{k_1}\left\{\frac{1}{[A]}\left(\frac{1}{k_2} + \frac{\phi}{[C]}\right)(1 + [P]K_0)\right\} + \frac{1}{k_2} + \frac{\phi}{[C]}}{\frac{1 + [P]K_0}{k_1[A]} + \frac{1}{[C]}\left(\frac{1}{k_3} + \frac{k_{-3}}{k_3 k_4}\right) + \frac{1}{k_4}}$

$$\begin{array}{ll}
 \text{C} & V'_m \quad \frac{[E_0]}{\frac{(1 + [P] K_0)}{k_1[A]} \left( 1 + \frac{k_{-1}}{[B] k_2} \right) + \frac{1}{k_2[B]} + \frac{1}{k_4}} \\
 & K'_m \quad \frac{\frac{k_{-1}}{k_1} \phi \frac{(1 + [P] K_0)}{[A][B]} + \frac{\phi}{[B]} + \frac{1}{k_3} + \frac{k_{-3}}{k_3 k_4}}{\frac{1 + [P] K_0}{k_1[A]} \left( 1 + \frac{k_{-1}}{[B] k_2} \right) + \frac{1}{k_2[B]} + \frac{1}{k_4}} \\
 & \phi = \frac{k_{-2}}{k_2 k_3} + \frac{k_{-2} k_{-3}}{k_2 k_3 k_4} \quad (26)
 \end{array}$$

Equations (26) show that the  $V'_m$  with respect to substrate A will be independent of P just as it was in the case involving two substrates. Consideration of mechanisms involving additional substrates show that the  $V'_m$  with respect to the first substrate in the ordered sequence is always independent of the product. The  $K'_m$ 's with respect to this substrate are linear functions of the product concentration. The second and third substrates cannot be distinguished in this manner since the product competes with substrate A. The  $V'_m$ 's and  $K'_m$ 's with respect to substrates B and C are all complicated functions of the product concentration.

It is possible to make certain generalizations which may be applied to more complicated cases of product inhibition from the kinetics derived from the relatively simple cases presented thus far. It has been shown that true initial rates should be used and that if rates are measured at times when the product concentration is large enough to cause the reverse reaction to occur appreciably, even the simplest enzymic reaction becomes quite complicated. The limiting velocity at infinite substrate concentration becomes a function of the product concentration and the  $v$  versus  $v/[S]$  plots become non-linear. It may be expected then that this would also occur in more complicated enzyme systems.

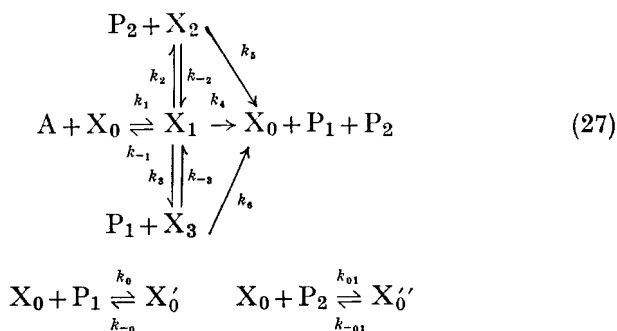
It has been pointed out that in the steady-state any enzyme associated with two substrates which add randomly will give non-linear  $v$  versus  $v/[S]$  plots. Certain simplifying assumptions which appear to be justified in consideration of the large number of linear plots reported from multi-substrate-enzyme systems were considered. These assumptions included a partial-quasiequilibrium

assumption, the quasiequilibrium assumption, and the ordered-sequence assumption. It was found that even in the simplest case of product inhibition where only one product is formed, it is possible that the limiting velocity is decreased by the presence of the inhibitory product even though no interaction at any site other than the active site was assumed.

#### IV. REACTIONS IN WHICH MORE THAN ONE PRODUCT IS FORMED BY ONE SUBSTRATE

If more than one product is produced in an enzymic reaction there are several ways in which the products can be desorbed from the enzyme in an ordered sequence. In addition, there is the possibility that the products will all be desorbed in a single step. Finally, it is possible that the products are desorbed one at a time in a completely random fashion. Naturally, it is possible that both the single-step displacement and the random multi-step displacements could occur simultaneously in the same reaction.

In the simplest case of this type, two products are formed from a single substrate. While the hydrolysis reactions are not true examples of this type reaction because two substrates are actually involved, they generally follow the kinetic characteristics of this type reaction because the second substrate, water, is generally in excess. The general mechanism is given as



The equilibrium constants,  $K_0$  and  $K_{01}$ , are defined as  $k_0/k_{-0}$  and  $k_{01}/k_{-01}$  respectively. Since both products arise from the same substrate and if the substrate concentration can be taken to be much

greater than the concentration of interaction sites on the enzyme, the net rates of formation of  $P_1$  and  $P_2$  must be the same. Then,

$$k_5 X_2 = k_6 X_3$$

and

$$k_5/k_6 = X_3/X_2$$

The rate equation based on the assumption that all forms of the enzyme are in the steady state is

$$v = \frac{(k_4 + k_5 \phi_1) [E_0]}{(k_{-1} + k_2 + k_3 + k_4 - k_{-2} [P_2] \phi_1 - k_{-3} [P_1] \phi_2)} \times \frac{K_1 [A]}{(1 + [P_1] K_0 + [P_2] K_{01}) + \phi_1 + \phi_2 + 1}$$

$$\phi_1 = \frac{k_2}{k_{-2} [P_2] + k_5} \quad \phi_2 = \frac{k_3}{k_{-3} [P_1] + k_6} \quad (28)$$

It can be shown that  $\phi_1$  and  $\phi_2$  are related to  $X_2$  and  $X_3$

$$k_5/k_6 = X_3/X_2 = \phi_2/\phi_1 \quad (28a)$$

In the  $v$  versus  $v/[S]$  form this equation becomes

$$v = \frac{(k_4 + k_5 \phi_1) [E_0]}{1 + \phi_1 + \phi_2} - \frac{(k_{-1} + k_2 + k_3 + k_4 - k_{-2} [P_2] \phi_1 - k_{-3} [P_1] \phi_2) \times (1 + [P_1] K_0 + [P_2] K_{01})}{1 + \phi_1 + \phi_2} \frac{v}{[S]} \quad (29)$$

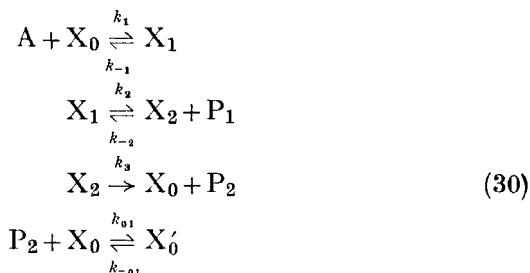
Since  $\phi_1$  and  $\phi_2$  are related as shown in Eq. (28a), only a single condition is required to make the  $V'_m$  independent of  $P_1$  or  $P_2$ . If  $k_{-2} [P_2] \ll k_5$ , then  $k_{-3} [P_1] \ll k_6$  and the  $V'_m$  becomes independent of  $P_1$  and  $P_2$ , but the  $K'_m$  may still remain a linear function of the concentration of each provided  $[P_1] K_0$  and  $[P_2] K_0 \gg 1$ . Physically this means that if the rate of breakdown of either enzyme-product complex,  $X_2$  or  $X_3$ , to free enzyme is much more rapid than its reaction with  $P_2$  or  $P_1$ , respectively, to reform  $X_1$ , the inhibition will be strictly competitive and due solely to the steps described by  $K_0$  and  $K_{01}$ . If, on the other hand, the  $k_{-3}$  and  $k_{-2}$  steps in Eq. (27) are of significant magnitude, the  $V'_m$  will be reduced in the presence of either product. A change in the  $V'_m$  was also found in the case

where the quasiequilibrium assumption is made for the mechanism described by Eqs. (27).<sup>14</sup> These results are summarized in Table V.

TABLE V. Condition When the Rate Parameters of the Mechanism Described by Eqs. (27) Become Independent of the Concentration of Either Product

Parameter that is independent of $P_1$ or $P_2$	$P_1$ or $P_2$	Conditions
$V'_m$	either	$k_{-2}[P_2] \ll k_5$ or $k_{-3}[P_1] \ll k_6$
$K'_m$	$P_1$	same as $V'_m$ and $K_0[P_1] \ll 1$
$K'_m$	$P_2$	same as $V'_m$ and $K_{01}[P_2] \ll 1$
$K'_m/V'_m$	either	same as $K'_m$

If a single substrate reacts with an enzyme to form two products and the products are desorbed from the enzyme in an ordered sequence, Eqs. (27) becomes



and  $K_{01} = k_{01}/k_{-01}$ . In this case

$$\begin{aligned}
 v &= \frac{[E_0]}{\frac{1}{k_3} + \phi} - \frac{\frac{k_{-1}}{k_1} \left( \frac{1}{k_{-1}} + \phi \right) (1 + [P_2] K_{01})}{\frac{1}{k_3} + \phi} \frac{v}{[S]} \\
 \phi &= \frac{k_{-2}[P_1]}{k_2 k_3} + \frac{1}{k_2}
 \end{aligned} \tag{31}$$

From Eq. (31) it can be seen that the first product,  $P_1$ , can be distinguished from  $P_2$  since the  $V'_m$  is a function of the concentration

of the second product only, whereas the  $K'_m$  depends linearly on the concentration of  $P_2$  and, in a somewhat less predictable manner, on the concentration of  $P_1$ . This mechanism can be distinguished from the mechanism described by Eqs. (27). This is, of course, in analogy with the arguments presented for the simpler case when only one product is formed from a single substrate, provided the step represented by  $k_3$  can be considered to be essentially "irreversible".

Since in Eqs. (30) there is no interaction between  $X_0$  and  $P_1$ , an interesting difference in the  $K'_m$ 's between the mechanisms described by Eqs. (27) and (30) arises when  $k_{-2}[P_1]$  is relatively small. Since  $K_0$  can be taken as zero in Eqs. (30), the  $K'_m$  will not depend upon the concentration of  $P_1$  provided  $k_{-2}[P_1] \ll k_3$  but it will be a linear function of the concentration of  $P_2$  if  $[P_2] K_{01}$  is significant. On the other hand, in the mechanism described by Eqs. (27) there is an interaction described by  $K_0$ . When  $k_{-2}[P_1]$  and  $k_{-3}[P_2]$  are relatively small compared with  $k_5$  and  $k_6$  respectively (here  $k_5$  is a rate constant describing a step kinetically similar to that described by  $k_3$  in Eqs. (30)), the  $K'_m$  will depend linearly on the concentrations of both products provided both  $K_0[P_1]$  and  $K_{01}[P_2]$  are significant. Physically this suggests that if the steps involving the reincorporation of product into the enzyme-substrate complex can be made relatively slow, and at the same time the reactions described by the equilibria  $K_0$  and  $K_{01}$  significant, it is possible to determine which products, if any, are concerned in reactions with  $X_0$  of the type described by  $K_0$  or  $K_{01}$ . This may be done by determining which products cause a linear increase in the  $K'_m$  term. In addition, this suggests that the mechanisms described by Eqs. (27) and (30) can be distinguished since the  $V'_m$  in (27) depends on both products once  $k_{-2}[P_1]$  and  $k_{-3}[P_2]$  become relatively large whereas the  $V'_m$  in (30) depends only on  $P_1$  as long as the reverse of the final reaction described by  $k_3$  remains relatively small. A summary of the conditions that cause the parameters in Eq. (31) to be independent of the concentration of either  $P_1$  or  $P_2$  is given in Table VI.

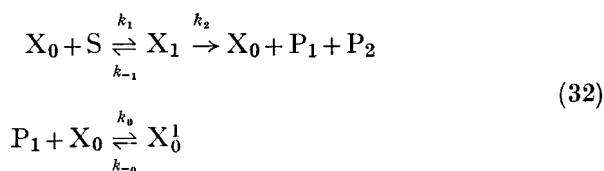
Perhaps the most thoroughly investigated enzyme with regard to product inhibition is chymotrypsin. In 1949 Harmon and Niemann<sup>16</sup> reported the inhibition of the trypsin-catalyzed hydrolysis of *N*-benzoyl-L-argininamide by *N*-benzoyl-L-arginine. They reported that the other product, ammonium ion, was not an

TABLE VI. Conditions When the Rate Parameters of the Mechanism Described by Eqs. (30) Become Independent of the Concentration of Either Product

Parameter that becomes independent	P <sub>1</sub> or P <sub>2</sub>	Conditions <sup>a</sup>
$V'_m$	P <sub>1</sub>	$\frac{k_{-2}}{k_3}[P_1] \ll 1$ or $\frac{k_{-2}}{k_2}[P_1] \ll 1$
$V'_m$	P <sub>2</sub>	Always
$K'_m$	P <sub>1</sub>	Same as $V'_m$
$K'_m$	P <sub>1</sub>	$\phi \gg 1/k_{-1}$ and $\phi \gg 1/k_3$
$K'_m$	P <sub>2</sub>	Never when $K_{01}$ is finite
$K'_m/V'_m$	P <sub>1</sub>	$\phi \ll 1/k_{-1}$
$K'_m/V'_m$	P <sub>2</sub>	Same as $K'_m$ (never when $K_{01}$ is finite)

<sup>a</sup>  $\phi$  in this case is defined in Eq. (31).

inhibitor. A short time later, Huang and Niemann and other associates<sup>17, 18, 19</sup> reported the inhibition of the  $\alpha$ -chymotrypsin-catalyzed hydrolysis of acetyl-L-tryptophanamide, nicotinyl-L-tryptophanamide, acetyl-L-tyrosinamide and nicotinyl-L-tyrosinamide by the corresponding acetylated amino acid products of each reaction. It was consistently found that ammonium ions did not inhibit the reaction even in concentrations up to 0.01M. Other examples of inhibition of chymotrypsin were subsequently investigated by Niemann and associates. The basic mechanism which they presumed was functioning is



where  $K_p = k_{-0}/k_0$ . This mechanism leads to the same rate expression that would be obtained if only one product were formed [Eqs. (5a)] and predicts that the inhibition by P<sub>1</sub> would be strictly competitive. Since every product studied by Niemann and his

associates which was found to inhibit did so competitively, even after 40 or 50% of the hydrolysis had occurred, the mechanism described by Eqs. (32) is the simplest mechanism possible and consistent with the experimental observations.

An integrated form of Eq. (6) based on the type mechanism described by Eqs. (30) for competitive product inhibition by  $j$  products was reported and tested by Niemann and associates<sup>20, 21, 22</sup>

$$k_2[E_0]t = K_m \left( 1 + [S_0] \sum_{j=1}^n \frac{1}{K_{Pj}} \right) \ln \frac{[S_0]}{[S]} + \left( 1 - K_m \sum_{j=1}^n \frac{1}{K_{Pj}} \right) ([S_0] - [S]) \quad (33)$$

This equation may be rearranged to

$$\frac{[S_0] - [S]}{t} = \frac{k_2[E_0]}{1 - \frac{K_m}{K_P}} - \frac{K_m \left( 1 + \frac{[S_0]}{K_P} \right) \ln \frac{[S_0]}{[S]}}{1 - \frac{K_m}{K_P}} \quad (33a)$$

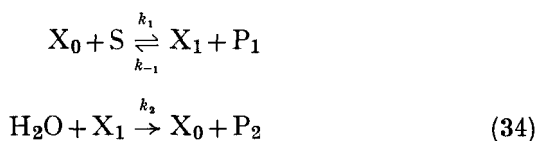
If  $([S_0] - [S])/t$ , the zero-order term, is plotted against  $(\ln[S_0]/[S])/t$ , the first-order term, a straight line is obtained which may be extrapolated back to initial conditions (when  $t = 0$ ). If a line is drawn through these extrapolated points, it will be the line which would have been obtained if initial rates had been used. The slope of this line will be equal to the negative of the apparent Michaelis constant. This provides a method of correcting for product inhibition of the type described by Eq. (6) or (32) when it is desired to calculate  $K_m$  and  $V_m$ . This method has been applied by Foster and Niemann<sup>20</sup> for the  $\alpha$ -chymotrypsin hydrolysis of acetyl-L-tyrosine hydroxamide.

Another hydrolytic enzyme that is subject to inhibition by a product is spleen NADase. Thus the hydrolysis of NAD to adenine-ribose-diphosphate-ribose (ARPPR) and nicotinamide is strongly retarded by nicotinamide but not by ARPPR when the spleen enzyme is used.<sup>23, 24</sup> NADase from other sources such as *Neurospora crassa* is not inhibited as much by nicotinamide.<sup>23</sup>



Using Lineweaver-Burk reciprocal plots, Zatman and co-workers<sup>23</sup> found that nicotinamide inhibited the spleen NADase-catalyzed hydrolysis in a manner that resembled non-competitive inhibition; that is, there was a large shift in the limiting velocity,  $V'_m$ , and a shift in the slope of the reciprocal plots,  $K'_m/V'_m$ . It was not established that the  $K'_m$  was independent of the presence of nicotinamide, nor was it established that the reciprocal of  $V'_m$  was a linear function of the nicotinamide concentration. It was established, however, that 42 to 49% inhibition was observed with  $2.5 \times 10^{-3}$  M nicotinamide over a NAD concentration range between  $6.5 \times 10^{-4}$  M and  $1.76 \times 10^{-2}$  M. The *Neurospora* enzyme, on the other hand, was inhibited by 79% when 0.2 M nicotinamide was added to  $6.7 \times 10^{-4}$  M NAD, but only 25% when 0.2 M nicotinamide was added to  $3.3 \times 10^{-2}$  M NAD. This indicated that the *Neurospora* enzyme was inhibited more or less competitively whereas the spleen enzyme was inhibited in another manner. In addition, it was found that certain analogs of nicotinamide such as nicotinic acid hydrazine reacted in the system containing the spleen enzyme to form corresponding analogs of NAD. Moreover, NAD containing  $^{14}\text{C}$  could be prepared by including nicotinamide labeled with  $^{14}\text{C}$  in the spleen enzyme reaction mixture. Finally, it was established that the observations were not due to a simple reverse of the whole hydrolysis since no NAD was formed from the incubation of ARPPR and nicotinamide with the enzyme.

These observations led Zatman and associates to suggest the following mechanism for the hydrolysis of NAD:



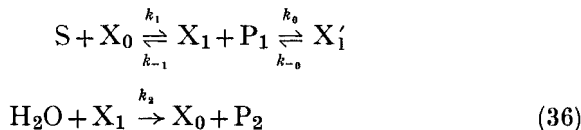
where S is NAD,  $\text{P}_1$  is nicotinamide, and  $\text{P}_2$  is ARPPR. However, the rate expression for this mechanism is

$$v = V_m - \left( \frac{k_{-1}[\text{P}_1] + k_2}{k_1} \right) \frac{v}{[\text{S}]} \quad (35)$$

It can be seen then that the mechanism described by Eq. (34) predicts that only the  $K'_m$  would be a function of  $[\text{P}_1]$  and that  $V'_m$  would

not. Since this result is inconsistent with Zatman's observations with spleen NADase, it must be discarded for that enzyme.

Zatman and associates offered a slight modification of the mechanism described by Eqs. (34) in which water still competes with nicotinamide for the  $X_1$  complex, but where nicotinamide is able to react also with the  $X_1$  complex to form an inactive complex,  $X'_1$ .



The resulting steady-state rate equation is

$$v = \frac{V_m}{\frac{k_{-1}}{k_1} \frac{[P_1]}{[S]} + [P_1] K_0 + 1} \quad (37)$$

where  $K_0 = k_0/k_{-0}$ .

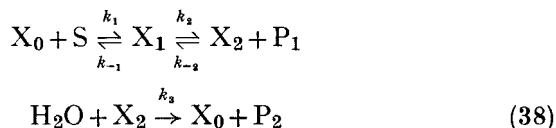
This mechanism leads to a change in the  $V'_m$  and  $K'_m/V'_m$  terms due to the presence of  $P_1$ . However, this mechanism does not appear particularly attractive since the product must react with  $X_1$  presumably at some site other than the one from which it was desorbed.

Another reaction which possesses certain similarities to the NADase reaction is the glucose-6-phosphatase catalyzed hydrolysis of glucose-6-phosphate to glucose and orthophosphate. A primary distinction between the reactions exists since both products of the glucose-6-phosphatase hydrolysis inhibit the reaction.<sup>25, 26, 28</sup>

Frieden and Mathews<sup>26</sup> observed that glucose inhibits glucose-6-phosphatase in a manner that is intermediate between non-competitive and uncompetitive, whereas Segal<sup>27</sup> reports that the glucose inhibition is strictly non-competitive. However, Hass and Byrne<sup>28</sup> have also observed that glucose inhibits in a way that is between non-competitive and uncompetitive and that the other product, orthophosphate, inhibits competitively.

As in the case of NADase, labeled glucose is rapidly incorporated into glucose-6-phosphate in the presence of glucose-6-phosphatase.<sup>27, 29</sup> The amount of  $^{14}\text{C}$ -glucose incorporated is equivalent to the difference in the amount of phosphate released in the inhibited and uninhibited reactions.

Segal,<sup>27</sup> Hass and Byrne,<sup>28</sup> and Walter and Frieden<sup>14</sup> have discussed several mechanisms in connection with apparent non-competitive and uncompetitive product inhibition. If, for example, an additional enzyme-substrate intermediate is included in the mechanism described by Eqs. (34), the mechanism becomes



The rate equation for this three-step process is the same as that given earlier in this chapter in Eq. (31), where  $K_{01} = 0$ . This equation is repeated in Eq. (39).

$$v = \frac{[E_0]}{\frac{1}{k_3} + \frac{1}{k_2} + \frac{k_{-2}[P_1]}{k_2 k_3}} - \frac{\frac{k_{-1}}{k_1} \left( \frac{1}{k_{-1}} + \frac{1}{k_2} + \frac{k_{-2}[P_1]}{k_2 k_3} \right)}{\frac{1}{k_3} + \frac{1}{k_2} + \frac{k_{-2}[P_1]}{k_2 k_3}} \frac{v}{[S]} \quad (39)$$

The cases where the parameters in this equation are independent of  $P_1$  have been summarized in Table VI. Briefly, it should be pointed out that the terms containing  $P_1$  drop out of the  $V'_m$  term only if  $(k_{-2}/k_3)[P_1] \ll 1$ , whereas they may drop out of the  $K'_m$  if

$$(k_{-2}/k_2)[P_1] \ll 1 \text{ and } (k_{-2}/k_3)[P_1] \ll 1$$

In addition,  $K'_m$  becomes independent of the product concentration if for any reason  $1/k_{-1} \ll 1/k_2 + k_{-2}[P_1]/k_2 k_3 \gg 1/k_3$ . Thus the terms in the  $K'_m$  will cancel and the  $K'_m$  will become equal to  $k_{-1}/k_1$  and the  $V'_m$  will become equal to  $k_2[E_0]/(1 + k_{-2}[P_1]/k_3)$ . Physically this situation requires that the enzyme-substrate complex,  $X_1$ , dissociate very slowly to  $X_2$  and glucose. In addition, it should be noted that the ratio  $K'_m/V'_m$  can be independent of the concentration of  $P_1$  any time  $k_{-2}[P_1]/k_2 k_3 \ll 1/k_{-1}$ . Physically this means that if the  $k_{-1}$  step in Eqs. (38) is slow, the reciprocal of  $V'_m$  is a linear function of the concentration of  $P_1$ , and the rate expression becomes homeomorphic to what is classically referred to as "uncompetitive" inhibition by  $P_1$ . Thus, it is possible that the mechanism described by Eqs. (38) would demonstrate kinetics which are characteristic of those expected on the basis of non-competitive product inhibition, uncompetitive product inhibition or of intermediate mechanisms

of inhibition. The possibility that both the NADase and the glucose-6-phosphatase reactions possess apparent uncompetitive character suggests that intermediate mechanisms may be functioning. The difference in type of inhibition observed by Frieden and Hass and Byrne from those observed by Segal may be explained on the basis of a slightly different relative value for the different steps in the mechanism described by Eqs. (38). This could be due to different characteristics of the enzyme used in the different laboratories.<sup>28</sup> It should be pointed out that Segal<sup>27</sup> has reported a proportionality between the reciprocal of the inhibited velocity and the glucose concentration, as would be expected from Eq. (39) if it is assumed that  $X_1$  dissociates to  $X_2$  and glucose very slowly, i.e. where the  $K'_m$  is independent of the concentration of  $P_1$ .

The values for the dissociation constant of the substrate complex,  $K_s$ , and the inhibition constant for glucose,  $K_i$ , reported by Segal<sup>27</sup> are:

$$\frac{k_{-1}}{k_1} = K_s = 8 \times 10^{-4} \text{ M} \quad \frac{k_{-2}}{k_3} = K_i = 1.2 \times 10^{-1} \text{ M}$$

The mechanism reported by Hass and Byrne for the glucose-6-phosphatase reaction is also identical to the one described by Eqs. (38). Since their data did not indicate strictly non-competitive product inhibition, it was not necessary to impose Segal's restrictions with regard to the relative values of the individual rate constants. The values reported by Hass and Byrne for the Michaelis constant,  $K'_m$ , the enzyme-substrate dissociation constant,  $K_s$ , and the inhibition constants,  $K_i$  and  $K_0$ , were:

$$K'_m = \frac{k_3(k_{-1} + k_2)}{k_1(k_2 + k_3)} = 6 \times 10^{-3} \text{ M}$$

$$K_s = \frac{k_{-1}}{k_1} = 8 \times 10^{-4} \text{ M}$$

$$K_i(\text{glucose}) = \frac{k_2 + k_3}{k_{-2}} = 8.8 \times 10^{-2} \text{ M}$$

$$K_0(\text{phosphate}) = \frac{k_0}{k_{-0}} = 5.5$$

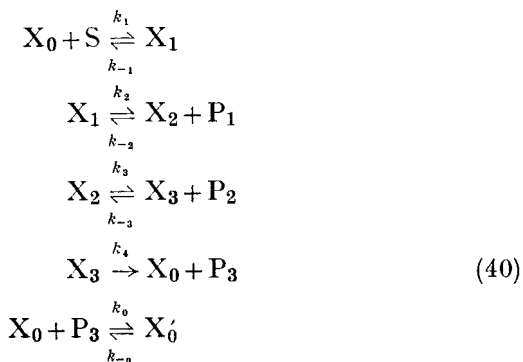
Byrne and Neuhaus<sup>30</sup> have suggested that the mechanism described by Eqs. (38) also accounts for the uncompetitive product

inhibition of another hydrolytic enzyme, *o*-phosphoserine phosphatase, by the product, serine. It has been pointed out that these equations predict a rate expression in which the reciprocal of the  $V'_m$  is a linear function of the product concentration but the ratio  $K'_m/V'_m$  is independent of  $P_1$  provided  $k_{-1}$  is very small compared to  $k_2k_3/k_{-2}[P_1]$ . These workers have also reported a proportionality between the reciprocal of the inhibited rate and the concentration of serine. It can readily be seen that this proportionality is expected when  $k_{-1} \ll k_2k_3/k_{-2}[P_1]$ .

Since in the case of glucose-6-phosphatase, both products inhibit the reaction, it is not possible that Eqs. (38), as they stand, describe the complete inhibition mechanism. As more information becomes available about the product inhibition by phosphate, it should be possible to distinguish between the mechanisms suggested for this enzyme.

It appears likely that a whole series of enzymic hydrolysis may follow a mechanism similar to Eqs. (23). It is probable that NADase, glucose-6-phosphatase, and *o*-phosphoserine phosphatase all follow a mechanism in which the products are desorbed from the enzyme in an ordered sequence. Further studies with product inhibition on these and other hydrolytic enzymes will yield valuable information which can also be used to eliminate possible mechanisms.

In the cases of the depolymerases it is possible that more than two products are formed during the enzymic reaction. Such a mechanism is described in Eqs. (40) for three products, each of which is desorbed in an ordered sequence.



In this mechanism, once again, the inhibition by an interaction

with the free enzyme is limited to a single product. It would be expected that  $P_3$  would be the most likely one to react with  $X_0$  since  $P_3$  and  $X_0$  are formed in the same step. In this case the rate expression is

$$v = \frac{[E_0]}{\phi_1 + \phi_2} - \frac{\frac{k_{-1}}{k_1} \left( \frac{1}{k_{-1}} + \phi_1 \right) (1 + [P_3] K_0)}{\phi_1 + \phi_2} \frac{v}{[S]} \quad (41)$$

$$\phi_1 = \frac{1}{k_2} + \frac{k_{-2}[P_1]}{k_2 k_3} + \frac{k_{-2}[P_1] k_{-3}[P_2]}{k_2 k_3 k_4} \quad \phi_2 = \frac{1}{k_3} + \frac{1}{k_4} + \frac{k_{-3}[P_2]}{k_3 k_4}$$

This equation is very similar to the one found in the case of two products. The generalization that may be made from Eqs. (30) and (40) is that it will always be possible to identify the final product formed provided it inhibits *and* assuming it is the product that reacts with  $X_0$ . In cases where more than one product react with  $X_0$ , the  $K'_m$  will be linear functions of each. Furthermore, it will become increasingly difficult to distinguish  $P_1$  from  $P_2$ , etc., since the  $V'_m$  and  $K'_m$  will depend on each similarly. The conditions under which the parameters in Eq. (41) become independent of the concentration of the product are summarized in Table VII.

## V. REACTIONS OF MORE THAN ONE SUBSTRATE TO FORM MORE THAN ONE PRODUCT

The simplest chemical reaction of this type is the one in which two substrates are converted to two products. This type of reaction embraces a large number of enzymic reactions. Prominent among these are the reactions in which one of the substrates is a coenzyme.

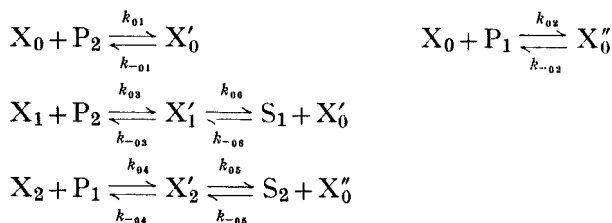
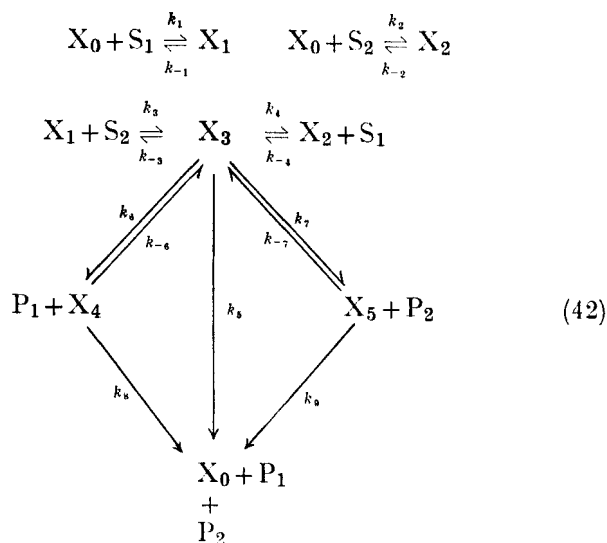
It would not be unexpected if enzymic reactions of this type demonstrated the following characteristics. If a random addition of substrates can occur, the enzyme-substrate-1 complex,  $X_1$ , should have affinity for substrate-2, and the enzyme-substrate-2 complex,  $X_2$ , should have affinity for substrate-1. In addition, since the products,  $P_2$  and  $P_1$ , differ from  $S_1$  and  $S_2$ , respectively, often in only a small way, it is reasonable to expect that  $X_1$  would combine with  $P_2$  and  $X_2$  would combine with  $P_1$ . In addition to this, the products of these combinations,  $X'_1$  and  $X'_2$ , respectively, may be formed by another route. If the free enzyme,  $X_0$ , forms inactive

TABLE VII. Conditions When the Rate Parameters of the Mechanism Described by Eqs. (40) Become Independent of the Concentration of the Products

Parameter that becomes independent	$P_1$ , $P_2$ , or $P_3$	Condition <sup>a</sup>
$V''_m$	$P_1$	$\frac{k_{-2}[P_1]}{k_3} + \frac{k_{-2}[P_1]k_{-3}[P_2]}{k_3k_4} \ll 1$
$V''_m$	$P_2$	$\frac{k_{-3}[P_2]}{k_3} + \frac{k_{-2}[P_1]k_{-3}[P_2]}{k_2k_3} \ll 1$
$V''_m$	$P_3$	Always
$K'_m$	$P_1$	Same as $V''_m$
$K'_m$	$P_1$	$\phi_1 \gg 1/k_{-1}$ and $\phi_1 \gg \phi_2$
$K'_m$	$P_2$	Same as $V''_m$
$K'_m$	$P_2$	$\frac{k_{-2}[P_1]k_{-3}[P_2]}{k_2k_3k_4} \geq \frac{k_{-2}[P_1]}{k_2k_3} + \frac{1}{k_{-1}} + \frac{1}{k_{-1}}$ and $\frac{k_{-3}[P_2]}{k_3k_4} \gg \frac{1}{k_3} + \frac{1}{k_4}$
$K'_m$	$P_3$	Never unless $K_0 = 0$
$K'_m/V''_m$	$P_1$	$\frac{k_{-2}[P_1]}{k_3} + \frac{k_{-2}[P_1]k_{-3}[P_2]}{k_3k_4} \ll 1$
$K'_m/V''_m$	$P_2$	$\frac{k_{-2}[P_1]k_{-3}[P_2]}{k_3k_4} \ll 1 + \frac{k_{-2}[P_1]}{k_3}$
$K'_m/V''_m$	$P_3$	Never unless $K_0 = 0$

<sup>a</sup> The meanings for  $\phi_1$  and  $\phi_2$  are given in Eq. (41).

complexes with  $P_2$  and  $P_1$ , which we will call  $X'_0$  and  $X''_0$ , respectively,  $X'_0$  would be expected to react with substrate-2,  $S_2$ , to form  $X'_2$  and  $X''_0$  would be expected to react with the substrate,  $S_1$ , to form  $X'_1$ . If the sites at which  $S_1$  and  $P_2$ , and  $S_2$  and  $P_1$  react are slightly different,  $P_2$  should be able to compete at a site with  $S_1$  but it may react at this site without competition with respect to  $S_2$ . Correspondingly,  $P_1$  may compete with  $S_2$  for the site at which these species react, but  $P_1$  may react at this site without competition with respect to  $S_1$ . This general mechanism is summarized in Eqs. (42).



Once again, if it is assumed that  $X_0$  is in equilibrium with each form of the substrate, but that the complexes  $X_1$ ,  $X_2$ , and  $X_3$  are in a steady state, certain equilibrium parameters may be defined.

$$K_1 = k_1/k_{-1}, \quad K_2 = k_2/k_{-2}, \quad K_{0n} = k_{0n}/k_{-0n} \quad n = 1, 2, 3, 4, 5, 6$$



The rate equations for this mechanism and for the mechanism in which all the equations described in (42) are in equilibrium have been derived elsewhere.<sup>14</sup> The  $V'_m$ 's with respect to  $S_1$  and  $S_2$ , respectively, for this mechanism in the partial steady-state are

$$\frac{\left(k_5 + \frac{k_8 k_6}{k_{-6}[P_2] + k_8}\right) [E_0]}{\frac{\phi(K_1 + K_{03} K_1 [P_2])}{[S_2]} + \frac{k_6}{k_{-6}[P_2] + k_8} + \frac{k_7}{k_{-7}[P_1] + k_9} + 1} \quad (43a)$$

$$\frac{\left(k_5 + \frac{k_8 k_6}{k_{-6}[P_2] + k_8}\right) [E_0]}{\frac{\phi(K_2 + K_{04} K_2 [P_1])}{[S_1]} + \frac{k_6}{k_{-6}[P_2] + k_8} + \frac{k_7}{k_{-7}[P_1] + k_9} + 1} \quad (43b)$$

The respective  $K'_m$ 's are

$$\frac{\frac{\phi}{[S_2]} (1 + K_2 [S_2] + K_{01} [P_1] + K_{02} [P_2] + K_{04} K_2 [S_2] [P_1])}{\frac{\phi(K_1 + K_{03} K_1 [P_2])}{[S_2]} + \frac{k_6}{k_{-6}[P_2] + k_8} + \frac{k_7}{k_{-7}[P_1] + k_9} + 1} \quad (43c)$$

$$\frac{\frac{\phi}{[S_1]} (1 + K_1 [S_1] + K_{01} [P_1] + K_{02} [P_2] + K_{03} K_1 [S_1] [P_2])}{\frac{\phi(K_2 + K_{04} K_2 [P_1])}{[S_1]} + \frac{k_6}{k_{-6}[P_2] + k_8} + \frac{k_7}{k_{-7}[P_1] + k_9} + 1} \quad (43d)$$

where  $\phi =$

$$\frac{k_{-3} + k_{-4} + k_5 + k_6 + k_7 - \frac{k_{-6} k_6 [P_2]}{k_{-6}[P_2] + k_8} - \frac{k_{-7} k_7 [P_1]}{k_{-7}[P_1] + k_9}}{K_1 k_3 + k_4 K_2} \quad (43e)$$

It is clear from these equations, (43a-e), that the  $V'_m$  with respect to either substrate will be a function of the concentration of both products,  $P_1$  and  $P_2$ . Furthermore, increasing the concentrations of non-variable substrates will not cause *all* the terms containing  $P_1$  or  $P_2$  to become small. The  $V'_m$ 's therefore may be functions of both product concentrations regardless of the concentration of the non-variable substrate. In the special circumstance where the non-variable substrate concentration is saturating, and

$$k_8 k_6 / (k_{-6}[P_2] + k_8) \gg k_5 \text{ and } k_6 / (k_{-6}[P_2] + k_8) \gg k_7 / (k_{-7}[P_1] + k_9) + 1$$

the  $V'_m$  becomes equal to  $k_8[E_0]$  and is independent of either product concentration. Physically, however, this means that the  $k_8$  or  $k_9$  steps are the only significant steps in which products are formed. It is clear that the  $V'_m$  will depend upon the relative amounts of the reactions,  $k_5$ ,  $k_8$  and  $k_9$ , contributing to it. Since in the steady state  $k_8$  and  $k_9$  are interdependent, it is possible to express the  $V'_m$  in terms of  $k_5$  and either of the other two constants. The relative contribution to the net reaction rate will in turn, for  $k_8$  or  $k_9$ , be a function of the concentrations of the products reversibly formed in the respective steps. When the product concentrations are made large, the relative contribution from the two-step displacement mechanisms will be lowered, and, as a consequence, the  $V'_m$  will be lowered. A similar result is obtained in the case when the equations described in (42) are all in equilibrium.<sup>14</sup>

The  $K'_m$ 's given in Eqs. (43c) and (43d) are both complicated functions of the concentrations of both products. The dependence of the  $K'_m$ 's on the concentrations of the products obtained when the mechanism described by Eqs. (42) is at quasiequilibrium is also similar and has been reported by Walter and Frieden.<sup>14</sup> The conditions under which the parameters in Eqs. (43) become independent of the concentration of  $P_1$  or  $P_2$  are summarized in Table VIII.

Several possible mechanisms, all of which are basically limitations of the mechanism described by Eqs. (42), for the enzymic conversion of two substrates to two products have been discussed. Alberty<sup>31</sup> has recently presented a number of these mechanisms and Walter and Frieden<sup>14</sup> have discussed others.

Dalziel<sup>32</sup> has pointed out that the overall enzymic conversion of  $S_1$  and  $S_2$  to  $P_2$  and  $P_1$  may be represented conveniently by

$$\frac{[E_0]}{v} = \varphi_0 + \frac{\varphi_1}{[S_1]} + \frac{\varphi_2}{[S_2]} + \frac{\varphi_{12}}{[S_1][S_2]} \quad (44)$$

Alberty<sup>31</sup> and Dalziel<sup>32</sup> have pointed out that  $\varphi_0$ ,  $\varphi_1$ ,  $\varphi_2$ , and  $\varphi_{12}$  can readily be obtained from experimental data. For example, if the concentration of  $S_1$  is held constant for a series of experiments at different concentrations of  $S_2$ , a plot of  $[E_0]/v$  versus  $1/[S_2]$  will be linear. This can be seen by putting Eq. (44) in the form

$$\frac{[E_0]}{v} = \left( \varphi_0 + \frac{\varphi_1}{[S_1]} \right) + \left( \varphi_2 + \frac{\varphi_{12}}{[S_1]} \right) \frac{1}{[S_2]} \quad (45)$$

TABLE VIII. Conditions When the Rate Parameters of the Mechanism Described by Eqs. (42) Become Independent of the Concentration of Either Product

Parameter that becomes independent of	P <sub>1</sub> or P <sub>2</sub>	With respect to	Conditions <sup>a</sup>
V' <sub>m</sub>	All P's	S <sub>1</sub>	$\frac{\phi}{[S_2]} (K_1 + K_{03} K_1 [P_2]) + \frac{k_6}{k_{-6}[P_2] + k_8} + \frac{k_7}{k_{-7}[P_1] + k_9} \ll 1$ and $\frac{k_8 k_6}{k_{-6}[P_2] + k_8} \ll k_3$
V'' <sub>m</sub>	All P's	S <sub>1</sub>	$\frac{k_8 k_6}{k_{-6}[P_2] + k_8} \gg k_3$ and $\frac{\phi}{[S_2]} (K_1 + K_{03} K_1 [P_2]) + \frac{k_7}{k_{-7}[P_1] + k_9} + 1 \ll \frac{k_6}{k_{-6}[P_2] + k_8}$
V'' <sub>m</sub>	P <sub>1</sub>	S <sub>1</sub>	$k_{-7}[P_1] \ll k_9$
V' <sub>m</sub>	P <sub>2</sub>	S <sub>1</sub>	$k_{-6}[P_2] \ll k_8$ and $\frac{\phi}{[S_2]} (K_1 + K_{03} K_1 [P_2]) \ll 1 + \frac{k_6}{k_8} + \frac{k_7}{k_{-7}[P_1] + k_9}$
V'' <sub>m</sub>	P <sub>1</sub>	S <sub>2</sub>	$k_{-7}[P_1] \ll k_9$ and $\frac{\phi}{[S_1]} (K_2 + K_{04} K_2 [P_1]) \ll 1 + \frac{k_7}{k_9} + \frac{k_6}{k_{-6}[P_2] + k_8}$
V'' <sub>m</sub>	P <sub>2</sub>	S <sub>2</sub>	$k_{-6}[P_2] \ll k_8$
K' <sub>m</sub>	P <sub>1</sub>	S <sub>1</sub>	Never as long as K <sub>01</sub> or K <sub>04</sub> is finite
K'' <sub>m</sub>	P <sub>2</sub>	S <sub>2</sub>	Never as long as K <sub>02</sub> or K <sub>03</sub> is finite

<sup>a</sup>  $\phi$  is defined in Eq. (43c).

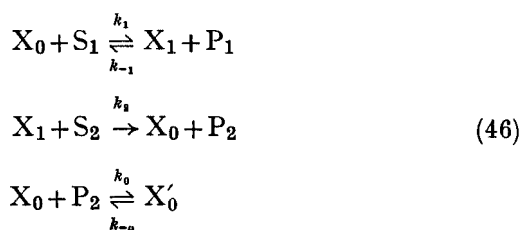
By plotting the intercept and slope of Eq. (45) versus  $1/[S_1]$  all four coefficients may be obtained from intercepts and slopes. In a refinement of these techniques, Mahler and Baker have programmed Eq. (44) for an IBM 650 computer.<sup>33</sup>

For convenience in relating the  $v$  versus  $v/[S]$  form of the rate equations to the coefficients of the Dalziel equation, the meanings of the  $K'_m$ 's and  $V'_m$ 's in terms of the  $\varphi$ 's are given in Table IX.

TABLE IX. The Relationship Between the Rate Parameters and the Dalziel Coefficients

Parameter	With respect to	Equals
$V'_m$	$S_1$	$\varphi_0 + \frac{\varphi_2}{[S_2]}$
$V'_m$	$S_2$	$\varphi_0 + \frac{\varphi_1}{[S_1]}$
$K'_m/V'_m$	$S_1$	$\varphi_1 + \frac{\varphi_{12}}{[S_2]}$
$K'_m/V'_m$	$S_2$	$\varphi_2 + \frac{\varphi_{12}}{[S_1]}$

If the substrates add to the enzyme in an ordered sequence in enzymic reaction of this type and the products are desorbed in an ordered sequence, the simplest possible mechanism involving a final uni-directional step and a re-association of  $P_2$  and  $X_0$  predicts that a portion of the leading substrate would be transferred to the enzyme in the first step:



The steady-state rate equations for this reaction sequence are:

$$v = k_2[E_0][S_2] - k_2[S_2] \frac{k_{-1}}{k_1} \left( \frac{1}{k_{-1}} + \frac{[P_1]}{k_2[S_2]} \right) (1 + [P_2]K_0) \frac{v}{[S_1]} \quad (47)$$

$$v = \frac{k_1[E_0][S_1]}{1 + [P_2]K_0} - \frac{k_1[S_1] \left\{ \frac{k_{-1}[P_1]}{k_1[S_1]k_2} (1 + [P_2]K_0) + \frac{1}{k_2} \right\}}{1 + [P_2]K_0} \frac{v}{[S_2]} \quad (48)$$

It can readily be seen that this mechanism is distinguished by the fact that the  $V'_m$ 's with respect to either substrate are linear functions of the concentration of the other substrate. Furthermore, in the absence of the first product it may be seen that the  $K'_m$  with respect to either substrate is also a linear function of the concentration of the other substrate. In addition, the ratio,  $K'_m/V'_m$  will be independent of the concentration of the non-variable substrate.

The  $V'_m$  with respect to  $S_1$  will never depend on either product. The reciprocal of the  $V'_m$  with respect to substrate  $S_2$ , however, will be a linear function of the concentration of  $P_2$  but will be independent of  $P_1$ . The  $K'_m$  with respect to substrate  $S_1$  will always be a linear function of the concentration of  $P_2$ . It is apparent that  $K_0$  can be calculated from either the  $K'_m$  with respect to  $S_1$  or the  $V'_m$  with respect to  $S_2$ .

The  $K'_m$  with respect to  $S_1$  will become independent of the concentration of  $P_1$  if  $[P_1]/k_2[S_2] \ll 1/k_{-1}$ . This result is consistent with those obtained from the discussion of other mechanisms in that increasing the concentration of the non-variable substrate will decrease the inhibition by  $P_1$ .

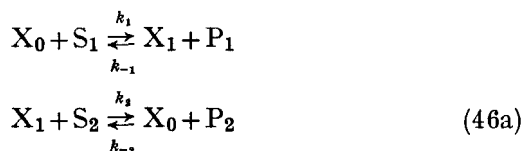
The  $K'_m$  with respect to  $S_2$  will become independent of  $P_1$  or of  $P_2$  whenever  $(k_{-1}/k_{-2})([P_1]/[S_1]k_2)(1 + [P_2]K_0) \ll 1/k_2$ . This result can also be brought about any time the concentration of  $S_1$  is made very large or when  $k_{-1}[P_1]$  is very small. These results are summarized in Table X(A).

If the mechanism described by Eqs. (46) is written in the fully reversible form, it is clear that the reaction of  $P_2$  with  $X_0$  must result in the formation of some substrate,  $S_2$ . Thus, in this case, the reaction between  $P_2$  and  $X_0$  in Eqs. (46) and the fully reversible

TABLE X(A). Conditions When the Rate Parameters of the Mechanism Described by Eqs. (46) Become Independent of the Concentration of Either Product

Parameter that becomes independent	P <sub>1</sub> or P <sub>2</sub>	With respect to	Conditions
$V'_m$	P <sub>1</sub>	S <sub>1</sub>	Always
$V'_m$	P <sub>2</sub>	S <sub>1</sub>	Always
$V'_m$	P <sub>1</sub>	S <sub>2</sub>	Always
$V'_m$	P <sub>2</sub>	S <sub>2</sub>	Never when $K_0$ is finite
$K'_m$	P <sub>1</sub>	S <sub>1</sub>	$\frac{[P_1]}{k_2[S_2]} \ll \frac{1}{k_{-1}}$
$K'_m$	P <sub>2</sub>	S <sub>1</sub>	Never when $K_0$ is finite
$K'_m$	P <sub>1</sub>	S <sub>2</sub>	$\frac{k_{-1}[P_1]}{k_1[S_1]k_2} (1 + [P_2]K_0) \ll \frac{1}{k_2}$
$K'_m$	P <sub>2</sub>	S <sub>2</sub>	$\frac{k_{-1}[P_1]}{k_1[S_1]k_2} (1 + [P_2]K_0) \gg \frac{1}{k_2}$
$K'_m/V'_m$	P <sub>1</sub>	S <sub>1</sub>	$\frac{[P_1]}{k_2[S_2]} \ll \frac{1}{k_{-1}}$
$K'_m/V'_m$	P <sub>2</sub>	S <sub>1</sub>	Never when $K_0$ is finite
$K'_m/V'_m$	P <sub>1</sub>	S <sub>2</sub>	$\frac{k_{-1}[P_1]}{k_1[S_1]k_2} (1 + [P_2]K_0) \ll \frac{1}{k_2}$
$K'_m/V'_m$	P <sub>2</sub>	S <sub>2</sub>	$\frac{k_{-1}[P_1]}{k_1[S_1]k_2} (1 + [P_2]K_0) \ll \frac{1}{k_2}$

mechanism, described by Eqs. (46a), lead to enzyme intermediates which must be different for these two mechanisms.



This suggests that the rate equations derived from Eqs. (46a) may be drastically different from those obtained from Eqs. (46). The  $v$

versus  $v/[S]$  forms of the rate equation obtained from Eqs. (46a) are:

$$v = [E_0] k_2 [S_2] - \left[ \frac{k_{-2}[P_2] + k_{-1}[P_1] + k_2[S_2]}{k_1} \right] \frac{v}{[S_1]} \quad (47a)$$

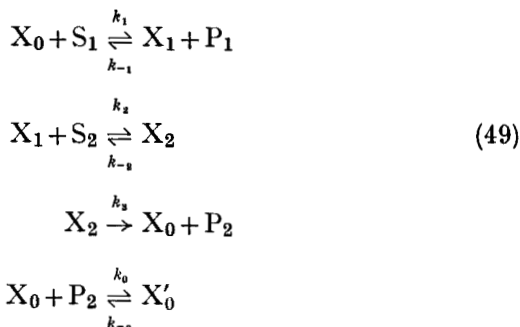
$$v = [E_0] k_1 [S_1] - \left[ \frac{k_{-2}[P_1] + k_{-1}[P_1] + k_1[S_1]}{k_2} \right] \frac{v}{[S_2]} \quad (48a)$$

It is clear from a comparison of Eqs. (47), (48), and (47a), (48a), that the two mechanisms described by Eqs. (46a) and (46) lead to different rate equations. The mechanism described by Eqs. (46a) is still distinguished by the fact that the  $V'_m$ 's with respect to either substrate are linear functions of the concentrations of the other substrate. However, in this mechanism, neither  $V'_m$  is affected by either product. Furthermore, unlike the results predicted for Eqs. (46), the  $K'_m$  with respect to  $S_2$  depends on the concentration of  $P_2$  even if the concentration of  $P_1$  is negligible, and the  $K'_m$  with respect to  $S_1$  can be made to be independent of  $P_2$  as well as  $P_1$  by allowing the concentration of  $S_2$  to be very large. The conditions under which these individual parameters become independent of the respective products for the fully reversible mechanism are summarized in Table X(B).

TABLE X(B). Conditions When the Rate Parameters of the Mechanism Described by Eqs. (46a) Become Independent of the Concentration of Either Product

Parameter that becomes independent	$P_1$ or $P_2$	With respect to	Conditions
$V'_m$	All P's	All S's	Always
$K'_m$	$P_1$	$S_1$	$k_{-2}[P_2] + k_2[S_2] \gg k_{-1}[P_1]$
$K'_m$	$P_2$	$S_1$	$k_{-1}[P_1] + k_2[S_2] \gg k_{-2}[P_2]$
$K'_m$	$P_1$	$S_2$	$k_{-2}[P_2] + k_1[S_1] \gg k_{-1}[P_1]$
$K'_m$	$P_2$	$S_2$	$k_{-1}[P_1] + k_1[S_1] \gg k_{-2}[P_2]$
$K'_m/V'_m$	All P's	All S's	Same as respective $K'_m$ 's

If it is assumed that in the mechanism described by Eqs. (46), a ternary enzyme complex between part of the first substrate and the second substrate is formed, a three-step mechanism must be considered:



The rate expressions are:

$$v = \frac{[E_0]}{\frac{\phi}{[S_2]} + \frac{1}{k_2}} - \frac{\frac{k_{-1}}{k_1} \left( \frac{1}{k_{-1}} + \frac{[P_1]\phi}{[S_2]} \right) (1 + [P_2]K_0)}{\frac{\phi}{[S_2]} + \frac{1}{k_3}} \frac{v}{[S_1]} \tag{50}$$

$$v = \frac{[E_0]}{\frac{1 + [P_2]K_0}{k_1[S_1]} + \frac{1}{k_3}} - \frac{\frac{k_{-1}}{k_1} \frac{[P_1]\phi}{[S_1]} (1 + [P_2]K_0) + \phi}{\frac{1 + [P_2]K_0}{k_1[S_1]} + \frac{1}{k_3}} \frac{v}{[S_2]} \tag{51}$$

where  $\phi = (1/k_2) + (k_{-2}/k_2 k_3)$ .

It can be seen that this mechanism leads to rate equations (50) and (51) which are distinctly different from those derived from Eqs. (46). Unless certain conditions are met the  $V'_m$  with respect to both substrates will not be linear functions of the concentrations of the non-variable substrate as they were in the mechanism described by Eqs. (46). If it happens that

$$1/k_3 \ll \phi/[S_2] \text{ or } 1/k_3 \ll (1 + [P_2]K_0)/k_1[S_1]$$

then the  $V'_m$ 's with respect to  $S_1$  and  $S_2$ , respectively, become linear functions of the non-variable substrate concentration. Physically,



however, this means that the final step ( $k_3$ ) in Eqs. (49) must be very fast.

As in the mechanism described by Eqs. (46) the  $V'_m$  with respect to substrate  $S_1$  will never depend upon  $P_1$  or  $P_2$  but the  $V'_m$  with respect to  $S_2$  will depend upon the concentration of  $P_2$  unless  $(1 + [P_2]K_0)/k_1[S_1] \ll 1/k_3$ . Apparently, then, it is possible in principle to make the  $V'_m$  with respect to  $S_2$  independent of the concentration of  $P_2$  by increasing the concentration of  $S_1$ . This should serve as another useful tool in distinguishing between the mechanisms outlined in Eqs. (46) and (49).

The  $K'_m$  with respect to  $S_1$  will always be a linear function of the concentration of  $P_2$  as long as  $K_0$  is finite, and will also depend on the concentration of  $P_1$  unless  $[P_1]\phi/[S_2] \ll 1/k_{-1}$ . Thus, if the  $k_{-1}$  step is very slow or if the concentration on the non-variable substrate,  $S_2$ , is made large enough, the  $K'_m$  with respect to  $S_1$  may become independent of  $P_1$ . The  $K'_m$  with respect to  $S_2$  can become independent of  $P_1$  if  $(k_{-1}[P_1]/k_1[S_1])(1 + [P_2]K_0) \ll 1$  and it can be made independent of  $P_2$  if  $(k_{-1}[P_1]/k_1[S_1])(1 + [P_2]K_0) \ll 1$  and  $(1 + [P_2]K_0)/k_1[S_1] \ll 1/k_3$  or if  $(k_{-1}[P_1]/k_1[S_1])(1 + [P_2]K_0) \gg 1$  and  $(1 + [P_2]K_0)/k_1[S_1] \gg 1/k_3$ . These results indicate that it is possible, at least in principle, to make the  $K'_m$  with respect to  $S_2$  independent of both  $P_1$  and  $P_2$  if the concentration of  $S_1$  is made large enough. These results are summarized in Table XI(A).

If the mechanism described by Eqs. (49) is written in the fully reversible form, the reaction of  $P_2$  with  $X_0$  does not result in the immediate formation of a substrate (as it did in the mechanism described by Eqs. (46a)). In this case, it is also necessary that the complex,  $X_2$ , decompose in the reverse direction to  $X_1$  and  $S_2$  in order for a substrate to be formed. This is illustrated in Eqs. (49a):

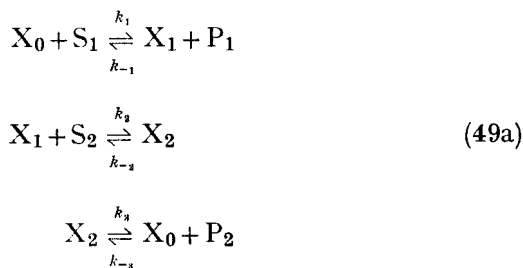


TABLE XI(A). Conditions When the Rate Parameters of the Mechanism Described by Eqs. (49) Become Independent of the Concentration of Either Product

Parameter that becomes independent	P <sub>1</sub> or P <sub>2</sub>	With respect to	Conditions <sup>a</sup>
$V'_m$	P <sub>1</sub>	S <sub>1</sub>	Always
$V'_m$	P <sub>2</sub>	S <sub>1</sub>	Always
$V'_m$	P <sub>1</sub>	S <sub>2</sub>	Always
$V'_m$	P <sub>2</sub>	S <sub>2</sub>	$\frac{1 + [P_2] K_0}{k_1[S_1]} \ll \frac{1}{k_3}$
$K'_m$	P <sub>1</sub>	S <sub>1</sub>	$\frac{[P_1] \phi}{[S_2]} \ll \frac{1}{k_{-1}}$
$K'_m$	P <sub>2</sub>	S <sub>1</sub>	Never if $K_0$ is finite
$K'_m$	P <sub>1</sub>	S <sub>2</sub>	$\frac{k_{-1}}{k_1} \left( \frac{[P_1]}{[S_1]} \right) (1 + [P_2] K_0) \ll 1$
$K'_m$	P <sub>2</sub>	S <sub>2</sub>	$\frac{k_{-1}[P_1]}{k_1[S_1]} (1 + [P_2] K_0) \ll 1$ and $\frac{1 + [P_2] K_0}{[S_1] k_1} \ll \frac{1}{k_3}$
$K'_m$	P <sub>2</sub>	S <sub>2</sub>	$\frac{k_{-1}[P_1]}{k_1[S_1]} (1 + [P_2] K_0) \gg 1$ and $\frac{1 + [P_2] K_0}{[S_1] k_1} \gg \frac{1}{k_3}$
$K'_m/V'_m$	P <sub>1</sub>	S <sub>1</sub>	$\frac{[P_1] \phi}{[S_2]} \ll \frac{1}{k_{-1}}$
$K'_m/V'_m$	P <sub>2</sub>	S <sub>1</sub>	Never if $K_0$ is finite
$K'_m/V'_m$	P <sub>1</sub>	S <sub>2</sub>	$\frac{k_{-1}[P_1]}{k_1[S_1]} (1 + [P_2] K_0) \ll 1$
$K'_m/V'_m$	P <sub>2</sub>	S <sub>2</sub>	$\frac{k_{-1}[P_1]}{k_1[S_1]} (1 + [P_2] K_0) \ll 1$

<sup>a</sup>  $\phi$  is defined in Eq. (51a).

The steady-state rate equations are:

$$v = \frac{[E_0]}{\frac{\phi}{[S_2]} + \frac{1}{k_3}} - \frac{\frac{1 + k_{-3}[P_2]/k_3}{k_1} + \frac{k_{-1}[P_1](k_2\phi + k_{-3}[P_2]/k_3) + k_{-2}k_{-3}[P_2]/k_3}{k_1 k_2 [S_2]}}{\frac{\phi/[S_2] + 1/k_3}{[S_1]}} \quad (50a)$$

$$v = \frac{[E_0]}{\frac{1 + (k_{-3}[P_2]/k_3)}{k_1[S_1]} + \frac{1}{k_3}} - \frac{\frac{\phi + k_{-1}[P_1](k_2\phi + k_{-3}[P_2]/k_3) + k_{-2}k_{-3}[P_2]/k_3}{k_1 k_2 [S_1]}}{\frac{1 + k_{-3}[P_2]/k_3}{k_1[S_1]} + \frac{1}{k_3}} \frac{v}{[S_2]} \quad (51a)$$

where  $\phi$  has the same meaning as in Eqs. (50) and (51).

It is clear from a comparison of Eqs. (50), (51), and (50a), (51a), that the two mechanisms described by Eqs. (49) and (49a) are very similar, but distinguishable. Note that the limiting rates with respect to both substrates depend on the products in exactly the same way. The  $K'_m$ 's appear to depend on the products similarly except that the Dalziel coefficient,  $\varphi_{12}$ , in the mechanism described by Eqs. (49) predicts that as  $[P_1] \rightarrow 0$ ,  $\varphi_{12} \rightarrow 0$  whereas the mechanism described by Eqs. (49a) predicts that as

$$[P_1] \rightarrow 0, \varphi_{12} \rightarrow k_{-2}k_{-3}[P_2]/k_1 k_2 k_3$$

The Dalziel coefficients for the four mechanisms described by Eqs. (46), (46a), (49), and (49a) are summarized in Table XI(B).

Theorell and Chance<sup>34</sup> suggested the following mechanism for the liver alcohol dehydrogenase reaction

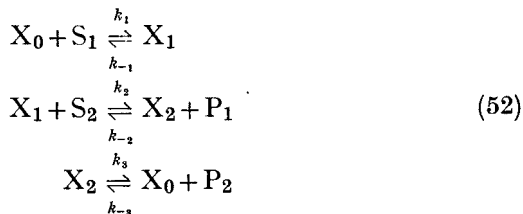


TABLE XI(B). Differences in the Dalziel Coefficients' Dependence on the Products in the Fully and Partially Reversible Enzyme Mechanism ( $P_1$  Formed Before  $S_2$  Adds)

Mechanism (text equations)	$\varphi_0$	$\varphi_1$	$\varphi_2$	$\varphi_{12}$
(46)	0	$\frac{1 + k_0[P_2]/k_{-0}}{k_1}$	$\frac{1}{k_2}$	$\frac{k_{-1}[P_1](1 + k_0[P_2]/k_{-0})}{k_1 k_2}$
(46a)	0	$\frac{1}{k_1}$	$\frac{1}{k_2}$	$\frac{k_{-1}[P_1] + k_{-2}[P_2]}{k_1 k_2}$
(49)	$\frac{1}{k_3}$	$\frac{1 + k_0[P_2]/k_{-0}}{k_1}$	$\frac{1 + k_{-2}/k_3}{k_2}$	$\frac{k_{-1}[P_1] \left( 1 + \frac{k_0[P_2]}{k_0} + \frac{k_{-2}}{k_3} + \frac{k_{-2} k_0 [P_2]}{k_3 k_{-0}} \right)}{k_1 k_2}$
(49a)	$\frac{1}{k_3}$	$\frac{1 + k_{-3}[P_2]/k_3}{k_1}$	$\frac{1 + k_{-2}/k_3}{k_2}$	$\frac{k_{-1}[P_1] \left( 1 + \frac{k_{-2}}{k_3} + \frac{k_{-3}[P_2]}{k_3} \right) + \frac{k_{-2} k_{-3} [P_2]}{k_3}}{k_1 k_2}$

If the final step in Eqs. (52) is taken to be "irreversible" but  $P_2$  can react with  $X_0$  to form  $X'_0$  (which should be similar to  $X_2$ ) the mechanism can be described by Eqs. (53) and (54):

$$v = \frac{[E_0]}{\frac{1}{k_3} + \frac{\phi}{[S_2]}} - \frac{\frac{k_{-1}}{k_1} \left( \frac{1}{k_{-1}} + \frac{\phi}{[S_2]} \right) (1 + [P_2] K_0)}{\frac{1}{k_3} + \frac{\phi}{[S_2]}} \frac{v}{[S_1]} \quad (53)$$

$$v = \frac{[E_0]}{\frac{1 + [P_2] K_0}{k_1 [S_1]} + \frac{1}{k_3}} - \frac{\frac{k_{-1}}{k_1} \frac{\phi}{[S_1]} (1 + [P_2] K_0) + \phi}{\frac{1 + [P_2] K_0}{k_1 [S_1]} + \frac{1}{k_3}} \frac{v}{[S_2]} \quad (54)$$

where  $\phi = \frac{1}{k_2} + \frac{k_{-2}[P_1]}{k_2 k_3}$ .

It may be seen from these equations that the  $V'_m$  with respect to  $S_2$  will not be a function of the concentration of  $P_1$ , whereas the  $V'_m$  with respect to  $S_1$  may be. In the general case, where  $k_{-2}[P_1]/k_3 \ll 1$ , no product inhibition by  $P_1$  will be observed. Once again, it is possible to decrease the effects of  $P_1$  simply by making the concentration of the non-variable substrate large. Both the  $K'_m$  and the  $V'_m$  with respect to  $S_1$  can be made independent of the concentration of  $P_1$  if  $S_2$  can be made saturating. The  $K'_m$  with respect to  $S_2$ , on the other hand, can be made a linear function of the concentration of  $P_1$  by using saturating levels of  $S_1$ , but it cannot be made independent of  $P_1$  by this method.

Once again, a coincidental case exists in which the reciprocal of the  $V'_m$  with respect to  $S_1$  can be made a linear function of the concentration of  $P_1$  and the  $K'_m$  can be made independent of  $P_1$ . These conditions are that  $1/k_{-1} \ll \phi/[S_2] \gg 1/k_3$ . Physically this means again that the reverse of the first and the forward third reactions are relatively fast.

The inhibition with respect to  $S_1$  by  $P_2$  will always be strictly competitive, whereas the  $V'_m$  with respect to  $S_2$  may become a function of the concentration of  $P_2$ . The reciprocal of the  $V'_m$  with respect to  $S_2$  may become a linear function of the concentration of  $P_2$  if  $(1 + [P_2] K_0)/k_1 [S_1] \gg 1/k_3$  and the  $K'_m$  becomes independent of  $P_2$  if this condition obtains and  $(k_{-1}/k_1)(1 + [P_2] K_0)/[S_1] \gg 1$ . These results are summarized in Table XII.

TABLE XII. Conditions When the Rate Parameters of the Mechanism Described by Eqs. (52) Become Independent of the Concentration of Either Product

Parameter that becomes independent of	P <sub>1</sub> or P <sub>2</sub>	With respect to	Conditions <sup>a</sup>
$V'_m$	P <sub>1</sub>	S <sub>1</sub>	$\frac{k_{-2}[P_1]}{k_3} \ll 1$ or $\frac{\phi}{[S_2]} \ll \frac{1}{k_3}$
$V'_m$	P <sub>2</sub>	S <sub>1</sub>	Always
$V'_m$	P <sub>1</sub>	S <sub>2</sub>	Always
$V'_m$	P <sub>2</sub>	S <sub>2</sub>	$\frac{1 + [P_2] K_0}{k_1[S_1]} \ll \frac{1}{k_3}$
$K'_m$	P <sub>1</sub>	S <sub>1</sub>	$\frac{k_{-2}[P_1]}{k_3} \ll 1$ , $\frac{\phi}{[S_2]} \ll \frac{1}{k_3}$ , and $\frac{\phi}{[S_2]} \ll \frac{1}{k_{-1}}$
$K'_m$	P <sub>1</sub>	S <sub>1</sub>	$\frac{\phi}{[S_2]} \gg \frac{1}{k_3}$ and $\frac{\phi}{[S_2]} \gg \frac{1}{k_{-1}}$
$K'_m$	P <sub>2</sub>	S <sub>1</sub>	Never if $K_0$ is finite
$K'_m$	P <sub>1</sub>	S <sub>2</sub>	$\frac{k_{-2}[P_1]}{k_3} \ll 1$
$K'_m$	P <sub>2</sub>	S <sub>2</sub>	$\frac{k_{-1}}{k_1} \frac{(1 + [P_2] K_0)}{[S_1]} \ll 1$ and $\frac{1 + [P_2] K_0}{k_1[S_1]} \ll \frac{1}{k_3}$
$K'_m$	P <sub>2</sub>	S <sub>2</sub>	$\frac{k_{-1}}{k_1} \frac{(1 + [P_2] K_0)}{[S_1]} \gg 1$ and $\frac{1 + [P_2] K_0}{k_1[S_1]} \gg \frac{1}{k_3}$
$K'_m/V'_m$	P <sub>1</sub>	S <sub>1</sub>	$\frac{k_{-2}[P_1]}{k_3} \ll 1$
$K'_m/V'_m$	P <sub>1</sub>	S <sub>1</sub>	$\phi/[S_2] \ll \frac{1}{k_{-1}}$
$K'_m/V'_m$	P <sub>2</sub>	S <sub>1</sub>	Never if $K_0$ is finite
$K'_m/V'_m$	P <sub>1</sub>	S <sub>2</sub>	$\frac{k_{-2}[P_1]}{k_3} \ll 1$
$K'_m/V'_m$	P <sub>2</sub>	S <sub>2</sub>	$\frac{k_{-1}}{k_1} \frac{(1 + [P_2] K_0)}{[S_1]} \ll 1$

<sup>a</sup>  $\phi$  is defined in Eqs. (53) and (54).

In terms of the coefficients defined in Eq. (44), the initial rate of the fully reversible version of the enzymic reaction described by Eqs. (52) will be determined by:

$$\varphi_0 = 1/k_3, \quad \varphi_1 = 1/k_1, \quad \varphi_2 = 1/k_2, \quad \text{and} \quad \varphi_{12} = k_{-1}/k_1 k_2 \quad (55)$$

$$\varphi'_0 = 1/k_{-1}, \quad \varphi'_1 = 1/k_{-3}, \quad \varphi'_2 = 1/k_{-2}, \quad \text{and} \quad \varphi'_{12} = k_3/k_{-2} k_{-3} \quad (56)$$

where the primed coefficients refer to the reverse reaction. Dalziel has pointed out that since  $\varphi_1 \varphi_2 / \varphi_{12} = \varphi'_0$  for this mechanism

$$\frac{\frac{1}{k_1} \times \frac{1}{k_2}}{\frac{k_{-1}}{k_1 k_2}} = \frac{1}{k_{-1}} \quad (57)$$

In addition, it is apparent that  $\varphi'_1 \varphi'_2 / \varphi'_{12} = \varphi_0$ . These identities provide two checks on whether the experimental data really can be represented in terms of the mechanism described by Eqs. (52). Additional checks may be obtained by use of experiments in which one of the products is added along with  $S_1$  and  $S_2$ :

$$\begin{aligned} \varphi_0 &= 1/k_3, \quad \varphi_1 = \frac{1}{k_1} \left( 1 + \frac{k_{-3}[P_2]}{k_3} \right) \quad \text{or} \quad \varphi_1 = \frac{1}{k_1}, \\ \varphi_2 &= \frac{1}{k_2} \quad \text{or} \quad \frac{1}{k_2} \left( 1 + \frac{[P_1] k_{-2}}{k_3} \right) \\ \varphi_{12} &= \frac{k_{-1}}{k_1 k_2} \left( 1 + \frac{k_{-3}[P_2]}{k_3} \right) \quad \text{or} \quad \frac{k_{-1}}{k_1 k_2} \left( 1 + \frac{k_{-2}[P_1]}{k_3} \right) \end{aligned} \quad (58)$$

Since  $P_2$  competes with  $S_1$  for the free enzyme, the terms in the rate equation containing  $S_1$  are inhibited competitively. The inhibition constant for  $P_2$  is simply the equilibrium constant for the third reaction of the mechanism described by Eqs. (52). Thus  $k_{-3}/k_3$  can be determined and, since  $k_3$  is known from  $\varphi_0$ ,  $k_{-3}$  can be determined. The identity

$$\frac{\varphi_0}{\frac{k_{-3}}{k_3}} = \varphi'_1 \quad (59)$$

provides a check to determine if the mechanism described by Eqs. (52) is consistent with experimental observations.

Since the addition of  $P_1$  tends to reverse the second reaction in Eqs. (52), there is a competitive effect on the terms in the rate equation containing  $P_1$ . The competitive inhibition constant in this case, however, is not an equilibrium constant but is equal to  $k_3/k_{-2}$ . Consequently it is possible to determine  $k_{-2}$ , since  $k_3$  is known from  $\varphi_0$ . The identity

$$\frac{\varphi_0}{k_{-2}/k_3} = \varphi'_2 \quad (60)$$

provides still another check to determine if the mechanism described by Eqs. (52) is operative.

Thus, by appropriate use of experiments of the type in which the two substrates and one of two products are added it is possible to determine all six rate constants from Eqs. (52). Several checks on the validity of the calculated rate constants have been pointed out. In addition to these, Alberty<sup>35</sup> has pointed out that  $\varphi'_{12}/\varphi_{12}$  must equal the equilibrium constant for the overall reaction.

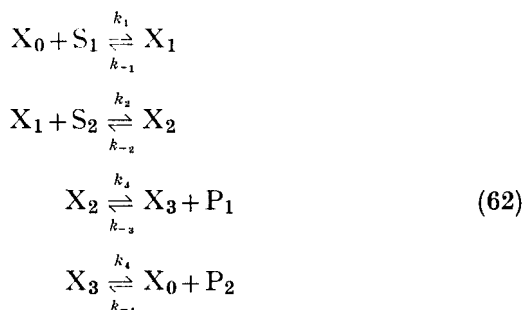
If an additional step is added to the mechanism described by Eqs. (52), in which  $P_1$  competes with  $S_1$  for the free enzyme, the rate expression becomes altered only by the presence of a significant concentration of  $P_1$ :

$$\begin{aligned} \frac{[E_0]}{v} = & \frac{1}{k_3} + \frac{1}{k_1[S_1]} \left( 1 + \frac{k_{-4}[P_1]}{k_4} \right) + \frac{1}{k_2[S_2]} \left( 1 + \frac{k_{-2}[P_1]}{k_3} \right) + \\ & + \frac{k_{-1}}{k_1 k_2 [S_1][S_2]} \left( 1 + \frac{k_{-4}[P_1]}{k_4} \right) \left( 1 + \frac{k_{-2}[P_1]}{k_3} \right) \end{aligned} \quad (61)$$

where  $X'_0 \xrightleftharpoons[k_{-4}]{k_4} X_0 + P_1$ . The consequence of the addition of this step is that the  $\varphi_{12}$  term now shows a more complicated dependence on the concentration of  $P_1$ . The binding constant for the additional step represented in Eq. (61) can most easily be obtained by determining the effect of  $P_1$  on the intercept of a plot of  $[E_0]/v$  versus  $1/[S_2]$ .

If a ternary complex is formed, the mechanism can be described by Eqs. (62),



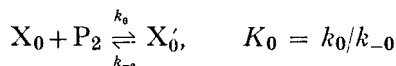


If the final step (4) is again taken to be "irreversible" but  $P_2$  can react with  $X_0$  to form  $X'_0$  (which should be similar to  $X_3$ ), the mechanism can be described by Eqs. (63) and (64):

$$v = \frac{[E_0]}{\frac{\phi_1}{[S_2]} + \phi_2} - \frac{\frac{k_{-1}}{k_1} \left( \frac{1}{k_{-1}} + \frac{\phi_1}{[S_2]} \right) (1 + [P_2] K_0)}{\frac{\phi_1}{[S_2]} + \phi_2} \frac{v}{[S_1]} \tag{63}$$

$$v = \frac{[E_0]}{\frac{1 + [P_2] K_0}{k_1[S_1]} + \phi_2} - \frac{\frac{k_{-1}}{k_1} \frac{\phi_1}{[S_1]} (1 + [P_2] K_0) + \phi_1}{\frac{1 + [P_2] K_0}{k_1[S_1]} + \phi_2} \frac{v}{[S_2]} \tag{64}$$

$$\phi_1 = \frac{1}{k_2} + \frac{k_{-2}}{k_2 k_3} + \frac{k_{-1} k_{-3} [P_1]}{k_2 k_3 k_4} \quad \phi_2 = \frac{1}{k_3} + \frac{1}{k_4} + \frac{k_{-3} [P_1]}{k_3 k_4}$$



It can be seen from these equations that the  $V'_m$  with respect to  $S_1$  depends upon the concentration of  $P_1$  but is independent of  $P_2$ . However, the  $V'_m$  with respect to  $S_2$  is a function of the concentration of both products. The  $K'_m$ 's are both dependent upon the concentrations of both products. Appropriate conditions such as have been assumed in the previous examples can be made in this case to make either the  $K'_m$ 's or the  $V'_m$ 's, or their ratios, independent of the concentration of  $P_1$ , and in some cases, of  $P_2$ . Again, it should be possible in this mechanism to distinguish between  $P_1$  and  $P_2$ . These conditions are summarized in Table XIII.

TABLE XIII. Conditions When the Rate Parameters of the Mechanism Described by Eqs. (62) Become Independent of the Concentration of Either Product

Parameter that becomes independent of	P <sub>1</sub> or P <sub>2</sub>	With respect to	Conditions <sup>a</sup>
V' <sub>m</sub>	P <sub>1</sub>	S <sub>1</sub>	$\frac{k_{-3}[P_1]}{k_3 k_4} \left( \frac{k_{-2}}{[S_2] k_2} + 1 \right) \ll \frac{1}{[S_2]} \left( \frac{1}{k_2} + \frac{k_{-2}}{k_2 k_3} \right) + \frac{1}{k_3} + \frac{1}{k_4}$
V' <sub>m</sub>	P <sub>2</sub>	S <sub>1</sub>	Always
V' <sub>m</sub>	P <sub>1</sub>	S <sub>2</sub>	$\frac{k_{-3}[P_1]}{k_3 k_4} \ll \frac{1}{k_3} + \frac{1}{k_4} + \frac{1 + [P_2]K_0}{k_1[S_1]}$
V' <sub>m</sub>	P <sub>2</sub>	S <sub>2</sub>	$\frac{1 + [P_2]K_0}{[S_1]k_1} \ll \phi_2$
K' <sub>m</sub>	P <sub>1</sub>	S <sub>1</sub>	$\frac{k_{-2}k_{-3}[P_1]}{k_3 k_4} \ll 1 + \frac{k_{-2}}{k_3}$ and $\frac{k_{-3}[P_1]}{k_3 k_4} \left( \frac{k_{-2}}{[S_2]k_2} + 1 \right) \ll \frac{1}{[S_2]} \left( \frac{1}{k_2} + \frac{k_{-2}}{k_2 k_3} \right) + \frac{1}{k_3} + \frac{1}{k_4}$
K' <sub>m</sub>	P <sub>1</sub>	S <sub>1</sub>	$\frac{k_{-2}k_{-3}[P_1]}{k_2 k_3 k_4} \gg \frac{1}{k_2} + \frac{k_{-2}}{k_2 k_3} + \frac{1}{k_{-1}}$ and $\frac{k_{-3}[P_1]}{k_3 k_4} \left( \frac{k_{-2}}{[S_2]k_2} + 1 \right) \gg \frac{1}{[S_2]} \left( \frac{1}{k_2} + \frac{k_{-2}}{k_2 k_3} \right) + \frac{1}{k_3} + \frac{1}{k_4}$

$K'_m$	$P_2$	$S_1$	Never if $K_0$ is finite
$K'_m$	$P_1$	$S_2$	$\frac{k_{-2}k_{-3}[P_1]}{k_3k_4} \ll 1 + \frac{k_{-2}}{k_3}$ and $\frac{k_{-3}[P_1]}{k_3k_4} \ll \frac{1}{k_3} + \frac{1}{k_4} + \frac{1+[P_2]K_0}{[S_1]k_1}$
$K'_m$	$P_1$	$S_2$	$\frac{k_{-2}k_{-3}[P_1]}{k_3k_4} \gg 1 + \frac{k_{-2}}{k_3}$ and $\frac{k_{-3}[P_1]}{k_3k_4} \gg \frac{1}{k_3} + \frac{1}{k_4} + \frac{1+[P_2]K_0}{[S_1]k_1}$
$K'_m$	$P_2$	$S_2$	$\frac{k_{-1}(1+[P_2]K_0)}{k_1[S_1]} \ll 1$ and $\frac{1+[P_2]K_0}{k_1[S_1]} \ll \phi_2$
$K'_m$	$P_2$	$S_2$	$\frac{k_{-1}(1+[P_2]K_0)}{k_1[S_1]} \gg 1$ and $\frac{1+[P_2]K_0}{k_1[S_1]} \gg \phi_2$
$K'_m/V'_m$	$P_1$	$S_1$	$\frac{k_{-2}k_{-3}[P_1]}{[S_2]k_2k_3k_4} \ll \frac{1}{k_{-1}} + \frac{1}{k_2} + \frac{k_{-2}}{k_2k_3}$
$K'_m/V'_m$	$P_2$	$S_1$	Never is $K_0$ is finite
$K'_m/V'_m$	$P_1$	$S_2$	$\frac{k_{-2}k_{-3}[P_1]}{k_3k_4} \ll 1 + \frac{k_{-2}}{k_3}$
$K'_m/V'_m$	$P_2$	$S_2$	$\frac{k_{-1}(1+[P_2]K_0)}{k_1[S_1]} \ll 1$

<sup>a</sup>  $\phi_1$  and  $\phi_2$  are defined in Eq. (64).

The coefficients in Eq. (44) for the fully reversible mechanism described by Eqs. (62) for the initial rates are:

$$\begin{aligned}\varphi_0 &= 1/k_3 + 1/k_4, \quad \varphi_1 = 1/k_1, \quad \varphi_2 = \frac{1 + (k_{-2}/k_3)}{k_2}, \\ \varphi_{12} &= \frac{k_{-1}[1 + (k_{-2}/k_3)]}{k_1 k_2} \\ \varphi'_0 &= \frac{1}{k_{-1}} + \frac{1}{k_{-2}}, \quad \varphi'_1 = \frac{1}{k_{-4}}, \quad \varphi'_2 = \frac{1 + (k_3/k_{-2})}{k_{-3}}, \\ \varphi'_{12} &= \frac{k_4[1 + (k_3/k_{-2})]}{k_{-3} k_{-4}}\end{aligned}\quad (65)$$

where the fourth step is now reversible but  $K_0 = 0$ . Alberty<sup>31</sup> has pointed out that by studying the initial steady-state rates of the forward reaction,  $k_1$ ,  $k_{-1}$ , and the quantities  $(1/k_3 + 1/k_4)$  and  $[1 + k_{-2}/k_3]/k_2$  may be calculated. Similarly from the reverse reaction,  $k_4$ ,  $k_{-4}$  and the quantities  $(1/k_{-1} + 1/k_{-2})$  and  $[1 + k_3/k_{-2}]/k_{-3}$  may be obtained. Combination of these data will give all eight rate constants associated with this mechanism. Since actual equilibrium constants of the reactions of the leading substrate with the free enzyme and the final product with the free enzyme can be determined with both this mechanism and the one described by Eqs. (52), it is possible to compare the values to those obtained by equilibrium measurements.

Dalziel<sup>32</sup> has pointed out that if  $k_{-2} \gg k_{-1}$  and  $k_3 \gg k_4$ , the identities given in Eq. (57) will also hold for the mechanism described by Eqs. (62). This means that if these conditions exist, the existence of a ternary complex would not be suggested from steady-state rates. Alberty points out,<sup>31</sup> however, that the existence of a ternary complex could be brought out by experiments in which the first product formed,  $P_1$ , was added initially.

If the second product formed,  $P_2$ , is added initially with the two substrates and initial rates are measured, the rate expression will be given by<sup>31</sup>

$$\begin{aligned}\frac{[E_0]}{v_0} &= \left( \frac{1}{k_3} + \frac{1}{k_4} \right) + \frac{1 + (k_{-4}[P_2]/k_4)}{k_1[S_1]} + \frac{1 + (k_{-2}/k_3)}{k_2[S_2]} + \\ &\quad + \frac{k_{-1}[1 + (k_{-2}/k_3)]}{k_1 k_2 [S_1][S_2]} \left( 1 + \frac{k_{-4}[P_2]}{k_4} \right)\end{aligned}\quad (66)$$

Alberty has pointed out that since  $P_2$  competes with  $S_1$  for  $X_0$ , the  $S_1$  terms are competitively inhibited and the inhibition constant is simply the equilibrium constant for the dissociation of the enzyme- $P_2$  complex. This means that addition of this product and subsequent measurement of initial rates is of no value in distinguishing between the mechanism described by Eqs. (52) and (62) since the effect of  $P_2$  will be identical in both mechanisms. It has been pointed out in this chapter that a distinction could be made, in principle, between these two mechanisms if other than true initial rates were measured or if a reaction between  $X_0$  and  $P_2$  ( $K_0$  in the equations) occurs.

If the first product,  $P_1$ , is added along with  $S_1$  and  $S_2$ , the rate expression becomes

$$\begin{aligned} \frac{[E_0]}{v_0} = & \left\{ \frac{1 + (k_{-3}[P_1]/k_4)}{k_3} + \frac{1}{k_4} \right\} + \frac{1}{k_1[S_1]} + \\ & + \frac{1 + (k_{-2}/k_3)\{1 + (k_{-3}[P_1]/k_4)\}}{k_2[S_2]} + \\ & + \frac{k_{-1}\{1 + (k_{-2}/k_3)\{1 + (k_{-3}[P_1]/k_4)\}\}}{k_1 k_2 [S_1][S_2]} \end{aligned} \quad (67)$$

Since  $P_1$  tends to bring about the reversal of the third reaction in Eqs. (62), the addition of  $P_1$  exerts a competitive effect on the terms containing  $k_3$ . However, Alberty points out that the inhibition constant,  $k_{-3}/k_4$ , cannot be calculated from the experimental data, but  $k_{-3}/(k_3 + k_4)$  and  $k_{-2}k_{-3}/(k_{-2} + k_3)k_4$  can. It should be noted that in this equation  $\varphi_0$  is affected by the concentration of  $P_1$ .

Alberty points out that since Eqs. (67) and (58) are of a different form, it is possible at least in principle to differentiate between the two mechanisms from which they were derived [Eqs. (52) and (63)] when  $P_1$  is added initially. This distinction can be made even though  $k_{-2} \gg k_{-1}$  and  $k_3 \gg k_4$  and the relationships between the coefficients of the forward and reverse reaction described by the identity given in Eq. (57) hold for both mechanisms. Attention is called once again to the dependence of  $\varphi_0$  on the concentration of  $P_1$  in Eq. (61) but not in (58). Thus it is possible to distinguish between two very similar mechanisms through the use of product inhibition.

If the additional reaction between  $X_0$  and  $P_1$  to form  $X'_0$  is added

to the mechanism described by Eqs. (62), the rate expression becomes<sup>31</sup>

$$\begin{aligned} \frac{[E_0]}{v_0} = & \left( \frac{1}{k_3} + \frac{1}{k_4} \right) \left( 1 + \frac{k_{-3}[P_1]}{k_3 + k_4} \right) + \frac{1 + (k_{-5}[P_1]/k_5)}{k_1[S_1]} + \\ & + \frac{1 + (k_{-2}/k_3)}{k_2[S_2]} \left( 1 + \frac{k_{-2}k_{-3}[P_1]}{(k_{-2} + k_3)k_4} \right) + \\ & + \frac{k_{-1}[1 + (k_{-2}/k_3)]}{k_1k_2[S_1][S_2]} \left( 1 + \frac{k_{-2}k_{-3}[P_1]}{(k_{-2} + k_3)k_4} \right) \left( 1 + \frac{k_{-5}[P_1]}{k_5} \right) \end{aligned} \quad (68)$$

where  $P_1 + X_0 \xrightleftharpoons[k_{-6}]{k_5} X'_0$ . Since  $P_1$  competes with  $S_1$  for  $X_0$ , as well as displacing the equilibrium in the third step, the terms containing  $S_1$  are inhibited by the factor  $(1 + k_{-5}[P_1]/k_5)$ . It has been pointed out that this mechanism can be distinguished from the one described by Eqs. (52) because of the effects of  $P_1$  on the limiting velocity.

In the preceding discussion we have considered the basic mechanisms described by Eqs. (52) in the fully reversible form (in which they are written) and in the form when the last step has not had the opportunity to reverse to such an extent that any substrate is reformed from  $P_2$ , but when  $P_2$  reversibly reacts with  $X_0$  to form some complex,  $X'_0$ . Equations (53) and (54) take into account the effect of both products in the mechanism with the last step uni-directional. Equations (55) and (56) define the Dalziel coefficients for the fully reversible version of Eqs. (52) when the concentrations of the products of the reaction are negligible. Equations (58) define these coefficients when the concentration of  $P_1$ , but not  $P_2$ , is negligible. In order to summarize these results, the values of the Dalziel coefficients for both these versions of the mechanism described by Eqs. (52) in the presence of both products are listed in Table XIII(A). Comparison of these results reveals that there is no detectable kinetic difference between these two mechanisms.

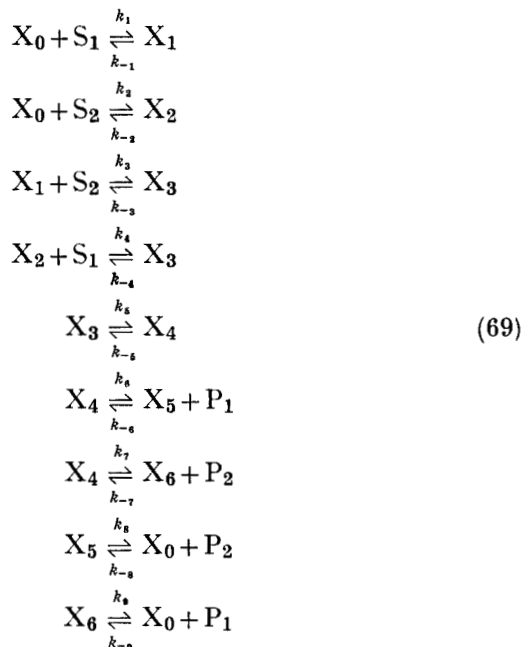
Similarly, we have considered the basic mechanism described by Eqs. (62) in both the fully and partially reversible forms. Equations (63) and (64) take into account the effect of both products in the mechanism with the last step uni-directional. Equation (65) defines the Dalziel coefficients for the fully reversible version of (62) when the concentrations of the products are negligible. Equation

TABLE XIII(A). Similarity of the Dalziel Coefficients' Dependence on the Products in the Fully and Partially Reversible Enzyme Mechanism ( $P_1$  Formed After  $S_2$  Adds)

Mechanism	$\phi_0$	$\phi_1$	$\phi_2$	$\phi_{12}$
$S_1 + X_0 \rightleftharpoons X_1$	$\frac{1}{k_3}$	$\frac{k_{-3}[P_2]}{1 + \frac{k_{-3}[P_2]}{k_3}}$	$\frac{k_{-2}[P_1]}{1 + \frac{k_{-2}[P_1]}{k_3}}$	$k_{-1} \left( 1 + \frac{k_{-2}[P_1]}{k_3} + \frac{k_{-3}[P_2]}{k_3} \right) + \frac{k_{-2}k_{-3}[P_1][P_2]}{k_3}$
$S_2 + X_1 \rightleftharpoons X_2 + P_1$				
$X_2 \rightleftharpoons X_0 + P_2$		$\frac{1}{k_1}$	$\frac{k_2}{k_2}$	$\frac{k_1 k_2}{k_3}$
$S_1 + X_0 \rightleftharpoons X_1$				
$S_2 + X_1 \rightleftharpoons X_2 + P_1$	$\frac{1}{k_3}$	$\frac{k_0[P_2]}{1 + \frac{k_0[P_2]}{k_{-0}}}$	$\frac{k_{-2}[P_1]}{1 + \frac{k_{-2}[P_1]}{k_3}}$	$k_{-1} \left( 1 + \frac{k_{-2}[P_1]}{k_3} + \frac{k_0[P_2]}{k_{-0}} + \frac{k_{-2}k_0[P_1][P_2]}{k_{-0}k_3} \right)$
$X_2 \rightarrow X_0 + P_2$		$\frac{1}{k_1}$	$\frac{k_2}{k_2}$	$\frac{k_1 k_2}{k_3}$
$P_2 + X_0 \rightleftharpoons X_0^1$				

(66) is the rate equation when the concentration of  $P_1$ , but not  $P_2$ , is small, and Eq. (67) is the rate equation when the concentration of  $P_2$ , but not  $P_1$ , is negligible. Comparison of the coefficients obtained from the fully and partially reversible versions of this mechanism in the presence of both products reveals that these two mechanisms are also similar.

Alberty has also discussed the rate equation for the mechanism



where the fifth step is the rate determining step and the other steps occur randomly and are in equilibrium. The rate equation for this mechanism for the forward reaction is

$$\frac{[E_0]}{v_0} = \frac{1}{k_5} \left( 1 + \frac{K_4}{[S_1]} + \frac{K_3}{[S_2]} + \frac{K_1 K_3}{[S_1][S_2]} \right) \tag{70}$$

and for the reverse reaction:

$$\frac{[E_0]}{v_0} = \frac{1}{k_{-5}} \left( 1 + \frac{K_7}{[P_2]} + \frac{K_6}{[P_1]} + \frac{K_7 K_9}{[P_1][P_2]} \right) \tag{71}$$

From measurements of the forward and reverse reaction,  $k_{-5}$ ,  $k_5$



and the eight equilibrium constants can be obtained<sup>31</sup> since  $K_1K_3 = K_2K_4$  and  $K_6K_8 = K_7K_9$ . If large amounts of  $P_2$  are added initially along with  $S_1$  and  $S_2$  and initial rates are determined, the rate expression is

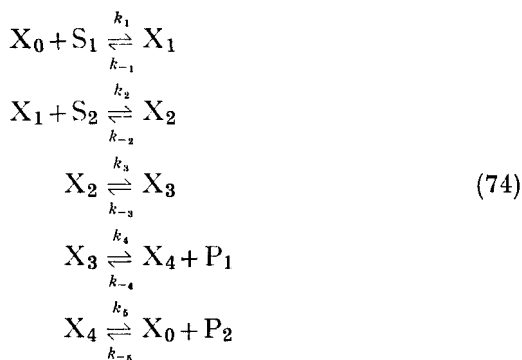
$$\frac{[E_0]}{v_0} = \frac{1}{k_5} \left\{ 1 + \frac{K_4}{[S_1]} + \frac{K_3}{[S_2]} + \frac{K_1K_3}{[S_2][S_2]} \left( 1 + \frac{[P_2]}{K_8} \right) \right\} \quad (72)$$

and similarly, if  $P_1$  is added

$$\frac{[E_0]}{v_0} = \frac{1}{k_5} \left\{ 1 + \frac{K_4}{[S_1]} + \frac{K_3}{[S_2]} + \frac{K_1K_3}{[S_1][S_2]} \left( 1 + \frac{[P_1]}{K_9} \right) \right\} \quad (73)$$

Equations (72) and (73) show that in this mechanism the effect of added product is restricted to the  $\phi_{12}$  term. Consequently, the effect of adding  $P_1$  or  $P_2$  is entirely different in the mechanism described by Eqs. (69) than in those described by (52) or (62). Moreover, it is important to note that the effect of added  $P_1$  is distinctly different in each of the three mechanisms considered.

Baker and Mahler<sup>33</sup> have suggested three additional mechanisms for the type of enzymic reaction under discussion. One of these only involves the insertion of a second ternary complex into the mechanism described by Eqs. (62).



Since it would be expected that this mechanism would be indistinguishable from the one described by Eqs. (62) unless  $X_2$  or  $X_3$  could be measured, it will not be discussed further.

The second additional mechanism suggested by Baker and Mahler was actually a simplification of Eqs. (69) in which the affinity

of the enzyme for  $S_1$  and  $S_2$  remains unchanged by binding to one of the substrates. In this case from Eqs. (69):

$$K_1 = K_4 \quad K_2 = K_3 \quad (75)$$

The third mechanism suggested by Baker and Mahler is similar to the mechanism described by Eqs. (62) except that

$$k_3 \gg k_4 \quad k_{-2} \gg k_{-1} \quad (76)$$

Baker and Mahler have pointed out that from the four values of  $\varphi$  and the four values of  $\varphi'$ , it is possible to distinguish between the mechanism represented by Eqs. (75) and the group (74) or (62), and the group (76) and (52), using the relationships between the  $\varphi$ 's suggested by Dalziel.<sup>32</sup> Case (69) remains indeterminate.

The use of product inhibition leads to an even greater possibility of distinctions between the six mechanisms described by Eqs. (52), (62), (69), (74), (75), and (76). It has already been pointed out how readily (52) and (62) can be distinguished by the addition of the product,  $P_1$ . Baker and Mahler<sup>33</sup> have extended the treatment given by Alberty to include the effect of the concentrations of the products on the initial velocities of the six mechanisms listed. In treating the general case, they point out that Eq. (44) is modified, in the presence of an inhibitory product, to

$$\frac{[E_0]}{v_0} = \Delta_0 \varphi_0 + \frac{\Delta_1 \varphi_1}{[S_1]} + \frac{\Delta_2 \varphi_2}{[S_2]} + \frac{\Delta_{12} \varphi_{12}}{[S_1][S_2]} \quad (77)$$

where  $\varphi_P(\text{inhibited})/\varphi_P(\text{uninhibited}) = \Delta_P$ . The mechanism dependence of the  $\Delta$  values reported by Baker and Mahler are given in Table XIV.

From Table XIV, it can be seen that product-inhibition studies of initial rates afford a method of distinguishing between cases (52) and (76), which cannot be distinguished by other criteria. Once again, this is due to the effect of  $P_1$  on the limiting velocity in the mechanism described by Eqs. (76). Baker and Mahler point out that the mechanisms described by Eqs. (75) and the group (52) and (76) can be distinguished from each other and from all other mechanisms from a study of the eight  $\varphi$  values of the forward and reverse reaction and the "Haldane relationship"

$$\varphi'_{12}/\varphi_{12} = K_{eq} \quad (78)$$

TABLE XIV. Mechanistic Dependence of the  $\Delta$  Values, Defined in Eq. (77)<sup>a</sup>

Mechanism (text equations)	P added	Identities	Equal to unity	Not equal to unity
(69), (75)	$P_1$ or $P_2$		$\Delta_0; \Delta_1; \Delta_2$	$\Delta_{12}$
(62), (74) and (76)	$P_2$	$\Delta_1 = \Delta_{12}$	$\Delta_0; \Delta_2$	None
	$P_1$	$\Delta_2 = \Delta_{12}$	$\Delta_1$	$\Delta_0$
(52)	$P_2$	$\Delta_1 = \Delta_{12}$	$\Delta_0; \Delta_2$	None
	$P_1$	$\Delta_2 = \Delta_{12}$	$\Delta_0; \Delta_1$	None

<sup>a</sup> Table taken from Mahler *et al.*<sup>33</sup>

It is possible, at least in principle, to distinguish among five of the six suggested mechanisms. As pointed out earlier, no distinction between the mechanisms described by Eqs. (62) and (74) will be possible by these methods.

Mahler and associates<sup>36, 37</sup> have applied the methods outlined above to determine the mechanism of the liver alcohol dehydrogenase reaction:



Since these workers found that the calculated  $\phi$  values generally had statistical errors ranging from 5 to 10%<sup>36</sup> it was difficult to set up meaningful comparisons between quotients or products of these coefficients with total errors as high as 30%. Therefore the results were compared with another method of mechanism characterization in which the effect of deuteration of the  $\alpha$  hydrogen of NADH to NADD or of the substitution of deuterium in  $CH_3CH_2OH$  to  $CH_3CHDOH$  on the rate constants was measured. An example of the technique used may be exemplified by its application to a reaction of the type which obeys Eqs. (52). No assumption is made with regard to the actual magnitude of the kinetic isotope effects

except that there is no isotope effect in the reactions which do not involve hydrogen or deuterium exchange. In this case, for the mechanism described by Eqs. (52),

$$\bar{\phi}'_1 = 1, \quad \bar{\phi}_0 = 1, \quad \bar{\phi}'_2 = \bar{\phi}'_{12}, \quad \text{and} \quad \bar{\phi}_1 \bar{\phi}_2 / \bar{\phi}_{12} = \bar{\phi}'_0 \quad (80)$$

where  $\phi_P(\text{deuterated})/\phi_P(\text{hydrogenated}) = \phi_P$ . The derivation of Eqs. (80) is straightforward. Since  $\bar{\phi}'_1$  and  $\bar{\phi}_0$  are related to  $k_3$  and  $k_{-3}$  there can be no isotope effect since the deuterium was already transferred in an earlier step. In  $\bar{\phi}'_2$ ,  $k_{-2}$  is probably isotope-dependent, but exactly the same effect is present in  $\bar{\phi}'_{12}$ . Finally,  $\bar{\phi}'_0$  is dependent on a possible isotope effect in  $k_{-1}$ , but this effect would be equal to that present in  $\bar{\phi}_1 \bar{\phi}_2 / \bar{\phi}_{12}$ . The mechanism dependence for the six mechanisms under discussion for the  $\bar{\phi}_P$  values is given in Table XV.

TABLE XV. Mechanistic Dependence of the  $\bar{\phi}$  Values, Defined in Eqs. (80)<sup>a</sup>

Mechanism (text equations)	Identities	Equal to unity
(69) and (75)	$\bar{\phi}'_0 = \bar{\phi}'_1; \bar{\phi}'_2 = \bar{\phi}'_{12}; \bar{\phi}'_0 = \bar{\phi}'_2; \bar{\phi}'_1 = \bar{\phi}'_{12}$	None
(62) and (74)	$\bar{\phi}'_2 = \bar{\phi}'_{12}$	$\bar{\phi}'_1$
(52) and (76)	$\bar{\phi}'_2 = \bar{\phi}'_{12}; \bar{\phi}_1 \bar{\phi}_2 / \bar{\phi}_{12} = \bar{\phi}'_0$	$\bar{\phi}'_1; \bar{\phi}_0$

<sup>a</sup> Table taken from Mahler *et al.*<sup>33</sup>

The results of these studies and the studies of the Haldane relationships, the Dalziel relationships, and the product inhibition relationships reported by Baker<sup>36</sup> are summarized in Table XVI.

The Haldane relationships given in Table XVI indicate that  $\phi'_{12}/\phi_{12}$  is not equal either to  $\phi_0 \phi'_1 \phi'_2 / \phi'_0 \phi_1 \phi_2$  or  $\phi'_0 \phi'_1 \phi'_2 / \phi_0 \phi_1 \phi_2$ . This criterion alone is enough to eliminate the mechanisms described by Eqs. (52), (75), and (76) from consideration. The Dalziel relationships given in Table XVI indicate that in all cases  $\phi_1 \phi_2 / \phi_{12} \neq \phi_0$  and  $\phi'_1 \phi'_2 \neq \phi'_0$ . This also excludes the mechanism described by Eqs. (52).  $\phi_1 \phi_2 / \phi_{12} \leq \phi'_0$  in the hydrogen case but it is  $\geq \phi'_1$  in the deuterium example. Similarly,  $\phi'_1 \phi'_2 / \phi_{12} \geq \phi_0$  in both the hydrogen and deuterium examples. Since this is the reverse of the Dalziel relation

TABLE XVI. Kinetic Results Obtained by Mahler and Associates in the Investigation of the Mechanism for Liver Alcohol Dehydrogenase

(A) Haldane relationships (between  $\varphi'_{12}/\varphi_{12}$  and  $\varphi_0\varphi'_1\varphi'_2/\varphi'_0\varphi_1\varphi_2$  or  $\varphi'_0\varphi'_1\varphi'_2/\varphi_0\varphi_1\varphi_2$ )

$K_{eq}$	Hydrogen	Deuterium
$\varphi'_{12}/\varphi_{12} \times 10^{-2}$	$3.56 \pm 0.24$	$3.41 \pm 0.28$
$\varphi_0\varphi'_1\varphi'_2/\varphi'_0\varphi_1\varphi_2 \times 10^{-1}$	$3.71 \pm 0.82$	$2.05 \pm 0.70$
$\varphi_0\varphi'_1\varphi'_2/\varphi_0\varphi_1\varphi_2 \times 10^{-3}$	$1.08 \pm 0.24$	$0.42 \pm 0.14$

(B) Dalziel relationships (between  $\varphi_1\varphi_2/\varphi_{12}$  and  $\varphi_0$  or  $\varphi'_0$ )

	Hydrogen	Deuterium
$\varphi_1\varphi_2/\varphi'_{12} \times 10^1$	$3.35 \pm 0.38$	$6.47 \pm 0.92$
$\varphi'_1\varphi'_2/\varphi_{12} \times 10^1$	$1.88 \pm 0.15$	$1.76 \pm 0.22$
$\varphi_0 \times 10^2$	$6.79 \pm 0.40$	$10.8 \pm 1.7$
$\varphi'_0 \times 10^1$	$3.67 \pm 0.13$	$4.86 \pm 0.04$

(C) Product inhibition (see Table XIV)

	$\varphi_P$ (No product)	$\varphi_P$ (+ Product)	$\Delta_P$
(1) Acetaldehyde + NADH $\rightarrow$ Ethanol ( $5.65 \times 10^{-4}M$ )			
$\varphi_0$	$6.79 \times 10^{-2}$	$8.24 \times 10^{-2} \pm 0.79$	$1.21 \pm 0.19$
$\varphi_1$	$2.85 \times 10^{-7}$	$2.40 \times 10^{-7} \pm 0.04$	$0.84 \pm 0.05$
$\varphi_2$	$1.41 \times 10^{-5}$	$2.39 \times 10^{-5} \pm 0.06$	$1.69 \pm 0.08$
$\varphi_{12}$	$1.20 \times 10^{-11}$	$2.26 \times 10^{-11} \pm 0.05$	$1.88 \pm 0.15$
(2) Acetaldehyde + NADH $\rightarrow$ NAD ( $2.51 \times 10^{-5}M$ )			
$\varphi_0$	$6.79 \times 10^{-2}$	$1.15 \times 10^{-1} \pm 0.16$	$1.68 \pm 0.33$
$\varphi_1$	$2.85 \times 10^{-7}$	$3.31 \times 10^{-7} \pm 0.22$	$1.16 \pm 0.12$
$\varphi_2$	$1.41 \times 10^{-5}$	$1.26 \times 10^{-5} \pm 0.02$	$0.90 \pm 0.04$
$\varphi_{12}$	$1.20 \times 10^{-11}$	$5.37 \times 10^{-11} \pm 0.04$	$4.47 \pm 0.28$

TABLE XVI—*continued*

	$\varphi_P$ (No product)	$\varphi_P$ (+ Product)	$\Delta_P$
(3) Ethanol + NAD $\rightarrow$ NADH ( $9.82 \times 10^{-7}$ M)			
$\varphi'_0$	$3.67 \times 10^{-1}$	$3.98 \times 10^{-1} \pm 0.12$	$1.08 \pm 0.07$
$\varphi'_1$	$4.21 \times 10^{-6}$	$8.07 \times 10^{-6} \pm 0.21$	$1.92 \pm 0.13$
$\varphi'_2$	$1.91 \times 10^{-4}$	$1.29 \times 10^{-4} \pm 0.05$	$0.67 \pm 0.04$
$\varphi'_{12}$	$4.27 \times 10^{-9}$	$3.20 \times 10^{-9} \pm 0.13$	$0.75 \pm 0.04$
(4) Acetaldehyde + $\alpha$ -D-NADH $\rightarrow$ Dideutroethanol ( $5.45 \times 10^{-4}$ M)			
$\varphi_0$	$1.08 \times 10^{-1}$	$1.67 \times 10^{-1} \pm 0.03$	$1.54 \pm 0.28$
$\varphi_1$	$4.63 \times 10^{-7}$	$2.09 \times 10^{-7} \pm 0.23$	$0.45 \pm 0.09$
$\varphi_2$	$4.02 \times 10^{-5}$	$4.38 \times 10^{-5} \pm 0.03$	$1.08 \pm 0.02$
$\varphi_{12}$	$2.87 \times 10^{-11}$	$5.39 \times 10^{-11} \pm 0.10$	$1.87 \pm 0.09$
(5) Acetaldehyde + $\alpha$ -D-NADH $\rightarrow$ NAD ( $2.42 \times 10^{-5}$ M)			
$\varphi_0$	$1.08 \times 10^{-1}$	$8.81 \times 10^{-2} \pm 0.63$	$0.82 \pm 0.19$
$\varphi_1$	$4.63 \times 10^{-7}$	$1.85 \times 10^{-6} \pm 0.02$	$4.00 \pm 0.38$
$\varphi_2$	$4.02 \times 10^{-5}$	$5.25 \times 10^{-5} \pm 0.02$	$1.30 \pm 0.02$
$\varphi_{12}$	$2.87 \times 10^{-11}$	$1.84 \times 10^{-10} \pm 0.01$	$6.40 \pm 0.23$
(6) Dideutroethanol + NAD $\rightarrow \alpha$ -D-NADH ( $1.63 \times 10^{-6}$ M)			
$\varphi'_0$	$4.86 \times 10^{-1}$	$5.18 \times 10^{-1} \pm 0.05$	$1.06 \pm 0.02$
$\varphi'_1$	$4.36 \times 10^{-6}$	$1.40 \times 10^{-5} \pm 0.02$	$3.20 \pm 0.21$
$\varphi'_2$	$3.94 \times 10^{-4}$	$1.51 \times 10^{-4} \pm 0.09$	$0.38 \pm 0.03$
$\varphi'_{12}$	$9.79 \times 10^{-9}$	$2.29 \times 10^{-8} \pm 0.03$	$2.34 \pm 0.15$
(7) Ethanol + NAD $\rightarrow \beta$ -D-NADH ( $3.06 \times 10^{-6}$ M)			
$\varphi'_0$	$3.67 \times 10^{-1}$	$4.09 \times 10^{-1} \pm 0.29$	$1.11 \pm 0.12$
$\varphi'_1$	$4.21 \times 10^{-6}$	$1.20 \times 10^{-5} \pm 0.04$	$2.84 \pm 0.21$
$\varphi'_2$	$1.91 \times 10^{-4}$	$1.79 \times 10^{-4} \pm 0.10$	$0.94 \pm 0.08$
$\varphi'_{12}$	$4.27 \times 10^{-9}$	$1.08 \times 10^{-8} \pm 0.01$	$2.53 \pm 0.06$

## (D) Isotope effects (see Table XV)

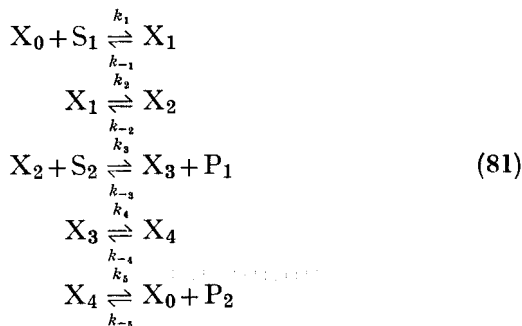
$\bar{\varphi}'_0 = 1.32 \pm 0.06$	$\bar{\varphi}_0 = 1.59 \pm 0.36$	
$\bar{\varphi}'_1 = 1.04 \pm 0.10$	$\bar{\varphi}_1 = 1.62 \pm 0.19$	$\bar{\varphi}_1 \bar{\varphi}_2 / \bar{\varphi}_{12} = 1.93 \pm 0.46$
$\bar{\varphi}'_2 = 2.06 \pm 0.10$	$\bar{\varphi}_2 = 2.84 \pm 0.09$	
$\bar{\varphi}'_{12} = 2.29 \pm 0.15$	$\bar{\varphi}_{12} = 2.39 \pm 0.20$	

Baker suggests that the actual mechanism must be a modification of one of the ordered sequence, ternary complex mechanisms.

The product inhibition studies also suggest one of the ordered sequence mechanisms with the coenzyme identified as  $S_1$  and  $P_2$ . These observations can be seen from Table XVI(C).

The isotope effects given in Table XVI(D) show that the identity,  $\bar{\phi}'_2 = \bar{\phi}'_{12}$ , which is common to all six mechanisms, is satisfied by the data. The identity  $\bar{\phi}'_0 = \bar{\phi}'_1$  is also satisfied, but  $\bar{\phi}'_0 \neq \bar{\phi}'_2$  and  $\bar{\phi}_1 \neq \bar{\phi}_{12}$ , excluding mechanisms (69) and (75). Also, since  $\bar{\phi}'_1$  equals unity, (69) and (75) are impossible. Since  $\bar{\phi}_0 \neq 1$  and probably  $\bar{\phi}'_0 \neq \bar{\phi}_1 \bar{\phi}_2 / \bar{\phi}_{12}$ , Baker<sup>36</sup> suggests that the mechanisms described by (52) and (76) are less likely than those described by (62) and (74).

The data presented in Table XVI suggest that the mechanism of liver alcohol dehydrogenase involves an ordered sequence of substrate binding and product desorption of the type described by Eqs. (62) or (74). However, the inverted Dalziel relationships observed by Baker<sup>36</sup> prompted Mahler, Baker and Shiner<sup>37</sup> to suggest a perturbation of one of these mechanisms as the actual mechanism for this enzyme. They point out that only two possibilities exist. One possible perturbation applied to the simplest example of a compulsory binding mechanism is

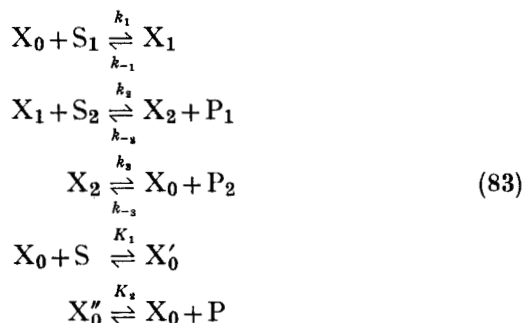


The coefficients for this mechanism reported by Mahler and associates<sup>37</sup> are

$$\begin{aligned}
 \varphi_0 &= \frac{k_2(k_4 + k_{-4} + k_5) + k_4 k_5}{k_2 k_3 k_4}, \quad \varphi_1 = \frac{k_{-1} + k_2}{k_1 k_2}, \quad \varphi_2 = \frac{k_{-2} + k_2}{k_2 k_3} \\
 \varphi_{12} &= \frac{k_{-1} + k_{-2}}{k_1 k_2 k_3}, \quad \varphi'_0 = \frac{k_{-4}(k_{-1} + k_2 + k_{-2}) + k_{-1} k_{-2}}{k_{-1} k_{-2} k_{-3}} \\
 \varphi'_1 &= \frac{k_{-4} + k_5}{k_{-4} k_{-5}}, \quad \varphi'_2 = \frac{k_4 + k_{-4}}{k_{-3} k_{-4}}, \quad \varphi'_{12} = \frac{k_4 k_5}{k_{-3} k_{-4} k_{-5}}
 \end{aligned} \tag{82}$$

It can be seen that in Eqs. (82), the ratio  $\varphi_1\varphi_2/\varphi_{12}$  may be equal to, smaller than, or greater than  $\varphi'_0$ , depending only on the relative magnitudes of  $k_{-1}$  and  $k_{-4}$ .

The second possible perturbation of this type of mechanism which can lead to inverted Dalziel relationships postulates the reversible formation of unreactive binary complexes.



If S and P, which react with  $X_0$  in Eqs. (83), are  $S_1$  and  $P_2$ ,

$$\begin{aligned}
 \varphi_0 &= \frac{k_1 + k_3 K_1}{k_1 k_3}, \quad \varphi_1 = \frac{1}{k_1}, \quad \varphi_2 = \frac{k_1 + k_{-1} K_1}{k_1 k_2}, \quad \varphi_{12} = \frac{k_{-1}}{k_1 k_2} \\
 \varphi'_0 &= \frac{k_{-3} + k_{-1} K_2}{k_{-1} k_{-3}}, \quad \varphi'_1 = \frac{1}{k_{-3}}, \quad \varphi'_2 = \frac{k_{-3} + k_3 K_2}{k_{-2} k_{-3}}, \\
 \varphi'_{12} &= \frac{k_3}{k_{-2} k_{-3}}
 \end{aligned} \tag{84}$$

If S and P are  $S_2$  and  $P_1$ ,

$$\begin{aligned}
 \varphi_0 &= \frac{1}{k_3}, \quad \varphi_1 = \frac{k_2 + K_1(k_{-1} + k_2[S_2])}{k_1 k_2}, \quad \varphi_2 = \frac{1}{k_2}, \quad \varphi_{12} = \frac{k_{-1}}{k_1 k_2} \\
 \varphi'_0 &= \frac{1}{k_{-1}}, \quad \varphi'_1 = \frac{k_{-2} + K_2(k_3 + k_{-2}[P_1])}{k_{-2} k_{-3}}, \quad \varphi'_2 = \frac{1}{k_{-2}}, \\
 \varphi'_{12} &= \frac{k_3}{k_{-2} k_{-3}}
 \end{aligned} \tag{85}$$

It should be noted that in Eqs. (85),  $[S_2]$  and  $[P_1]$  appear in  $\varphi_1$  and  $\varphi'_1$ . Therefore, there is a possibility that unless  $k_2[S_2] \ll k_{-1}$  and  $k_{-2}[P_1] \ll k_3$ , the reciprocal plots will be non-linear.



The mechanism described by Eqs. (84), which is the mechanism suggested by Mahler and associates<sup>37</sup> for the liver alcohol dehydrogenase reaction, predicts an interesting identity. That is:

$$\varphi_0 + \varphi'_0 = \varphi_1 \varphi_2 / \varphi_{12} + \varphi'_1 \varphi'_2 / \varphi'_{12} \quad (86)$$

This relationship was found to be obeyed in the data of Mahler and associates, at least to a first approximation. These data are shown in Table XVII. Thus it has been shown that the combination of the study of product inhibition with other kinetic experiments can lead to valuable information which may be used to eliminate mechanisms which may otherwise be considered possible.

TABLE XVII. Additional Results Obtained by Mahler *et al.* in the Investigation of the Mechanism of Liver Alcohol Dehydrogenase<sup>37</sup>

Atom transferred	$\varphi_0 + \varphi'_0$	$\varphi_1 \varphi_2 / \varphi_{12} + \varphi'_1 \varphi'_2 / \varphi'_{12}$
Hydrogen	$0.435 \pm 0.017$	$0.523 \pm 0.053$
Deuterium	$0.594 \pm 0.057$	$0.823 \pm 0.114$

Fromm and Nelson<sup>38</sup> have used product inhibition as a tool for the investigation of the mechanism of ributol dehydrogenase. Since the substrate, NAD, protected the enzyme from thermal inactivation but the other substrate, ribitol, did not,<sup>38</sup> an ordered sequence of substrate addition with NAD as the leading substrate was indicated. Fromm and Nelson, however, also considered the possibility of a random binding mechanism in their product inhibition studies.

Fromm and Nelson<sup>38</sup> report that the inhibition of the ribitol dehydrogenase reaction with respect to NAD by the sugar product D-ribulose resulted in a significant shift in the limiting velocity and a slight shift in the slope of the reciprocal plots. The inhibition by this product with respect to the sugar substrate, ribitol, on the other hand, resulted in a small, almost indiscernible shift in the limiting velocity and a significant shift in the slope of the reciprocal plots.

The inhibition by NADH with respect to NAD was found to be strictly competitive. The inhibition by NADH with respect to ribitol, on the other hand, resulted in non-linear reciprocal plots in which it appeared that the limiting velocity was decreased by the presence of inhibitory product.

Fromm and Nelson point out that cursory inspection of these results suggests that the data are consistent with the mechanism for an ordered sequence of substrate binding to the enzyme, leading to one or more ternary complexes.<sup>38</sup> The elimination of the random addition mechanism described by Eqs. (42) and (69) by data of this type has been discussed in detail in this chapter.

According to Eq. (66), if  $1/v_0$  is plotted versus  $1/[S_1]$ , in the presence of different concentrations of the first product formed, and if the ordinate intercept values of the curve without added  $P_1$  are subtracted from those obtained in the presence of  $P_1$ , a linear proportional increase in ordinate intercept with increasing concentrations of  $P_1$  should result. Fromm and Nelson<sup>38</sup> report that in the case of ribitol dehydrogenase this increase is non-linear and possibly parabolic. Similarly, if reciprocal plots of  $1/v$  versus  $1/[S_2]$  are made in the presence of different concentrations of  $P_1$ , and the slopes of the curve in the absence of  $P_1$  are subtracted from those in the presence of  $P_1$ , a linear increase in slope with increasing concentrations of  $P_1$  should result. The intercept values should also increase proportionately in the  $1/[S_2]$  plot. The obvious discrepancies with respect to the slopes of the  $1/[S_2]$  plots and the intercepts of the  $1/[S_1]$  plots led Fromm and Nelson<sup>38</sup> to the conclusion that  $P_1$ , besides reversing the reaction in which it was formed, also competes with ribitol for the enzyme-NAD complex,  $X_1$ . The comparison of slope and intercept changes calculated from Eq. (66) and those determined experimentally by Fromm and Nelson<sup>38</sup> for the forward reaction of ribitol dehydrogenase in the presence of D-ribulose are given in Table XVIII.

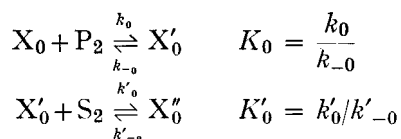
It can be seen from Table XVIII that there is a large discrepancy between the values predicted by Eq. (66) and the values observed by Fromm and Nelson.<sup>38</sup> These workers point out that in all probability the large slope alterations they observed in their  $1/v$  versus  $1/[S_2]$  plot could not have been discernible if Eq. (66) had been applicable.

Fromm and Nelson<sup>38</sup> suggest that abortive ternary complexes

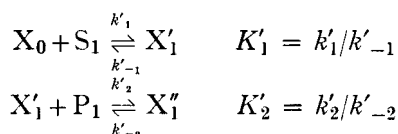
TABLE XVIII. Results from Product Inhibition Studies of Ribitol Dehydrogenase Obtained by Fromm and Nelson, Indicating the Existence of Abortive Ternary Complexes

[P <sub>1</sub> ] × 10 <sup>-3</sup> M	Intercept changes from 1/v versus 1/[S <sub>1</sub> ] plots		Slope changes from 1/v versus 1/[S <sub>2</sub> ] plots	
	Theoretical	Experimental	Theoretical	Experimental
0.77	5200	6600	12	60
1.54	10,400	13,000	24	126
2.31	15,600	22,800	36	221

between fully oxidized or reduced reactants and the free enzyme are formed:



and



The complete equations for the mechanisms described by Eqs. (52), (62) and (69) in which the abortive ternary complexes are formed reported by Fromm and Nelson<sup>38</sup> are:

(I) For the mechanism represented by Eqs. (52), the addition of P<sub>1</sub>:

$$\begin{aligned}
 \frac{[E_0]}{v_0} &= \frac{1}{k_3} + \frac{1}{k_1[S_1]} + \frac{(1 + [P_1] K_1) \left(1 + \frac{k_{-2}}{k_3} [P_1]\right)}{k_2[S_2]} + \\
 &\quad + \frac{k_{-1} \left(1 + \frac{k_{-2}[P_1]}{k_3}\right)}{k_1 k_2 [S_1] [S_2]} \quad (87)
 \end{aligned}$$

of  $P_2$ :

$$\frac{[E_0]}{v_0} = \frac{1}{k_3} + \frac{1 + \frac{k_{-3}[P_2](1 + [S_2]K'_0)}{k_3}}{k_1[S_1]} + \frac{1}{k_2[S_2]} + \frac{k_{-1} \left\{ \frac{1 + k_{-3}[P_2](1 + [S_2]K'_0)}{k_3} \right\}}{k_1 k_2 [S_1][S_2]} \quad (88)$$

instead of Eqs. (58).

(2) For the mechanism represented by Eqs. (62); the addition of  $P_1$ :

$$\begin{aligned} \frac{[E_0]}{v_0} = & \frac{1 + \frac{k_{-3}[P_1]}{k_4}}{k_3} + \frac{1}{k_4} + \frac{1}{k_1[S_1]} + \\ & + \frac{(1 + [P_1]K'_1) \left\langle \frac{1 + k_{-2}\{1 + (k_{-3}[P_1]/k_4)\}}{k_3} \right\rangle}{k_2[S_2]} + \\ & + \frac{k_{-1} \left\langle \frac{1 + k_{-2}\{1 + [k_{-3}[P_1]/k_4]\}}{k_3} \right\rangle}{k_1 k_2 [S_1][S_2]} \end{aligned} \quad (89)$$

of  $P_2$ :

$$\begin{aligned} \frac{[E_0]}{v_0} = & \frac{1}{k_3} + \frac{1}{k_4} + \frac{1 + \frac{k_{-4}[P_2](1 + [S_2]K'_0)}{k_4}}{k_1[S_1]} + \frac{1 + \frac{k_{-2}}{k_3}}{k_2[S_2]} + \\ & + \frac{k_{-1} \left( 1 + \frac{k_{-2}}{k_3} \right) \left( 1 + \frac{k_{-4}[P_2](1 + [S_2]K'_0)}{k_4} \right)}{k_1 k_2 [S_1][S_2]} \end{aligned} \quad (90)$$

instead of Eqs. (66).

(3) For the random sequence pathway, Eqs. (69), the addition of  $P_1$ :

$$\begin{aligned} \frac{[E_0]}{v_0} = & \frac{1}{k_1} + \frac{K_4 \left( 1 + \frac{[P_1]}{K_1} \right)}{k_1[S_1]} + \frac{K_3}{k_1[S_2]} + \\ & + \frac{K_1 K_3 \left\langle \frac{1 + [P_1]\{1 + ([S_2]/K_{ii})\}}{K_8} \right\rangle}{k_1[S_1][S_2]} \end{aligned} \quad (91)$$

of  $P_2$ :

$$\frac{[E_0]}{v_0} = \frac{1}{k_1} + \frac{K_4}{k_1[S_2]} + \frac{K_3 \left( 1 + \frac{[P_2]}{K_i} \right)}{k_1[S_2]} + \frac{K_1 K_3 \left\langle 1 + \frac{[P_2] \{ 1 + ([S_1]/K_{ii}) \}}{K_9} \right\rangle}{k_1[S_1][S_2]} \quad (92)$$

instead of Eqs. (72) and (73) and where

$$K_i = [ES_2][P_2]/[ES_2P_2] \text{ in Eq. (91) and } [ES_1][P_1]/[ES_1P_1] \text{ in Eq. (92)}$$

$$K_{ii} = [EP_2][S_2]/[ES_2P_2] \text{ in Eq. (91) and } [EP_1][S_1]/[ES_1P_1] \text{ in Eq. (92)}$$

It can be seen that from these equations it is not possible to distinguish between the three mechanisms under consideration when only inhibition by  $P_1$  is considered. However, it should be possible to evaluate the effect for the forward reaction when NADH, which is  $P_2$ , is present.

The value for  $K'_0$  obtained by Fromm and Nelson from the change in  $V'_m$  observed from the reciprocal plots involving NAD as the variable substrate was  $1.9 \pm 0.2 \times 10^{-3}M$ , for three concentrations of D-ribulose. The values calculated from the change of slope of the plots involving ribitol as the variable substrate was  $0.6 \pm 0.1 \times 10^{-3}M$  for three concentrations of D-ribulose. An average value of  $1.1 \times 10^{-3}M$  was reported for  $K'_0$ . The value for  $K'_1$  obtained from the change in the slope of the plots involving NAD as the variable substrate was  $0.43 \pm 0.02 M$  for three concentrations of NADH. The reciprocal plots involving ribitol in the presence of NADH were, as expected from Eqs. (88), (90) and (92) and the high value of  $K'_1$ , only slightly non-linear.

On the other hand, it would be expected that in the reverse reaction in which the  $K'_0$  for the oxidized ternary complex is about  $10^{-3}M$ , there should be a significant decrease in the initial rate at high concentrations of the second substrate, D-ributol, in the presence of NAD and NADH.<sup>38</sup>

Figure 1, which has been reproduced from the paper by Fromm

and Nelson,<sup>38</sup> illustrates this point. The initial rate actually decreases as the concentration of the variable substrate, ribulose, is increased, provided an appropriate concentration of NAD, now  $P_2$ , is present. This rather unique result could be quantitatively predicted from Eq. (88).

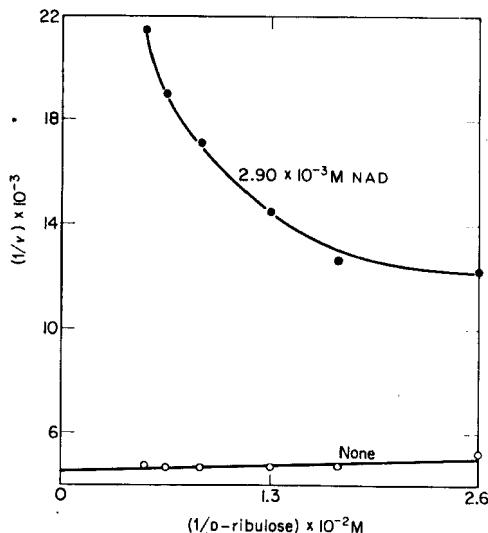


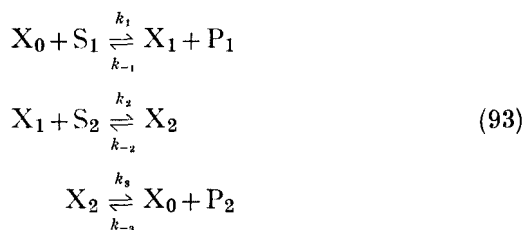
Fig. 1. Plot of reciprocal of initial reaction velocity ( $v$ ) versus reciprocal of molar concentration of D-ribulose. NADH was held constant at  $2.73 \times 10^{-4}$ M, and D-ribulose varied in the range of  $3.85 \times 10^{-3}$ M to  $1.92 \times 10^{-2}$ M.

Thus, the product inhibition results obtained by Fromm and Nelson suggest that the mechanism of ribitol dehydrogenase involves an ordered sequence of substrate addition and product desorption. The coenzyme substrate has been identified as  $S_1$  and  $P_2$  and the existence of one or more ternary complexes is indicated. In addition, these findings are consistent with the hypothesis that two abortive ternary complexes between the fully oxidized or fully reduced reactants and the free enzyme are formed.

Another reaction of the type under discussion here for which a mechanism has been suggested from product inhibition studies is the hexokinase catalyzed reaction of glucose and ATP to form glucose-6-phosphate and ADP. Crain and Sols<sup>39,40</sup> studied the

hexokinase reaction in 1954 and concluded that the non-competitive inhibition by the product, glucose-6-phosphate, involved an attachment by the inhibitor to different combinations of groups on the enzyme than does the substrate. However, the results of Crain and Sols were based on analogy with binding studies with other inhibitors of the hexokinase reaction and their interpretation has been questioned recently.<sup>41</sup> ADP, on the other hand, was reported in preliminary investigations to be a competitive inhibitor of hexokinase.<sup>42</sup>

Fromm and Zewe<sup>43</sup> have recently presented a detailed study of the kinetics of the hexokinase reaction. They have reported that reciprocal plots of velocity and either substrate concentration produced a series of parallel lines for each concentration of the non-variable substrate. There was no tendency for these plots to converge at or to the left of the  $1/v$  axis. These data may be taken to mean that the two substrates, glucose and ATP, are not present on the enzyme simultaneously. The simplest mechanism describing this situation is that described earlier in Eqs. (49a):



where  $S_1$ ,  $S_2$ ,  $P_1$ , and  $P_2$  represent ATP, glucose, ADP, and glucose-6-phosphate respectively. The steady-state rate equation from Eqs. (50a) and (51a) when the concentration of  $P_2$  is negligible is:

$$\frac{[E_0]}{v_0} = \frac{1}{k_3} + \frac{1}{k_1[S_1]} + \frac{1 + (k_{-2}/k_3)}{k_2[S_2]} + \frac{k_{-1}[P_1]\{1 + (k_{-2}/k_3)\}}{k_1 k_2 [S_1][S_2]} \quad (94)$$

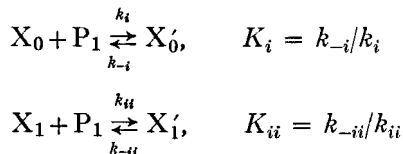
It should be noted that in this mechanism,

$$\begin{aligned} \varphi_0 &= \frac{1}{k_3}, \quad \varphi_1 = \frac{1}{k_1}, \quad \varphi_2 = \frac{1 + (k_{-2}/k_3)}{k_2}, \\ \varphi_{12} &= \frac{k_{-1}[P_1]\{1 + (k_{-2}/k_3)\}}{k_1 k_2} \end{aligned} \quad (95)$$

Fromm and Zewe did not observe that ADP inhibition of hexokinase is competitive with respect to either substrate as did Crane and Sols. Thus a significant shift occurs in the  $V'_m$  with respect to both substrates when constant levels of ADP are added to the reaction mixture. The slope of the reciprocal plots with respect to glucose is independent of the concentration of ADP over the concentration range  $7.15 \times 10^{-4}$  to  $1.43 \times 10^{-3}\text{M}$ . The slopes with respect to the other substrate, ATP, increase slightly as the concentration of ADP is raised. These data are most readily explained if it is assumed that ADP reacts with the free enzyme as well as with  $X_1$  in Eqs. (93).

$$\frac{[E_0]}{v_0} = \frac{1}{k_3} \left( 1 + \frac{[P_1]}{K_{ii}} \right) + \frac{1 + ([P_1]/k_i)}{k_1[S_1]} + \frac{1 + (k_{-2}/k_3)}{k_2[S_2]} + \frac{k_{-1}[P_1]\{1 + (k_{-2}/k_3)\}}{k_1 k_2 [S_1][S_2]} \quad (96)$$

where



The values calculated for  $K_i$  and  $K_{ii}$  by Fromm and Zewe from both reciprocal plots of  $1/[S_1]$  and  $1/[S_2]$  agree within 7%. The values are  $K_i = 4.2 \times 10^{-4}\text{M}$  and  $K_{ii} = 1.9 \times 10^{-3}\text{M}$ .

Since the slopes of the reciprocal plots with respect to glucose in the presence of ADP are parallel it may be concluded that  $k_{-1}[P_1]$  is small, even in the presence of added ADP.<sup>43</sup> Thus  $\varphi_{12}$  in Eqs. (94) and in (96) may be taken as zero even in the presence of up to  $1.43 \times 10^{-3}\text{M}$  ADP. Thus, it is concluded by Fromm and Zewe that the reversal of the first step of the hexokinase reaction is relatively slow. Physically this may indicate that once the enzyme-phosphoryl intermediate is formed, it has a much greater tendency to react with glucose than with ADP. This, of course, would be expected since the energy of the glucose-6-phosphate bond is far less than that of the ADP-phosphate bond.

It has been pointed out that when the assumption that  $k_{-2}$  is small is made in Eqs. (93), the rate equation becomes of a type



similar to that expected where both substrates are present simultaneously on the enzyme. However, the ADP inhibition, as has been pointed out, eliminates this possibility.

Fromm and Zewe have observed that the product, glucose-6-phosphate, inhibits the hexokinase reaction uncompetitively with respect to glucose but strictly competitively with respect to ATP. Thus the reciprocal plots involving glucose form a series of parallel straight lines for each concentration of glucose-6-phosphate. These workers have pointed out that when kinetic studies of the forward reaction of the mechanism given by Eqs. (93) are conducted in the presence of the second product,  $P_2$ , the rate equation becomes

$$\frac{[E_0]}{v_0} = \frac{1}{k_3} + \frac{1 + (k_{-3}[P_2]/k_3)}{k_1[S_1]} + \frac{1 + (k_{-2}/k_3)}{k_2[S_2]} + \frac{k_{-2}k_{-3}[P_2]}{k_1k_2k_3[S_1][S_2]} \quad (97)$$

It can be seen from Eq. (97) that reciprocal plots of velocity and ATP concentration, where ATP is  $S_1$ , in the absence and presence of glucose-6-phosphate,  $P_2$ , should give a common intercept on the  $1/v$  axis. On the other hand, the reciprocal plots of velocity and glucose concentration observed by Fromm and Zewe would appear to be at variance with Eq. (97) unless the  $\varphi_{12}$  term can be deleted from the equation. These workers have pointed out that if it is assumed that the ratio of  $k_{-2}/k_3 < 6.45 \times 10^{-5} \text{M/min}$ , the  $\varphi_{12}$  term will not appear as a significant factor in Eq. (97) at the concentrations of ATP used.

Thus kinetic data utilizing the powerful tool of product inhibition have been presented to suggest that the mechanism of the hexokinase reaction is one in which the product of the first substrate dissociates before the second substrate adds to the enzyme. This means that the mechanism may involve a phosphoryl-enzyme intermediate.

Zewe and Fromm<sup>44</sup> have also studied the effects of added products on both the forward and reverse reaction catalyzed by rabbit muscle lactic dehydrogenase. The results of these experiments with product inhibition were then used to determine certain features about the mechanism for this lactic dehydrogenase. The possible mechanisms that were considered and the subsequent rate equations have been discussed in the theoretical section of this chapter and in the sections on ribitol dehydrogenase and hexokinase. The

rational for distinguishing between the possible mechanisms has also been presented in detail.

Zewe and Fromm<sup>44</sup> were able to eliminate the mechanisms described by Eqs. (46) and (49) on the basis that the slopes and intercepts of reciprocal plots of initial rates and substrate concentration in the presence of different amounts of the non-variable substrate depended on the concentration of the non-variable substrate. In addition, the intercepts of these plots were a linear function of the concentration of the non-variable substrate and the intercepts of plots of the reciprocal of the limiting velocity and the concentration of the non-variable substrate were found to converge at a common point on the  $1/V'_m$  axis.

The product, pyruvate, was found to inhibit competitively with respect to lactate, but with respect to NAD the inhibition was not competitive. Similarly in the reverse reaction, NAD was found to inhibit competitively with respect to NADH but the inhibition was not competitive with respect to pyruvate.

The other product of the forward reaction, NADH, was found to inhibit competitively with respect to NAD but the inhibition was not competitive and the reciprocal plots were non-linear with respect to lactate. The other product of the reverse reaction, lactate, was found to inhibit competitively with respect to pyruvate but the inhibition was not competitive with respect to NAD. The reciprocal plots involving NAD were non-linear in the presence of lactate.

Zewe and Fromm<sup>44</sup> point out that these data suggest an ordered sequence of substrate addition for rabbit muscle lactic dehydrogenase in which the coenzyme substrates bind the free enzyme. The existence of a kinetically significant ternary complex between two substrates and the free enzyme was not suggested as in the case of ribitol dehydrogenase.<sup>43</sup> However, abortive ternary complexes similar to those postulated in the ribitol dehydrogenase mechanism were suggested. The dissociation constant for the fully oxidized ternary complex, i.e. the complex between the free enzyme, NAD, and pyruvate, was found to be  $2 \times 10^{-4} \text{M}$  from the four plots involving product inhibition by the oxidized products. The dissociation constant for the fully reduced ternary complex, i.e. the complex between the free enzyme, NADH, and lactate was found to be  $0.2 \text{ M}$  from the four plots involving product inhibition by the reduced products.

## VI. GENERAL COMMENTS ON THE METHODS EMPLOYED

Some general comments on the examples that have been discussed appear to be in order. Mahler and associates<sup>33</sup> have already pointed out that the use of product inhibition to determine enzymic mechanisms is severely limited by the requirement for a high degree of accuracy in the rate measurements.

The actual relationships between the limiting velocity or the apparent Michaelis constant and the concentration of the product are often ignored. The importance of determining whether or not the reciprocal of the limiting velocity is actually a linear function of the concentration of the product was recently shown by Fromm and associates<sup>38, 44</sup> in their work on ribitol and lactic dehydrogenases. In addition, many examples of product inhibition have been called "non-competitive" simply because a change in slope and intercept occurs in the reciprocal plots. The examination of the actual independence of the apparent Michaelis constant on the product concentration should be done over a wide range of product concentrations before the classical term "non-competitive" inhibition can correctly be applied. In other cases the inhibition may be referred to as "mixed inhibition" in classical terms, or as "not competitive" as has been used here.

Hofstee<sup>3</sup> pointed out several years ago that the use of reciprocal plots is not the best way to present kinetic data for enzyme reactions. Due to the extremely biased form of this type of plot, it is often not possible to detect significant deviations from linearity. The use of the  $v$  versus  $v/[S]$  plot was shown to be superior in that it minimizes the danger of misinterpretation of the resulting points to define a non-existent straight line. Non-linear reciprocal or  $v$  versus  $v/[S]$  plots are expected in enzymic reactions involving more than one substrate unless certain *mechanistic* assumptions such as the ordered sequence assumption or the quasiequilibrium assumption are made. The non-linearity may very easily be masked in the reciprocal plots, but is more easily detected in the  $v$  versus  $v/[S]$  plot.

Despite the fact that this danger was pointed out almost ten years ago, practically all the kinetic studies with product inhibition have been presented in the form of reciprocal plots. Some of the data is so obviously non-linear that no attempt was made to

define a straight line from the plots. In most of the other cases, however, the points appeared by cursory inspection to be linear but must be considered linear with considerable reservation.

For example, Zewe and Fromm<sup>44</sup> make the explicit statement that their reciprocal plots obtained in the absence of added product from the rabbit muscle lactic dehydrogenase reaction are linear. Careful examination of these plots, as well as Fromm and Zewe's plots from the hexokinase study,<sup>43</sup> reveals that they may possess a significant amount of concave up curvature. Examination of the reciprocal plots in the presence of added products reveals that the amount of non-linearity probably is increased by the addition of any of the inhibitory products. Since this non-linearity is not predicted by the ordered sequence mechanism proposed by Fromm and Zewe for either enzymic reaction, the conclusions of these investigators as to the mechanism of these enzymes' action must be regarded as approximate. It should be made clear that the data of Fromm and Zewe are referred to here only as an *example* of how the mechanistic conclusions drawn by practically all other investigators using reciprocal plots of kinetic data may be subject to a readily testable criticism.

In order to test the indication that the reciprocal plots reported by Zewe and Fromm for lactic dehydrogenase were not linear, the data were replotted in the  $v$  versus  $v/[S]$  form. Even in cases where no inhibitory product had been added, a smooth curvature in the  $v$  versus  $v/[S]$  plots was observed, especially when the coenzyme was the variable substrate. For example, from the data given in Fig. 2 of ref. 44 on lactic dehydrogenase it can be shown that the apparent Michaelis constant with respect to NAD decreases over ten-fold in the presence of  $7.2 \times 10^{-3}\text{M}$  lactate as the NAD concentration is increased from  $6 \times 10^{-5}$  to  $2 \times 10^{-4}\text{M}$ .

It is not possible to determine the reason for the curvature in these plots; however, several alternatives immediately suggest themselves. The observed curvature may be due to the impurity of the enzyme preparation used,<sup>44</sup> due to a physical limitation of the impracticality of measuring true initial rates before enough product has accumulated to cause inhibition, or due to a significant contribution of a random sequence mechanism that is not at quasiequilibrium.<sup>2</sup> Since, as was pointed out before, two of these explanations depend on the mechanism of the enzyme's action, it is

of great importance to determine if curvature exists in plots which are expected, from the proposed mechanism, to be linear.

Many other types of enzymic reactions in which more than two substrates and/or two products are formed are possible. The steady-state rate equations for the possible combinations of ordered sequences of substrate addition and product desorption have been derived, but there is little point in presenting a series of such complicated equations since most of the principles illustrated by these equations have already been shown in the simpler cases already presented. However, two rules may be inferred from these equations. The first is that the resulting rate expressions become increasingly complex as the number of species involved in the reaction is increased. The possibilities are plainly limitless as are the possible complexities of the rate equations. The second principle is that both the  $V'_m$  and  $K'_m$  with respect to any given substrate will generally be a function of the concentration of all products formed after that substrate reacts with the enzyme. The notable exception is that the last product formed in an "irreversible" step will not inhibit at all unless a special reaction between it and the free enzyme is written.

### ACKNOWLEDGEMENT

I gratefully acknowledge the technical assistance of Dr. Earl Frieden for the help extended for the preparation of this manuscript. I also gratefully acknowledge Dr. Manuel Morales, in whose laboratory this chapter was finally written.

### References

1. Henri, V., *Lois Générales de l'Action des Diastases*, Hermann, Paris, 1903.
2. Hearon, J. Z., Bernhard, S. A., Friess, S. L., Botts, D. J., and Morales, M. F., *The Enzymes*, Vol. 1, Chapter 2, Academic Press, New York, 1959.
3. Hofstee, B. H., *Science* **116**, 329 (1952).
4. Morales, M. F., and Goldman, D. E., *J. Am. Chem. Soc.* **77**, 6069 (1955).
5. Hommes, F. A., *Arch. Biochem. Biophys.* **96**, 28-40 (1962).
6. Alberty, R. A., and Koerber, B. M., *J. Am. Chem. Soc.* **79**, 6379 (1957).
7. Morales, M. F., *Federation Proc.* **15**, 133 (1956).
8. King, E. L., *J. Phys. Chem.* **60**, 1375 (1956).
9. Alberty, R. A., *The Enzymes*, Vol. 1, Chapter 3, Academic Press, New York, 1959.
10. Peller, L., and Alberty, R. A., *J. Am. Chem. Soc.* **81**, 5907 (1959).

11. Eigen, M., *Discussions Faraday Soc.* **17**, 194 (1954).
12. Hammes, G. G., and Alberty, R. A., *J. Am. Chem. Soc.* **82**, 1564 (1960).
13. Alberty, R. A., and Hammes, G. G., *Z. Elektrochem.* **64**, 124 (1960).
14. Walter, C. F., and Frieden, E., *Advan. Enzymol.* **25**, 167 (1963).
15. Segal, H. L., Kachmar, J. F., and Boyer, P. D., *Enzymologia* **15**, 187 (1952).
16. Harmon, K. M., and Niemann, C., *J. Biol. Chem.* **178**, 743 (1949).
17. Huang, H. T., and Niemann, C., *J. Am. Chem. Soc.* **73**, 1541 (1951).
18. Huang, H. T., Foster, R. J., and Niemann, C., *J. Am. Chem. Soc.* **74**, 105 (1952).
19. Foster, R. J., Shine, H. J., and Niemann, C., *J. Am. Chem. Soc.* **77**, 2378 (1955).
20. Foster, R. J., and Niemann, C., *Proc. Natl. Acad. Sci. U.S.* **39**, 999 (1953).
21. Jennings, R. R., and Niemann, C., *J. Am. Chem. Soc.* **77**, 5432 (1955).
22. Booman, K. A., and Niemann, C., *J. Am. Chem. Soc.* **77**, 5733 (1955).
23. Zatman, L. J., Kaplan, N. O., and Colowick, S. P., *J. Biol. Chem.* **200**, 197 (1953).
24. Zatman, L. J., Kaplan, N. O., Colowick, S. P., and Ciotti, M. M., *J. Biol. Chem.* **209**, 453 and 467 (1954).
25. Beaufay, H., and de Duve, C., *Bull. Soc. Chim. Biol.* **36**, 1939 (1954).
26. Frieden, E., and Matthews, H., unpublished observations.
27. Segal, H. L., *J. Am. Chem. Soc.* **81**, 4047 (1959).
28. Hass, L. F., and Byrne, W. L., *J. Am. Chem. Soc.* **82**, 947 (1960).
29. Hass, L. F., and Byrne, W. L., *Science* **131**, 991 (1960).
30. Neuhaus, F. C., and Byrne, W. L., *J. Biol. Chem.* **235**, 2019 (1960).
31. Alberty, R. A., *J. Am. Chem. Soc.* **80**, 1777 (1958).
32. Dalziel, K., *Acta Chem. Scand.* **11**, 1706 (1957).
33. Baker, R. H., and Mahler, H. R., *Biochemistry* **1**, 35 (1962).
34. Theorell, H., and Chance, B., *Acta Chem. Scand.* **5**, 1127 (1951).
35. Alberty, R. A., *J. Am. Chem. Soc.* **75**, 1928 (1953).
36. Baker, R. H., *Biochemistry* **1**, 41 (1962).
37. Mahler, H. R., Baker, R. H., and Shiner, V. J., *Biochemistry* **1**, 47 (1962).
38. Fromm, H. J., and Nelson, D. F., *J. Biol. Chem.* **237**, 215 (1962).
39. Crane, R. K., and Sols, A., *J. Biol. Chem.* **203**, 273 (1953).
40. Crane, R. K., and Sols, A., *J. Biol. Chem.* **210**, 597 (1954).
41. Fromm, H. J., *Federation Proc.* **21** (1962).
42. Sols, A., and Crane, R. K., *J. Biol. Chem.* **206**, 925 (1954).
43. Fromm, H. J., and Zewe, V., *J. Biol. Chem.* **236**, 1661 (1962).
44. Zewe, V., and Fromm, H. J., *J. Biol. Chem.* **236**, 1668 (1962).

## AUTHOR INDEX

The names of authors and joint authors of chapters in the present book, and the page numbers at which these chapters begin, are printed in **heavy type**. Page numbers of bibliographical references as listed at the ends of the chapters are in *italics* and page numbers of citations in the text are in ordinary type.

- Ablov, A. B., **405**  
Abragam, A., **501**, **531**, **535**, **554**, **579**  
Ackerman, E., **621**, **626**  
Adams, O. W., **79**  
Adams, W. H., **79**  
Adrian, F. J., **563**, **579**  
Akamatu, H., **321**, **335**, **336**  
Akimov, I., **407**  
Albert, A., **79**  
Alberty, R. A., **649**, **650**, **651**, **652**,  
**653**, **680**, **694**, **698**, **699**, **723**, **724**  
Alcañiz, **80**  
Aldous, E., **598**, **601**  
Alexander, H. E., **220**, **237**  
Alexander, P., **263**, **264**, **265**, **267**,  
**269**, **277**, **279**  
Alger, R. S., **579**  
Allen, B. T., **639**, **644**  
Allen, E., **267**, **279**  
Allen, L. C., **79**  
Alper, T., **600**  
Amberg, C. H., **243**, **257**  
Amos, A. T., **79**  
Anderson, R. S., **549**, **551**, **579**, **581**  
Anderson, T. H., **579**  
Androes, G. M., **181**  
Andros, G. W., **335**  
Angell, C. L., **496**  
Aono, S., **580**  
Appel, K., **78**, **156**, **157**  
Ard, W. B., **267**, **280**  
Arnold, W., **643**  
Ashraf El Bayoumi, M., **156**  
Astbury, W. T., **266**, **279**  
Atherton, N. M., **549**, **552**, **579**  
Augenstein, L., **232**, **236**  
Avery, E. C., **644**  
Backstrom, H. L., **579**  
Bailey, A. J., **272**, **274**, **279**  
Baker, R. H., **682**, **703**, **704**, **706**, **709**,  
**724**  
Ballhausen, C. J., **197**  
Ballio, A., **406**  
Bardeen, J., **255**, **258**  
Barnett, L., **156**  
Basilio, C., **157**  
Basolo, F., **406**  
Bass, L. W., **497**  
Bath, J. D., **239**, **257**  
Baudet, J., **49**, **79**  
Baudet, P., **357**  
Bawdon, F. C., **593**, **600**  
Baxter, S., **251**, **258**  
Bayer, E., **611**, **626**  
Bear, R. S., **279**  
Beaufay, H., **724**  
Beauregard, L. G., **279**  
Beaven, G. H., **156**  
Beetlestone, J., **405**, **611**, **627**  
Bell, F. O., **279**  
Bellamy, L. J., **497**  
Bendall, J. R., **272**, **279**  
Benes, H. A., **574**, **579**  
Bennema, P., **579**  
Bennett, J. E., **406**  
Benson, S. W., **242**, **243**, **257**  
Berlin, A. A., **357**  
Bernal, J. D., **257**  
Bernhard, S. A., **723**

- Berry, G., 576, 581  
 Bersohn, R., 540, 579  
 Berthier, G., 49, 51, 72, 74, 79, 82, 83, 357  
 Berthold, H., 406  
 Bertinchamps, A., 156, 358  
 Bierstedt, P. E., 337  
 Bigeleisen, J., 581  
 Blackwell, L., 338  
 Blinder, S. M., 563, 579  
 Bloch, F., 531  
 Bloembergen, N., 531  
 Blois, M. S., 340, 350, 353, 357  
 Blomgren, G. E., 331, 335  
 Blout, E. R., 436, 456, 459, 463, 493, 497, 498  
 Blum, H. F., 600  
 Blumenfeld, L. A., 263, 279, 340, 345, 350, 351, 352, 357, 358  
 Boedtker, H., 219, 236, 466, 497  
 Boer, E. de, 579, 583  
 Boggus, J. D., 582  
 Bolton, J. R., 579  
 Booman, K. A., 724  
 Bose, M., 337, 338  
 Botts, D. J., 723  
 Bowers, V. A., 563, 579, 581  
 Bowes, J. H., 271, 272, 274, 279  
 Boyd, H. M., 422  
 Boyer, P. D., 724  
 Boyes-Watson, J., 257  
 Boys, S. F., 79  
 Bozóky, L., 156  
**Braams, R., 259, 271, 273, 279, 627**  
 Bradbury, E. M., 436, 491, 497, 498  
 Bradley, D. F., 633, 643  
 Bragg, J. K., 231, 237  
 Bragg, L., 257  
 Brandt, C. L., 600, 601  
**Braterman, P. S., 359**  
 Bray, R. C., 606, 621, 626  
 Bree, A., 312, 335  
 Brenner, S., 156  
 Brill, A. S., 406, 605, 608, 614, 616, 621, 626  
 Brodie, A. F., 595, 599, 601  
 Broomhead, J. M., 451, 497  
 Brovetto, P., 537, 579  
 Brown, A. E., 279  
 Brown, D. J., 497  
 Brown, W. G., 23, 28, 44, 82  
 Brucker, W., 638, 639, 644  
 Bubnov, N. N., 634, 635, 643  
 Bull, H. B., 240, 244, 257  
 Byrne, W. L., 672, 673, 674, 724  
 Cabannes, J., 420  
 Cabin, M., 181  
 Cagnasso, A., 197  
 Cahill, A. E., 403, 407  
 Calvin, M., 298, 301, 302, 331, 335, 336, 337, 338, 402, 406, 407, 553, 581, 603, 627, 632, 633, 643  
 Cambi, L., 197, 609, 626  
 Camiscoli, J. F., 338  
 Cantarow, A., 79  
 Cantelmo, P., 592, 600  
 Cardew, M. H., 240, 241, 242, 243, 244, 245, 257  
 Carrington, A., 562, 579  
 Carswell, D. J., 335  
 Carter, L. A., 643  
 Cassel, J., 271, 274, 279  
 Castellán, G. W., 255, 258  
 Chain, E. B., 406  
 Chalvet, O., 60, 79  
 Chance, B., 689, 724  
 Chapman, D., 417  
 Chargaff, E., 498  
 Charlesby, A., 264, 265, 279  
 Chestnut, D. B., 536, 537, 540, 579, 581  
 Chiu, Y. N., 561, 579  
 Ciotto, M. M., 724  
 Clark, J. B., 585, 600  
 Clementi, E., 82  
 Closs, G. L., 407  
 Closs, L. E., 407  
 Coates, G. E., 406  
 Cochran, E. L., 563, 579, 581  
 Cockbain, E. G., 406  
 Cockran, W., 497  
 Coelho, R., 276, 280



- Cole, T., 536, 541, 542, 545, 579, 580, 581  
 Coleman, P., 279  
 Collman, J. P., 406  
 Colowick, S. P., 724  
 Commoner, B., 629, 630, 631, 637, 643  
 Compton, D. M. J., 313, 335  
 Conger, A., 641, 644  
 Coolidge, A. S., 16, 81  
 Corey, R. B., 264, 280, 498  
 Cornet, N., 156, 358  
 Coryell, C. D., 181, 183, 197, 198  
 Coulson, C. A., 8, 14, 36, 41, 42, 79, 80, 156, 540, 573, 580  
 Craig, D. P., 33, 79, 565, 580  
 Crane, R. K., 716, 717, 718, 724  
 Crawford, V. A., 540, 580  
 Creeth, J. M., 497  
 Crick, F. H. C., 86, 103, 107, 148, 156, 158, 270, 281, 498  
 Cullis, A. F., 181, 257  
 Cusachs, L. C., 80  
  
 Dalziel, K., 627, 680, 698, 704, 724  
 Daudel, R., 6, 79, 80, 156, 197  
 David, K. M., 258  
 Davidson, E., 257  
 Davidson, N. R., 536, 580  
 Davies, D. R., 181, 257, 498  
 Davies, D. W., 156  
**Davies, R. C., 359, 406**  
 Davis, S., 244, 254, 257  
 Davydov, A. S., 335, 567, 580  
 Day, P., 406  
 Debye, P., 348, 357  
 de Duve, C., 724  
 de Groot, J. H., 556, 583  
 Dekker, C. A., 80  
 den Hartog, H., 608, 614, 616, 626  
 Depireux, J., 156, 358  
 Deutsch, H. F., 614  
 Dewar, M. J. S., 40, 80  
 Dexter, D. L., 567, 573, 574, 580  
 Dezelic, M., 407  
 Dibeler, V. H., 299  
 Dickenson, R. E., 181, 257  
  
 DiMarzio, E. A., 227, 229, 232, 233, 236  
 Dimond, A., 223, 236  
 Divies, P. L., 573, 580  
 Dobriner, K., 419  
 Dole, M., 244, 257  
 Domingo, R., 48, 80  
 dos Santos-Veiga, J., 579  
 Doty, P., 219, 221, 231, 236, 237, 466, 497, 498  
**Douzou, P., 339, 358**  
 Drain, L. E., 257  
 Drake, M. P., 279  
 Dravnieks, F., 562, 579  
 DuBridge, L. A., 336  
 Dubuisson, 414  
 Ducanson, W. E., 14, 80  
 Duchesne, J., 80, 146, 340, 358  
 Dulbecco, R., 593, 600  
 Duval, C., 420, 421, 423, 429  
 Dwyer, F. P., 403, 406  
  
 Eastman, J. W., 335, 336  
 Edgell, 218  
 Edwards, J. O., 348, 357  
 Egami, F., 498  
**Ehrenberg, A., 281, 602, 603, 604, 608, 609, 614, 618, 619, 620, 623, 624, 625, 626, 627, 640, 641, 644**  
 Ehrenberg, L., 281, 623, 624, 625, 627, 640, 641, 644  
 Eidus, L. Kh., 275, 276, 277, 279  
 Eigen, M., 156, 724  
 Eigner, J., 219, 221, 236  
 Eiler, J. J., 497  
 Eisinger, J., 358  
 El Bayoumi, M. A., 358  
 Elder, E., 582  
**Eley, D. D., 146, 156, 238, 240, 241, 242, 243, 244, 245, 257, 258, 319, 336, 340, 358**  
 Elliot, A., 279  
 Ellis, D. A., 243, 257  
 Ellis, J. W., 239, 257  
 Ellison, F. D., 82  
 Elöd, E., 269, 279  
 Elvidge, J. A., 402, 406

- Emmett, P. H., 245, 257  
 Engelsma, G., 336  
 Engelsman, G., 407  
 Erb, E., 546, 583  
 Ermolaev, V., 566, 567, 580  
 Eyring, H., 208, 236  
  
 Falk, J. E., 406  
 Farmer, J. B., 580  
 Felsenfeld, G., 497  
 Fermi, E., 534, 580  
**Fernández-Alonso, J. I., 3, 45, 47, 48, 80**  
 Ferraro, J. R., 498  
 Ferroni, S., 537, 579  
 Fessenden, R. W., 536, 542, 545, 580, 581  
 Fielding, P. E., 309, 336  
 Fields, M., 497  
 Filippov, M. P., 405  
 Fischer, J. J., 531  
 Fischer-Hjalmars, 62, 65, 75  
 Floodmark, 64  
 Fock, V., 15, 33, 80  
 Foissac, L., 276, 280  
 Foley, K. A., 46, 81  
 Foner, S. N., 581  
 Förster, T., 567, 571, 574, 580  
 Foss, J. G., 246, 257  
 Foster, R. J., 580, 670, 724  
 Fowler, R. H., 257  
 Fox, D., 336, 580  
 Fox, M., 279  
 Frady, J., 585, 600  
 Fraenkel, G. K., 583  
 Franck, J. A., 272, 276, 277, 278, 280, 336  
 Francq, J. C., 358  
 Franklin, R. E., 497  
 Fraser, M. J., 436, 467, 497  
 Fraser, R. D. B., 436, 467, 497  
 Fresco, J. R., 466  
 Frey, H. J., 257  
 Fricke, H., 276, 279, 280  
 Fridovich, I., 620, 627  
 Frieden, E., 653, 672, 673, 680, 724  
 Friess, S. L., 723  
 Frisch, H. L., 232, 236  
 Fritsch, A., 276, 280  
 Fritsch, O., 255, 258  
 Fritze, E. R., 269, 279, 281  
 Froese, G., 268, 281  
 Fromm, H. J., 711, 712, 713, 715, 716, 717, 718, 719, 720, 721, 722, 724  
 Frosch, R. P., 565, 566, 583  
 Fueno, T., 37, 43, 80  
 Fujita, J., 197  
 Fujumori, E., 46, 59, 80  
 Fukui, K., 45, 61, 66, 80  
 Furberg, S., 497  
 Fuson, N., 426  
  
 Gajewskae, 227  
 Galanin, M. D., 573, 574, 580  
 Ganassi, E. E., 275, 279  
 Gardner, C. L., 580  
 Garrett, C. G. B., 336  
 Garrison, W. M., 272, 280  
 Geiduschek, E. D., 232, 237  
 Geirer, A., 497  
 George, P., 403, 405, 406, 611, 627  
 Gerlich, D., 309, 337  
 Geske, D. H., 582  
 Ghosh, D. K., 541, 547, 548, 580  
 Gibbs, J. H., 227, 229, 232, 233, 236  
 Gibson, G. E., 565, 580  
 Gibson, J. F., 172, 175, 181, 616, 627  
 Giese, A. C., 592, 594, 600, 601  
 Giffe, J. W., 279  
 Gillespie, J. M., 280  
 Gillies, N. E., 600  
 Gilmore, E. H., 565, 580  
 Ginoza, W., 219, 221, 222, 236  
 Girard, M., 423  
 Glinkin, A. A., 357  
 Goepfert-Mayer, M., 32, 80, 561, 580  
 Goldman, D. E., 648, 723  
 Goodgal, S. H., 601  
 Goodman, L., 79  
 Gordy, W., 50, 264, 265, 267, 268, 273, 278, 280, 547, 548, 549, 550, 552, 553, 581, 582, 638, 639, 644  
 Gosling, R. G., 497  
 Goudot, 46, 67, 76

- Gouterman, M., 406, 558, 561, 580  
 Grabe, B., 45, 62, 63, 65, 66, 68, 69, 70, 80  
 Grant, P. M., 552, 580  
 Green, D. W., 281  
 Green, S. I. E., 406  
 Greer, S., 219, 236  
 Griffith, J. S., 72, 81, 172, 179, 181, 197, 405, 609, 610, 611, 614, 627  
 Griffiths, J. H. E., 554, 580  
 Groot, M. S. de, 554, 557, 562, 565, 566, 580  
 Guilbert, T. L., 82  
 Guild, W. R., 229, 236  
 Guillemin, V., 81  
 Gulland, J. M., 497  
 Gurney, R. W., 255, 258  
 Gustavson, K. H., 280  
 Gutman, F., 309, 336  
 Gutowsky, H. S., 513, 531
- Haddow, A., 81  
 Hadni, A., 428  
 Haffermann, 23  
 Hall, D., 406  
 Hall, F. R., 337  
 Ham, N. S., 559, 561, 580  
 Hameka, H. F., 561, 580  
 Hamilton, L. D., 157, 497  
 Hamilton, L. D. G., 277, 279  
 Hammes, G. G., 651, 652, 653, 724  
 Handler, P., 620, 627  
 Hanss, M., 354, 358  
 Harbury, H. A., 46, 81  
 Harhash, A. W., 638, 644  
 Harm, W., 591, 592, 596, 599, 601  
 Harmon, K. M., 668, 724  
 Harnik, E., 309, 337  
 Harrington, W. F., 280  
 Hart, R. G., 181, 257  
 Hartree, D. R., 14, 15, 33, 81  
 Hartree, E. F., 197  
 Haselkorn, R., 466  
 Hass, L. F., 673, 674, 724  
 Hausser, K. H., 611, 626  
 Hearle, J. W. S., 251, 258  
 Hearon, J. Z., 723
- Hedén, C. G., 156  
 Hedges, R. M., 301, 336  
 Heer, J. de, 156  
 Heidenreich, R. D., 358  
 Heise, J. J., 629, 630, 631, 643  
 Heitler, W., 197  
 Helfrich, W., 292, 336, 337  
 Heller, C., 541, 542, 543, 545, 579, 580, 581  
 Hellmann, H., 156  
 Helmkamp, G. K., 497  
 Henri, V., 647, 648, 723  
 Henriksen, T., 627  
 Herriot, R. M., 601  
 Herzberg, G., 580  
 Higuchi, I., 258, 580  
 Hildebrand, D., 280  
 Hildebrand, J. H., 574, 579  
 Hill, J. A., 406  
 Hill, T. L., 65, 81, 244, 245, 257  
 Hillebrandt, B., 591, 592, 596, 601  
 Hinshelwood, C. N., 153, 156  
 Hippel, P. H. von, 280  
 Hnojewyj, W. S., 257  
 Hodes, M. E., 498  
 Hoesterey, D., 327, 336  
**Hoffmann, T. A., 84, 156**  
 Hofstee, B. H., 721, 723  
 Hoistine, G. J., 579  
 Holiday, E. R., 156  
 Hollaender, A., 598, 600, 601  
 Holmes, B., 280  
 Hommes, F. A., 648, 723  
 Hooper, C. W., 157, 497  
 Hoover, S. R., 257  
 Hopkins, G. R., 477, 498  
 Hornig, A. W., 556, 580  
 Horsfield, A., 543, 545, 546, 548, 550, 580, 582  
 Hotchkiss, R. D., 221, 237  
 Howells, E. R., 257  
 Howitt, F. O., 279, 280  
 Howland, J. J., 603, 627  
 Hoyland, J. R., 79  
 Huang, H. T., 669, 724  
 Hubbard, P. G., 509, 531  
 Huber, R., 644

- Hudson, R. F., 265, 279  
 Hückel, E., 26, 34, 46, 81  
 Huggins, C. M., 336  
 Hutchison, C. A., Jr., 553, 554, 556,  
     562, 565, 566, 581  
 Hyde, J. S., 556, 580
- Ikeda, K., 336  
 Imamura, A., 80  
 Ingram, D. J. E., 170, 172, 175, 181,  
     406, 581, 627, 644  
 Inokuchi, H., 335, 336  
 Iredale, T., 335  
 Isenberg, I., 46, 81, 353, 358  
 Iso, K., 231, 237  
 Iverson, R., 600
- Jackson, J. E., 422  
 Jacobson, C., 601  
 Jacques, J., 469, 497  
**Jagger, J., 584, 588, 592, 601**  
 James, B. R., 406  
 James, H. M., 16, 81  
 Janot, 421  
 Jardetsky, C. D., 531  
**Jardetsky, O., 499, 531**  
 Jarnagin, R. C., 338  
 Jarrett, H. S., 581  
 Jaseja, T. S., 549, 551, 579, 581  
 Jayko, M. E., 272, 280  
 Jen, C. K., 581  
 Jennings, R. R., 724  
 Jennings, T. J., 258  
 Jillot, B. A., 406  
 Johnson, D. A., 279  
 Johnson, E. A., 156  
 Johnson, E. M., 227  
 Johnson, F. H., 236  
 Jolit, M., 601  
 Jones, R. N., 419  
 Jordan, D. O., 156, 497  
 Jorgensen, C. K., 406  
 Josien, L. M., 424, 426  
 Josse, J., 135, 156  
 Joyner, L. G., 245, 257
- Julg, A., 81  
 Jung, F., 186, 198, 406, 627
- Kaa, J. M. van der, 156  
 Kachmar, J. F., 724  
 Kaiser, A. D., 156  
 Kalamkarova, M. B., 275, 279  
 Kalckar, H., 62, 81  
 Kallmann, H., 327, 328, 336, 338  
 Kalmanson, A. E., 279, 357, 358  
 Kanda, Y., 338  
 Kaplan, N. O., 724  
 Karo, A. M., 79  
 Karplus, M., 536, 538, 581  
 Karpovich, I. A., 338  
 Kasha, M., 23, 81, 130, 156, 346, 347,  
     358, 553, 578, 581  
 Kashket, E. R., 595, 599, 601  
 Katayama, M., 547, 548, 581  
 Kauzman, W., 81  
 Kayushin, L. P., 275, 279  
**Kearns, D. R., 282, 298, 302, 331,**  
     337, 338  
 Keilin, B., 257  
 Keiner, A., 591, 592, 601  
 Kendrew, J. C., 160, 181, 239, 257,  
     280  
 Kepler, R. G., 291, 295, 296, 301,  
     317, 337  
 Khalil, M. S. H., 636, 643  
 Kida, S., 197  
 King, E. L., 650, 723  
 King, G., 254, 258  
 Kirby, R. D., 266, 280  
 Kiszely, G., 156  
 Kittleman, E. J., 406  
 Kleczkowski, A., 593, 600  
 Klemperer, E., 497  
 Klevens, H. B., 581, 582  
 Kobayashi, M., 197  
 Koerber, B. M., 723  
 Köhnlein, W., 627  
 Koenig, V. L., 279  
 Kolos, W., 16, 81  
 Kommandeur, J., 312, 321, 324, 326,  
     331, 335, 337, 338

- Kon, H., 81  
Koopmans, T., 45, 81  
Korn, A. H., 257  
Kornberg, A., 156  
**Kotani, M.**, 159, 181, 191, 197, 385  
Koutecký, J., 99, 156  
Krasnovskii, A. A., 634, 643  
Kronick, P. L., 337  
Krumholtz, P., 377, 406  
Kumler, W. D., 497  
Kuntz, E., 272, 280  
Kurita, Y., 547, 548, 549, 550, 553, 581, 582  
Kuroda, H., 336  
Kyogoku, T., 497  
**Kyogoku, Y.**, 435, 456, 469, 472, 481, 485, 498  
  
Labes, M. M., 337, 338  
**Ladik, J.**, 78, 84, 156, 157  
Lambe, J., 579  
Landmann, W., 276, 280  
Lane, D., 221, 236  
Langridge, R., 129, 157, 497  
Lauffer, M. A., 223, 236  
Lea, D., 275, 280  
LeBlanc, O. H., 291, 293, 294, 295, 296, 336, 337  
**Lecomte, J.**, 408, 421  
Lefebvre, R., 80, 81, 156, 197  
Legallais, V., 608, 626  
Lehninger, A. L., 81  
Leidy, G., 220, 237  
Lemberg, R., 406  
Lengyel, P., 157  
Lenormant, H., 436, 463, 497  
Leone, C. A., 276, 280  
Leslie, J., 157  
**Leslie, R. B.**, 238  
Leveau, M., 280  
Levene, P. A., 441, 497  
Lever, A. B. P., 406  
Lewis, G. N., 553, 564, 576, 581  
Lewis, J. T., 8, 79  
Liang, C. Y., 157  
Lin, W. C., 542, 545, 548, 550, 581  
Linnett, J. W., 81  
Linschitz, H. M., 576, 581  
Lipkin, D., 553, 576, 581  
Lipman, F., 62, 81  
Lippincott, B. B., 631, 643  
Litt, M., 466, 497  
Little, K., 264, 265, 271, 280  
Livingston, H. K., 257  
Livingston, R., 567, 576, 581  
Loach, P. A., 407  
Löfroth, G., 623, 627  
Löwdin, P. O., 8, 9, 16, 81, 157  
London, F., 197  
Longuet-Higgins, H. C., 5, 81  
Loos, G. M., 600  
Low, B. W., 243, 257  
Lozé, C., 430, 436, 497  
Ludwig, G. D., 618, 627  
Lupinski, J. H., 579  
Lykos, P. G., 81, 82  
Lykos, R. G., 79  
Lyons, J. R., 406  
Lyons, L. E., 254, 258, 286, 287, 288, 298, 301, 302, 307, 311, 312, 314, 318, 324, 335, 337  
McClure, D. S., 564, 565, 566, 580, 581  
Maccoll, A., 406  
McConnell, H. M., 536, 537, 541, 542, 545, 557, 561, 579, 580, 581, 582  
McDowell, C. A., 542, 543, 545, 548, 550, 580, 581  
McGlynn, S. P., 81, 319, 332, 337, 358, 573, 578, 582  
Mackie, J. C., 311, 312, 314, 337  
McKim, F. R., 610, 627  
McLachlan, A. D., 536, 538, 539, 562, 579, 582  
McLaren, A. D., 240, 242, 244, 257  
McLear, A. D., 82  
McMillan, J. A., 563, 582  
McWeany, R., 22, 81  
McWeeny, R., 561, 582  
Mahler, H. R., 682, 703, 704, 705, 706, 707, 709, 711, 721, 724  
Maki, A. H., 582  
Malcolm, B. R., 279

- Maling, J. E., 340, 350, 353, 357  
 Malmström, B. G., 626  
 Mangum, B. W., 553, 556, 565, 566, 581  
 Mann, D. E., 582  
 Many, A., 309, 320, 337  
 Mark, P., 292, 336  
 Markham, R., 280  
 Marmur, J., 219, 221, 236, 466, 497  
 Marsh, R. E., 264, 280  
 Marshall, J. R., 497  
 Maruma, Y., 336  
 Marvin, D. A., 497  
 Mason, H. S., 627, 639, 644  
 Mason, R., 153, 157  
 Mason, S. F., 49, 81  
 Matage, N., 157  
 Matheson, M. S., 536, 582  
 Mathieu, J. P., 469, 497  
 Matsen, F. A., 301, 336  
 Matsunaga, Y., 323, 335, 337  
 Matsuo, K., 498  
 Matthaei, J. H., 157  
 Matthews, H., 672, 724  
 Matthews, M. R., 600  
 Matveeva, N. G., 357  
 Medley, J. A., 254, 258  
 Meir, H., 337  
 Mellon, E. F., 257  
 Mercer, E. H., 265, 280  
 Merkbam, E., 407  
 Merrifield, R. E., 337  
 Mette, H., 337  
 Michaelis, L., 602, 627  
 Michaels, G., 219, 236  
 Miki, K., 588, 591, 592, 601  
 Miles, H. T., 455, 456, 459, 497, 498  
 Mira, J., 80  
 Miyagawa, I., 280, 547, 548, 549, 550, 552, 582, 638, 639, 644  
 Miyake, A., 498  
 Mizushima, S., 498  
 Moffit, W. E., 36, 81, 558, 580  
 Mogel, T. T., 553, 581  
 Monfils, A., 340, 358  
 Monnier, 414  
 Monod, J., 601  
 Mooney, R. C. L., 498  
 Moore, W., 337  
 Moore, W. J., 257  
 Morales, M. F., 65, 81, 648, 650, 723  
 Morell, D. B., 406  
 Morgan, R. S., 456, 459, 493, 498  
 Morokuma, K., 63, 66, 80  
 Morpurgo, G., 406  
 Morpurgo, L., 406  
 Morris, G. C., 298, 301, 337  
 Morrison, J. A., 257  
 Mortensen, E. M., 83  
 Morton, J. R., 543, 545, 546, 548, 550, 580, 582  
 Moser, C., 80, 156, 197  
 Moss, J. A., 271, 272, 274, 279  
 Mott, N. F., 255, 258  
 Mourre, R., 81  
 Müller, A., 627, 644  
 Muirhead, H., 181, 257  
 Mulliken, R. S., 17, 28, 45, 64, 81, 82, 396, 406, 573, 582  
 Muramatsu, N., 498  
 Murrell, J. N., 82, 296, 337, 396, 406  
 Nagata, C., 63, 66, 80  
 Nakagawa, I., 498  
 Nakajima, T., 59, 82  
 Nakamoto, K., 197  
 Nakamura, T., 606, 627  
 Naves, Y. R., 422  
 Nelson, D. F., 711, 712, 713, 715, 716, 724  
 Neuhaus, F. C., 674, 724  
 Nicholls, P., 627  
**Nicolau, C., 628, 636, 639, 643, 644**  
 Niemann, C., 668, 669, 670, 724  
 Nirenberg, M. W., 157  
 Nishimoto, K., 157  
 Norberg, R. E., 631, 643  
 North, A. C. T., 181  
 Northrop, D. C., 307, 308, 313, 318, 333, 335, 337  
 Nowotny, H., 269, 279  
 Nutter, R. L., 477, 498  
 Nygaard, A. P., 618, 627

- Ochoa, S., 135, 136, 157  
 O'Connel, R. A., 266, 280  
 O'Hagan, J. E., 406  
 Ohno, K., 99, 157  
 Onsager, L., 313, 337  
 Orgel, L. E., 72, 81, 181, 191, 197, 406  
 Osterhoff, L. J., 579  
 Otarova, G. K., 275, 279  
 Owen, J., 197, 554, 580  
  
 Pake, G. E., 582, 629, 643  
 Paldus, J., 156  
 Palmer, K. J., 240, 257  
 Paoloni, L., 110, 157, 233, 236  
 Pappas, P., 531  
 Parfitt, G. D., 336, 358  
 Pariser, R., 35, 36, 37, 49, 60, 68, 82, 98, 101, 157, 562, 564, 582  
 Parks, J. M., 23, 82  
 Parosot, A., 280  
 Parr, R. G., 23, 35, 36, 37, 49, 60, 68, 82, 98, 101, 157  
 Parris, M., 406  
 Paschke, R. F., 422  
 Passoneau, J. U., 631, 643  
 Pastor, R. C., 337  
 Patch, C. T., 233, 236  
 Pauli, W., 337  
 Pauling, L., 18, 19, 21, 30, 47, 68, 82, 181, 183, 184, 189, 197, 198, 240, 242, 257, 264, 280, 498, 602, 627  
 Pearson, G. L., 258  
 Pearson, R. G., 406  
 Peller, L., 650, 723  
 Peppard, D. F., 498  
 Peradejordi, F., 79  
 Perault, A., 50, 61, 82  
 Perlitsh, M., 601  
 Perrin, D. D., 406  
 Perrin, F., 573, 574, 582  
 Perron, R. R., 271, 280  
 Perry, M. J., 336, 358  
 Perutz, M. F., 160, 181, 238, 257, 280  
  
 Peters, L., 265, 280  
 Peters, R. H., 258  
 Peterson, D. L., 582  
 Petterson, R., 626  
 Pfannmüller, H., 269, 279, 281  
 Phillips, D. C., 181, 257  
 Pick, H., 337  
 Piette, L., 627  
 Pinset, I., 280  
 Pinset-Harström, I., 276, 280  
 Platt, J. R., 385, 395, 406, 559, 581, 582  
 Platzman, R. L., 272, 276, 277, 278, 280  
 Pochettino, 338  
 Pohlit, H., 268, 280  
**Pollard, E., 201, 223, 224, 226, 236, 237, 280**  
 Pollisar, M. J., 236  
 Polonsky, J., 358  
 Polyani, M., 402, 406  
 Pon, N. G., 632, 643  
 Pooley, D., 545, 546, 582  
 Pope, M., 327, 328, 336, 338  
 Pople, J. A., 35, 37, 82, 98, 157, 564, 582  
 Porter, G., 566, 575, 582  
 Pound, R. V., 531  
 Powell, W. F., 212, 213, 236  
 Pratt, J. M., 406  
 Preuss, H., 157  
 Price, W. C., 223, 236, 237, 436, 497, 498  
 Pringsheim, P., 567, 582  
 Pritchard, H. O., 98, 157, 536, 580  
 Pritchard, M. O., 64, 83  
 Prout, K. C., 406  
 Pryce, M. H. L., 535, 554, 579  
 Ptak, M., 350, 354, 358  
 Pullman, A., 6, 38, 39, 44, 49, 51, 53, 54, 59, 60, 63, 66, 67, 68, 70, 74, 75, 76, 82, 104, 110, 153, 157, 358, 623, 627  
 Pullman, B., 6, 38, 39, 44, 49, 50, 51, 53, 54, 60, 61, 63, 66, 67, 68, 70, 72, 74, 75, 76, 79, 82, 83, 98, 104, 110, 153, 157, 158, 357, 358, 623, 627

- Purcell, E. M., 531  
 Putzeiko, E., 407
- Rabinowitch, E., 636, 637, 643  
 Rae, A. D., 406  
 Raistrick, A. S., 271, 279  
 Rajewski, B., 268, 269, 280, 281  
 Randall, J. T., 281  
 Randolph, M. L., 627, 641, 644  
 Ransil, J., 82  
 Read, M., 358  
 Reaume, S. H., 223, 236  
 Redhardt, A., 268, 269, 280, 281  
 627  
 Reinhardt, 639  
 Reitz, J. R., 157  
 Reucroft, P. J., 306, 338  
 Reyerson, L. H., 246, 255, 257  
 Rhodes, D. N., 272, 279  
 Rhodes, W., 128, 156, 157  
 Rice, S. A., 232, 237, 498  
 Rich, A., 270, 281, 497, 498  
 Richards, F. M., 243, 257  
 Riehl, N. V., 253, 254, 258, 338  
 Rieke, C., 28, 82  
 Ristau, O., 198, 627  
 Roberts, J. D., 82  
 Roberts, R. B., 598, 601  
 Robertson, J. M., 406  
 Robertson, R. E., 582  
 Robinson, G. W., 358, 565, 566, 582,  
 583  
 Robinson, J. C., 600  
 Roger, M., 221, 237  
 Rogers, G. E., 270, 281  
 Roggen, L. van, 550, 582  
 Roginsky, S. Z., 257  
 Rondoni, P., 157  
 Roothaan, C. C. J., 16, 33, 34, 81, 83,  
 157  
 Ropars, C., 358  
 Rosen, D., 279  
 Rosenberg, B., 251, 253, 258, 290,  
 316, 332, 336, 338  
 Rosenkrantz, H., 411  
 Rossman, M. G., 181, 257  
 Rowen, J. W., 240, 242, 257
- Rowlands, J. R., 543, 545, 582  
 Rudy, O. N., 337  
 Ruedenberg, K., 27, 29, 36, 37, 83,  
 559, 561, 580  
 Rupert, C. S., 594, 596, 601  
 Rupprecht, A., 156  
 Rushbrooke, G. S., 41, 79  
 Rutherford, H. A., 264, 265, 266,  
 280, 281  
 Ruud, B., 211
- Sadron, C., 339, 340, 354, 358**  
 Sanders, R. T., 601  
 Sandros, K., 579  
 Sarachek, A., 601  
 Satlow, G., 264, 265, 266, 269, 270,  
 281  
 Scalco, E. G., 157  
 Schaad, L. J., 36, 79  
 Scheimising, H. N., 80  
 Scheler, W., 186, 198, 406, 627  
 Schellman, J. A., 216, 231, 232, 237  
 Schepartz, B., 79  
 Scherr, C. W., 83  
 Schildkraut, C., 221, 236  
 Schingu, H., 80  
 Schmeising, H. V., 40, 82  
 Schmitt, F. C., 83  
 Schmitt, F. O., 281  
 Schneider, W. G., 258, 312, 313, 335,  
 337  
 Schnepf, O., 580  
**Schoffa, G., 182, 186, 198, 365, 385,**  
**397, 406, 610, 627, 638, 644**  
 Schonland, D., 175, 181  
 Schramm, G., 497  
 Schröder, E., 644  
 Schuler, R. N., 580  
 Schwartz, G., 156  
 Schweitzer, D., 576, 581  
 Scregg, G., 406  
 Seeds, W. E., 497, 498  
 Seehof, J. M., 243, 244, 257  
 Seery, V. L., 531  
 Segal, H. L., 672, 673, 674, 724  
 Seher, P., 579



- Sehn Pei Gen, *357, 358*  
 Sehr, R., *337, 338*  
 Seitz, F., *255, 258*  
 Setlow, J., *223, 236, 593, 601*  
 Shack, J., *218, 237*  
 Shaw, T. M., *240, 257*  
 Shepard, D. C., *601*  
 Sherwood, H. K., *643*  
 Shibata, K., *643*  
 Shields, H., *264, 265, 267, 268, 273, 280*  
**Shimanouchi, T., 435, 456, 469, 497, 498**  
 Shine, H. J., *724*  
 Shiner, V. J., *709, 724*  
 Shiobara, K., *498*  
 Shlypintokh, V. Ya., *634, 643*  
 Shoosmith, J., *580*  
 Shore, V. C., *181, 257*  
 Short, L. N., *497, 498*  
 Shugar, D., *157, 227, 594, 597, 601*  
 Shuler, K. E., *536, 573, 582*  
 Shull, H., *565, 582*  
 Shulman, R. G., *340, 350, 353, 358*  
 Silver, M., *336, 337, 338*  
 Simmonds, D. H., *280*  
 Simms, H. S., *441, 497*  
 Simpson, O., *307, 308, 313, 318, 333, 335, 337*  
 Simpson, W. T., *582*  
 Sinanoğlu, O., *83*  
 Singer, L. S., *324, 338*  
 Sinsheimer, R. L., *477, 498*  
 Skinner, H. A., *64, 83, 98, 157*  
 Sklar, A. L., *561, 580*  
 Sklar, S. L., *32, 80*  
 Slater, J. C., *13, 18, 21, 83, 119, 157, 198*  
 Sloan, G. J., *581*  
 Slough, W., *338*  
**Smaller, B., 532, 536, 563, 566, 582, 637, 644**  
 Smith, K. M., *280*  
 Snart, R. S., *258*  
 Sogo, P. B., *632, 633, 643*  
 Sols, A., *716, 717, 718, 724*  
 Souda, R., *498*  
 Spanjard, C., *72, 74, 82*  
 Sparrman, B., *624, 627, 641, 644*  
 Spencer, M., *157*  
 Speyer, J. F., *157*  
 Spivey, D. I., *146, 156, 257, 258, 358*  
 Sponer, H., *316, 338*  
 Sponsler, O. L., *239, 257*  
 Stacey, K. A., *279*  
 Stafford, R. S., *592, 601*  
 Stainsby, G., *281*  
 Stearn, A., *227*  
 Stent, G. S., *157*  
 Stern, A., *407*  
 Stevens, K. W. H., *582*  
 Stitt, F., *197*  
 Stokes, A. R., *498*  
 Stone, F. S., *249, 258*  
 Strandberg, B. E., *181, 257*  
 Strathdee, J., *541, 545, 582*  
 Streitwieser, A., *6, 26, 46, 83*  
 Sturtevant, J. M., *232, 237*  
 Sueko, N., *219, 236*  
 Sutherland, G. B. B. M., *436, 491, 498*  
 Suzuki, I., *498*  
 Swensen, P. A., *601*  
 Switzer, D. I., *338*  
 Symons, M. C. R., *562, 579*  
 Szegoe, E. L., *609, 626*  
 Szent-Györgyi, A., *46, 81, 83, 152, 153, 157, 339, 348, 358*  
 Szymanski, B. M., *358*  
 Takenishi, T., *498*  
 Tamm, C., *498*  
 Tanabe, Y., *198*  
 Tanaka, C., *495, 498*  
 Tanner, E. M., *498*  
 Taube, H., *403, 407*  
 Taylor, C. P. S., *258*  
 Taylor, H. A., *258*  
 Taysum, D. H., *336, 358*  
 ten Bosch, J. J., *627*  
 Terenin, A., *338, 407, 553, 566, 567, 573, 574, 576, 580, 582, 583*

- Teszler, O., 264, 265, 266, 281  
 Thaxton, G. D., 338  
 Theorell, H., 603, 604, 608, 614, 618, 627, 689, 724  
 Thom, H. G., 636, 639, 643, 644  
 Thompsett, J. M., 218, 237  
 Thompson, H. W., 498  
 Thon, N., 258  
 Thornberry, H. H., 227  
 Thuillier, J. M., 358  
 Tinoco, I., 96, 97, 128, 158  
 Tolberg, W., 422  
 Tollin, G., 337, 338, 643  
 Tomkinson, J., 407  
 Torriani, A. M., 601  
 Townsend, J., 629, 630, 643  
 Tristam, G. R., 257  
 Tsepalov, V. E., 634, 643  
 Ts'o, P. O. P., 497  
**Tsuboi, M., 435, 436, 455, 456, 469, 491, 497, 498**  
 Tsuchida, R., 197, 198  
 Tüdös, F., 152, 158  
 Turcsányi, B., 152, 158  
 Turkevich, J., 337  
 Tuttle, T., 583  
 Tuttle, T. P., Jr., 536, 583  
  
 Ubbelohde, A. R., 338  
 Udvardy, A., 156  
 Uebersfeld, J., 546, 583  
 Ulbert, K., 277, 281  
 Umrichina, A. V., 634, 643  
 Ur, H., 338  
  
 Vänngård, T., 626  
 Valdemoro, C., 50, 82, 157  
 Valteau, W. D., 227  
 Van der Kaa, J., 358  
 van der Waals, J. H., 554, 556, 557, 562, 565, 566, 580, 583  
**Van Herpen, G., 259**  
 Van Tubergen, R. P., 229, 236  
 Van Vleck, J. H., 167, 181, 192, 198  
 van Voorst, J. D. W., 579  
 Van Wazer, J. R., 498  
  
 Varney-Cebe, N., 280  
 Vartanian, A. T., 258, 338  
 Vaughan, W. R., 581  
 Vavilov, S. I., 567, 583  
 Veillard, A., 49, 51, 83, 98, 158  
 Verne, 414  
 Vidale, G. L., 232, 236  
 Villessov, F. I., 301, 338  
 Vincow, G., 583  
 Vittorio, D. V., 406  
 Vivo, J. L., 583  
 Vozvyshaeva, L. V., 358  
  
 Wacks, M. E., 299  
 Waddington, T. C., 258, 313, 335, 338  
 Wade, N. G., 531  
 Walden, M. K., 266, 280  
 Walker, J., 497  
 Walsh, W. M., Jr., 353, 358  
**Walter, C. F., 645, 653, 673, 680, 724**  
 Ward, R. B., 552, 580  
 Ward, R. L., 583  
 Warner, R. C., 498  
 Watabe, M., 638, 639, 644  
 Watanabe, I., 497, 498  
 Waters, T. N., 406  
 Watson, J. D., 86, 103, 107, 148, 156, 158, 498  
 Watts-Tobin, R. I., 156  
 Weatherwax, R. S., 587, 591, 592, 598, 601  
 Webb, L. A., 579  
 Wegman, 414  
 Weiner, N., 531  
 Weisman, S. I., 579  
 Weissman, S. I., 535, 536, 554, 583, 629, 643  
 Wells, P. H., 600  
 Werner, R. L., 496  
 Wertz, J. E., 583  
 Whalley, M., 407  
 Wheeler, D. H., 422  
 Wheland, G. W., 28, 30, 47, 49, 68, 82, 83  
 Whiffen, D. H., 541, 543, 545, 546, 547, 548, 549, 550, 552, 579, 580, 582, 583

- White, E., 272, 280  
Wilbur, K. M., 638, 639, 644  
Wilhelm, F., 338  
Wilk, M., 338  
Wilkins, M. H. F., 157, 497, 498  
Wilkinson, F., 575, 582  
Wilkinson, G. R., 436, 497, 498  
Will, G., 181  
**Williams, R. J. P.**, 198, 359, 406, 407, 614  
Willis, M. R., 336  
Wilson, E. B., 82  
Wilson, H. R., 157, 497, 498  
Windsor, M. W., 566  
Wise, W. C., 601  
Wiseman, T. J., 406  
Wissmann, G., 337  
Woese, C. R., 158, 224, 233, 237  
Woessner, D. E., 513, 531  
Wolf, H. C., 583  
Woods, H. J., 265, 279, 280  
Wright, B. A., 271, 280  
Wright, M. R., 565, 566, 583  
Wulff, D. L., 601  
Wurz, H., 280  
Yakushigi, E., 643  
Yamamoto, A., 407  
Yamamoto, H., 456, 498  
Yamazaki, I., 606, 616, 627  
Yasaitis, E., 582  
Yockey, H. P., 158  
Yonetani, T., 620, 627  
Yonezawa, T., 80  
Zablow, L., 411  
Zahariasen, W. M., 498  
Zahn, H., 266, 269, 270, 279, 281  
Zahradnik, R., 156  
Zamenhof, S., 219, 220, 236, 237  
Zatman, L. J., 671, 672, 724  
Zeldovich, J., 257  
Zener, C., 13, 81  
Zewe, V., 717, 718, 719, 720, 722, 724  
Zimm, B. H., 219, 221, 222, 231, 236  
Zimmer, K. G., 278, 281, 640, 644  
Ziomek, J. S., 484, 498  
Zubay, G., 498

## SUBJECT INDEX

Page numbers in **heavy type** denote the beginning of a chapter about the stated subject, where a list of the chapter subdivisions may be found. Not all such subdivision heads are repeated here. The letters ff indicate that the stated subject is mentioned again on one or both of the next two following pages.

- Absorption spectrum, 98  
Acetyl acetate, 376  
*N*-Acetylglycine, 547  
Acetyl phosphate, 66  
Acid dissociation constants of oxime complexes, 374  
Activated state, 209  
Activation energy, 147, 212  
    effect of impurities, 307 ff  
Active centres, 124  
Adenine, 47 ff, 52, 85  
    internuclear distance, 87  
    molecular diagrams, 94  
    transition moment vector, 95  
Adenine-thymine pairs, 54 ff  
Adenosine  
    diphosphate, 63 ff  
    hydrochloride, 447  
    infrared spectra, 445 ff, 452, 457 ff  
    monophosphate, 66  
    substrates, 716 ff  
    triphosphate, 63, 64  
ADP: *see* Adenosine diphosphate  
Adenylic acid, 349  
Adipic acid radical, 546  
Adsorption  
    isotherms, 239 ff  
    thermodynamics, 244  
After effect, 46  
Ageing, 85  
*Agrostis stolonifera*, 625  
    free radicals from irradiation, 640  
Alanine radical, 550  
    24\*
- Alkaloids, infrared spectroscopy, 421  
Allowed energy values, 204  
Alloxazine ring, 70  
Alpha- ( $\alpha$ ) and  $\beta$ -bands, 382  
Alternate hydrocarbons, 37, 41  
Aminidases, 74  
Amino acids, 265, 546  
    constants, 548  
    protein, 135  
    radicals, 546 ff  
Angular momentum  
    mechanical, 164  
    orbital, 162  
    quantum number, 10  
    total, 163  
Anisotropic dipolar interaction, 540 ff  
Annealing, 221  
Anthracene  
    carrier mobilities' temperature dependence, 304  
    electron and hole mobilities, 294  
    ionization potential, 302  
Antibiotics, structure of, 422  
Antibodies, 262  
Anti-bonding  
    levels, 144  
    molecular orbital, 19 ff, 168  
    orbitals, 92  
Antigenic effect, 262  
Antiserum combining with virus, 223  
Antitumor activity, 60 ff  
Aperiodic crystals, 202

- Apurinic acid, infrared spectra of, 466
- Aromatics, 305
- electrical properties, 305
  - homogeneous complexes, 321 ff
  - hydrocarbons, 152
  - magnetic properties, 323 ff
  - photoconduction, 310
  - (pyridine type) N atom, 91
  - ring nitrogens, basicity of, 59
- Ashiem-Zondek reaction, 433
- Aspartic acid radicals, 551
- Atomic magnetic moments, 166
- Atomic orbitals, 10 ff
- ATP: *see* Adenosine triphosphate
- Aufbau process, 27
- Avena sativa*, 634
- Azauracil, 53
- Bacillus subtilis*, 220
- Bacterial viruses, photoreactivation, 586
- Bacteriophage, 223, 233
- Band theory calculations, 293
- Banfield and Kenyon's radical, 319
- Barium diethylphosphate, absorption band, 488
- Barium dimethylphosphate, 484
- Base pairs
- anomalous and normal, 111, 115
  - donor-acceptor, 148 ff
  - electronic structure, 108
  - stereochemical investigations, 109
  - Watson-Crick, 148 ff
- Bases
- superimposed, 122 ff
  - total  $\pi$ -electron energy of, 93
- Basicity order, 366
- B.E.T.: *see* Brunauer-Emmett-Teller
- Betagalactosidase, 212
- Bile pigments, absorption spectra, 398
- Bilirubin, 399
- Biocatalyzed reactions, electronic interpretation, 61 ff
- Biochemical genetics, 130 ff
- Biological substances
- infrared spectroscopy prospects, 408
  - structural determination, 418
- Block condition, 138
- Bohr magneton number, 121, 166 ff, 171, 180
- Boltzmann factor, 502
- Bond orders, 41 ff, 50, 53, 98
- Bonding molecular orbitals, 92, 168
- Bone, 270
- Born-Oppenheimer approximation, 8, 85
- Bound states of molecule, 7
- Bovine plasma albumin, 254
- Bovine serum albumin, 243
- Brownian motion, 506, 509
- Brunauer-Emmett-Teller equation, 240
- monolayer, 249
- Caffeine-riboflavin complex, 46
- Calf thymus, 128
- Cancer, 85
- antitumor activity, 60 ff
- Cancerous information, 154
- Carboxyl phosphate, 63 ff
- Carcinogenic hydrocarbons, 152 ff
- Carcinogens, 152 ff
- Carriers, 288
- mobilities, 290 ff
  - photogeneration, 288
  - thermal generation, 288
- Catalase, 160, 182, 615
- Catecholamine, 522
- Catochrome, 72
- Cells, ultraviolet photoprotection, 584
- Cerebral samples, infrared spectroscopy, 414
- Chain ligands, 380
- Charge densities, 98, 121
- Charge transfer, 363, 368
- bond, 250
  - complex, 70
  - spectra, 368 ff
  - theory, 44, 45 ff

- Chelation, 426  
Chemical bond, 11, 16 ff, 183  
Chemical protectors, 261  
Chemical reactivity, 43 ff  
Chemical shifts, 500  
Chemically induced mutation, 85  
CH<sub>3</sub> group, hyperconjugation, 90  
Chloranil, as electron acceptor, 254  
*Chlorella*, electron spin resonance, 637  
Chlorins, 386  
Chlorocruorin, 386  
Chloroplast, 629  
    electron spin resonance, 629  
    luminescence, 634  
    semiconductor action, 633  
Choline phenyl ethers, 77  
Chromophore, 586, 593 ff  
Chymotrypsin, product inhibition, 668  
*Cis* effect, 374, 376  
*Cis-trans* isomerism, 422  
Closed set, 9  
Closed-shell configurations, 45  
Cobalamin spectra, 400  
Coding problem, 130  
CO, effect on ferrous spectrum, 394  
Coenzymes DPN, FAD, electronic structure, 67 ff  
Collagen, 264, 270 ff  
Competitive inhibitor, 650  
Complete set, 9  
Computers, 88  
Conductivity, 85  
    and adsorbed water, 251  
Configurational change, 207, 210  
Configurational entropy, 246  
Conformation partition function, 229  
Conjugated organic ligands, 380 ff  
Copper acetyl-acetonate, 370  
Coppering's radical, 319  
Correlation, 8  
Corrins, 386, 399  
    system, 380  
Cortical cells, 269  
Coulomb integral, 25, 99  
Coupling constants, 500  
Covalent bonds, 17, 203  
Covalent porphyrins, 74  
Cross-linking, protective effect of, 277  
Crystal, 286  
    electron affinity, 286  
    field splitting, 362  
    ionization potential, 286  
Cupric dimethylglyoximate, 370  
Curie's law, 167  
Curie-Weiss law, 610  
Cystein or cysteamine, 261  
Cystine, 267  
    no orientation dependence, 268  
Cystine dihydrochloride radical, 550  
Cytidine infrared spectra, 441 ff, 455  
Cytidylic acid, 349  
Cytochrome *a*, 386, 392  
Cytochrome oxidase, 620  
Cytochromes, 160, 182, 377, 620  
    electron carriers, 74  
    electronic structure, 71  
Cytosine, 52 ff, 85, 97, 456  
    internuclear distance, 87  
    molecular diagrams, 94  
    transition moment vector, 95  
Dalziel relationship, 682, 689, 698, 706, 710  
Dark electrical conductivity, 303  
    of aromatic molecular solids, 303 ff  
    temperature dependence, 304  
Dark reactions, 5  
*d-d* transitions, 363, 371  
Degeneracy, 205  
Delocalization energy, 38 ff, 50, 116, 150  
Delocalization of pi-electrons, 146  
Delocalized bonds, 21 ff  
Delocalized electron, expectation value of Hamiltonian of, 138  
Delocalized  $\pi$ -electrons, 87, 90, 116  
Denaturation, 216  
Deoxyadenosine, 349

- Deoxycorticosterone, 411  
  spectrum varying with sample preparation, 411
- Deoxycorticosterone acetate, 419  
  infrared spectroscopy, 419
- Deoxyguanosine, 349
- Deoxyribonuclease, 461 ff
- Deoxyribonucleate, 467, 489  
  infrared dichroism, 467  
  spectra, 484 ff
- Deoxyribonucleic acid (DNA), 349, 436  
  absorption spectrum, 128  
  band structures, 146  
  chain configuration, 344  
  charge carriers in conduction band, 148  
  complementary chains of bases, 217  
  d.c. conductivity, 146  
  delocalized  $\pi$ -electron system, 137  
  double helix, 86 ff, 103, 144, 148 ff  
    configuration of salts, 436  
  double-stranded model, 342 ff  
  duplication frequency, 152  
  duplication, tumor development and, 148  
  electronic properties, 339, 346 ff  
  electronic structure, 88  
  electron spin resonance, 351  
  impurities and crystal imperfections, 147  
  macromolecule, 142, 145  
  magnetic properties, 351  
  molecular structure, 341 ff  
  nucleic acids, 460  
  oscillator strength, 128  
  photoreactivation, 586  
  polarization, 151, 153  
  polarized molecule, 148  
  quantum mechanical considerations on some properties of, 84  
  radiation level, 152  
  real, band structure of, 142 ff  
  secondary structure in solutions, 436  
  semiconductivity, 146  
  superimposed bases, 128  
  synthesis rate, 153 ff  
  transforming, 587, 593  
  transitions on heating, 217  
  ultraviolet absorption maximum, 114
- DNA-RNA-P(protein) coding, 135
- Depolymerases, enzymic reaction, 675
- Determinantal equations, 124, 143
- Deuterated chlorophyll, 637
- Deuteration, 563  
  acceptor and donor, 575  
  triplet state EPR effects, 563, 566
- Dialkylphosphate anions, spectra, 484 ff
- Dicarboxylic acid  
  free radicals, 541 ff  
  hyperfine coupling constants, 544
- Diethyl phenyl phosphates, 77
- Digonal hybrids, 19
- Dimethylglyoximate complexes, 369 ff  
  spectra, 371 ff
- Dimethylglyoxime radicals, 552
- Dimethylphosphate anion, 484 ff
- Diphosphoglyceric acid, 62
- Diphosphorpyridine nucleotide, 67
- Dipoles, 128
- Dipositive bond, 75
- Dipyrrylmethene, 398, 404
- Dirac theory, 164
- Disulphide bonds, 266
- DNA: *see* Deoxyribonucleic acid
- D<sub>2</sub>O medium, 228
- Donor-acceptor  
  complexes, 320 ff  
  theory, 286 ff, 333 ff
- Dose-reduction factor, 586
- Double helix, 86 ff, 436, 459, 493
- Double linkage, 20
- Doublets, Kramer's theorem, 172 ff, 175
- dRNA, 219
- E. coli*: *see* *Escherichia coli*
- Effective magnetic moment, 171, 180

- Effective principal quantum number, 13
- Eigenfunctions, eigenvalues, 8, 31
- Electromagnetic radiations, 260
- Electron, 302
- affinities, 46, 302 ff
  - affinity of the *i*-th atom, 98
  - configuration, 6
  - of cations, 375
  - interaction integrals, 99
  - orbitals of metals, 360
  - paramagnetic resonance (EPR), 159
  - of free radicals, 532 ff
  - in methanol, 577
  - spectroscopy, recent advances in, 532
  - promotion, 28
  - relativistic theory, 164
  - repulsion terms of cation, 364
  - spin resonance (ESR), 603
    - absolute calibration, 606
    - investigations on plant systems, 628
    - measurements, 330 ff
    - spectroscopy, 264, 278, 605 ff
  - transfer, 368
    - between water and proteins, 239
    - theory, 45 ff
  - transition, 93
- Electronic conduction in organic molecular solids, 282
- Electronic configuration, 6
- Electronic properties
- of DNA, 339
  - of DNA and its components, comparison of, 347 ff
  - supermolecular, 354
- Electronic structure of hemoproteins, particularly hemoglobins, 159
- Electronic structures in quantum biochemistry, 3
- Electronic wave function, 8
- Electrophilic reagent, 67
- Electrophilic substitution, 44
- Electrostatic field, effect on biological objects, 155
- Electrostatic repulsions, 13
- Elementary cell, 139
- Elovich equation, 247
- Embryos X-rayed, 640
- Endergonic reactions, 62
- Energy
- absorption units, 261
  - bands, 140 ff
  - forms, 203 ff
  - indices, 31
    - of pteridines, 59
    - of purine bases, 51
    - of pyrimidine bases, 54
  - levels, perturbation of, 133
  - richness, 5
  - transfer, 567 ff
  - transfer models, 572
- Energy-rich bonds, 61 ff
- Enolic forms, 104
- Enthalpy and entropy, 226
- Entropies of adsorption, 239
- Enzymatic hydrolysis, 74
- hypotheses, 76
- Enzyme action, determined by product inhibition and other kinetic methods, 645
- Enzyme activity loss, 211
- Enzyme hydrolysis, 665, 675
- Enzyme inactivation, 212
- Enzyme radicals, ESR spectrum, 619
- Enzyme reaction rates, 211 ff
- Enzyme systems, 607
- magnetic properties, 607 ff
- Enzymes, 262
- Epinephrine, 518 ff
- relaxation times, 520 ff
- Epinephrine-ATP complex, temperature dependence of relaxation times, 524
- EPR: *see* Electron paramagnetic resonance
- Equilibrium mixtures of spin states, 365
- Equilibrium state of electron distribution, 147



- Escherichia coli*, 587  
  photoprotection, 587  
  ribosomes, 462 ff  
ESR: *see* Electron spin resonance  
Esterases, 74  
Ethylenic linkage, 20  
Ethyl radical, EPR spectrum, 538  
Excitation energies, 112 ff, 129  
Excited state radical, 378  
Expectation value, 138  
Eyring's formulation of energy changes, 208 ff  
Eyring and Polanyi theory, 78  
  
Far ultraviolet radiation, 584  
  photoprotection from, 584  
Feather, 265  
Ferric dimethylglyoximate complex, 372  
Ferricytochrome, 72  
Ferriheme, 190  
Ferrihemoglobin, 169 ff  
  azide, 172  
  complexes, 185  
  cyanide, 196  
  fluoride, 174, 189  
Ferrihemoproteins, reactions with peroxides, 612  
Ferrimyoglobin complexes, 185  
Ferrocytochrome, 72  
Ferroelectricity, 85  
Ferrohemoglobin, 169 ff  
  electronic structure of iron in, 177 ff  
Ferroporphyrin, 72 ff  
Ferrous (low spin) porphyrins, 390  
Ferroverdin, 378  
Fibrous proteins, 262  
  experiments on, 263 ff  
Five coordination, 370  
Fixed ligand, stability of complexes, 366  
Flavin free radicals, 617  
Flavoprotein, 67, 617 ff  
Fluororacil, 53  
Folic acid coenzymes, 77  
Forbidden band width, 147  
Forbidden charge transfer, 395  
Forbidden transitions, 542, 556  
  of phosphors, 558  
Formamide, 461  
Free-electron methods, 32, 44  
Free-electron orbital model, 559  
Free energy, 206, 226  
  variation of in macromolecule, 209  
Free radicals, 261  
  concentration of, 606  
  in *Agrostis stolonifera*, 640  
  in plant material, 629  
  radiation-induced, 621  
Free-valence index, 42  
Frontier-electron method, 32, 44  
  
Gall stones, infrared spectroscopy, 413  
Gamma-rays, 260  
Genetical considerations, 130 ff  
Genetic markers, 220  
Glutaric acid radical, 546  
Glycine radical, 546 ff  
Glycollic acid,  
  constants, 548  
  radical, 552  
Glycosidases, 74 ff  
Glycyl-glycine, 265  
Goepfert-Mayer and Sklar method, 32 ff  
Gouy balance, 603 ff  
Grating spectrographs, 409  
Grotthuss proton conduction, 253  
Guanidine phosphate, 66  
Guanine, 47 ff, 50 ff, 85, 349  
  internuclear distance, 87  
  molecular diagrams, 94  
  transition moment vector, 95  
Guanine-cytosine pairs, 54 ff  
Guanosine, infrared spectra, 449 ff  
Guanylic acid, 349  
G-Value, 261  
  
Haem a  
  complexes, 394  
  ferric complexes, 392  
Haematoporphyrin, 634

- Haemin derivatives, absorption spectra, 397  
 Haemoglobin (hemoglobin), 182, 395  
   adsorption isotherms, 240  
   electronic structure, 159  
   hydration, 243  
   magnetic properties, 159  
   metabolic breakdown, 77  
   protein content, 242  
   water adsorption, 238  
*Hæmophilus influenzae*, 220, 593  
 Haem-proteins (hemoproteins), 71, 375  
   chemical bond, 182  
   electronic structure, 159  
   magnetic properties, 159, 607 ff  
   magnetic susceptibilities and the chemical bond, 182  
   peroxide compounds of, magnetic properties, 614  
   temperature dependence of magnetic susceptibility, 609 ff  
 Hair, 265  
 Haldane relationship, 704 ff  
 Hamiltonian, 25  
 Hamiltonian operator, 7 ff  
 Harmonic oscillator, 204  
 Hartree-Fock-Brueckner SCF theory, 16  
 Hartree-Fock equations, 15, 33  
 Heat inactivation effects, 221  
 Helical form, 207  
 Hellman-Feynman theorem, 18  
 Hemes, 167  
 Hemoglobin: *see* Haemoglobin  
 Hemotropin, 609  
 Hermitian, 25  
 Hermitian operator, 7  
*Herpes simplex*, 222  
 Heteroatoms, 30 ff  
 Heterocyclic bases, interaction, 346 ff  
 Heteromolecules, 37  
 Hexokinase reaction, kinetics, 717  
 High-energy phosphate bond, 70  
 High spin, 169 ff  
   ferric porphyrins, 391  
   states in equilibrium with low, 375 ff  
*Hordeum vulgare*, 634 ff  
 Horn, 265  
 Hückel approximation, 26 ff, 88, 96, 108, 111, 124, 136 ff, 147, 150  
 Hund's rule, 162, 187, 193  
 Hybridization, 18  
 Hybridized (pyrrole type) N atom, 91  
 Hydrocarbons, carcinogenic and not, 152  
 Hydrogen bond energy, 232  
 Hydrogen bonds, 86 ff, 111, 203, 207  
 Hydrolases, 74 ff  
 Hydrolytic deaminases, 74  
 Hydrolyzable linkages, 62  
 Hydroxylamine poison of photo-synthesis by, 636  
 Hydroxymethylcytosine, 52 ff  
 Hyperchromicity, 128  
 Hyperfine interaction, 533 ff  
 Hyperfine structure, 562  
   of triplet state, 562 ff  
 Hypophosphite anion, infrared and Raman spectra, 478 ff  
 Hypoxanthine, 47 ff, 50 ff  
 Imidazole groups, absence of orientation in, 369  
 Imino (keto) forms, 104  
 Impurity atoms, 255  
 Impurity levels between energy bands, 147  
 Inactivation, 225 ff  
 Incomplete shells, 161  
 Infrared spectra  
   of nucleic acids and related compounds, 435  
   of sodium deoxyribonucleate, 437  
 Infrared spectroscopy  
   biological use, 408  
   correlation tables, 419  
   importance of correct dispersion, 409  
   medical applications, 432  
 Inosine, 451  
   infrared spectra, 451

- Internal energy, 205  
Intermolecular electronic transfers, 45  
Inter- or intramolecular bonds, detection of, 423 ff  
Ionization energy of donors, 255  
Ionization potentials, 46, 52, 64, 98  
Ionizing radiations, effects on fibrous proteins, 259  
Iron-porphyrin complexes, 182  
Irradiation resistance of dyed wool, 266  
Isoalloxazine, 617  
Isomers, structural differences, 416  
Isopropyl alcohol, infrared spectra, 494  
Isotropic hyperfine constants, 536  
Isotropic hyperfine interaction, 534  
Isovaline radicals, 551  
  
Kasha's flow chart, 24  
Kekulé structures, 40  
Keratin, 251, 254, 263, 264 ff  
    ionizing radiation effects, 266  
Kirkwood-Bauer-Magat line, 425  
Koopman's theorem, 45  
Kramer's theorem of doublets, 172 ff, 175  
  
"Labelled" elements, 431  
Laguerre polynomials, 10  
Lamellar complexes, 326  
Landé *g*-factor, 165  
Langmuir-Adam trough, 240  
Laplacian operator, 7  
Large molecules: *see* Macromolecule  
Larmor period, 510  
Lattice, 502  
LCAO method, 23  
LCAO-MO calculation, 116  
LCAO-MO method, 88  
Legendre functions, 10  
Levels shift by interaction of bases, 133  
Ligand-field  
    splitting parameters, 361  
    theory, 167 ff, 187, 190, 613  
    transitions, 363 ff  
Ligands  
    bound on *z*-axis, stability of, 374  
    decreasing polarizability, 400  
    reactivity of, 376 ff  
    substitution reactions, 376  
Light, action of, 379 ff  
Light-excited state, 631  
Lincoln wool, 269  
Lineweaver-Burk reciprocal plots, 671  
Liver alcohol dehydrogenase, 707 ff, 711  
Living seeds, 623 ff  
Localization energies, 42  
Localized adsorption on polar groups, 250  
Localized bonds, 21 ff  
London attractions, 203  
Longitudinal relaxation, 503  
Low spin, 169 ff, 172  
    complexes, 370  
    ferric porphyrin, 393  
    states, 368  
    in equilibrium with high, 375 ff  
Luminescence of chloroplasts, 634  
Lysogenic *E. coli*, 588  
  
Macromolecules, 525  
    action of heat on, 210  
    binding to small molecules, 523 ff  
    secondary and tertiary structure, 202  
    swelling of, 210  
    variation of free energy, 209  
Magnesium phthalocyanide, 634  
Magnetic anisotropy, 610  
Magnetic methods, 607  
Magnetic moment, 164 ff  
    incompletely quenched, 170  
Magnetic performance data: Gouy, Rankine, ESR, 607 ff  
Magnetic susceptibility measurements, 183 ff  
Magnetization vector, 503  
Majority carrier, 311

- Malonic acid radical, 541  
Manganous phthalocyanine, 402  
Mataga-Nishimoto approximation, 99  
Mesitylene, 514  
Mesobilene, 399  
Messenger RNA, 219 ff  
Metal ions, 182  
Metal porphyrins, properties of, 359  
Metal porphyrins, chlorins, phthalocyanines, 380  
Metal protoporphyrin complexes, 389  
Methene bridges, 376 ff, 383  
    carbon atoms, 397, 404  
Methyl cytosine, 52 ff  
Methyl group pseudo-atom  $H_3$ , 91  
Methyl radical, 537, 576  
    EPR spectra, 537  
Michaelis constants, 653, 670 ff, 674, 721 ff  
    simple enzymic reactions, 653  
Michaelis-Menten mechanism, 648  
Microorganisms, photoprotection from UV damage, 592  
Microspectrographs, 409  
Mirror microspectrographs, 412  
Mitochondria, 238  
Mitosis, 85, 89  
    frequency, 152  
Molecular biology, 4  
Molecular diagram, 42  
Molecular electronic indices, 38  
Molecular orbital (MO) combinations, 194 ff  
Molecular orbital energies, 104 ff, 126, 143, 144  
Molecular orbital method, 191  
Molecular orbitals, 19, 22  
Molecular structure and infrared spectroscopy, 420  
Molecules, 525  
    small, binding with macromolecules, 523  
Monoalkylphosphate anions, spectra of, 476 ff  
Monodehydroascorbic acid, electron spin resonance, 636  
Monoglycerides, infrared spectroscopy, 413  
Monolayer, 246  
    coverages, 239  
Monomethylphosphate anion, spectra of, 476  
Mononucleotides, 468, 477 ff  
Mulliken-Wheland method, 28 ff  
Muscle, infrared spectroscopy, 413  
Mushroom, 638 ff  
Myoglobin, 160, 182, 239, 395, 615  
Myosin, 274 ff  
  
NAD, NADH substrates, 715, 720  
Nail, 265  
Naphthalene, ionization potential, 302  
Near ultraviolet radiation, 586  
Nephelaxetic series, 364 ff, 401  
*Neurospora crassa*, 670 ff  
Neutral free radicals, 319 ff  
*Nicotiana tabacum*, electron spin resonance, 629  
Nicotinamide, 670 ff  
Nicotinamide adenine dinucleotide (NADH), 586  
NO groups, 377  
Non-alternant hydrocarbons, 37  
Non-degenerate MO, 93  
Non-localized bonds, 21 ff  
Non-ohmic currents, 313 ff  
Normalization integral, 8  
Nuclear dipoles, Zeeman energy of, 534  
Nuclear magnetic measurements, 499  
Nuclear magnetic resonance, 500  
Nucleic acids, 52  
    and compounds, 435  
    biological activity loss, 220  
    denaturation, 217  
    fundamental bases, 56  
    infrared spectra, 435, 460 ff  
    luminescence, 347  
    photoprotection of modifiable site, 594 ff

- Nucleic acids—*contd.*  
  secondary structure, 466  
  thermal effects on, 201  
  UV absorption, 585
- Nucleohistone, 462  
  base pairings, 463
- Nucleophilic attack, 67, 377 ff
- Nucleophilic substitution, 44
- Nucleosides  
  infrared spectra of, 440 ff  
  mixed products, 452 ff
- Nucleotide bases  
  molecular diagrams, 94  
  sequence, 88, 130 ff  
  tautomeric molecular diagrams, 106  
  transition moment vectors, 95  
  unusual tautomeric forms, 104  
  wavelengths and *f*-values, 96
- Nylon-66, 264
- Old yellow enzyme, 618
- One-electron energies, 27
- Opposed resonance of ADP and ATP, 65
- Optical rotation, 216
- Orbital angular momentum, 162
- Orbital contribution to total energy, 27
- Orbital energies, 178
- Orbital function, 161
- Orbital, Hartree-Fock approximation, 161
- Orbitals, 11  
  ligand, 168  
  splitting, 167 ff
- Organic molecular solids, electronic conduction in, 282
- Organic phosphors, 556 ff
- Ortholocalization, 44
- Orthonormal set, 14
- Oscillator strengths, 94, 100  
  values of, 114, 129
- Oscilloscope trace, 504
- Ovalbumin, 216
- Overlap atomic orbitals, 17 ff
- Overlap electron clouds in superimposed rings, 87
- Overlap integrals, 17, 64, 116, 121 ff, 131
- Overlap maximum, 17
- Oxime complexes, 374
- Oxime oxidation, 377
- Oxygen  
  increases effect of ionizing radiations, 261  
  superdelocalizability, 67
- Oxyhemoglobin, 72
- Oxypurines, 47
- Oxytetracycline PMR spectrum, 528
- Para-localization energy, 43
- Paramagnetic species of biological interest, 602
- Paramagnetism, temperature independent, 167
- Pariser and Parr method, 35 ff
- Partial bond order, 41
- Partition function, 206, 226, 229 ff
- Pauli exclusion principle, 8, 11, 186, 557
- Pauling-Slater principle, 17
- Pauling-Wheland method, 30 ff
- Penetration effect, 13
- Penicillin  
  albumin concentration affecting relaxation rate, 525  
  relaxation rates, 514, 525 ff  
  -protein system, 527  
  spectra, 524
- Peophytine, 634
- Peptidases, 74
- Peptide chains, 262
- Peptide groups, water vapour adsorption on, 242
- Periodic boundary condition, 138
- Periodic model sequences, 88
- Peritoneal fat, infrared spectroscopy, 414
- Peroxydase, 160, 182, 615
- Perturbation method, 9

- Phenanthrene and naphthalene, triplet state, 569
- Phosphate, 467  
  groups, absorption bands of, 467 ff  
  high-energy bond, 70  
  ion, 64
- Phosphenol pyruvate, 66
- Phosphite anions  
  infrared and Raman spectra, 469 ff  
  vibrational spectra, 472 ff
- Phospho-diester link, 219
- Phosphomonoester group, 468
- Phosphorus, superdelocalizability, 67
- Photochemical *cis*-effect, 403
- Photochemical processes, triplet state, 576
- Photoconductivity, 290  
  impurity effects, 318 ff  
  in aromatic molecular solids, 310  
  intensity dependence in aromatics, 317 ff  
  pre-exponential factor, 308 ff  
  pressure dependence, 297 ff  
  pulsed, 290 ff  
  temperature dependence, 296 ff  
    in aromatics, 316 ff
- Photoprotection, **584**, 586 ff  
  from far ultraviolet, **584**  
  killing in *E. coli* B, 589  
  of *Colpidium colpoda*, 594  
  of *E. coli* B, action spectrum, 590, 596  
  of microorganisms from UV damage, 592  
  of *Pseudomonas aeruginosa*, 591, 594  
  of *Streptomyces griseus conidia*, 591  
  of subcellular systems, 593  
  temperature independence of, 590, 595  
  X-ray effects, 585
- Photoreactivation, 589  
  killing in *E. coli* B/r, 589
- Photosynthesis  
  ESR investigation of, 628 ff  
  main sequences, 636 ff
- Photosynthetic materials, electron spin resonance of, 632
- Photosynthetic reactions, 379
- Phthalocyanines, 370, 383, 402  
  metal substituents, 387
- Phycomyces*, 638 ff  
  melanin content, 639
- Pi ( $\pi$ ) bonds, 18 ff
- Pi ( $\pi$ )-donors, 363  
  character of metals, 395  
  metal ions, 390
- Pi ( $\pi$ )-electron  
  approximation, 22  
  charges or densities, 53  
  energies, 111, 115, 124, 128  
  interaction of orbitals, 87  
  orbitals, 117
- Piezoelectricity, 85
- Pigments, photoreduction, 635
- Piperidine, photoreduction with ascorbic acid, 635
- Plant systems, ESR investigations on, **628**
- Plants, 628  
  electron spin resonance investigations of, **628**  
  irradiation of, 640 ff  
  non-photosynthetic material, 638 ff
- Plant viruses, photoreactivation of, 586 ff
- PMR: *see* Proton magnetic resonance
- Pneumococcus, 220
- Polarization  
  energy, 286  
    of central cation, 361  
  measurements, 329  
  of ligand by cation, 361
- Polio virus, 222
- Polyadenylic acid, 493  
  infrared spectra, 456
- Polycytidylic acid, infrared spectra, 455
- Polynucleotides, 136 ff, 140, 144  
  chains, 86 ff  
  emission characteristics, 347 ff

- Polypeptides, 135  
  chains, 239  
    close together, 203  
    formation of, 220
- Polyribonucleotides, 135, 454  
  synthetic, infrared spectra of, 454 ff
- Polyuridylic acid, 459, 514  
  infrared spectra, 459 ff  
  relaxation rates, 514
- Porphyrin, 72, 380, 383  
  compounds, photochemistry of, 404 ff  
  energy comparisons, 73  
  spectra, 381
- Position vector of electron, 93
- Potassium hypophosphite, 479  
  spectra of, 479
- PR enzyme, 587, 596
- Primary photochemical process, 631
- Principal quantum number, 10
- Prism spectrographs, 409
- Product inhibition in determination of enzyme action, 645
- Prosthetic group, 160
- Protein-chloranil complex, 254
- Proteins  
  absolutely dry state, 243  
  crystals, van der Waals adsorption on, 249  
  current carriers in wet, 253  
  denaturation, 216  
  diamagnetic contribution, 171  
  fibrous, ionizing radiation effects on, 259  
  globular, 262  
  radiation effects on, 262  
  solid, water adsorption on, 238  
  swelling, 228  
  synthesis rate, 153 ff  
  theoretical partition functions, 229  
  thermal effects on, 201  
  thermal expansion, 224
- Protohaem complexes, 393
- Proton magnetic resonance, 511  
  non-rigid molecules relaxation rates, 514  
  proton relaxation rates, 517  
  relaxation rates, 517 ff  
  simplification for high resolution, 511 ff  
  spectra of epinephrine, 519 ff
- Protonated adenosine, 446, 459
- Protonated aniline, 443
- Protonated cytidine, 442
- Protonated pyridine, 443
- Protoporphyrin, 72
- Pseudoyohambine, 414
- Pteridines, 55  
  energy indices, 59
- Pulsed photoconductivity, 290 ff
- Pu-Py base interactions, 131
- Purines, 47 ff  
  A and G, 97  
  bases, energy indices of, 51  
  removal from RNA by heat, 219
- Purpurins, 398
- Pycnometer, radioactive counting, 224
- Pyridine  
  deuteriochloride, 444  
  energy indices of bases, 54  
  hydrochloride, 444  
  nucleotide enzymes, 67
- Pyridoxal phosphate enzymes, 77
- Pyrimidines, 52 ff  
  effect of substitution in, 385 ff  
  U, T and C, 97
- Pyrrole rings, 385
- Quantum biochemistry  
  applications, 44 ff  
  electronic structures in, 3
- Quantum chemistry, pure, semi-empirical and empirical theories of, 27
- Quantum mechanics, 5  
  application to DNA properties, 84  
  fundamentals, 6 ff  
  rules, 204
- Quantum numbers, 10
- Quenching, 170
- Rabies virus*, 222

- Racah parameters, 364 ff  
Radiation  
  electromagnetic, 203  
  fundamental, 5  
  mutation induced by, 85  
  natural, 146 ff, 152  
  resistance to, 271  
Radical attack, 44  
Radical scavengers, 272  
Rad (unit), 261  
Raman spectra, 469 ff, 476 ff, 478, 484 ff  
Random coil, 207  
  power of confusion, 229  
  transition from helix, 231  
Rankine balance, 605  
Rayleigh-Ritz method, 9  
Reaction coordinate, 209  
Relaxation measurements  
  interpreted by molecular events, 505 ff  
  interpreted by molecular interactions, 515 ff  
  non-rigid molecules, 514  
Relaxation times, 500  
Resonance, 116  
Resonance integrals, 124  
Resonance transfer, 571  
Resonator cavity, chloroplasts in, 630  
Respiratory coenzymes, 67  
Rhodamine B, 266  
Rhodofying carbonyl group, 386  
Ribitol dehydrogenase, 712 ff  
Ribonuclease, 246, 462  
Ribonucleates, infrared spectra, 492 ff  
Ribonucleic acid (RNA), 84, 436  
  magnetic properties, 351  
  nucleic acids, 460  
  photoreactivation, 586  
  scission, 219  
  secondary structure, 436  
  synthesis rate, 153  
  trinucleotides, 135, 136  
Ribose, infrared spectra, 494  
Ribosomes, 219  
Ring chelates, chemical reactivity, 402 ff  
Ring ligands, 380  
RNA: *see* Ribonucleic acid  
Roentgen (unit), 261  
Roginsky-Zeldovich equation, 247 ff  
Roginsky-Zeldovich kinetics, 255  
Roothaan's equations, 33  
Rotation, 203  
Rotational energy, 205  
Rotational isomers, 416 ff  
  structural determination, 485  
Rowin's theory, 76  
Russell-Saunders coupling, 197  
  
*Sancheria*, 634  
Sandwich cells, 311 ff  
Saturated ligands, 362  
Saturation of spin system, 502  
SCF-LCAO-MO method, 102  
Schrödinger equation, 7, 12, 187  
  for hydrogen-like atoms, 10  
Scission, 219, 224  
Sclera, 270  
Screening, 13  
Secular determinants, 92, 100, 124  
Secular equations, 93  
Seeds, 623  
  irradiated by X-rays, 641  
Self-consistent field (SCF) method, 14  
Self-consistent molecular orbital method, 33  
Semi-empirical atomic orbitals, 13  
Semi-empirical method, 35  
"Set" of keratin fibres, 266  
Sigma bonds, 18  
Sigma-donors, 363  
Silk, 240, 264 ff  
Single bases  
  electronic system, 90 ff  
  MO energies, 92  
  mutation and tautomerism, 103 ff  
  spectroscopical properties, 90  
Single-substrate, single-product reactions, 648 ff



- Singlet-singlet excitation, 96  
Singlet state, 331 ff  
    theory, 287  
Singlet-triplet excitation, 96  
Skin, 270  
Slater-type orbitals (STO), 13  
Small molecules  
    binding to macromolecules, 523  
    interactions between, 518  
Sodium hypophosphite-*d*, spectra of, 480  
Sodium ribonucleate, infrared spectra of, 463 ff  
Solid state  
    electron affinities, 298, 303  
    ionization potentials, 298 ff  
    physics, 137  
Soret band, 382  
    positions of, 393  
Specific molecular interactions  
    studied by nuclear magnetic relaxation measurements, 499  
Spectra of band systems, 95  
Spectra of conjugated chains, 398 ff  
Spectrochemical series, 363 ff, 371  
Spectroscopical properties, 90 ff  
Spectroscopy, EPM, advances in, 532  
Spin, 11, 365  
    angular momentum, 162  
    density, 537 ff  
    Hamiltonian, 554  
    high and low, 167  
    orbital, 162  
    pairing, 365  
    saturation, 502  
    system, definitions of, 501  
Spin-forbidden transitions, 396  
Spin-lattice relaxation, 502 ff  
"Spin-only" value, 170  
Spin-orbit coupling constant, 163 ff  
Spin-spin relaxation, 502  
Spin states, 376  
    change of, 365 ff  
    thermal equilibria between, 376  
Spontaneous mutation, 85  
Spreading pressure, 245  
sRNA, 219  
State function, 6  
Stationary states, 6  
Steroids, infrared spectroscopy, 413  
Strength of bonds, 19  
Structural indices, 31  
Substituents, 30 ff  
Succinic acid, 543 ff  
Sugar groups, 494  
    absorption bands, 494 ff  
Sulfadiazine spectra, 528  
Sulfonamides, nuclear magnetic resonance, 528 ff  
Sulfur bridges, 232  
Supercontraction, 266 ff  
Superdelocalizability, 67  
Superimposed bases, split and double shifts, 134  
Surface cell and layer, 311 ff  
Swelling, 266  
    of heated macromolecules, 210, 228  
Target theory, 263  
Tartrate ion, 421  
Tautomeric forms, 103 ff  
Tautomeric rearrangement, 115, 154  
Temperature-independent paramagnetism, 167  
Tendon, 270  
    protection by cross-linking, 277  
Tetraaminopyrimidine, 53  
Tetragonal field, 371  
Tetrahedral orbitals, 18  
Tetrahydrofuran, infrared spectra, 494 ff  
Tetrapyrroles, 380, 399  
Thermal effects on protein, nucleic acid and viruses, 201  
Thiodiglycollic acid radical, 553  
Thymine, 52 ff, 85, 349  
    internuclear distance, 87  
    molecular diagrams, 94  
    transition moment vector, 95

- Tobacco mosaic virus, 222  
   photoreactivation, 586  
 Total electron energy, 38 ff  
*Trans* effect, 374  
 Transelectronases, electronic structure, 71  
 Transition moment integrals, 93, 100  
 Transitions, 113 ff  
   of electronic relocation, 45  
*Trans*-labilizing effects, 367  
 Transverse relaxation, 503  
 Trapped charges, 314  
 Trigonal hybrids, 19  
 Trinucleotides, 135 ff  
 Triplet state, 553  
   EPR studies of, 553 ff  
   hyperfine structure, 562 ff  
   lifetime studies, 564 ff  
   of chlorophyll, 632  
   photochemical processes, 576 ff  
 Triplet state theory, 287, 332  
 Triplet-triplet transfer, 568  
*Triticum vulgare*, 634 ff  
 Tryptophan, 59, 267, 579  
   triplet state, characteristics of, 579  
 Tryptophan-pteridine complex, 46  
 Tryptophan-riboflavin complex, 46  
 Tumor development, 89, 148 ff, 154  
   hypothesis, 148  
 Tyrosine, 267
- ::::::::::::::
- Ultraviolet absorption spectra, 85  
 Ultraviolet adsorption changes in DNA, 218  
 Ultraviolet radiation, 584  
   definitions, 585 ff  
   killing and mutation, 584  
   photoprotection from, 584  
 Uniform states, 6  
 Unpaired electron density, 537  
 Unsaturated ligand, 362, 366  
 Unzipping or unraveling, 230  
 Uracil, 52 ff, 92  
   excitation energy, 100 ff  
   molecular diagrams, 94, 102  
   oscillator strength values, 101  
   transition moment vector, 95  
 Urea radicals, 551  
 Uridine, infrared spectra of, 447 ff, 453  
 Uridylic acid, 514
- Vaccinia*, 222  
 Vacuum microbalance, 247  
 Valence band positive holes, 146  
 Valence bond method, 21  
 Valence bond theory, 187 ff  
 van der Waal's attractions, 203  
 Variation method and theorem, 9  
 Vectorial form, 9  
 Vibration, 203  
 Vibrational energy, 205  
 Virial theorem, 25  
 Virus, combining with antiserum, 223  
 Viruses, 414, 433  
   attachment and entry, 223  
   heat effects on, 222 ff  
   infectivity loss, 233  
   infrared spectroscopy, 414, 433  
   multiplication of, 223  
   sterilization of, 211  
   thermal effects on, 201  
 Visible radiation, 586  
 Vitamin B<sub>12</sub>, 369, 399  
 Vitamins, 433
- Warburg apparatus, 637  
 Water  
   bound in polypeptide chains, 203  
   in inactivation process, 227  
   molecule, 239  
 Water adsorption  
   and conductivity, 251 ff  
   experimental kinetics of, 247  
   heats and entropies of, 244  
   hysteresis effects, 243 ff  
   interpretation of kinetics, 249

- Water adsorption—*contd.*  
  isotherms, 240 ff  
  on solid protein, **238**  
  thermodynamics of, **244**  
Watson-Crick model, 54, 116,  
  **342** ff  
Watson-Crick stereo-model, 86  
Wave function, 6  
Weiss constant, **611**  
Wiener-Khinchin theorem, 507  
Wiggles, 504  
Wilkins model, **344**  
Wool, 266  
  protection by cross-linking, **277**  
Xanthine, 47 ff, 50 ff  
Xanthine oxidase, 77, 620  
X-rays, 260  
  diffraction diagrams of natural  
    fibres, 264  
Yohimène, 414  
 $z$ -Axis ligands, 371, 376, 393, 400  
Zeeman energy, 177  
Zeeman splitting, 166  
Zero differential overlap, 36  
Zero-field splittings, 554  
Zero-order function, 12  
Zustandsumme, 206